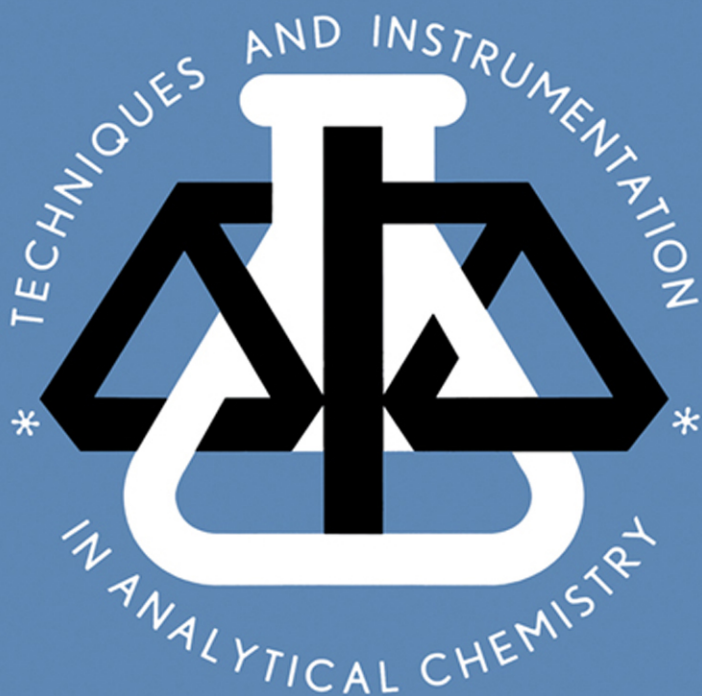


23



# **MOLECULARLY IMPRINTED POLYMERS**

**MAN-MADE MIMICS OF ANTIBODIES  
AND THEIR APPLICATIONS  
IN ANALYTICAL CHEMISTRY**

**edited by  
B. SELLERGREN**

**ELSEVIER**

TECHNIQUES AND INSTRUMENTATION IN ANALYTICAL CHEMISTRY – VOLUME 23

# **MOLECULARLY IMPRINTED POLYMERS**

**Man-made mimics of antibodies and their applications in analytical chemistry**

## TECHNIQUES AND INSTRUMENTATION IN ANALYTICAL CHEMISTRY

- Volume 1 **Evaluation and Optimization of Laboratory Methods and Analytical Procedures. A Survey of Statistical and Mathematical Techniques**  
by D.L. Massart, A. Dijkstra and L. Kaufman
- Volume 2 **Handbook of Laboratory Distillation**  
by E. Krell
- Volume 3 **Pyrolysis Mass Spectrometry of Recent and Fossil Biomaterials. Compendium and Atlas**  
by H.L.C. Meuzelaar, J. Haverkamp and F.D. Hileman
- Volume 4 **Evaluation of Analytical Methods in Biological Systems**  
**Part A. Analysis of Biogenic Amines**  
edited by G.B. Baker and R.T. Coutts  
**Part B. Hazardous Metals in Human Toxicology**  
edited by A. Vercruysse  
**Part C. Determination of Beta-Blockers in Biological Material**  
edited by V. Marko
- Volume 5 **Atomic Absorption Spectrometry**  
edited by J.E. Cantle
- Volume 6 **Analysis of Neuropeptides by Liquid Chromatography and Mass Spectrometry**  
by D.M. Desiderio
- Volume 7 **Electroanalysis. Theory and Applications in Aqueous and Non-Aqueous Media and in Automated Chemical Control**  
by E.A.M.F. Dahmen
- Volume 8 **Nuclear Analytical Techniques in Medicine**  
edited by R. Cesareo
- Volume 9 **Automatic Methods of Analysis**  
by M. Valcárcel and M.D. Luque de Castro
- Volume 10 **Flow Injection Analysis — A Practical Guide**  
by B. Karlberg and G.E. Pacey
- Volume 11 **Biosensors**  
by F. Scheller and F. Schubert
- Volume 12 **Hazardous Metals in the Environment**  
edited by M. Stoeppler
- Volume 13 **Environmental Analysis. Techniques, Applications and Quality Assurance**  
edited by D. Barceló
- Volume 14 **Analytical Applications of Circular Dichroism**  
edited by N. Purdie and H. Brittain
- Volume 15 **Trace Element Analysis in Biological Specimens**  
edited by R.F.M. Herber and M. Stoeppler
- Volume 16 **Flow-through (Bio)Chemical Sensors**  
by M. Valcárcel and M.D. Luque de Castro
- Volume 17 **Quality Assurance for Environmental Analysis**  
edited by Ph. Quevauviller, E.A. Maier and B. Griepink
- Volume 18 **Instrumental Methods in Food Analysis**  
edited by J.R.J. Paré and N.M.R. Bélanger
- Volume 19 **Trace Determination of Pesticides and their Degradation Products in Water**  
by D. Barceló and M.-C. Hennion
- Volume 20 **Analytical Pyrolysis of Natural Organic Polymers**  
by S.C. Moldoveanu
- Volume 21 **Sample Handling and Trace Analysis of Pollutants**  
edited by D. Barceló
- Volume 22 **Interlaboratory Studies and Certified Reference Materials for Environmental Analysis: the BCR approach**  
by Ph. Quevauviller and E.A. Maier
- Volume 23 **Molecularly Imprinted Polymers**  
**Man-made mimics of antibodies and their applications in analytical chemistry**  
edited by B. Sellergren

TECHNIQUES AND INSTRUMENTATION IN ANALYTICAL CHEMISTRY VOLUME 23

# MOLECULARLY IMPRINTED POLYMERS

**Man-made mimics of antibodies and  
their applications in analytical  
chemistry**

**Edited by Börje Sellergren**

*Department of Inorganic Chemistry and Analytical Chemistry  
Johannes Gutenberg University Mainz  
Duesbergweg 10–14  
D-55099 Mainz, Germany*



**ELSEVIER**

**Amsterdam–Lausanne–New York–Oxford–Shannon–Singapore–Tokyo**



ELSEVIER SCIENCE BV.  
Sara Burgerhartstraat 25  
P.O. Box 211, 1000 AE Amsterdam, The Netherlands

© 2001 Elsevier Science BV. All rights reserved.

This work is protected under copyright by Elsevier Science, and the following terms and conditions apply to its use:

#### Photocopying

Single photocopies of single chapters may be made for personal use as allowed by national copyright laws. Permission of the Publisher and payment of a fee is required for all other photocopying, including multiple or systematic copying, copying for advertising or promotional purposes, resale, and all forms of document delivery. Special rates are available for educational institutions that wish to make photocopies for non-profit educational classroom use.

Permissions may be sought directly from Elsevier Science Global Rights Department, PO Box 800, Oxford OX5 1DX, UK; phone: (+44) 1865 843830, fax: (+44) 1865 853333, e-mail: [permissions@elsevier.co.uk](mailto:permissions@elsevier.co.uk). You may also contact Global Rights directly through Elsevier's home page (<http://www.elsevier.nl>), by selecting 'Obtaining Permissions'.

In the USA, users may clear permissions and make payments through the Copyright Clearance Center, Inc., 222 Rosewood Drive, Danvers, MA 01923, USA; phone: (978) 7508400, fax: (978) 7504744, and in the UK through the Copyright Licensing Agency Rapid Clearance Service (CLARCS), 90 Tottenham Court Road, London W1P 0LP, UK; phone: (+44) 171 631 5555; fax: (+44) 171 631 5500. Other countries may have a local reprographic rights agency for payments.

#### Derivative Works

Tables of contents may be reproduced for internal circulation, but permission of Elsevier Science is required for external resale or distribution of such material.

Permission of the Publisher is required for all other derivative works, including compilations and translations.

#### Electronic Storage or Usage

Permission of the Publisher is required to store or use electronically any material contained in this work, including any chapter or part of a chapter.

Except as outlined above, no part of this work may be reproduced, stored in a retrieval system or transmitted in any form or by any means, electronic, mechanical, photocopying, recording or otherwise, without prior written permission of the Publisher.

Address permissions requests to: Elsevier Science Global Rights Department, at the mail, fax and e-mail addresses noted above.

#### Notice

No responsibility is assumed by the Publisher for any injury and/or damage to persons or property as a matter of products liability, negligence or otherwise, or from any use or operation of any methods, products, instructions or ideas contained in the material herein. Because of rapid advances in the medical sciences, in particular, independent verification of diagnoses and drug dosages should be made.

First edition 2001

Second impression 2003

Library of Congress Cataloging in Publication Data

A catalog record from the Library of Congress has been applied for.

ISBN: 0-444-82837-0

© The paper used in this publication meets the requirements of ANSI/NISO Z39.48-1992 (Permanence of Paper).  
Printed in The Netherlands.

## Contents

|                                   |      |
|-----------------------------------|------|
| <b>Preface</b> .....              | xvii |
| <b>List of Contributors</b> ..... | xix  |
| <b>Abbreviations</b> .....        | xxii |

### CHAPTER 1. A HISTORICAL PERSPECTIVE OF THE DEVELOPMENT OF MOLECULAR IMPRINTING

|         |   |    |
|---------|---|----|
| 1.1     | Introduction .....  | 1  |
| 1.2     | Polyakov invents molecular imprinting.....                  | 1  |
| 1.3     | The contributions of Pauling and Dickey .....               | 3  |
| 1.3.1   | Theories of antibody formation .....                        | 3  |
| 1.3.2   | Bio-imprinting in the 1940s .....                           | 5  |
| 1.3.3   | Dickey invents molecular imprinting .....                   | 6  |
| 1.4     | Methods for preparing molecularly imprinted silicas .....   | 6  |
| 1.5     | The mechanism(s) of selectivity .....                       | 7  |
| 1.5.1   | More studies on Dickey's system—molecular footprints? ..... | 9  |
| 1.5.2   | An association mechanism? .....                             | 9  |
| 1.5.3   | Objections to the association mechanism .....               | 10 |
| 1.6     | Applications of molecularly imprinted silicas .....         | 11 |
| 1.6.1   | Separation .....  | 11 |
| 1.6.1.1 | Column chromatography.....                                  | 11 |
| 1.6.1.2 | Thin layer chromatography .....                             | 12 |
| 1.6.2   | Structure elucidation.....                                  | 13 |
| 1.6.3   | Catalysis.....  | 13 |
| 1.6.4   | Other applications .....                                    | 14 |
| 1.6.5   | Making money using molecular imprinting? .....              | 15 |
| 1.7     | The decline of imprinted silica research .....              | 15 |
| 1.8     | Molecular imprinting in organic polymers .....              | 15 |
| 1.9     | Conclusions .....   | 17 |
|         | Acknowledgements.....                                       | 17 |
|         | References .....  | 17 |

### CHAPTER 2. FUNDAMENTAL ASPECTS ON THE SYNTHESIS AND CHARACTERISATION OF IMPRINTED NETWORK POLYMERS

|     |                    |    |
|-----|--------------------|----|
| 2.1 | Introduction ..... | 21 |
|-----|--------------------|----|

|            |   |    |
|------------|---|----|
| 2.2        | Free radical polymerisation .....   | 23 |
| 2.2.1      | Initiation.....   | 23 |
| 2.2.2      | Propagation .....   | 25 |
| 2.2.3      | Termination .....   | 25 |
| 2.2.4      | Steady state.....   | 26 |
| 2.2.5      | Chain transfer .....  | 26 |
| 2.2.6      | Inhibition.....   | 27 |
| 2.2.7      | Copolymerisation .....  | 27 |
| 2.2.8      | Tacticity .....   | 28 |
| 2.3        | Copolymers of divinyl monomers and monovinyl monomers.....                      | 29 |
| 2.3.1      | Pre-gel regime and kinetics .....   | 29 |
| 2.3.1.1    | The EDMA–MMA system .....   | 29 |
| 2.3.1.2    | The EDMA–MAA molecularly imprinted polymer (MIP) system: primary structure..... | 32 |
| 2.3.1.3    | The EDMA–MAA MIP system: secondary structure .....                              | 32 |
| 2.3.2      | Build-up of the porous structure: the tertiary structure .....                  | 33 |
| 2.4        | Site stability, integrity and accessibility.....                                | 35 |
| 2.5        | Polymer porosity and swelling .....   | 37 |
| 2.6        | Thermochemically versus photochemically initiated polymerisations .             | 39 |
| 2.7        | The cross-linking monomer .....   | 41 |
| 2.8        | Extraction of template .....  | 43 |
| 2.9        | Functional group titrations.....  | 44 |
| 2.10       | Binding site location .....   | 46 |
| 2.11       | Characterisation techniques for cross-linked vinyl polymers and MIPS            | 47 |
| 2.11.1     | Elemental analysis .....  | 48 |
| 2.11.2     | Gravimetric analysis .....  | 48 |
| 2.11.3     | Nuclear magnetic resonance spectroscopy .....                                   | 49 |
| 2.11.4     | Infrared spectroscopy.....  | 49 |
| 2.11.5     | Fluorescence probes of network solvation.....                                   | 49 |
| 2.11.6     | Pore structure in the dry state.....  | 50 |
| 2.11.6.1   | Gas sorption measurements .....   | 51 |
| 2.11.6.2   | Mercury penetration.....  | 52 |
| 2.11.6.3   | Surface areas .....   | 53 |
| 2.11.6.4   | Pore volume .....   | 53 |
| 2.11.6.5   | Pore size distribution.....   | 53 |
| 2.11.7     | Pore structure in the swollen state.....  | 54 |
| 2.11.8     | Thermal analysis.....   | 55 |
| References | .....   | 55 |

### **CHAPTER 3. THERMODYNAMIC PRINCIPLES UNDERLYING MOLECULARLY IMPRINTED POLYMER FORMULATION AND LIGAND RECOGNITION**

|     |   |    |
|-----|---|----|
| 3.1 | Introduction.....   | 59 |
| 3.2 | Physical principles underlying MIP preparation .....        | 59 |
| 3.3 | Physical principles underlying MIP–ligand recognition ..... | 64 |

|     |                       |    |
|-----|-----------------------|----|
| 3.4 | Conclusions .....     | 68 |
|     | Acknowledgements..... | 68 |
|     | References .....      | 68 |

## **CHAPTER 4. MOLECULAR IMPRINTING WITH COVALENT OR STOICHIOMETRIC NON-COVALENT INTERACTIONS**

|       |   |     |
|-------|---|-----|
| 4.1   | Introduction .....  | 71  |
| 4.2   | The concept of imprinting.....  | 72  |
| 4.3   | The optimisation of the polymer structure.....  | 74  |
| 4.4   | The role of the binding-site interactions .....   | 81  |
| 4.5   | Examples of covalent interactions in molecular imprinting.....                          | 82  |
| 4.5.1 | Boronic acid-containing binding sites.....  | 82  |
| 4.5.2 | Other types of covalent binding.....  | 85  |
| 4.5.3 | Covalent binding during imprinting and non-covalent binding during equilibration.....   | 95  |
| 4.6   | Molecular recognition and catalysis with stoichiometric non-covalent interactions ..... | 97  |
|       | Acknowledgements.....   | 107 |
|       | References .....  | 107 |

## **CHAPTER 5. THE NON-COVALENT APPROACH TO MOLECULAR IMPRINTING**

|         |  |     |
|---------|--|-----|
| 5.1     | Introduction .....   | 113 |
| 5.2     | Structure–binding relationships.....                                     | 118 |
| 5.2.1   | Examples of imprinted chiral stationary phases (CSPs).....               | 118 |
| 5.2.1.1 | High enantioselectivity, high substrate selectivity .....                | 118 |
| 5.2.1.2 | High enantioselectivity, low substrate selectivity .....                 | 121 |
| 5.2.2   | Antibody-like recognition.....   | 121 |
| 5.3     | Adsorption isotherms and site distribution .....                         | 126 |
| 5.3.1   | Batch rebinding experiments .....  | 127 |
| 5.3.2   | Results from frontal analysis.....                                       | 129 |
| 5.4     | Adsorption–desorption kinetics and chromatographic band broadening ..... | 132 |
| 5.4.1   | Adsorption–desorption kinetics in batch rebinding experiments.....       | 132 |
| 5.4.2   | Peak dispersion and asymmetry in chromatography using MIP-phases.....    | 133 |
| 5.5     | Factors influencing the recognition properties of MIPs.....              | 138 |
| 5.5.1   | Choice of the functional monomer.....                                    | 138 |
| 5.5.2   | Influence of the number of template interaction sites.....               | 146 |
| 5.5.3   | Thermodynamic considerations .....                                       | 147 |
| 5.5.3.1 | Concentration of functional monomer and template .....                   | 149 |
| 5.5.3.2 | Polymerisation temperature .....   | 149 |
| 5.5.3.3 | Polymerisation pressure.....   | 151 |

|         |   |     |
|---------|---|-----|
| 5.5.3.4 | Polymerisation diluent.....   | 153 |
| 5.5.4   | Influence of the template shape.....  | 154 |
| 5.5.5   | Influence of the monomer–template rigidity.....                                   | 156 |
| 5.5.6   | Studies of the monomer-template solution structures.....                          | 156 |
| 5.6     | Post-treatments affecting affinity, selectivity and mass transfer properties..... | 161 |
| 5.6.1   | Thermal annealing or curing.....  | 161 |
| 5.6.2   | Esterification.....   | 164 |
| 5.6.3   | Hydrolysis.....   | 165 |
| 5.7     | Medium dependence in the rebinding to MIPs.....                                   | 165 |
| 5.7.1   | Effect of swelling and porosity in different media.....                           | 165 |
| 5.7.2   | Chromatographic retention modes.....  | 167 |
| 5.7.2.1 | Electrostatic interactions – Organic mobile phases ..                             | 167 |
| 5.7.2.2 | Ion exchange retention mode.....  | 173 |
| 5.7.2.3 | Hydrophobic interactions – Aqueous mobile phases                                  | 176 |
| 5.7.3   | Mobile phase optimisation.....  | 179 |
| 5.8     | Conclusions.....  | 180 |
|         | References.....   | 180 |

## **CHAPTER 6. METAL-ION COORDINATION IN DESIGNING MOLECULARLY IMPRINTED POLYMERIC RECEPTORS**

|       |   |     |
|-------|---|-----|
| 6.1   | Introduction.....   | 185 |
| 6.2   | Binding site interactions in molecularly imprinted polymers.....                      | 186 |
| 6.3   | Advantages of metal-coordination interactions in molecular recognition.....           | 186 |
| 6.4   | Design of molecularly imprinted polymers based on metal-coordination interaction..... | 187 |
| 6.4.1 | Bulk polymerised metal-coordinating polymeric receptors.....                          | 187 |
| 6.4.2 | Surface modified metal-coordinating imprinted polymers.....                           | 191 |
| 6.5   | Applications of metal-coordinated imprinted polymers.....                             | 192 |
| 6.5.1 | Sorbents for separation media.....  | 193 |
| 6.5.2 | Recognition and binding of proteins.....  | 195 |
| 6.5.3 | Catalysis.....  | 197 |
| 6.5.4 | Sensors.....  | 197 |
| 6.6   | Conclusions and outlook.....  | 199 |
|       | References.....   | 201 |

## **CHAPTER 7. COVALENT IMPRINTING USING SACRIFICIAL SPACERS**

|     |  |     |
|-----|--|-----|
| 7.1 | Introduction.....  | 203 |
| 7.2 | Sacrificial spacer method.....                                       | 204 |
| 7.3 | Combination of non-covalent and sacrificial spacer methodologies ... | 206 |
| 7.4 | Amino acid sequence specific polymers.....                           | 208 |
| 7.5 | Conclusions.....   | 211 |

|                       |     |
|-----------------------|-----|
| Acknowledgements..... | 211 |
| References.....       | 211 |

## **CHAPTER 8. MOLECULAR IMPRINTING APPROACHES USING INORGANIC MATRICES**

|       |   |     |
|-------|---|-----|
| 8.1   | Introduction .....                          | 213 |
| 8.1.1 | Sol-gel chemistry .....                     | 214 |
| 8.2   | Two-dimensional matrices.....               | 217 |
| 8.3   | Three-dimensional matrices.....             | 221 |
| 8.3.1 | Thin films .....                            | 221 |
| 8.3.2 | Bulk structures.....                        | 222 |
| 8.3.3 | Separations.....                            | 233 |
| 8.3.4 | Catalysis.....                              | 235 |
| 8.4   | Zeolites and supramolecular imprinting..... | 239 |
| 8.5   | Conclusion .....                            | 241 |
|       | Acknowledgements.....                       | 241 |
|       | References .....                            | 242 |

## **CHAPTER 9. IMPRINTING POLYMERISATION FOR RECOGNITION AND SEPARATION OF METAL IONS**

|       |  |     |
|-------|--|-----|
| 9.1   | Introduction .....   | 245 |
| 9.2   | Survey of preparation methods of metal ion-imprinted resins.....                                     | 245 |
| 9.3   | Early studies on metal ion-imprinting .....  | 247 |
| 9.3.1 | Method 1 in Scheme 9.1 .....   | 247 |
| 9.3.2 | Method 2 in Scheme 9.1 .....   | 248 |
| 9.4   | Metal ion-imprinted microspheres prepared by reorganisation of coordinating groups on a surface..... | 250 |
| 9.4.1 | The concept of surface imprinting by the use of seed emulsion polymerisation .....                   | 250 |
| 9.4.2 | Preparation and physicochemical characterisation of the microspheres .....                           | 251 |
| 9.4.3 | Metal adsorption behaviour of the microspheres.....  | 252 |
| 9.4.4 | FT-IR and ESR studies on Cu(II)-loaded microspheres.....   | 253 |
| 9.5   | Metal ion-imprinted resins prepared by o/w emulsion polymerisation .....                             | 255 |
| 9.5.1 | Surface imprinting by use of O/W emulsion .....  | 255 |
| 9.5.2 | Potassium oleate and dioleoyl hydrogen phosphate as functional monomers .....                        | 256 |
| 9.5.3 | Metal ion-imprinted resins by O/W emulsion polymerisation ..   | 256 |
| 9.6   | Metal ion-imprinted resins prepared by W/O emulsion polymerisation .....                             | 260 |
| 9.6.1 | Imprinting polymerisation in W/O emulsion .....  | 260 |
| 9.6.2 | Dioleoyl phosphate (DOLPA) as functional monomer with $\gamma$ -ray irradiation .....                | 263 |
| 9.7   | Applications of metal ion-imprinted resins and future aspects .....                                  | 264 |

|       |   |     |
|-------|---|-----|
| 9.7.1 | Biomimetic applications .....                     | 264 |
| 9.7.2 | Chemical sensor and applications.....             | 265 |
| 9.7.3 | Other techniques using metal ion-imprinting ..... | 266 |
| 9.8   | Conclusion.....                                   | 267 |
|       | References .....                                  | 268 |

## **CHAPTER 10. BIO-IMPRINTING: POLYMERIC RECEPTORS WITH AND FOR BIOLOGICAL MACROMOLECULES**

|          |  |     |
|----------|--|-----|
| 10.1     | Introduction.....  | 271 |
| 10.2     | Molecular imprinting using biological macromolecules as matrix forming materials .....                   | 272 |
| 10.2.1   | Molecularly imprinted matrices using proteins as the precursors .....                                    | 272 |
| 10.2.1.1 | Molecularly imprinted protein matrices for recognition and separation.....                               | 273 |
| 10.2.1.2 | Molecularly imprinted protein matrices for catalysis .....   | 276 |
| 10.2.2   | Molecularly imprinted matrices using carbohydrates as the precursors .....                               | 282 |
| 10.3     | Molecular imprinting of biological macromolecules and assemblies...                                      | 283 |
| 10.4     | Protein mimetic imprinted gels: responsive hydrogels exhibiting biomolecular recognition properties..... | 289 |
| 10.5     | Conclusions and outlook.....   | 291 |
|          | References .....   | 293 |

## **CHAPTER 11. SURFACE IMPRINTING OF MICROORGANISMS**

|      |                                   |     |
|------|-----------------------------------|-----|
| 11.1 | Introduction.....                 | 295 |
| 11.2 | Imprinting of microorganisms..... | 295 |
| 11.3 | Methodology.....                  | 296 |
| 11.4 | Potential applications.....       | 301 |
| 11.5 | Conclusions .....                 | 303 |
|      | References .....                  | 303 |

## **CHAPTER 12. POLYMERISATION TECHNIQUES FOR THE FORMATION OF IMPRINTED BEADS**

|        |  |     |
|--------|--|-----|
| 12.1   | Introduction.....  | 305 |
| 12.2   | Special considerations relevant to molecularly imprinted beads.....                | 306 |
| 12.3   | Techniques that have been used to make molecularly imprinted beads .....           | 307 |
| 12.4   | Imprinted bead production methods.....   | 307 |
| 12.4.1 | Utilising the pores in preformed beads (method I in Table 12.1) .....              | 307 |
| 12.4.2 | Suspension polymerisation in water (method IIa in Table 12.1) .....                | 311 |
| 12.4.3 | Suspension polymerisation in fluorocarbon liquids (method IIb in Table 12.1) ..... | 312 |
| 12.4.4 | Dispersion polymerisation methods (method III in Table 12.1) .....                 | 315 |
| 12.4.5 | Aqueous two-step swelling method (method IV in Table 12.1) .....                   | 317 |

|  |     |
|--|-----|
| 12.4.6. Aerosol polymerisation methods (method V in Table 12.4).....           | 319 |
| 12.4.7 Surface rearrangement of latex particles (method VI in Table 12.1)..... | 320 |
| 12.5 Conclusions and future perspective .....                                  | 321 |
| Acknowledgements.....  | 322 |
| References .....   | 322 |

### **CHAPTER 13. TECHNIQUES FOR THE *IN SITU* PREPARATION OF IMPRINTED POLYMERS**

|   |     |
|---|-----|
| 13.1 Introduction .....   | 325 |
| 13.1.1 Molecular-level design .....                                   | 325 |
| 13.1.2 Morphology design.....   | 325 |
| 13.2 <i>In situ</i> imprinted polymer rods .....                      | 327 |
| 13.2.1 Polymer rods as chromatographic stationary phases.....         | 327 |
| 13.2.2 Tool for selecting functional monomer.....                     | 330 |
| 13.3 <i>In situ</i> dispersion polymers.....                          | 332 |
| 13.3.1 Use of imprinted affinity media in SPE .....                   | 332 |
| 13.3.2 Use of imprinted affinity media in electrophoresis.....        | 333 |
| 13.4 <i>In situ</i> molecular imprinting for batch applications ..... | 335 |
| 13.4.1 Batch-type <i>in situ</i> polymer preparation.....             | 335 |
| 13.4.2 Combinatorial method for molecular imprinting.....             | 335 |
| 13.5 Conclusions .....  | 339 |
| References .....  | 340 |

### **CHAPTER 14. APPLICATION OF MOLECULARLY IMPRINTED POLYMERS IN COMPETITIVE LIGAND BINDING ASSAYS FOR ANALYSIS OF BIOLOGICAL SAMPLES**

|   |     |
|---|-----|
| 14.1 Introduction .....   | 341 |
| 14.2 Use of molecularly imprinted polymers (MIPs) as antibody mimics... | 342 |
| 14.3 Organic solvent-based assays.....                                  | 344 |
| 14.4 Aqueous buffer-based assays.....                                   | 346 |
| 14.5 Selectivity .....  | 348 |
| 14.6 Sensitivity .....  | 349 |
| 14.7 Non-radioactive assays .....                                       | 350 |
| 14.8 Conclusions and future outlook.....                                | 351 |
| References .....  | 353 |

### **CHAPTER 15. MOLECULARLY IMPRINTED POLYMERS IN SOLID PHASE EXTRACTIONS**

|  |     |
|--|-----|
| 15.1 Introduction .....                      | 355 |
| 15.2 Multi-purpose SPE phases .....          | 356 |
| 15.3 High affinity SPE phases.....           | 358 |
| 15.4 Molecularly imprinted SPE (MISPE) ..... | 358 |



|          |   |     |
|----------|---|-----|
| 15.4.1   | Off-line protocols .....  | 364 |
| 15.4.1.1 | Sample clean-up of biological fluids.....                       | 364 |
| 15.4.1.2 | Extraction of analytes of environmental concern ....            | 366 |
| 15.4.2   | On-line protocols.....  | 368 |
| 15.4.2.1 | Extraction of nicotine.....                                     | 368 |
| 15.4.2.2 | MISPE with pulsed elution .....                                 | 370 |
| 15.4.2.3 | On-line coupled column approaches .....                         | 370 |
| 15.5     | The development of new MISPE protocols.....                     | 370 |
| 15.6     | Template bleeding: an unresolved issue in MISPE protocols ..... | 371 |
| 15.7     | Conclusions .....   | 373 |
|          | Acknowledgements.....   | 373 |
|          | References .....  | 373 |

## CHAPTER 16. CAPILLARY ELECTROCHROMATOGRAPHY BASED ON MOLECULAR IMPRINTING

|          |   |     |
|----------|---|-----|
| 16.1     | Introduction.....   | 377 |
| 16.2     | CEC.....  | 377 |
| 16.2.1   | Short introduction to CEC.....  | 377 |
| 16.2.2   | Equipment .....   | 379 |
| 16.3     | Molecular imprinting — a brief history: preparation and application ..... | 380 |
| 16.4     | CEC based on molecular imprinting.....                                    | 381 |
| 16.4.1   | Adjustment of MIPs to columns of capillary format.....                    | 381 |
| 16.4.1.1 | <i>In situ</i> dispersion polymerisation .....                            | 381 |
| 16.4.1.2 | Gel-entrapped MIP particles .....   | 382 |
| 16.4.1.3 | MIPs as pseudo-stationary phase .....                                     | 383 |
| 16.4.1.4 | MIP coatings.....   | 383 |
| 16.4.1.5 | <i>In situ</i> prepared MIP monoliths .....                               | 383 |
| 16.4.2   | Electrochromatographic separations.....                                   | 387 |
| 16.5     | Conclusions and future outlook .....                                      | 391 |
|          | References .....  | 392 |

## CHAPTER 17. MOLECULARLY IMPRINTED POLYMERS IN ENANTIOMER SEPARATIONS

|        |   |     |
|--------|---|-----|
| 17.1   | Introduction.....                       | 395 |
| 17.1.1 | Covalent molecular imprinting.....      | 396 |
| 17.1.2 | Non-covalent molecular imprinting ..... | 396 |
| 17.2   | Polymer systems .....                   | 397 |
| 17.2.1 | Monomers and cross-linkers .....        | 397 |
| 17.2.2 | Polymerisation solvents .....           | 398 |
| 17.2.3 | Polymerisation methods .....            | 399 |
| 17.3   | Chiral chromatography .....             | 400 |
| 17.3.1 | HPLC.....                               | 401 |

|                            |     |
|----------------------------|-----|
| 17.3.2 TLC .....           | 410 |
| 17.3.3 CE and CEC .....    | 412 |
| 17.3.4 Other methods ..... | 413 |
| 17.4 Conclusions .....     | 413 |
| References .....           | 414 |

## **CHAPTER 18. BIOMIMETIC ELECTROCHEMICAL SENSORS BASED ON MOLECULAR IMPRINTING**

|   |     |
|---|-----|
| 18.1 Introduction .....   | 417 |
| 18.2 Chemical sensor technology .....   | 417 |
| 18.2.1 Chemical sensors .....   | 417 |
| 18.2.2 The transducer .....   | 418 |
| 18.2.2.1 Electrochemical transducers .....  | 418 |
| 18.2.2.2 Other transducers .....  | 420 |
| 18.2.3 The recognition element .....  | 421 |
| 18.2.3.1 Physicochemical recognition elements .....   | 421 |
| 18.2.3.2 Biological recognition elements .....  | 422 |
| 18.2.3.3 Biomimetic recognition elements .....  | 423 |
| 18.3 Sensors utilising molecularly imprinted recognition sites .....                            | 423 |
| 18.3.1 Approaches using imprinted macroporous methacrylate,<br>acrylate or vinyl polymers ..... | 424 |
| 18.3.1.1 Early approaches .....   | 424 |
| 18.3.1.2 Sensors based on accumulation in the polymer .....                                     | 424 |
| 18.3.1.3 Sensors based on permeation through the polymer ..                                     | 426 |
| 18.3.2 Templated inorganic materials .....  | 428 |
| 18.3.3 Gate sites in surface monolayers .....   | 429 |
| 18.3.4 Templating in conducting and redox polymers .....  | 431 |
| 18.3.4.1 Ion sieving .....  | 431 |
| 18.3.4.2 More complex systems .....   | 432 |
| 18.3.4.3 Redox polymers .....   | 433 |
| 18.3.4.4 Composite materials .....  | 434 |
| 18.4 Conclusions and outlook .....  | 434 |
| References .....  | 436 |

## **CHAPTER 19. IONIC SENSORS BASED ON MOLECULARLY IMPRINTED POLYMERS**

|   |     |
|---|-----|
| 19.1 Introduction .....   | 441 |
| 19.2 Synthesis of ion-selective molecularly imprinted polymers (MIPs) ..... | 442 |
| 19.2.1 Monomer selection and preparation .....                              | 442 |
| 19.2.2 Preparation of complexes .....                                       | 443 |
| 19.2.3 Preparation of polymers .....  | 443 |
| 19.2.4 Testing for selectivity .....  | 445 |
| 19.3 Electrochemical sensors .....  | 447 |

|        |  |     |
|--------|--|-----|
| 19.3.1 | Conductivity .....                     | 447 |
| 19.3.2 | ISEs .....                             | 447 |
| 19.3.3 | Imprinted polymer ISEs .....           | 449 |
| 19.4   | Spectroscopic sensors .....            | 451 |
| 19.4.1 | Transition metal ion chromophores..... | 452 |
| 19.4.2 | Lanthanide ion chromophores .....      | 453 |
| 19.4.3 | Organic chromophores.....              | 458 |
| 19.4.4 | Optical probes.....                    | 461 |
| 19.5   | FIA .....                              | 461 |
| 19.6   | Prospects .....                        | 463 |
|        | Acknowledgements.....                  | 464 |
|        | References .....                       | 464 |

## CHAPTER 20. TOWARD OPTICAL SENSORS FOR BIOLOGICALLY ACTIVE MOLECULES

|           |   |     |
|-----------|---|-----|
| 20.1      | Introduction.....   | 467 |
| 20.2      | Optical sensors .....   | 468 |
| 20.2.1    | Ellipsometry.....   | 468 |
| 20.2.2    | Linear dichroism .....  | 468 |
| 20.2.3    | Colorimetric detection of solvent vapours using MIPs<br>deposited on quartz crystals..... | 470 |
| 20.2.4    | Surface plasmon resonance.....  | 472 |
| 20.2.5    | Fluorimetry.....  | 473 |
| 20.2.5.1  | Fibre optic detection of fluorescent template .....                                       | 473 |
| 20.2.5.2  | Effect of template on formation of fluorophores<br>within the MIP .....                   | 474 |
| 20.2.5.3  | Competition of template and fluorescent reporter ...                                      | 474 |
| 20.2.5.4  | Imprinting of silicas with fluorophores.....  | 475 |
| 20.2.5.5  | Covalent and non-covalent imprinting using<br>fluorophores as functional monomers .....   | 477 |
| 20.2.5.6  | Formation of fluorescent complex upon binding of<br>metal ion template .....              | 478 |
| 20.2.5.7  | Interaction of ancillary ligand with fluorescent metal<br>complexes within the MIP .....  | 478 |
| 20.2.5.8  | Determination of fluorophores using MIPs formed on<br>quartz crystals.....                | 479 |
| 20.2.5.9  | Quenching of functional monomer fluorescence upon<br>binding of analyte .....             | 480 |
| 20.2.5.10 | Competitive fluoroimmunoassay.....  | 481 |
| 20.2.6    | Sensors based on liquid chromatography (LC) .....   | 482 |
| 20.2.6.1  | Chloramphenicol (CAP) sensors.....  | 484 |
| 20.2.6.2  | Fluorescent detection of $\beta$ -estradiol [40].....                                     | 488 |
| 20.3      | Latest developments.....  | 490 |
| 20.3.1    | Liquid chromatographic detection of L-phenylalanine amide..                               | 490 |

|  |     |
|--|-----|
| 20.3.2 Fluorescent detection of PAHs in water .....        | 491 |
| 20.3.3 MIPs and infrared evanescent wave spectroscopy..... | 491 |
| 20.3.4 Competitive chemiluminescence assay .....           | 494 |
| 20.3.5 A fluorescent sensor for L-tryptophan.....          | 494 |
| 20.3.6 An enzyme-linked MIP sorbent assay .....            | 496 |
| 20.3.7 A fluorescent FIA sensor for flavonol .....         | 497 |
| 20.4 Outlook.....  | 498 |
| Acknowledgements.....                                      | 499 |
| References .....   | 500 |

## **CHAPTER 21. NON-COVALENT MOLECULARLY IMPRINTED SENSORS FOR VAPOURS, POLYAROMATIC HYDROCARBONS AND COMPLEX MIXTURES**

|  |     |
|--|-----|
| 21.1 Introduction .....  | 503 |
| 21.2 Chemical sensors.....   | 503 |
| 21.3 Evidence for molecular recognition.....                           | 506 |
| 21.4 Principles of non-covalent imprinting for sensors .....           | 507 |
| 21.5 Optical sensor applications.....                                  | 510 |
| 21.6 Mass-sensitive devices.....                                       | 515 |
| 21.7 Differences between chromatographic and chemosensory applications | 519 |
| 21.8 Conclusions .....   | 522 |
| References .....   | 524 |

This Page Intentionally Left Blank

## Preface

The ability of biological hosts to strongly and specifically bind to a particular molecular structure is a key factor in the biological machinery. Well known examples are the sensitivity of the immune response, where antibodies are generated in response to minute amounts of a foreign antigen, or the energy saved by enzymes due to their ability to stabilise the transition state of the reaction to be catalysed. With biological examples as models, chemists hope to be able to mimic these properties for various applications. For instance, stable recognition elements capable of strongly and selectively binding molecules could be used in robust, sensitive analytical methods for the analysis of trace levels of compounds in complex matrices. Alternatively, such recognition elements could be used to separate undesirable compounds from foods or biological fluids, for targeted delivery of drugs or for demanding separations at preparative level in the fine chemical industry. If the sites can be made to catalyse chemical reactions, a new tool to achieve efficient catalysis by design is at the chemist's disposal.

Robust molecular recognition elements with antibody-like ability to bind and discriminate between molecules or other structures can today be synthesised using molecular imprinting techniques. This includes the synthesis of cross-linked polymers in the presence of templates which may be small molecules, biological macromolecules, microorganisms or whole crystals. Removal of the template from the formed polymer thus generates a structure complementary to the template structure or to an analogous structure. This simple and appealing concept is the topic of this book. With 21 chapters written by the world's leading groups in the field and covering most aspects of the synthesis and applications of imprinted materials, this book provides the first complete coverage of the area of molecular imprinting available to date.

The book is divided into five sections starting with a historical perspective and fundamental aspects on the synthesis and recognition by imprinted polymers. The second section contains eight up-to-date overview chapters on current approaches to molecular and ion imprinting. This is followed by two chapters on new material morphologies and, in the last two sections, various analytical applications of imprinted polymers are given, with the last four chapters devoted to the promising field of imprinted polymers in chemical sensors.

It should be noted that the authors have widely different backgrounds, mainly polymer chemistry, organic chemistry, biochemistry or analytical chemistry. The book therefore has an interdisciplinary character and should, in my view, appeal to a broad audience. With these words I would like to thank the authors for preparing

their manuscripts and the referees for their critical reviews. Special thanks also go to my co-workers Dr. Andrew J. Hall, and Dr. Francesca Lanza for their many hours spent reading and correcting the manuscript.

Börje Sellergren

## List of Contributors

- C. ALEXANDER *Institute of Food Research, Norwich Research Park, Colney, Norwich NR4 7UA, UK*
- H.S. ANDERSSON *Bio-organic Chemistry Group, Institute of Natural Sciences, University of Kalmar, PO Box 905, S-391 29 Kalmar, Sweden*
- L.I. ANDERSSON *AstraZeneca R&D Södertälje, S-151 85 Södertälje, Sweden*
- R.J. ANSELL *School of Chemistry, University of Leeds, Leeds LS2 9JT, UK*
- A. BIFFIS *Institute of Organic Chemistry and Macromolecular Chemistry, Heinrich Heine University, Universitätsstrasse 1, D-40225 Düsseldorf, Germany*
- P.K. DHAL *GelTex Pharmaceuticals, Inc., 153 Second Avenue, Waltham, MA 02451, USA*
- F.L. DICKERT *Institute of Analytical Chemistry, University of Vienna, Währingerstrasse 38, A-1090 Vienna, Austria*
- A.J. HALL *Department of Inorganic Chemistry and Analytical Chemistry, Johannes Gutenberg University Mainz, Duesbergweg 10-14, D-55099 Mainz, Germany*
- O. HAYDEN *Institute of Analytical Chemistry, University of Vienna, Währingerstrasse 38, A-1090 Vienna, Austria*
- I. KARUBE *Research Center for Advanced Science and Technology, University of Tokyo, 4-6-1 Komaba, Meguro-ku, Tokyo 153-8904, Japan*
- M. KEMPE *Department of Organic Chemistry 1, University of Lund, Chemical Centre, PO Box 124, S-221 00 Lund, Sweden*
- D. KRIZ *European Institute of Science, S-223 70 Lund, Sweden*
- M.G. KULKARNI *National Chemical Laboratory, Pune 411 008, India*
- F. LANZA *Department of Inorganic Chemistry and Analytical Chemistry, Johannes Gutenberg University Mainz, Duesbergweg 10-14, D-55099 Mainz, Germany*



- M. MAEDA *Department of Materials Physics and Chemistry, Graduate School of Engineering, Kyushu University, Fukuoka 812-8581, Japan*
- R.A.MASHELKAR *National Chemical Laboratory, Pune 411 008, India*
- J. MATSUI *Laboratory of Synthetic Biochemistry, Faculty of Information Sciences, Hiroshima City University, 3-4-1 Ozukahigashi, Asaminami-ku, Hiroshima 731-3194, Japan*
- A.G.MAYES *School of Chemical Sciences, University of East Anglia, Norwich NR4 7TJ, UK*
- S. MCNIVEN *Research Center for Advanced Science and Technology, University of Tokyo, 4-6-1 Komaba, Meguro-ku, Tokyo 153-8904, Japan*
- M. MURATA *Department of Materials Physics and Chemistry, Graduate School of Engineering, Kyushu University, Fukuoka 812-8581, Japan*
- G.M. MURRAY *Department of Chemistry and Biochemistry, University of Maryland Baltimore County, 1000 Hilltop Circle, Baltimore, MD 21250, USA and Applied Physics Laboratory, Johns Hopkins University, 11100 Johns Hopkins Road, Laurel, MD 20723-6099, USA*
- I.A. NICHOLLS *Bio-organic Chemistry Group, Institute of Natural Sciences, University of Kalmar, PO Box 905, S-391 29 Kalmar, Sweden*
- S. NILSSON *Division of Technical Analytical Chemistry, Centre for Chemistry and Chemical Engineering, Lund University, PO Box 124, S-221 00 Lund, Sweden*
- N. PEREZ *Institute of Food Research, Norwich Research Park, Colney, Norwich NR4 7UA, UK*
- D.Y. SASAKI *Organic Materials Synthesis and Degradation, Sandia National Laboratories, PO Box 5800, Albuquerque, NM 87185-1407, USA*
- L. SCHWEITZ *Division of Technical Analytical Chemistry, Centre for Chemistry and Chemical Engineering, Lund University, PO Box 124, S-221 00 Lund, Sweden*
- B. SELLERGREN *Department of Inorganic Chemistry and Analytical Chemistry, Johannes Gutenberg University Mainz, Duesbergweg 10-14, D-55099 Mainz, Germany*

- T. TAKEUCHI *Laboratory of Synthetic Biochemistry, Faculty of Information Sciences, Hiroshima City University, 3-4-1 Ozukahigashi, Asaminami-ku, Hiroshima 731-3194, Japan*
- K. TSUKAGOSHI *Department of Chemical Engineering and Materials Science, Faculty of Engineering, Doshisha University, Tanabe, Kyoto 610-03, Japan*
- O.M. UY *Applied Physics Laboratory, Johns Hopkins University, 11100 Johns Hopkins Road, Laurel, MD 20723-6099, USA*
- E.N. VULFSON *Institute of Food Research, Norwich Research Park, Colney, Norwich NR4 7UA, UK*
- M.J. WHITCOMBE *Institute of Food Research, Norwich Research Park, Colney, Norwich NR4 7UA, UK*
- G. WULFF *Institute of Organic Chemistry and Macromolecular Chemistry, Heinrich Heine University, Universitätsstrasse 1, D-40225 Düsseldorf, Germany*

## List of Abbreviations

|          |  |
|----------|--|
| 2,4-D    | 2,4-Dichlorophenoxyacetic acid                           |
| 2,4-DB   | 2,4-Dichlorophenoxybutyric acid                          |
| 2,4-DOMe | 2,4-Dichlorophenoxyacetic acid methyl ester              |
| 9EA      | 9-Ethyladenine   |
| AAM      | Acrylamide   |
| ABDV     | 2,2'-Azo-bis-(2,4-dimethyl-valeronitrile)                |
| Ac.PABA  | <i>N</i> -Acryloyl-para-aminobenzamidine                 |
| AIBN     | 2,2'-Azobisisobutyronitrile                              |
| AME      | Ametryn  |
| AMP      | Adenosine monophosphate                                  |
| AMPSA    | 2-(Acrylamido)-2-methylpropanesulphonic acid             |
| ANN      | Artificial neural networks                               |
| ATP      | Adenosine triphosphate                                   |
| ATR      | Atrazine   |
| BA       | Benzylamine  |
| BDMA     | Butylene dimethacrylate                                  |
| BET      | Brunauer–Emmett–Teller (isotherm)                        |
| BSA      | Bovine serum albumin                                     |
| cAMP     | Cyclic adenosine monophosphate                           |
| CAP      | Chloramphenicol  |
| CE       | Capillary electrophoresis                                |
| CEC      | Capillary electrochromatography                          |
| CHEMFET  | Chemically sensitive field effect transistor             |
| CMMC     | 7-Carboxymethoxy-4-methylcoumarin                        |
| CP MAS   | Cross-polarisation magic angle spinning                  |
| CPOAc    | 4-Chlorophenoxyacetic acid                               |
| CSP      | Chiral stationary phase                                  |
| CV       | Cyclic voltammetry                                       |
| CVD      | Chemical vapour deposition                               |
| CWE      | Coated wire electrode                                    |
| DAD      | Diode array detection                                    |
| DB       | 1,4-Dibromobutane  |
| DCP      | 2,4-Dichlorophenol                                       |
| DDDPA    | 1,12-Dodecanediol- <i>O,O'</i> -diphenyl phosphonic acid |
| DEAEMA   | <i>N,N</i> -Diethyl-2-aminoethylmethacrylate             |
| DEGDMA   | Diethyleneglycol dimethacrylate                          |

|          |   |
|----------|---|
| DEO      | <i>N,N</i> -Diethyl- <i>p</i> -phenylazoaniline         |
| DMMB     | 3,5-Dimethyl methyl benzoate                            |
| DMO      | <i>N,N</i> -Dimethyl- <i>p</i> -phenylazoaniline        |
| DOLPA    | Dioleyl phosphate                                       |
| DSC      | Differential scanning calorimetry                       |
| DVB      | Divinylbenzene  |
| DVMB     | Divinyl methylbenzoate                                  |
| EDMA     | Ethylene glycol dimethacrylate                          |
| ELISA    | Enzyme-linked immuno-sorbent assay                      |
| EO       | Ethyl orange  |
| EOF      | Electroosmotic flow                                     |
| FIA      | Flow injection analysis                                 |
| FTIR     | Fourier-transform infrared spectroscopy                 |
| GCB      | Graphitised carbon black                                |
| GMA      | Glycidoxypromethylmethacrylate                          |
| HEMA     | 2-Hydroxyethyl methacrylate                             |
| HPLC     | High-performance liquid chromatography                  |
| IA       | Immunoaffinity  |
| ICP-AES  | Inductively coupled plasma atomic emission spectrometry |
| ICP-MS   | Inductively coupled plasma mass spectrometry            |
| ISE      | Ion-selective electrode                                 |
| ISFET    | Ion-selective field effect transistor                   |
| LB       | Langmuir–Blodgett (films)                               |
| LC       | Liquid chromatography                                   |
| LOD      | Limit of detection                                      |
| L-PA     | L-Phenylalanine anilide                                 |
| L-PMA    | L-Phenylalanine- <i>N</i> -methylanilide                |
| MA       | Methacrylate  |
| MAA      | Methacrylic acid  |
| MIA      | Molecularly imprinted sorbent assay                     |
| MIP      | Molecularly imprinted polymer                           |
| MISPE    | Molecularly imprinted solid phase extraction            |
| MISPE-PE | MISPE with pulsed elution                               |
| MMA      | Methyl methacrylate.                                    |
| MO       | Methyl orange   |
| MTES     | Methyltriethoxysilane                                   |
| NAD      | Nicotinamide adenine dinucleotide                       |
| NATA     | <i>N</i> -acetyltryptophanamide                         |
| O/W      | Oil/water   |
| ODS      | Octadecylsilane   |
| ODS      | Octadecyltrichlorosilane                                |
| PAH      | Polycyclic aromatic hydrocarbon                         |
| PAM      | Pentamidine   |
| PETEA    | Pentaerythritol tetraacrylate                           |
| PETRA    | Pentaerythritol triacrylate                             |

|        |   |
|--------|---|
| PLS    | Partial least squares                               |
| PMA    | Poly(methacrylates)                                 |
| PMP    | Pinacolyl methyl phosphonate                        |
| POAc   | Phenoxyacetic acid                                  |
| PRO    | Prometryn   |
| PS-DVB | Styrene-divinyl benzene copolymers                  |
| PSt    | Poly(styrenes)                                      |
| PVC    | Polyvinylchloride                                   |
| PVI    | Polyvinylimidazole                                  |
| PVP    | Poly(4-vinylpyridine)                               |
| QCM    | Quartz crystal microbalance                         |
| RAM    | Restricted access materials                         |
| SAM    | Self-assembling monolayers                          |
| SAW    | Surface acoustic wave                               |
| SAWS   | Surface acoustic wave sensor                        |
| SDS    | Sodium dodecyl sulphate                             |
| SEM    | Scanning electron microscopy                        |
| SERRS  | Surface enhanced Raman scattering                   |
| SPE    | Solid phase extraction                              |
| SPR    | Surface plasmon resonance                           |
| STW    | Shear transverse acoustic wave                      |
| TACN   | 1,4,7-Triazacyclononane                             |
| TAM    | Thiamphenicol                                       |
| TCDD   | 2,3,7,8-Tetrachlorodibenzodioxin                    |
| TEA    | Triethylamine                                       |
| TEOS   | Tetraethoxysilane                                   |
| TFA    | Trifluoroacetic acid                                |
| TFM    | Trifluoromethyl acrylic acid                        |
| TFM    | 2-(Trifluoromethyl)acrylic acid                     |
| TGA    | Thermal gravimetric analysis                        |
| THF    | Tetrahydrofuran                                     |
| TLC    | Thin-layer chromatography                           |
| TOP    | Tobacco peroxidase                                  |
| TPCK   | Tosyl phenyl alanyl chloromethyl ketone             |
| TRIM   | Trimethylol propane trimethacrylate                 |
| TSA    | Transition state analogues                          |
| V70    | 2,2'-Azo-bis-(4-methoxy-2,4-dimethyl-valeronitrile) |
| VOC    | Volatile organic compound                           |
| VPY    | Vinylpyridine                                       |
| W/O    | Water/oil   |
| XPS    | X-ray photoelectron spectroscopy                    |

## A historical perspective of the development of molecular imprinting

HÅKAN S. ANDERSSON AND IAN A. NICHOLLS

### 1.1. INTRODUCTION

Here we review the history of molecular imprinting, from the introduction of the technique in conjunction with silica matrices in 1931 until the beginning of the 1970s, when the technique was first applied to organic polymers. The theories used to explain the nature of the selective molecular recognition exhibited by imprinted silicas, the methods for their preparation, as well as the attempts to apply them for practical use, are discussed. Finally, a brief overview is given regarding the evolution of molecular imprinting in organic polymers.

Molecular imprinting is currently attracting wide interest from the scientific community as reflected in the 80 original papers published in the field during 1997 (Fig. 1.1). However, although interest in the technique is new, the concept itself has a long history. 1972 marked the start of molecular imprinting technology as we know it today, when the laboratories of Wulff [1] and Klotz [2] independently reported the preparation of organic polymers with predetermined ligand selectivities. Template molecules which were present during polymerisation, or derivatives thereof, were recognised by the resultant *molecularly imprinted polymer* (MIP). Nonetheless, some 40 papers describing conceptually similar approaches had appeared dating back to the early 1930s. This body of work pertains to the preparation of ligand-selective recognition sites in the inorganic matrix silica. The aim of this chapter is to review this “pre-history” of molecular imprinting, which serves as a reminder to us all that good science can be older than the time span covered by computer databases.

### 1.2. POLYAKOV INVENTS MOLECULAR IMPRINTING

At the beginning of this century much effort was devoted to the development of new materials and techniques for application in chromatography [3]. Although it had already been described during the mid-19th century by Schönbein and Goppelsröder [4], it was not until the development of zonal chromatography by Tswett in 1906 [5] that its usefulness as a method for purifying and/or analysing single compounds from crude mixtures was truly highlighted.

Among the many scientists active in this field was the Soviet chemist M.V.

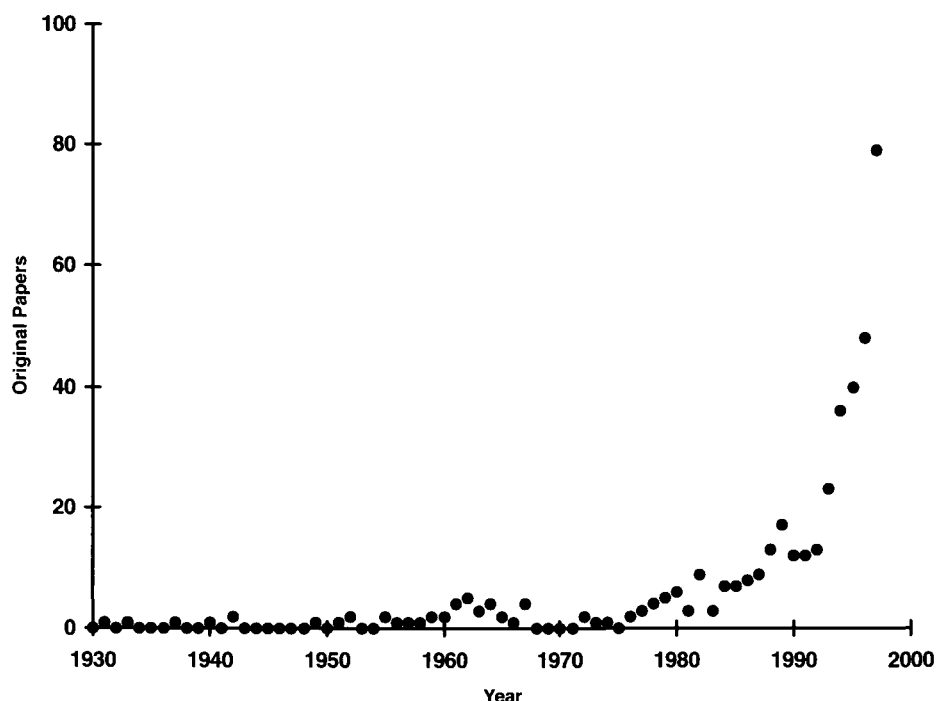


Fig. 1.1. Graphical representation illustrating the number of original papers published within the field of molecular imprinting between 1931 and 1997 [86].

Polyakov, who performed a series of investigations on silica for use in chromatography. Polyakov prepared his silica by the acidification of sodium silicate solutions, which after drying of the gelatinous silica polymer, afforded a rigid matrix. In a paper published in 1931 [6], the effects on silica pore structure of the presence of benzene, toluene or xylene during drying were reported. After 20–30 days of drying at room temperature, the additive was washed off using hot water. When  $\text{H}_2\text{SO}_4$  was used as the polymerisation initiator (acidifying agent), a positive correlation was found between surface areas, e.g. load capacities, and the molecular weights of the respective additives. However, when  $(\text{NH}_4)_2\text{CO}_3$  was instead used as the initiator, the results differed markedly from the above. When the silica was placed in a desiccator containing a beaker with one of the additives, the extent of adsorption of the different additives was shown to be dependent upon the structure of the additive present during the drying process (Table 1.1).

Polyakov concluded that differences in the rate and extent of silica polymerisation due to the weaker acidifier  $(\text{NH}_4)_2\text{CO}_3$  were the key factors underlying the apparent selectivity. The effect was ascribed to alterations in the silica structure induced by the presence of the additive, which was anticipated to replace water molecules on the silica surface. Later work, published in 1933 [7] and 1937 [8], contained more detailed investigations of this selective molecular recognition

TABLE 1.1

REBINDING DATA [6] FOR SILICAS PREPARED USING  $(\text{NH}_4)_2\text{CO}_3$  AS THE ACIDIFIER

|                    | Analyte, % adsorbed by silica |             |             |
|--------------------|-------------------------------|-------------|-------------|
|                    | Benzene                       | Toluene     | Xylene      |
| Gel prepared with: |                               |             |             |
| Benzene            | <b>87.5</b>                   | 80.6        | 80.1        |
| Toluene            | 88.5                          | <b>87.2</b> | 86.7        |
| Xylene             | 75.1                          | 79          | <b>68.3</b> |

phenomenon. Importantly, selectivity was suggested to arise from structural changes in the silica which were a consequence of the chemical nature of the additive. In other words, the additives were considered as templates which directly affected the resultant silica surfaces. To the best of our knowledge, this was the first time that experiments of this kind were accompanied by explanations of this nature.

Polyakov's studies went largely unnoted by the scientific community, with only a handful of citations which were almost exclusively from other Eastern European scientists. Not deterred, Polyakov continued until the late 1950s [9,10] writing reviews of the area, though mainly devoted to establishing his founding role in the development of molecular imprinting.

### 1.3. THE CONTRIBUTIONS OF PAULING AND DICKEY

Over the years following Polyakov's three papers, much attention was being focused on biochemical processes and the structures of biomolecules. Linus Pauling, at the Gates and Crellin Laboratories at the California Institute of Technology, Pasadena, was perhaps the most important contributor to the area at the time. After his work with valence bond theory, he shifted the direction of his research to the practical implications of the nature of the chemical bond, especially with respect to protein structure and function. The  $\alpha$ -helix and  $\beta$ -sheet structures, the molecular-level explanation to sickle-cell anaemia, and an early transition-state theory of catalysis, were all products of his research [11]. In addition, he carefully examined the selectivity exhibited by antibodies. The following section describes Pauling's efforts together with Frank Dickey, which constituted an independent development of molecular imprinting in silica matrices.

#### 1.3.1. Theories of antibody formation

Mankind has for decades benefited from the *in vitro* use of antibodies. Nevertheless, the basic mechanisms of antibody formation *in vivo* have been known for less



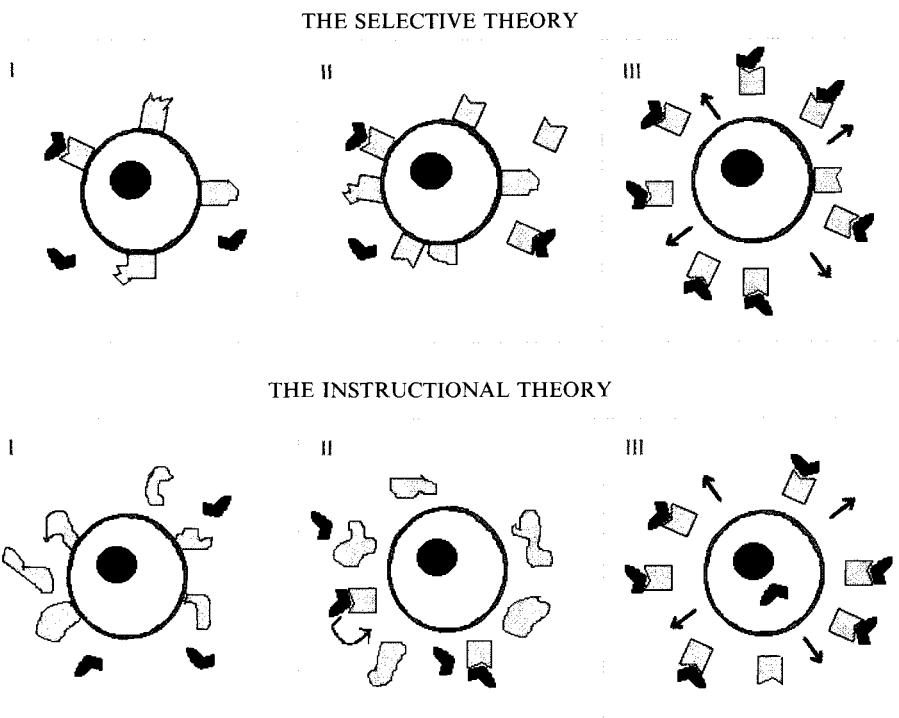


Fig. 1.2. Schematic representation of the selective and instructional theories used to explain the origin of the antigen selectivity of antibodies.

than 30 years, on account of the efforts of Burnet, Jerne, Talmadge and others [12,13]. Prior to the emergence of the *clonal-selection theory*, two divergent concepts evolved to explain the mechanism of antibody formation; the *selective theory* and the *instructional theory* (Fig. 1.2). The selective theory was first formulated in 1900 by Ehrlich [14], who postulated that a white blood cell's surface bore various antibodies to one of which the antigen became chemically linked. The interaction would prompt the cell to produce copies of the selected antibody in great excess. The instructional theory was first proposed by Breinl and Haurowitz in 1930 [15], though soon thereafter both Mudd [16] and Pauling [17] followed with related interpretations. They proposed that antibody formation took place in the presence of an antigen which served as a template for antibody formation.

Pauling's theory differed from those of the others in that he suggested that the primary structure of any antibody was identical and that selectivity arose from differences in the conformation of the antibody induced by the antigen template. Although this theory was later proven to be incorrect, the method he suggested to validate this hypothesis was imaginative:

*“An interesting possible method to producing antibodies from serum or globulin solution outside of the animal is suggested by the theory. The globulin would be*

*treated with a denaturing agent or condition sufficiently strong to cause the chain ends to uncoil; after which this agent or condition would be removed slowly while antigen or hapten is present in the solution in considerable concentration. The chain ends would then coil up to assume the configurations stable under these conditions, which would be configurations complementary to those of the antigen or hapten."* [17]

### 1.3.2. Bio-imprinting in the 1940s

In two publications from 1942 [18,19] Pauling and Campbell reported the "production of antibodies *in vitro*". The method by which this was claimed to have been accomplished was derived from that which is quoted in the section above. Two dye stuffs, methylene blue and 1,3-dihydroxy-2,4,6-tri(*p*-azophenylarsonic acid)benzene, and the polysaccharide *Pneumococcus polysaccharide Type III*, were employed as the antigens/templates. Polyclonal (non-immunised)  $\gamma$ -globulin serum was incubated together with high concentrations of antigen under denaturing conditions. In a typical experiment; a mixture of antigen, protein and NaOH, at a pH of approximately 11, was incubated for 15–30 min, whereafter a fraction was removed and continuously dialysed against a stream of phosphate buffer at pH 7.5. This was expected to give the opportunity for the antibodies to slowly renature to configurations stable in neutral solutions and in the presence of the antigen. After 72 h of dialysis the pH of the sample had reached 7.5, and there were only traces of antigen left in solution; the rest had been removed *via* the dialysis or incorporated in antibody precipitates formed during neutralisation. An increase in precipitate formation and antigen incorporation was interpreted as an indication that affinity maturation had occurred in the proteins. Temperature denaturation was found to affect the antibody in a similar way, though no change in affinity for the antigen was observed when the denaturing agent was either acid (pH 2.5) or urea (3.5 M). In experiments where the precipitated antibodies were redissolved after removal of the antigen (*Pneumococcus polysaccharide Type III*) and analysed with respect to selectivity, it was seen that the resulting antibody could efficiently precipitate the polysaccharide antigen, but not a related sugar polymer, *polysaccharide Type I*.

It appears pointless to discuss the validity of these findings today, but it is noteworthy that the procedure was in essence similar to what today is called bio-imprinting [20,21], a technique whereby a protein or other biopolymer is used as the matrix for molecular imprinting instead of an abiotic polymer. Moreover, the apparent success in preparing antibodies *in vitro* led Pauling to initiate an investigation of the application of the selective theory in an abiotic system, as is evident from the following recollection:

*"There was some criticism of our work — contradictory results reported by another investigator. I felt satisfied with what we had done, and did not go to the trouble of carrying out more studies, except that I got a senior student, Frank Dickey, to carry out the study with hydrated silica — precipitated silicic acid polymer."* [22]

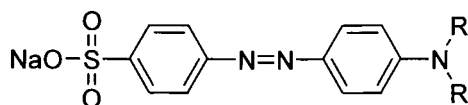
### 1.3.3. Dickey invents molecular imprinting

At a lecture delivered in Philadelphia's Franklin Institute on March 17, 1949, Pauling reported some of the results from Dickey's experiments [23]. Silica gels had been prepared "*by procedures analogous to the formation of antibodies*", i.e. in accordance with the selective theory, and the study was published later the same year [24]. The method described involved polymerisation of sodium silicate in the presence of a dye. Four different dyes were used, namely methyl, ethyl, *n*-propyl and *n*-butyl orange (Fig. 1.3). As much as possible of the dye was subsequently removed, and in rebinding experiments it was found that silica prepared in the presence of any of these "*pattern molecules*" would bind the pattern molecule in preference to the other three dyes. Table 1.2 shows the selective increase in pattern dye sorption capacities of the gels as related to a control gel, prepared in the absence of dye.

Shortly after this work had appeared, several research groups pursued the preparation of specific adsorbents using Dickey's method. The following section discusses the various approaches and systems used.

### 1.4. METHODS FOR PREPARING MOLECULARLY IMPRINTED SILICAS

The conditions under which the template molecules were introduced to the polymerisation system were shown to play an important role in the generation of



R= Me, Et, *n*-Pr or *n*-Bu

Fig. 1.3. Structures of the alkyl orange dyes.

TABLE 1.2

RELATIVE ADSORPTION POWERS: THE AMOUNT ADSORBED ON THE SILICA RELATED TO A NON-IMPRINTED SILICA PREPARATION [24]

Relative adsorption power for:

|                     | Methyl orange | Ethyl orange | Propyl orange | Butyl orange |
|---------------------|---------------|--------------|---------------|--------------|
| Gels prepared with: |               |              |               |              |
| Methyl orange       | <b>3.5</b>    | 1.6          | 1.1           | 1.1          |
| Ethyl orange        | 2.5           | <b>9</b>     | 2.1           | 2.2          |
| Propyl orange       | 2.3           | 5            | <b>20</b>     | 6            |
| Butyl orange        | 1.5           | 2.8          | 5             | <b>15</b>    |

ligand-selective recognition. The difference that is most evident when comparing the approaches of Polyakov and Dickey was that the latter had the template present in the sodium silicate pre-polymerisation mixture, whereas Polyakov introduced the template after the silica framework had been formed (Fig. 1.4). In this respect Dickey's method is more similar to present methodology, and it was this method that became the most widely used in subsequent studies. However, the method of Polyakov reappeared in the hands of Patrikeev and co-workers [25–29]. One advantage of this method is that it allows water insoluble compounds to be imprinted, as it was shown that water could be replaced by methanol for improved solubilisation of the template during the imprinting process [28]. No direct comparison between the two methods has been reported, though it would seem that Dickey's method is likely to have produced a more pronounced influence on the structure of the silica.

Several variations of Dickey's method were introduced. The initiation and propagation of the polymerisation process was controlled by the pH, and Dickey evaluated oxalic acid, acetic acid and HCl as the acidifiers [30]. It was found that a pH of 3.0, or lower, was optimal for polymerisation with respect to selective adsorptive properties, supposedly as a direct consequence of the lower rigidity acquired from high pH. The low buffer capacity of the reaction mixture made pH control difficult, and sometimes yielded very low pH values when using HCl, which could affect the stability of the template. In the case of HOAc, evaporation during the polymerisation process led to a rise in pH, which resulted in a less selective material, though load capacity was higher than that obtained with the other two acidifiers. Oxalic acid was found to be the best choice, as this did not affect pH as dramatically as HCl and did not evaporate as did acetic acid. Despite this, HCl remained the most frequently used acidifier.

Another stage in the imprinting process that was subjected to investigation was the template extraction procedure. Extraction had to be carried out after careful drying of the silica, otherwise the selectivity would be lost [31]. Dickey extracted the dyes by extensive washing in methanol. Later work by Morrison *et al.* [32] indicated that Dickey's washing procedure was not sufficient to remove the dye from the silica, and that additional washing with water or aqueous HCl was required. The amount of residual template could be estimated by dissolving the silica in aqueous NaOH and analysing the resulting solution by spectroscopy [32,33]. As the mechanism of recognition was under debate, various agents were added to destroy unextractable template in order to minimise the possible influence of bound template on silica selectivity. Examples of such agents include  $\text{H}_2\text{O}_2$  [28] and  $\text{H}_2\text{SO}_3$  [34], but neither of these compounds alone could fully remove/destroy all template [30]. However, Soxhlet extraction with methanol followed by treatment with a combination of  $\text{HNO}_3$  and  $\text{H}_2\text{O}_2$  proved to be an efficient procedure [34].

## 1.5. THE MECHANISM(S) OF SELECTIVITY

The mechanism of selectivity proposed by Polyakov [8] was vague and, as stated, did not receive much attention. Moreover, the instructional theory from which

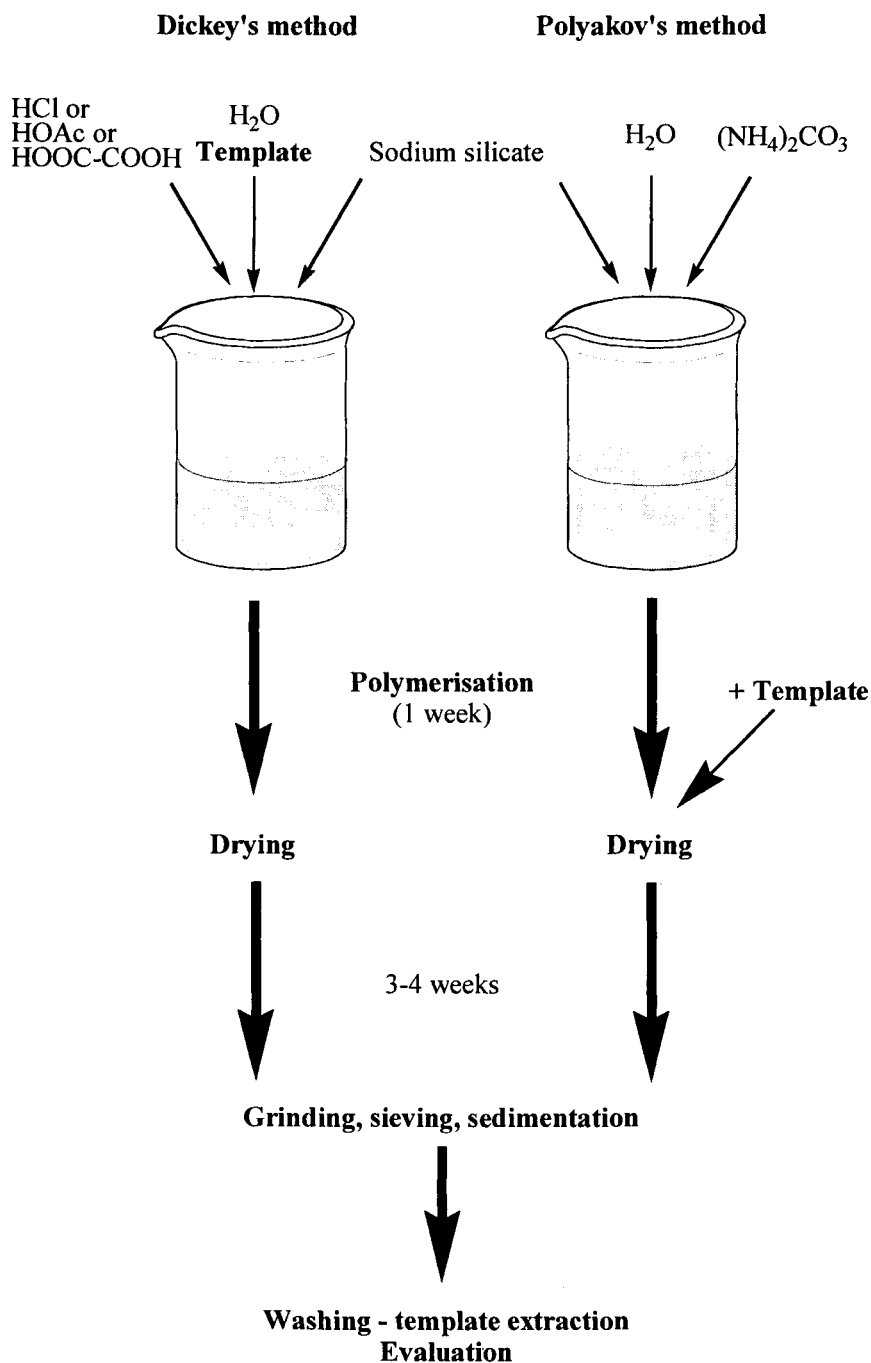


Fig. 1.4. Schematic illustration of the methods for imprinted silica preparation developed by Dickey and Polyakov.

Dickey had found inspiration for his work was under debate, which obviously influenced the credibility of its application to the silica system. An active scientific debate ensued regarding the nature of the mechanisms responsible for ligand recognition in these imprinted silicas, with two opposing schools of thought.

### 1.5.1. More studies on Dickey's system — molecular footprints?

In his first work, Dickey had provided only a cursory discussion of the possible mechanisms underlying the specific adsorption. His experiments were largely repeated by Bernhard [35], who confirmed Dickey's results. In 1955, Haldeman and Emmett [33] reported a reinvestigation of Dickey's silica samples, where they found selectivity to be significantly lower than originally described, a problem that had been described by Dickey [30] as the result of ageing of the silica. However, their interpretation of the basis of silica–ligand selectivity was more clearly presented than previously:

*“When a gel is formed in the presence of a dye, it seems likely that most of the combined dye will be situated on or near the surface, since such interactions should generate defects in the gel structure. . . . It seems reasonable to suppose that in the process of methanol extraction, which follows gel formation and drying, dye molecules on or near the surface are removed leaving micropores (“footprints”) of geometry and properties characteristic of the dye. The number of such pores should increase with the basicity of the dyes.” [33]*

They implied that the high adsorptive capacities of imprinted silica reported by Dickey were inconsistent with the footprint theory, as the surface coverage, if resulting from such high sorption capacities, would be significantly *above* 100%. Based on observations of the colour of the adsorbed dye, Haldeman and Emmett concluded that the interaction was non-ionic, and that the interaction between dye and silica consisted mainly of hydrogen and van der Waals' bonding. The theory was analogous to that presented by Dickey the same year [30]. The findings that electrostatic interactions dominated the recognition process were later supported by Waksmundzki *et al.*, who investigated template–silica binding in various solvents, and identified a negative correlation between the degree of adsorption and the dielectric constant of the solvent [36]. In addition, Curti and Colombo had demonstrated that stereoselectivity could be introduced through the footprinting procedure [37–39], which indicated that the footprints were of three-dimensional character, i.e. “*imprints*”, a term which first occurred in the publication by Haldeman and Emmett. This conclusion was later to be supported by Beckett and co-workers [40–43], though the interpretation was questioned by Bartels *et al.* [34].

### 1.5.2. An association mechanism?

In 1959, a Canadian research group led by Morrison challenged the footprint theory [32]. This work was, also a re-examination of Dickey's system. Although their results concurred with those reported by Dickey [30], they noted that the

residual dye constituted an appreciable fraction of the amount of dye that could be specifically adsorbed. The adsorption isotherms were concave in relation to the concentration axis, but linear at higher concentrations. Linearity was, however, seen throughout the whole interval on a non-imprinted reference gel, except in the cases of propyl and butyl orange, which also exhibited the non-linear segment on the reference gel. These effects were ascribed to the formation of complexes between ligand and template entrapped in the silica after the extraction procedure. While Dickey had pointed out that acid washing yielded higher specific adsorption capacity, Morrison *et al.* found that acid washing did not lead to any significant extraction of template. Thus they concluded that the enhancement of specific adsorption following acid washing could not be explained by the removal of template molecules from footprints, but rather by an enhanced accessibility to remaining dye molecules, which constituted nucleation centres.

Waksmundzki *et al.* extensively examined the surface areas and microporosities of imprinted silica surfaces [44]. It was found that although the template itself had little effect on the total surface area, the sizes of the micropores were positively correlated to the size of the template. Subsequent studies on the sorption of template to silicas imprinted with pyridine [45–50], quinoline and acridine [45–47], and 2-picoline, 2,4-lutidine and 2,4,6-collidine [50], combined with thermodynamic studies on the heat of wetting of template or methanol/water sorption [47,51–53], led to the conclusion that these templates were adsorbed as multilayers to the silica. This observation supported the association mechanism hypothesis. The possibility of a footprint mechanism and an association mechanism coexisting in a concentration dependent fashion does not appear to have been considered.

### **1.5.3. Objections to the association mechanism**

The association mechanism was challenged by Beckett and Youssef [43], who had conducted a study on quinine-selective silica which had shown that selectivity could be abolished as a result of treatment with steam or by deactivation using dry organic solvents. They proposed five points in support of the footprint theory: (i) If a molecule trapped in the adsorbent is an optical isomer, and if this isomer forms a racemic compound with its optical antipode, this would be expected to yield a more stable complex than would be obtained from self-association. The reverse effect was observed with imprinted silica. (ii) If the trapped molecules led to selective attraction, it would be expected that an increase in the concentration of trapped molecules would yield an increase in the selectivity of the control. No such correlation was seen in this study. (iii) Selectivity was reduced relative to the control upon the passing of dry organic solvents through the silica, although the trapped molecules were not extracted by this procedure. No difference in the adsorption of an unrelated compound, 5-aminoacridine, was observed after this treatment. Deactivation of quinine footprints was interpreted as the most likely explanation to this effect. (iv) Storage of the silica for some months produced changes in the silica structure which permitted further extraction of template. This reduction in the concentration of trapped quinine increased the adsorptive power of the adsorbent, while the same

procedure did not result in any change in the adsorptive capacity of the control. (v) Changes in selectivity observed in this study when steam was forced through the adsorbent could be better explained by changes in footprint structure than by alterations in the attractive forces of trapped molecules.

More detailed studies of the polymerisation process were carried out by Bartels [54] who showed, using UV spectroscopy, an inter-relationship between oligo-silicic acids in the polymerisation mixture and the template (1,10-phenanthroline). This result indicated specific pre-organisation of silicic acids around the template prior to or during polymerisation. Comparison of Debye–Scherrer spectra of the imprinted and non-imprinted silicas suggested that the template acted as an order-inducing agent which yielded a regular two-dimensional crystal. Further condensation in the environment surrounding the template was interpreted to be of random order, which was explained by the fact that no order-inducing agent was present other than the template. In summary, although there was not enough evidence to refute the footprint theory in these systems, the possibility that an association mechanism plays a significant role could not be overlooked.

## 1.6. APPLICATIONS OF MOLECULARLY IMPRINTED SILICAS

It is interesting to note that many of the concepts and application areas currently being pursued with molecular imprinting technology were already considered during the early silica imprinting years. Although these attempts apparently failed to attract sufficient attention to motivate further work on them, they were ahead of their time in many respects. Earlier sections of this chapter have been focused upon the development of the technique and the mechanisms underlying it, but a significant part of the work from the 1960s involved attempts to use imprinted materials for practical purposes, as discussed below.

### 1.6.1. Separation

#### 1.6.1.1. Column chromatography

The first group to use imprinted silicas as solid phases in chromatography were Curti *et al.*, who reported the partial resolution of both mandelic acid and camphorsulphonic acid enantiomers using a frontal analytical system [37–39] (Fig. 1.5). The racemic camphorsulphonic acid was applied onto a column containing silica imprinted against the *d*-antipode, and polarimetric analyses of the eluate fractions indicated that a 30% enrichment in *l*-camphorsulphonic acid had been achieved. An analogous experiment, where racemic mandelic acid was used, yielded an enrichment of 10%. Alkyl oranges were analysed similarly and selectivity was demonstrated. It is noteworthy that these affinity separations were reported more than 15 years before the breakthrough of affinity chromatography [55].

The group of Patrikeev prepared silicas imprinted against harmine and a derivative, and employed these materials as stationary phases for zonal liquid



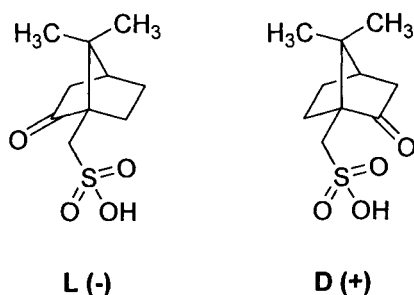


Fig. 1.5. The enantiomers of camphorsulphonic acid.

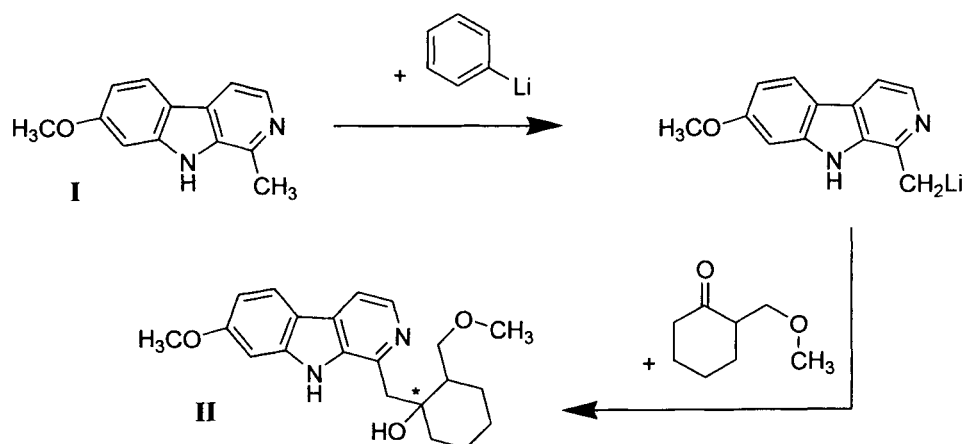


Fig. 1.6. Synthesis of 3-(2'-methoxymethyl-1'-hydroxycyclohexyl-1'-methyl)norharminine (II) from harmine (I), according to Patrikeev *et al.* [31].

chromatography in a coupled column format [28]. Elution was performed with organic solvents. The approach was found to be successful in resolving a series of by-products resulting from the synthesis of 3-(2'-methoxymethyl-1'-hydroxycyclohexyl-1'-methyl)norharminine (Fig. 1.6). The separation of steroids (testosterone derivatives) was also reported in this paper. However, the chromatographic performances of the systems reported by Curti *et al.* and Patrikeev *et al.* are not possible to ascertain from the data available.

#### 1.6.1.2. Thin layer chromatography

Patrikeev *et al.* also employed imprinted silicas for thin layer chromatography. The silica was mixed with plaster and immobilised on a plate for use in the separation and identification of gramines [31] and for the resolution of amino acid derivatives [29]. In the latter experiment it was found that the influence of the amino acid protective group, dinitrophenol, was too dominant to allow the separation of

dinitrophenyl derivatised amino acids. Nevertheless, selectivity in relation to other amino acid derivatives was observed.

Independently, Erlenmeyer and Bartels performed similar studies using starch as the immobilising agent [56]. They demonstrated that imprinted silicas could be used to distinguish between dimethyl- and diethyl-aniline, a distinction that the native silica was unable to make in the solvent mixture used (ethyl acetate/methanol/HOAc (5 M); 60:30:10).

### 1.6.2. Structure elucidation

In a 1957 publication in *Nature* [40], the group of Beckett presented an innovative method for determining the absolute configuration of organic molecules. The adsorption of stereoisomers of unknown configurations onto silicas imprinted by a single stereoisomer of a related compound of known configuration, allowed the configuration of the analyte to be deduced. This was demonstrated using quinine- and quinidine-selective silicas, where the relative adsorptions of cinchonine, cinchonidine, 9-deoxyquinine, 9-deoxycinchonidine and 9-deoxyquitenine led to correct assignments of the absolute configurations. This work was later extended to morphine and related compounds [41,42], as well as atropine analogues [41].

The group of Bartels described silica footprints as being analogous to biological receptors. Furthermore, the possibility of using the presence or absence of binding to the silanol groups as the basis for a binary code was considered, and used for producing “*information-theory interpretations*” of the selectivities of imprinted silicas [31]. Such structure-selectivity relationships were extensively examined *via* the crosswise comparison of the retention of a series of related compounds by a series of silicas imprinted against the same series of compounds [57]. These studies were further extended to shed light on the importance of the types of functional groups for the footprinting effect [58,59]. Similar crosswise comparisons were also made by the group of Waksmundzki [60]. Powerful tools for multivariate analyses were unavailable at the time, but this approach of gathering structural data from crosswise comparisons of adsorption data is the same as has been used in recent years for the development of various sensor systems, such as electronic noses.

### 1.6.3. Catalysis

In Dickey's 1949 paper [24], he presented the idea that specific catalysis, analogous to that of enzymes, was a possible application for silicas imprinted against selected reactants or products. This idea does not appear to have been realised until 1962, when the group of Patrikeev demonstrated what could be regarded as an early synthetic enzyme [27]. The reaction studied was the polycondensation of amino acid esters, a reaction known to yield both linear polypeptides (4%) and cyclic peptides (diketopiperazine, 96%) (Fig. 1.7).

By preparing the silica in the presence of either a tripeptide (ala-ala-gly) or a diketopiperazine, according to Polyakov's method the product ratios could be significantly shifted in favour of the template. The rate enhancement of the

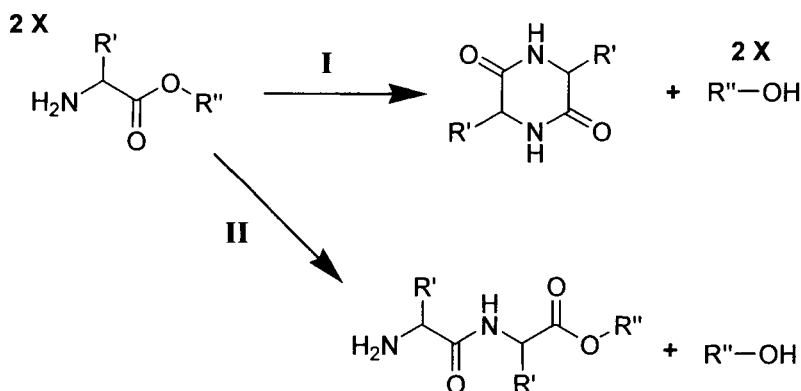


Fig. 1.7. The formation of diketopiperazine (I) and linear peptide (II), as catalysed by the MIP artificial enzymes of Patrikeev *et al.* [27].

TABLE 1.3

RELATIVE MASS RATIOS FOR THE  
POLYMERISATION OF AMINO ACID ESTERS IN THE  
PRESENCE OF VARIOUS SILICAS [27]

| Gels prepared with: | Mass ratio<br>diketopiperazine/linear polypeptide |
|---------------------|---|
| Nothing (reference) | 96/4  |
| Diketopiperazine    | 96.5/3.5  |
| Tripeptide          | 86/14   |
| Casein              | 50/50   |

tripeptide imprinted silica relative to the solution reaction was 72-fold, and the product ratios resulting from silicas prepared with the tripeptide (Table 1.3), shifted 2.5 times in favour of the linear peptide. An even more dramatic improvement was achieved when using casein as the template (12.5 times), though despite the impressive results the role of residual template was not examined.

#### 1.6.4. Other applications

A type of bacteria-mediated imprinting has recently been reported [61]. Interestingly, the multifaceted group of Patrikeev reported an equally spectacular experiment in 1962, using silica as the matrix [26]. A *Pseudomonas fluorescens* or *Bacillus mycoides* culture was introduced during vacuum drying of the newly formed silica at room temperature. After some time, the temperature was raised to 120°C and the silica was dried until a constant weight was reached. Subsequent treatment with H<sub>2</sub>O<sub>2</sub> at 90–95°C, to destroy the bacteria, was followed by repeated drying. The

resulting “bacteria-imprinted” silica was found to promote the growth of the imprinted bacteria species better than both non-imprinted silica, silica imprinted with other bacteria, or sand. In another study, footprints introduced by the chiral surface of *B. mycoides* were examined [25]. According to the authors, this species exists in both a right-hand and a left-hand form. Silica prepared in the presence of either bacteria culture was claimed to yield pronounced stereoselectivity, though some stereoselectivity of the control silica was also reported.

### **1.6.5. Making money using molecular imprinting?**

One difficulty which appears to remain to this day is the commercialisation of molecularly imprinted polymers. Although no molecularly imprinted silica product ever reached the market, at least two patents, apparently on molecular imprinting [27], were held by the group of Patrikeev [62,63]. That some commercial interest existed is also confirmed by the fact that Merck patented a nicotine filter invented by Erlenmeyer [64], consisting of nicotine imprinted silica, able to adsorb 10.7% more nicotine than non-imprinted silica. The material was intended for use in cigarette filters.

## **1.7. THE DECLINE OF IMPRINTED SILICA RESEARCH**

After a steady flow of publications over a period of 15 years, the interest in imprinted silica experienced a temporary decline (it has been pursued more recently by several groups). We have not been able to find any direct explanations from studying the literature, other than those put forward in the excellent review by Bartels and Prijs [31], which principally relate to the limitations in stability and reproducibility of the imprinted silica materials.

The silica lost its memory for the template over time. This fact had been noted by Dickey, but although treatment with HCl was found to somewhat reverse the process, no real progress was made over the years to overcome this problem. Moreover, the difficulties in repeating a silica batch preparation were significant and the adsorption capacities were reported to vary by 30% between batches (although 10% variations could be achieved under standardised conditions). The choice of template was restricted to water soluble compounds which had to be fairly stable in acid, although these limitations could be surmounted by the methods of Polyakov and Patrikeev. Another limitation was that the only templates amenable to imprinting were those that bound relatively strongly to native silica in water [65]. In conclusion, progress in the 40 year long development of the technique was limited by the performance of the silica matrix.

## **1.8. MOLECULAR IMPRINTING IN ORGANIC POLYMERS**

It was in 1972 that the groups of Klotz and Wulff independently presented the first examples of molecular imprinting in synthetic organic polymers. Briefly, the

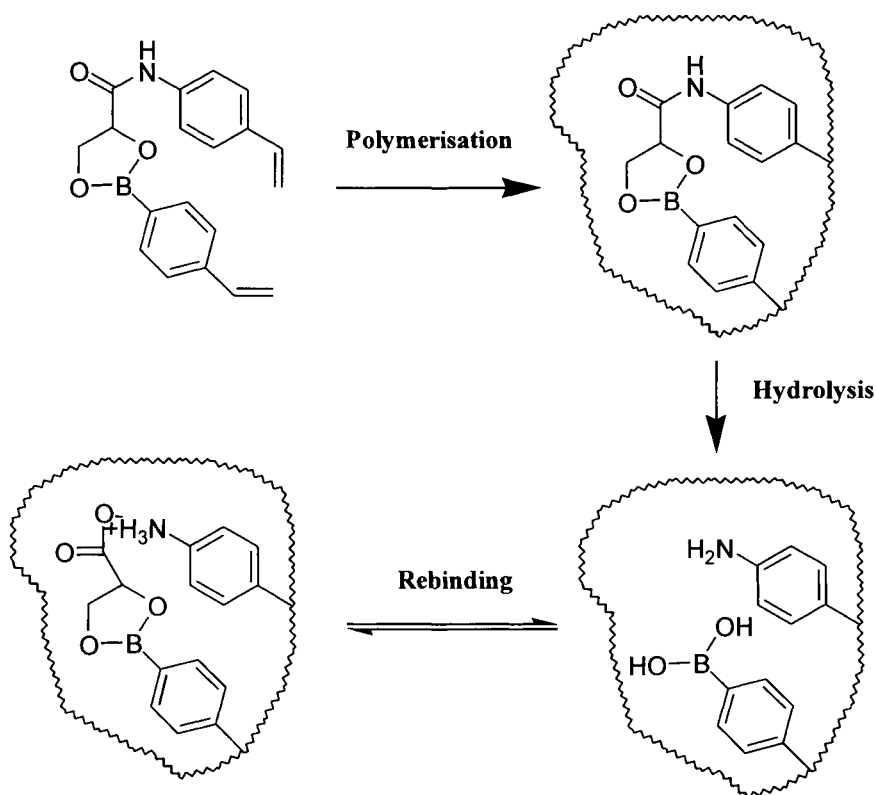


Fig. 1.8. The covalent approach to molecular imprinting in organic polymers, as introduced by the group of Wulff, exemplified by the D-glyceraldehyde MIP reported in 1972 [1].

first report of Wulff and Sarhan described a “controlled distance method”, involving the copolymerisation of D-glyceraldehyde-(*p*-vinylanilide)-2,3-O-*p*-vinylphenylboronate and divinylbenzene. Subsequent hydrolysis of the glycerate moiety disclosed imprints exhibiting chiral recognition of D-glyceraldehyde [1] (Fig. 1.8). This work was followed by extensive investigations during the 1970s and 1980s by the same group, resulting in some 30 original works. As these achievements will be covered in subsequent chapters they will not be discussed in further detail here.

Takagishi and Klotz had previously shown that the binding of small molecules in aqueous media to organic polymers could be enhanced *via* the introduction of pendant hydrophobic groups to the otherwise hydrophilic polymer [66], and that the introduction of disulphide cross-linkages, restricting the mobility of the polymer chains, led to enhanced capacities [67]. As the last in this series of papers, they combined these approaches [2]. The introduction of caproyl or lauroyl groups in polyethyleneimine polymers and subsequent incubation with the template (methyl orange), followed by moderate cross-linking *via* the formation of disulphide bridges from thiobutylolactone monomer, yielded MIPs which exhibited a higher

adsorption capacity towards methyl orange than the reference systems. These binding studies were carried out in aqueous media. No information with regard to selectivity was provided in this work, and the system does not appear to have been further characterised, though analogous studies on poly(vinylpyrrolidone) were carried out by Takagishi *et al.* in the 1980s [68–73].

The scientific activity within the field during the 1970s and early 1980s is outside the scope of this text, but has previously been thoroughly reviewed by Wulff [74]. Mention of the molecular imprinting of metal ions [75] is warranted, as this methodology was later expanded by others to a metal-coordination approach [76,77] by which organic templates could be imprinted. A most important development was the introduction of a general non-covalent approach by the group of Mosbach in the early 1980s [78,79], which significantly broadened the scope of molecular imprinting. While activity within the field was relatively low through the 1970s and 1980s, this trend began to change around 1990 (Fig. 1.1). The reasons for this are not obvious, but a series of papers, as exemplified by references [80–84], demonstrating the versatility of the non-covalent approach probably played a role. Work published by Vlatakis *et al.* in 1993 [85], by far the most cited filed in the area, in which it was shown that a MIP system could demonstrate selectivity comparable to that of biological receptors, was significant in generating interest for the technique.

The past few years have witnessed an almost exponential increase in interest in molecular imprinting, as illustrated by the number of publications appearing in the area. From 1931 to the time of writing, around 500 original papers have been published by close to 700 co-authors from more than 100 groups [86]. MIPs *anno 1998* are indeed stable, batch reproducibility is excellent and a wide range of compound classes can be successfully imprinted.

## 1.9. CONCLUSIONS

The history of molecular imprinting is longer than generally perceived and is comprised of several different independently developed approaches. This chapter acknowledges the efforts of the first workers in this area.

## ACKNOWLEDGEMENTS

The authors thank Dr Sergey Piletsky at the National Academy of Science in Ukraine, Kiev and Ms Jeanna Klinth at the University of Kalmar, Sweden, for translating some of the papers cited here. This work was supported by the University of Kalmar Research Fund.

## REFERENCES

- 1 G. Wulff and A. Sarhan, *Angew. Chem.*, **84**, 364 (1972).
- 2 T. Takagishi and I.M. Klotz, *Biopolymers*, **11**, 483 (1972).
- 3 H.H. Strain, *Anal. Chem.*, **23**, 25 (1951).

- 4 F. Goppelsröder, *Ver. Naturforsch. Ges.*, **3**, 268 (1861).
- 5 M.S. Tswett, *Ber. D. Botan. Ges.*, **24**, 316 (1906).
- 6 M.V. Polyakov, *Zhur. Fiz. Khim.*, **2**, 799 (1931).
- 7 M.V. Polyakov, P.M. Stadnik, M.W. Paryckij, I.M. Malkin and F.S. Duchina, *Zhur. Fiz. Khim.*, **4**, 454 (1933).
- 8 M.V. Polyakov, L.P. Kuleshina and I.E. Neimark, *Zhur. Fiz. Khim.*, **10**, 100 (1937).
- 9 Z. Vysotskii and M.V. Polyakov, *Zhur. Fiz. Khim.*, **30**, 1901 (1956).
- 10 Z. Vysotskii and M.V. Polyakov, *Dokl. Akad. Nauk SSSR*, **129**, 831 (1959).
- 11 S.F. Mason, *Chem. Soc. Rev.*, **29** (1997).
- 12 N.K. Jerne, *Sci. Amer.*, **229**, 52 (1973).
- 13 G.L. Ada and G. Nossal, *Sci. Amer.*, **257**, 50 (1987).
- 14 P. Ehrlich, *Proc. Royal Soc. Lond.*, **66**, 424 (1900).
- 15 F. Breinl and F. Haurowitz, *Z. Physiol. Chem.*, **19**, 245 (1930).
- 16 S. Mudd, *J. Immunol.*, **23**, 423 (1932).
- 17 L. Pauling, *J. Am. Chem. Soc.*, **62**, 2643 (1940).
- 18 L. Pauling and D.H. Campbell, *Science*, **95**, 440 (1942).
- 19 L. Pauling and D.H. Campbell, *J. Exp. Med.*, **76**, 211 (1942).
- 20 L. Braco, K. Dabulis and A.M. Klibanov, *Proc. Natl. Acad. Sci. USA*, **87**, 274 (1990).
- 21 M. Ståhl, M-O. Månsson and K. Mosbach, *Biotechnol. Lett.*, **12**, 161 (1990).
- 22 L. Pauling, *Personal communication* (1994).
- 23 Anonymous, *Chem. Eng. News*, **27**, 913 (1949).
- 24 F.H. Dickey, *Proc. Natl. Acad. Sci. USA*, **35**, 227 (1949).
- 25 V.V. Patrikeev, A.A. Balandin, E.I. Klabunovskii, J.S. Mardaszew and G.I. Maksimova, *Dokl. Akad. Nauk SSSR*, **132**, 850 (1960).
- 26 V.V. Patrikeev, Z.S. Smirnova and G.I. Maksimova, *Dokl. Akad. Nauk SSSR*, **146**, 707 (1962).
- 27 V.V. Patrikeev, T.D. Kozarenko and A.A. Balandin, *Izvest. Akad. Nauk SSSR, Otdelenie Khim.*, **1**, 170 (1962).
- 28 V.V. Patrikeev, A.F. Scholin and I.A. Nikiforova, *Izvest. Akad. Nauk SSSR, Otdelenie Khim.*, **6**, 1031 (1963).
- 29 V.V. Patrikeev and A.F. Scholin, *Molekul. Khromatogr., Akad. Nauk SSSR, Just. Fiz. Khim.*, **66** (1964).
- 30 F.H. Dickey, *J. Phys. Chem.*, **59**, 695 (1955).
- 31 H. Bartels and B. Prijs, *Adv. Chromatogr.*, **11**, 115 (1974).
- 32 J.L. Morrison, M. Worsley, D.R. Shaw and G.W. Hodgson, *Can. J. Chem.*, **37**, 1986 (1959).
- 33 R.G. Haldeman and P.H. Emmet, *J. Phys. Chem.*, **59**, 1039 (1955).
- 34 H. Bartels, B. Prijs and H. Erlenmeyer, *Helv. Chim. Acta*, **49**, 1619 (1966).
- 35 S.A. Bernhard, *J. Am. Chem. Soc.*, **74**, 4946 (1952).
- 36 A. Waksmundzki, J. Oscik, J. Rozylo and R. Nasuto, *Ann. Univ. Mariae Curie-Skłodowska, Lublin-Polonia: Sect. AA*, **19**, 9 (1964).
- 37 R. Curti and U. Colombo, *Chim. Ind.*, **23**, 103 (1951).
- 38 R. Curti and U. Colombo, *J. Am. Chem. Soc.*, **74**, 3961 (1952).
- 39 R. Curti, U. Colombo and F. Clerici, *Gazz. Chim. Ita.*, **82**, 491 (1952).
- 40 A.H. Beckett and P. Anderson, *Nature*, **179**, 1074 (1957).
- 41 A.H. Beckett and P. Anderson, *J. Pharm. Pharmacol.*, **11**, 258T (1959).
- 42 A.H. Beckett and P. Anderson, *J. Pharm. Pharmacol.*, **12**, 228T (1960).
- 43 A.H. Beckett and H.Z. Youssef, *J. Pharm. Pharmacol.*, **15**, 253T (1963).
- 44 A. Waksmundzki, J. Oscik, J. Matusiewicz, R. Nasuto and J. Rozylo, *Przemysl. Chem.*, **40**, 387 (1961).
- 45 A. Waksmundzki, *Roczniki Chem.*, **32**, 323 (1958).
- 46 A. Waksmundzki, J. Oscik, J. Rozylo and R. Nasuto, *Przemysl. Chem.*, **40**, 527 (1961).
- 47 A. Waksmundzki, J. Oscik, J. Rozylo and R. Nasuto, *Przemysl. Chem.*, **40**, 565 (1961).
- 48 A. Waksmundzki, J. Oscik, J. Rozylo and J. Matusiewicz, *Folia Soc. Sci. Lublin*, **2**, 149 (1962).

- 49 A. Waksmundzki, J. Oscik, R. Nazuto and J. Rozylo, *Przemysl. Chem.*, **42**, 193 (1963).
- 50 A. Waksmundzki, J. Oscik, J. Rozylo and R. Nasuto, *Przemysl. Chem.*, **46**, 287 (1967).
- 51 A. Waksmundzki, J. Oscik, R. Nazuto and J. Rozylo, *Przemysl. Chem.*, **40**, 432 (1961).
- 52 A. Waksmundzki, J. Oscik, J. Rozylo and R. Nasuto, *Folia Soc. Sci. Lublin*, **2**, 145 (1962).
- 53 A. Waksmundzki, J. Oscik, R. Nazuto and J. Rozylo, *Przemysl. Chem.*, **46**, 159 (1967).
- 54 H. Bartels, *J. Chromatogr.*, **30**, 113 (1967).
- 55 P. Cuatrecasas, M. Wilchek and C.B. Anfinsen, *Proc. Natl. Acad. Sci. USA*, **61**, 636 (1968).
- 56 H. Erlenmeyer and H. Bartels, *Helv. Chim. Acta*, **47**, 46 (1964).
- 57 H. Erlenmeyer and H. Bartels, *Helv. Chim. Acta*, **47**, 1285 (1964).
- 58 H. Bartels and H. Erlenmeyer, *Helv. Chim. Acta*, **48**, 284 (1965).
- 59 H. Bartels, *Z. Anorg. Allg. Chem.*, **350**, 143 (1967).
- 60 A. Waksmundzki, T. Wawrzynowicz and T. Wolski, *Ann. Univ. Mariae Curie-Skłodowska, Lublin-Polonia: Sect. AA*, **17**, 27 (1962).
- 61 A. Aherne, C. Alexander, M.J. Payne, N. Perez and E.N. Vulfson, *J. Am. Chem. Soc.*, **118**, 8771 (1996).
- 62 V.V. Patrikeev, E.I. Klabunovskii and J.S. Mardashev, *USSR Pat. no. 125491*, in *Chem. Abs.* **XX**, 16,694g (1960).
- 63 V.V. Patrikeev and Z.S. Smirnova, *USSR Pat. no. 136096*.
- 64 E.A. Merck, *Ger. Pat. no. 1218918*, in *Chem. Abs.* **65**, 17,386e (1966).
- 65 H. Erlenmeyer and H. Bartels, *Helv. Chim. Acta*, **48**, 301 (1965).
- 66 I.M. Klotz, G.P. Royer and A.R. Sloniewsky, *Biochemistry*, **8**, 4752 (1969).
- 67 I.M. Klotz and J.U. Harris, *Biochemistry*, **10**, 923 (1971).
- 68 T. Takagishi, A. Hayashi and N. Kuroki, *J. Polym. Sci. Polym. Chem. Ed.*, **20**, 1533 (1982).
- 69 T. Takagishi, T. Sugimoto, H. Hamano, Y.-J. Lim, N. Kuroki and H. Kuzoka, *J. Polym. Sci. Polym. Lett. Ed.*, **22**, 283 (1984).
- 70 T. Takagishi, T. Sugimoto, H. Hamano, Y.-J. Lim and N. Kuroki, *J. Polym. Sci. Polym. Chem. Ed.*, **22**, 4035 (1984).
- 71 T. Takagishi, H. Hamano, T. Shimokado and N. Kuroki, *J. Polym. Sci. Polym. Lett. Ed.*, **23**, 545 (1985).
- 72 T. Takagishi and M. Okada, *Chem. Express*, **1**, 359 (1986).
- 73 H. Kozuka, T. Takagishi, K. Yoshikawa, N. Kuroki and M. Mitsuishi, *J. Polym. Sci. Polym. Chem. Ed.*, **24**, 2695 (1986).
- 74 G. Wulff, *ACS Symp. Ser.*, **308**, 186 (1986).
- 75 H. Nishide and E. Tsuchida, *Makromol. Chem.*, **177**, 2295 (1976).
- 76 Y. Fujii, K. Matsutani and K. Kikuchi, *J. Chem. Soc. Chem. Commun.*, 415 (1985).
- 77 P.K. Dhal and F.H. Arnold, *Macromolecules*, **25**, 7051 (1992).
- 78 R. Arshady and K. Mosbach, *Makromol. Chem.*, **182**, 687 (1981).
- 79 L. Andersson, B. Sellergren and K. Mosbach, *Tetrahedron Lett.*, **25**, 5211 (1984).
- 80 B. Sellergren, M. Lepistö and K. Mosbach, *J. Am. Chem. Soc.*, **110**, 5853 (1988).
- 81 L.I. Andersson, D.J. O'Shannessy and K. Mosbach, *J. Chromatogr.*, **513**, 167 (1990).
- 82 L. Fischer, R. Müller, B. Ekberg and K. Mosbach, *J. Am. Chem. Soc.*, **113**, 9358 (1991).
- 83 K.J. Shea, D.A. Spivak and B. Sellergren, *J. Am. Chem. Soc.*, **115**, 3368 (1993).
- 84 B. Sellergren and K.J. Shea, *J. Chromatogr.*, **635**, 31 (1993).
- 85 G. Vlatakis, L.I. Andersson, R. Müller and K. Mosbach, *Nature*, **361**, 645 (1993).
- 86 The Society for Molecular Imprinting: <http://www.ng.hik.se/~SMI>



This Page Intentionally Left Blank

## Fundamental aspects on the synthesis and characterisation of imprinted network polymers

BÖRJE SELLERGREN AND ANDREW J. HALL

### 2.1. INTRODUCTION

As is apparent from other chapters in this book, most examples of high fidelity molecular imprinting have been demonstrated using highly cross-linked organic polymers as the imprinting matrix. Most of these are synthesised by free radical copolymerisation of functional vinyl monomers with an excess of cross-linking divinyl monomers in the presence of a diluent (which may be a pore-forming agent, porogen), usually a solvent for the monomers. In addition, a template or template-monomer adduct is added prior to polymerisation in order to form the imprinted sites. This results in a porous organic polymeric material equipped with binding sites for the template ion or molecule. Well known examples of such materials outside the molecular imprinting arena are copolymers of a functionalised styrene with technical grade divinylbenzene (DVB) or copolymers of functionalised methacrylates or acrylamides with di- or tri-functionalised cross-linkers (Fig. 2.1) [1–3]. These materials have found widespread use as adsorbents, ion exchange resins, supports for solid phase synthesis or as chromatographic stationary phases. The aim of this chapter is to give a fundamental description of the formation and structure of cross-linked network polymers formed by free radical polymerisation and to give the reader an insight into the main factors influencing the molecular imprinting process. Finally, a list of the most common techniques applied for the structural characterisation of this type of materials is given.

The polymeric adsorbents are usually prepared by variations of two-phase suspension processes. These refer to systems where microdroplets of monomers and solvent are converted into solid beads upon polymerisation. In the case where the monomers are not water soluble, as in the case of styrene-based polymers and many methacrylate-based polymers, the monomers, a solvent and a droplet stabiliser are suspended as droplets by stirring in water and then polymerised (o/w suspension polymerisation). The particle size and dispersity can be influenced by the stirring speed and the type of stabiliser. So far, only a few examples of the preparation of imprinted polymers in bead format have been described [4–8] and these are thoroughly reviewed in Chapter 12. In non-covalent imprinting, the main limitation to the use of these techniques is that the imprinting method often requires the use of polar partly water soluble monomers or templates in combination with less polar water insoluble components. Use of the o/w suspension method

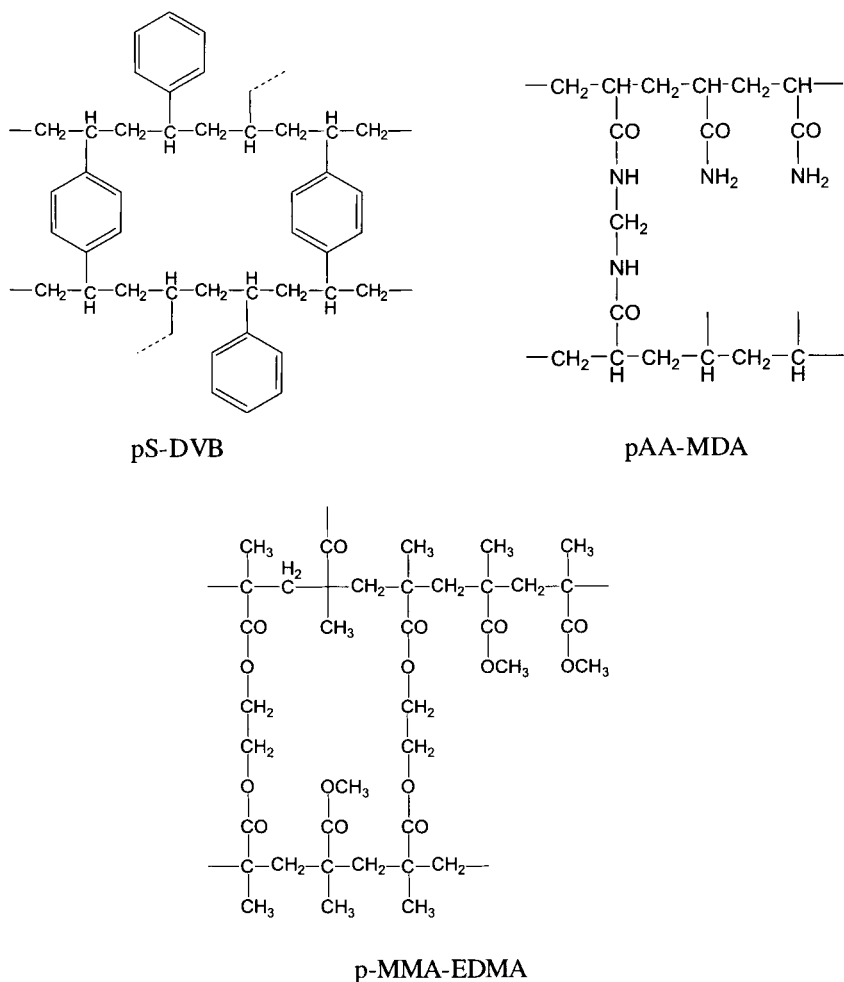


Fig. 2.1. Structure of different types of support materials for chromatography, adsorption, catalysis and solid phase synthesis, *co*-poly-(styrene-divinylbenzene) (pS-DVB), *co*-poly-(acrylamide-methyldiacrylamide) (pAA-MDA), *co*-poly-(methylmethacrylate-ethylene glycol dimethacrylate) (pMMA-EDMA).

is thus often prevented due to partitioning of the monomers and/or template into the aqueous phase. Therefore, most materials described to date have been prepared by the so-called monolith technique. This refers to homogeneous solution/precipitation polymerisation methods giving polymer monoliths that need to be ground and sieved prior to use. The main disadvantages of this technique are the loss of material in the sieving process, the irregular particle shapes, the large size distribution of particles and the poor heat dissipation, and thereby temperature control, when scaling up the batch sizes [9].

## 2.2. FREE RADICAL POLYMERISATION

The double bonds in most vinylidene compounds of the general structure  $\text{CH}_2=\text{CR}_1\text{R}_2$  are reactive towards free radicals, cations or anions, forming transient species with a life-time long enough to add to another double bond containing molecule [10]. This generates a new active centre and repetition of this addition process leads to the formation of polymer. The growth of the chain is then stopped by various termination mechanisms. The key steps in addition polymerisations are thus (i) initiation, (ii) propagation and (iii) termination (Fig. 2.2).

### 2.2.1. Initiation

In most olefinic monomers the group  $\text{R}_1$  is either H or  $\text{CH}_3$ . The group  $\text{R}_2$  is then classified depending on its electron withdrawing or donating properties. This, in turn, provides information on whether the monomer is suited for polymerisation using anionic or cationic initiators respectively [10]. Ionic polymerisation is more limited with respect to the monomer structure than free radical polymerisation. Due to its electrical neutrality, the free radical is a less selective and generally more useful initiator. There are other reasons why these systems are particularly useful in molecular imprinting.

Free radical reactions are little affected by the presence of acids or bases or by changes in the polarity of solvents [11]. This allows molecular imprinting to be carried out under a variety of different conditions. The free radical initiator can be

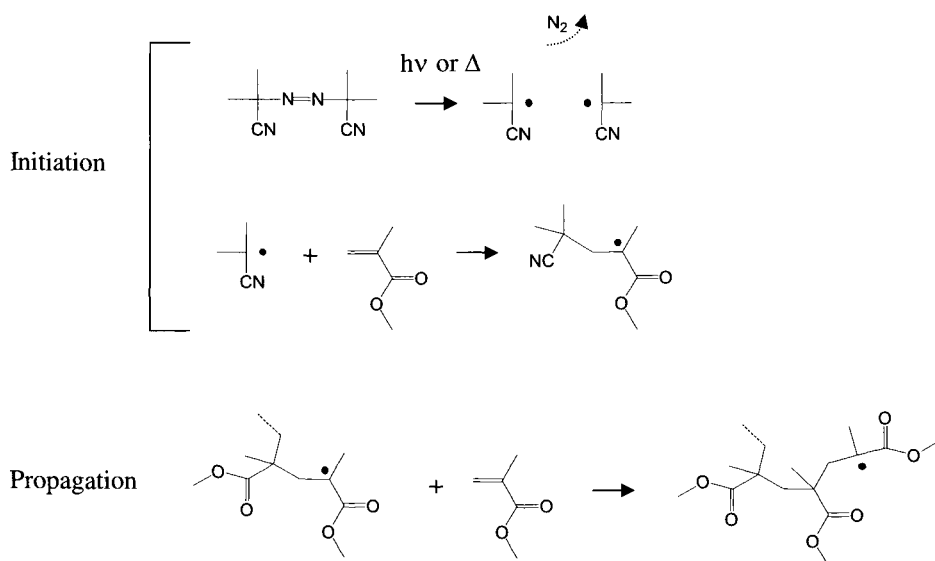


Fig. 2.2. Free radical addition polymerization of MMA using AIBN as initiator.

generated by thermal or photochemical means at different temperatures, increasing the versatility regarding the imprinting of thermally labile templates or poorly soluble templates. This also allows conditions to be chosen where the interactions occurring between monomer and template prior to polymerisation are particularly strong [12–14]. Initiation by radiation allows spatially controlled polymerisations *in situ* [10].

Initiation of free radical polymerisations can occur *via* high energy radiation or *via* addition of initiator molecules which, when subjected to heat, electromagnetic radiation, or chemical reaction, will homolyse to form radicals with higher reactivity than the monomer radicals. However, the reactivity must be low enough to allow the initiator radical to react with the monomer. Azo- and peroxide initiators, with bond energies of 105–170 kJ/mol, are particularly useful in this regard and are the most commonly used initiators in molecular imprinting (Table 2.1).

The free radicals may be generated in different ways. For azo-initiators the free radicals are generated either by UV radiation at the wavelength for maximum absorption or thermally at a temperature providing a suitable rate of decomposition. Since the rate of decomposition is slower than the rate of reaction of the initiator radical the initiation rate can be written as the rate of decomposition:

$$v_i = d[RM\bullet]/dt = 2k_d f [I] \quad (1)$$

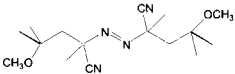
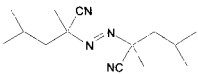
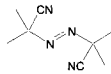
where 2 relates to the two radicals generated per initiator molecule,  $f$  is the efficiency of the radicals to propagate chains,  $[I]$  is the initiator concentration and  $[RM]$  is the concentration of propagating species. For photoinitiated polymerisations using a photosensitive initiator the rate is written as:

$$v_i = 2\phi\epsilon I_0 [I] \quad (2)$$

where  $\phi$  is the quantum yield,  $\epsilon$  is the extinction coefficient and  $I_0$  is the incident light intensity. If the rate is too high, a large concentration of reactive centres will be generated leading to early termination and low molecular weights, where-as if the rate is too low the polymerisation will not reach completion within a practicable time frame. For an initiator concentration of 0.1 M the decomposition rate should typically be  $10^{-6}$ – $10^{-7}$  M/s, corresponding to a  $k_d$  of  $10^{-5}$ – $10^{-6}$ /s in the temperature range 50–150°C. For the common initiator 2,2'-azobisisobutyronitrile (AIBN) (Table 2.1) the homolysis reaction (Fig. 2.2) occurs either by irradiation at the  $\lambda_{max}$  at 345 nm using a mercury vapour lamp or by heating the reaction near the temperature given in Table 2.1. In the imprinting protocols developed thus far, *ca.* 1% (w/w) AIBN is added based on total monomer and the thermally initiated polymerisations are generally carried out at 60°C. Given the rate constant for decomposition at this temperature ( $k \approx 1.9 \times 10^{-5}$ /s) [10], the rate of radical production should satisfy the above rate criteria. In the case of the photochemically initiated polymerisations, other considerations must be made. The intensity of the UV light, the distance from the light source and the penetration depth (depending on  $\epsilon$ ) will determine the rate of radical production.

TABLE 2.1

## FREE RADICAL INITIATORS WITH DECOMPOSITION TEMPERATURE RANGES SUITABLE FOR USE AND APPLICATIONS IN MOLECULAR IMPRINTING

| Type  | Initiator                                   | Initiation temperature | Reference to MIPs        |
|---|---|------------------------|--------------------------|
| Peroxide:   | RC(O)OO(O)CR: R=ethyl                       | 110 - 130 °C [10]      | -                        |
|   | R= benzoyl                                  | 40 - 70 °C             | -                        |
|   | R = tert-butyl                              | 100 - 120 °C           | -                        |
| Persulphate:  | S <sub>2</sub> O <sub>8</sub> <sup>2-</sup> | 90 °C [21]             | Acrylamide MIPs [56]     |
| Azo:  | V-70 <sup>b</sup>                           | 30 °C <sup>a</sup>     | For use of V-68 see [14] |
|   | ABDV (V-65) <sup>b</sup>                    | 50 °C <sup>a</sup>     | [12, 14, 46]             |
|   | AIBN (V-60) <sup>b</sup>                    | 65 °C <sup>a</sup>     | [52]                     |
| Ionizing radiation  | γ-rays                                      | 15 °C                  | [80]                     |
| <div style="display: flex; justify-content: space-around; align-items: flex-end;"> <div style="text-align: center;">  <p>V70</p> </div> <div style="text-align: center;">  <p>ABDV</p> </div> <div style="text-align: center;">  <p>AIBN</p> </div> </div> |   |                        |                          |

(a) Approximate temperature at  $t_{1/2} = 10$  h

(b) Trade name of Waco Chemicals, Inc. (Osaka, Japan).

Although the rate of decomposition can be estimated, a number of side reactions prevent all generated radicals from initiating the growth of a polymer chain (reflected in  $f$  or  $\phi$ ). For instance, a considerable rate of recombination of the initiator can occur, depending on the solvent used.

### 2.2.2. Propagation

A chain carrier is formed from the reaction of a free radical and a new monomer unit and propagation occurs rapidly by addition of new monomers to produce primary linear polymer chains.



with the rate of propagation given by:

$$v_p = k_p[M][M\cdot] \quad (4)$$

where  $[M\cdot]$  represents the concentration of growing reactive ends. The reaction can be followed by the disappearance of monomer.

### 2.2.3. Termination

Propagation continues until the free radical reacts to form an inactive covalent bond. This can occur when the concentration of free radicals is high or when chain transfer agents are present. Termination can occur in many ways: (i) the interaction

of two active chain ends; (ii) the reaction of an active chain end with an initiator radical; (iii) termination by transfer of the active centre to another molecule, which may be solvent, initiator, monomer or template; or (iv) interaction with impurities (e.g. oxygen) or inhibitors. Type (i), the most important, can occur by two different mechanisms (Fig. 2.3): (a) combination and (b) disproportionation. In the polymerisation of methyl methacrylate (MMA) mechanism (a) is the most common at temperatures below 330 K whereas (b) predominates above 330 K. The rate of termination is given by:

$$v_t = 2k_t[M\cdot][M\cdot] \quad (5)$$

### 2.2.4. Steady state

At steady state, the rate of production of free radicals equals the rate of consumption, i.e.

$$2k_i[M\cdot]^2 = 2k_d[I] \quad (6)$$

This can be put into equation (4) giving the rate of polymerisation:

$$v_p = k_p\{fk_d[I]/k_t\}^{1/2}[M] \quad (7)$$

for thermally initiated polymerisations. Thus the rate can be estimated based on experimentally determined rate constants. In the polymerisation of MMA,  $k_p$  is *ca.*  $4 \times 10^4/\text{M}/\text{min}$  [10,15].

### 2.2.5. Chain transfer

The chain length in free radical polymerisations is usually lower than would be expected from the mechanism of termination. The reason for this discrepancy is that the growing polymer chain can transfer the radical to other species, leading to termination of one chain, and thus generating a new radical that will react further. The following transfer mechanisms may occur:

Transfer to monomer: This type of transfer involves abstraction of hydrogen radicals from the monomer and is negligible in the copolymerisation of MMA and ethylene glycol dimethacrylate (EDMA) [15].

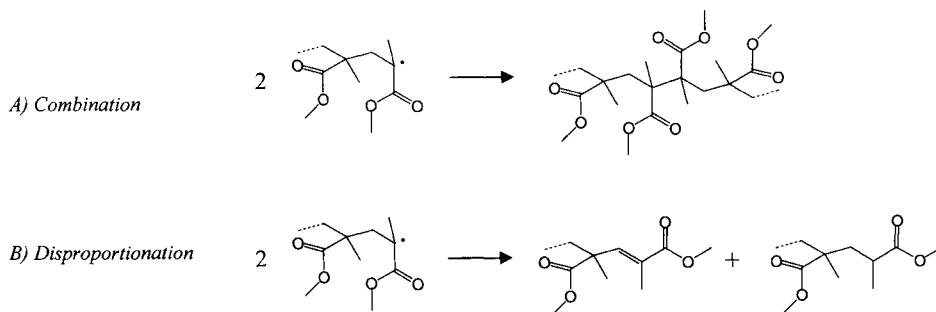


Fig. 2.3. Termination mechanisms in the free radical polymerization of MMA.

*Transfer to initiator:* This type of transfer involves transfer of radicals to the initiator. Organic peroxides are particularly susceptible to this kind of transfer whereas azo-initiators are not as reactive in this respect [10].

*Transfer to polymer:* This type of transfer leads to branching of the polymer and is negligible in the copolymerisation of MMA and EDMA [15].

*Transfer to solvent:* A number of solvents are reactive towards free radicals. Halogenated solvents belong to this group and  $\text{CCl}_4$  is particularly reactive. They react with the growing polymer chain by abstraction of a chlorine radical and the resulting solvent radical can then initiate a new chain or terminate a growing chain [10].

*Transfer to template:* Several templates are not compatible with free radical reactions since they are either monomers themselves or are capable of transferring free radicals to either the growing polymer or the initiator (see Section 2.8). Reactivity of this kind should be established prior to polymerisation by model reactions on a small scale.

### 2.2.6. Inhibition

Some reagents react with the initiating radical to give unreactive substances, a process known as inhibition. A common inhibitor for vinyl polymerisations is hydroquinone, which reacts by the transfer of two hydrogen radicals to the initiator radicals (Fig. 2.4). This gives quinone and unreactive initiator and has the net effect of causing a lag time in the polymerisation and a decrease in the initiator concentration. Monomers are often stored in the presence of inhibitor in order to prevent polymerisation. The amount and type of inhibitor may vary depending on the monomer batch and the manufacturer. For inter-laboratory comparisons of materials to be possible, it is therefore important to remove the inhibitor and purify the monomers prior to use [13].

### 2.2.7. Copolymerisation

Most of the imprinted polymers described to date are copolymers, i.e. polymers formed by incorporating two monomers in the polymer. Depending on the relative reactivity of the monomers different types of polymers are formed [10]. For linear vinyl polymers these are:

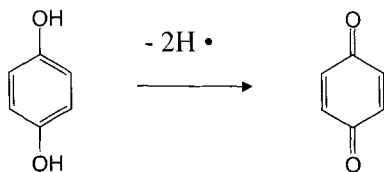


Fig. 2.4. Hydroquinone as inhibitor.



(i) statistical copolymers, formed when the monomers enter the chain in a statistical fashion; (ii) alternating copolymers, when there is an alternating tendency among the monomers to react with each other; or (iii) block copolymers where, conversely to (ii), the monomers tend to react with themselves.

In order to predict the extent of formation of these structures, the relative reactivity of the monomers must be estimated. For this purpose the corresponding reaction kinetics must be defined:



$k_{11}$ ,  $k_{22}$  and  $k_{12}$ ,  $k_{21}$  are the rate constants for the corresponding self-propagating and cross-propagating reactions. The reactivity ratios,  $r_1 = k_{11}/k_{12}$  and  $r_2 = k_{22}/k_{21}$ , give information about the tendency of the monomers to form blocks or alternating structures when copolymerised with another given monomer. These quantities allow the composition of the polymer to be determined at any given moment. If  $r_1 = r_2 = 1$ , the copolymerisation is considered ideal and the monomers will be randomly incorporated in the polymer. When both  $r_1$  and  $r_2$  are large, a tendency for block formation will be seen, while when the values are small an alternating tendency will be observed. To avoid these structures the product  $r_1 r_2$  should be close to 1 [10].

## 2.2.8. Tacticity

If the substituents on one of the vinyl carbons are different from each other, polymerisation will yield pseudochiral centres along the polymer chain. Depending on the stereochemistry at each centre, the polymer can be stereoregular; isotactic if the configurations are the same throughout the chain or syndiotactic if they are alternating. If no repeating configuration is seen the structure is atactic. The stereoregularity has a major influence on the physical and chemical properties of the polymer. For instance, the flexibility of a chain of p-MMA in solution decreases in the order syndiotactic > atactic > isotactic, whereas the glass transition temperature varies in the opposite direction [10]. In molecular imprinting, an important issue is whether the template is capable of inducing a preferred tacticity that may eventually influence the molecular recognition properties. For chiral templates this translates to the interesting question of whether induction of configuration chirality in the polymer main chain is possible. This question has been extensively investigated by Wulff and co-workers, using monosaccharides linked as boronate esters to monomers [42]. From these studies it was concluded that chirality in the main chain could not account for the enantioselectivity exhibited by the imprinted polymers.

## 2.3. COPOLYMERS OF DIVINYL MONOMERS AND MONOVINYL MONOMERS

### 2.3.1. Pre-gel regime and kinetics

#### 2.3.1.1. The EDMA–MMA system

The bulk copolymerisation of divinyl monomers with monovinyl monomers leads initially to the formation of primary chains where the pendant double bonds then engage in the cross-linking process. The tacticity and regularity of the primary chains are determined by the same factors as in the formation of linear polymers. Kinetic and structural aspects of the copolymerisation of MMA and EDMA have been studied by many groups during the last 50 years [16–19]. Most of this work has been based on studies of the pre-gel regime of the thermochemically initiated bulk copolymerisation of low levels of divinyl monomer ( $< 25\%$ ) with monovinyl monomer using AIBN as initiator. In the copolymerisation of these monomers at  $70^\circ\text{C}$ , the following reactivity ratios were determined by Li *et al.* [15]:  $r_1 = 0.67$  and  $r_2 = 1.49$ , where  $M_1 = \text{MMA}$  and  $M_2 = \text{EDMA}$ . This implies that these monomers have a tendency to form alternating primary chains. During polymerisation, pendant double bonds are created that can either react or remain unreacted. Those that react can either react with another growing chain, forming a cross-link, or they can react intramolecularly forming cycles [18]. After a certain number of cross-links has been formed, the polymer viscosity becomes so high that the mixture is no longer freely flowing and a gel is formed. The onset of gelation occurs when the weight average chain length of the copolymer tends to infinity. However, if only cyclisation occurs, linear polymer is obtained and the mixture remains freely flowing. Thus, the time to reach the gel point depends on a number of parameters. The degree of cyclisation and reactivity of the pendant double bonds are two of these factors. In the bulk polymerisation it was found that the pendant double bonds were, on average, half as reactive as the monomeric double bonds [18]. It was further found that a few per cent of the pendant double bonds reacted by cyclisation. Both these factors contributed to a delay in the gel point. However, the influence of these factors will be strongly dependent on the chain length, the concentration of divinyl monomer and the type of solvent (a bad solvent favouring cyclisation).

At the levels of divinyl monomer used in the formation of imprinted polymers the gel point is typically reached after a few minutes and at low conversion of monomer, usually below 5% [18,19]. In a study using 25% EDMA and AIBN as initiator at  $70^\circ\text{C}$ , high conversions were reached rapidly with over 90% conversion after just 20 min. (Fig. 2.5A) [19]. At this point, however, the viscosity is so high that the propagation becomes diffusion controlled and the rate of initiation decreases at the expense of initiator radical recombination. The Tromsdorff effect also sets in [1]. This is related to a slower termination by recombination, leading to an increase in the concentration of free radicals. By plotting the conversion  $X$  versus time, the variation of the product  $k_p[M\cdot]$  with time can be calculated (Fig. 2.5B):

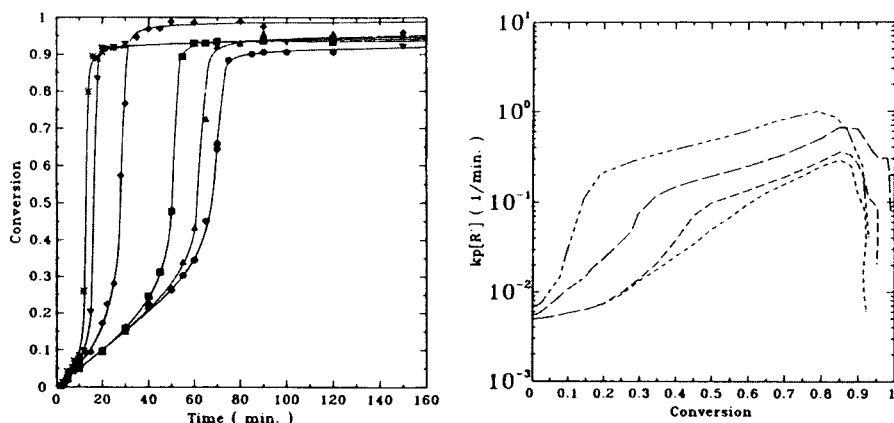


Fig. 2.5. (A) Conversion versus time for the polymerization of MMA/EDMA at 70°C using various levels of EDMA. Circle 0%, pyramid: 0.3%, square: 1.0%, diamond: 5.0%, triangle: 15.0%, double cross: 25.0%. Initiator: 0.3% (w/w) AIBN. Reproduced from Li *et al.* [19]. (B) Variation of the product  $k_p[R^*]$  with conversion for the polymerization of MMA/EDMA at 70°C at the indicated levels of EDMA. Reproduced from Li *et al.* [19].

$$dX/dt = k_p[M\cdot](1 - X) \quad (9)$$

where  $k_p$  = propagation rate constant and  $[M\cdot]$  = concentration of free radicals.

It is seen that  $k_p[M\cdot]$  increases in the interval between 0 and 80% conversion. This is attributed to an increase in the free radical concentration;  $k_p$  is believed to be roughly constant. Due to the dense network and poor accessibility when using high levels of divinyl monomer (greater than 50%), up to about 10% of the double bonds remain unreacted. The kinetic parameters estimated for the above system [15] are given in Table 2.2.

TABLE 2.2

ESTIMATION OF KINETIC PARAMETERS IN THE COPOLYMERISATION OF MMA AND EDMA [15]

| Parameter         | Constant      | Estimate                           |
|-------------------|---------------|------------------------------------|
| Initiation (AIBN) | $k_d$         | $2.06 \times 10^{-3}/\text{M/min}$ |
| Propagation       | $k_{p11}$     | $2.77 \times 10^4/\text{M/min}$    |
|                   | $k_{p22}$     | $5.65 \times 10^4/\text{M/min}$    |
| Termination       | $(k_{111})_0$ | $1.24 \times 10^9/\text{M/min}$    |
| Reactivity ratios | $r_1$         | 0.67                               |
|                   | $r_2$         | 1.49                               |

Where  $M_1$  = MMA and  $M_2$  = EDMA. The polymers were prepared at 70°C.

It should be noted that this study was carried at 70°C, where the half life of AIBN is relatively short, in the order of a few hours [10]. In a study by Svec and co-workers on the copolymerisation of EDMA with glycidoxypromethylmethacrylate (GMA), polymerisations were carried out at 50 or 60°C using cyclohexanol–octanol as porogen [20]. This resulted in considerably slower rates of polymerisation than in the work by Li *et al.* [19]. In contrast to the study by Li *et al.* the rate of polymerisation decreased with increasing fraction of EDMA in the monomer mixture, although a maximum fraction of 80% was used compared to a maximum fraction of 25% in the work by Li *et al.* (Fig. 2.6). Two factors are of importance. The half life of the initiator responds logarithmically to the temperature; thus the initiator decomposition half life at 60°C is more than 10 h and at 50°C it is more than 50 h. This, together with the system being more dilute due to the presence of solvent, explains the lower rate of polymerisation. The decrease in propagation rate with increasing fraction of EDMA was explained by the fact that the conversion depends on reaction of only one of the double bonds of the divinyl monomer. If only one double bond in EDMA is considered as active, then the concentration of active double bonds is decreasing with increasing concentration of EDMA. In the later stages of the polymerisation the remaining double bond will become less reactive due to the poor accessibility within the highly cross-linked domains of the polymer.

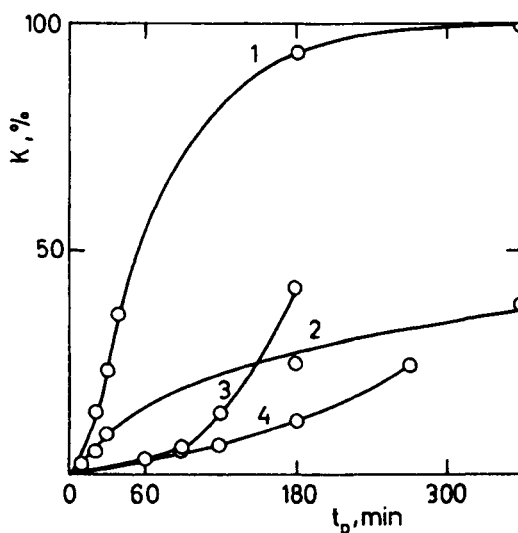


Fig. 2.6. Conversion versus time curves for the polymerization of GMA/EDMA and MMA/EDMA. Volume ratio: monomer/inert components = 2/3, inert components: dodecanol/cyclohexanol: 1/9. GMA/EDMA = 17/3 (1), = 3/17 (2); MMA/EDMA = 17/3 (3), = 3/17 (4). Initiator: AIBN, 0.5% (w/w). Polymerization temperature: 50°C.  $K$  = conversion,  $t_p$  = polymerization time. Reproduced from Horák *et al.* [20].

### 2.3.1.2. The EDMA–MAA molecularly imprinted polymer (MIP) system: primary structure

One common system in molecular imprinting is based on copolymers of EDMA and MAA. Although the structure of the primary chains is not known, useful information can be obtained from data on analogous linear polymers. The MMA ( $M_1$ )–MAA ( $M_2$ ) system has reactivity ratios  $r_1 = 0.37$  and  $r_2 = 2.2$ , giving a product  $r_1 r_2 = 0.81$ . This indicates that MAA has a tendency for homopolymerisation, whereas MMA prefers to react with MAA [21]. Theoretically this will produce a polymer with a slight excess of MAA in the initial stages of polymerisation and a slight excess of MMA in the later stages of polymerisation. However, reactivity ratios of polar monomers are strongly influenced by solvent, temperature and the presence of templates, i.e. factors that complicate the picture. Other common monomers used in molecular imprinting are based on the styrene monomer unit. Copolymerisation of styrene with MMA tends to produce alternating polymers given that  $r_1$  and  $r_2$  are less than one [10].

Polymers of MAA often exhibit syndiotacticity, the extent being influenced by the template effect (Figure 2.7B) [22], solvent and temperature. To what extent the tacticity influences the recognition properties of the materials is not clear.

### 2.3.1.3. The EDMA–MAA MIP system: secondary structure

In molecular imprinting, the rate of propagation relative to the rate of dissociation of the complex of the template and the functional monomers is an important issue (Fig. 2.7). Thus, if this ratio is high the template–monomer complexes can be expected to be essentially “frozen” upon incorporation. However, this assumes that a high level of cross-linker is used and that no additional strain in the polymer is built up, thus affecting the geometry after removal of solvent and template. However, if the ratio is low, the template will have time to dissociate before the three-dimensional shape of the site is defined. In this case the sites may be formed by an alternative mechanism where multidentate interactions are formed, involving functional groups of the same polymer chain followed by fixation of these structures (Fig. 2.7A). The stability and life time of such complexes would be much higher. The well documented template effect occurring upon polymerisation of functional monomers, e.g. acrylic acid, [22] or vinylimidazole [23], shows that functional oligomers can act as a template for the monomer, leading to enhanced rates (autoacceleration) and structural control (tacticity) (Fig. 2.7B). This favours the “freezing in” mechanism, but is expected to be of less importance for MAA [22].

Also of considerable importance is the mechanism of site formation. At what stage in the polymerisation are the high energy sites formed and stabilised? Does the solution structure of the monomer–template assemblies reflect the disposition of functional groups at the binding sites [24]? (See Chapter 5 for a further discussion.) Attempts to correlate the association constants determined for the monomer–template interactions in homogeneous solution with the rebinding association

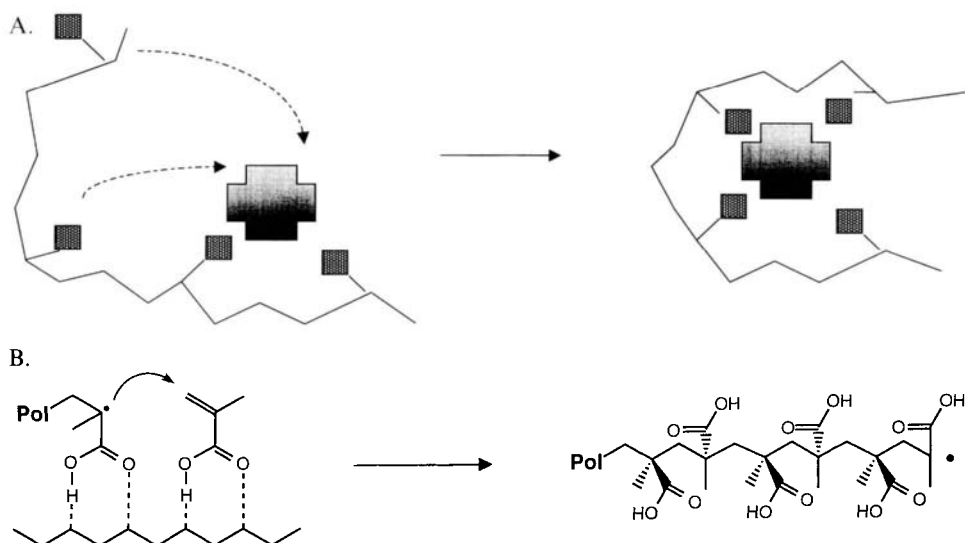


Fig. 2.7. Influence of the template on polymer chain conformation (A) or polymer chain growth (B).

constant have been made using 9-ethyladenine [25,26] and L-phenylalanine anilide (L-PA) [27] respectively as model templates.

### 2.3.2. Build-up of the porous structure: the tertiary structure

In the case of solution polymerisations, the properties of the solvent determine whether the polymer precipitates or whether it stays solvated during polymerisation. Polymerisation of a divinyl monomer in the presence of a good solvent will result in a more uniform distribution of cross-links while in the presence of a poor solvent a heterogeneous distribution of cross-links can be expected and a permanently porous polymer will be formed (see Figure 2.12). Solvents with pore-forming properties are called porogens; otherwise the more general term diluent is used. Much work has been devoted to elucidating the structure of styrenic supports [1,28–31]. Here, macroporous resins can, depending on the diluent used, form when the polymerisation is carried out using more than 5% DVB as the cross-linking monomer. During polymerisation, permanent pores are formed that, upon drying, collapse to different extents depending on the quality of the solvent. Small molecules can diffuse freely into the pores if the latter are sufficiently large. In micropores with diameters below 20 Å the diffusion is slow due to capillary forces. Three main classes of porogens exist; solvents for the polymer structure, non-solvents and polymers [1]. The use of polymers usually gives rise to large pores (> 1000 Å). In the case where a non-solvent is used the resulting polymer contains agglomerates of microspheres (1000–2000 Å) and each microsphere shows smaller nuclei (50–300 Å) more or less connected (Fig. 2.8). Between the nuclei there is a family of very small

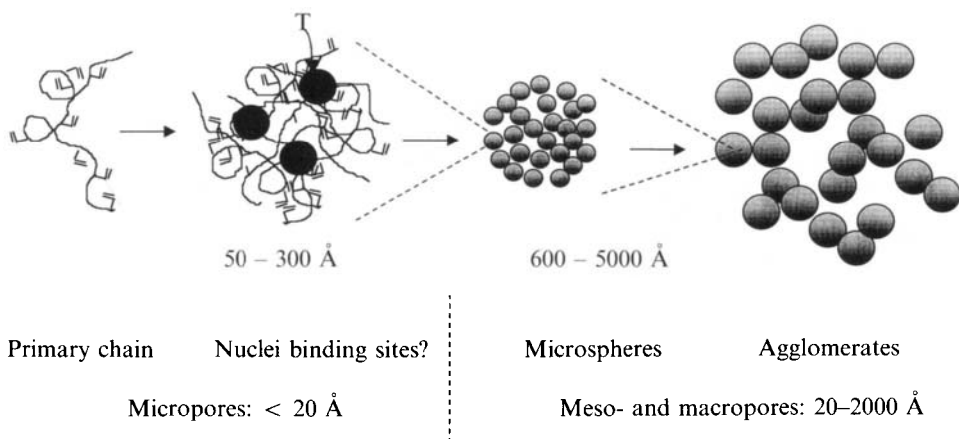


Fig. 2.8. Build-up of the porous structure of a macroporous adsorbent in presence of a template (T).

pores (50–150 Å) which are mainly responsible for the high surface area of the materials. Increasing the level of cross-linker reduces the contact between the nuclei and the average pore size is shifted to smaller pore sizes including mesopores (200–500 Å). Increasing the amount of diluent leads to an increase in the amount of large pores between the agglomerates. The effects of these parameters are best illustrated in a phase diagram (Fig. 2.9), showing that a macroporous morphology is seen only in a limited domain. The location of the boundaries depends on the nature of the diluent. Attempts to correlate the changes in porous structure with the solubility parameters are usually unsuccessful.

Copolymers of GMA and EDMA have been extensively studied by the group of Svec [20,32–38]. The general trends established in the polymerisation of styrene and

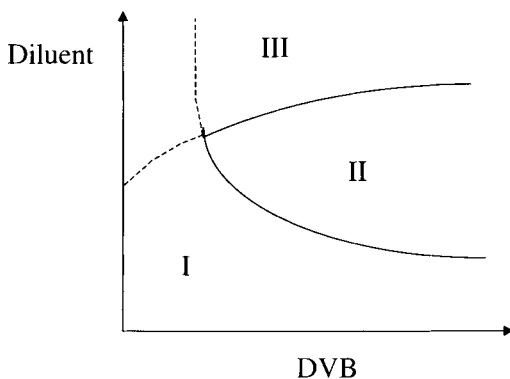


Fig. 2.9. Phase diagram for the copolymerization of styrene-DVB in the presence of a non-solvent diluent. I: gel type domain, II: macroporous domain, III: domain where the microspheres have been covered before the end of the polymerization. From Guyot [1].

DVB were valid in this system as well. These concern the dependence of surface area and pore volume on the amount of diluent and cross-linker. The surface area increases with the amount of EDMA and goes through a maximum with increasing amount of diluent. Using cyclohexanol–dodecanol as a solvent–non-solvent pair, the factors of importance for the structure and morphology of the polymers were studied by experimental design [34]. In these experiments the concentration of the diluent mixture was varied between 20 and 77% (volume/total volume), the concentration of EDMA between 25 and 100% (volume/monomer volume), the concentration of initiator (AIBN) between 0.2 and 4% (w/w), the concentration of non-solvent (dodecanol), between 0 and 15% (v/v) and the polymerisation temperature between 70° and 90°C. The surface area (determined by nitrogen sorption), pore volume (determined by mercury porosimetry) (see Section 2.11.6.) and the mechanical properties were chosen as responses.

The specific surface area was mainly affected by the concentration of the diluents and the concentration of EDMA. When varying the former factor, a maximum of 460 m<sup>2</sup>/g was observed between 60 and 66% (v/v) of diluent, using an EDMA concentration of 100% (v/v). This behaviour is explained as follows. At low diluent concentrations, the polymer becomes dense and impenetrable leading to a low surface area, whereas when the amount of diluent is high the density of the polymer nuclei is small. They may grow undisturbed and form larger submicroscopic particles with a low divided surface area. Close to the optimum concentration of diluent, the surface area is mainly controlled by the concentration of EDMA. Thus the surface area increases with the concentration of EDMA. This is explained by the decrease in the size of the nuclei and microspheres. The concentration of initiator and the polymerisation temperature had little influence on the morphological properties. With increasing concentration of the non-solvent the surface area decreased. With regards to the porosity, an increase was observed with increasing amount of EDMA at lower levels of cross-linking.

Similar studies have been carried out by the groups of Schmid *et al.* [39] and Reinholdsson and co-workers [40,41] for the polymerisation of trimethylol propane trimethacrylate (TRIM) using toluene as solvent and iso-octane as non-solvent.

## 2.4. SITE STABILITY, INTEGRITY AND ACCESSIBILITY

For the formation of defined recognition sites, the structural integrity of the monomer–template assemblies must be preserved during polymerisation to allow the functional groups to be fixed in space in a stable arrangement complementary to the template. This is achieved by the use of a high level of cross-linking. In Fig. 2.10 it can be seen that at least 50% of the total monomer in the MAA–EDMA system must be the cross-linker (EDMA) for recognition to be seen [12]. This is confirmed by independent observations using other imprinting systems [42]. However, the role of the polymer matrix is not only to contain the binding sites in a stable form, but also to provide porosity to allow easy access for the



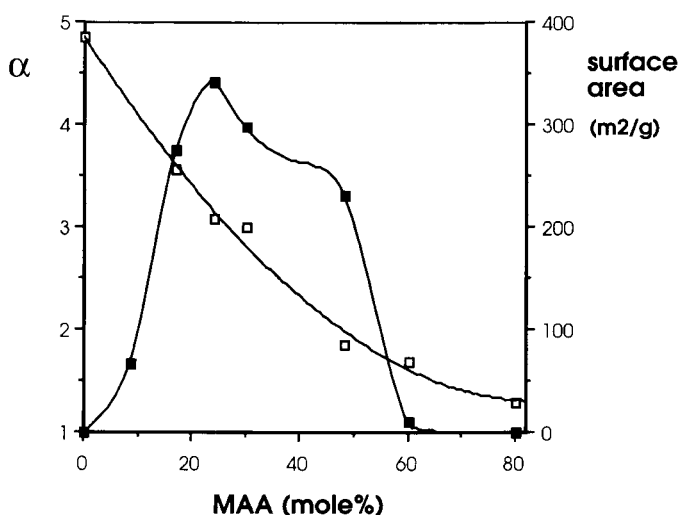


Fig. 2.10. Enantiomer separation factor ( $\alpha$ ) and specific surface area versus the level of MAA in the monomer mixture for the chromatographic resolution of D,L-PA on an L-PA imprinted polymer using acetonitrile as inert solvent. Eluent: 5% acetic acid in acetonitrile. Column temperature 80°C and flow rate: 0.2 ml/min. From Sellergren [12].

template to all sites. As shown in the previous section, porosity is achieved by carrying out the polymerisation in the presence of a porogen. Most of the cross-linked network polymers used for molecular imprinting have a wide distribution of pore sizes associated with various degrees of diffusional mass transfer limitations and a different degree of swelling. Based on the above criteria, i.e. site accessibility, integrity and stability, the sites may be classified into different types (Fig. 2.11). The sites associated with meso- and macro-pores ( $> 20 \text{ \AA}$ , site A) are expected to be easily accessible compared to sites located in the smaller micropores ( $< 20 \text{ \AA}$ , site B) where the diffusion is slow. The number of the latter type of sites may be higher since the surface area of micropores, for a given pore volume, is higher than that of macropores. One undesirable effect of adding an excess of template is the loss of site integrity due to coalescence of the binding sites (site D), which is related to the extent of template self-association. The optimum amount of template is usually about 5% of the total amount of monomer, but can be higher when trivinyl monomers are used as cross-linkers (where a larger fraction of functional monomer is used) [43]. The amount of template is of course also limited by its solubility and availability, although recycling is possible.

Often the materials swell to different extents depending on the type of diluent (see Chapter 5). The swelling is normally high in solvents and low in non-solvents for the polymer. Unfortunately, this may lead to large changes in the accessibility and density of the binding sites when the solvent is changed (see Chapter 5). Moreover if rebinding of the template to the sites occurs in a swelling solvent and

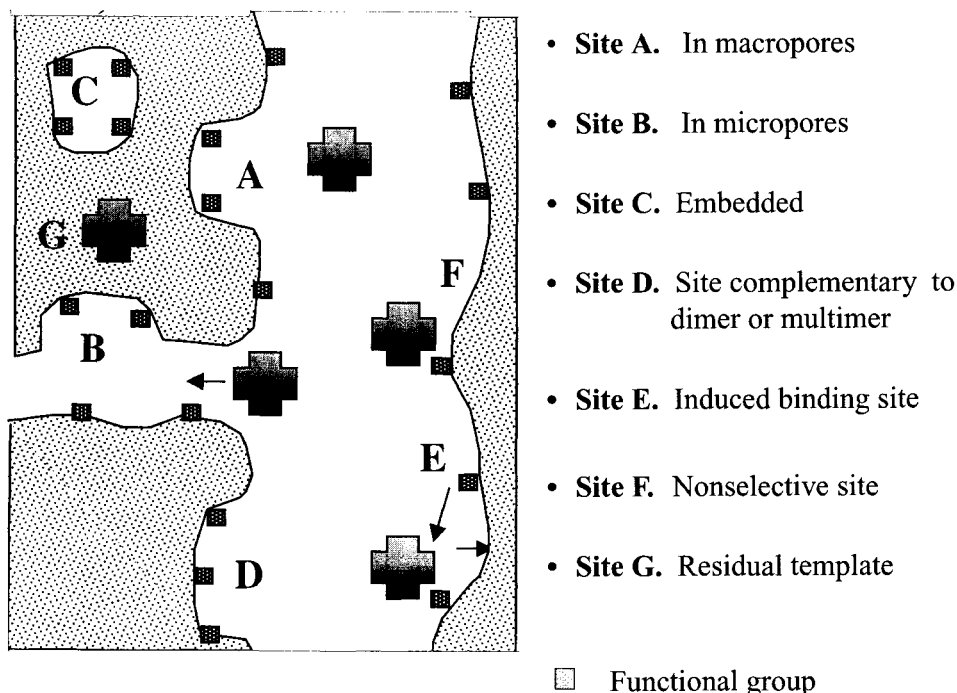


Fig. 2.11. Different types of binding sites in polymers containing micro- meso- and macropores.

desorption is carried out in a non-swelling solvent the template risks being entrapped in the smaller pores of the network [44]. For most applications in liquid media, permanent porosity and a large surface area of accessible meso- and macropores are therefore preferred. This gives materials mainly containing accessible sites of type A. The results discussed in Chapter 5 show that for this purpose the volume of diluent should be slightly larger than the volume of monomers, the level of cross-linking should be relatively high ( $> 50$  mol %) and that the swelling and porosity should be controlled by the type of solvent–non-solvent mixture during polymerisation. It is important to keep in mind that the latter also affect the stability of the monomer–template assemblies [13].

## 2.5. POLYMER POROSITY AND SWELLING

Depending on whether a solvent or a non-solvent is used as diluent, large differences in swelling between the materials may be seen [13,40]. In the molecular imprinting of L-PA (model system), a number of MIPs were prepared using a standard recipe with 83% cross-linker but with different diluents (see also Chapter 5) [13]. To what extent do the solubility parameters then correlate with the polymer morphology or, in other words, which solvents are good and which are bad in the polymerisation of EDMA and MAA. As described in Chapter 5, maximum

solvation of the growing polymer chains occurs when the solubility parameters,  $\delta$ , of the polymer and the solvent are the same. However, a correct estimate of  $\delta$  of the polymer is difficult, firstly because it is a copolymer and secondly because it is cross-linked [10]. Often the solubility parameter is close to the one of the polymer of the predominating monomer. As seen in Tables 2.3 and 2.4 the  $\delta$ , values of the solvents are all in the range of either p-MMA, p-MAA or the terpolymer MAA-MMA-EA. Thus there are no obvious conclusions to be drawn from this comparison. However, it is interesting to note that among the solvents used, only  $\text{CH}_2\text{Cl}_2$  and  $\text{CHCl}_3$  are listed as good solvents for p-MMA in *The polymer handbook* [45]. This is in agreement with the finding that the corresponding polymers are gel-like with high swelling factors, typical of cross-linked polymers prepared in the presence of good solvents [13].

The difference in swelling among the photoinitiated polymers appears to be unrelated to the number of unreacted double bonds, in view of the similar intensity of the band attributed to the C=C stretch of unreacted double bonds at 1638/cm in the infrared spectra. Furthermore,  $^{13}\text{C}$ -CP-MAS-NMR results indicated that the number of unreacted double bonds was less than 10% in polymers prepared using tetrahydrofuran (THF) as porogen. Also, no chain transfer is expected to occur in this system [15], although in some cases transfer to the template may occur. Rather it is related to the heterogeneity of the cross-links, which in turn will affect the stiffness of the chains linking the agglomerates or microspheres together during phase separation [1]. This is influenced by the ability of the porogen to solvate the

TABLE 2.3

SOLUBILITY PARAMETERS, HYDROGEN BOND CAPACITY AND REFRACTIVE INDICES OF SOLVENTS USED FOR PREPARING MIPs

| Solvent                  | $\delta_d$ | $\delta_p$ | $\delta_h$ | $\delta (\text{MPa})^{0.5}$ | H-bond | $N_D$ |
|--------------------------|------------|------------|------------|-----------------------------|--------|-------|
| MeCN                     | 15.3       | 18.0       | 6.1        | 24.6                        | P      | 1.34  |
| THF                      | 16.8       | 5.7        | 8.0        | 19.4                        | M      | 1.41  |
| $\text{CHCl}_3$          | 17.8       | 3.1        | 5.7        | 19.0                        | P      | 1.45  |
| $\text{C}_6\text{H}_6$   | 18.4       | 0          | 2.0        | 18.6                        | P      | 1.50  |
| DMF                      | 17.4       | 13.7       | 11.3       | 24.8                        | M      | 1.43  |
| $\text{CH}_2\text{Cl}_2$ | 18.2       | 6.3        | 6.1        | 20.3                        | P      | 1.42  |
| <i>i</i> -propanol       | 15.8       | 6.1        | 16.4       | 23.5                        | S      | 1.38  |
| HOAc                     | 14.5       | 8.0        | 13.5       | 21.3                        | S      | 1.37  |
| MeOH                     | 15.1       | 12.3       | 29.3       | 29.7                        | S      | —     |
| Toluene                  | 18.0       | 1.4        | 2.0        | 18.6                        | P      | —     |
| $\text{H}_2\text{O}$     | 15.5       | 16.0       | 42.4       | 47.9                        | S      | —     |
| Cyclohexane              | 16.8       | 0          | 0.2        | 16.8                        | P      | —     |

The solubility parameter  $\delta$  has been divided into one dispersive term  $\delta_d$ , one polar term  $\delta_p$  and one hydrogen bonding term  $\delta_h$ . H-bond is a measure of the hydrogen bonding capacity of the solvent in terms of both donor and acceptor ability: P = poor, M = moderate and S = strong.  $n_D$  = refractive index.

TABLE 2.4

SOLUBILITY PARAMETERS ( $\delta$  [(MPa)<sup>0.5</sup>]) OF LINEAR POLYMERS IN SOLVENTS WITH DIFFERENT HYDROGEN BONDING CAPACITY

|                                 | Solvent hydrogen bonding capacity |           |           |
|---------------------------------|-----------------------------------|-----------|-----------|
|                                 | Poor                              | Moderate  | Strong    |
| PMMA                            | 18.2–26                           | 17.4–27.2 | 0         |
| PMAA                            | 0                                 | 20.3      | 26.0–29.7 |
| MMA/EA/MAA<br>(40/40/20 mole %) | 0                                 | 18.2–22.1 | 19.4–29.7 |

See reference [13] and [45]. EA = ethylacrylate.

growing polymer chains (Fig. 2.12). For instance, in a poor solvent agglomeration is promoted, leading to the formation of densely cross-linked microspheres, where the phase separation occurs when the microspheres precipitate. This gives a relatively open pore structure with strong links between the microspheres. Such materials exhibit permanent porosity and low swelling. With a good solvent, intermolecular cross-links are favoured and a material is obtained which is built up of loosely linked grains of solvent swollen gel particles. These materials exhibit low pore volume and high swelling and often similar specific swelling (see Chapter 5) to the materials prepared in the presence of a non-solvent [40]. Therefore the swollen state morphology probably varies less between the materials.

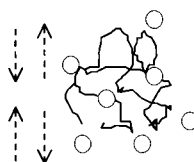
## 2.6. THERMOCHEMICALLY VERSUS PHOTOCHEMICALLY INITIATED POLYMERISATIONS

As mentioned in Section 2.2.1, the rate of initiation by UV irradiation is proportional to the intensity of the incident light. The half life of AIBN at 0°C when irradiated with a “standard laboratory light source” with emission maximum at 366 nm was estimated to be 8 h [14]. This contrasts with initiations using higher intensity medium or high pressure mercury vapour lamps [13,38]. In these cases significantly shorter half lives can be expected. The medium pressure lamp used in the L-PA model system [13] was of 550 W, delivering intensities in the order of 10–100 mW/cm<sup>2</sup> with the reactions occurring at 10–30 cm from the lamp. In a study by Viklund *et al.* on the photoinitiated copolymerisation of GMA and TRIM using AIBN as initiator, a UV light source delivering an incident intensity of 10 mW/cm<sup>2</sup> was used [38]. The polymerisations were in this case judged to be complete within 1 h.

Although the generation of free radicals may be faster by photolytic homolysis the propagation rate should be slower due to the low temperature of polymerisation (–20 to +15°C as compared to *ca.* 60°C when using thermochemical initiation).

- **Good solvation of the growing chains**

- Primary chain mechanism
- Homogenous network with small pores in the dry state
- Flexible internuclei connections
- High swelling factors



- **Poor solvation of the growing chains**

- Primary particle mechanism
- Macropores ( $> 500 \text{ \AA}$ )
- Microspheres
- Low swelling factors

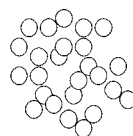


Fig. 2.12. Properties of network polymers prepared in good solvents and bad solvents for the growing polymer chain.

The gel point is still reached at about the same time in both systems. Even if the number of unreacted double bonds is similar for materials prepared using different porogens it is markedly higher, about two times, for polymers prepared by photoinitiation compared to polymers prepared by thermal initiation, i.e. *ca.* 10% versus *ca.* 5% [13]. This is also seen in the swelling factors, which are higher for photopolymerised MIPs compared to the corresponding thermally polymerised MIPs (see Chapter 5). A reduction in the number of unreacted double bonds and thereby an increased stability of the materials may be achieved by subjecting the polymers to thermal curing at elevated temperatures after an initial period of reaction at lower temperatures [12,13,46]. This should increase the double bond conversion, partly in the form of cross-links.

Another difference between the two polymerisation techniques is that they result in materials with different mass transfer kinetics. The thermally prepared polymers are usually associated with a slow mass transfer which makes it necessary to perform many of the chromatographic evaluations at elevated column temperatures (up to  $90^{\circ}\text{C}$ ). This often results in separation factors and resolutions in the same order as photoinitiated polymers evaluated at ambient temperature [27,47]. Meanwhile, using photochemically polymerised materials, good recognition and resolution are often obtained at ambient temperature [14]. Often, the end result is two materials that exhibit similar selectivity at high column temperature but significantly different selectivities at ambient temperatures (Fig. 2.13). Moreover, many examples have shown that the sample load capacity of the MIPs prepared by thermal initiation [13,46] is higher than corresponding MIPs prepared by photochemical initiation [48,49]. The above differences may be associated with the extent of micropores in the materials. In the dry state the thermally prepared materials have a larger population of micropores than the photopolymerised materials [13].

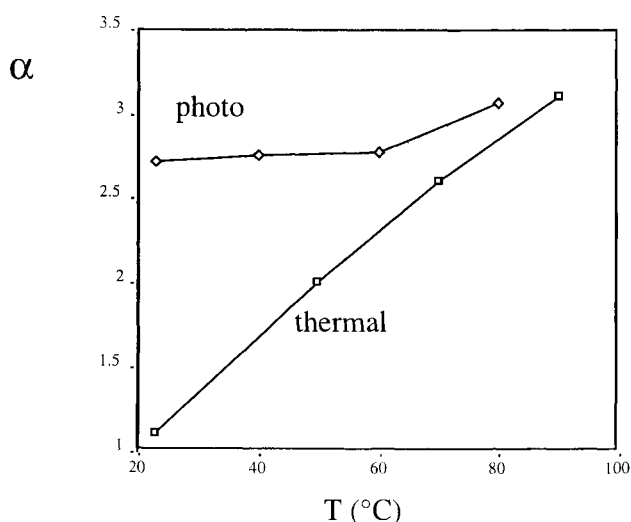


Fig. 2.13. Separation factor ( $\alpha$ ) versus column temperature in the chromatographic resolution of D,L-PA on L-PA imprinted polymers prepared by thermochemical initiation at 60/90/120°C (24 h at each temperature) using acetonitrile as porogen and photochemical initiation at 15°C for 24 h using dichloromethane as porogen. For the thermochemically polymerised material the mobile phase was 5% acetic acid in acetonitrile and for the photochemically polymerised material the mobile phase was acetonitrile/water/acetic acid: 92.5/2.5/5 (v/v/v). From Sellaergren *et al.* [27] and Sellaergren and Shea [13].

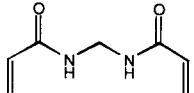
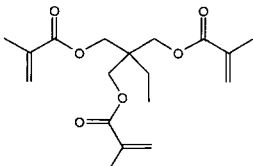
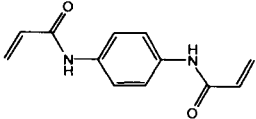
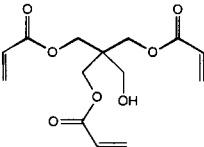
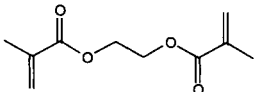
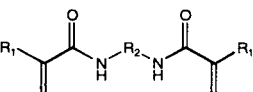
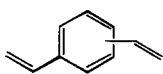
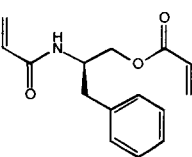
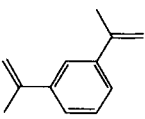
Even if this does not reflect the swollen state porosity, it would lead to increased diffusional limitations and a larger specific surface area. The photopolymers probably have a more open pore structure in the swollen state giving the template more rapid access to the sites, which are in this case confined to a smaller surface area. The difference in the conversion of pendant double bonds, and thereby the difference in cross-linking densities between the two types of materials, is probably also a factor that comes into play. An increase in chain flexibility at the sites is likely to cause an increase in the template adsorption-desorption rate coefficients. In this context it is interesting to note that increased rate enhancements were observed upon controlled hydrolysis of the polymer backbone of an imprinted esterase model [73].

## 2.7. THE CROSS-LINKING MONOMER

Several cross-linking monomers have been evaluated in molecular imprinting (Table 2.5). Wulff *et al.* made a systematic comparison of styrene-based MIPs with MIPs based on methacrylates [42]. Resins prepared from DVB exhibited lower selectivity, poorer chromatographic performance and lower thermal stability than the methacrylate-based resins. Replacing DVB with meta-di-isopropenylbenzene led to some improvements in this regard [50, 54]. One reason for the poor performance

TABLE 2.5

## VARIOUS CROSS-LINKING MONOMERS USED IN MOLECULAR IMPRINTING

|   |          |  |          |
|---|----------|--|----------|
|    | [56]     |   | [49]     |
| <i>N,N'</i> -methylenediacylamide   |          | <i>Trimethylolpropane trimethacrylate (TRIM)</i>                                   |          |
|    | [56]     |   | [49]     |
| <i>N,N'</i> -diacryloyl-1,4-diaminobenzene  |          | <i>Pentaerythritol triacrylate (PETRA)</i>   |          |
|    | [42]     |   | [56, 54] |
| <i>Ethyleneglycoldimethacrylate (EDMA)</i>  |          | <i>Diacrylamides<br/>Dimethacrylamides</i>   |          |
|   | [42]     |  | [81]     |
| <i>Divinylbenzene (DVB)</i>   |          | <i>N,O-diacryloylphenylalaninol</i>  |          |
|  | [51, 54] |  |          |
| <i>m-diisopropenylbenzene</i>   |          |  |          |

of the DVB resins is that they are poorly solvated by many of the common solvents used in chromatography and in the rebinding experiments [51]. They are also more rigid, as seen in the lower swelling when comparing otherwise identically prepared resins (in methanol the swelling was 1.27 and 1.64 for polymers prepared from DVB and EDMA respectively [42]; porogen: acetonitrile/benzene: 1/1). EDMA is the most commonly used cross-linker for the methacrylate-based systems, primarily because it provides materials with mechanical and thermal stability, good

wettability in most rebinding media and rapid mass transfer with good recognition properties [52]. Except for trimethacrylate monomers, such as TRIM, no other cross-linking monomer provides similar recognition properties for such a large variety of target templates. In the imprinting of peptides, TRIM has been used to prepare resins possessing a higher sample load capacity and a better performance than similar resins prepared using EDMA as cross-linker [43]. It has also been successfully used in the preparation of MIP-filled fused silica capillaries [53]. Amide-based cross-linkers are interesting since they provide a polar, more protein-like microenvironment, which is different from the less polar methacrylates and styrene-based resins [54]. This may be beneficial in the imprinting of polar templates with limited solubility in organic solvents. The early work by Arshady and Norrl w and their co-workers should be mentioned in this regard [55–57].

## 2.8. EXTRACTION OF TEMPLATE

One problem in molecular imprinting concerns the small amount of template that remains strongly bound to the polymer after attempted extraction (site G in Fig. 2.11). This usually amounts to more than 1% of the amount of template given to the monomer mixture and remains bound even after careful washing of the polymer [13,58–60]. This may not constitute a problem in preparative separations or catalysis, but when the materials are used for sample preparation prior to analytical quantification of low levels of analytes, bleeding of this fraction will cause false results (see Chapter 15) [59,60]. In spite of careful washing, slow leakage of template often occurs upon exchange of solvents. This problem may be reduced by thermal posttreatment of the materials [44] (see Chapter 5) or prevented by the use of a template analogue as template [59]. Also more effective wash procedures may lead to less bleeding [60]. The question is then how the template is incorporated in the polymer. Some templates may react with free radicals and become covalently incorporated in the matrix. In order to establish whether this is occurring, model reactions between the template, the initiator and, possibly, a small amount of monovinyl monomer should be carried out. By this mechanism no leakage can occur since the template would be covalently bound to the polymer. However, leakage is possible if the template is physically entrapped in the densely cross-linked regions of the nuclei [44]. Swelling and shrinkage of the polymer may then cause slow bleeding of this fraction.

It has also been speculated that the unextracted template may act as a nucleation site for template cluster formation [61]. Since the solvating properties of the medium are changing during polymerisation the template may form clusters which would then be the actual species imprinted. This mechanism may contribute to the recognition seen in some systems but can hardly explain the excellent recognition seen in a number of systems and the fact that recognition or catalytic activity often improves with the yield of template recovery [73].

It is important to carefully determine the recovery of the template and to verify the identity of the recovered template. The recovery can be estimated by



determining either the amount of template in the extracts or the amount of template in the polymer [13,62]. For this purpose solution  $^1\text{H}$ -NMR, HPLC, GC, elemental analysis and scintillation counting have been used (see Section 2.11). By NMR the identity of the extracted fraction is easily verified, along with the amount of unreacted monomer. Quantification can be done by comparing the integrals of the template to those of an internal standard. More accurate quantification of the amount of template in the extract can be obtained by the use of chromatography [13]. On the other hand elemental analysis on a heteroatom existing preferably only in the template can be used to determine the recovery. Higher sensitivities are obtained using trace analytical techniques (see Section 2.11.). High sensitivities are also obtained using a radioactively labelled template. The amount of template in the polymer before and after extraction is then compared by scintillation counting on the polymer or by total combustion of the polymer followed by counting of the isotopes [62].

## 2.9. FUNCTIONAL GROUP TITRATIONS

Potentiometric pH-titrations of protolytic functional groups in cross-linked materials provide information about their local environment and accessibility [63–65]. Titrations of highly cross-linked carboxylic acid containing polymers (i.e. weak cation exchangers) are mostly used in order to determine ion-exchange capacity, buffering range and the average  $\text{p}K_{\text{a}}$  of the polymer [64,66]. In a fundamental characterisation of the L-PA model system, potentiometric pH-titrations were performed on a MIP and its corresponding blank polymer [67]. In Fig. 2.14 the obtained pH-titration profiles in organic–aqueous systems and the corresponding  $\text{p}K_{\text{a}}$  distribution profile are shown. The titrations of the polymers were compared to a titration of an amount of acetic acid corresponding to one equivalent of carboxylic acid groups in the polymer. As can be seen from these curves, most of the carboxylic acid groups originally added as monomers have been titrated, indicating that they are accessible. A lower accessibility (60–70%), was seen in the titration in a pure aqueous system compared to that in an aqueous–organic system (75–85%). This may be related to the lower swelling observed in water leading to a more compact structure and a lower accessibility [13]. Furthermore the polymers have a buffer capacity over a wide pH range. This is somewhat higher in the organic–aqueous system than in the fully aqueous system. The physical meaning of this difference is unclear, since the method to standardise the pH meter renders the pH readings in the organic–aqueous system only apparent values [65].

In the titration of polyelectrolytes, neighbouring group effects largely influence the pH-titration profile [68]. For instance, in polyacrylic acid the ionisation of the most acidic group may be facilitated by hydrogen bonding to a neighbouring carboxylic acid group. However, as the polymer ionises progressively the net increase in negative charge on the polymer will make it more difficult to ionise the next carboxylic acid group. It has been shown that the apparent  $\text{p}K_{\text{a}}$  increases with the degree of ionisation ( $\alpha^*$ ) according to:

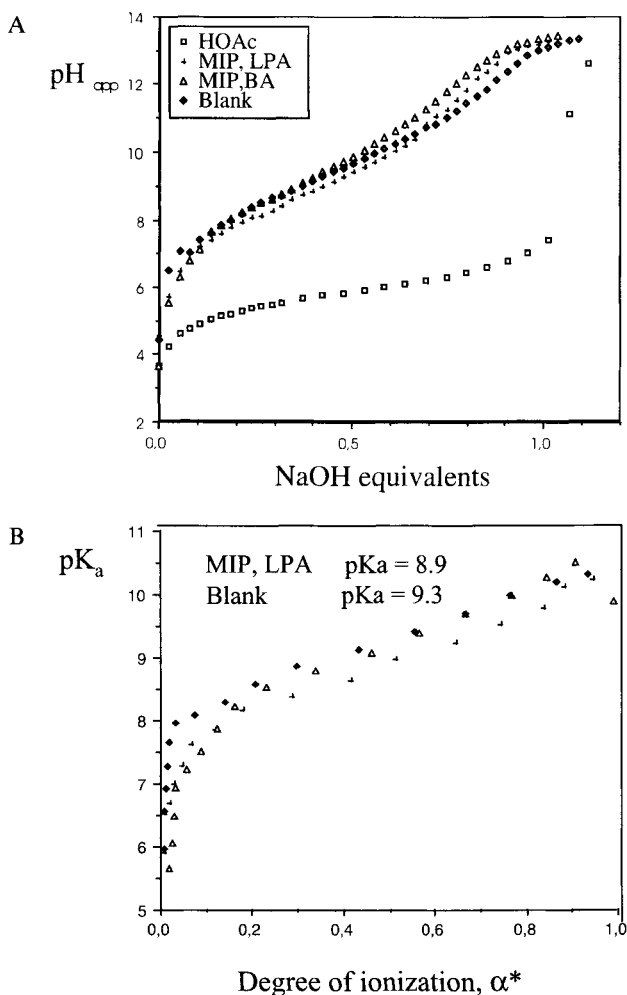


Fig. 2.14. (A) Potentiometric titration curves of a polymer imprinted with L-PA (PLPA), a polymer imprinted with benzylamine (PBA), a blank non-imprinted polymer (PBL) and acetic acid in MeCN/0.1M NaCl: 70/30 (v/v). The NaOH equivalents (x-axis) are calculated based on the theoretical amount of carboxylic acid groups present in the polymer. In (B) is seen the calculated  $\text{pK}_a$  distribution as a function of the degree of ionization ( $\alpha^*$ ). The polymer swelling (ml/ml) in this solvent system was constant in the pH interval 3–12 and was for PLPA: 1.32 and for PBL: 1.26. From Sellergren and Shea [67].

$$\text{pK}_a = \text{pH} \log[\alpha^*/(1 - \alpha^*)] \quad (10)$$

A plot of  $\text{pK}_a$  as a function of  $\alpha^*$  can thus be regarded as a measure of the ease of proton removal from the polyion at a given degree of ionisation. The shape of the  $\text{pK}_a$  versus  $\alpha^*$  plot depended on the polymer being titrated. However, the polymers exhibited buffering capacity at higher pH values than commonly found

for weak cation exchangers [64,66]. This difference may be related to the charge densities of the materials. The more weakly cross-linked cation exchange resins are quite swellable and can thus expand and reduce the build-up of electrostatic repulsion, leading to a titration curve that approaches that of the free acid [68]. The imprinted materials are less swellable and no change in swelling was observed when the pH was varied. On the other hand the L-PA imprinted polymer showed significantly larger swelling than corresponding blank non-imprinted polymers prepared without template or with benzylamine as template. In the organic-aqueous system the difference between the titration curves of imprinted polymer and the blank polymer can thus be explained by their different swelling factors. A contribution from the structural organisation of the carboxylic acid groups in the polymer is also possible (which may *per se* be the reason for the difference in swelling). In the blank polymer, the absence of template during polymerisation will leave the carboxylic acid groups to interact mainly with themselves, forming acid dimers. However, in the presence of template, some acid groups will also interact with the template molecule. After freeing the polymers from template these acid groups have lost their hydrogen bond partner and are thus in a more isolated environment than the acid groups in the blank material. Such an arrangement would result in a lower  $pK_a$  for the more isolated acid groups compared to the  $pK_a$  of the associated groups. Indeed the  $pK_a$  of the L-PA MIP was slightly lower than that of the blank polymer.

## 2.10. BINDING SITE LOCATION

In the course of characterisation of the chromatographic and structural properties of MIPs, a number of results have been obtained that have shed some light upon the question concerning the location of the binding sites in the polymer. Some of these are contradictory. In view of the heterogeneous cross-link density of the network polymers, the highly cross-linked primary particles or nuclei formed early in the polymerisation [31] should be better able to preserve the three-dimensional structure of the binding site than the less cross-linked external regions of the microspheres or the interconnecting chain segments. On the other hand, the former type of sites should be less accessible than the latter ones. It was shown that the swelling of MIPs, identically prepared except for the solvent used, had little effect on the selectivity of the materials (see Chapter 5) [13]. This makes it unlikely that the sites are located in the interconnecting segments. This is also indicated by the study of thermally annealed materials, where the annealing led to large changes in swelling but no impairment of the selectivity of the materials (Chapter 5). Unfortunately no other conclusions can be drawn from these studies concerning the location of the sites.

An interesting study on the rebinding of diketones to imprinted polymers was reported by Shea and Sasaki [69]. Polymers were prepared by copolymerisation of the corresponding *bis*-ketal as template with meta-di-isopropenylbenzene as cross-linking monomer (Fig. 2.15). The *bis*-ketal is hydrolysed with acid freeing the

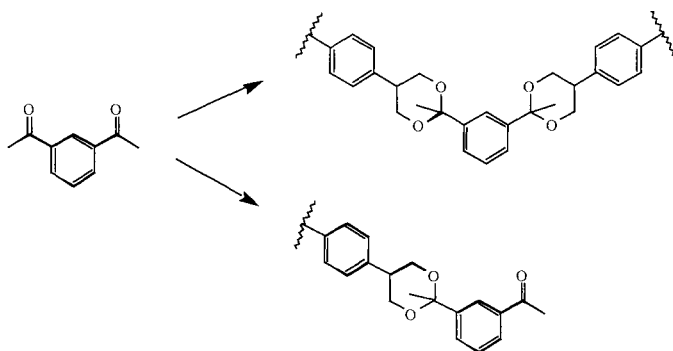


Fig. 2.15. Possible one- and two-point binding of aryldiketones to diol functionalised templated binding sites. From Shea and Sasaki [69].

polymer from the diketone and leaving behind a site equipped with two diol groups positioned to rebind the template. The rebinding was analysed spectroscopically by  $^{13}\text{C}$ -CP-MAS NMR and FTIR spectroscopy (see next section) by quantifying the extent of one and two point rebinding respectively. Sites that are well defined are expected to allow mainly two point binding, whereas templates bound to poorly defined sites will be mainly linked at one point only. Since the rebinding occurred under irreversible conditions the mode of rebinding with time revealed the accessibility of the different types of sites. Early in the rebinding experiment, a large percentage of two point binding was observed while later on the percentage of one point binding increased. This indicates that the most selective sites also are the most accessible. Interestingly, the opposite conclusion was reached for rebinding of bisnaphthol, as a transition metal ligand, to shape-selective templated sites. [82]

## 2.11. CHARACTERISATION TECHNIQUES FOR CROSS-LINKED VINYL POLYMERS AND MIPs

In order to draw conclusions of how variables related to the preparation of porous solids affect their useful properties, it is necessary to characterise the structure and morphology of the materials. First it should be established that the polymerisation has proceeded to full conversion of the monomers and, ideally, the regularity and structure of the primary chains should be studied. It is also important to determine the accessibility and microenvironment of the functional groups and binding sites. In chromatography, these factors are directly related to the sample load capacity and mass transfer kinetics of the stationary phase. In molecular imprinting the number of these binding sites depends on the amount of template that can be recovered by various washing procedures. Sensitive methods for quantifying this amount must be found. Knowledge about dynamic processes, such as polymer chain mobility or side chain mobility and rates of transport of small molecules within the pores, is important to understand the behaviour of MIPs. A more far reaching goal is to find methods allowing the binding sites to be characterised at

- **Pore system, surface areas, texture**
  - Porosimetry (N<sub>2</sub> sorption, Hg penetration)
  - Microscopy (SEM)
  - Swelling and solvent uptake
- **Conformational transitions, thermostability**
  - Thermal analysis (TGA, DSC)
- **Polymer yield, composition**
  - Elemental analysis
  - CP-MAS-solid state NMR
- **Chemical and structural information**
  - Potentiometric titrations
  - FTIR
  - CP-MAS-solid state NMR
  - Fluorescence probes

Fig. 2.16. Techniques used in the characterization of MIPs.

a molecular level. Until now the methods shown in Fig. 2.16 have been used to gain information related to the above properties.

### 2.11.1. Elemental analysis

Elemental analysis is the classical method to obtain information about the elemental composition of an unknown substance [70,71]. A known amount of unknown substance is converted to simple, known compounds containing only the element to be quantified. For instance carbon and hydrogen are determined in organic compounds by conversion through combustion to carbon dioxide and water followed by quantitative analysis of the latter compounds. Likewise nitrogen is converted to nitrogen gas. An exact match between the theoretical composition, calculated assuming a quantitative yield of polymerisation, and the analytical results indicates that the polymerisation has incorporated all monomers stoichiometrically in high yield [72]. Reactions with the polymer, for instance removal of template, are most easily detected when the removed or added species contain an element such as nitrogen, halogen, sulphur or phosphorus. For instance in the imprinting of phosphorus transition state analogues for ester hydrolysis the amount of phosphorus in the polymer was determined by trace elemental analysis prior to (0.081%) and after (0.0015%) splitting, giving a splitting yield of about 98% [73].

### 2.11.2. Gravimetric analysis

A rough measure of the yield of polymerisation is obtained by weighing the dry polymer after removal of unreacted monomer, solvent and template by continuous extraction and comparing the weight to the total weight of added monomer [13].

### 2.11.3. Nuclear magnetic resonance spectroscopy

$^1\text{H}$ -NMR and  $^{13}\text{C}$ -NMR are useful tools for the determination of regularity and tacticity in soluble polymers [10]. In the polymerisations leading to insoluble polymers solution NMR can be used to study the polymers formed prior to gelation and the kinetics of the polymerisation [18]. However, for insoluble polymers solid state  $^{13}\text{C}$ -NMR has so far provided the most useful information [1,41,74]. Based on cross-polarisation magic angle spinning (CP-MAS) experiments, estimates of the relative amounts of different types of carbon atoms have been made. For instance, this is a widely used technique for the estimation of the amount of unreacted double bonds remaining in materials after the polymerisation of divinyl monomers. Moreover it has been used to monitor rebinding to imprinted polymers [69]. Due to some shortcomings of the CP-MAS technique, single pulse excitation techniques are now considered to be more accurate for quantitative purposes [74].

### 2.11.4. Infrared spectroscopy

Infrared spectra of insoluble polymers are easily obtained from KBr pellets of the polymer [75]. By first comparing bands of the monomers to those of the polymer, the extent of incorporation of the monomers can be established. In the MIPs formed from EDMA and MAA there are a number of useful bands informative about the structure and local environment of the polymer chains (Fig. 2.17). The bands at  $1638/\text{cm}^{-1}$  and  $950/\text{cm}^{-1}$  are informative about the extent of unreacted double bonds in the material and have been quantitatively evaluated [54,76]. The position of the carbonyl band at about  $1700/\text{cm}^{-1}$  is sensitive to the extent of hydrogen bonding to the carbonyl oxygens. However, this band is composed of both the ester carbonyl bands and the carboxylic acid carbonyls and is therefore not informative about the extent of hydrogen bonding to the carboxylic acid groups. Nevertheless, ionisation of the acid group should lead to the appearance of a peak at around  $1570/\text{cm}^{-1}$ . The extent and mode of hydrogen bonding is also revealed by the intensity and position of the O-H stretching band at around  $3300\text{--}3500/\text{cm}^{-1}$ . Here a band at  $3300/\text{cm}^{-1}$  has been attributed to carboxylic acid cyclic dimers, while one at  $3440/\text{cm}^{-1}$  has been attributed to isolated groups [77]. In the spectra of the L-PA imprinted polymers a maximum is seen at  $3440/\text{cm}^{-1}$ , with an inflection at  $3300/\text{cm}^{-1}$  [13]. However, strong absorbance was also observed at higher wavenumbers, indicating a population of isolated carboxylic acid groups. The intensity of these bands is highly sensitive to water remaining in the samples.

### 2.11.5. Fluorescence probes of network solvation

The dry state morphology obtained from gas sorption experiments does not reveal how the material interacts with solvents. In addition to the measurement of swelling and solvent uptake, fluorescent probes can be incorporated in the polymer network and used to measure the extent of solvation of the polymer in a given solvent [51,54]. For this purpose Shea and co-workers incorporated dansyl

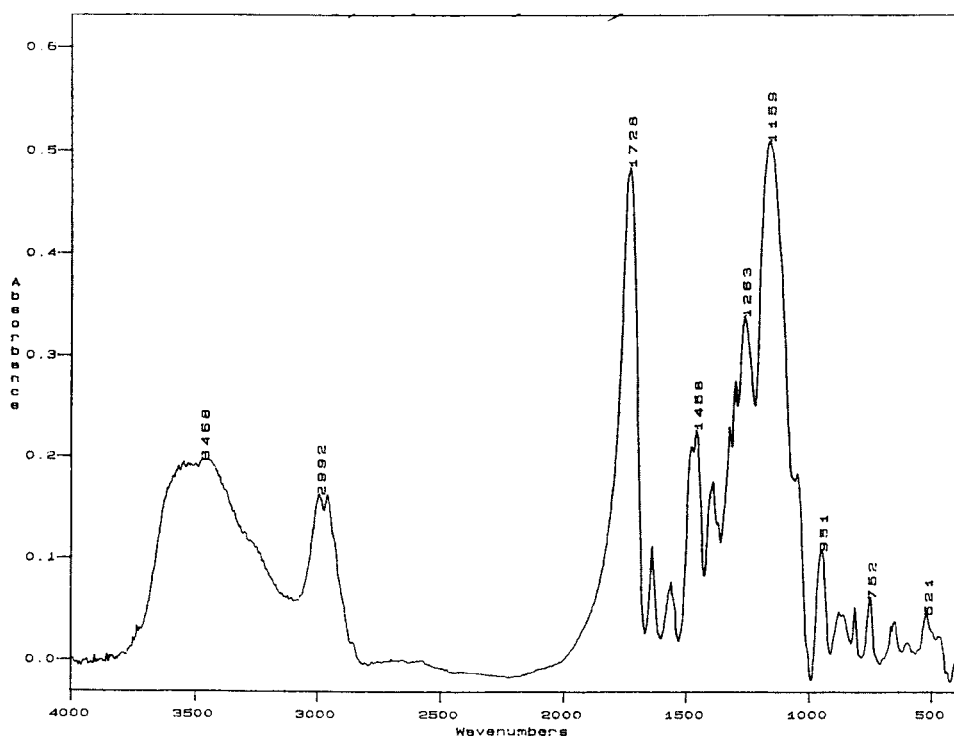


Fig. 2.17. Infrared spectrum (KBr) of a copolymer of EDMA (83 mol %) and MAA (17 mol %) imprinted with L-PA using  $\text{CH}_2\text{Cl}_2$  as porogen. The peak assignments were as follows:  $>3440\text{ cm}^{-1}$  OH stretch, COOH monomeric;  $3300\text{ cm}^{-1}$  OH stretch, COOH dimers;  $2840\text{--}3000\text{ cm}^{-1}$  CH stretch, aliphatic CH,  $1728\text{ cm}^{-1}$  CO stretch, ester CO and COOH;  $1630\text{ cm}^{-1}$  vinyl C=C stretch (unreacted vinyl groups); *ca.*  $1600\text{ cm}^{-1}$ ,  $\text{COO}^-$ ;  $1380\text{--}1470\text{ cm}^{-1}$  -O- $\text{CH}_2$ -bending;  $1263\text{ cm}^{-1}$  C-O bend, ester;  $1163\text{ cm}^{-1}$ , ester;  $955\text{ cm}^{-1}$  C- $\text{CH}_3$  rocking,  $750\text{--}800\text{ cm}^{-1}$  CH vinyl out of plane bending,  $750\text{--}850\text{ cm}^{-1}$   $\text{CH}_2$  rocking.

monomers into highly cross-linked resins. The extent of solvation could then be estimated based on shifts in the emission maximum of the polymer bound probe imbibed in a solvent when compared to the probe dissolved in the same solvent (Fig. 2.18). For some solvents the emission maxima are found to be close to that of the probe in a dry material, indicating little or no penetration of the solvent into the pores.

#### 2.11.6. Pore structure in the dry state

The pore structure of porous substances is characterised by the following parameters:

Specific surface area,  $S$  ( $\text{m}^2/\text{g}$ )

Specific pore volume,  $V_p$  ( $\text{mL/g}$ )

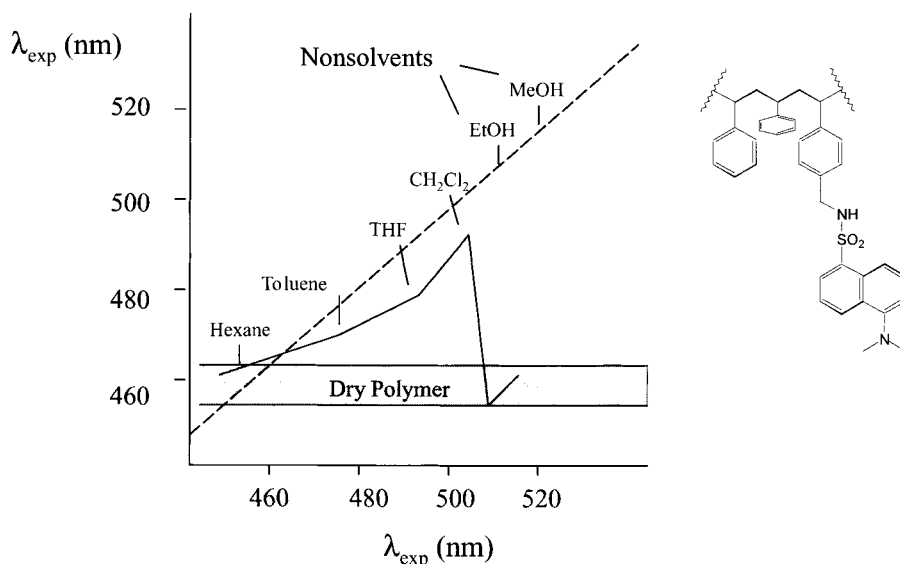


Fig. 2.18. Fluorescence emission maxima measured for prelabelled polystyrene immersed in different solvents versus calculated emission maxima. The straight line represents the emission maxima measured for the probe dissolved in the solvents whereas the curve represents doped polystyrene. From Shea *et al.* [51].

Average pore diameter,  $D_p$  (Å)

Pore size distribution  $dV_p/dD_p$

These parameters can be determined from gas adsorption–desorption measurements, usually nitrogen, and from mercury penetration measurements [78,79].

#### 2.11.6.1. Gas sorption measurements

Experimentally a gas is dosed in small amounts into an evacuated sample chamber containing a known amount of dry solid at the gas boiling point. By registering the equilibrium pressure after each addition and, knowing the amount of gas added, an adsorption isotherm showing the quantity of adsorbed gas,  $x_a$ , as a function of the relative pressure ( $p/p_0$ ) in the range  $0 < p/p_0 < 1$  can be plotted ( $p$  = equilibrium pressure,  $p_0$  = saturation vapour pressure of the pure liquid adsorptive). The mechanism of gas adsorption depends on the ratio between the molecular diameter  $d_m$  and the pore diameter  $D_p$ . If the average pore diameter is much larger than  $d_m$  the pore wall may be regarded as a planar surface, whereas if the diameters are similar, dispersion forces related to the pore curvature will influence the adsorption. With large pores the gas diffuses rapidly and equilibrium is rapidly reached. Due to the low surface area of large pores the amount of gas adsorbed is relatively low giving adsorption isotherms of type II or, for non-porous solids, of type III (Fig. 2.19). For small pores the diffusion is slow



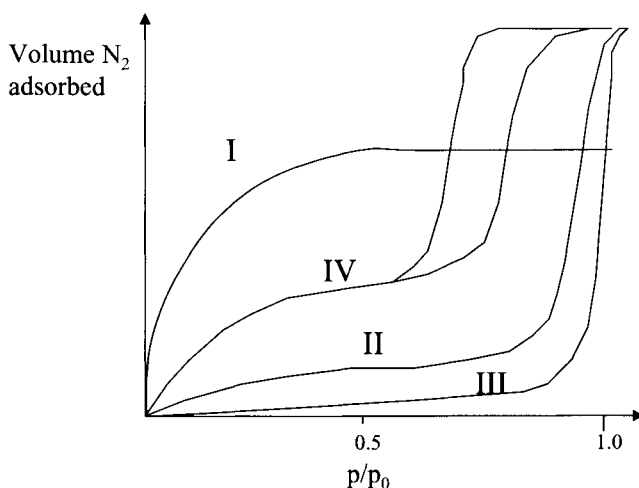


Fig. 2.19. Adsorption isotherms as classified by Gregg and Sing [78].

and depends strongly on the size of the gas molecule. Here, interactions occur in three dimensions instead of the layer interactions occurring in the larger pores. After pore filling at increasing pressure no more gas is adsorbed, resulting in a Langmuir type I isotherm. Depending on the isotherm the sorbent is classified as microporous if it contains only micropores ( $D_p < 20 \text{ \AA}$ ) or macroporous if it contains only macropores ( $D_p > 500 \text{ \AA}$ ). In between are mesoporous adsorbents ( $20 < D_p < 500 \text{ \AA}$ ) which exhibit a type IV isotherm. The hysteresis loop is explained by different mechanisms of filling and emptying of the pores in this size range. Based on the adsorption isotherm the porous characteristics can be estimated.

#### 2.11.6.2. Mercury penetration

In mercury penetration measurements, mercury is forced under various pressures into the pores of the material. Due to the large contact angle ( $\theta$ ) of mercury in contact with most materials, the pressure required to force mercury into the pores can be expressed as a function of the pore radius:

$$pr = -2\sigma\cos\theta \quad (11)$$

where  $p$  is the applied pressure,  $r$  is the pore radius and  $\sigma$  the surface tension of mercury. Mercury penetration is a destructive technique and requires that the material is mechanically stable. The experimental results are evaluated by several methods making assumptions about the process of adsorption or about the state of the adsorbed material, giving models showing good agreement with the isotherms in certain regions. From these models the above named quantities can be deduced.

### 2.11.6.3. Surface areas

For a given pore volume the surface area increases with decreasing pore size. Approximate values are:

|                         |                          |
|-------------------------|--------------------------|
| Microporous adsorbents: | > 500 m <sup>2</sup> /g  |
| Mesoporous adsorbents:  | 10–500 m <sup>2</sup> /g |
| Macroporous adsorbents: | < 10 m <sup>2</sup> /g   |

Depending on the pore sizes in a given adsorbent, different models are applied in the calculation of the surface areas. For meso- and macroporous adsorbents the surface areas are best calculated using the BET method from the region  $0.05 < p/p_0 < 0.35$  of the isotherm. Multiplying the amount of adsorbed gas corresponding to a monolayer,  $x_m$ , with the area per molecule gives the surface area of the material. For the type I Langmuir isotherm this amount is simply obtained by the Langmuir equation:

$$p/x_a = 1/(Bx_m) + p/x_m \quad (12)$$

where  $x_a$  is the amount of gas adsorbed and  $B$  is a constant depending on the surface character.

From mercury penetration the surface area is determined knowing the surface tension and contact angle of mercury and the total volume of penetrated mercury. Measurements agree with the BET measurements below surface areas of 100 m<sup>2</sup>/g.

### 2.11.6.4. Pore volume

The specific pore volume can be determined from nitrogen adsorption measurements if the adsorbent is meso- or microporous. For macroporous adsorbents with pore diameters above 1000 Å, the pore volume can be determined by mercury penetration measurements by integrating the pressure–volume curve. The total pore volume of meso- and microporous adsorbents can be calculated by assuming that, in the range  $0.95 < p/p_0 < 1$ , all pores in the adsorbent are filled with condensed gas. The total pore volume is then simply calculated as:

$$v_p = x_a V \text{ (mL/g)} \quad (13)$$

The volume of micropores can be obtained using the Dubinin equation [78].

### 2.11.6.5. Pore size distribution

As for the pore volume, the pore sizes of meso- and microporous adsorbents are characterised using gas sorption measurements, whereas the pore sizes of macroporous adsorbents are best estimated using mercury penetration measurements or by electron microscopy. The function  $\partial v_p / \partial d_p = f(d_p)$  can be calculated using various models. In gas sorption on sorbents with mesopores the function is obtained using the Kelvin equation describing capillary condensation.

### 2.11.7. Pore structure in the swollen state

In most applications of porous adsorbents they are used in a liquid medium. Depending on the affinity of the polymer for a particular solvent and depending on the degree and distribution of cross-links it will swell to varying extents [1]. The porosity in the swollen state is therefore of particular interest. Polymeric adsorbents usually swell more in a good solvent for the corresponding non-cross-linked polymer than in a non-solvent for that polymer. In order to assess interactions between polymers and liquids one can use the semi-empirical approach introduced by Hildebrand, based on the assumption that like dissolves like [10,45]. This is expressed in terms of solubility parameters ( $\delta$ ) related to the energy of vapourisation of the solvent or the polymer. Knowing  $\delta$  for the solvent and the polymer allows an estimate of the heat of mixing per unit volume according to:

$$\Delta H_m/V = (\delta_1 - \delta_2)^2 \phi_1 \phi_2 \quad (14)$$

where  $\delta_1$  is related to the energy of vapourisation of species 1 and  $\phi_1$  its volume fraction in the mixture (species 1 and 2 are assumed to be non-interacting). A minimum  $\Delta G$  is obtained when  $\delta_1 = \delta_2$ , implying a maximum solvation of the growing polymer chains (good solvent). Usually,  $\delta$  for a polymer is assumed similar to  $\delta$  of the solvent that produces maximum swelling. In a more detailed description,  $\delta$  is divided into dispersive, dipole-dipole and hydrogen bonding terms (Table 2.3):

$$\delta = (\delta_D^2 + \delta_P^2 + \delta_H^2)^{1/2} \quad (15)$$

Depending of the size of the hydrogen bonding term the solvents have been further classified as either poorly, moderately or strongly hydrogen bonding. A correct estimate of  $\delta$  for highly cross-linked polymers is difficult due to their cross-linked nature, which gives rather small swelling factors. Often, however, the solubility parameter is close to that of the predominating monomer. As can be seen in Tables 2.3 and 2.4, all solvents have  $\delta$  values in the range of either p-MAA, p-MMA or p-MMA/MAA/EA, linear polymers similar to the cross-linked methacrylates commonly used in molecular imprinting.

Pore size distributions in the swollen state can be obtained by a technique called thermoporosimetry [1,2]. This is based on measurements of the freezing point of solvents inside the pores. This is usually lower in the smaller pores and an empirical relationship has been found:

$$R_p = 131.6/\Delta T - 0.79 \quad (16)$$

Thus, by scanning calorimetry at lower temperatures, a distribution curve is obtained allowing one to estimate the pore size distribution. Another alternative technique consists of freeze drying of the polymer and thereafter measuring the pore size distribution by the conventional gas sorption technique [2].

The swelling is also dependent on the level of cross-linking in the resin, i.e. the higher the cross-linking the lower the swelling. For heterogeneously cross-linked resins, as in the case of permanently porous, mesoporous or macroporous

polymers, the situation is more complex. Here the pores are filled with liquid and the cross-link density is heterogeneous. Thus, the inaccessible regions of the nuclei will be less swollen than their outer shells and the internuclei space [1]. Swelling is measured by allowing a given volume of dry polymer, with a known particle size and weight, to equilibrate in a solvent whereafter the volume of the swollen particles is measured. This gives the volume swelling and the volume swelling ratio is calculated as:

$$\text{Volume swelling ratio} = \frac{\text{Bed volume of swollen particles}}{\text{Bed volume of dry particles}} \quad (17)$$

Since the weight of the bed volume of the dry particles is known, the apparent density,  $d_{app}$ , can be calculated:

$$d_{app} = \frac{\text{Weight of dry particles}}{\text{Bed volume of dry particles}} \quad (18)$$

and the weight specific swelling is then given as:

$$\text{Weight swelling ratio} = \frac{\text{Volume swelling ratio}}{d_{app}} \quad (19)$$

Materials with different volume swelling ratios but with similar weight swelling ratios have a similar pore volume in the swollen state. For information about the total pore volume in the non-swollen state a non-swelling solvent is often used to measure the solvent uptake of the polymer [13,54]. Thus, as in the swelling experiment, a given weight and volume of particles is placed in a non-swelling solvent. The excess solvent is then removed and allowed to evaporate until the particles are freely flowing and separate. At this point only the pores are assumed to be filled with solvent and the volume uptake is calculated as:

$$\text{Solvent uptake} = \frac{((\text{Weight filled particles} - \text{Weight dry particles})/d_{\text{solv}})}{\text{Weight dry particles}} \quad (20)$$

#### 2.11.8. Thermal analysis

When a polymer undergoes a physical or chemical change a corresponding change in enthalpy is observed. Measurement of the associated heat released or taken up by the polymers and the change in mass forms the basis of differential scanning calorimetry (DSC) and thermal gravimetric analysis (TGA) respectively [10]. The sample (a few mg) is placed in a pan located on a heating block, which is warmed at a uniform rate together with a reference pan. The differential energy needed to keep the reference at the same temperature as the sample is proportional to the energy released in exothermic transitions or taken up in endothermic transitions in the sample.

## REFERENCES

- 1 A. Guyot, In: *Synthesis and separations using functional polymers*, D.C. Sherrington, P. Hodge Eds, John Wiley & Sons Ltd., p. 1 (1988).

- 2 D.C. Sherrington, *Macromol. Chem., Macromol. Symp.*, **70/71**, 303 (1993).
- 3 R. Arshady, *J. Chromatogr.*, **586**, 181 (1991).
- 4 A.G. Mayes and K. Mosbach, *Anal. Chem.*, **68**, 3769 (1996).
- 5 R.J. Ansell and K. Mosbach, *J. Chromatogr. A*, **787**, 55 (1997).
- 6 K. Hosoya, K. Yoshizako, N. Tanaka, K. Kimata, T. Araki and J. Haginaka, *Chem. Lett.*, 1437 (1994).
- 7 J. Matsui, M. Okada, M. Tsuruoka and T. Takeuchi, *Anal. Commun.*, **34**, 85 (1987).
- 8 L. Ye, P. Cormack and K. Mosbach, *Anal. Commun.*, **36**, 35 (1999).
- 9 A.G. Mayes and K. Mosbach, *Trends Anal. Chem.*, **16**, 321 (1997).
- 10 J.M.G. Cowie, *Polymers: chemistry and physics of modern materials*, Blackie and Son Ltd. (1991).
- 11 J. March, *Advanced organic chemistry*, John Wiley & Sons (1992).
- 12 B. Sellergren, *Makromol. Chem.* **190**, 2703 (1989).
- 13 B. Sellergren and K.J. Shea, *J. Chromatogr.*, **635**, 31 (1993).
- 14 D.J. O'Shannessy, B. Ekberg and K. Mosbach, *Anal. Biochem.*, **177**, 144 (1989).
- 15 W.-H. Li, A.E. Hamielec and C.M. Crowe, *Polymer*, **30**, 1518 (1989).
- 16 C. Walling, *J. Am. Chem. Soc.*, **67**, 441 (1945).
- 17 M. Gordon and R.-J. Roe, *J. Polym. Sci.*, **21**, 27 (1956).
- 18 D.T. Landin and C.W. Macosko, *Macromolecules*, **21**, 846 (1988).
- 19 W.-H. Li, A.E. Hamielec and C.M. Crowe, *Polymer*, **30**, 1513 (1989).
- 20 D. Horák, F. Svec, C.M.A. Ribeiro and J. Kálal, *Angew. Makromol. Chem.*, **87**, 127 (1980).
- 21 S. R. Sandler and W. Karo, *Polymer syntheses, Vol. II*, Academic Press (1977).
- 22 A. Chapiro, *Pure and Appl. Chem.*, **53**, 643 (1981).
- 23 H.T. van de Grampel, Y.Y. Tan and G. Challa, *Macromolecules*, **25**, 1041 (1992).
- 24 B. Sellergren *et al.*, in preparation (2000).
- 25 D. Spivak, M.A. Gilmore and K.J. Shea, *J. Am. Chem. Soc.*, **119**, 4388 (1997).
- 26 G. Lancelot, *J. Am. Chem. Soc.*, **99**, 7037 (1977).
- 27 B. Sellergren, M. Lepistö and K. Mosbach, *J. Am. Chem. Soc.*, **110**, 5853 (1988).
- 28 R.L. Albright, *React. Polym.*, **4**, 155 (1986).
- 29 K. Dusek, H. Galina and J. Mikes, *Polym. Bull.*, **3**, 19 (1980).
- 30 K.A. Kun and R. Kunin, *J. Polym. Sci., Part A-1* **6**, 2689 (1968).
- 31 H. Kast and W. Funke, *Makromol. Chem.*, **180**, 1335 (1979).
- 32 F. Svec, J. Hradil, J. Coupek and J. Kálal, *Angew. Makromol. Chem.*, **48**, 135 (1975).
- 33 E. Kálalová, Z. Radová, F. Svec and J. Kálal, *Eur. Polym. J.*, **13**, 293 (1977).
- 34 D. Horák, F. Svec and J. Kálal, *Angew. Makromol. Chem.*, **95**, 109 (1981).
- 35 D. Horák, F. Svec, M. Ilavsky, M. Bleha, J. Baldrián and J. Kálal, *Angew. Makromol. Chem.*, **95**, 117 (1981).
- 36 F. Svec, *Angew. Makromol. Chem.*, **144**, 39 (1986).
- 37 V. Smígel and F. Svec, *J. Appl. Polym. Sci.*, **46**, 1439 (1992).
- 38 C. Viklund, E. Pontén, B. Glad, K. Irgum, P. Hörstedt and F. Svec, *Chem. Mat.*, **9**, 463 (1997).
- 39 A. Schmid, L.-L. Kulin and P. Flodin, *Makromol. Chem.*, **192**, 1223 (1991).
- 40 P. Reinholdsson, T. Hargitai, R. Isaksson and B. Törnell, *Angew. Makromol. Chem.*, **192**, 113 (1991).
- 41 T. Hjertberg, T. Hargitai and P. Reinholdsson, *Macromolecules*, **23**, 3080 (1990).
- 42 G. Wulff, R. Kemmerer and J. Vietmeier, *Nouv. J. Chim.*, **6**, 681 (1982).
- 43 M. Kempe, *Anal. Chem.*, **68**, 1948 (1996).
- 44 Å. Zander, P. Findlay, T. Renner, B. Sellergren and S. A., *Anal. Chem.*, **70**, 3304 (1998).
- 45 J. Bandrup and E.H. Immergut, *The polymer handbook*, Wiley (1989).
- 46 B. Sellergren, *Chirality*, **1**, 63 (1989).
- 47 B. Sellergren and K.J. Shea, *J. Chromatogr. A*, **690**, 29 (1995).
- 48 D.J. O'Shannessy, L.I. Andersson and K. Mosbach, *J. Mol. Recognit.*, **2**, 1 (1989).
- 49 M. Kempe and K. Mosbach, *J. Chromatogr. A*, **691**, 317 (1995).

- 50 K.J. Shea, *Polym. Prepr.* **35**, 992 (1994).
- 51 K.J. Shea, D.Y. Sasaki and G.J. Stoddard, *Macromolecules*, **21**, 1722 (1989).
- 52 G. Wulff, *Angew. Chem., Int. Ed. Engl.*, **34**, 1812 (1995).
- 53 L. Schweitz, L.I. Andersson and S. Nilsson, *Anal. Chem.*, **69**, 1179 (1997).
- 54 K.J. Shea, G.J. Stoddard, D.M. Shavelle, F. Wakui and R.M. Choate, *Macromolecules*, **23**, 4497 (1990).
- 55 R. Arshady and K. Mosbach, *Macromol. Chem.*, **182**, 687 (1981).
- 56 O. Norrlöw, M. Glad and K. Mosbach, *J. Chromatogr.*, **299**, 29 (1984).
- 57 O. Norrlöw, Doctoral Thesis, University of Lund (1986).
- 58 K.J. Shea, D.A. Spivak and B. Sellergren, *J. Am. Chem. Soc.*, **115**, 3368 (1993).
- 59 L.I. Andersson, A. Paprica and T. Arvidsson, *Chromatographia*, **46**, 57 (1997).
- 60 B.A. Rashid, R.J. Briggs, J.N. Hay and D. Stevenson, *Anal. Commun.*, **34**, 303 (1997).
- 61 J.L. Morrison, M. Worsley, D.R. Shaw and G.W. Hodgson, *Can. J. Chem.*, **37**, 1986 (1959).
- 62 B. Sellergren, B. Ekberg and K. Mosbach, *J. Chromatogr.*, **347**, 1 (1985).
- 63 D.C. Sherrington and P. Hodge Eds. *Synthesis and separations using functional polymers*, J. Wiley and Sons (1988).
- 64 F. Helfferich, *Ion exchange*, McGraw-Hill Inc. (1962).
- 65 E.P. Serjeant, *Potentiometry and potentiometric titrations*, John Wiley and Sons (1984).
- 66 D.J. Pietrzyk, In: *Packings and stationary phases in chromatographic techniques*, Vol. 47, K.K. Unger Ed., Marcel Dekker Inc., p. 585 (1990).
- 67 B. Sellergren and K.J. Shea, *J. Chromatogr. A*, **654**, 17 (1993).
- 68 P. Molyneux, *Water-soluble synthetic polymers: properties and behaviour*, Vol. II, CRC Press, Inc. (1984).
- 69 K.J. Shea and D.Y. Sasaki, *J. Am. Chem. Soc.*, **113**, 4109 (1991).
- 70 D.A. Skoog, D.M. West and F. J. Holler, *Fundamentals of analytical chemistry*, Saunders College Publishing (1992).
- 71 T.S. Ma and R.C. Rittner, *Modern organic elemental analysis*, Marcel Dekker (1979).
- 72 G. Wulff, W. Vesper, R. Grobe-Einsler and A. Sarhan, *Makromol. Chem.*, **178**, 2799 (1977).
- 73 B. Sellergren and K.J. Shea, *Tetrahedron Assym.*, **5**, 1403 (1994).
- 74 R.V. Law, D.C. Sherrington, C.E. Snape, I. Ando and H. Kurosu, *Macromolecules*, **29**, 6284 (1996).
- 75 L.J. Bellamy, *The infrared spectra of complex molecules*, Chapman and Hall (1980).
- 76 M. Bartholin, G. Boissier and J. Dubois, *Makromol. Chem.*, **182**, 2075 (1981).
- 77 Y. Kikihira and H. Yamamura, *Macromol. Chem.*, **186**, 423 (1985).
- 78 S.J. Gregg and K.S.W. Sing, *Adsorption, surface area and porosity*, Academic Press Inc., (1982).
- 79 K. Unger, *Angew. Chem. Int. Ed.*, **11**, 267 (1972).
- 80 S.S. Milojkovic, D. Kostoski, J.J. Comor and J.M. Nedeljkovic, *Polymer*, **38**, 2853 (1997).
- 81 L. Andersson, B. Ekberg and K. Mosbach, *Tetrahedron Lett.*, **26**, 3623 (1985).
- 82 N.M. Brunkan, M.R. Gagné, *J. Am. Chem. Soc.* **122**, 6217 (2000).

This Page Intentionally Left Blank

## **Thermodynamic principles underlying molecularly imprinted polymer formulation and ligand recognition**

IAN A. NICHOLLS AND HÅKAN S. ANDERSSON

### **3.1. INTRODUCTION**

As measured by the dramatic increase in the number of publications in the area over recent years [1], the field of molecular imprinting has gained acceptance as a unique area of scientific endeavour, which lies at the cross-roads of polymer, organic, analytical, physical and bio-chemistries. Both the technique itself and its range of applications have been comprehensively reviewed [2–18].

Although a vast number of papers has appeared describing systems prepared using new template structures, monomers and polymerisation formats and presenting new applications, less effort has been directed towards characterising and understanding the physical mechanisms underlying molecularly imprinted polymer (MIP) formation and MIP–ligand recognition (Fig. 3.1). The development of a true understanding of these mechanisms will assist in the design and application of new and improved MIP systems and in the interpretation of polymer–ligand recognition events. In this overview of the state of the art in this aspect of molecular imprinting, we will deal first with the physical aspects of MIP formation, and secondly with the physical nature of MIP–ligand binding.

### **3.2. PHYSICAL PRINCIPLES UNDERLYING MIP PREPARATION**

Much research effort has been devoted to the development of a general understanding of the physical basis of molecular recognition, i.e. why two molecules do, or do not, interact. The paradigms of Jencks [19,20] have been utilised by several groups in this regard. In particular, two related semi-empirical approaches have been independently developed by the groups of Andrews [21], a “back of the envelope” approach to the prediction of ligand–receptor binding constants, and Williams [22–24], a detailed factorisation of the energetic contributions to binding. These approaches attempt to define the physical terms which govern a binding (recognition) event. The general thermodynamic treatment developed by Williams, equation (1), is the more instructive in this regard, and can be utilised as a basis for better understanding the recognition events that give rise both to the imprinting effect during MIP synthesis and to ligand–MIP binding events, as has been described in a series of recent papers [25–27].



$$\Delta G_{\text{bind}} = \Delta G_{\text{t+r}} + \Delta G_{\text{r}} + \Delta G_{\text{h}} + \Delta G_{\text{vib}} + \Sigma \Delta G_{\text{p}} + \Delta G_{\text{conf}} + \Delta G_{\text{vdW}} \quad (1)$$

where the Gibbs free energy changes are:  $\Delta G_{\text{bind}}$ , complex formation;  $\Delta G_{\text{t+r}}$ , translational and rotational;  $\Delta G_{\text{r}}$ , restriction of rotors upon complexation;  $\Delta G_{\text{h}}$ , hydrophobic interactions;  $\Delta G_{\text{vib}}$  residual soft vibrational modes;  $\Sigma \Delta G_{\text{p}}$ , the sum of interacting polar group contributions;  $\Delta G_{\text{conf}}$ , adverse conformational changes; and  $\Delta G_{\text{vdW}}$ , unfavourable van der Waals' interactions.

Although molecular imprinting is conceptually elegant in its simplicity, as reflected in the *highly schematic representations of the imprinting process* depicted in many papers, the molecular level events taking place in the polymerisation mixture are very complex. A vast range of variables play a role in determining the success, or otherwise, of a polymerisation. The basis for the molecular memory of MIPs lies in the formation of template–functional monomer solution adducts in the pre-polymerisation reaction mixture. The relative strengths of these interactions range from weak van der Waals' forces to reversible covalent bonds. The position of the equilibrium for formation of self-assembled solution adducts between templates and attendant monomers,  $\Delta G_{\text{bind}}$ , determines the number of resultant sites and degree of receptor site heterogeneity. The more stable and regular the template–functional monomer complex, the greater the number, and fidelity, of resultant MIP receptors. The extent of “optimal” template coordination by functional monomer is dependent upon the nature of each of the chemical components present in the polymerisation mixture, and upon the physical environment (temperature and pressure). The relative strengths of monomer(s)–monomer(s), template–template, solvent–template, and solvent–monomer(s) interactions influence the extent and quality of functional monomer–template interactions, which in turn govern the quality of the resultant receptor population. In cases utilising reversible covalent functional monomer–template interactions, complex stability is guaranteed, though the shape-complementarity arising from the cross-linking monomer is controlled by non-covalent processes.

It is interesting to note that although apparently unaware of the development of molecular imprinting, Pande *et al.* [28] proposed the use of thermodynamic control for the preparation of synthetic polymer systems with a memory for a template structure. Monte Carlo computer simulations were performed to validate their hypothesis. From these calculations they identified the formation of non-random polymer sequences arising from an evolution-like *preferred selection* of various monomer components by similar species. These studies have since been expanded upon using statistical mechanics to examine the consequences for protein folding [29].

Direct evidence for the formation of non-covalent monomer–template interactions, the extent of which is reflected in the total binding term,  $\Delta G_{\text{bind}}$ , was first presented in an elegant NMR study by Sellergren *et al.* [30]. In this seminal study, a combination of line-broadening and chemical shift arguments was used by the authors to establish the formation of functional monomer (methacrylic acid)–template (phenylalanine anilide (PA)) complexes. Their results also suggested the minor presence of template self-association and higher order complexes.

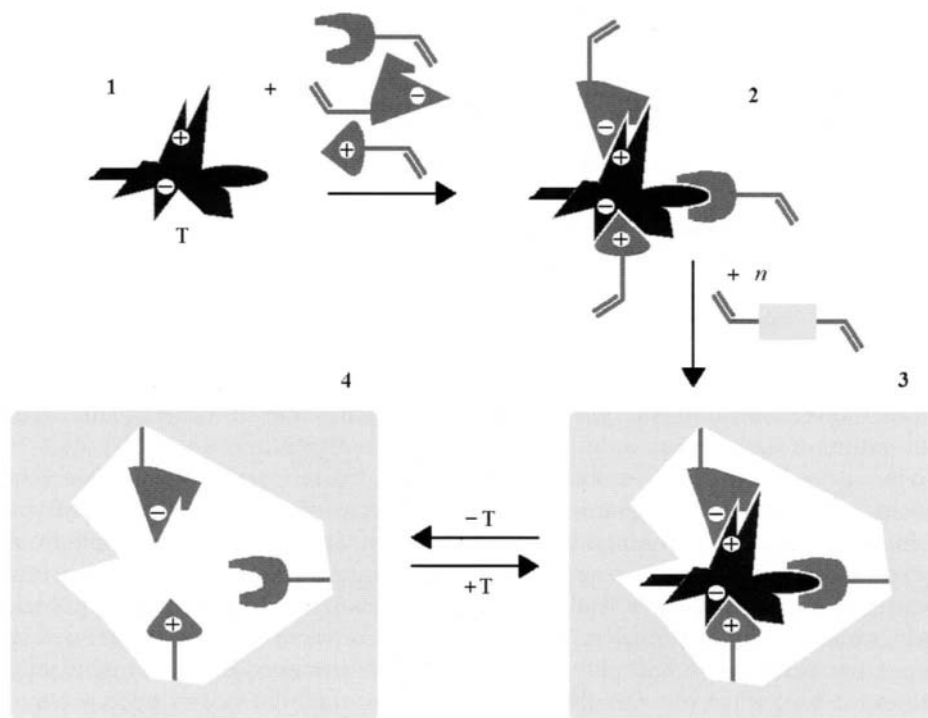


Fig. 3.1. A highly schematic representation of the molecular imprinting process. A monomer mixture with chemical functionality complementary to that of the template is allowed to form solution adducts through the complementary interacting functionalities (reversible covalent or non-covalent interactions). Polymerisation in the presence of a cross-linking agent, followed by removal of the template, leads to the defining of recognition sites of complementary steric and functional topography to the template molecule.

More recently, a UV titration approach has been used to calculate the dissociation constants for the solution adducts and the relative concentration of fully complexed template in the polymerisation mixture [31]. Although the concentration ranges accessible with UV studies are often below those used in standard imprinting polymerisation techniques, the identification of complex formation, or otherwise, is a useful tool. This approach was also used to verify the inert nature of the cross-linking agent ethylene glycol dimethacrylate and for the screening of candidate functional monomers [32]. A similar approach was adopted by Whitcombe *et al.* [33], where NMR chemical shift studies allowed the calculation of dissociation constants and a potential means for predicting the binding capacities of MIPs. The NMR characterisation of functional monomer–template interactions has also been applied to the study of the interaction of 2,6-bis(acrylamido)pyridine and barbiturates [34], and of 2-aminopyridine and methacrylic acid [35].

The position of the equilibrium between free template–monomer(s) and their corresponding complexes is a product of both temperature and pressure. Lower

temperatures of polymerisation can be used advantageously for the preparation of electrostatic interaction-based MIPs, as demonstrated by O'Shannessy *et al.* [36], though elevated temperatures (120°C) were shown by Sellergren and Shea [37] to yield polymers with improved performance characteristics. In this latter study, the influence of porogen (solvent of polymerisation) on template–monomer complexes was also addressed in conjunction with the morphology and properties, temperature stability and swelling capacity, of the resultant polymers. Recently the Sellergren group showed that high pressure (1000 bar) polymerisation can be used to enhance the selectivity of the resultant imprinted polymers [38]. However, the influence of pressure and temperature effects on the polymerisation process (e.g. reaction rate) and polymer structure (e.g. pore structure and swelling properties) make the drawing of direct conclusions regarding their influence on the mechanisms of complex formation difficult. This is made even harder due to the template dependent nature of the pressure induced selectivity enhancement.

The use of non-covalent interactions for molecular imprinting is inherently limited by the stability constant(s) for the formation of solution adducts. Moving to higher functional monomer–template ratios, in order to push the equilibrium towards complex formation, leads to increased numbers of randomly oriented functional groups, which in turn lead to increased levels of non-specific binding. Much lower ratios, a non-imprinted polymer being the extreme case, lead to lower site population densities in the polymer. However, many more detailed optimisation studies are warranted in order to better understand the influence of polymerisation mixture composition on template complexation, and thus polymer recognition characteristics. That we still have much to learn regarding polymer optimisation is reflected in the results from a study by Mayes & Lowe [39]. Here they demonstrated that the quality and number of high affinity morphine selective sites is of the same order of magnitude in polymers prepared using only 2% of the template concentration as in polymers prepared using *standard* protocols [40]. These results have been supported by another recent paper utilising unusual polymerisation mixture compositions, where the Mosbach group have described the synthesis of imprinted microspheres with binding parameters superior to conventional imprinted particles [41]. The utility of this development for expediting polymer synthesis, and the potential of this new imprinted polymer format in a range of application areas is exciting.

The  $\Delta G_{t+r}$  term in equation (1) reflects the change in translational and rotational Gibbs free energy associated with combining two or more free entities in a complex, a process which is entropically unfavourable. This term carries implications for the order (number of components) of complexes that may be formed. It can be stated that functional monomer systems capable of simultaneous interactions of correct geometry, relative to multiple single point interacting monomers, should yield higher concentrations of complexed template, due to a reduction in the adverse loss of translational and rotational free energy, an entropically unfavourable process. From a semantic perspective, the use of multiple coordinating monomers in molecular imprinting lies between the concepts of traditional non-covalent molecular imprinting (mono-dentate monomers) and supramolecular

chemistry. A number of examples of the application of multiple functional monomer–template interactions have recently appeared [34,42–44].

The selectivities observed for MIPs prepared with rigid templates are superior to those of less rigid structures, which is a direct consequence of  $\Delta G_r$ . The origin of this effect lies in the fact that the more rigid the structure, the lower the number of possible solution conformations and thus solution complexes. This in turn renders a narrower site distribution in the resultant polymer. This is supported by the observation that the highest MIP–ligand affinities thus far observed have been for rigid templates such as the alkaloids morphine [40] and yohimbine [45]. This is further underscored by the affinity of the morphine MIP for its template being superior to that of the opioid receptor binding neuropeptide leucine enkephalin for an enkephalin-imprinted polymer, even though the peptide has a greater number of potential electrostatic interaction points.

The number and relative strengths of different template–functional monomer interactions, as given by the  $\Sigma\Delta G_p$  term, dictates the degree of selectivity of the resultant polymer [46]. In terms of electrostatic interactions, several reports have been made of enhanced selectivity through the use of more strongly interacting functional monomers which favour template–monomer complex stability. The Takeuchi group has presented a series of studies using trifluoromethylacrylic acid as a functional monomer [47–50], and demonstrated that it can be used to augment template recognition. The lower  $pK_a$  of this monomer enhances ion pairing and ion–dipole interactions.

The use of metal ion coordination of templates has been shown to be advantageous in a number of studies. The possibility of multiple interactions with the template, in conjunction with the greater relative strengths of template–metal ion interactions, lends to their use in highly polar solvents, such as methanol, as exemplified by work from the Arnold group in a study using Cu(II) coordination of imidazole containing templates [51]. In work by the Murray group, the coordination and luminescent properties of Eu(III) have been used to selectively bind hydrolysis products from the nerve agent Soman [52], and Pb(II) selective matrices have been prepared and evaluated [53]. Metal ions have also featured in a series of papers describing MIPs with catalytic activities, where their capacity to engage in multiple simultaneous interactions is used to coordinate reacting groups Co(II) [54–56] and Ti(IV) [57].

The vast majority of MIPs reported to date have described the use of organic (non-polar) solvent soluble templates and polymer systems, and their evaluation in organic (non-polar) solvent systems. The often impressive ligand selectivities obtained are a reflection of the strengths of electrostatic interactions in non-polar media. Nonetheless, for many potential applications, in particular those of an environmental or biomedical nature, the templates of interest, e.g. peptides, proteins, oligonucleotides, sugars, are often incompatible with such polymerisation media. Another option when using water as the solvent of polymerisation is the use of hydrophobic moiety selective functional monomers, which can contribute to solution adduct formation through the hydrophobic effect, the contribution of which is reflected in the  $\Delta G_h$  term of equation (1). Alternatively, functional

monomers capable of sustaining electrostatic interactions at such high polarities, e.g. metal ion chelation can be employed, as discussed above. With this in mind, a number of groups have been working towards the development of water-compatible polymer systems for use in molecular imprinting.

The groups of Nicholls and Sreenivasan have independently developed cyclodextrin-based functional monomers as a general approach to imprinting in water [58–60]. These polymer systems have been effectively applied to the imprinting of steroids [60] and organic solvent insoluble species, in particular amino acids [58,59]. Another, quite unique, approach has been the use of crown ethers to solubilise highly polar, e.g. *zwitterionic*, species at low polarities [61]. This work, by Andersson and Ramström, provides an interesting basis for further studies, in particular through the use of polymerisable crown ether derivatives.

In relation to the other terms described in equation (1), the extent to which soft vibrational modes,  $\Delta G_{\text{vib}}$ , contribute to solution adduct homogeneity is a direct product of the temperature employed for the polymerisation process. The conformational,  $\Delta G_{\text{conf}}$ , and van der Waal's,  $\Delta G_{\text{vdW}}$ , energy terms in equation (1) reflect the need for compromise of template conformation and effective solvation in order to form solution adducts. Determination of the significance of these terms can be made using molecular modelling.

To summarise, each of the thermodynamic terms contributing to the stability and uniformity of the solution adducts formed during the molecular imprinting pre-arrangement process play a role in determining  $\Delta G_{\text{bind}}$ . How these terms influence the non-covalent MIP–ligand recognition will be discussed in the following section.

It can be concluded that the exclusive use of non-covalent template–functional monomer interactions is inherently limited by the stabilities of the template–functional monomer complexes. The subsequent heterogeneity of the template selective recognition sites, their polyclonal nature, is a direct consequence of the extent of template complexation. A small number of studies have attempted to combine the versatility of non-covalent interaction-based molecular imprinting with the benefits afforded by the constraint of functional monomer and template through reversible covalent bonds [62–65]. This approach, although requiring the synthesis of template derivatives, offers much scope for enhancing the fidelity of template selective recognition sites.

### 3.3. PHYSICAL PRINCIPLES UNDERLYING MIP–LIGAND RECOGNITION

Although the thermodynamic terms derived from equation (1) can also be used to shed light on the recognition of an analyte by a MIP, solvent–analyte, analyte–analyte interactions and macroscopic effects (e.g. solvent and analyte diffusion rates and surface areas) also play a critical role in determining the binding characteristics of a polymer and its suitability for use in a given application. Unfortunately, very little in the way of direct physical analysis of polymer bound ligand has been reported, though a study by the group of Shea using solid state NMR techniques deserves special mention [66].

In terms of ligand binding to a MIP recognition site, the conformational,  $\Delta G_{\text{conf}}$ , and van der Waals',  $\Delta G_{\text{vdw}}$ , energy terms in equation (1) reflect the need for compromise of template conformation and degree of effective solvation, so long as rebinding takes place in the polymerisation solvent. As both the pre-arrangement phase and ligand rebinding are under thermodynamic control, we may assume that the template population will not possess, on average, conformational strain, nor adverse van der Waals' interactions. This statement relates to the central dogma of molecular imprinting, namely that the solution adducts are reflected in the recognition sites presented in the bulk polymer. Thus for the study of template rebinding equation (1) can be simplified (equation (2)).

$$\Delta G_{\text{bind}} = \Delta G_{\text{t+r}} + \Delta G_{\text{r}} + \Delta G_{\text{h}} + \Delta G_{\text{vib}} + \Sigma \Delta G_{\text{p}} \quad (2)$$

In terms of the thermodynamics of MIP–ligand binding, the rigidity of templates contributed to the fidelity of the resultant receptor site populations. The binding of a ligand to a MIP recognition site is governed by the same thermodynamic constraints. Thus, all other factors being equal, a more flexible ligand will incur a larger energetic (entropic) penalty,  $\Delta G_{\text{r}}$ , in order to bind (5–6 kJ mol<sup>-1</sup>, i.e. one order of magnitude in terms of binding constant).

The role of electrostatic interactions,  $\Sigma \Delta G_{\text{p}}$ , on ligand recognition has been examined through the study of the influence of solvent polarity on MIP–ligand selectivity and by using template analogues. By examining enantiomer capacity factors and MIP enantioselectivity as a function of eluent water content, the relative strength of non-covalent electrostatic interactions has been studied in methacrylic acid–ethylene glycol dimethacrylate [67]. The inclusion of increasing amounts of water in the eluent has a more profound effect upon the capacity factor for the imprinted enantiomer than its antipode. This was interpreted in terms of the greater involvement of hydrogen bonding modes in specific template recognition than in non-specific binding modes. Other studies by the Mosbach group using acrylamide MIPs [68–70] demonstrated similar effects and, in addition, a contribution from hydrophobic interactions was observed, as the ligand solubilities allowed study at high water concentrations, up to 70% in acetonitrile. In the latter study [70], it was shown that polymer performance improved at higher ionic strength, though the influence of aqueous solvent ionic strength on the swelling characteristics of polymers of this type remains to be examined. This approach has also been utilised to examine the relative contribution of ionic and hydrophobic interactions on MIP–ligand interactions in a Tröger's Base MIP [71], the first example of synthetic receptors for a substances containing chiral nitrogen centres.

The presence of water, as described above, is adverse with respect to electrostatic interactions, though it is conducive to hydrophobic interactions. The group of Lars I. Andersson has undertaken a series of thorough studies on the application of MIPs prepared in organic solvents for binding studies in aqueous environments [40,72,73]. Through careful optimisation of ligand binding studies it is possible to enhance, in some cases, the polymer selectivities. Most interestingly, converse effects have been reported when using organic solvents on polymers imprinted in water [58,59]. Thus, when a combination of hydrophobic and

electrostatic interacting functional monomers is employed, a balance of entropically motivated hydrophobic effect interactions and enthalpically driven electrostatic interactions is necessary for optimal binding. As more polar environments lead to a weakening of electrostatic interactions and less polar environments a weakening of the hydrophobic effect, a balance of these leads to entropy–enthalpy compensation effects. This phenomenon has also been used for the development of synthetic receptor binding assays for herbicides by the Mosbach group [74,75], where they demonstrated that imprinting in vinyl pyridine–ethylene glycol dimethacrylate copolymers was possible in methanol containing 20% water.

Although molecular level studies of MIP–ligand interactions are scarce, a number of significant quantitative and semi-quantitative chromatographic analyses of MIP–ligand binding phenomena have been presented, which have helped to shed light on the mechanisms of ligand–MIP binding and augment the information derived from ligand binding data. In one such study Sellergren and Shea [76] extensively examined the influence of pH, temperature and polymer heat treatment on chromatographic response. Using the influences of flow rate and sample loading on peak asymmetry they identified that non-linear binding adsorption isotherms are associated with the binding of template structures. In addition, the influence of polymer heat treatment on the retention characteristics for enantiomers of PA on an L-enantiomer MIP showed that the retention of the non-imprinted antipode bears resemblance to that of weak cation exchange resins. Furthermore, they demonstrated using variable temperature chromatographic studies that the nature of the mobile phase and its interaction with the solubilised analyte produce marked differences in chromatographic behaviour. Van't Hoff analyses allowed dissection of the entropic and enthalpic contributions to binding under different elution conditions, from which inference to the nature of the solvation state of the analyte and its influence on binding could be drawn. A similar approach has since been adopted by Lin and co-workers in an electrochromatographic study [77].

In another study Sellergren and Shea [78] modelled the chromatographic behaviour of a solute, PA, on imprinted and non-imprinted polymers using a simple cation-exchange model, and were able to describe the behaviour as a function of mobile phase pH. Moreover, the model they proposed was sufficient to explain the differences in selectivity between the two polymers.

In a recent study Sajonz *et al.* [79] have examined in detail the thermodynamics and mass transfer kinetics of the enantiomers of PA on a PA-imprinted polymer using staircase frontal analysis. The adsorption data for both enantiomers were fitted to both Freundlich and bi-Langmuir isotherms, the former being indicative of higher template solvation states. They characterised the concentration and enantiomer dependence of the mass flow properties that led to the identification of a low concentration of very high affinity (nM) sites. This case provides a good example of how physical chemical studies of ligand binding behaviour can yield information regarding the polymer micro-environment.

The role of template–template self-association in molecular imprinting was the subject of extensive debate during the early work with silica-based systems [1]. Its involvement in organic polymer imprinting has, however, attracted much less

attention, though Sellergren *et al.* have observed evidence for a minor component of template–template self-association in NMR studies of PA–methacrylic acid pre-polymerisation mixtures [30]. Recently, Andersson *et al.* [80] observed chromatographic responses indicative of the presence of higher order template complex binding sites in the study of a series of (–)-nicotine-imprinted polymers prepared with varying amounts of template (up to 10 M). They observed that higher sample loadings resulted in longer retention times and increases in MIP enantioselectivity representative of those of cooperative binding phenomena in earlier affinity chromatographic studies [81]. The results suggest the presence of sites selective for template–template complexes, which in turn indicate their presence in the polymerisation mixture. Although a self-association model best suited the results obtained with some of the polymers in this study, others were perhaps better explained using the solvation model previously suggested by Sellergren [79]. Nonetheless, although the extent to which template solvation and self-association/cooperative processes contribute to MIP–ligand binding is undoubtedly system dependent, thus neither mechanism can be disregarded. Consequently, these factors should be taken into consideration when examining MIP preparation and MIP–ligand binding (Fig. 3.2).

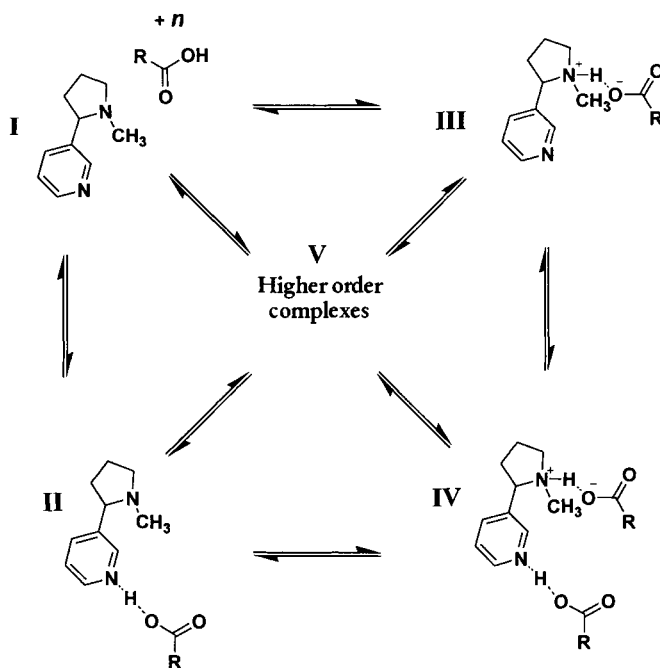


Fig. 3.2. A schematic representation of the molecular imprinting pre-arrangement phase (corresponding to 2 in Fig. 3.1), here using (–)-nicotine as the template and carboxylic acid containing functional monomers. In this case a total of five states of complexation are proposed: I, non-complexed template; II, weak single point interaction; III, strong single point interaction; IV, combination of weak and strong interactions; V, higher order complexes e.g. monomer interactions with template–template self-association complexes, higher monomer solvation levels.



### 3.4. CONCLUSIONS

In conclusion, the thermodynamic factorisation presented here provides a basis for identifying the physical factors significant for interpretation of the molecular imprinting process, and MIP–ligand binding. Together with an understanding of the macroscopic properties associated with polymer performance one can begin to talk of *rational* polymer design for a specific end use. Collectively, the efforts from many laboratories underscore the significance of the general conclusions presented.

Although much progress has been made towards the development of a better understanding of the mechanisms underlying molecular imprinting, much remains to be understood. Without doubt, there is much valuable information to be obtained from thermodynamic and spectroscopic studies of the self-assembly, polymerisation and MIP–ligand binding processes.

### ACKNOWLEDGEMENTS

We thank our co-workers, Dr Börje Sellergren, Dr Lars I. Andersson and Dr Andrew G. Mayes for valuable advice and discussions. The financial support of the Swedish Engineering Sciences Research Council (TFR), Carl Tryggers Stiftelsen and the Crafoord Stiftelsen are most willingly acknowledged.

### REFERENCES

- 1 H.S. Andersson and I.A. Nicholls, In: *Molecularly imprinted polymers. Man made mimics of antibodies and their application in analytical chemistry*, B. Sellergren Ed., Elsevier (2000).
- 2 K. Haupt and K. Mosbach, *Trends Biotechnol.*, **16**, 468 (1998).
- 3 G. Wulff, *Chemtech*, **28**, 19 (1998).
- 4 H.S. Andersson and I.A. Nicholls, *Recent Res. Develop. Pure Appl. Chem.*, **1**, 133 (1997).
- 5 A.G. Mayes and K. Mosbach, *Trends Anal. Chem.*, **16**, 321 (1997).
- 6 B. Sellergren, *Amer. Laboratory*, **29**, 14 (1997).
- 7 B. Sellergren, *Trends Anal. Chem.*, **16**, 310 (1997).
- 8 M.J. Whitcombe, C. Alexander and E.N. Vulfson, *Trends Food. Sci. Technol.*, **8**, 140 (1997).
- 9 R.J. Ansell, O. Ramström and K. Mosbach, *Clin. Chem.*, **42**, 1506 (1996).
- 10 K. Mosbach and O. Ramström, *Bio/Technology*, **14**, 163 (1996).
- 11 M.T. Muldoon and L.H. Stanker, *Chem. Ind.*, **18**, 204 (1996).
- 12 T. Takeuchi and J. Matsui, *Acta Polymerica*, **47**, 471 (1996).
- 13 M. Kempe and K. Mosbach, *J. Chromatogr. A*, **694**, 3 (1995).
- 14 I.A. Nicholls, L.I. Andersson, K. Mosbach and B. Ekberg, *Trends Biotechnol.*, **13**, 47 (1995).
- 15 J. Steinke, D.C. Sherrington and I.R. Dunkin, *Adv. Polym. Sci.*, **123**, 80 (1995).
- 16 S. Vidyasankar and F.H. Arnold, *Curr. Opin. Biotechnol.*, **6**, 218 (1995).
- 17 G. Wulff, *Angew. Chem. Int. Ed. Engl.*, **34**, 1812 (1995).
- 18 K.J. Shea, *Trends Polym. Sci.*, **2**, 16 (1994).

- 19 M.I. Page and W.P. Jencks, *Proc. Natl. Acad. Sci. USA*, **68**, 1678 (1971).
- 20 W.P. Jencks, *Adv. Enzymol.*, **43**, 219 (1975).
- 21 P.R. Andrews, D.J. Craik and J.L. Martin, *J. Med. Chem.*, **27**, 1648 (1984).
- 22 D.H. Williams, J.P.L. Cox, A.J. Doig, M. Gardner, U. Gerhard, P.T. Kaye, A.R. Lal, I.A. Nicholls, C.J. Salter and R.C. Mitchell, *J. Am. Chem. Soc.*, **113**, 7020 (1991).
- 23 M. Searle, D.H. Williams and U. Gerhard, *J. Am. Chem. Soc.*, **114**, 10,704 (1992).
- 24 S.E. Holroyd, P. Groves, M.S. Searle, U. Gerhard and D.H. Williams, *Tetrahedron*, **49**, 9171 (1993).
- 25 I.A. Nicholls, *Chem. Lett.*, 1035 (1995).
- 26 I.A. Nicholls, *Adv. Molec. Cell Biol.*, **15**, 667 (1996).
- 27 I.A. Nicholls, *J. Molec. Recogn.*, **11**, 79 (1998).
- 28 V.S. Pande, A.Y. Grosberg and T. Tanaka, *Proc. Natl. Acad. Sci. USA*, **91**, 12,976 (1994).
- 29 T. Tanaka, T. Enoki, A.Y. Grosberg, S. Masamune, T. Oya, Y. Takaoka, K. Tanaka, C.N. Wang and G.Q. Wang, *Ber. Bunsen Ges. Phys. Chem.*, **102**, 1529 (1998).
- 30 B. Sellergren, M. Lepistö and K. Mosbach, *J. Am. Chem. Soc.*, **110**, 5853 (1988).
- 31 H.S. Andersson and I.A. Nicholls, *Bioorg. Chem.*, **25**, 203 (1997).
- 32 J. Svenson, H.S. Andersson, S.A. Piletsky and I.A. Nicholls, *J. Molec. Recogn.*, **11**, 83 (1998).
- 33 M.J. Whitcombe, L. Martin and E.N. Vulfson, *Chromatographia*, **47**, 457 (1998).
- 34 K. Tanabe, T. Takeuchi, J. Matsui, K. Ikebukuro, K. Yano and I. Karube, *J. Chem. Soc., Chem. Comm.*, 2303 (1995).
- 35 Z. Jie and H. Xiwen, *Anal. Chim. Acta*, **381**, 85 (1999).
- 36 D.J. O'Shannessy, B. Ekberg and K. Mosbach, *Anal. Biochem.*, **177**, 144 (1989).
- 37 B. Sellergren and K.J. Shea, *J. Chromatogr.*, **635**, 31 (1993).
- 38 B. Sellergren, C. Dauwe and T. Schneider, *Macromolecules*, **30**, 2454 (1997).
- 39 A. Mayes and C.R. Lowe, In: *Methodological surveys in bioanalysis of drugs*, vol. 25, E. Reid, H.M. Hill and I.D. Wilson Eds, Royal Society of Chemistry, Cambridge, p. 28 (1998).
- 40 L.I. Andersson, R. Müller, G. Vlatakis and K. Mosbach, *Proc. Natl. Acad. Sci. USA*, **92**, 4788 (1995).
- 41 L. Ye, P.A.G. Cormack and K. Mosbach, *Anal. Commun.*, **36**, 35 (1999).
- 42 L. Fischer, R. Müller, B. Ekberg and K. Mosbach, *J. Am. Chem. Soc.*, **113**, 9358 (1991).
- 43 G. Wulff, T. Gross and R. Schönfeld, *Angew. Chem. Int. Ed. Engl.*, **36**, 1962 (1997).
- 44 M. Knutsson, H.S. Andersson and I.A. Nicholls, *J. Molec. Recogn.*, **11**, 87 (1998).
- 45 J. Berglund, I.A. Nicholls, C. Lindbladh and K. Mosbach, *Bioorg. Med. Chem. Lett.*, **6**, 2237 (1996).
- 46 H.S. Andersson, A.-C. Koch-Schmidt, S. Ohlson and K. Mosbach, *J. Mol. Recogn.*, **9**, 675 (1996).
- 47 J. Matsui, Y. Miyoshi and T. Takeuchi, *Chem. Lett.*, 1007 (1995).
- 48 J. Matsui, I.A. Nicholls and T. Takeuchi, *Tetrahedron: Asymmetry*, **7**, 1357 (1996).
- 49 J. Matsui, O. Doblhoff Dier and T. Takeuchi, *Anal. Chim. Acta*, **343**, 1 (1997).
- 50 J. Matsui and T. Takeuchi, *Anal. Commun.*, **34**, 199 (1997).
- 51 S. Vidyasankar, P.K. Dhal, S.D. Plunkett and F.H. Arnold, *Biotechnol. Bioengn.*, **48**, 431 (1995).
- 52 A.L. Jenkins, O.M. Uy and G.M. Murray, *Anal. Chem.*, **71**, 373 (1999).
- 53 X.F. Zeng and G.M. Murray, *Sep. Sci. Technol.*, **31**, 2403 (1996).
- 54 A. Leonhardt and K. Mosbach, *React. Polym.*, **6**, 285 (1987).
- 55 J. Matsui, I.A. Nicholls, I. Karube and K. Mosbach, *J. Org. Chem.*, **61**, 5414 (1996).
- 56 J. Matsui, I.A. Nicholls, T. Takeuchi, K. Mosbach and I. Karube, *Anal. Chim. Acta*, **335**, 71 (1996).
- 57 B.P. Santora, A.O. Larsen and M.R. Gagne, *Organometallics*, **17**, 3138 (1998).
- 58 S.A. Piletsky, H.S. Andersson and I.A. Nicholls, *J. Molec. Recogn.*, **11**, 94 (1998).
- 59 S.A. Piletsky, H.S. Andersson and I.A. Nicholls, *Macromolecules*, **32**, 633 (1999).

- 60 K. Sreenivasan, *Appl. Polym. Sci.*, **70**, 15 (1998).
- 61 H.S. Andersson and O. Ramström, *J. Mol. Recogn.*, **11**, 103 (1998).
- 62 B. Sellergren and L. Andersson, *J. Org. Chem.*, **55**, 3381 (1990).
- 63 S.E. Byström, A. Börje and B. Åkermark, *J. Am. Chem. Soc.*, **115**, 2081 (1993).
- 64 M.J. Whitcombe, M.E. Rodriguez, P. Villar and E.N. Vulfson, *J. Am. Chem. Soc.*, **117**, 7105 (1995).
- 65 M. Lübke, M.J. Whitcombe and E.N. Vulfson, *J. Am. Chem. Soc.*, **120**, 13,342 (1998).
- 66 K.J. Shea and D.Y. Sasaki, *J. Am. Chem. Soc.*, **113**, 4109 (1991).
- 67 I.A. Nicholls, O. Ramström and K. Mosbach, *J. Chromatogr. A*, **691**, 349 (1995).
- 68 C. Yu and K. Mosbach, *J. Org. Chem.*, **62**, 4057 (1997).
- 69 C. Yu and K. Mosbach, *J. Mol. Recogn.*, **11**, 69 (1998).
- 70 C. Yu, O. Ramström and K. Mosbach, *Anal. Lett.*, **30**, 2123 (1997).
- 71 K. Adbo, H.S. Andersson, J. Ankarloo, J.G. Karlsson, M.C. Norell, L. Olofsson, J. Svenson, U. Örtengren and I.A. Nicholls, *Bioorg. Chem.*, **27**, 363 (1999).
- 72 L.I. Andersson, *Anal. Chem.*, **68**, 111 (1996).
- 73 L.I. Andersson, R. Müller and K. Mosbach, *Macromol. Res. Comm.*, **17**, 65 (1996).
- 74 K. Haupt, A. Dzgoev and K. Mosbach, *Anal. Chem.*, **70**, 628 (1998).
- 75 K. Haupt, A.G. Mayes and K. Mosbach, *Anal. Chem.*, **70**, 3936 (1998).
- 76 B. Sellergren and K.J. Shea, *J. Chromatogr. A*, **690**, 29 (1995).
- 77 J.M. Lin, T. Nakagama, K. Uchiyama and T. Hobo, *Biomed. Chromatogr.*, **11**, 298 (1997).
- 78 B. Sellergren and K.J. Shea, *J. Chromatogr. A*, **654**, 17 (1993).
- 79 P. Sajonz, M. Kele, G.M. Zhong, B. Sellergren and G. Guiochon, *J. Chromatogr. A*, **810**, 1 (1998).
- 80 H.S. Andersson, J.G. Karlsson, S.A. Piletsky, A.-C. Koch-Schmidt, K. Mosbach and I.A. Nicholls, *J. Chromatogr. A*, **848**, 39 (1999).
- 81 P. Cuatrecasas, M. Wilchek and C.B. Anfinsen, *Proc. Natl. Acad. Sci. USA*, **61**, 636 (1968).

## Molecular imprinting with covalent or stoichiometric non-covalent interactions

GÜNTER WULFF AND ANDREA BIFFIS

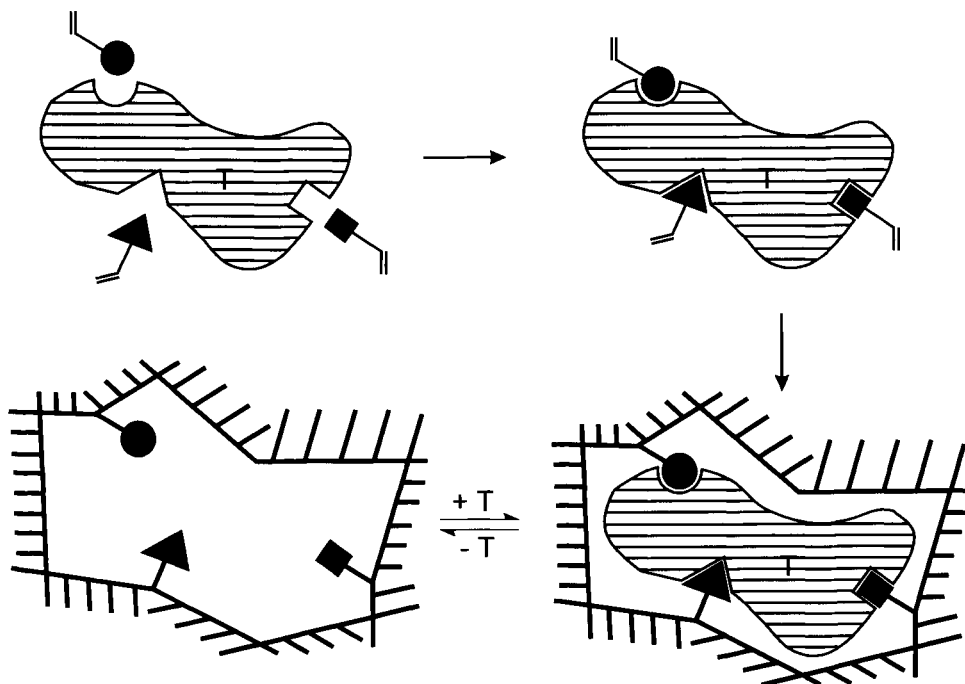
### 4.1. INTRODUCTION

Molecular imprinting in synthetic polymers was reported for the first time in 1972 [1–4]. The initial idea was to obtain in the polymer highly specific binding clefts with a predetermined size, shape and three-dimensional arrangement of functional groups. Later on, further experiments demonstrated that such functionalised cavities could be tailored to mimic the active sites of enzymes (“enzyme analogue built polymer”).

The molecular imprinting procedure is generally based on the linkage of suitable monomers containing functional groups (binding site monomers) to template molecules by covalent (later also non-covalent) interactions. Subsequent copolymerisation of the resulting template monomer assembly with an excess of a cross-linking agent in the presence of a porogenic solvent produces rigid macroporous polymers. Removal of the template molecules (see Scheme 4.1) leaves behind cavities in the polymer whose size, shape and three-dimensional arrangement of binding sites are determined by the structure of the template molecules.

In the earlier years of molecular imprinting, the development of the basic concepts and the optimisation of the imprinted polymer structure were undertaken using almost exclusively covalent interactions [6]. Later on, non-covalent interactions (e.g. electrostatic or hydrogen bonding) became attractive since they are usually more easily employed [7–9]. However, when covalent interactions are used, the binding site monomers can be employed in the exact stoichiometric ratio to the template molecule, whereas with non-covalent interactions the binding constants are generally rather low so that the imprinting procedure requires the binding site monomers to be present in large excess. In this way, the binding sites in the resulting polymer are not exclusively located inside the cavities; this represents a considerable drawback, especially for catalytic applications or preparative chromatographic purposes, as we will see in the following sections. Non-covalent interactions can be employed in a stoichiometric fashion only if interactions with very high binding constants ( $K_a = 10^2$ – $10^7$ ) are used. It is interesting to note that at present the most efficient catalytic systems based on imprinted polymers can only be obtained with covalent or stoichiometric non-covalent interactions [10–13].

The imprinting technique resembles the formation of antibodies from haptens. Indeed, an imprinting-like mechanism was formerly postulated for the formation of



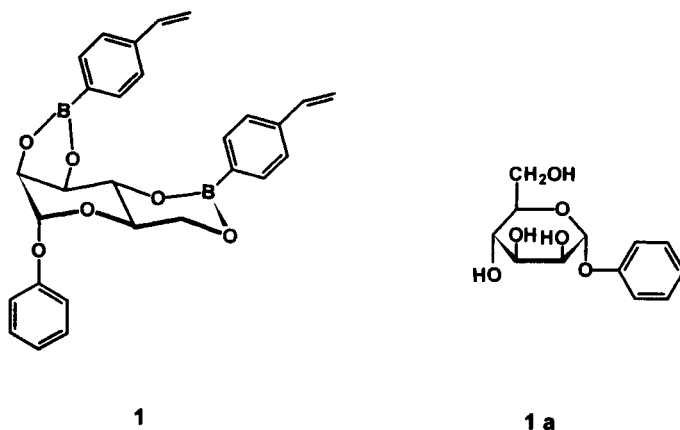
Scheme 4.1. Schematic representation of the imprinting of specific cavities in a cross-linked polymer by a template (T) with three different binding groups [4,5].

antibodies [14]. It is important to remark that the functional groups in the imprinted cavities are located on different polymer chain segments, which are held in a definite mutual orientation simply by cross-links. Thus, the information is not carried by a low-molecular-weight part of the polymer. Instead, the entire arrangement of polymer chains (the topochemistry) is responsible for the molecular recognition. This is reminiscent of the structure of the active centres of enzymes. The relationship between the template and the imprinted cavity corresponds to the key-and-lock principle proposed by Emil Fischer for enzyme catalysis around 100 years ago [15]. The imprinting process has a certain analogy to F.H. Dickey's attempts to imprint silica gel by precipitation in the presence of template molecules [16].

## 4.2. THE CONCEPT OF IMPRINTING

The imprinting procedure can be exemplarily described by considering the polymerisation of the template monomer **1**, which was used for the optimisation of the method [5,17–19]. In this case, phenyl- $\alpha$ -D-mannopyranoside **1a** acts as the template molecule. Two molecules of 4-vinylbenzeneboronic acid (the binding site monomer) are covalently bound by diester linkages to the template. The template monomer

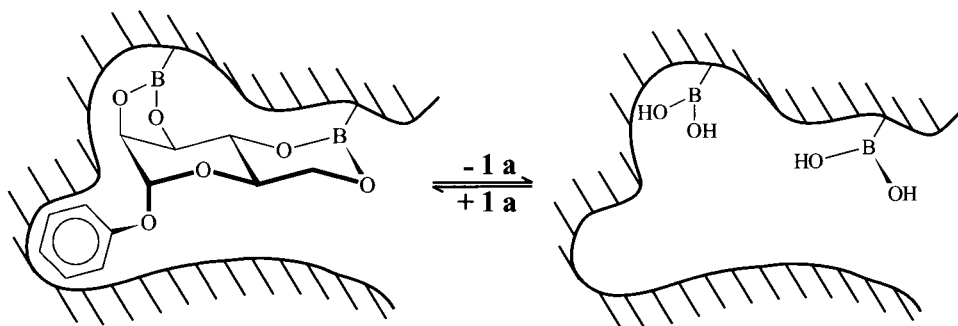
can be copolymerised by free radical initiation in the presence of a porogenic solvent and a large amount of a cross-linking agent. The polymers thus obtained are macroporous, hence they possess a system of permanent pores and a high inner surface area. Such polymers are characterised by a good accessibility through their macropore system as well as by a rather rigid structure with low mobility of the polymer chains.



The template **1a** can be split off by water or methanol to an extent of up to 95% (see Scheme 4.II). The accuracy of the steric arrangement of the binding sites in the resulting imprinted cavity can be tested by the ability of the polymer to resolve the racemate of the template, namely phenyl- $\alpha$ -D,L-mannopyranoside. The polymer was equilibrated in a batch procedure with a solution of the racemate under conditions that allowed a thermodynamically controlled partition of the enantiomers between polymer and solution. The enrichment of the antipodes in the polymer and in solution was determined and the separation factor  $\alpha$ , i.e. the ratio of the distribution coefficients of the D- and L-enantiomer between polymer and solution, was calculated. After extensive optimisation of the procedure,  $\alpha$  values between 3.5 and 6.0 were obtained [4]. This is an extremely high selectivity for racemic resolution that cannot be reached by most other methods.

Polymers obtained by this procedure can be used for the chromatographic separation of the racemates of the corresponding template molecules [4,5,19–22]. The selectivity of the separation process is fairly high (separation factors up to  $\alpha = 4.56$ ), and under particular conditions (high temperatures, gradient elution; see the discussion in Section 4.5.) resolution values of  $R_s = 4.2$  with baseline separation have been obtained (Fig. 4.1). These sorbents can be prepared conveniently and possess excellent thermomechanical stability. Even when used at 80°C under high pressure for a long time, no leakage of the stationary phase or decrease of selectivity during chromatography was observed.

Meanwhile, a large number of different templates has been investigated by us and many other groups in the world (for reviews see [4,8,9,23–26]). An interesting extension of the concept of molecular imprinting was introduced by Mosbach and



Scheme 4.II. Schematic representation of the polymerisation of **1** to obtain a specific cavity. The template **1a** can be removed with water or methanol, leaving behind the free cavity [4].

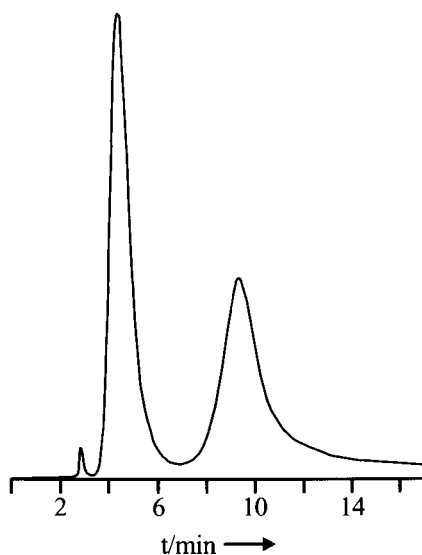


Fig. 4.1. Chromatographic resolution of D,L-**1a** on a polymer imprinted with **1** (elution with a solvent gradient at 90°C) [19].

co-workers [8] who exclusively used non-covalent interactions; this aspect is dealt with in Chapter 5.

### 4.3. THE OPTIMISATION OF THE POLYMER STRUCTURE

The optimisation of the polymer structure proved to be rather complicated. On the one hand, the polymers should be rather rigid to preserve the structure of the cavity after the template is split off. On the other hand, a certain flexibility of the polymer chain is necessary to facilitate the attainment of a fast equilibrium between

release and re-uptake of the template in the cavity. These two properties are contradictory to each other and a careful optimisation has to be performed in all cases. Furthermore, a good accessibility of as many cavities as possible should be guaranteed and a reasonable thermal and mechanical stability is also necessary. Up to now, macroporous polymers have been employed in nearly all cases. Such polymers possess a high inner surface area (100–600 m<sup>2</sup>/g) and show, after optimisation, a good accessibility as well as a satisfactory thermomechanical stability.

The selectivity is mostly influenced by the kind and amount of cross-linking agent employed in the imprinted polymer synthesis. Figure 4.2 shows the dependence of the selectivity on the polymer cross-linking degree in the racemic resolution of the racemate of **1a** with polymers prepared from **1** [17,18]. No selectivity can be observed below a certain amount of cross-linking (around 10%); the cavities are then not sufficiently stabilised. Above 10% cross-linking, a steady increase in selectivity occurs. Between 50 and 66% the increase in selectivity is surprisingly high, especially if ethylene dimethacrylate (EDMA) is used as cross-linker.

In this investigation EDMA appears to be a superior cross-linker compared to *p*-divinylbenzene (*p*-DVB) or butylene dimethacrylate (BDMA). To evaluate other possible cross-linkers, we tested pure *o*-, *p*- and *m*-DVB and a number of dimetha-

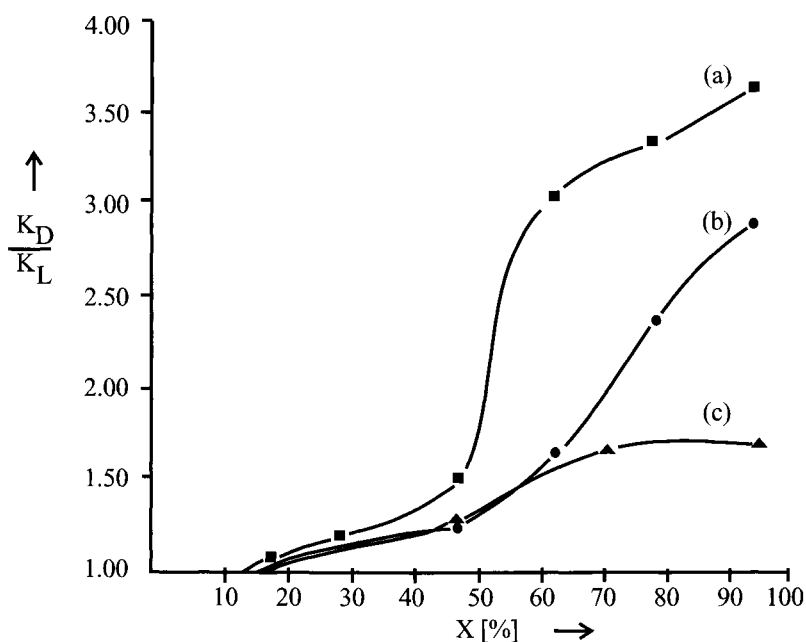
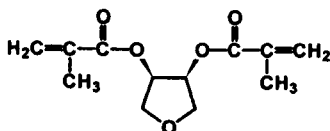


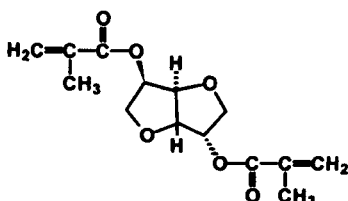
Fig. 4.2. Selectivity of polymers as a function of the type and amount (*X*) of cross-linking agent [17]. The polymers were prepared in the presence of **1** with various proportions of the cross-linking agents; (a) EDMA, (b) tetramethylene dimethacrylate, and (c) DVB. After removal of the template **1a**, the separation factor  $\alpha = K_D/K_L$  was determined for the resolution of D,L-**1a** in a batch process.



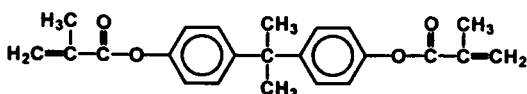
crylates of varying rigidity and flexibility [18]. The obtained polymers were investigated for their properties, i.e. inner surface area, splitting percentage of the template, swellability in methanol and selectivity.



2



3



4

Table 4.1 shows the influence of different cross-linking agents on the properties of the polymers. The swellability of the polymers is an indication of their flexibility. The use of *o*-, *m*- and *p*-DVBs gives only low selectivity; swellability and splitting percentage are also rather unsatisfactory. These cross-linking agents produce highly rigid cavities such that the more specific cavities cannot be freed from the template. EDMA, in contrast, produces cavities which are flexible enough for fast template splitting and rebinding. An even higher flexibility of the cross-linking agent, as in the case of diethylene glycol dimethacrylate (DEGDMA in **P-F** (Table 4.1)) and triethyleneglycol dimethacrylates (TEGDMA in **P-G**), results again in less selective cavities. The use of the new cross-linkers **2** and **3** (**3** is optically active) does not give any additional increase in selectivity compared to EDMA. The same is true for the very rigid cross-linker **4**. Recently, good results have been reported for the trifunctional cross-linker trimethylolpropane trimethacrylate (TRIM) [27,28], but this cross-linker has not been employed to a large extent.

In order to use the stabilising effect of a rather rigid cross-linked polymer in

TABLE 4.1

DEPENDENCE OF THE PROPERTIES OF THE POLYMERS ON THE KIND OF CROSS-LINKING AGENT [18]

| Polymer    | Cross-linking agent | Comonomer | Percentage of cross-linking (%) | Inner surface area (m <sup>2</sup> /g) | Splitting percentage (%) | Swellability | Separation factor ( $\alpha$ ) |
|------------|---------------------|-----------|---------------------------------|--|--------------------------|--------------|--------------------------------|
| <b>P-A</b> | <i>o</i> -DVB       | Styrene   | 71                              | 348                                    | 49.2                     | 1.45         | 1.64                           |
| <b>P-B</b> | <i>m</i> -DVB       | Styrene   | 71                              | 577                                    | 42.4                     | 1.26         | 1.65                           |
| <b>P-C</b> | <i>p</i> -DVB       | Styrene   | 71                              | 661                                    | 42.2                     | 1.36         | 1.67                           |
| <b>P-D</b> | <i>p</i> -DVB       | —         | 95                              | 825                                    | 41.3                     | 1.27         | 1.70                           |
| <b>P-E</b> | EDMA                | —         | 95                              | 383                                    | 81.7                     | 1.69         | 3.66                           |
| <b>P-F</b> | DEGDMA              | —         | 95                              | 30                                     | 90.0                     | 2.42         | 1.24                           |
| <b>P-G</b> | TEGDMA              | —         | 95                              | n.d.                                   | n.d.                     | 2.71         | 1.41                           |
| <b>P-H</b> | BDMA                | —         | 95                              | 128                                    | 92.3                     | 2.27         | 2.88                           |
| <b>P-I</b> | <b>2</b>            | —         | 95                              | 214                                    | 81.4                     | 2.04         | 2.05                           |
| <b>P-J</b> | <b>3</b>            | —         | 95                              | 344                                    | 77.6                     | 2.28         | 2.68                           |
| <b>P-K</b> | <b>4</b>            | —         | 95                              | 339                                    | 86.5                     | 1.96         | 1.78                           |

In all cases, 5% of **1**, the cross-linking agent, and (sometimes) additional monomer were copolymerised radically in the inert solvent mixture acetonitrile/benzene 1:1 (1 g of monomer mixture/1 mL of solvent mixture). Swellability: ratio of the specific gel bed volume to the bulk volume. Splitting percentage: percentage of templates that could be split off.

combination with a more flexible one, we prepared interpenetrating networks [18]. The best polymer in this investigation consisted of a mother polymer from **1** and EDMA with a relatively large inner pore volume. After template removal, this unmodified polymer showed a separation factor  $\alpha = 2.68$ . The polymer that still contained the template was swollen with a solution of technical grade DVB and polymerised once more. The second polymerisation was expected to stabilise the more flexible initial structure without affecting the kinetic exchange. The selectivity was somewhat higher ( $\alpha = 2.81$ ), but the splitting percentage was considerably lower than for the macroporous polymer **P-E**.

There is a strong influence of the nature of the porogenic solvent used during polymerisation on the polymer structure [6], but the influence on the selectivity is astonishingly low (see Table 4.2). A strong influence on the selectivity is observed if the amount of porogenic solvent during polymerisation is changed from 0.29 up to 1.76 mL/g monomer mixture, the optimum being around 1.0 [29].

Apart from a high selectivity, the polymers should possess some flexibility to improve the rate of the reversible binding of the template within the cavities. Cavities of accurate shape but without any flexibility present a kinetic hindrance to reversible binding. In order to obtain a fast attainment of equilibrium during batch or chromatographic separations, the amount of cross-linking agent needs to be reduced. Thus, a balance between selectivity and good kinetic behaviour must be reached [30].

Polymers obtained with EDMA as cross-linker retained their selectivity for a long period. Even under high pressure in an HPLC column, the selectivity remained unchanged for months. This was true even when the column was used at 70–80°C. On the other hand, polymers cross-linked with DVB gradually lost their resolving power at higher temperatures. Interestingly, at 60°C the  $\alpha$  value for racemic resolution increased further to 5.11. Higher selectivity at elevated temperature had already been observed during earlier chromatographic studies [20,21].

TABLE 4.2

DEPENDENCE OF POLYMER PROPERTIES ON THE KIND OF SOLVENT USED<sup>a</sup> [6]

| Polymer      | Solvent                  | Inner surface area (m <sup>2</sup> /g) | Splitting percentage (%) | Separation factor ( $\alpha$ ) |
|--------------|--------------------------|--|--------------------------|--------------------------------|
| <b>P-E a</b> | Acetonitrile/<br>Benzene | 383                                    | 81.7                     | 3.66                           |
| <b>P-E b</b> | Acetonitrile             | 290                                    | 76.6                     | 2.68                           |
| <b>P-E c</b> | Benzene                  | 453                                    | 54.6                     | 2.86                           |
| <b>P-E d</b> | DMF                      | 208                                    | 90.9                     | 2.59                           |
| <b>P-E e</b> | DMSO                     | 117                                    | 87.6                     | 2.68                           |
| <b>P-E f</b> | Ethyl acetate            | 380                                    | 75.6                     | 2.74                           |
| <b>P-E g</b> | Dioxane                  | 211                                    | 79.2                     | 2.65                           |

<sup>a</sup>The polymers were prepared as in the case of **P-E**, but the kind of solvent was varied.

In most cases the macroporous imprinted polymers are prepared in bulk and are then crushed and sieved. This involves a rather tedious procedure providing irregularly broken polymer particles. Conventional suspension polymerisation is, in most cases, not viable since water interferes with the interactions between the template and the binding site monomers, thus hampering efficient imprinting. Suspension polymerisation can, however, be applied if water-stable covalent linkages are employed (see Chapter 12). This is not the case with, for example, boronic ester bonds. Fortunately, with the newly developed amidine binding site monomer [11,12,31] (see Section 4.6.) suspension polymerisation can be applied even in combination with non-covalent imprinting [13]. In this case the binding interaction is strong enough to avoid components being extracted in the aqueous phase. This facilitates the polymer preparation and yields spherical beads of a desired particle diameter. Soluble, highly cross-linked microgels can also be prepared with those systems [32].

Another possibility is represented by running suspension polymerisation in media other than water. For example, a suspension polymerisation may also involve a perfluorinated liquid alkane as the dispersing phase [33]. In other examples, a two-step swelling and polymerisation method was applied to prepare molecularly imprinted beads [34].

Still another possibility is the use of silica-based supports, which are available in a broad range of bead sizes and pore diameters. These beads can be easily modified by silanising reagents carrying polymerisable groups. In a second step, the beads can be coated with thin layers of imprinted polymers for the separation of dyes [35], enantiomeric sugars [36,37], bisimidazoles [38] and enzymes [39]. These coated silicas show very good properties as chromatographic supports, the only drawback being their somewhat lower loading capacity when compared to macroporous polymers. It is also possible to use TRIM-based beads and to coat them as described above [40a,b].

Usually, the chiroptical properties of highly cross-linked polymers cannot be measured. The asymmetry of the empty cavities can be deduced from their excellent racemate resolution ability, but under special conditions it can also be directly detected by optical activity measurements [41]. For this, the polymer is suspended in a solvent that has the same refractive index as the polymer, a technique which was developed for other types of insoluble polymers. The values of molar optical rotation thus determined are shown in Table 4.3.

If we compare the value ( $-61.7^\circ$ ) for a polymer prepared from **1** (calculated for the molar content of **1**), still containing the template, with the value  $-448.9^\circ$  for the template monomer **1**, it becomes apparent that the molar optical rotation value is considerably decreased as a result of polymerisation. This can have several causes, one being the influence of the polymer matrix. Its effect can be determined by removing the optically active template **1a**. If the boronic acids are then converted with ethylene glycol to the corresponding achiral ester, the polymer shows a positive molar rotation  $[\text{M}]_{546}^{20} = +110.0^\circ$ . Apparently, in **P-E** the imprints generated in the polymer make a positive contribution to the optical rotation value. Measuring the optical rotation in the solid phase allows the

TABLE 4.3

## MOLAR OPTICAL ROTATION VALUES FOR POLYMERS WITH CHIRAL CAVITIES [41]

|                  | Template<br>monomer <b>1</b> | Polymer <b>P-E'</b><br>with template <b>1a</b> | Polymer <b>P-E</b><br>template <b>1a</b> split off <sup>a</sup> |
|------------------|------------------------------|--|---|
| $[M]_{546}^{20}$ | -448.9                       | -61.7  | + 110.0   |

<sup>a</sup>As the ethylene glycol ester.

properties of chiral cavities in the polymer to be directly determined. Information on parameters such as the binding situation of a bound template molecule or the swelling degree can also be gained.

If, for example, a polymer with empty cavities is recharged with the template, the resulting polymer, in contrast to **P-E'** (with template), has a very large positive rotation value  $[M]_{546}^{20} = +323^\circ$ . If this loaded polymer is heated in acetonitrile in the presence of molecular sieves (3 Å), the molar rotation  $[M]_{546}^{20}$  changes to  $-68^\circ$ , i.e. to about the same value as for the original polymer with template. Evidently, most of the template molecules are first bound by a one-point binding (i.e. by esterification of only one boronic acid group in the cavity), and this situation changes then to a two-point binding. At higher temperatures most of the template is quickly bound by a two-point binding.

The optical rotation of such imprinted polymers after template removal is clearly not caused by individual chiral centres, as is usually the case, but by the boundaries of the empty cavities as a whole. Their chiral construction is stabilised by means of the cross-linking of the polymer chains. This type of chirality can arise from the asymmetric configuration of the cross-linking points as well as from asymmetric conformations of the polymer chains which are stabilised by cross-linking. The extent to which these two factors contribute is not known.

The possibility that a chiral configuration of linear polymer chain segments could make a contribution to the asymmetry of the cavities was also considered, since binding site monomers linked to a chiral template molecule were sometimes found to give optically active vinyl polymers in an asymmetric cyclocopolymerisation reaction [42,43]. However, monomers with a structure like **1** do not tend to undergo such asymmetric cyclocopolymerisations. One must therefore conclude that it is not the configuration but a fixed asymmetric conformation of the polymer chains that is responsible for the asymmetry. With other types of template monomers, however, such contributions of backbone-chiral portions of the polymer might be expected.

Another possible reason for the observed racemic resolution could be the existence of a few optically active templates that could not be split off. Careful investigations showed that racemic resolution is not brought about by the interaction of the racemate with the remaining templates [6].

#### 4.4. THE ROLE OF THE BINDING-SITE INTERACTIONS

The binding groups have several functions in the imprinting procedure [4,44–48]. The desirable properties during polymerisation, template removal and subsequent rebinding of a suitable substrate in a batch or chromatographic separation are quite different and can be summarised as follows:

- (1) During polymerisation:
  - a. stoichiometric interactions between template and binding site monomers are desirable,
  - b. bonding should be stable during polymerisation, and
  - c. the bonding orientation should be fixed in space
- (2) During template removal:
  - a. cleavage of the template should be possible under mild conditions, and
  - b. cleavage of the template should be as complete as possible
- (3) During rebinding:
  - a. very quick and reversible interactions should be involved,
  - b. the rebinding equilibrium should possess a favourable position that can easily be shifted in any direction,
  - c. the rebinding should be as selective as possible, and
  - d. the binding site interactions should be fixed in space

The first point implies the need for thermodynamically and kinetically stable interactions, whereas readily reversible interactions are demanded to satisfy the other two points. Interactions can be either covalent or non-covalent. The use of covalent or stoichiometric non-covalent interactions has the advantage of the exact stoichiometry: the binding groups are precisely fixed in space during the polymerisation, after which they are exclusively located in the imprinted cavities of the resulting polymer. Covalent interactions are especially suitable if a high percentage of the template can be removed from the polymer and the interactions with substrates can be strongly accelerated by catalysis; examples of this strategy will be discussed in the next section. In principle, binding through metal coordination can also be regarded as a special kind of covalent interaction. However, it will not be discussed here since the topic is treated in other chapters of this book (see Chapter 6). With the usual non-stoichiometric non-covalent interactions, a considerable excess (usually at least four-fold) of binding site monomers is required in the polymerisation mixture to ensure the complete complexation of the template molecule. In this way, the majority of the binding groups are incorporated at random. As was recently found [49], under these conditions only 15% of the imprinted cavities can re-uptake a template, the remaining 85% are irreversibly lost for separation. This may be due to shrinking of the majority of cavities. On the contrary, with stoichiometric interactions template removal usually leads to swelling of the cavities, which guarantees a high proportion (90–95%) of template re-uptake and a quick mass transfer during rebinding [4]. Upon template re-uptake the cavity shrinks to its original volume (induced fit). It can be concluded that imprinted polymers based on non-stoichiometric, non-covalent interactions are generally not well suited for

preparative separations. On the other hand, the template is usually very easily removed and reversible interactions with substrates are in principle fast. It is the structure of the template molecule and the kind of application that determine which interactions are the most favourable in each specific case. When producing chromatographic materials for analytical purposes, simple non-covalent interactions are usually preferred, as the materials are more readily obtained and an excess of binding groups apparently does not have a detrimental effect on the separations. For the construction of catalysts, the location and orientation of binding groups and catalytically active groups in the cavities are of greater significance, such that covalent and stoichiometric non-covalent interactions should be considered more advantageous in this case.

Detailed investigations have shown that the selectivity in enantiomeric resolution depends both on the arrangement of the functional groups inside the cavities and on the shape of the cavities [50–53]. The dominating factor, however, is the functional group arrangement [50,51]. If two binding sites per template have been used, one-point binding can occur in several fashions, but there is only one possibility for two-point binding [4,37]. It can be inferred that the two-point binding will be the most selective. Therefore, the occurrence of the two-point binding has to be increased, which is possible, e.g. by raising the temperature [41], as will be discussed in detail in the next section.

## 4.5. EXAMPLES OF COVALENT INTERACTIONS IN MOLECULAR IMPRINTING

### 4.5.1. Boronic acid-containing binding sites

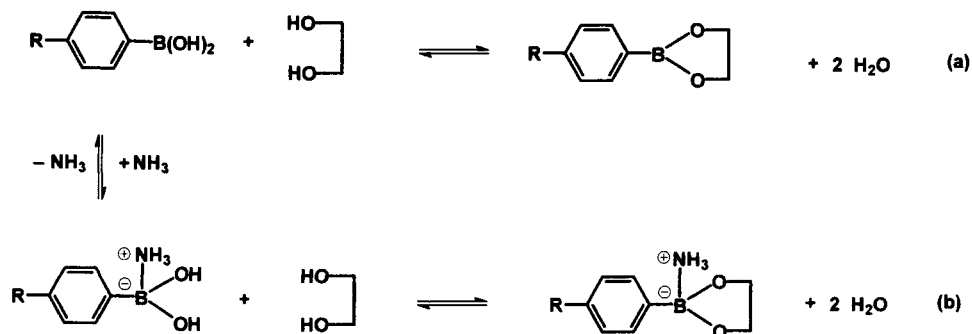
The boronic acid group is very suitable for covalent binding. Polymers of 4-vinylphenylboronic acid are commercially available as stationary phases for chemo-selective affinity chromatography of diol-containing compounds in alkaline aqueous solution [54]. Binding site monomers of this kind can also be used in a similar way for molecular imprinting; in this case, relatively stable trigonal boronic esters are formed with diol-containing templates (equation (a)).

Ester formation occurs with complete stoichiometric conversion at relatively low reaction rates ( $t_{1/2}$  100–600 s). In the absence of water no back reaction takes place. There is a very slow ester–ester exchange reaction ( $t_{1/2} \approx 5000$  s). The boronic ester moieties can be readily cleaved in water/alcohol. This reaction is, in principle, fast and complete ( $t_{1/2} \approx 100$  s), so that the template can be released from an imprinted macroporous polymer in 85–95% yield.

The re-uptake of template in the imprinted polymer is relatively slow (consider the rates of formation of boronic esters listed above), but more than 90% of the free cavities can be reoccupied. Fortunately, in aqueous alkaline solution or in the presence of certain nitrogen bases (for example  $\text{NH}_3$  or piperidine) tetragonal boronic esters are formed (equation (b)), which equilibrate extremely rapidly with tetragonal boronic acid and diol [47,55]. In these cases the rate of equilibration

( $t_{1/2} \approx 10^4$  s) is comparable to typical values for non-covalent interactions. At the molar ratios corresponding to equation (b), conversion amounts to 97%. The extent of reaction can be controlled by addition of water or methanol.

These equilibria can be even more rapid if the interaction with nitrogen bases occurs intramolecularly (see Table 4.4 entry k) [46,47,56,57]. In those cases in which a basic nitrogen atom is located at a favourable distance from the boronate ester, a rate acceleration of  $10^8$ – $10^9$  fold compared to the unsubstituted phenylboronate can be observed [56,57].



Investigation on boronic acid-containing imprinted polymers led to the first examples of successful chromatographic racemic separations using imprinted materials. The addition of nitrogen bases to the mobile phase resulted in an enhancement of the mass transfer in such a way that complete chromatographic separations were possible in a few minutes. With further optimisation of the chromatographic procedure, coupled with higher temperatures, we were able in 1986 to perform for the first time a complete racemate resolution with  $R_s = 2.1$  [21]. Later on, we achieved resolutions of  $R_s = 4.3$  by using gradient elution [19] (see Fig. 4.1).

Remarkably, the more strongly retarded enantiomer (corresponding to the template molecule) gives a much more pronounced peak broadening in these separations if a solvent gradient is omitted during chromatography. The number of theoretical plates for this compound is at most half that of the less strongly retarded enantiomer. The reason must be essentially the two-point binding of the template molecule compared to the one-point binding of the other enantiomer.

This difference is also evidenced by the temperature dependence of the number of theoretical plates for the two enantiomers. The template molecule shows hardly any temperature dependence because of increased two-point binding with slow binding rates at higher temperatures, whereas the number of theoretical plates for the second enantiomer increases rapidly, as expected (see Fig. 4.3a) [21]. The effect of concentration on retention is also very different for two enantiomers (see Fig. 4.3b). The 'wrong' enantiomer does not show much effect, whereas retention of the template molecule is greatly increased at lower concentrations, at which only the most selective cavities are occupied by the template molecule. The selectivity therefore increases sharply [49]. It is interesting to notice that this chromatographic



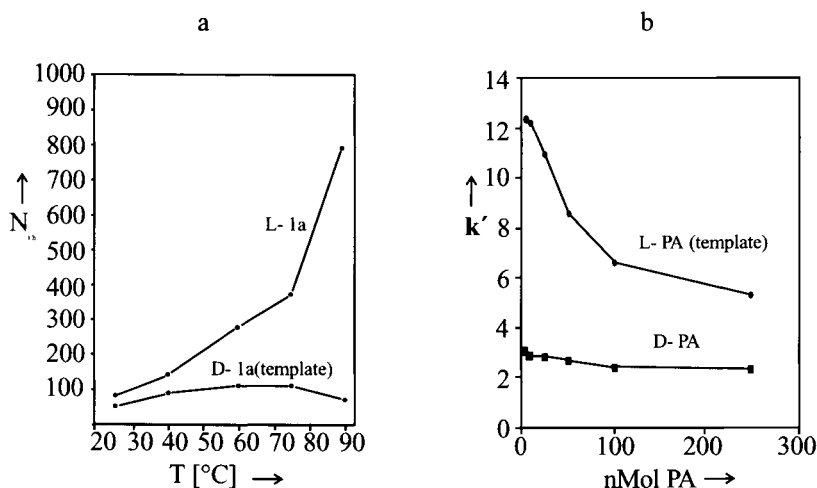


Fig. 4.3. Differences in the effect of temperature on the number of theoretical plates and of the amount of chromatographed substance on the retention of template molecules and their enantiomers. (a) Temperature dependence of the number of theoretical plate ( $N_{th}$ ) in the resolution of D-1a and L-1a on a polymer imprinted with 1 [21]. (b) Dependence of the capacity factor  $k'$  on the amount of chromatographed substance in the resolution of L- and of D-phenylalanine anilide on a polymer imprinted with L-phenylalanine anilide [49].

behaviour is observed not only for covalent interactions but for all other interaction types, hence it seems to be a typical characteristic of imprinted polymers.

Preparative chromatographic separations are also possible. For example, 30 mg of the racemate of 1a were efficiently resolved by 20 g of polymer [22].

In Table 4.4 a number of examples of molecular imprinting using boronic acid-containing binding sites are shown. Mostly templates with diol groups have been used. Entries a, e and j show templates which are bound by one boronic acid *via* a boronic ester bond. Imprinted polymers with higher selectivity are obtained if two boronic acid binding sites are attached to the templates (see entries b, c, g, h, i and k). The optimisation of the imprinted polymer structure was mainly carried out using phenyl- $\alpha$ -D-mannopyranoside (1a) as the template. Recently, the resolution of the racemates of free sugars (fructose, mannose and galactose) was also accomplished with polymers prepared for this purpose. Thus, for the first time, sugar racemates could be resolved without the need for previous derivatisation [19,50,51].

One might expect that three covalent interactions should be especially favourable for imprinting and for subsequent molecular recognition. However, it has been shown that three boronic acid interactions [2,3,58], three different covalent interactions [36], or three or more non-covalent interactions [75,76] all lead to poorer resolving power (that is, a smaller number of theoretical plates  $N_{th}$ ) for the polymers. Here the main factor must be the low rate of formation of polymer-substrate complexes.

The effect of the flexibility of the binding group on the resolving power of the polymers was also investigated with boronic acids [19,77,78]. For this, nine different

polymerisable boronic acids with different degrees of flexibility were used, with phenyl- $\alpha$ -D-mannopyranoside as the template. As the mobility of the groups in the cavity increased, the selectivity in racemate resolution decreased.

$\alpha$ -Hydroxy carboxylic acids, such as mandelic acid (entry j), also bind to boronic acids, and imprinted polymers of this type possess remarkably good resolving power for the racemate of mandelic acid [68–70].

Boronic acid binding sites can also be used in combination with other covalent or non-covalent interactions. Glyceric acid derivatives were thus bound as boronic esters with additional electrostatic, hydrophobic, charge transfer or hydrogen bonding interactions with other binding site monomers [79,80]. A boronic ester bond combined with an imine bond has been used for the imprinting of L-DOPA [63,64]. Template rebinding to these polymers is again considerably accelerated by addition of nitrogen bases, as discussed before.

As shown in entries h and i, it is also possible to couple silane-containing boronic acids to the surface of silica. Recently, Shinkai and co-workers attached a reactive boronic diester saccharide to the surface of (60)-fullerenes [65] and in this way obtained soluble (60)-fullerenes with two boronic acids at a defined distance for the selective binding of saccharides.

The boronic acid binding site can also be used for interactions with monoalcohols. In the presence of an *ortho*-hydroxymethylene group (see entry l), an intramolecular cyclic monoester is formed (boronophthalide). This compound still has one hydroxyl group left for the esterification of monoalcohols, a reaction that can be used in the imprinting procedure [46,47,72]. Recently this method has been revived for the binding of steroid alcohols [73,98b,c].

#### 4.5.2. Other types of covalent binding

The suitability of Schiff bases for covalent binding was also extensively investigated (see Table 4.5, entries a–f). Schiff bases are in principle suitable for molecular imprinting, since the position of the equilibrium for the imino bond formation is favourable. The rate of bond formation and breaking is often too low for rapid chromatography [46,81], but it can be considerably increased by using suitable intramolecular neighbouring groups [46,82] (see entries h, i). Use of Schiff bases allows the binding site to be either an amine (entries a, b, c) or an aldehyde (entries d, e, f). Aldehyde-containing binding sites have been successfully employed for the imprinting with amino acid derivatives [63,64,81]. In this case, the application of amino acid templates in the form of anilides turned out to be especially suitable, as shown for phenyl alanine anilide **5** derivatives.

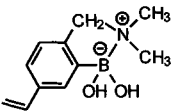
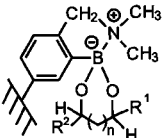
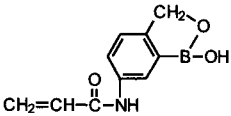
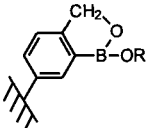
The use of Schiff bases mostly involved amine-containing binding sites and a two-point binding of the template (entries a, b, c). Thus, with the aid of bisaldehydes of differing structure, two amino groups could be introduced into microcavities of different shape. Remarkable selectivities for template rebinding were obtained (see entry a) [83,84]. In connection with these experiments the question arose as to whether or not the distance between two binding groups on a surface, hence a two-dimensional arrangement of functional groups, could also lead

TABLE 4.4

## BORONIC ACID-CONTAINING BINDING SITES

| Entry | Template                  | Binding site | Binding during equilibrium | References      |
|-------|---------------------------|--------------|----------------------------|-----------------|
| a     | Diols                     |              |                            | [58]            |
| b     | Polyols                   | „            | „                          | [2,3,58]        |
| c     | Saccharides               | „            | „                          | [5,17–19,50,51] |
| d     | Sialic acid               | „            | „                          | [59,60]         |
| e     | Glyceric acid derivatives | „            | „                          | [1–3,29,61,62]  |
| f     | L-DOPA                    | „            | „                          | [63,64]         |
| g     | Saccharides               |              |                            | [65]            |
|       |                           |              | at [60]-fullerenes         |                 |
| h     | Saccharides               |              |                            | [22,66]         |
|       |                           |              | at SiO <sub>2</sub>        |                 |
| i     | Glycoproteins             |              |                            | [67]            |
|       |                           |              | at SiO <sub>2</sub>        |                 |
| j     | Mandelic acid             |              |                            | [68–70]         |

TABLE 4.4 *continued*

| Entry | Template           | Binding site  | Binding during equilibrium  | References    |
|-------|--------------------|---|---|---------------|
| k     | Diols, saccharides |  |  | [46,47,71]    |
| l     | Monoalcohols       |  |  | [46,47,72,73] |

to substrate selectivity [83,84]; in the typical imprinting of polymers or silica gels, the functional group arrangement within the imprinted cavities is three-dimensional.

Bisazomethines derived from suitable dialdehydes were condensed on the surface of wide-pore silica gels for testing the distance selectivity. The most promising substances for the condensation were of the type  $\text{RSi}(\text{CH}_3)(\text{OCH}_3)_2$  (entry c). The residual free silanol groups on the surface were then blocked by hexamethyldisilazane to prevent non-specific adsorption. After cleavage of the template, two amino groups were left behind at a definite distance apart (Fig. 4.4).

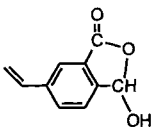
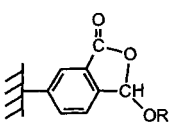
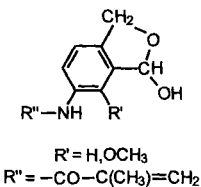
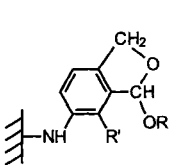
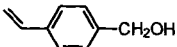
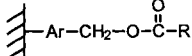
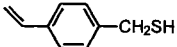
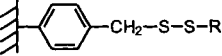
If good selectivity is to be obtained, the number of condensed templates must not be too high to avoid template rebinding through adjacent amino groups that did not originally form a pair. If dialdehydes in which the aldehyde groups are at varying distances apart are exposed to such modified silica gels, the dialdehyde that was used to carry out the imprinting is bound preferentially [4,83,84,86]. Dicarboxylic acids with different distances between the carboxyl groups can also be very effectively separated on these silica gels (Table 4.6) [86]. From Table 4.6 it can be seen that terephthalic acid, with the correct distance between the carboxyl groups (0.70 nm), is the most retarded and those acids in which the distance is greater or smaller are less strongly retained. Remarkably high  $\alpha$  values can be obtained in this way. In the example shown, the binding during imprinting is covalent, whereas during equilibration non-covalent interactions prevail. More examples of this method are given in Table 4.7. If an aldehyde is used as the binding group and a diamine as the template, diamines should also be separable after removal of the diamine and oxidation of the aldehyde to carboxyl groups. Moreover, if the remaining silanol groups are blocked with space-filling silanes (for example, phenyldimethylmethoxysilane) prior to template removal from the surface, contours of the size of the templates are obtained once the template is split off (Fig. 4.4) [83,84]. Long-chain aliphatic silanes can also be used for this purpose [95].

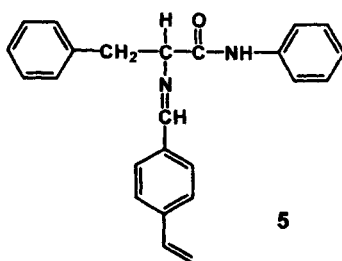
TABLE 4.5

## COVALENT BINDING AS SCHIFF BASES, KETALS, ESTERS AND DISULPHIDES

| Entry | Template  | Binding site               | Binding during equilibrium | Reference     |
|-------|-----------|----------------------------|----------------------------|---------------|
| a     | Aldehydes |                            |                            | [83,84]       |
| b     | Aldehydes |                            |                            | [83–85]       |
| c     | Aldehydes |                            |                            | [4,86]        |
| d     | Amines    |                            |                            | [46,63,64,81] |
| e     | Amines    |                            |                            | [74]          |
|       |           | $R' = -NH-CO-C(CH_3)=CH_2$ |                            |               |
|       |           | $R' = -CH=CH_2$            |                            |               |
| f     | Amines    |                            |                            | [6,36,37]     |
| g     | Ketones   |                            |                            | [53,87–89]    |

TABLE 4.5 *continued*

| Entry | Template                      | Binding site  | Binding during equilibrium  | Reference |
|-------|-------------------------------|---|---|-----------|
| h     | Amines                        |    |    | [46]      |
| i     | Alcohols                      |    |    | [46,82]   |
| j     | Cyclobutane-dicarboxylic acid |    |    | [90-92]   |
| k     | Disulphide                    |  |  | [93,94]   |



Using a trialdehyde as template it was also possible to introduce three amino groups as a TRIPOD on the silica surface [85].

Another possibility to introduce two functional groups at a predetermined distance was investigated by polymerising the disulphide **6** under imprinting conditions (see entry k). Subsequent reduction of the disulphide bond with diborane provides polymers with two closely positioned mercapto groups (see Scheme 4.III).

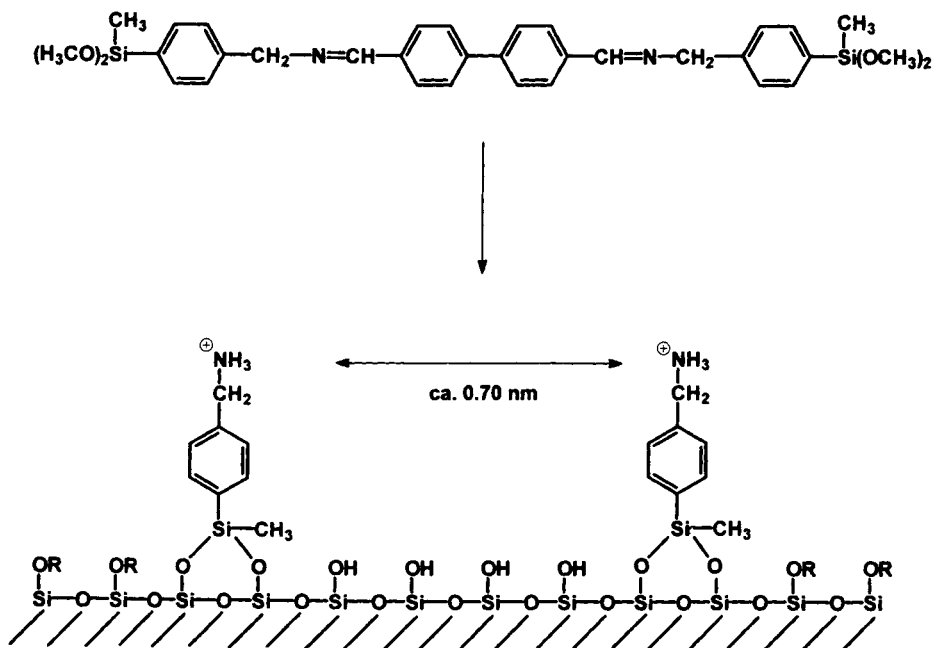


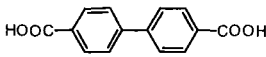
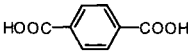
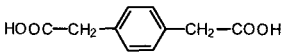
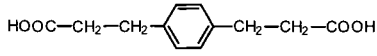
Fig. 4.4. Preparation of a silica gel surface functionalised with pairs of amino groups at a definite distance apart. The distance between the groups (about 0.70 nm) is fixed by using biphenyl-4,4'-dialdehyde as the template [4.86].

Under comparable conditions, polymers with randomly distributed mercapto groups were obtained from (4-vinylbenzyl)-thioacetate. The degree of cooperativity of each of the two mercapto groups was determined quantitatively by oxidation with  $I_2$ . The percentage of reoxidation by  $I_2$  to disulphide depends on the exact position of each pair of mercapto groups, which in turn depends on the degree of cross-linking of the polymer, the concentration of the mercapto groups, the degree of swelling and the reoxidation temperature. Under proper conditions, reoxidation of polymers from **6** was achieved in 99% yield. On the contrary, polymers with randomly distributed mercapto groups showed, under certain conditions, complete site separation and no reoxidation [93,94].

Shea *et al.* [53,87–89] used ketals (entry g) for introducing binding groups. Diketones with various distances between the keto groups were functionalised by ketal formation with polymerisable diols. The resulting imprinted polymers showed considerable selectivity for their own diketone template when they were reloaded with a mixture of diketones. Unlike the rebinding experiments mentioned earlier, ketal bond formation takes place slowly; hence template rebinding appears to be kinetically controlled, in contrast to the rebinding reactions described so far, which are thermodynamically controlled. In this case, if the arrangement of functional groups in the substrate molecules is the same, the size

TABLE 4.6

HPLC SEPARATIONS WITH THE SILICA GEL DESCRIBED IN FIG. 4.4 (LOADING:  $4.23 \times 10^2$  MMOL  $\text{NH}_2$  GROUPS PER GRAM). CAPACITY FACTORS ( $k'$ ) OF SOME DICARBOXYLIC ACIDS WITH VARIOUS DISTANCES ( $d$ ) BETWEEN THE CARBOXYL GROUPS AND SEPARATION FACTORS  $\alpha$  FOR CERTAIN PAIRS OF SUBSTANCES ARE GIVEN.

| Entry | Chromatographed substance   | $d$ [nm] | $k'$  | $\alpha$              |
|-------|---|----------|-------|-----------------------|
| 1     |  | 1.14     | 0.015 | —                     |
| 2     |  | 0.70     | 0.314 | $\alpha_{2,1} = 20.9$ |
| 3     |  | 0.85     | 0.226 | $\alpha_{3,1} = 15.1$ |
| 4     |  | 1.11     | 0.037 | $\alpha_{3,4} = 6.1$  |

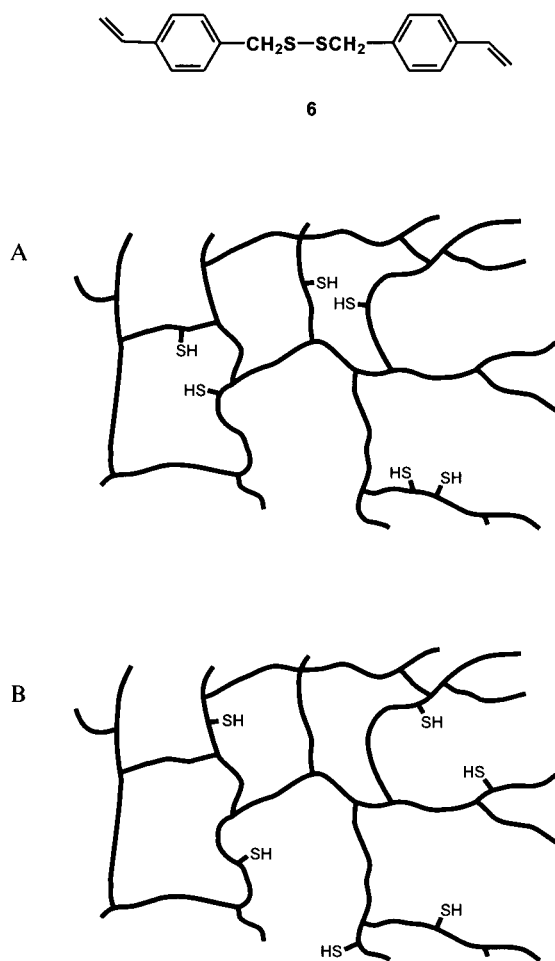
Eluent: 2-propanol/acetonitrile/formic acid 67.9/32.0/0.1 [4,86]. The distance of the two- $\text{NH}_3$ -groups attached to the silica is around 0.70 nm calculated for the distance of the outer spheres in a probable conformation of the groups. Similarly, the distance of the carboxyl groups in the dicarboxylic acids is calculated from the distance of the outer spheres of the dianions.

and shape of the rest of the molecule become important factors for the extent of rebinding.

With these template monomers very careful investigations on the mechanism of the imprinting procedure have been performed by Shea's group. The influence of the cooperativity of binding sites, of the shape of the cavity, and of the occurrence of one- or two-point binding has been taken into consideration.

In the very early years of imprinting, carboxylic acid ester moieties were used as binding groups. The aim was the preparation of microreactors for regio- and stereo-selective reactions. For this, the cavity was first imprinted with a possible product of the reaction and a precursor was then embedded into the cavity. The idea was to favour the formation of the product used as template by running the reaction within the imprinted cavity. The first experiments were carried out by the research groups of Shea [90,91] and Neckers [92], who performed cycloadditions that led to cyclopropanedicarboxylic and cyclobutanedicarboxylic acids, respectively. The latter

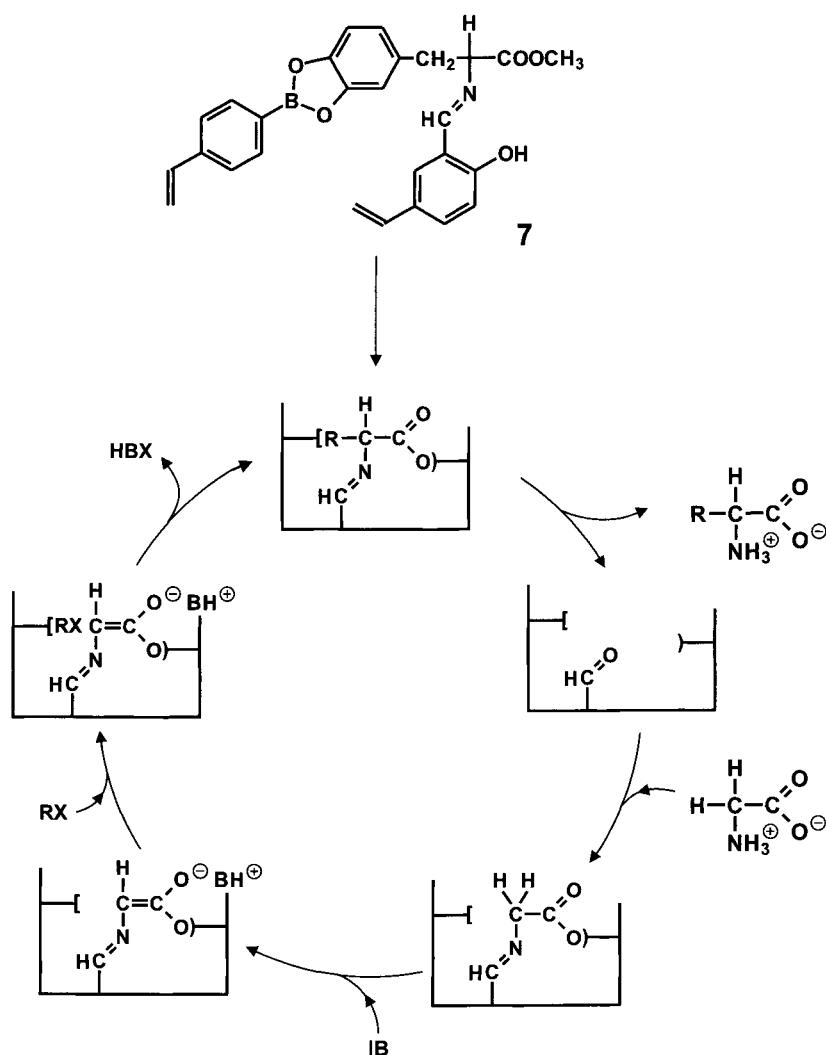




Scheme 4.III. Mercapto groups as nearest neighbours by copolymerisation of **6** and subsequent reduction (A) or distributed at random by copolymerisation of (4-vinylbenzyl)thioacetate and subsequent reduction (B) [93,94].

were obtained with remarkable regio- and diastereo-selectivity. Belokon *et al.* [74] (entry e) used Schiff base formation for binding and established that, on removal of a proton from an amino acid template located in a cavity, the intermediate carbanion maintains its original configuration (unlike in solution) and therefore reacts under retention. Sarhan and El-Zahab [69] were able to use this strategy to perform a stereospecific inversion of the configuration of mandelic acid.

The first asymmetric syntheses in a chiral cavity were achieved in our research group [63,64]. Enantio-selective C-C bond formation was attempted inside a chiral cavity with the objective of preparing optically active amino acids. The synthetic



Scheme 4.IV. Schematic representation of the asymmetric synthesis of  $\alpha$ -amino acids using imprinted polymers [63,64].

approach is outlined in Scheme 4.IV. Template monomer **7**, with L-DOPA as template possessing boronic acid and salicylaldehyde binding sites was, used for imprinting.

After removal of the template, glycine was embedded in the cavity, deprotonated, and alkylated. The highest enantiomeric excesses (36% ee) reported so far with imprinted polymeric reagents have been achieved with amino acids prepared in this way. This enantiomeric excess is purely a result of the asymmetric induction of the cavity.

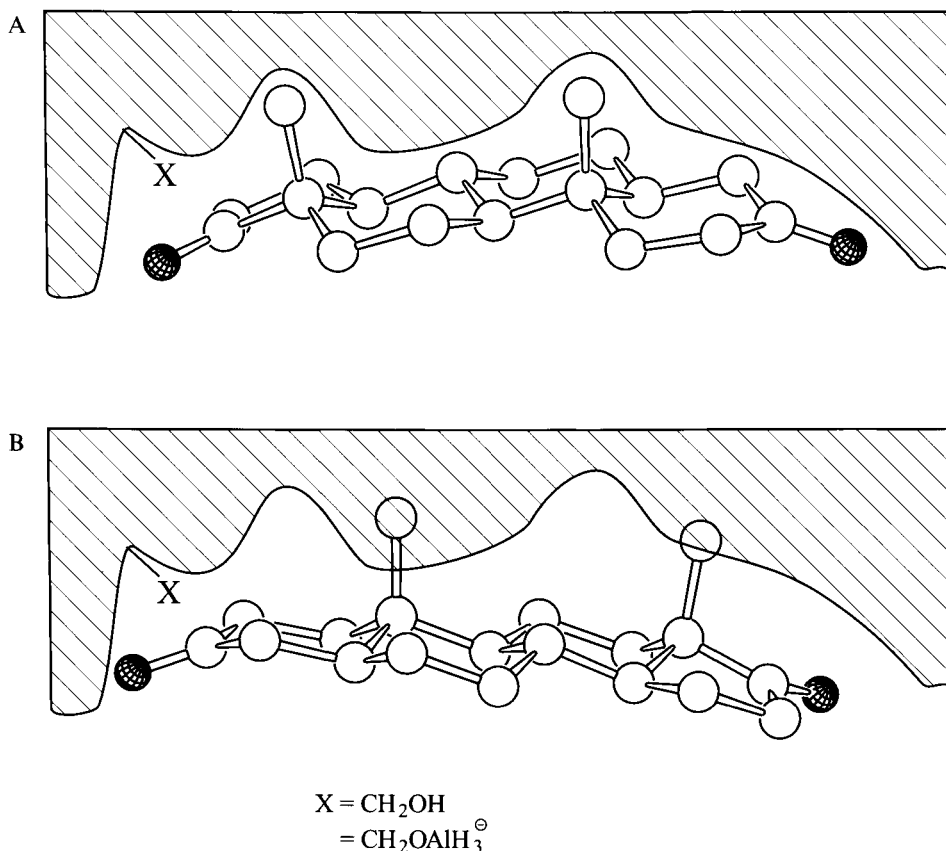
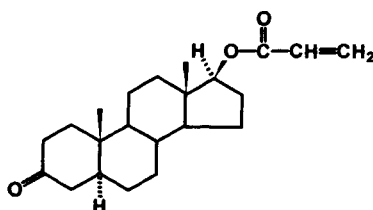


Fig. 4.5. Schematic representation of the embedding of androstane-3,17-dione in a cavity produced by imprinting with **8** ( $\text{X} = \text{CH}_2\text{OH}$  or  $\text{CH}_2\text{OAlH}_3^\ominus$  [96]. Embedding examples with the 17-keto group (a) and the 3-keto group (b) in close proximity to the X group. Poor fitting is obtained in (b) [96].

Very remarkable regio- and stereo-selective reactions were performed by Byström *et al.* [96]. They used an ester bond for binding a steroid during imprinting (see monomer **8**). The template was removed by reductive cleavage, thus producing a cavity with a  $\text{CH}_2\text{OH}$  group in a particular position. The hydroxyl group was then converted to an active hydride species with  $\text{LiAlH}_4$ . On reacting androstane-3,17-dione with this polymer, only the carbonyl group in position 17 was reduced to the alcohol, whereas in solution or with a polymer with statistically distributed hydride groups the position 3 was exclusively reduced. Figure 4.5 shows that the shape of the cavity indeed favours reduction only at position 17. A considerable stereochemical preference (ratio of  $\alpha$ - to  $\beta$ -OH groups formed) was also observed.



8

#### 4.5.3. Covalent binding during imprinting and non-covalent binding during equilibration

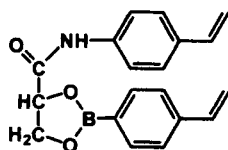
It has already been mentioned that covalent binding during the imprinting procedure has the advantage of stability and exact stoichiometry, whereas readily reversible non-covalent interactions are better suited for the equilibration of the free cavities with the substrate. As a consequence, some researchers tried to prepare imprinted polymers using covalent binding and then to switch to non-covalent binding site interactions during equilibration. This principle had already been used in the first published example of molecular imprinting in polymers [1,3] (see entry a, Table 4.7). In this case, D-glyceric acid was bound at the carboxyl group by an amide bond and at the diol group by a boronic ester (see 9). After polymerisation and removal of the template, rebinding occurs through a boronic ester bond and through simple electrostatic attraction between the acid and the amine functional group. Similarly, templates containing an alcohol function have been bound as esters. After template removal, carboxylic acid groups are left in the cavity, which can give hydrogen bonds to the template alcohol or interact ionically with amine-containing substrates [97a,b] (entry b). The disadvantage of this strategy is often the stability of the covalent bond, which is responsible for splitting percentages of only around 20%. As already mentioned, reductive cleavage of the ester group is somewhat better suited for this approach (entry c). A further problem arises when considering that different kinds of interaction during imprinting and rebinding imply different bond distances between the binding sites in the cavity and the template molecule (entries a and b).

The drawbacks of this method are less pronounced in Whitcombe's [98a] approach. This group uses carbonate esters (see entry d), which are easier to hydrolyse producing hydroxyl groups which rebind the template by hydrogen bonding with a similar bond distance. Even easier to hydrolyse are Schiff bases, which have already been discussed in Table 4.5, entries a–f. In this way, amine groups are positioned in the cavities, as has already been described in Table 4.6; the distance of the amino groups is then defined and causes a good selectivity not only for the original template, but also for dicarboxylic acids by electrostatic interaction if these compounds possess the right spacing between their functional groups. Similarly, this principle allows catalytically active imprinted polymers to be prepared, as shown by Shea and co-workers [10]. In this case, one takes advantage of covalent

TABLE 4.7

## COVALENT BINDING DURING IMPRINTING AND NON-COVALENT INTERACTION DURING EQUILIBRATION

| Entry | Template         | Binding site                        | Binding during imprinting                            | Binding during equilibration | Reference      |
|-------|------------------|-------------------------------------|--|------------------------------|----------------|
| a     | Carboxylic acids |                                     |  |                              | [1-3,29,61,62] |
| b     | Alcohols         | $\text{CH}_2=\text{CH}-\text{COOH}$ | $\text{CH}_2=\text{CH}-\text{C}(=\text{O})\text{OR}$ |                              | [97]           |
| c     | Alcohols         | $\text{CH}_2=\text{CH}-\text{COOH}$ | $\text{CH}_2=\text{CH}-\text{C}(=\text{O})\text{OR}$ |                              | [96]           |
| d     | Alcohols         |                                     |  |                              | [98]           |
| e     | Dialdehyde       |                                     |  |                              | [4,86]         |
| f     | Dialdehyde       |                                     |  |                              | [10]           |



9

imprinting to place in each cavity two amino groups in a strictly defined position, which then act cooperatively in the catalytic process *via* non-covalent interactions.

#### 4.6. MOLECULAR RECOGNITION AND CATALYSIS WITH STOICHIOMETRIC NON-COVALENT INTERACTIONS

It has already been stated that covalent as well as non-covalent non-stoichiometric interactions have advantages and disadvantages when employed for molecular imprinting. In the last 10 years, many research efforts have been directed towards the development of imprinting strategies able to combine the advantages of covalency and non-covalency without suffering their disadvantages. One method uses covalent binding during imprinting and non-covalent binding during equilibration, as described above. Another approach involves the use of novel kinds of interactions between template molecule and binding sites. Ideally, the interaction should be stoichiometric in nature, yet allow a high yield in template splitting and fast rebinding kinetics without the need for special reaction conditions.

A possible solution for this problem is based on the application of coordinative bonds based on metal complexes, in which the metal centres act as mediators by inclusion in the same coordination sphere of both the binding site monomer and the template molecule. Such an approach is discussed in detail in Chapter 6. A further possibility is represented by the use of stoichiometric, non-covalent interactions, which has provided very promising results in the last five years. In most cases, the kind of interaction employed was mainly based on multiple hydrogen bonding. In general, when two or more hydrogen bonds are formed between the template molecule and a binding site monomer, very stable assemblies with large association constants can form in aprotic media, which in turn are easily cleaved in solvents such as water or alcohols. On the other hand, owing to the high value of the association constants, no excess binding site monomer is needed to shift the formation of the template assembly to completion so that, after polymerisation, the functional groups are exclusively located within the imprinted cavities. In this way, the high splitting yields and fast rebinding kinetics usually observed with non-covalent, non-stoichiometric interactions are combined with the precise location of functional groups and the high accessibility of the free cavities for molecular recognition that is typical for covalent imprinting. This combination is extremely important for the development of imprinted polymers possessing catalytic activity, as will be discussed below. Finally, it is important to remark that stoichiometric,

non-covalent interactions amenable to application in molecular imprinting are by no means limited to multiple hydrogen bonds. Very recently, an alternative approach appeared in the literature making use of host–guest chemistry [99], a possibility which is undoubtedly worth further investigation (see below). Examples of binding site monomers and corresponding templates which have been employed in molecular imprinting with stoichiometric non-covalent interactions are summarised in Table 4.8.

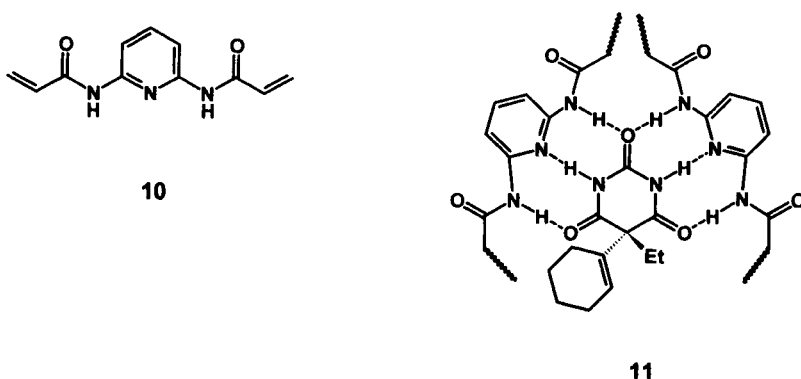
In 1995, Tanabe and co-workers and Takeuchi and co-workers [26,105] introduced the polymerisable 2,6-diaminopyridine derivative **10** as a novel binding site monomer that is able to interact with barbiturates through multiple hydrogen bonds. The existence of such an interaction was qualitatively assessed by observing the changes in the chemical shifts of the signals in the  $^1\text{H}$  NMR spectrum upon complexation. Interestingly, in this case the binding site monomer also acted as a cross-linker. The imprinted polymers prepared by this method showed an up to 100-fold enhanced adsorption of their own template molecule in comparison to a non-imprinted analogue. The postulated structure **11** of the imprinted cavity closely resembles supramolecular receptors that were originally developed by Hamilton and co-workers for the same purpose [110]; however, molecular imprinting appears to provide a much simpler route to synthetic receptors with respect to traditional organic chemistry.

Another binding site able to give multiple hydrogen bonds was investigated in our institute [100,106,107,111]. First, the binding of amido-pyrazoles with dipeptides was carefully investigated with low-molecular-weight model substances. In this case it is expected that one amido-pyrazole interacts with the top face of the dipeptide by a three-point binding, whereas a second amido-pyrazole is bound to the bottom face by a two-point binding. Complexation should stabilise the  $\beta$ -sheet conformation in the dipeptide (see Fig. 4.6). NMR titrations of Ac-L-Val-L-Val-OMe with 3-methacryloyl-amino-pyrazole show large but markedly different down-

TABLE 4.8

## STOICHIOMETRIC NON-COVALENT INTERACTIONS

| Entry | Template                                  | Polymerisable binding site | Reference       |
|-------|---|----------------------------|-----------------|
| 1     | Carboxylic acids                          | Amidines                   | [12,31,100,101] |
| 2     | Phosphonic acid monoesters                | Amidines                   | [11,12]         |
| 3     | Phosphoric esters                         | Amidines                   | [13]            |
| 4     | Phosphoric and phosphonic acid monoesters | Guanidines                 | [102]           |
| 5     | Amidines                                  | Carboxylic acid            | [103,104]       |
| 6     | Barbiturates                              | Diaminopyridines           | [26,105]        |
| 7     | Oligopeptides                             | Aminopyrazoles             | [100,106,107]   |
| 8     | Steroids                                  | $\beta$ -Cyclodextrins     | [99,108,109]    |



field shifts for both peptide amide protons. When one equivalent of 5-amido-pyrazole is added, only complexation of the peptide top face by three-point binding is observed with an association constant  $K_a$  of 80 L/mol. On further addition of 5-amido-pyrazole, complexation of the bottom face by a two-point binding occurs, with an association constant of only 2.0 L/mol. In both complexes the dipeptide possesses a  $\beta$ -sheet conformation. By tailoring the amide function in the binding site the association constant can be substantially increased ( $K_a = 890$  L/mol for  $\text{CF}_3\text{CO}-$ ). The binding site monomer **12** has been used for imprinting with dipeptides; the resulting polymer was successfully employed in the resolution of the racemate of the template dipeptide [111].

The amidine group is a very efficient new binding site able to form multiple hydrogen bonds as well as electrostatic interactions. It strongly interacts with oxyanions, such as carboxylates and phosphonates, and represents an excellent mimic of the guanidinium group of the natural amino acid arginine. Sellergren [103,104] was the first to use amidine-carboxylic acid interactions to develop polymers imprinted

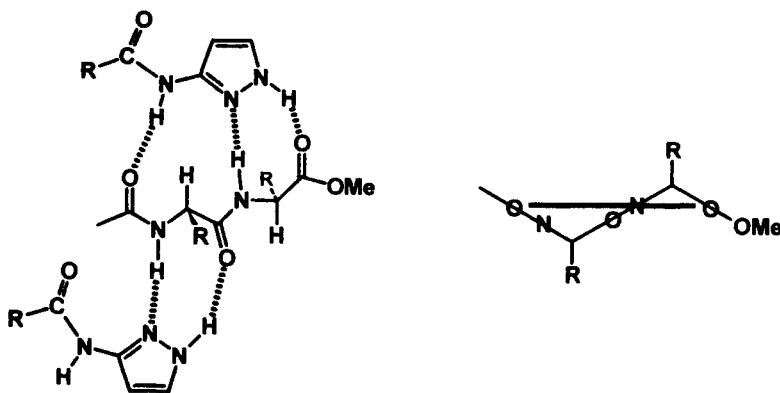
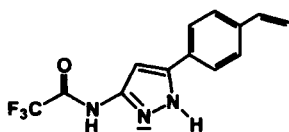


Fig. 4.6. Side and top view of the computer-calculated dipeptide-amidopyrazole 2:1 complex [106,107]; when seen from above, the heterocycle on the top-side is symbolised by a horizontal bar (for a better overview, the second heterocycle is omitted).



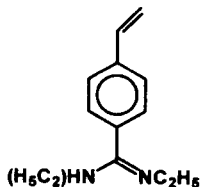
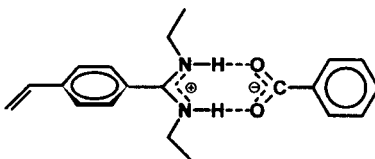
**12**

with the template pentamidine, a drug possessing two amidine functionalities. He employed methacrylic acid as the binding site monomer; however, he always worked with an excess of methacrylic acid even if the association constants would probably have allowed him to use a stoichiometric quantity of the binding site monomer. Our group was the first to use polymerisable amidines as binding site monomers for stoichiometric non-covalent molecular imprinting [11,12,31,100,101]. For this we developed polymerisable *N,N'*-bisalkylamidines such as **13** [31]. The *N*-substitution by alkyl groups offers the advantage of improved solubility of the amidine/substrate complex in aprotic solvents. NMR titration of amidine-carboxylic acid complexes such as **14** gave an association constant of  $3.4 \times 10^6$  L/mol (in  $\text{CDCl}_3$  at  $25^\circ\text{C}$ ), enough to ensure the formation of stoichiometric non-covalent interactions with carboxylate-containing template molecules. By contrast, the association constants for the binding site monomers traditionally employed in non-covalent molecular imprinting do not normally exceed 10 L/mol.

The usefulness of these novel amidine binding site monomers in molecular imprinting was demonstrated by their application in the preparation of polymers that were imprinted with optically active *N*-(4-carboxybenzoyl)-phenylglycine (**15**); the resulting materials could discriminate between the enantiomers of the template molecule with  $\alpha$  values of up to 2.8 [12].

The special advantage of amidine-based stoichiometric non-covalent interactions is illustrated in Fig. 4.7. The templates **15** were removed from an imprinted polymer and then the polymer was re-offered different amounts of template **15** in methanol for rebinding. Figure 4.7 shows a nearly stoichiometric uptake with a reloading yield of about 99%. This is in marked contrast to non-stoichiometric non-covalent interactions in which only around 15% of the cavities can be reloaded.

It is important to notice that the amidine moiety can act as a binding group and as a base at the same time. The importance of this dual nature will become apparent below, when we discuss the catalytic properties of imprinted polymers prepared using this functional group.

**13****14**

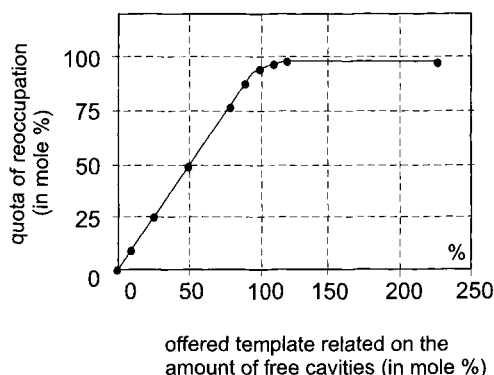
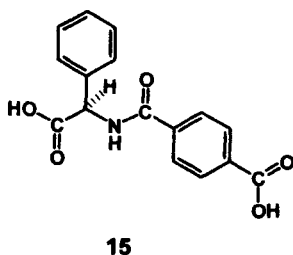


Fig. 4.7. Template re-uptake of a polymer imprinted with a monomer consisting of **15** and two moles of **13** in dependence to the offered amount of template **15**.



Shea and co-workers [102] prepared synthetic receptors for phosphates and phosphonates on the surface of  $\text{SiO}_2$  xerogels by functionalisation with guanidinium groups. In a surface imprinting procedure the binding site monomer, a 3-trimethoxysilylpropyl-1-guanidinium salt, was combined with the templates (phosphates or phosphonates) and attached to the silica surface. The affinities of the template molecules for these materials improved by about an order of magnitude compared to analogous low molecular weight receptors reported in the literature.

It has been demonstrated that a skilled use of multiple hydrogen bonding can result in the design of efficient imprinted polymers based on stoichiometric non-covalent interactions. Recently, a novel strategy has been devised for the development of imprinted polymers specific for steroids [99,108,109]. In this case, stoichiometric non-covalent interactions based on host-guest chemistry were employed. Komiyama and co-workers [108] prepared suitable polymerisable  $\beta$ -cyclodextrins; these molecules form well-defined 3:1 complexes with cholesterol [112]. Copolymerisation of such a complex in the presence of a cross-linker followed by template removal left cavities with a predefined cyclodextrin array that is able to selectively recognise and rebind the template. Although the binding capacity of the polymers seems to be rather low, these reports could be the prelude to novel developments in the molecular imprinting with stoichiometric, non-covalent interactions based on the combined action of receptors which selectively bind a particular part of the substrate.

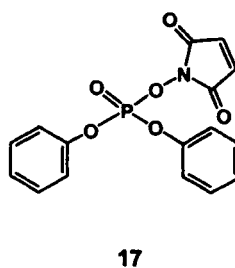
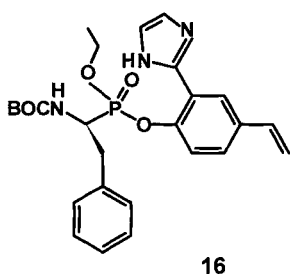
The concept of molecular imprinting was originally aimed at designing artificial materials able to mimic the properties of natural antibodies and enzymes. For many years the greatest advances in this research field have been related to the improvement of the molecular recognition properties of the polymers, while mimicking another typical feature of natural enzymes, namely their ability to catalyse reactions with high activity and selectivity, has been less successful. Only in the course of the last ten years have the advances in the molecular imprinting technology made it possible to address the problem of mimicking enzyme catalysis with some success. Interestingly, considering the contributions published to date, the performance of the most efficient imprinted polymer catalysts appears to be strictly connected with the application of stoichiometric interactions in the imprinting procedure. In fact, the need to achieve “true” catalysis, that is, high turnover numbers, necessarily implies the use of interactions which allow both a fast binding of the reagents and an efficient release of the products. On the other hand, since the binding sites serve in most cases as the catalytically active functionalities as well, an exact placement of the functional groups within the cavity and the absence of functionalities outside the cavities is crucial for the catalytic performance of the imprinted polymer.

It has already been reported that antibodies prepared against the transition state of a reaction show considerable catalytic activity [113]. For example, antibodies prepared against a phosphonic ester (as a transition state analogue for alkaline ester hydrolysis) enhanced the rate of ester hydrolysis by  $10^3$ – $10^4$  fold. Recently, similar systems based on imprinted polymers which display high catalytic activity have been successfully prepared. Initial attempts were performed by several groups [114–117] with imprinted polymers based on non-stoichiometric, non-covalent interactions, which, however, gave results far below those obtained with antibodies. Rate enhancements up to 6.7-fold were reached in one case.

Sellergren and Shea [115] tried to catalyse the same reaction by utilising an interesting covalent–non-covalent approach aimed at creating, within the imprinted cavity, a “charge relay” system similar to that found in chymotrypsin. The enantiomerically pure monomer **16** was copolymerised with methacrylic acid and a cross-linker. After hydrolysis of the phosphonic ester function of the template, the phenolic residue, together with the imidazole moiety and a methacrylic acid group interacting with the imino nitrogen in the imidazole ring, were intended to form the catalytic triad. Unfortunately, the catalytic activity of these polymers turned out to be rather low; however, a certain degree of substrate enantio-selectivity was observed.

In a similar approach, very recently an imprinting procedure using labile covalent interactions was employed with quite some success [118]. Template monomer **17** was used to imprint a transition state analogue structure and to introduce at the same time a dicarboxylate moiety in the cavity. In this case a 120-fold rate enhancement compared to the solution and 55-fold compared to a control polymer containing statistically distributed dicarboxylates was observed.

The catalysis of some other reactions by imprinted polymers also showed promising results. The dehydrofluorination of 4-fluoro-4-(4-nitrophenyl)butanone



was studied by Beach and Shea [119] and Mosbach and co-workers [120]. Shea used benzylmalonic acid as the template to precisely position two polymerisable amines within the cavity. After template removal, this catalyst enhanced the dehydrofluorination rate by a factor of 8.6.

Even stronger accelerations (25-fold) were obtained in the decarboxylation of 3-carboxybenzoxazoles [10]. In this case two amino groups were placed a suitable distance apart in the cavity by means of a polymerisable di-Schiff base.

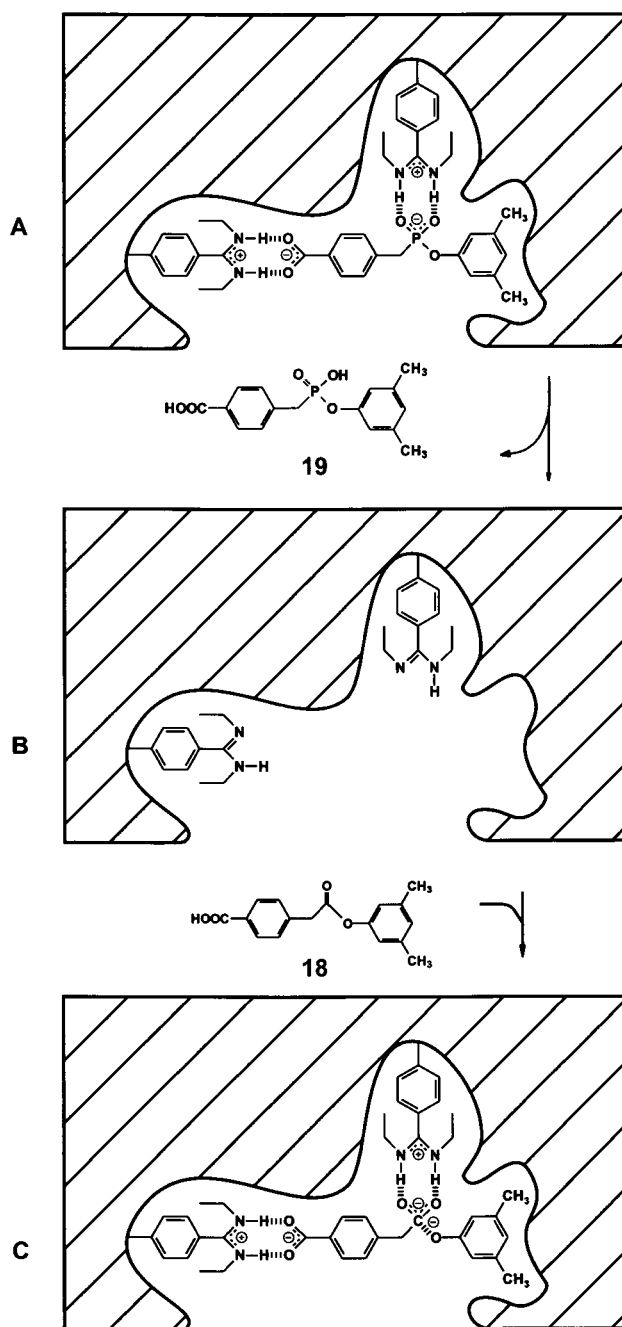
From the previous examples it is apparent that simple imprinting with a transition state analogue does not lead to cavities with sufficient catalytic activity; in addition, catalytically active groups have to be placed in proper position within the cavity. This is also true for catalytic antibodies since it was shown that for, example, a guanidinium group (of the amino acid L-arginine) plays an important role in the catalysis of the basic hydrolysis of esters by a catalytic antibody.

We had therefore turned to the application of amidine groups for both binding and catalysis as we started to investigate the alkaline hydrolysis of ester **18** (Scheme 4.V) [11]. Phosphonic monoester **19** was used as the transition state analogue; addition of two equivalents of the new binding site monomer **13** provided the bisamidinium salt. By the usual polymerisation, work-up and template removal procedures, catalytically active cavities were obtained with two amidine groups each. Owing to the stoichiometric interactions employed, the amidine groups are located in the cavities exclusively.

At pH 7.6, the imprinted polymer accelerated the rate of hydrolysis of ester **18** by more than 100-fold compared to the reaction in solution at the same pH (see equation (c) and Table 4.9). Addition of an equivalent amount of monomeric amidine to the solution only slightly increased the rate. A control polymer prepared from the amidinium-benzoate salt gave a somewhat stronger rate enhancement.

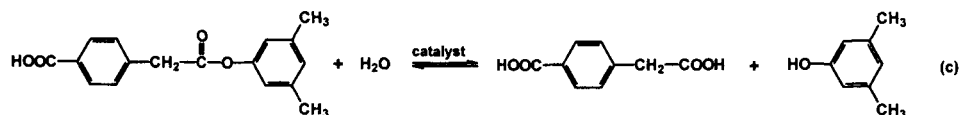
These and the following examples show the strongest catalytic effects for ester hydrolysis obtained so far by the imprinting method. Compared to antibodies, such imprinted polymers are less efficient by just one order of magnitude (see later results). This is especially remarkable since we used "polyclonal" active sites and rigid, insoluble polymers. It should also be mentioned that these hydrolyses occur with non-activated phenol esters and not, as in nearly all other reported cases, with activated 4-nitrophenyl esters.

In order to see whether or not these polymers display typical enzyme-analogue properties, we investigated the kinetics of the catalysed reaction in the presence



Scheme 4.V. Schematic representation of the polymerisation of template **19** in the presence of two equivalents of binding site monomer **13** (A), removal of **19** (B), and catalysis causing alkaline hydrolysis of **18** through a tetrahedral transition state [11].

TABLE 4.9



RELATIVE REACTION RATE CONSTANTS OF THE BASIC HYDROLYSIS OF THE ESTER 18

| pH value | Solution + amidine vs. solution | Control polymer vs. solution | TSA imprinted polymer vs. solution |
|----------|---------------------------------|------------------------------|------------------------------------|
| 7.0      | 1.5                             | 10.9                         | 49.0                               |
| 7.6      | 2.4                             | 20.5                         | 102.2 (235.3) <sup>a</sup>         |
| 9.0      | 1.9                             | 4.7                          | 17.6                               |

Kinetics were followed by HPLC determining the diacid released. The ratios refer to the reaction in buffer/acetonitrile at the same pH. This value is defined as 1.0.

<sup>a</sup>Relative enhancement on determination of the phenol released.

of various substrate to catalyst ratios. Figure 4.8 shows the observed typical Michaelis–Menten kinetics. Saturation phenomena occur at higher concentrations. This indicates that all active sites are then occupied and the reaction becomes independent of substrate concentration. In contrast, much slower kinetics, with a linear relationship are observed in solution and in solution with the addition of amidine. The polymer prepared from amidinium benzoate also exhibits Michaelis–Menten kinetics to some extent. Benzoate seems therefore to act as a less effective template.

The Michaelis constant was determined to be  $K_m = 0.60$  mM. Turnover numbers are relatively low ( $k_{cat} = 0.4 \times 10^{-2}/\text{min}$ ) but are definitely present. Furthermore, we found that the template molecule itself is a powerful competitive inhibitor with  $K_i = 0.025$  mM, i.e. it is bound more strongly than the substrate by a factor of 20. It is remarkable that such a strong binding of substrate or template occurs in water–acetonitrile 1:1. Binding in aqueous solution by the usual electrostatic interactions or hydrogen bonding is much weaker.

Similar to catalytic antibodies, we observed some product inhibition. In the case mentioned, the reaction rate was calculated from the amount of released acid. If the calculation is based on phenol release, the rate enhancement turned out to be nearly doubled. Hydrolysis of carbonates should avoid this difficulty. Therefore, diphenyl phosphate was used as template, and the hydrolysis of diphenyl carbonate was then investigated [13]. Compared to solution an enhancement of 982-fold was obtained and typical Michaelis–Menten kinetics were observed ( $V_{max} = 0.023$  mM/min,  $K_m = 5.01$  mM,  $k_{cat} = 0.0115/\text{min}$ ,  $k_{cat}/K_m = 2.30/\text{min/M}$ ).

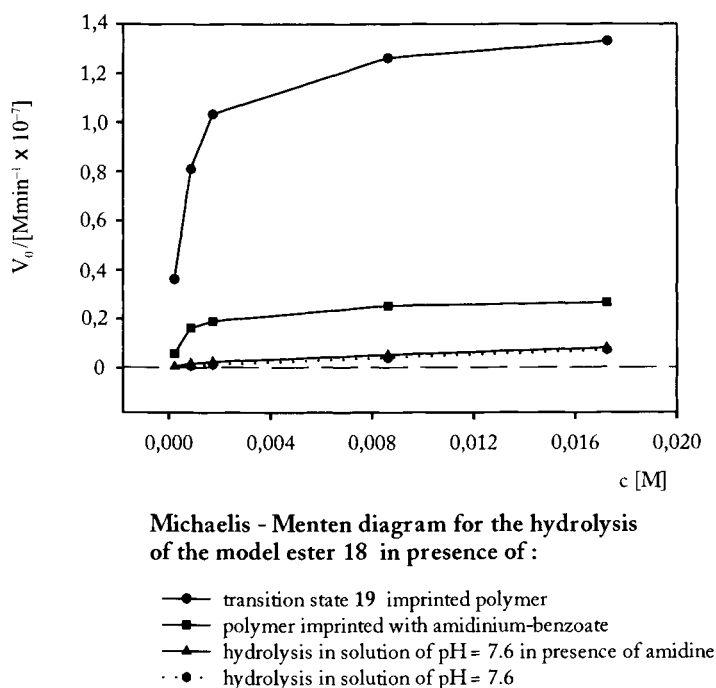


Fig. 4.8. Michaelis–Menten kinetics of the hydrolysis of **18** according to equation (c) in the presence of different catalysts. The initial rates versus substrate concentration are plotted.

Finally, the last few years have seen the first examples of the use of molecular-imprinted, polymer-supported catalysts for achieving product selectivity. The imprinted cavities are tailored in such a way that the course of a chemical reaction is directed towards one of the possible products. In the previous section it has already been shown that molecularly imprinted polymers used as microreactors are able to impart to a given reaction a different regio- and stereo-selectivity with respect to the same reaction in solution. Attempts towards an imprinted enantio-selective catalyst were reported by Gamez and co-workers who employed as template monomer an optically active, polymerisable ruthenium complex bearing in its coordination sphere an enantiomerically pure alkoxide [121]. After polymerisation, the alkoxide was split off and the resulting polymer-supported catalyst was used for enantio-selective hydride transfer reductions. The obtained selectivity was higher than for a polymer prepared without the optically active alkoxide but lower than for the same ruthenium complex in solution.

A similar approach was employed in our laboratory for the development of molecularly imprinted catalysts for the enantio-selective reduction of prochiral ketones with borane (CBS reaction) [122]. A stable, polymerisable transition state analogue of this reaction leading to the formation of one particular enantiomer product was prepared (Fig. 4.9). After polymerisation, the template molecule can

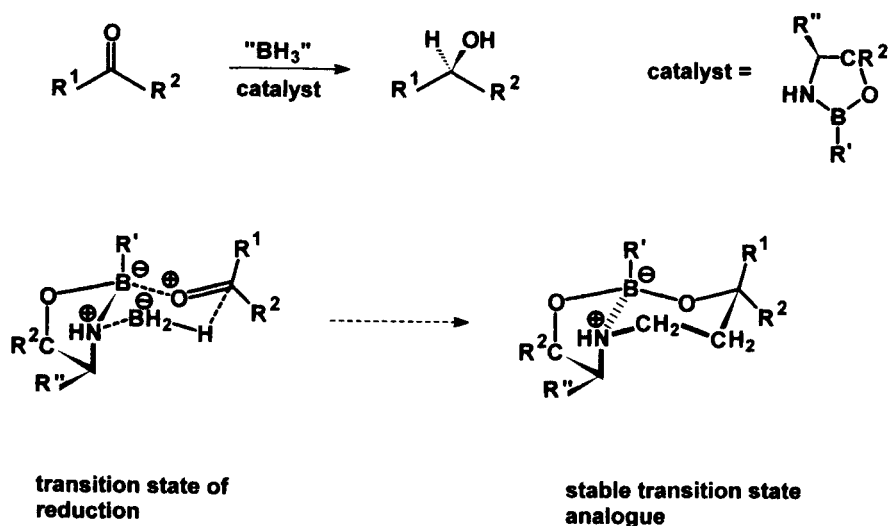


Fig. 4.9. Enantio-selective reduction of prochiral ketones using oxazaborolidines as catalysts. The transition state of the reaction and a stable transition state analogue are represented.

be hydrolysed, leaving polymer-bound boronic acid groups which can be subsequently coupled with aminoalcohols to give polymer-bound oxazaborolidines embedded within imprinted cavities complementary to a predetermined transition state of the reaction.

However, also in this case enantio-selectivities never exceeded the values obtained with the oxazaborolidine in solution, probably because of diffusional limitations within the polymer support, which enhanced the contribution of the non-selective, direct borane reduction of the ketone. In spite of the rather low imprinting effects obtained in these initial attempts, we feel that this approach still represents a most interesting application of molecularly imprinted polymers in catalysis and deserves further attention in the near future.

## ACKNOWLEDGEMENTS

These investigations were supported by financial grants from the Deutsche Forschungsgemeinschaft, the Minister für Wissenschaft und Forschung des Landes Nordrhein-Westfalen, and the Fonds der Chemischen Industrie.

## REFERENCES

- 1 G. Wulff and A. Sarhan, *Angew. Chem. Int. Ed. Engl.*, **11**, 341 (1972).
- 2 G. Wulff and A. Sarhan, *German patent application (Offenlegungsschrift)* DE-A 2242796 (1974), *Chem. Abstr.* **83**, P 60300w (1974).



- 3 G. Wulff, A. Sarhan and K. Zabrocki, *Tetrahedron Lett.*, **44**, 4329 (1973).
- 4 G. Wulff, *Angew. Chem. Int. Ed. Engl.*, **34**, 1812 (1995).
- 5 G. Wulff, W. Vesper, R. Grobe-Einsler and A. Sarhan, *Makromol. Chem.*, **178**, 2799 (1977).
- 6 G. Wulff, In: *Polymeric reagents and catalysts*, W.T. Ford Ed., *ACS Symp. Ser.*, Vol. 308, p. 186, Washington, 1986.
- 7 B. Sellergren, M. Lepistö and K. Mosbach, *J. Am. Chem. Soc.*, **110**, 5853 (1988).
- 8 K. Mosbach and O. Ramström, *Biotechnology*, **14**, 163 (1996).
- 9 B. Sellergren, In: *Practical approach to chiral separations by liquid chromatography*, G. Subramanian Ed., VCH, Weinheim, p. 69 (1994).
- 10 S. Kato and K.J. Shea, unpublished results presented at the ACS Spring Meeting in San Francisco (1997).
- 11 G. Wulff, T. Gross and R. Schönfeld, *Angew. Chem. Int. Ed. Engl.*, **36**, 1961 (1997).
- 12 G. Wulff and R. Schönfeld, *Adv. Materials*, **10**, 957 (1998).
- 13 A. Strikowsky, D. Kasper, M. Grün, B.S. Green, J. Hradil and G. Wulff, *J. Am. Chem. Soc.*, **122**, 6295 (2000).
- 14 L. Pauling, *J. Am. Chem. Soc.*, **62**, 2643 (1940).
- 15 E. Fischer, *Ber. Dtsch. Chem. Ges.*, **27**, 2985 (1894).
- 16 F.H. Dickey, *Proc. Natl. Acad. Sci. USA*, **35**, 227 (1949).
- 17 G. Wulff, R. Kemmerer, J. Vietmeier and H.-G. Poll, *Nouv. J. Chim.*, **6**, 681 (1982).
- 18 G. Wulff, J. Vietmeier and H.-G. Poll, *Makromol. Chem.*, **188**, 731 (1987).
- 19 G. Wulff and M. Minárik, *J. Liq. Chromatogr.*, **13**, 2987 (1990).
- 20 G. Wulff and W. Vesper, *J. Chromatogr.*, **167**, 171 (1978).
- 21 G. Wulff and M. Minárik, *J. High Resolut. Chromatogr. Commun.*, **9**, 607 (1986).
- 22 G. Wulff and M. Minárik, In: *Chromatographic chiral separations*, M. Zief and L.J. Crane Eds, Marcel Dekker, New York, p. 15 (1988).
- 23 R.A. Bartsch and M. Maeda (Eds), *Molecular and ionic recognition with imprinted polymers*, ACS-Symposium Series, Washington, **703** (1998).
- 24 K.J. Shea, *Trends Polym. Sci.*, **2**, 166 (1994).
- 25 J.H.G. Steinke, I.R. Dunkin and D.C. Sherrington, *Adv. Polym. Sci.*, **123**, 81 (1995).
- 26 T. Takeuchi and J. Matsui, *Acta Polym.*, **47**, 471 (1996).
- 27 M. Kempe and K. Mosbach, *J. Chromatogr. A*, **691**, 317 (1995).
- 28 M. Kempe and K. Mosbach, *Tetrahedron Lett.*, **36**, 3563 (1995).
- 29 A. Sarhan and G. Wulff, *Makromol. Chem.*, **183**, 85 (1982).
- 30 G. Wulff, In: *Molecular interactions in bioseparations*, T.T. Ngo Ed., Plenum Press, New York, p. 363 (1993).
- 31 G. Wulff, R. Schönfeld, M. Grün, R. Baumstark, G. Wildburg and L. Häußling (BASF AG), *German Open DE A 19720345* (1998), *Chem. Abstr.*, **128**, 49,155 (1998).
- 32 A. Biffis, G. Siedlaczek and S. Stalberg, G. Wulff, *Macromol. Chem. Phys.*, in press.
- 33 A.G. Mayes and K. Mosbach, *Anal. Chem.*, **68**, 3769 (1996).
- 34 K. Hosoya, K. Yoshizako, N. Tanaka, K. Kimata, T. Araki and J. Haginaka, *Chem. Lett.*, 1437 (1994).
- 35 O. Norrlöw, M. Glad and K. Mosbach, *J. Chromatogr.*, **299**, 29 (1984).
- 36 G. Wulff, D. Oberkobusch and M. Minárik, *React. Polym. Ion Exch. Sorbents I*, **3**, 261 (1985).
- 37 G. Wulff, D. Oberkobusch and M. Minárik, In: *Proceedings of the XVIIIth Solvay Conference on Chemistry, Brussels 1983*, G. v. Binst, Ed., Springer Verlag, Berlin, p. 229 (1986).
- 38 S.D. Plunkett and F.H. Arnold, *J. Chromatogr. A*, **708**, 19 (1995).
- 39 K. Hirayama, M. Burow, Y. Morikawa and N. Minoura, *Chem. Lett.*, 731 (1998).
- 40a P.K. Dhal, S. Vidyasankar and F.H. Arnold, *Chem. Mater.*, **7**, 154 (1995).
- 40b F.H. Arnold, S. Plunkett, P.K. Dhal and S. Vidyasankar, *Polymer Preprints*, **36**, 97 (1995).
- 40c M. Glad, P. Reinholdsson and K. Mosbach, *React. Polym.*, **25**, 47 (1995).

- 41 G. Wulff and G. Kirstein, *Angew. Chem. Int. Ed. Engl.*, **29**, 684 (1990).
- 42 G. Wulff, *Angew. Chem. Int. Ed. Engl.*, **28**, 21 (1989).
- 43 G. Wulff, In: *Synthesis of polymers*, A.D. Schlüter Ed., Wiley-VCH Verlag, Weinheim, p. 375 (1998).
- 44 G. Wulff, *TIBTECH*, **11**, 85 (1993).
- 45 G. Wulff, *Mol. Cryst. Liq. Cryst.*, **276**, 1 (1996).
- 46 G. Wulff, *Pure and Appl. Chem.*, **54**, 2093 (1982).
- 47 G. Wulff, W. Dederichs, R. Grotstollen and C. Jupe, In: *Affinity chromatography and related techniques*, T.C.J. Gribnau, J. Visser and R.J.F. Nivard Eds, p. 207, Elsevier, Amsterdam 1982.
- 48 I.A. Nicholls, *Adv. Molec. Cell. Biol.*, **15**, 667 (1996).
- 49 B. Sellergren and K.J. Shea, *J. Chromatogr.*, **635**, 31 (1993).
- 50 G. Wulff and J. Schauhoff, *J. Org. Chem.*, **56**, 395 (1991).
- 51 G. Wulff and J. Haarer, *Makromol. Chem.*, **192**, 1329 (1991).
- 52 D.J. O'Shannessy, L.I. Andersson and K. Mosbach, *J. Mol. Recognit.*, **2**, 1 (1989).
- 53 K.J. Shea and D.Y. Sasaki, *J. Am. Chem. Soc.*, **111**, 3442 (1989).
- 54 A. Bergold and W.H. Scouten, In: *Solid phase biochemistry*, W.H. Scouten Ed., Wiley, New York, p. 149 (1983).
- 55 M. Lauer and G. Wulff, *J. Chem. Soc. Perk. Trans. II.*, 745 (1987).
- 56 G. Wulff, M. Lauer and H. Böhnke, *Angew. Chem. Int. Ed. Engl.*, **23**, 741 (1984).
- 57 M. Lauer, H. Böhnke, R. Grotstollen, M. Salehnia and G. Wulff, *Chem. Ber.*, **118**, 246 (1985).
- 58 G. Wulff, I. Schulze, K. Zabrocki and W. Vesper, *Makromol. Chem.*, **181**, 531 (1980).
- 59 S.A. Piletsky, E.V. Piletskaya, K. Yano, A. Kugimiya, A.V. Elgersma, R. Levi, U. Kahlow, T. Takeuchi and I. Karube, *Analyt. Letters*, **29**, 157 (1996).
- 60 S.A. Piletsky, E.V. Piletskaya, T.I. Pansyuk, A.V. El'skaya, A.E. Rachhov, R. Levi, I. Karube and G. Wulff, *Macromolecules*, **31**, 2137 (1998).
- 61 A. Sarhan and G. Wulff, *Makromol. Chem.*, **183**, 1603 (1982).
- 62 G. Wulff and A. Sarhan, In: *Chemical approaches to understanding enzyme catalysis: biomimetic chemistry and transition state analogs*, B.S. Green, Y. Ashani and D. Chipman Eds, Elsevier, Amsterdam, p. 106 (1982).
- 63 G. Wulff and J. Vietmeier, *Makromol. Chem.*, **190**, 1727 (1989).
- 64 G. Wulff and J. Vietmeier, *Makromol. Chem.*, **190**, 1717 (1989).
- 65 T. Ishii, K. Nakashima and S. Shinkai, *Chem. Commun.*, 1047 (1998).
- 66 G. Wulff and T. Huver, unpublished results, see T. Huver, PhD Thesis, University of Düsseldorf (1987).
- 67 M. Glad, D. Norrlöw, B. Sellergren, N. Siegbahn and K. Mosbach, *J. Chromatogr.*, **347** 11 (1985).
- 68 A. Sarhan, M.M. Ali and M.Y. Abdelaal, *React. Polym.*, **11**, 57 (1989).
- 69 A. Sarhan and M.A. El-Zahab, *Macromol. Chem. Rapid Commun.*, **555**, 8 (1987).
- 70 A. Sarhan, *Macromol. Chem. Rapid Commun.*, **3**, 489 (1982).
- 71 D. James, P. Linnane and S. Shinkai, *Chem. Commun.*, 281 (1996).
- 72 G. Wulff and W. Dederichs, unpublished results, see W. Dederichs, PhD Thesis, University of Düsseldorf (1983).
- 73 C.R. Smith, M.J. Whitcombe and E.N. Vulfson, In: *Separations for biotechnology: 3* D.L. Pyle Ed., Royal Society of Chemistry, Cambridge, p. 482, 1994.
- 74 Y.N. Belokon, V.J. Tararov, T.F. Savelëva, M.M. Vorobiev, S.U. Vitt, U.F. Sizov, N. A. Sukhacheva, G.U. Vasilev and V.M. Belikov, *Makromol. Chem.*, **184**, 2213 (1983).
- 75 A. Moradian and K. Mosbach, *J. Mol. Recognit.*, **2**, 167 (1989).
- 76 B. Sellergren, *Chirality*, **1**, 63 (1989).
- 77 G. Wulff and J. Gimpel, *Makromol. Chem.*, **183**, 2469 (1982).
- 78 G. Wulff and H.-G. Poll, *Makromol. Chem.*, **188**, 741 (1987).
- 79 G. Wulff, A. Sarhan, J. Gimpel and E. Lohmar, *Chem. Ber.*, **107**, 3364 (1974).
- 80 G. Wulff and E. Lohmar, *Isr. J. Chem.*, **18**, 279 (1979).

- 81 G. Wulff, W. Best and A. Akelah, *Reactive Polymers*, **2** 167 (1984).
- 82 G. Wulff and G. Wolf, *Chem. Ber.*, **119**, 1876 (1986).
- 83 G. Wulff, B. Heide and G. Helfmeier, *J. Am. Chem. Soc.*, **108**, 1089 (1986).
- 84 G. Wulff, B. Heide and G. Helfmeier, *React. Polym. Ion Exch. Sorbents*, **6**, 299 (1987).
- 85 D.C. Tahmassebi and T. Sasaki, *J. Org. Chem.*, **59**, 679 (1994).
- 86 G. Wulff and T. Görlich, unpublished results, see T. Görlich, PhD Thesis, University of Düsseldorf (1991).
- 87 K.J. Shea and T.K. Dougherty, *J. Am. Chem. Soc.*, **108**, 109 (1986).
- 88a K.J. Shea and D.Y. Sasaki, *J. Am. Chem. Soc.*, **113**, 4109 (1991).
- 88b K.J. Shea and D.Y. Sasaki, *J. Am. Chem. Soc.*, **111**, 3442 (1989).
- 89 K.J. Shea, D.Y. Sasaki and G.J. Stoddard, *Macromolecules*, **22**, 1722 (1989).
- 90 K.J. Shea and E. A. Thompson, *J. Org. Chem.*, **43**, 4253 (1978).
- 91 K.J. Shea, E.A. Thompson, S.D. Pandey and P.S. Beauchamp, *J. Am. Chem. Soc.*, **102**, 3149 (1980).
- 92 I. Damen and D.C. Neckers, *J. Am. Chem. Soc.*, **102**, 3265 (1980).
- 93 G. Wulff and I. Schulze, *Angew. Chem. Int. Ed. Engl.*, **17**, 537 (1978).
- 94 G. Wulff and I. Schulze, *Isr. J. Chem.*, **17**, 291 (1978).
- 95 Y.-T. Tao and Y.-H. Ho, *J. Chem. Soc., Chem. Commun.*, 417 (1988).
- 96 S.E. Byström, A. Börje and B. Åkermarck, *J. Am. Chem. Soc.*, **115**, 2081 (1993).
- 97a B. Sellergren and L. Andersson, *J. Org. Chem.*, **55**, 3381 (1990).
- 97b J.W. Ellis, E.S. Miroeva, J. Hilton and J.N. BeMiller, *Polym. Preprints*, **38**, 391 (1997).
- 98a M.J. Whitcombe, M.E. Rodriguez, P. Villar and E.N. Vulfson, *J. Am. Chem. Soc.*, **117**, 7105 (1995).
- 98b M.J. Whitcombe, C. Alexander and E.N. Vulfson, *Trends Food Sci. Technol.*, **8**, 140 (1997).
- 98c C. Alexander, C.R. Smith, M.Y. Whitcombe and E.N. Vulfson, *J. Am. Chem. Soc.*, **121**, 6640 (1999).
- 99 H. Asanuma, M. Kakazu, M. Shibata, T. Hishiyama and M. Komiyama, *J. Chem. Soc., Chem. Commun.*, 1971 (1997).
- 100 G. Wulff, T. Groß, R. Schönfeld, T. Schrader and C. Kirsten, In: *Molecular and ionic recognition with imprinted polymers*, R.A. Bartsch and M. Maeda Eds, ACS-Symposium Series **703**, p. 10, Washington, 1998.
- 101 G. Wulff, *CHEMTECH* **28**, 19 (1998); G. Wulff, In: *Templated organic synthesis*, F. Diederich and P.J. Stang Eds, Wiley-VCH, Weinheim, p. 39, 1999.
- 102 D.Y. Sasaki, D.J. Rush, C.E. Daitch, T.M. Alam, R.A. Assink, C.S. Ashley, C.J. Brinker and K.J. Shea, In: *Molecular ionic recognition with imprinted polymers*, R.A. Bartsch and M. Maeda Eds, ACS-Symposium Series **703**, p. 314, Washington, 1998.
- 103 B. Sellergren, *Anal. Chem.*, **66**, 1578 (1994).
- 104 B. Sellergren, *J. Chromatogr. A*, **673**, 133 (1994).
- 105 K. Tanabe, T. Takeuchi, J. Matsui, K. Ikebukuro, K. Yano and I. Karube, *J. Chem. Soc., Chem. Commun.*, 2303 (1995).
- 106 T. Schrader and C. Kirsten, *J. Chem. Soc., Chem. Commun.*, 2089 (1996).
- 107 C. Kirsten and T. Schrader, *J. Am. Chem. Soc.*, **119**, 12061 (1997).
- 108 H. Asanuma, M. Kakazu, M. Shibata, T. Hishiyama and M. Komiyama, *Supramol. Sci.*, **5**, 417 (1998).
- 109 K. Sreenivasan, *J. Appl. Polym. Sci.*, **70**, 19 (1998).
- 110 S.K. Chang, D.V. Engen, E. Fan and A.D. Hamilton, *J. Am. Chem. Soc.*, **113**, 7640 (1991).
- 111 T. Schrader, C. Kirsten and G. Wulff, unpublished results, see C. Kirsten, PhD Thesis, University of Düsseldorf (1997).
- 112 P. Claudy, J.M. Letoffe, P. Germain, J.P. Bastide, A. Bayol, S. Blasquez, R.C. Rao and B. Gonzalez, *J. Thermal. Anal.*, **37**, 2497 (1991).
- 113 See, for example, R.A. Lerner, S.J. Benkovic and P.G. Schultz, *Science*, **252**, 659 (1991).

- 114 D.K. Robinson and K. Mosbach, *J. Chem. Soc., Chem. Commun.*, 969 (1989).
- 115 B. Sellergren and K.J. Shea, *Tetrahedron Asymmetry*, **5**, 1403 (1994).
- 116 K. Ohkubo, Y. Urata, S. Hirota, Y. Honda and T. Sagawa, *J. Mol. Catal.*, **87**, L21 (1994).
- 117 M.E. Davis, *CATTECH*, 19 (1997).
- 118 J.-M. Kim, K.-D. Ahn, A. Strikowsky and G. Wulff, *Macromol. Chem. Phys.*, in press.
- 119 J.V. Beach and K.J. Shea, *J. Am. Chem. Soc.*, **116**, 379 (1994).
- 120 R. Müller, L.I. Andersson and K. Mosbach, *Makromol. Chem., Rapid Commun.*, **14**, 637 (1993).
- 121 P. Gamez, B. Dunjic, C. Pinel and M. Lemaire, *Tetrahedron Lett.*, **36**, 8779 (1996).
- 122 A. Biffis and G. Wulff, unpublished results, see A. Biffis, PhD Thesis, University of Düsseldorf (1998).

This Page Intentionally Left Blank

## The non-covalent approach to molecular imprinting

BÖRJE SELLERGRÉN

### 5.1. INTRODUCTION



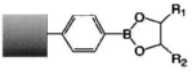
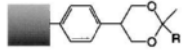
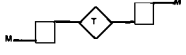

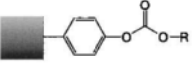
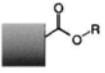


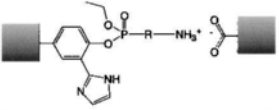
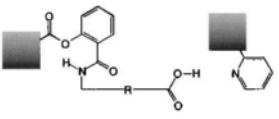
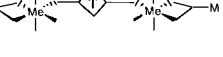
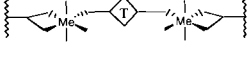
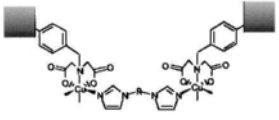

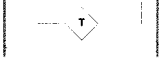
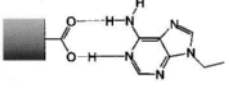
Molecularly imprinted polymers (MIPs) may be prepared according to a number of approaches that are different in the way the template is linked to the functional monomer and subsequently to the polymeric binding sites (Table 5.1) (see Chapter 4). Thus, the template can be linked and subsequently recognised by virtually any combination of cleavable covalent bonds, metal ion coordination or non-covalent bonds. The first example of molecular imprinting of organic network polymers introduced by Wulff (see Chapter 4) was based on a covalent attachment strategy, i.e. covalent monomer–template, covalent polymer–template [1]

Currently, the most widely applied technique to generate molecularly imprinted binding sites is represented by the non-covalent route developed by the group of Mosbach [2]. This is based on non-covalent self-assembly of the template with functional monomers prior to polymerisation, free radical polymerisation with a cross-linking monomer and then template extraction followed by rebinding *via* non-covalent interactions. Although the preparation of a MIP by this method is technically straightforward, it relies on the success of stabilisation of the individually weak non-covalent interactions between the template and the functional monomers. This stabilisation will in turn result in the incorporation of the functional binding groups into the templated sites. As exemplified by biological recognition elements, binding sites containing only a few, convergent, correctly positioned functional groups, may bind a substrate with very high binding energies (see Chapter 3). The imprinted materials can be synthesised and evaluated in any standardly equipped laboratory within a reasonable time and some of the MIPs exhibit binding affinities and selectivities in the order of those exhibited by antibodies for their antigens (see Chapter 14). Nevertheless, in order to develop a protocol for the recognition of any given target molecule, all the alternative linking strategies may have to be taken into account. The relative merits of the covalent and non-covalent routes are discussed in Chapters 4, 6 and 7.

Most MIPs are synthesised by free radical polymerisation of functional mono-unsaturated (vinyl, acrylic, methacrylic) monomers with an excess of cross-linking di- or tri-unsaturated (vinyl, acrylic, methacrylic) monomers, resulting in porous organic network materials. These polymerisations have the advantage of being relatively robust, allowing polymers to be prepared in high yield using different

TABLE 5.1

## APPROACHES FOR IMPRINTING SMALL MOLECULES

| Synthesis  | Rebinding  | Attachments   | Reference |
|--|--|---|-----------|
| <p><i>Covalent</i></p>              | <p><i>Covalent</i></p>              |    | [44]      |
|  |  |    | [45]      |
| <p><i>Covalent</i></p>              | <p><i>Noncovalent</i></p>           |    | [30]      |
|  |  |    | [149]     |
| <p><i>Covalent-Noncovalent</i></p>  | <p><i>Noncovalent</i></p>           |    | [122]     |
|  |  |  | [150]     |
| <p><i>Metal ion-mediated</i></p>  | <p><i>Metal ion-mediated</i></p>  |  | [151]     |
| <p><i>Noncovalent</i></p>         | <p><i>Noncovalent</i></p>         |  | [24]      |

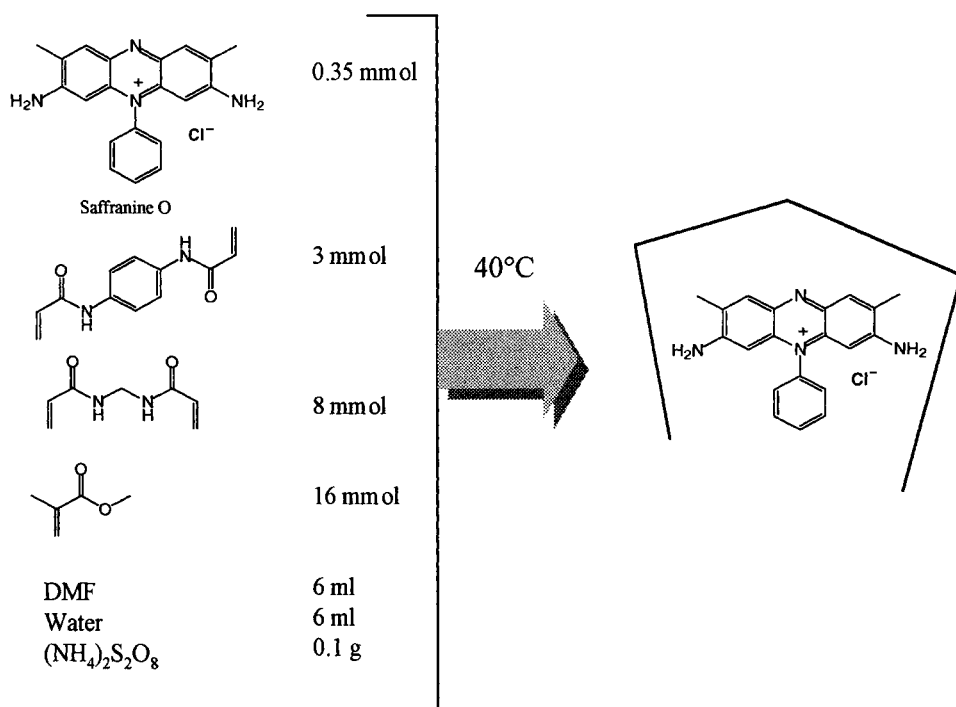


Fig. 5.1. Imprinting of saffranine O in cross-linked polyacrylamide gel [5].

solvents (aqueous or organic) and at different temperatures (see Chapter 2) [3]. Thus, conditions that are compatible with the different solubilities and stabilities of the template molecules can be chosen.

In the first examples of non-covalent imprinting in organic polymers, various dyes and alkaloids were imprinted in polyacrylamide gels (Fig. 5.1). Cross-linking monomers (<50%), usually a mixture of *N,N'*-methylenediacylamide and *N,N'*-1,4-phenylenediacylamide, and methylmethacrylate (MMA) plus in some cases a functional monomer, such as dimethylaminoethyl methacrylate, were polymerised in the presence of the dye (e.g. saffranine, rhodanil blue) using DMF/water mixtures as solvents. The resulting gels were subsequently studied with regards to their retention characteristics for the dyes in chromatography. In most cases the dye used as template was slightly more retained on the imprinted gel [4,5]. In view of the low nominal cross-link density, these materials were quite swellable (2.9 mL/g in DMF) and upon drying lost their recognition properties. Furthermore, the selectivities obtained were not remarkable and, due to the large swelling factors and the limited mechanical stability, the chromatographic efficiency was poor. By coating the polymers onto wide pore silica (1000 Å) modified with methacrylate groups (see Chapter 12) a slightly higher efficiency was observed, although the selectivity factors remained similar to that of the bulk material. It is likely that the



poor recognition was caused by the use of polar solvents, required to solubilise the amide monomers, and a low cross-link density.

The most successful non-covalent imprinting systems are based on commodity acrylic or methacrylic monomers, such as methacrylic acid (MAA), cross-linked with ethyleneglycol dimethacrylate (EDMA). Initially, derivatives of amino acid enantiomers were used as templates for the preparation of imprinted stationary phases for chiral separations (MICSPs), but the system has proven generally applicable to the imprinting of templates which are capable of allowing hydrogen bonding or electrostatic interactions to develop with MAA [6,7]. The procedure applied to the imprinting of L-phenylalanine anilide (L-PA) is outlined in Fig. 5.2. In the first step, the template (L-PA), the functional monomer (MAA) and the cross-linking monomer (EDMA) are dissolved in an aprotic solvent (diluent or porogen, the latter term being used when the resulting material contains permanent pores) of low to medium polarity. The free radical polymerisation is then initiated with an azo initiator, commonly 2,2'-azo-bisisobutyronitrile (AIBN), either by photochemical homolysis below room temperature [7,8] or thermochemically at 60°C or higher [6]. Lower thermochemical initiation temperatures down to 40 or 30°C may be employed, using 2,2'-azo-bis-(2,4-dimethyl-valeronitrile) (ABDV) and 2,2'-azo-bis-(4-methoxy-2,4-dimethyl-valeronitrile) respectively, or other designed initiators (see Chapters 2 and 12) [8,9]. In the final step, the resultant polymer is crushed by mortar and pestle or in a ball mill, extracted using a Soxhlet apparatus, and sieved to a particle size suitable for chromatographic (25–38  $\mu\text{m}$ ) or batch

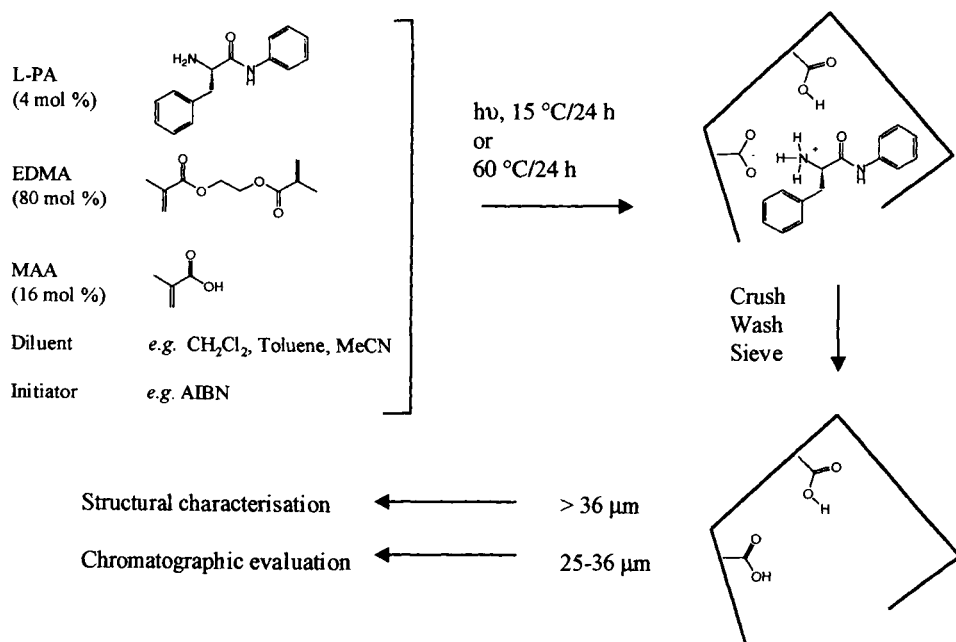


Fig. 5.2. Preparation of MIPs using L-PA as template. The L-PA model system [6].

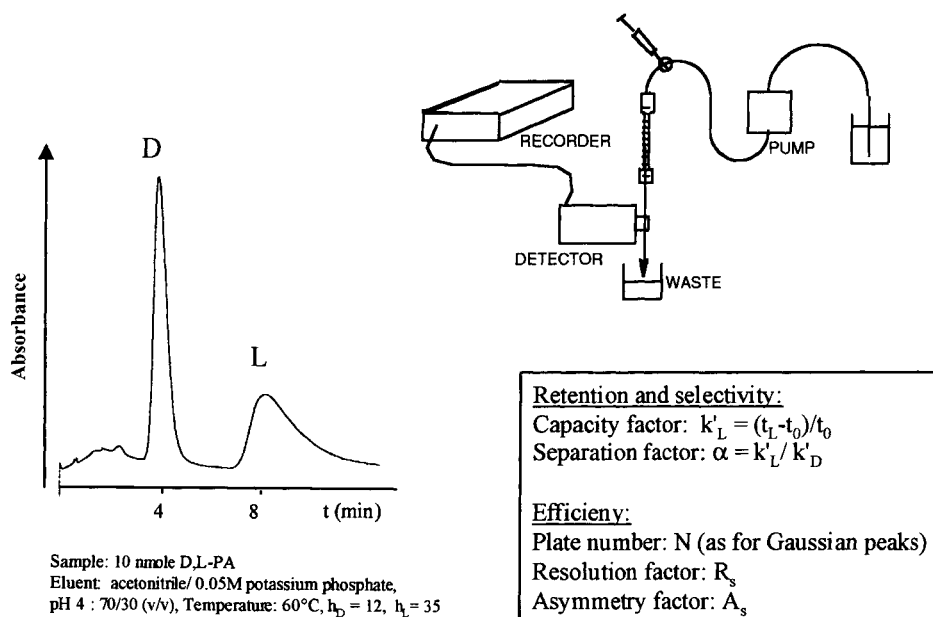


Fig. 5.3. Principle of the chromatographic evaluation of the recognition properties of MIPs.

(150–250  $\mu\text{m}$ ) applications [7]. The recognition properties of the polymers are then assessed in batch rebinding experiments, by measuring the amount of template taken up by the polymers at equilibrium, or in chromatography, by comparing the retention time or capacity factor ( $k'$ ) [10] of the template with that of structurally related analogues when using the imprinted and control polymers as stationary phases (Fig. 5.3). The latter technique can only be applied to systems where a significant part of the binding to the templated sites occurs on the time scale of the chromatographic run. As discussed in Chapter 4 this is rarely the case in systems relying on reversible covalent bonds. The system shown in Fig. 5.2 will be referred to as the L-PA model system.

In the elucidation of retention mechanisms, an advantage of using enantiomers as model templates is that non-specific binding, which affects both enantiomers equally, will cancel out. Therefore the separation factor ( $\alpha$ ) uniquely reflects the contribution to binding from the enantioselectively imprinted sites. As an additional comparison, the retention on the imprinted phase is compared with the retention on a non-imprinted reference phase. The efficiency of the separations is routinely characterised by estimating a number of theoretical plates ( $N$ ), a resolution factor ( $R_s$ ) and a peak asymmetry factor ( $A_s$ ) [10]. These quantities are affected by the quality of the packing and mass transfer limitations, as well as the amount and distribution of the binding sites.

Some restrictions of this molecular imprinting technique are obvious. The template must be available in preparative amounts, it must be soluble in the

monomer mixture and it must be stable and unreactive under the conditions of the polymerisation. The solvent must be chosen considering the stability of the monomer–template assemblies and whether it gives rise to the porous structure necessary for rapid kinetics in the interaction of the template with the binding sites. However, if these criteria are satisfied, a robust material capable of selectively rebinding the template can be easily prepared and evaluated in a short time.

## 5.2. STRUCTURE–BINDING RELATIONSHIPS

### 5.2.1. Examples of imprinted chiral stationary phases (CSPs)

As reviewed by Kempe in Chapter 17, a large number of racemates have been successfully resolved on tailor-made MIPs. Using MAA as functional monomer, good recognition is obtained for templates containing Brønsted-basic or hydrogen bonding functional groups close to the stereogenic centre. On the other hand templates containing acidic functional groups are better imprinted using a basic functional monomer, such as vinylpyridine (VPY). This emphasises the importance of functional group complementarity when designing MIPs. Furthermore, the separation factors are high and higher than those observed for many of the widely used commercial CSPs [11]. However, the columns are tailor-made and the number of racemates resolved nearly equals the number of stationary phases, i.e. each column can resolve only a limited number of racemates. Although the separation factors are high, the resolution factors are low. However, the performance can often be enhanced by running the separations at higher temperatures [6] and by switching to an aqueous mobile phase (Fig. 5.3) [7]. Enhanced performance may also be obtained by performing the imprinting *in situ* in fused silica capillaries for use in capillary electrochromatography [12,13]. At low sample loads, the retention on the MICSPs is extremely sensitive to the amount of sample injected, indicating overloading of the small amount of high energy binding sites [14]. Moreover, the peaks corresponding to the template are usually broad and asymmetric. This is ascribed to the site heterogeneity together with a slow mass transfer (see below).

#### 5.2.1.1. High enantioselectivity, high substrate selectivity

MIPs showing high selectivity for their respective template molecules were obtained when using L-PA and L-phenylalanine-*N*-methylanilide (L-PMA) respectively as templates (comparing a secondary and tertiary amide) (Fig. 5.4) [15]. The racemate corresponding to the template was well resolved on the corresponding MIP, whereas the analogue racemate was less retained and only poorly resolved. Similar results were obtained when comparing a polymer imprinted with L-phenylalanine ethyl ester and one imprinted with its phosphonate analogue and have also been observed in comparisons between a primary (1) and tertiary (2) amine [16] and two diacids, *N*-protected aspartic (3) and glutamic (4) acid [17]. Pronounced discrimination of minor structural differences have also been reported

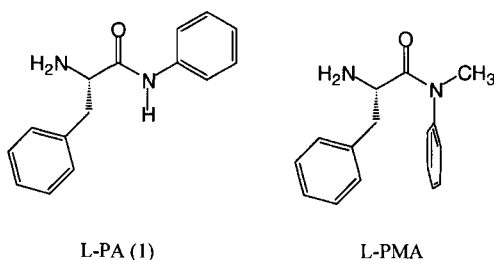
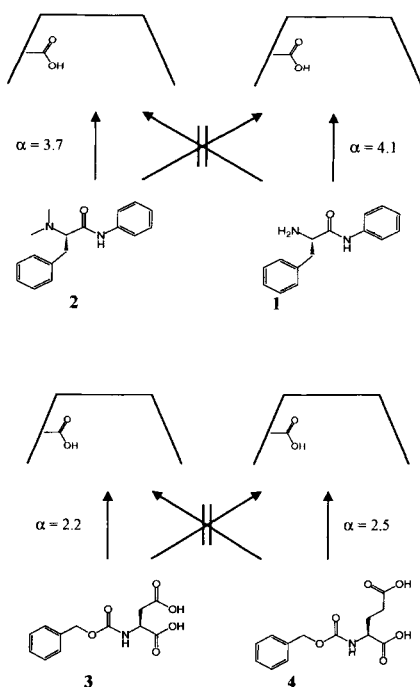
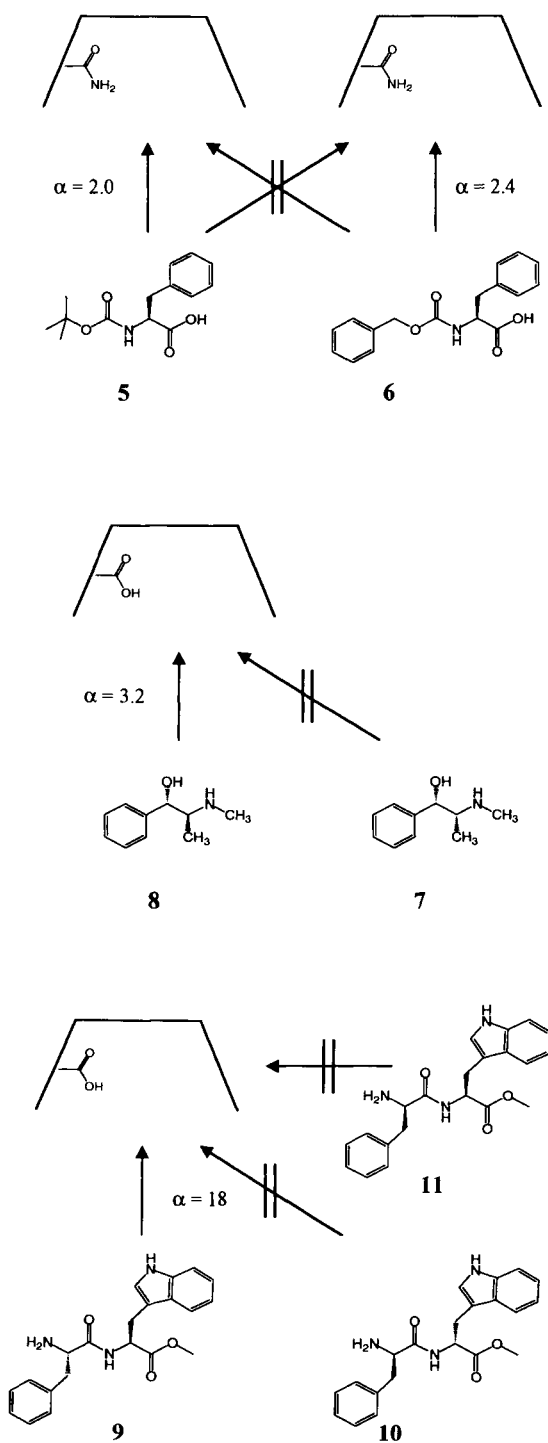


Fig. 5.4. Minimum energy conformations of L-PA and L-PMA based on molecular mechanics calculations and UV and NMR spectroscopic characterisations. From Lepistö and Sellergren [15].



in the imprinting of *N*-protected amino acids, such as (5) and (6) [18], aminoalcohols like ephedrine (7) and pseudoephedrine (8) [19], monosaccharides [20] and peptides like (9–11) [21]. Since the polymers imprinted with templates containing bulky substituents discriminated against those containing smaller substituents, the recognition is not purely a size exclusion effect. Instead it probably depends on shape complementarity between the site and the substrate as well as on conformational differences between the derivatives. It was concluded, on the basis of  $^1\text{H}$ -NMR, Nuclear Overhauser Enhancement experiments and molecular mechanics



calculations, that L-PA and the *N*-methylanilide exhibit large conformational differences. Thus, the torsional angles between the anilide ring plane and the amide plane, as well as the *E-Z* preference in the amide bond, were different [15]. The low energy conformer of the anilide has the phenyl group in a *cis*-conformation to the carbonyl oxygen with a torsional angle of about 30°, whereas in the *N*-methylanilide the phenyl group is found in a *trans*-conformation twisted almost 90° out of the amide plane. This will result in a different arrangement of the functional groups at the site. In this context it is interesting to note that the polymer imprinted with the *N*-methylanilide is less selective for its template, i.e. a lower separation factor is seen for the template compared with that observed using the L-PA imprinted polymer and, furthermore, a significant separation of the enantiomers of D,L-PA is also observed. This can be explained by considering the smaller spatial requirements of D,L-PA, which can thus be forced into a conformation matching the site of the *N*-methylanilide.

#### 5.2.1.2. High enantioselectivity, low substrate selectivity

Numerous examples of MIPs that are capable of resolving more than the racemate corresponding to the template have been reported [22,23]. In these cases some structural variations are tolerated without seriously compromising the efficiency of the separation. For instance, a polymer imprinted with L-PA resolved amino acid derivatives with different side chains or amide substituents [22]. Anilides of all aromatic amino acids were resolved, along with  $\beta$ -naphthylamides and *p*-nitroanilides of leucine and alanine (Table 5.2). Furthermore, in aqueous mobile phases, the free amino acid phenylalanine could also be baseline resolved on an L-PA imprinted polymer [23]. Apparently, substitution of groups that are not involved in potential binding interactions only leads to a small loss in enantioselectivity. Also, it was noted that the dipeptide D,L-phenylalanylglycine anilide was resolved, while glycyl-D,L-PA was not. This observation emphasises the importance of the spatial relationship between the functional groups at the sites and indicates that substitutions made some distance away from the centre of chirality are permitted.

#### 5.2.2. Antibody-like recognition

The first demonstration of high affinity, high selectivity binding to imprinted polymers was the imprinting of nitrogen heterocycles (Table 5.3) [24–26]. Here the functional monomer, MAA, could interact with many of the templates forming stable cyclic hydrogen bonds. The detection of binding of this order of strength requires methods that can measure low concentrations, down to 10<sup>-9</sup> M. This can be done by the use of labelled probes (using radioactive isotopes or fluorescent groups) competing with the target molecule for the binding site in the polymer (these methods have been thoroughly reviewed by Andersson in Chapter 14). Using such methods, a small class of high affinity binding sites and a larger class of low affinity sites are usually observed. When these polymers are evaluated in

TABLE 5.2

## RESOLUTION OF AMINO ACID DERIVATIVES ON A MIP IMPRINTED WITH L-PA

| Racemate                            | $k'_L$ | $\alpha$ |
|-------------------------------------|--------|----------|
| <i>Phenylalanine anilide</i>        | 3.5    | 2.3      |
| <i>Tyrosine anilide</i>             | 2.9    | 2.2      |
| <i>Tryptophane anilide</i>          | 2.4    | 2.0      |
| <i>Phenylalanine p-nitroanilide</i> | 3.1    | 2.1      |
| <i>Leucine p-nitroanilide</i>       | 2.1    | 1.6      |
| <i>Alanine p-nitroanilide</i>       | 2.0    | 1.6      |

Data from [22].

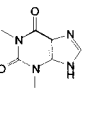
chromatography or in batch rebinding, the sites with highest affinity and selectivity for the template are not seen. Thus, most of the previously described MIPs prepared using MAA as functional monomer presumably contained high affinity site classes as well, although these were not probed. It is also apparent, from Table 5.3, that recognition is seen most often in organic solvents, but in a number of cases also in aqueous media; this medium dependence will be discussed later. When the polymers in Table 5.3 were compared with a commercial immunoassay for the same target analytes, good correlations were often observed with respect to cross-reactivities, i.e. specificity [25,26]. Comparing antibodies with MIPs, what then are the main similarities and differences in their structure function and the method of their synthesis?

Antibodies or immunoglobulins are large, soluble, globular proteins that are synthesised by an animal in response to the presence of a foreign substance [27]. They are synthesised in plasma cells called B-lymphocytes and are capable of recognising the foreign substance, or antigen, with high fidelity. The antigen is a macromolecule, i.e. protein, polysaccharide or DNA, of which a part (epitope) is recognised by the antibody. Therefore, small molecules do not stimulate antibody formation on their own, but have to be coupled (conjugated) to a macromolecular carrier (protein) in order to generate the immunoresponse. The thereby elicited antibodies can subsequently recognise the attached as well as the free molecule (hapten). A typical preparation of antibodies against a target compound starts with the design of the hapten and the choice of carrier [28]. This includes the attachment chemistry, where care has to be taken not to modify the part of the molecule for which specificity is desired. The antigen is then injected into an animal (e.g. rabbit, mouse, rat) 3 weeks apart and the immunoresponse allowed to develop over a few weeks (Fig. 5.5). At this time blood can be drawn from the immunised animal and the antibodies isolated. When the response is effective the blood can contain over several mg/mL concentrations of antibodies. In view of their affinity towards the hapten, they can be isolated by affinity chromatography using the hapten as the

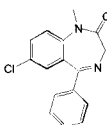
TABLE 5.3

## ASSOCIATION CONSTANTS AND SITE DENSITIES CALCULATED FROM COMPETITIVE RADIOLIGAND BINDING ASSAYS USING MIPs

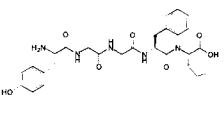
| TEMPLATE          | ASSAY MEDIUM               | ASSOCIATION CONSTANT<br>$K_a$ ( $M^{-1}$ ) |                               | BINDING SITE DENSITY<br>$n$ ( $\mu\text{mol/g}$ ) |                   | REF  |
|-------------------|----------------------------|--|-------------------------------|---|-------------------|------|
|                   |                            | CLASS 1                                    | CLASS 2                       | CLASS 1   | CLASS 2           |      |
|                   |                            |  |                               | 1   | 2                 |      |
| (1) Theophyllin   | MeCN-HOAc <sup>a</sup>     | $2.9 \cdot 10^6$                           | $1.5 \cdot 10^4$              | 0.016   | 1.3               | [25] |
| (2) Diazepam      | Toluene-Hept. <sup>b</sup> | $5.6 \cdot 10^7$                           | $4.3 \cdot 10^5$ <sup>c</sup> | 0.0062  | 0.17 <sup>c</sup> | [25] |
| (3) Enkephalin    | MeCN-HOAc <sup>a</sup>     | $7.7 \cdot 10^6$                           | $2.3 \cdot 10^4$              | 0.017   | 1.0               | [26] |
|                   | Aq. pH 4.5 <sup>d</sup>    | $1.0 \cdot 10^7$                           | $8.3 \cdot 10^4$ <sup>c</sup> | 0.004   | 0.72 <sup>c</sup> | [26] |
| (4) Morphine      | Toluene-HOAc <sup>c</sup>  | $1.1 \cdot 10^7$                           | $1.1 \cdot 10^5$              | 1.2   | 39                | [26] |
|                   | Aq. pH 6 <sup>d</sup>      | $8.3 \cdot 10^5$                           | $4.2 \cdot 10^4$              | 0.8   | 6.9               | [26] |
| (5) S-Propranolol | Toluene-HOAc <sup>c</sup>  | $2.5 \cdot 10^7$                           | $4.4 \cdot 10^4$              | 2.0   | 38                | [34] |
|                   | Aq. pH 6 <sup>d</sup>      | $2.5 \cdot 10^8$                           | $2.4 \cdot 10^5$              | 0.63  | 28                | [34] |



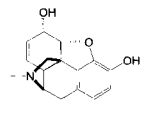
(1)



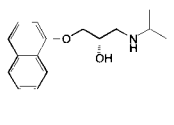
(2)



(3)



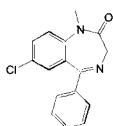
(4)



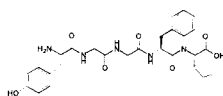
(5)



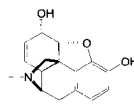
(1)



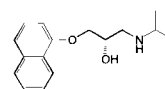
(2)



(3)



(4)



(5)

(a) Acetonitrile/acetic acid : 99/1 in the assay of (1) and 95/5 (v/v) in the assay of (3).

(b) Toluene/heptane : 3/1 (v/v).

(c) A third class of binding sites was also present with  $K_a = 1.7 \cdot 10^4 M^{-1}$  and  $n = 1.2 \mu\text{mol/g}$  in the assay of (1) and  $K_a = 2.3 \cdot 10^3 M^{-1}$  and  $n = 36 \mu\text{mol/g}$  in the assay of (3).

(d) Sodium citrate buffer (20 mM) containing 10 % or 2 % (in the assay of (5)) ethanol.

(e) Toluene/acetic acid : 98/2 (v/v) in the assay of (4) and 99.5/0.5 (v/v) in the assay of (5).

affinity ligand. The antibodies isolated after the maturation period are of the immunoglobulin G-type, with a mass of 150 kDa (Fig. 5.6). They consist of two light ( $C_L$  25 kDa) and two heavy chains ( $C_H$  50 kDa) linked by disulphide bridges, while the antigen binding occurs at the tip of the two variable (V) regions (obtained by cleavage with papain). The binding of the hapten is strong and specific, with association constants ranging from  $10^4$  to  $10^{10}/M$ , i.e. 6–15 kcal/mol. Each immunisation results in a heterogeneous population of antibodies, where each antibody-producing cell produces an antibody with a given affinity and specificity for the antigen, a polyclonal distribution. By fusing the lymphocyte cells with cancerous myeloma cells, a homogeneous population of antibodies, monoclonal antibodies,



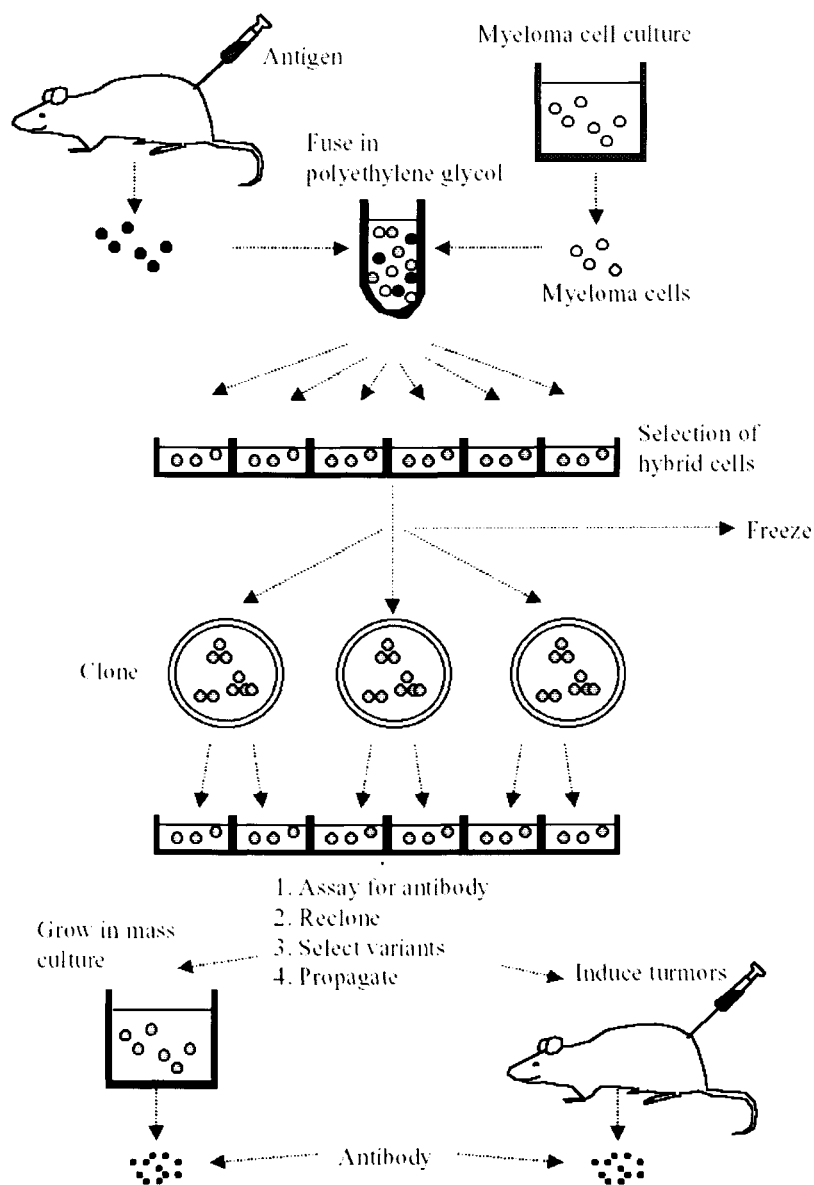
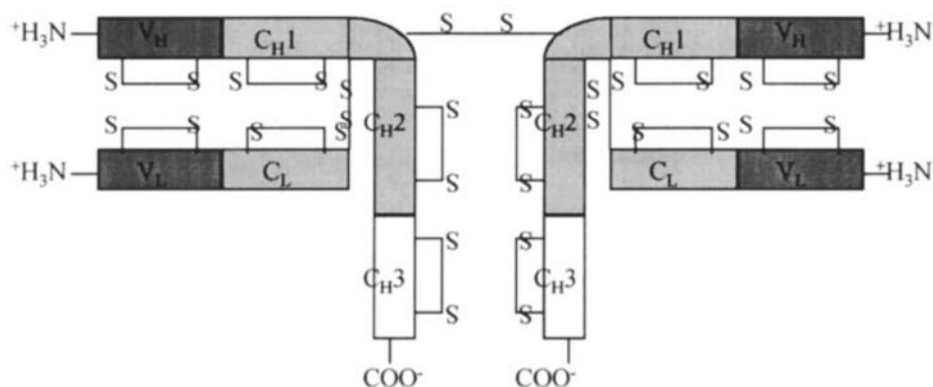


Fig. 5.5. Procedure for the preparation of monoclonal antibodies according to Milstein [148].

can be isolated. As in enzyme–substrate binding, recognition occurs by a combination of hydrogen bonding, van der Waals and ionic interactions in a site of low polarity. In contrast to enzyme–substrate recognition, however, the binding involves relatively small conformational changes in the protein.



**Fig. 5.6. Schematic structure of immunoglobulin G (IgG).**

The main difference in the synthesis of antibodies and imprinted polymers is the role of the molecular template. Whereas imprinted polymers are synthesised in the presence of a template, according to the “*instructive theory*” (see Chapter 1) once believed to be the way antibodies were synthesised [27,29], the immunor-response is rather an increase in the level of expression of already existing genes. MIPs are also polyclonal in their nature, although some templates can generate a homogeneous site population of relatively high density (see Chapter 4) [24,30,31]. In these cases the net density of binding sites is high, particularly in comparison with immobilised antibodies, and preparative scale applications should be feasible. Another difference is the medium in which these recognition elements function best. MIPs often display good recognition in organic solvents, whereas significant non-specific binding is seen in aqueous solvents [32]. However, some templates are well recognised in aqueous solvents as well [33,34]. These are usually somewhat more hydrophobic and here the hydrophobic effect contributes specifically to the recognition [32]. The MIPs are more stable and robust than antibodies [7,35]. They can withstand temperatures over 120°C [14], treatment with strong acid and base, as well as treatment with any organic solvent, with only small losses in selectivity [35]; antibodies need to be stored at low temperatures and can often only be reused in a limited number of assays or separations.

Other recognition elements are being generated by combinatorial techniques, making use of phage display peptide libraries or synthetic libraries containing many different compounds [36,37]. These can be screened according to a number of criteria in addition to the strength and specificity of binding. Thus, screening can also be done for stability and on/off kinetics, making these elements ideal for use in biosensors or as chromatographic selectors. This technology is expected to offer a competitive alternative to antibodies, providing smaller monoclonal recognition elements for a number of target compounds, with stability and affinity superior to those of antibodies.

### 5.3. ADSORPTION ISOTHERMS AND SITE DISTRIBUTION

Adsorption isotherms yield important information concerning binding energies, modes of binding and site distributions in the interaction of small molecules with adsorbent surfaces [38]. In the liquid phase applications of MIPs, a molecule in solution interacts with binding sites in a solid adsorbent. The adsorption isotherms are then simply plots of the equilibrium concentrations of bound ligand (adsorbate) versus the concentration of free ligand. The isotherms can be fitted using various models where different assumptions are made. The most simple is the Langmuir type adsorption isotherm (equation (1)), where the adsorbent is assumed to contain only one type of site; adsorbate–adsorbate interactions are assumed not to occur and the system is assumed ideal. This isotherm depends on two parameters: the saturation capacity (site density),  $q_{s1}$  (equation (2)) and the binding constant,  $b_1$ , related to  $K_a$  as shown in equation (3), with  $M_w$  being the molecular weight of the adsorbate [39,40].

$$q = \frac{a_1 C}{1 + b_1 C} \quad (1)$$

$$q_{s1} = a_1/b_1 \text{ (g/l)} \quad (2)$$

$$K_a = b_1 M_w \text{ (/M)} \quad (3)$$

The bi-Langmuir model (equation (4)) or tri-Langmuir model, the sum of two or three Langmuir isotherms, correspond to models that assume the adsorbent surface to be heterogeneous and composed of two or three different site classes. Finally the Freundlich isotherm model (equation (5)) assumes no saturation capacity, but instead, a continuous distribution of sites of different binding energies.

$$q = \frac{a_1 C}{1 + b_1 C} + \frac{a_2 C}{1 + b_2 C} \quad (4)$$

$$q = aC^{1/n} \quad (a \text{ and } n = \text{numerical parameters}) \quad (5)$$

Depending on the template–functional monomer system, the type of polymer, the conditions for its preparation and the concentration interval covered in the experiment, the adsorption isotherms of MIPs have been well fitted with all the isotherm models [24,25,41,30].

Thus, most MIPs suffer from a heterogeneous distribution of binding sites. In non-covalent imprinting, two effects contribute primarily to the binding site heterogeneity. Due to the amorphous nature of the polymer, the binding sites are not identical, somewhat similar to a polyclonal preparation of antibodies. The sites may, for instance, reside in domains with different cross-linking density and accessibility [43]. Secondly, this effect is reinforced by the incompleteness of the monomer–template association [6]. In most cases the major part of the functional monomer exists in a free or dimerised form, not associated with the template. As a consequence, only a part of the template added to the monomer mixture gives rise to selective binding sites. This contrasts with the situation in covalent imprinting

[30,42,44,45] or stoichiometric non-covalent imprinting [31] where, theoretically, all of the template split from the polymer should lead to a templated binding site. The poor yield of binding sites results in a strong dependence of selectivity and binding on sample load, at least within the low sample load regime (see later Fig. 5.25).

To determine the adsorption isotherm, the equilibrium concentrations of bound and free template have to be reliably measured within a large concentration interval. Since the binding sites are part of a solid this experiment is relatively simple. Thus, it can be done in a batch equilibrium rebinding experiment or by frontal analysis.

### 5.3.1. Batch rebinding experiments

The adsorption isotherm can be obtained by adding incremental amounts of template to a given amount of polymer, allowing the system to equilibrate and then measuring the concentration of free template in solution; the concentration of adsorbed template is then obtained by subtraction [9,24]. This has some similarities with equilibrium dialysis experiments when evaluating associations between small molecules and protein receptors [38]. The sensitivity of the method for measuring the concentrations will determine the highest measurable binding constant. This means that the use of templates containing fluorophores or radioactive isotopes will allow lower concentrations to be measured, which may reveal the existence of site classes with larger binding constants [25,26,33]. For isotherms adhering to the Langmuir isotherm model, the binding constant and saturation capacity can be estimated graphically from a linearised version of the isotherm. This is preferably done by plotting the isotherm in a Scatchard format (or  $x$  reciprocal format), where each linear region of the isotherm is fitted with a straight line by linear regression; the binding constant is calculated from the slopes and the saturation capacity from the  $y$ -intercepts (equation 6).

$$\frac{q}{C} = bq_s - bq \quad (6)$$

Figure 5.7A shows a Scatchard plot of the isotherm data for the batch rebinding of 9-ethyladenine (9EA) to a 9EA imprinted polymer prepared according to the imprinting protocol shown in Fig. 5.2 [24]. As may be seen, the plot reveals two linear regions representing two classes of binding sites. Fitting this to a bi-Langmuir model gives a pair of binding constants and site densities. The binding sites generated by non-covalent imprinting are commonly described by 2- or 3-site models, where a majority of the sites are responsible for non-specific binding, i.e. they are not template imprinted. The question is whether subtraction of the binding to a non-imprinted blank polymer from the binding to the imprinted polymer allows identification of the imprinted site classes. By subtracting the amount of 9EA bound to a blank polymer imprinted with benzylamine (BA) from the amount of 9EA bound to the 9EA-templated polymer, an adsorption isotherm adhering to a Langmuir monosite model was obtained (Fig. 5.7B). Interestingly,

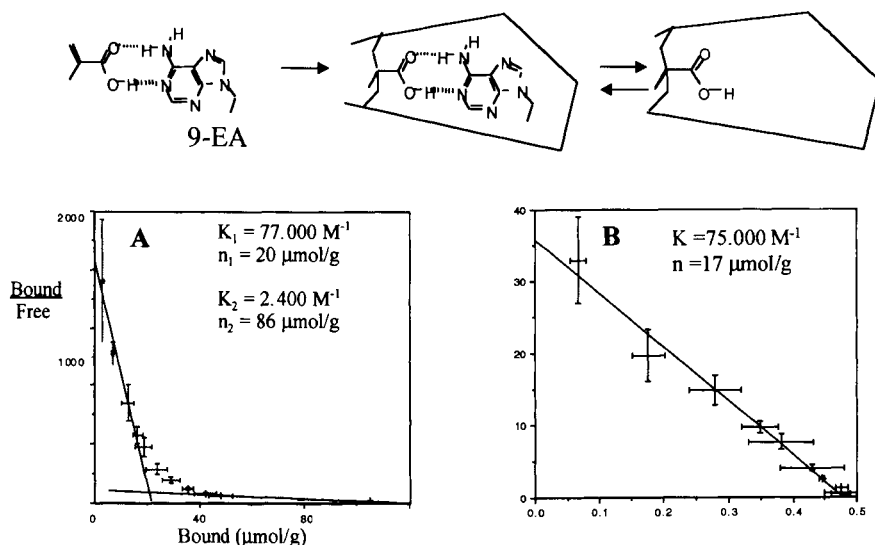


Fig. 5.7. (A) Scatchard plot of the adsorption isotherm in  $\text{CHCl}_3$  of 9EA to a MIP imprinted with 9EA (P9EA) and (B) Scatchard plot of the differential binding to PEA after subtraction of the binding to a MIP imprinted with BA. From Shea *et al.* [24].

the binding constant and saturation capacity obtained from the Scatchard plot agreed well with those obtained from the direct plot of the binding data. This shows that the second low energy site class is indeed responsible for non-specific binding in this polymer. Furthermore, in view of the linear Scatchard plot, the high energy sites appear to be uniform and isolated, which stands in contrast to the isotherms obtained for other non-covalently imprinted polymers [9,46,47]. These sites amount to *ca.*  $20 \text{ μmol/g}$  polymer, corresponding to a yield of imprinted sites of *ca.* 35%, based on the amount of template added to the monomer mixture. This value is not typical for MIPs, where instead saturation capacities in the range of  $1 \text{ μmol/g}$  or lower are seen; this corresponds to a yield of binding sites of less than 1% [9,48]. Again this depends on the sensitivity of the technique used to measure the concentrations. The particular efficiency of the 9EA template in generating uniform high energy sites is believed to be due to the favourable cyclic hydrogen bonded structures it forms with carboxylic acids in chloroform (see below). It should also be noted that the strongest binding was observed using chloroform as solvent, i.e. the same solvent used in the preparation of the materials. Considerably lower binding constants were observed in more polar protic solvents (Table 5.4). That recognition is more efficient in organic solvents is a commonly observed phenomenon. However, a number of templates are also well recognised in aqueous solvents [32,34,40,49]. The 9EA-templated sites are highly selective. Thus the 9EA imprinted polymers retained adenine bases over other purine or pyrimidine bases and nucleosides (Table 5.5).

TABLE 5.4

## ASSOCIATION CONSTANTS FOR THE BINDING OF 9EA TO MIPs

| Polymer | Solvent                 | Site class | $K_a$ (/M)           | $n$ ( $\mu\text{mol/g}$ ) |
|---------|-------------------------|------------|----------------------|---------------------------|
| P(EA)   | $\text{CHCl}_3$         | 1          | $7.5 \times 10^4$    | 19                        |
|         |                         | 2          | $2.4 \times 10^3$    | 86                        |
| P(BA)   |                         | 1          | $1.4 \times 10^3$    | 53                        |
|         |                         | 2          | 0.3                  | 120                       |
| P(EA)   | $\text{MeCN/HOAc aq}^a$ |            | $0.7 \times 10^{3a}$ | 23                        |
| P(BA)   |                         |            | $0.4 \times 10^3$    | 12                        |

The data are average results of three independent batch binding experiments where the association constants  $K_a$  have been determined from the linear regions of the corresponding Scatchard plots. The site classes have been identified from a biphasic behaviour of the plots. P(EA) refers to a MIP imprinted with 9EA and P(BA) to a MIP imprinted with BA. Data from [24].

<sup>a</sup>Acetonitrile/acetic acid/water: 92.5/5/2.5 (v/v/v).

### 5.3.2. Results from frontal analysis

One powerful technique for the study of the interactions between solutes and stationary phases and for the investigation of the parameters of these interactions is frontal analysis [50]. This method allows accurate determination of adsorption and kinetic data from simple breakthrough experiments and the technique has proven its validity in a number of previous studies. It has also been used to estimate the adsorption energies and saturation capacities in the binding of templates to MIPs, but often the data have been modelled only at one temperature and graphically evaluated using a simple Langmuir mono-site model, which in most cases gives a poor fit of the data [46]. Furthermore, the breakthrough curves are interpreted assuming thermodynamic equilibrium, which is often an invalid assumption in view of the slow mass transfer in these systems. Instead, based on the mass balance equation and by assuming kinetic and isotherm values to best fit isotherms and elution profiles obtained at different temperatures, a more accurate picture of the thermodynamics and mass transfer of the system can be obtained [50].

The isotherms for the two enantiomers of phenylalanine anilide were measured at 40, 50, 60 and 70°C and the data fitted to each of the models given in equations (1), (4) and (5), using the transport model of chromatography (see Fig. 5.8) [40]. The

TABLE 5.5

## CHROMATOGRAPHIC RETENTION VOLUMES OF PURINES AND PYRIMIDINES ON 9EA (PEA) AND BA (PBA) IMPRINTED MIPs

| Solute                                   | <i>V</i> (ml) on PEA | <i>V</i> (ml) on PBA |
|--|----------------------|----------------------|
| 9-ethyladenine (9EA)                     | <b>49</b>            | 2.5                  |
| Benzylamine (BA)                         | 1.7                  | <b>3.1</b>           |
| 1-Cyclohexyluracil                       | 2.1                  | 1.8                  |
| 1-Propyl cytosine                        | 1.8                  | 1.9                  |
| 1-Propyl thymidine                       | 1.9                  | 1.7                  |
| Adenine                                  | <b>24</b>            | —                    |
| Guanine                                  | 1.8                  | 1.6                  |
| Uracil                                   | 2.0                  | 1.7                  |
| Cytosine                                 | 2.8                  | 2.0                  |
| Thymine                                  | 2.1                  | 1.8                  |
| Adenosine                                | <b>15</b>            | 3.0                  |
| Guanosine                                | 4.9                  | 3.5                  |
| Uridine                                  | 2.0                  | 1.7                  |
| Cytidine                                 | 2.2                  | 2.6                  |
| Thymidine                                | 1.9                  | 1.7                  |
| 2'-deoxy-Adenine                         | <b>17</b>            | 2.8                  |
| 2'-deoxy-Guanine                         | 3.9                  | 2.7                  |
| 2'-deoxy-Uridine                         | 2.0                  | 1.7                  |
| 2'-deoxy-Cytidine                        | 2.1                  | 2.0                  |
| 2'-5'-deoxy-Cytidine                     | 1.9                  | 1.9                  |
| 2',3',5'-tri- <i>O</i> -acetyl-Adenosine | <b>5.1</b>           | 1.8                  |
| 2',3',5'-tri- <i>O</i> -acetyl-Guanosine | 1.9                  | 1.6                  |
| 2',3',5'-tri- <i>O</i> -acetyl-Uridine   | 1.6                  | 1.5                  |
| 2',3',5'-tri- <i>O</i> -acetyl-Cytidine  | 1.6                  | 1.5                  |
| 3',5'-di- <i>O</i> -acetyl-Thymidine     | 1.7                  | 1.6                  |
| 2',3'-isopropylidene-Adenosine           | <b>9.7</b>           | 2.4                  |
| 2',3'-isopropylidene-Guanosine           | 2.7                  | 2.0                  |

The chromatographic investigation was performed using acetonitrile/acetic acid/water: 92.5/5/2.5 (v/v/v) as mobile phase. 10  $\mu$ l of a 1.0 mM solution of each solute were injected. Guanine and guanosine were injected as 0.1 mM solutions. Data from [24]

lines in the main figure illustrate the best fits of the experimental data to the bi-Langmuir isotherm equation at 40, 50, 60 and 70°C respectively. The top-left insert shows their best fits to the Langmuir isotherm equation and the bottom-right inset to the Freundlich isotherm equation. The isotherms obtained by fitting the data to the Langmuir equation are of a lower quality than the other two. Both the Freundlich and the bi-Langmuir model gave good fits. A comparison of the residuals reveals that the different isotherms of D-PA are best fitted to a bi-Langmuir model, while the isotherms for L-PA are slightly better fitted to a Freundlich isotherm

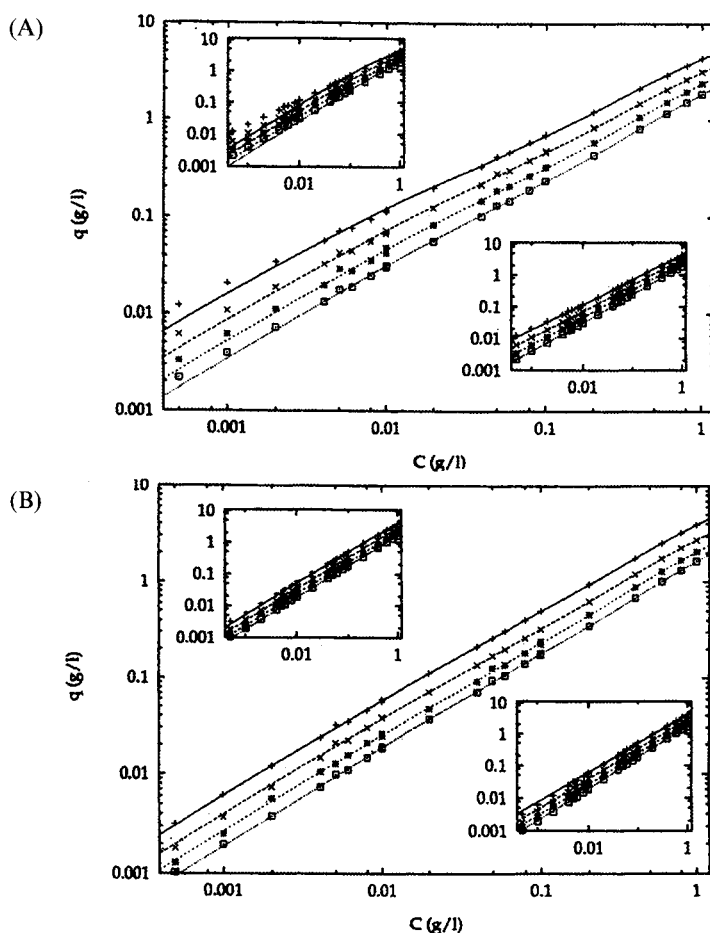


Fig. 5.8. Frontal analysis of the binding of D- and L-PA to an MIP imprinted with L-PA. The MIP was prepared using dichloromethane as diluent following the procedure shown in Fig. 5.2. Fitting (lines) of the experimental isotherm data (symbols) for L-PA (A) and D-PA (B) to the bi-Langmuir model (main figure), the Langmuir model (left inset) and the Freundlich model (right inset). For the runs at 40°C: solid lines and plus symbols, at 50°C: long dashed lines and crosses, at 60°C: short dashed lines and stars, at 70°C: dotted lines and squares. Mobile phase: MeCN/potassium phosphate buffer 0.05 M, pH 5.85: 70/30 (v/v). From Sajonz *et al.* [40].

model, particularly at low temperatures. However, at concentrations higher than  $17 \mu\text{M}$  ( $4 \times 10^{-3} \text{ g/l}$ ), the isotherm data of L-PA are equally well fitted to the Freundlich and to the bi-Langmuir isotherm models, suggesting the existence of binding sites with higher binding energies ( $K > 50,000/\text{M}$ ). The binding constants and the saturation capacities agree well with values determined in other studies [9]. At 40°C, for L-PA, these are respectively 84/M and 90  $\mu\text{mol/g}$  for the class 2 sites



and 16,000/M and 1  $\mu\text{mol/g}$  for the class 1 sites. For D-PA, the respective values are 48/M and 136  $\mu\text{mol/g}$  for the class 2 sites and 5520/M and 0.4  $\mu\text{mol/g}$  for the class 1 sites. In view of the small saturation capacities observed for D-PA on these sites, with the exception of the result obtained at 40°C, the first site class appears to be nearly specific for L-PA.[14]. Finally, in agreement with previous findings, the class 2 sites exhibit a certain selectivity for L-PA.

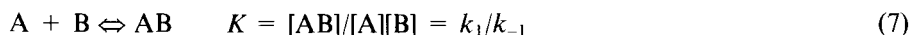
The fact that the isotherm data for L-PA were better fitted to the Freundlich isotherm at lower concentrations agrees with previous studies on other template systems, where the isotherm data were often best fitted to tri-Langmuir models [25]. Competitive assays using radiolabelled substrates allowed the identification of a class of sites with a very low surface coverage (*ca.* 1 nmol/g) and high binding constants (up to  $1 \times 10^9/\text{M}$ ) (Table 5.3).

## 5.4. ADSORPTION-DESORPTION KINETICS AND CHROMATOGRAPHIC BAND BROADENING

For most applications of specific molecular recognition elements, fast association-dissociation kinetics in the host-guest interactions are important. In chemical sensors, the response time depends on the association rate between the sensor-bound receptor and the target analyte, whereas the dissociation rate affects how fast the sensor can be regenerated [51]. The kinetics thus influence the sample throughput of the analysis, i.e. how many samples can be analysed in a certain time interval. Furthermore, in catalysis, the binding kinetics, if being the rate limiting step, determine the rate of the chemical transformation and, in chromatographic separations, it will influence the spreading of the chromatographic peaks.

### 5.4.1. Adsorption-desorption kinetics in batch rebinding experiments

As follows from the equilibrium expression for the association of two molecules [38],



the association kinetics are second order and the dissociation kinetics first order:

$$v_1 = k_1[\text{A}][\text{B}] \quad (8)$$

$$v_{-1} = k_{-1}[\text{AB}] \quad (9)$$

In the homogeneous binding of antigens to antibodies, the association rate is usually diffusion controlled and the rate constant is therefore found to be in the order of  $10^7$  to  $10^8/\text{M.s}$ . The dissociation, on the other hand, depends on the affinity of the antibody for the antigen and is usually found to be in the range  $10^{-7}/\text{s}$  to  $10^2/\text{s}$  [52]. The rates become slower in heterogeneous systems due to additional diffusional mass transfer limitations. On/off kinetics in antibody-antigen interactions have been thoroughly studied using surface plasmon resonance instruments [53]. In these studies the typical association and dissociation rate constants

were in the order of  $10^5/\text{M/s}$  and  $10^{-3}/\text{s}$  respectively. The latter constants should be compared with the heterogeneous kinetics in the binding of templates to MIP binding sites. Only a few reports on batch rebinding kinetics have been published (see Chapter 18). In the binding of 9EA to 9EA imprinted polymers, a minimum value of  $k_1$  of  $10^2 \text{ M/s}$  and of  $k_{-1}$  of  $10^{-2}/\text{s}$  was estimated (Fig. 5.9). These rate constants result in lengthy equilibration times, most often in the order of several hours [35,54]. It is also clear that in the timescale of a chromatographic experiment these processes will contribute significantly to the broadening of the chromatographic peaks.

#### 5.4.2. Peak dispersion and asymmetry in chromatography using MIP-phases

When a solute band passes through a chromatographic column it is continuously broadened due to various dispersion processes [55,56]. These include processes that show little or no flow rate dependence, such as eddy-diffusion or extracolumn effects, and flow rate dependent processes, such as (i) axial diffusion, (ii) mass transfer processes, including mobile phase, intra-particle and stationary phase diffusion, and (iii) slow kinetic processes upon interaction with the stationary phase. Other factors, such as non-linear binding isotherms and slow desorption rates, affect the symmetry of the peak [57,58]. Together these processes counteract the separation of two compounds and lead to poorer resolutions. An understanding of their origin is important in order to improve the separations and also to gain insight into the kinetics and mechanism of solute retention.

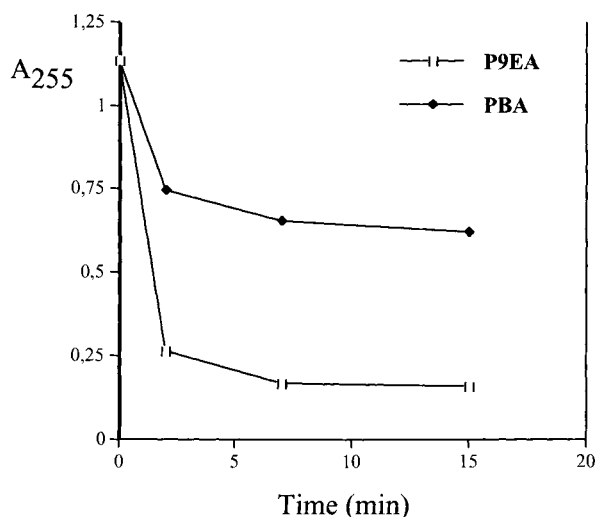


Fig. 5.9. Room temperature kinetics of the adsorption of 9EA (2 mL of a 0.1 mM solution in chloroform) to a MIP imprinted with 9EA (P9EA, 50 mg) and one with BA (PBA).

In enantiomer separations of D,L-PA on L-PA imprinted CSPs the dependence of the chromatographic parameters on flow rate and sample load was studied [59]. Using a thermally annealed stationary phase, a strong dependence of the asymmetry factor ( $A_s$ ) of the L-form on sample load and a weak dependence on flow rate suggested that column overloading contributed strongly to the peak asymmetry (Fig. 5.10). This is to be expected in view of the site heterogeneity discussed in the previous section. However, slow kinetic processes are another contributing factor to the pronounced band broadening in chromatography using MIP-based columns. In view of the high binding constants observed for MIPs, the desorption rate at the high energy binding sites should be much slower than that at the low energy sites.

Since the retention of the template on the imprinted polymers strongly depends on the sample load (see later Fig. 5.25), the theoretical models describing the various dispersion processes are not applicable. Nevertheless, on an imprinted CSP for L-PA, the least retained enantiomer, D-PA, elutes as a fairly Gaussian peak (Fig. 5.3), which should be governed by the same band broadening mechanisms that are considered in the models. A measure of the dispersion of a Gaussian peak is the deviation from its mean value, which is reflected in the reduced plate height as:

$$h = H/d_p = L/(d_p N) \quad (10)$$

where  $d_p$  is the average particle diameter,  $H$  is the height equivalent to a theoretical plate,  $L$  is the column length and  $N$  the number of theoretical plates. If the contributions to peak broadening operate independently from each other (not applicable in non-linear chromatography),  $h$  can be expressed as a sum of these contributions:

$$h = h_{ax} + h_c + h_{ediff} + h_{idiff} + h_{kin} \quad (11)$$

where  $h_{ax}$  is the contribution from axial diffusion in the mobile and stationary phases,  $h_c$  is the contribution from eddy-diffusion,  $h_{ediff}$  is the film resistance to mass transfer at the particle boundary,  $h_{idiff}$  is the contribution from slow intra-

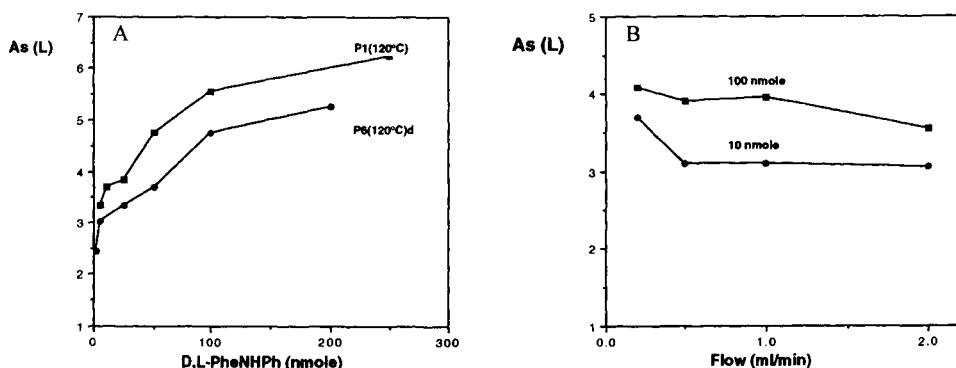


Fig. 5.10. Peak asymmetry versus sample load (A) and flow rate (B) in the chromatography of D,L-PA (10 nmol) injected on an L-PA imprinted stationary phase. Mobile phase: MeCN/0.05 M potassium phosphate buffer, pH 4: 70/30 (v/v).

particle diffusion and  $h_{\text{kin}}$  is the contribution from slow kinetic processes in the interactions with the stationary phase. The sum of the latter two terms is commonly known as the mass transfer term.

For porous ion exchange resins it has been found that  $h$  depends on  $u$  approximately as:

$$h = Cu^\beta \quad (12)$$

$$\ln h = \ln C + \beta \ln u \quad (13)$$

where  $\beta$  is a function of the packing, particle size and the exchanging solute and  $C$  a function of the rate of intra-particle diffusion and sorption-desorption [60]. It follows that  $\ln h$  should be a linear function of  $\ln u$  with slope  $\beta$  and intercept  $\ln C$ .

In Fig. 5.11 this plot is seen for D- and L-PA and a non-retained acetone void marker at two temperatures on a column packed with an L-PA MIP. This MIP was prepared using benzene as porogen and evaluated at neutral pH [59]. The plots are all linear and seem to adhere to equation (12). Thus, at 20°C,  $\beta$  of the retained solutes is slightly higher than  $\beta$  for the non-retained acetone and  $C$  increases with increasing retention. At 45°C, however,  $\beta$  for the retained solutes is the same as that of acetone. The plots for acetone do not change with temperature, indicating that the diffusion of neutral solutes in the mobile phase does not control the band spreading. Interestingly, the plots in Fig. 5.11 are similar to plots obtained in anion

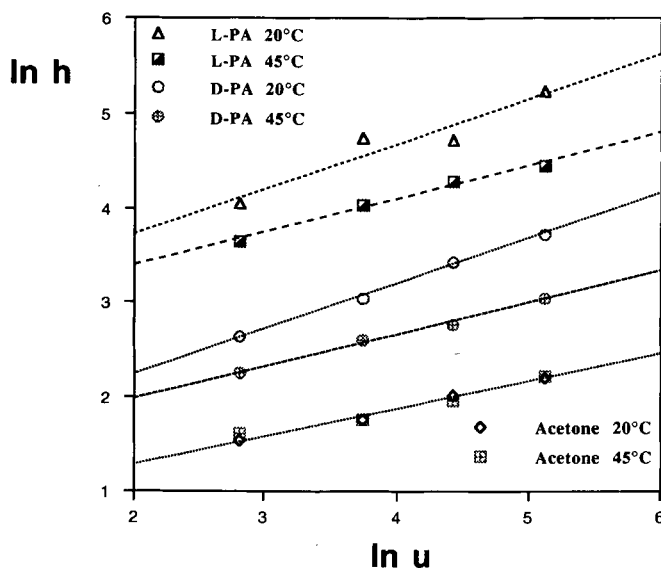


Fig. 5.11. Double logarithmic plot of the reduced plate height ( $h$ ) versus the linear mobile phase velocity ( $u$ ) in the chromatography of D,L-PA (100 nmol) on an L-PA MIP prepared using benzene as diluent at two different column temperatures. At 20°C  $k'_L \approx 6$ ,  $k'_D \approx 2.5$ . At 45°C:  $k'_L \approx 2.1$ ,  $k'_D \approx 1.0$ . Mobile phase: MeCN/potassium phosphate buffer 0.05 M, pH 7 : 70/30 (v/v). From Sellergren and Shea [59].

exchange chromatography of nucleosides, where  $C$  increases with  $k'$  and where both  $C$  and  $\beta$  decrease with temperature [61]. Here, the mass transfer is believed to be limited by slow intra-particle diffusion. This contrasts with bonded phase chromatography where the plots are non-linear but parallel and where no significant mass transfer problems are present [56].

In the frontal analysis experiment described in Section 5.3.2, the transport model of chromatography was used to fit the experimental data [40]. Neglecting axial and eddy diffusion, band broadening was accounted for by one single mass transfer rate coefficient. The mass transfer rate coefficients estimated were small and strongly dependent on the temperature and solute concentration, particularly the rate coefficients corresponding to the imprinted L-enantiomer (Fig. 5.12). Above a concentration of *ca.* 0.1 g/L the mass transfer rate coefficients of the two enantiomers are similar.

Figure 5.13 shows overloaded elution profiles obtained for three different injection volumes of solutions of the same concentrations of the two enantiomers of PA (dashed lines). The solid lines in these figures show the band profiles numerically calculated for a concentration dependent mass transfer coefficient  $k_f$  (main figure), a low concentration value of  $k_f$  (upper inset) and a high concentration value of  $k_f$  (lower inset). For the L-enantiomer, the best fit of the data is obtained using the concentration dependent rate constant, while for the D-enantiomer the best fit is obtained using a constant value of  $k_f$  equal to 35/min (low concentration value).

The concentration dependence of the rate coefficients can be accounted for by assuming the existence of a small number of high energy sites, exhibiting slow

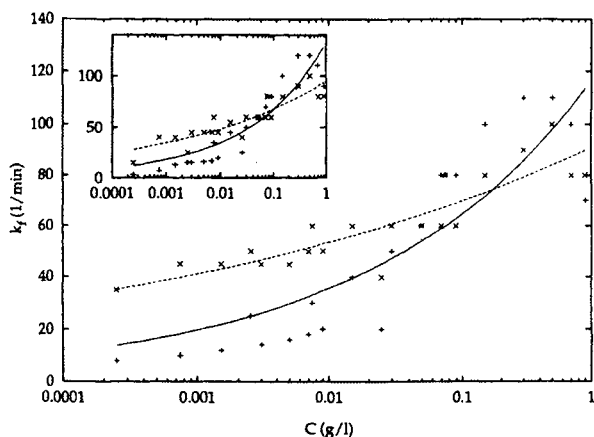


Fig. 5.12. The concentration dependence of  $k_f$  obtained from frontal analysis for L- (solid lines and plus symbols) and D- (dashed lines and crosses) PA at 40°C using a bi-Langmuir isotherm (main figure) or a Freundlich isotherm (inset) to fit the data. Experimental data (symbols) were fitted (lines) to the function:  $k_f = k_{f,0}C^n$ . Mobile phase: MeCN/potassium phosphate 0.05 M, pH 5.85; 70/30 (v/v). The MIP was prepared using L-PA as template and dichloromethane as diluent following the procedure shown in Fig. 5.2. From Sajonz *et al.* [40].

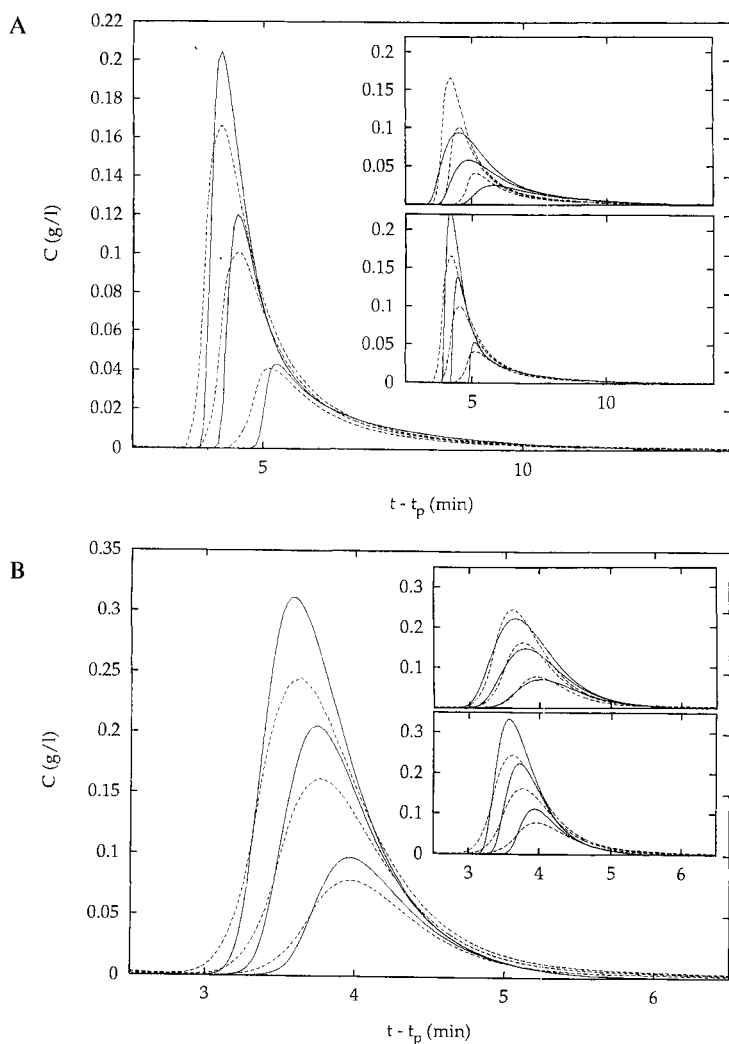


Fig. 5.13. Example of overloaded elution profiles from the frontal analysis runs described in Fig. 5.8 and Fig. 5.12. D,L-PA was injected at sample volumes of 240, 160 and 80  $\mu\text{l}$  at a sample concentration of 1 g/L and a temperature of 40°C. Experimental data: dotted lines. Numerical calculations: solid lines. (A) L-PA, main figure:  $k_f = 117.3 \text{ C}^{0.2582}/\text{min}$ , upper inset:  $k_f = 10/\text{min}$ , lower inset:  $k_f = 110/\text{min}$ . (B) D-PA, main figure:  $k_f = 90.9 \text{ C}^{0.1147}/\text{min}$ , upper inset:  $k_f = 35/\text{min}$ , lower inset:  $k_f = 90/\text{min}$ . Mobile phase: MeCN/potassium phosphate buffer 0.05 M, pH 5.85: 70/30 (v/v). From Sajonz *et al.*[40].

exchange kinetics, and less selective sites where the substrates are bound and released more rapidly.

Slow mass transfer processes have also been observed in other chromatographic separations using MIP stationary phases. For instance, studies of the retention

mechanism of both enantiomers of dansyl-phenylalanine on a dansyl-L-phenylalanine MIP led to similar conclusions [62]. However, it should be noted that this factor, apart from depending on the concentration interval, strongly depends on the system studied, i.e. template–monomer system, cross-linking monomer, diluent and method of polymerisation.

## 5.5. FACTORS INFLUENCING THE RECOGNITION PROPERTIES OF MIPs

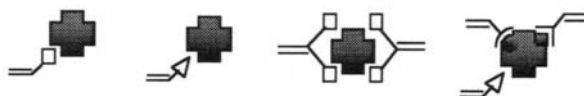
It is of obvious importance that the functional monomers strongly interact with the template prior to polymerisation, since the solution structure of the resulting assemblies presumably defines the subsequently formed binding sites. By stabilising the monomer–template assemblies it is possible to increase the number of imprinted sites. At the same time the number of non-specific binding sites will be minimised, since there will be a reduction in the amount of free, non-associated functional monomer. For any particular template, the following factors that are likely to affect the recognition properties of the site have been identified (Fig. 5.14).

### 5.5.1. Choice of the functional monomer

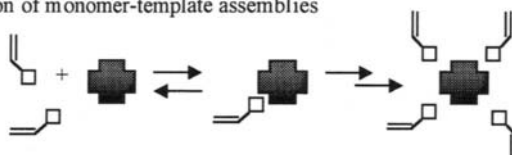
The strength and positioning of the monomer–template interactions are of importance to obtain materials with good molecular recognition properties. The broad applicability of MAA as a functional monomer is related to the fact that the carboxylic acid group serves well as a hydrogen bond and proton donor as well as a hydrogen bond acceptor [63]. In aprotic solvents such as acetonitrile, carboxylic acids and amine bases form contact hydrogen bonded assemblies where the association strength for a given acid increases with the basicity of the base [64]. Thus, templates containing Brønsted-basic or hydrogen bonding functional groups are potentially suitable templates for the MAA/EDMA system [6]. Furthermore, more stable cyclic hydrogen bonds can form with templates containing acid [17], amide [16] or functionalised nitrogen heterocycles [24,25]. For the pre-polymerisation complexes discussed thus far, the electrostatic interactions are sensitive to the presence of polar protic solvents. However, exceptions are the complexes formed between carboxylic acids and guanidines or amidines [65,66]. Here cyclic hydrogen bonded ion pairs are formed with stability constants that are an order of magnitude higher than those previously discussed (see later Table 5.12). This allows amidines such as pentamidine (**12**) to be imprinted using *iso*-propanol/water as a porogenic solvent mixture, resulting in polymers that bind pentamidine strongly in aqueous solvents [67].

Apart from the successful examples discussed above, the recognition for many templates is far from that required for the particular application, even after careful optimisation of the other factors affecting the molecular recognition properties. Often, a large excess of MAA in the synthesis step is required for recognition to be observed and then only in solvents of low to medium polarity and hydrogen bond capacity [68]. In fact, in these cases the optimum rebinding solvent is often the solvent used as diluent (see under Section 5.7.) [69]. Thus the polymer exhibits

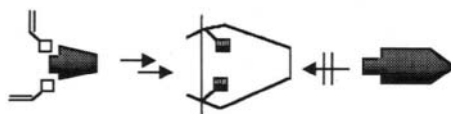
- Choice of the functional monomer



- Stabilisation of monomer-template assemblies



- Template size and shape



- Monomer-template conformational rigidity



Fig. 5.14. Factors affecting the recognition properties of MIPs related to the monomer-template assemblies.

memory for the diluent as well as the template. Moreover, the excess of functional monomer results in a portion not being associated with imprinted sites. These sites interact non-selectively with solutes with affinity for carboxylic acids and limit the degree of separation that can be achieved. Hence MAA, although broadly applicable, is not a universal monomer for the generation of high affinity sites. Instead, for the recognition of any given target molecule, access to functional monomers targeted towards structural features specific for particular compounds or classes of compounds is required. (Table 5.6).

Based on the structural features of the templates that generate good sites, an interesting possibility would be to incorporate these structures in new functional monomers for the recognition of carboxylic acids. This concept is somewhat similar to the reciprocity concept in the design of CSPs [70]. Thus Wulff *et al.* synthesised *N,N'*-disubstituted *p*-vinylbenzamidines (see **13** in Table 5.6B) and showed that these monomers could be used to generate high fidelity sites for the molecular

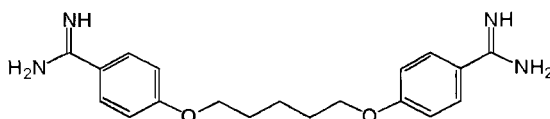
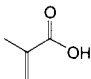
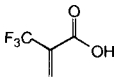
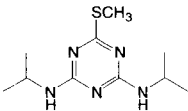
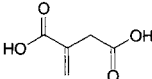
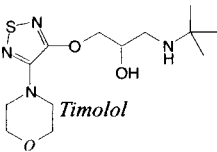
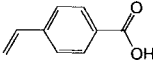
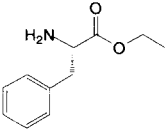
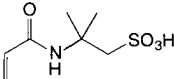
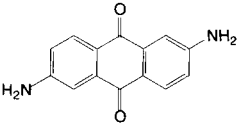




TABLE 5.6A

## ACIDIC FUNCTIONAL MONOMERS GIVING ENHANCED REBINDING SELECTIVITY IN NON-COVALENT MOLECULAR IMPRINTING

| Monomer  | Example of template   | Note   | Reference |
|--|---|--|-----------|
| <br>MAA   | <i>Hydrogen bond and proton accepting compounds</i>   |  | [130]     |
| <br>Trifluoromethyl acrylic acid (TFM)              | <br>Prometryn (PRO)              | <i>Enhanced selectivity in terpolymer with MAA</i>         | [87]      |
| <br>Itaconic acid (ITA)                             | <br>Timolol                      | <i>Similar results as with MAA</i>                         | [152]     |
| <br>p-Vinylbenzoic acid (PVB)                      | <br>L-Phenylalanine ethyl ester | <i>Using DVB as crosslinker</i>                            | [153]     |
| <br>Acrylamidomethylpropane sulfonic acid (AMPSA) | <br>2,6-diaminoantraquinone    | <i>No selectivity seen using MAA as functional monomer</i> | [154]     |

recognition of chiral carboxylic acids (see Chapter 4) [66]. The binding is strong enough to provide efficient recognition in aqueous solvents too. Furthermore, due to the strong binding, the functional monomer is quantitatively associated with the template, minimising non-specific binding. Functional group complementarity is thus the basis for the choice of functional monomer.

In this context other commodity monomers may also be used. Thus, for templates containing acid groups, basic functional monomers are preferably chosen

(Table 5.6B). 2- or 4-VPY are particularly well suited for the imprinting of carboxylic acid templates and provide materials with selectivities of the same order as those obtained using MAA for basic templates [71,72]. However, these polymers are susceptible to oxidative degradation and require special handling.

In the imprinting of carboxylic acids and amides high selectivities are also seen using acrylamide (AAM) as functional monomer [18], while the use of *N,N*-diethyl-2-aminoethylmethacrylate (DEAEMA) has led to materials showing high selectivity for alcohols, e.g. chloramphenicol [73], and polar templates such as nucleotides [74,75]. Other amino monomers, such as *N,N,N*-trimethyl-2-aminoethylmethacrylate and allylamine, have been used in combination with *p*-vinylbenzeneboronic acid in the imprinting of sialic acid in DMF. The resulting polymers exhibited recognition for sialic acid in aqueous media [76–78]. Finally 2-aminoethyl methacrylate has been used in the imprinting of diacids for the construction of a catalytic site for dehydrofluorination [79]. Some hydrophilic templates, some poorly soluble in organic solvents, can be imprinted using 2-hydroxyethylmethacrylate (HEMA) in polar diluents [77,80–82]. Thus, polymers exhibiting high selectivity for creatinine [83] and salicylic acid [84] in aqueous solvents have been prepared using methanol/water mixtures as diluents. Also, using HEMA as functional monomer, in combination with a fluorescent cationic monomer, cyclic adenosine monophosphate (cAMP) was successfully imprinted [85]. The resulting polymer was used as a fluorescence sensor for the template. Furthermore, combinations of two or more functional monomers, giving terpolymers or higher, have in a number of cases given polymers with better recognition ability than the recognition observed from the corresponding copolymers [54,71,72,86,87]. These systems are particularly complex when the monomers constitute a donor–acceptor pair, since monomer–monomer association will compete strongly with template–monomer association if neither of the monomers has a particular preference for the template. In a recent series of papers by the group of Liangmo, careful optimisation showed that a combination of AAM and 2-VPY gave significantly higher enantioselectivities in the imprinting of *N*-protected amino acids than the combination of 2-VPY with MAA [88]. Furthermore, better results were obtained using acetonitrile as the diluent in contrast to other systems where solvents of lower polarity (e.g. toluene, dichloromethane, chloroform) give the best results. These results show that adequate performance can only be achieved after careful optimisation where the related factors are varied systematically.

The search for the optimal structural motif to complement the template functionality may also be guided by results from the area of host–guest and ligand–receptor chemistry. Thus, based on a receptor developed by Hamilton *et al.* for the molecular recognition of barbiturates [89], a diacryloyl-diaminopyridine was used to complement the imide structural motif found in barbiturates [90]. In the case of poorly polar to apolar templates, with few polar functional groups that can provide interaction sites for polar functional monomers, it may instead be beneficial to use amphiphilic monomers, stabilising the monomer–template assemblies by hydrophobic and Van der Waals' forces. Thus, cyclodextrins have been used to template binding sites for cholesterol [91] or to enhance the selectivity in the imprinting of

TABLE 5.6B

## BASIC AND CHARGED FUNCTIONAL MONOMERS GIVING ENHANCED REBINDING SELECTIVITY IN NON-COVALENT MOLECULAR IMPRINTING

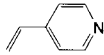
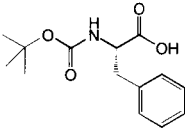
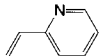
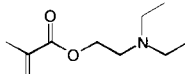
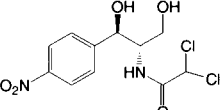
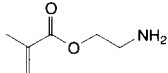
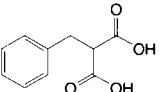
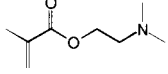
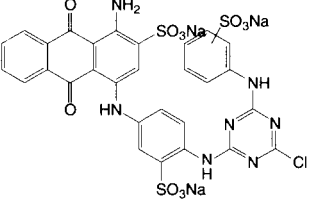
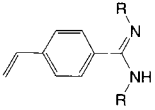
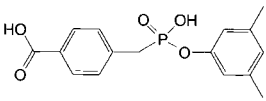
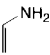
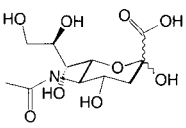
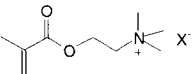
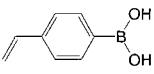
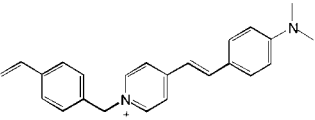
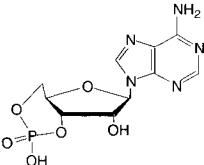
| Monomer  | Example of template   | Note  | Reference    |
|--|---|---|--------------|
| <br>4-vinylpyridine (4VPY)                                | <br><i>N</i> -tBOC- <i>L</i> -phenylalanine<br>2,4-D ( <i>vide infra</i> ) | Often enhanced selectivity as terpolymer with MAA or AA | [71,133,155] |
| <br>2-vinylpyridine (2VPY)                                | see 4VPY  | see 4VPY  | [72]         |
| <br><i>N,N</i> -diethyl-2-aminoethylmethacrylate (DEAEMA) | <br>Chloramphenicol<br>Nucleotides   | Competitive assay developed                             | [73]         |
| <br>2-aminoethylmethacrylate (AEMA)                     | <br>Benzylmalonic acid   | Dehydro-fluorination catalyst                           | [79]         |
| <br><i>N,N</i> -dimethyl-2-aminoethylacrylate           | <br>Cibachron blue   |   | [156]        |

TABLE 5.6B *continued*

| Monomer  | Example of template  | Note   | Reference |
|--|--|--|-----------|
| <br>4-vinyl-1-( <i>N,N'</i> -dialkylamidino)benzene ( <b>13</b> ) | <br>Transition state-analogue | Hydrolytic enzyme models                                     | [31]      |
| <br>Allylamine  | <br>Sialic acid               | Used in combination with <i>p</i> -vinylphenyl-boronic acid: | [78]      |
| <br>Monomers with quarternary ammonium groups                     |                               |  | [77]      |
| <br>X <sup>-</sup>   | <br>cAMP                     | Used in combination with HEMA                                | [85]      |

enantiomers of amino acids [92]. Monomers based on bile acids or cholesterol (**14A** in Table 5.6C) have also been used to generate binding sites for cholesterol (**14B** in Table 5.6C) [93]. In a comparison of a number of common adsorbents, the adsorbents imprinted with cholesterol exhibited the largest uptake of cholesterol from intestinal-mimicking fluids at physiologically relevant concentrations.

Based on chiral functional monomers such as (**15**) in Table 5.6C MIPs capable of chiral resolution can be prepared using a racemic template. Thus, using racemic *N*-(3,5-dinitrobenzoyl)- $\alpha$ -methylbenzylamine (**16** in Table 5.6C) as template, a polymer capable of racemic resolution of the template was obtained [86]. Another chiral monomer based on L-valine (**17**) was used to prepare MIPs for the separation of dipeptide diastereomers [94]. In these cases, the configurational chirality inherent in the pendant groups of the polymer are to some extent themselves chiral selectors and the effect of imprinting is merely to enhance the selectivity. Alternative approaches to imprint peptides *via* strong monomer–template association have recently been

TABLE 5.6C

UNCHARGED FUNCTIONAL MONOMERS GIVING ENHANCED REBINDING SELECTIVITY IN NON-COVALENT MOLECULAR IMPRINTING

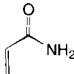
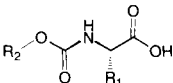
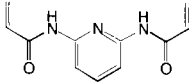
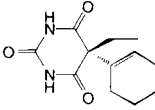
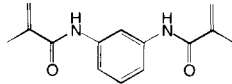
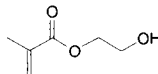
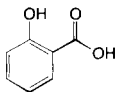
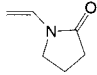
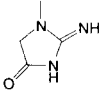
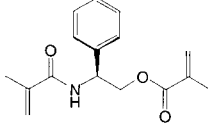
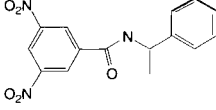
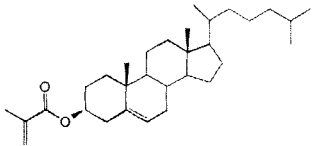
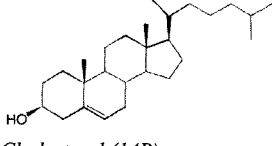
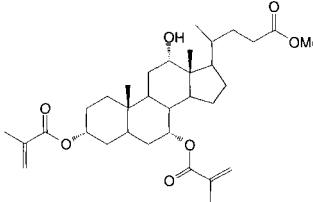
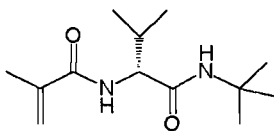
| Monomer   | Example of template   | Note   | Reference |
|---|---|--|-----------|
| <br><i>Acrylamide (AAM)</i>                        | <br><i>N-protected amino acids</i>                           | <i>Sometimes in combination with VPY</i>       | [18, 133] |
| <br><i>N,N'-bisacryloyl-diaminopyridine</i>        | <br><i>Cyclobarbital</i>                                     | <i>Rebinding in chloroform</i>                 | [90]      |
| <br><i>N,N'-bismethacryloyl-1,3-diaminobenzene</i> | <i>L-PA</i>   | <i>Used in combination with MAA</i>            | [7]       |
| <br><i>2-hydroxyethylmethacrylate (HEMA)</i>      | <br><i>Salicylic acid</i>                                   |  | [80, 84]  |
| <br><i>N-vinylpyrrolidone</i>                    | <br><i>Creatinine</i>                                      | <i>Highest selectivity was seen using HEMA</i> | [83]      |
| <br><i>N,O-dimethacryloylphenylglycinol</i> (15) | <br><i>N-(3,5-dinitrobenzoyl)-α-methylbenzylamine</i> (16) | + MAA  | [157]     |

TABLE 5.6C *continued*

| Monomer  | Example of template  | Note   | Reference |
|--|--|--|-----------|
| <br>3-β-methacryloylcholesterol(14A)                | <br>Cholesterol (14B) | +MAA<br>Rebinding of<br>cholesterol from<br>gastrointestinal<br>mimicking fluids | [93]      |
| <br>3α,7α-dimethacryloylcholic acid<br>methyl ester | Cholesterol  | +MAA   | [93]      |

reported (see Chapter 4), although no results of the chromatographic application of these phases have been shown. Strong complexation capable of inducing a  $\beta$ -sheet conformation was possible using a designed functional monomer [95].

Thus, enhanced separations can be obtained using configurationally chiral monomers (selectors) in combination with molecular imprinting. What about selectors with conformational chirality? Can chirality be induced by molecular imprinting? This concept was elegantly demonstrated by Welch using a brush-type stationary phase containing a slowly interconverting (in the order of a day) racemic atropisomer (**18**) as imprintable selector (Fig. 5.15) [96]. Leaving the selector in contact with an enantiomerically pure template molecule (selectand) (**19**) for more than 2 weeks led to induction of the most stable selector-selectand complex. After washing out the selectand, the selector could be used to separate the racemate of (**19**) with a similar separation factor to that obtained using the reciprocal phase. However, due to interconversion, the chiral phase racemised over a period of 2–3 days, a period that can possibly be extended by storing the phase at low temperatures. Also mentioned was the interesting possibility of using a selection of slowly



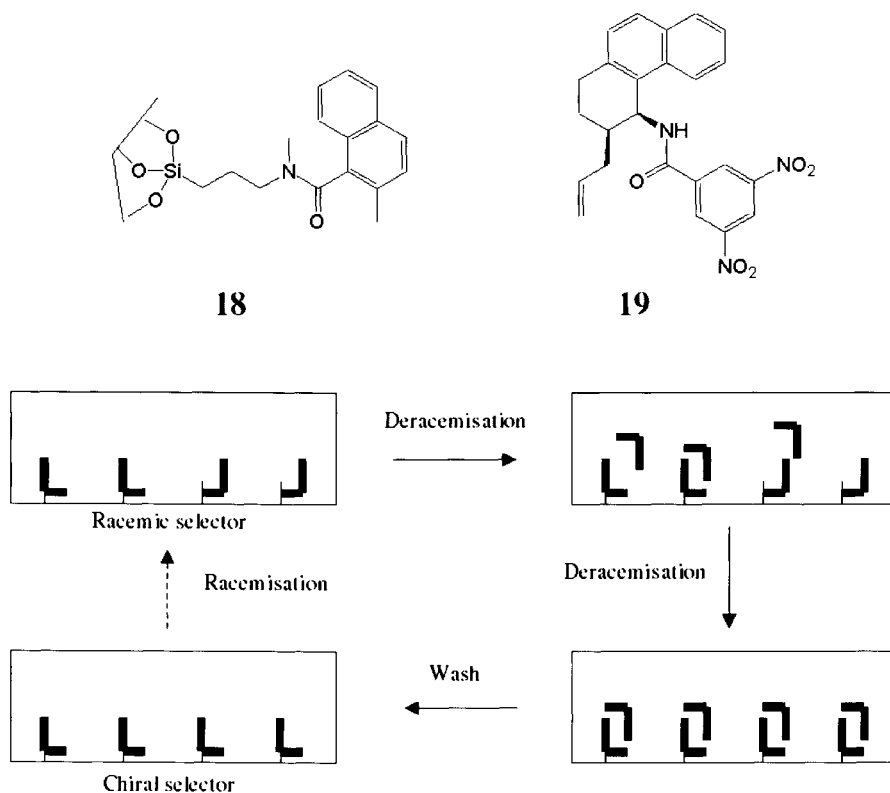


Fig. 5.15. Imprintable brush type selectors by Welch [96].

interconverting selectors to achieve a broadly applicable system for atropisomer-based imprinting.

### 5.5.2. Influence of the number of template interaction sites

Molecular recognition in biological systems takes place by the combination of several complementary weak interactions between a biological binding site and the molecule to be bound [97]. A larger number of complementary interactions will increase the strength and fidelity of the recognition. Thus, templates offering multiple sites for interaction with the functional monomer are likely to yield binding sites of higher specificity and affinity for the template [1]. One example of this effect was observed in a study of the molecular imprinting of enantiomers of phenylalanine derivatives (Fig. 5.16) [6,98]. Starting with L-phenylalanine ethyl ester as the template, interactions with carboxylic acids in acetonitrile should consist of the ammonium carboxylate ion pair, as well as a weak ester-carboxylic acid hydrogen bond (indicated by arrows). By replacing either the ester group with the stronger hydrogen bonding amide group or by introducing an aromatic amino

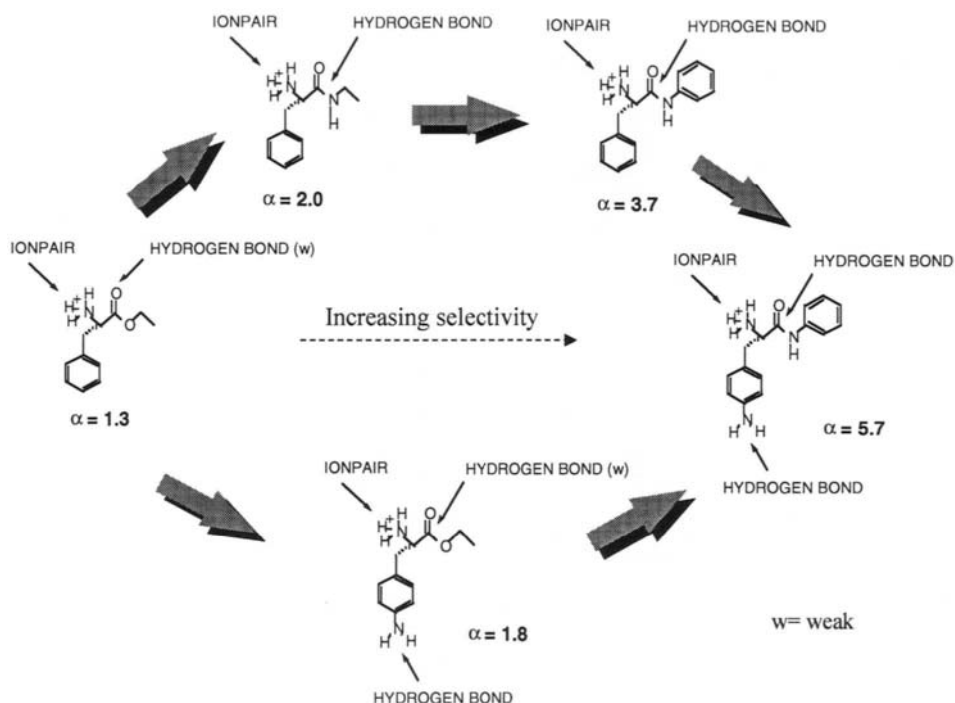


Fig. 5.16. Influence of the number of basic interaction sites of the template versus the separation factor measured in chromatography for the corresponding racemate. The templates were imprinted using MAA as functional monomer by thermochemical initiation at 60/90/120°C (24 h at each temperature) and using acetonitrile as diluent. From Sellergren *et al.* [6].

group, which allows an additional hydrogen bond interaction with another carboxylic acid group, the enantiomeric selectivity increased. In L-PA, where the ethyl amide substituent has been replaced by an anilide group, an additional increase in selectivity is seen. Combining the structural modifications in one molecule, *p*-amino-phenylalanine-anilide, gave rise to the highest separation factor. Similar observations have been made in the imprinting of a number of different classes of compounds and thermodynamic evidence for the existence of multiple additive interactions in the sites has been provided [99]. In the search for optimal synthetic conditions for MIPs, useful start-up information can be obtained from the vast literature existing on solution studies of molecular interactions and molecular recognition [100–102].

### 5.5.3. Thermodynamic considerations

An important part of the optimisation process is the stabilisation of the monomer–template assemblies by thermodynamic considerations (Fig. 5.17). The



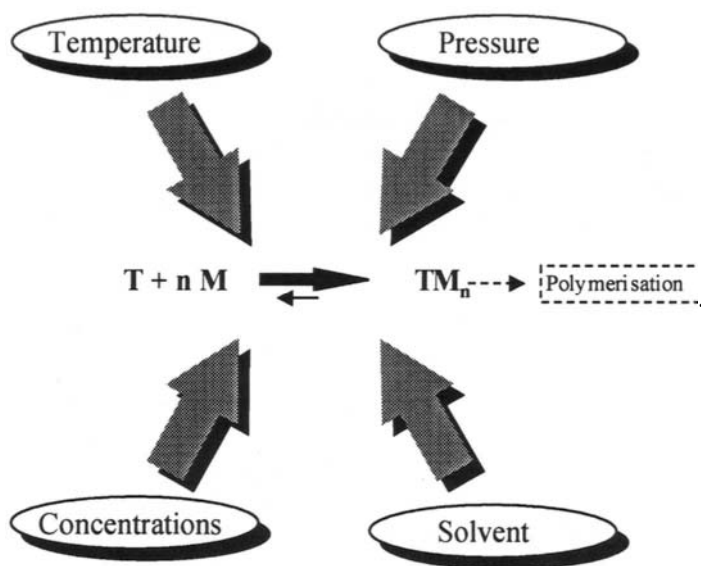


Fig. 5.17. Stabilisation of monomer template assemblies by thermodynamic considerations.

enthalpic and entropic contributions to the association will determine how the association will respond to changes in the polymerisation temperature. The change in free volume of interaction will determine how the association will respond to changes in polymerisation pressure. Finally, the solvent interaction with the monomer–template assemblies, relative to the free species, indicates how well it will stabilise the monomer–template assemblies in solution. Here each system has to be optimised individually. Another option is to simply increase the concentration of the monomer or the template. In the former case, assuming a constant monomer/solvent ratio, the nominal cross-linking level will decrease, while the potential number of non-selective binding sites will increase. In the latter case, the site integrity will be compromised. The above factors have been studied for the L-PA model system. In aprotic media of low polarity, MAA and templates containing polar functional groups are only weakly solvated and the interactions holding the monomer template–assemblies together are mainly electrostatic in nature [97]. In such cases the association of the monomer and template is associated with a loss of one set of rotational and translational degrees of freedom, which leads to a net decrease in entropy (see Chapter 3) [103]. From this it follows that the interaction will be weakened at increased temperatures. On the other hand, when the monomer and the template are more strongly solvated, the association may lead to the release of part of the solvent shell, leading in turn to a net increase in rotational and translational entropy. In this case the interaction will be favoured by increasing the temperature.

### 5.5.3.1. Concentration of functional monomer and template

MIPs for L-PA were prepared using various molar ratios of MAA to EDMA and characterised in the chromatographic mode for their ability to retain and separate D- and L- PA (see Fig. 2.10, in Chapter 2) [9]. The separation factor increased continuously, reaching a maximum of 4.5 at around 25 mol % MAA, and then a slight decrease was seen up to 50 mole %. Increasing the concentration of MAA from 50 to 60 mol % caused the loss of enantioselectivity. This agrees with results obtained by Wulff and co-workers on a template model system based on covalent bonds between the template and the monomer (see Chapter 4) [104]. The loss in selectivity was accompanied by a significant reduction in the capacity factors for both enantiomers. By increasing the MAA concentration the surface area also decreased. As seen in Chapter 2, upon a decrease in cross-linking, the morphology is likely to change from a material with permanent porosity to a gel-like material with low surface area and pore volume in the dry state. The increase in MAA also leads to excessive peak broadening. Based on these results, a concentration of *ca.* 25 mol % MAA (the rest being the cross-linking monomer) has been chosen in most studies. As discussed in Section 5.5.6, the extent of complex formation can be estimated based on NMR chemical shift changes [6], UV-spectral changes [105] or chromatographic retention [6] as a function of the concentration of the functional monomer. At monomer concentrations where the respective curves level off, complexation is assumed complete and higher monomer concentrations will contribute only to non-specific binding and counteract the separation. In the L-PA model system, this appears to be a valid assumption in view of the agreement between the complex distribution curves in Section 5.5.6 and the concentration of MAA beyond which recognition was not improved.

Knowledge of the association constants between the template and the monomer in solution may thus be used to predict suitable starting concentrations of monomer and template, leading to a larger fraction of high affinity sites. The latter parameter is of particular importance when the template is available only in small amounts, when it is poorly soluble in the common diluents or for analytical applications, when only a limited saturation capacity is required. In such cases it has proven possible to reduce the template concentration by more than a factor of 10 without significant loss of the recognition properties of the material [106].

### 5.5.3.2. Polymerisation temperature

Table 5.7 shows data from the chromatographic investigation of MIPs for L-PA prepared by thermochemical initiation at either 40 or 60°C using ABDV and AIBN as initiators respectively [9]. The differences in conversion between the materials, caused by the different initiation temperatures, were reduced by subsequently curing the polymers at 90 and 120°C. The polymers prepared at the lower temperature exhibited stronger retentions, although the separation factors were largely similar for the two polymers. In a separate study, it was shown that L-PA imprinted polymers prepared at lower temperature exhibited higher separation factors than

TABLE 5.7

CHROMATOGRAPHIC RESULTS OBTAINED USING L-PA IMPRINTED MIPs  
POLYMERISED AT DIFFERENT TEMPERATURES AND EVALUATED AT TWO  
TEMPERATURES

| Polym.<br>temp. (°C) | Column<br>temp. (°C) | Resolution<br>(Rs) | Capacity<br>factor (L-<br>PA) ( $k'_L$ ) | Separation<br>factor ( $\alpha$ ) | Solvent<br>uptake<br>(ml/g) | Surface<br>area (m <sup>2</sup> /g) |
|----------------------|----------------------|--------------------|--|-----------------------------------|-----------------------------|-------------------------------------|
| 60/90/120            | 23                   | 0.5                | 1.5                                      | 2.9                               | 1.28                        | 229                                 |
| 40/90/120            | 23                   | 0.8                | 3.5                                      | 3.1                               | 1.23                        | 204                                 |
| 60/90/120            | 80                   | 1.0                | 3.2                                      | 4.6                               | —                           | —                                   |
| 40/90/120            | 80                   | 2.3                | 6.2                                      | 4.3                               | —                           | —                                   |

The polymers were prepared using acetonitrile as diluent and AIBN (60°C) or ABDV (40°C) as initiators. Polymerisation was started at the indicated temperatures and allowed to proceed for 24 h at each temperature. In the chromatographic evaluation the mobile phase was acetonitrile/acetic acid: 90/10 (v/v). Each enantiomer (10 nmol) was injected separately. Data from [9].

their counterparts prepared at higher temperature, particularly when evaluating them at lower temperature (Fig. 5.18) [8]. The discrepancies between these studies may be related to the curing step, which was omitted in the latter study.

Different results were also obtained for L-PA imprinted polymers evaluated in the CEC mode for the separation of D,L-phenylalanine [23]. In this study, polymers prepared at 4°C by photoinitiated polymerisation and at 40 and 60°C by thermally initiated polymerisation exhibited similar separation factors when evaluated in the CEC mode, whereas the retention and resolution increased with decreasing polymerisation temperature. These results indicate that the materials have a different morphology, perhaps related to the conversion of pendant double bonds, which is likely to increase with increasing polymerisation temperature [107]. The solvent uptake and surface area of L-PA imprinted materials prepared at two different temperatures appeared similar (Table 5.7), indicating that the stronger retention is due to an increased accessibility to imprinted sites [9]. Similar observations have been made in a number of cases of MIPs prepared by photochemical initiation. Here polymerisations at temperatures as low as -20°C have been performed, resulting in stronger retentions but often with a similar selectivity to the corresponding polymers prepared at temperatures of 10–20°C. The fact that the thermally polymerised materials exhibit similar selectivities to the photopolymerised materials at elevated column temperatures (see Chapter 2) shows that the site accessibility, rather than the stability of the monomer–template complexes, is the main factor behind this behaviour. The different morphologies of these type of materials have been extensively discussed in Chapter 2.

More hydrophobic templates, such as 2,4-dichlorophenoxy acetic acid (Fig. 5.19), are best imprinted in combination with vinyl pyridine as functional monomer in

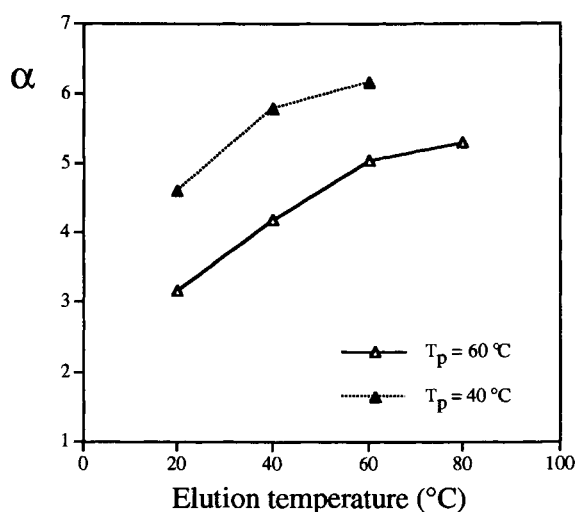


Fig. 5.18. Effect of polymerisation and elution temperature on the enantiomer separation factor ( $\alpha$ ) in the separation of D- and L-PA on L-PA imprinted polymers. Polymers were prepared by thermochemical initiation at either 60 or 40°C using AIBN or ABDV respectively as initiators. The samples consisted of *ca.* 20 nmol of each of D- and L-PA and BOC-L-PA as void marker. Flow rate: 0.5 mL/min. Mobile phase: MeCN/acetic acid: 95/5 (v/v). The columns were thermostatted by immersing them in a circulating water bath at the indicated temperature. From O'Shannessy *et al.* [8].

polar solvents and by thermal initiation at elevated temperatures [33]. This suggests an entropically driven association, as is the association between cholesterol and steroid monomers (**14**) or cyclodextrin monomers.

#### 5.5.3.3. Polymerisation pressure

The pressure effects on molecular associations are usually small and considerably smaller than the effects of temperature and solvent [108,109]. The response of intermolecular associations in solution to pressure depends on the change in free volume ( $\Delta V^\circ$ ) upon association according to equation (14):

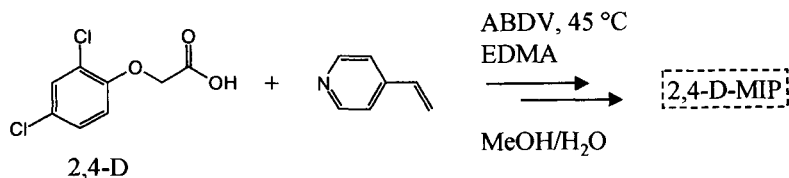


Fig. 5.19. Molecular imprinting of 2,4-dichlorophenoxyacetic acid using 4-VPY as functional monomer and methanol as diluent as described by Haupt *et al.* [33].

$$\left[ \frac{\partial RT \ln K}{\partial RT} \right]_T = -\Delta V^\circ \quad (14)$$

where  $K$  is the association constant of the complex,  $R$  the gas constant,  $T$  the absolute temperature,  $P$  the pressure and  $\Delta V^\circ$  the difference in volume occupied by the products and the reactants (reaction volume). If the association leads to a net decrease in volume ( $\Delta V^\circ < 0$ ), it follows that the association constant increases with increasing pressure. For instance, if  $\Delta V^\circ = -10 \text{ cm}^3/\text{mol}$ ,  $K$  increases by a factor of 1.5 at 1000 bar and 60 at 10000 bar, while if  $\Delta V^\circ = -20 \text{ cm}^3/\text{mol}$  these factors are 2.2 and 3500 respectively, as is evident from the logarithmic dependence of  $K$  on  $P$  and  $\Delta V^\circ$  seen in equation (14).

Network polymers of MAA and EDMA were prepared in the presence of the triazines atrazine (ATR) or ametryn (AME) as templates (for structures see later Table 5.15), by thermochemically initiated free radical polymerisation at either 1 or 1000 bar in three different diluents [110]. After washing, the materials properties were characterised and they were chromatographically evaluated for rebinding selectivity. Comparing the ATR imprinted materials prepared using different porogens the results confirmed results obtained using the L-PA model system [7]. Thus, the affinity and selectivity in the rebinding step decreased with increasing hydrogen bonding capacity of the diluent, which is in the order dichloromethane < acetonitrile < isopropanol. This is attributed to destabilisation of the monomer–template assemblies due to stronger solvation of the free monomer and template (see following section). Furthermore, the polymer dry state morphology and swelling appeared to have little influence on the selectivity.

Comparing the materials prepared at the two pressures, no pronounced difference was seen using ATR ( $\text{p}K_a = 1.7$ ) as template, whereas when using the more basic AME ( $\text{p}K_a = 4.1$ ) as template and isopropanol as diluent, a significant effect of the pressure applied during polymerisation on the affinity and selectivity for AME was seen (Table 5.8). The capacity factor for AME was *ca.* 30% higher on the polymer prepared at 1000 bar than on the one prepared at normal pressure at a sample load of 100 nmol and *ca.* 40% higher when the same comparison was done

TABLE 5.8

CHROMATOGRAPHIC RETENTION OF TRIAZINES (10 NMOLE INJECTED SEPARATELY) ON AME IMPRINTED POLYMERS PREPARED AT DIFFERENT PRESSURES [110]

| Pressure | AME  |                      | ATR  |                      | CYA  |                      | Ref. |                      |
|----------|------|----------------------|------|----------------------|------|----------------------|------|----------------------|
|          | $k'$ | $k'/k'_{\text{AME}}$ | $k'$ | $k'/k'_{\text{AME}}$ | $k'$ | $k'/k'_{\text{AME}}$ | $k'$ | $k'/k'_{\text{AME}}$ |
| 1 bar    | 2.3  | 1                    | 1.2  | 0.50                 | 0.44 | 0.19                 | 1.6  | 0.68                 |
| 1000 bar | 3.2  | 1                    | 1.4  | 0.44                 | 0.63 | 0.20                 | 1.6  | 0.50                 |

The chromatographic evaluation was done using acetonitrile as mobile phase. The polymers were prepared at 60°C, using isopropanol as diluent and at the pressures given in the table.

at a sample load of 10 nmol. The retention of other triazines and of the reference also increased, but not to the same extent. This is shown by the relative retentions of these compounds, which are lower on the 1000 bar polymer than on the one prepared at normal pressure. The enhanced retention induced by pressure was lost upon ageing and thermal treatment of the materials.

#### 5.5.3.4. Polymerisation diluent

In a study of the influence of the diluent properties on the recognition properties of MIPs, a series of L-PA MIPs was prepared in the presence of various solvents (diluent) with different polarity and hydrogen bonding properties (Table 5.9) [7]. The structure and morphology of the polymers were then studied by measurement of swelling and solvent uptake and pore structure by nitrogen sorption and mercury penetration analysis. They were further characterised spectroscopically by FTIR and NMR spectroscopy and by scanning electron microscopy. The recognition properties of the polymers were then studied chromatographically.

The hydrogen bonding capacity of the diluent, an average of donor and acceptor capacity [111], was the only parameter that correlated with the recognition properties of the materials (Table 5.9). Thus, the polymers prepared using the poorly hydrogen bonding diluents exhibited higher enantioselectivities than those prepared using the moderately or strongly hydrogen bonding diluents. Interestingly, these polymers comprise both mesoporous (diluent: acetonitrile or benzene), low swelling materials and non-porous (diluent: chloroform or dichloromethane), swellable materials. Therefore, no correlation is evident between polymer morphology and the rebinding properties of the polymers. Concerning the influence of the solubility parameters on the polymer morphology, see Chapter 2. For clarity, it should be noted that diluents comprise solvents and non-solvents for the polymer, which can result in polymers with porous or non-porous morphologies. The term porogen should be used only in those cases where a permanently porous structure is obtained.

The above findings are in agreement with a number of similar studies of MIPs targeted towards less polar templates interacting mainly by electrostatic interactions with the monomers (see also previous section) [110,112]. However, in the case of stronger electrostatic interactions such as in the hydrogen bonded ion pairs formed between amidines and carboxylic acids [31,67], polymerisation can be carried out in more competitive solvents, such as mixtures of alcohols and water, resulting in good recognition properties. This is also possible for some hydrophilic templates using other hydrogen bonding monomers such as HEMA [77,80–82] and DEAEMA [74] (Table 5.6). Increasing the aqueous content is also favoured in the imprinting of templates of lower polarity which interact *via* hydrophobic interactions with the functional monomer. This has been observed in the imprinting of 2,4-dichlorophenoxy acetic acid, using VPY as functional monomer (Fig. 5.19) [33], and in the imprinting of cholesterol with polymerisable bile acids or cholesterol (**14**) [93].

TABLE 5.9

EFFECT OF DILUENT AND THERMAL TREATMENT ON POLYMER MORPHOLOGY, THERMAL STABILITY AND CHROMATOGRAPHIC PERFORMANCE OF MIPs USING L-PA AS TEMPLATE

| Diluent                         | H-bond type | Temperature at 50% mass loss (°C) | Swelling (ml/ml) | Pore volume (ml/g) | Surface area (m <sup>2</sup> /g) | Separation factor $\alpha$ (= $k'_L/k'_D$ ) at sample load of D,L-PA |          |
|---------------------------------|-------------|-----------------------------------|------------------|--------------------|----------------------------------|--|----------|
|                                 |             |                                   |                  |                    |                                  | 12.5 nmol  | 100 nmol |
| MeCN                            | P           | 404                               | 1.36             | 0.60               | 256                              | 5.8  | 2.6      |
| CHCl <sub>3</sub>               | P           | —                                 | 2.11             | 0.007              | 3.5                              | 4.5  | 2.6      |
| C <sub>6</sub> H <sub>6</sub>   | P           | —                                 | 1.55             | 0.43               | 216                              | 6.8 (1.6) <sup>d</sup>   | 2.4      |
| CH <sub>2</sub> Cl <sub>2</sub> | P           | 419                               | 2.01             | 0.007              | 3.8                              | 8.2 (6.4) <sup>d</sup>   | 2.4      |
| DMF                             | M           | —                                 | 1.97             | 0.17               | 127                              | 2.0 <sup>a</sup>   | NR       |
| THF                             | M           | 397                               | 1.84             | 0.24               | 194                              | 4.1  | 1.5      |
| <i>i</i> -propanol              | S           | —                                 | 1.10             | 0.86               | 49                               | 3.5 <sup>a</sup>   | 2.4      |
| HOAc                            | S           | —                                 | 1.45             | 0.52               | 267                              | 1.9 <sup>a</sup>   | NR       |
| MeCN <sup>b</sup>               | P           | 375                               | 1.19             | 0.89               | 317                              | 3.1  | NR       |
| THF <sup>b</sup>                | M           | 357                               | 1.27             | 0.73               | 382                              | 1.6  | NR       |
| MeCN <sup>c</sup>               | P           | 400                               | 1.35             | 0.65               | 266                              | 3.7  | 2.4      |

The polymers were prepared by photochemical initiation except for (b). The chromatographic separations were carried out using acetonitrile/acetic acid/water: 92.5/5/2.5 (v/v/v %) as mobile phase and applying two different sample loads of D,L-PA. NR = non-resolved peak maxima.

<sup>a</sup>Mobile phase acetonitrile/acetic acid/water: 96.3/2.5/1.25 (v/v %).

<sup>b</sup>Prepared by thermochemical initiation.

<sup>c</sup>After photochemical initiation and polymerisation at low temperature post-treatment at 120°C for 24 h was carried out.

<sup>d</sup>Results after annealing of the polymers under vacuum in the dry state at 120°C for 24 h and heating of the polymers at 130°C for 4 h in the mobile phase. The MIP using benzene (C<sub>6</sub>H<sub>6</sub>) as diluent was evaluated using acetonitrile/0.05 M potassium phosphate buffer, pH 7: 7/3 (v/v) as mobile phase. The separation factor prior to the heat treatment was 4.1 in this mobile phase. Data from [7]

### 5.5.4. Influence of the template shape

The template shape itself may be sufficient to create the necessary steric complementarity for efficient discrimination between two molecules. The first unambiguous evidence for the influence of template shape on the recognition properties of MIPs was obtained using a covalent template system [113]. Thus, diol-containing binding sites for aryl-1,3-diketones with different aryl groups exhibited memory for the respective aryl group (Fig. 5.20). Shape complementarity was also suggested as

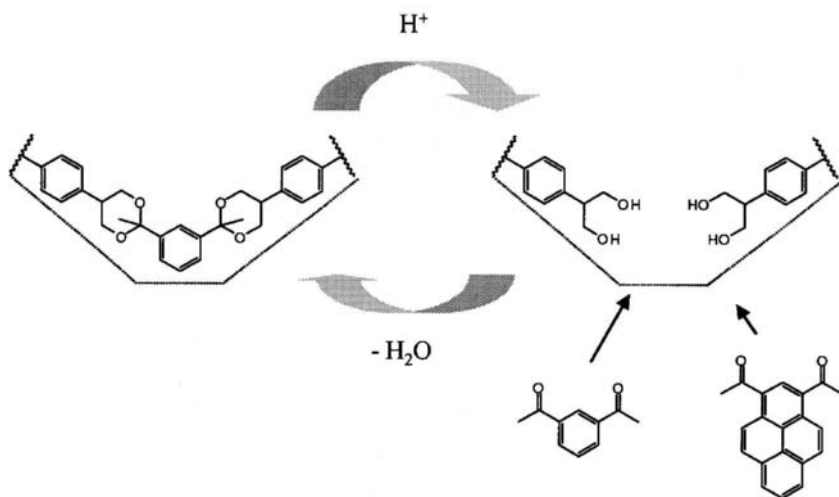


Fig. 5.20. Competitive rebinding experiment to a polymer imprinted with the bisketal of 1,3-diacetylbenzene [113].

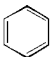
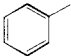
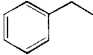
one contributing factor in the ability of MIPs for L-PA, and the corresponding *N*-methylanilide, L-PMA, to discriminate between their complementary templates (see Section 5.2.1.1) [15]. A number of other examples suggest that shape complementarity contributes to the recognition in MIPs. For instance, polymers imprinted with BA are capable of recognising its template compared with structurally related compounds (see Section 5.7.2.2). Another striking example of shape recognition is the porogen imprinting effect observed by Hosoya *et al.* (Table 5.10) [114]. Pronounced shape complementarity and size exclusion effects were recently observed in the imprinting of amino acids with different *N*-protecting groups.[18].

A practically important example is the discrimination between the alkylated guanines *O*6-methylguanine and *O*6-ethylguanine, by corresponding imprinted polymers (Table 5.11). These DNA base adducts are the results of DNA alkylations that may lead to genetic damage and to cancer. DNA adducts may occur at a number of sites within the DNA molecule, usually by alkylation, i.e. addition of electrophiles (activated PAHs, epoxides, nitrosamines, halogens) to nucleophilic sites within the DNA molecule [115]. Guanine bases are the predominant site for attack (Fig. 5.21). Due to the latency of the human cancer process, early determination of such biomarkers after exposure is obviously of great interest. MIPs targeted towards these structures could become a valuable aid in the development of corresponding analytical methods. In view of the conformational rigidity of these molecules the discrimination is likely to be the result of steric exclusion or Van der Waals' complementarity. The fact that both polymers recognise their corresponding template indicates a level of recognition similar to the most efficient biological recognition elements [97].



TABLE 5.10

## POROGEN IMPRINTING EFFECTS

| Template porogen   | $k'_{\text{toluene}}/k'_{\text{benzene}}$ | $k'_{\text{ethylbenzene}}/k'_{\text{toluene}}$ |
|--|---|--|
| <br><i>Benzene</i>      | 1.11                                      | 1.10   |
| <br><i>Toluene</i>      | 1.25                                      | 1.10   |
| <br><i>Ethylbenzene</i> | 1.28                                      | 1.22   |

Separation factors obtained for stationary phases imprinted with the indicated templates as porogens. Mobile phase: 80% aqueous methanol. Data from [158].

### 5.5.5. Influence of the monomer–template rigidity

As shown by Wulff and Gimpel [116] and discussed by Nicholls [103] (see Chapter 3), the more conformationally defined the monomer and the template, the lower the number of stable conformers that will be imprinted and the more defined the recognition sites will be. The rebinding will also occur without much loss of rotational entropy, further promoting strong binding [97,103]. The importance of pre-organisation is well known in the area of host–guest chemistry [117]. Thus, the better the fit between the site and the template, the less entropy will be lost due to conformational changes in the site, as well as in the template, upon binding. This will increase the affinity and selectivity of the recognition. It should be mentioned that some of the best working MIPs are those imprinted with rigid templates, such as nitrogen heterocycles [24–26].

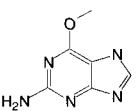
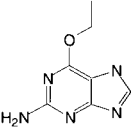
### 5.5.6. Studies of the monomer–template solution structures

To what extent do the solution complexes formed between the monomer and the template in solution reflect the architecture of the polymeric binding sites? This question is important, since a thorough characterisation of the monomer–template assemblies may assist in deducing the structure of the binding sites in the polymer and thus have a predictive value.

As discussed in Section 5.5.3.1., the potential for a given monomer–template pair to produce templated sites can be predicted by measuring the stability constants, e.g. by spectroscopic techniques, in a homogeneous solution mimicking the

TABLE 5.11

RECOGNITION BY POLYMERS IMPRINTED WITH *O*-6-METHYL-GUANINE (O6MG) AND *O*-6-ETHYLGUANINE (O6EG)

| MIP template   | <i>k'</i> O6MG |      | <i>k'</i> O6EG |
|--|----------------|------|----------------|
| <br><i>O6MG</i> | MeCN/HOAc      | MeCN | MeCN/HOAc      |
|  | 2.8            | > 80 | 1.6            |
| <br><i>O6EG</i> | 3.2            |      | 2.9            |
| Reference polymer  | 0.7            | 13   | 0.6            |

The polymers were evaluated using either acetonitrile/acetic acid/water: 92.5/5/2.5 (v/v/v) or acetonitrile as mobile phase. 10 nmol of solute were injected in 10  $\mu$ l of the mobile phase.

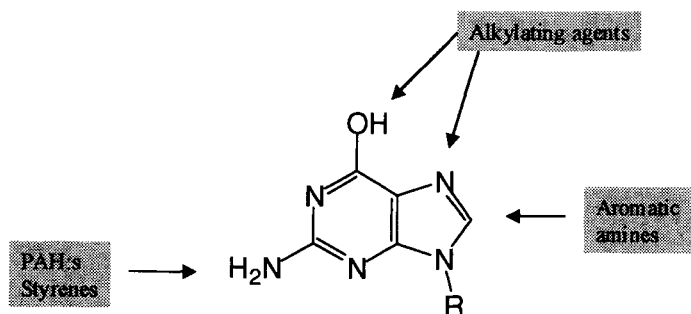


Fig. 5.21. Most common sites for alkylation of guanine by various carcinogens.

monomer mixture prior to polymerisation [6,124,105,118]. This can ultimately be used as a preliminary screening procedure to search for suitable functional monomers. Thus, estimated solution association constants can be compared with the heterogeneous binding constants determined in the rebinding step to the imprinted sites, as given in Table 5.12 for some common templates.

<sup>1</sup>H-NMR spectroscopy and chromatography were used to study the association

TABLE 5.12

ASSOCIATION CONSTANTS FOR COMPLEXES BETWEEN CARBOXYLIC ACIDS AND NITROGEN BASES IN APROTIC SOLVENTS AND CORRESPONDING ASSOCIATION CONSTANTS AND SITE DENSITIES FOR BINDING OF THE BASE TO A MIP

| Acid                 | Base  | Solvent         | $K_a$ (/M)                                     | $n$ (mol/g) | Ref.  |
|----------------------|---|-----------------|--|-------------|-------|
| Acetic acid          | ATR   | $\text{CCl}_4$  | 210  | —           | [101] |
| Butyric acid         | 9-EA  | $\text{CDCl}_3$ | (1) 114<br>(2) 41<br>(3) 5<br>> $10^6$         | —           | [100] |
| 4-methylbenzoic acid | 4-vinyl-1-( $N,N'$ -dialkylamidino)-benzene | $\text{CDCl}_3$ | > $10^6$                                       | —           | [66]  |
| PMAA                 | ATR   | $\text{CHCl}_3$ | (1) $8.3 \times 10^4$<br>(2) $1.0 \times 10^4$ | 20<br>40    | [118] |
| PMAA                 | 9-EA  | $\text{CHCl}_3$ | (1) $7.6 \times 10^4$<br>(2) $2.4 \times 10^3$ | 20<br>86    | [24]  |

PMAA refers to polymers imprinted with respective base using MAA as functional monomer.

between MAA and L-PA in solution as a mimic of the pre-polymerisation mixture [6]. The  $^1\text{H}$ -NMR chemical shifts of either the template or the monomer versus the amount of added MAA, as well as the chromatographic retention of D,L-PA versus the amount of acid in the mobile phase (Fig. 5.22), varied in accordance with the formation of multimolecular complexes between the template and the monomer in the mobile phase. A 1:2 template–monomer complex was proposed to exist prior to polymerisation, based on the modelled complex distribution curves (Fig. 5.23). Based on these results, hydrogen bond theory and the assumption that the solution structure was preserved after the polymerisation, a structure for the template bound to the site was proposed (Fig. 5.24). Since these initial studies, a number of other examples support this model, i.e. the recognition is due to functional group complementarity and a correct positioning of the functional groups in the sites, as well as a steric fit in the complementary cavity [45,99,113,119].

Rebinding to sites formed from residual non-extracted template has also been proposed as a contributing factor to the observed recognition [120,121]. This suggests that template remaining in the polymer after attempted template removal is capable of acting as a nucleation site for the template in the rebinding experiment. Thus, the actual binding sites are complementary to small clusters of the template. This is an interesting theory which may explain the adsorption behaviour in some systems (note in particular the use of cholesterol monomers to imprint cholesterol (14)) [93], particularly at low site occupancy. However, in most imprinted systems rebinding selectivity or catalytic efficiency increase with

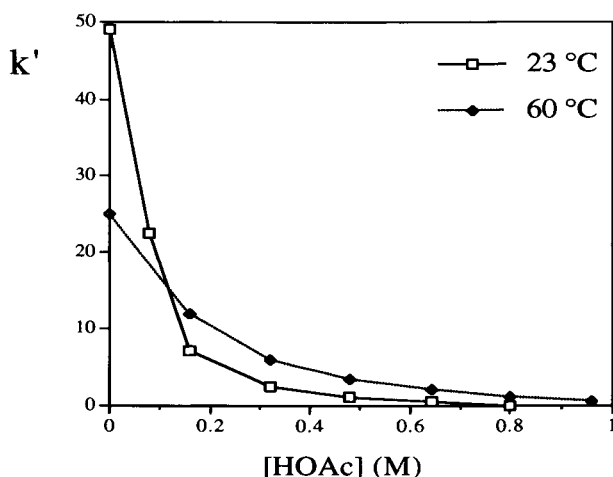


Fig. 5.22. Retention ( $k'$ ) of D-PA at 23°C and at 60°C on an L-PA imprinted polymer versus the concentration of acetic acid (HOAc) in the mobile phase (MeCN). From Sellergren *et al.* [6].

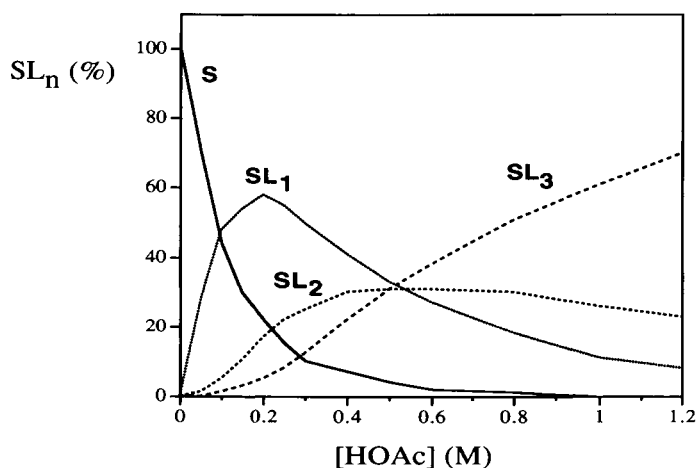


Fig. 5.23. Distribution of complexes at room temperature estimated from the data in Fig. 5.22 assuming the same concentration of PA (0.1 M) as prior to polymerisation. From Sellergren *et al.* [6].

increasing recovery of the template [122]. Also, the commonly observed bi- or tri-Langmuir adsorption isotherms indicate true receptor behaviour, with separated sites each interacting with one template molecule [14].

In the triazine and 9EA MIP model systems predictions may be made based on previous studies of closely related solution complexes. Of particular relevance is the work by Welhouse and Bleam [101] on solution complexes of ATR formed by hydrogen bonding with various small molecules and the work by Lancelot on the

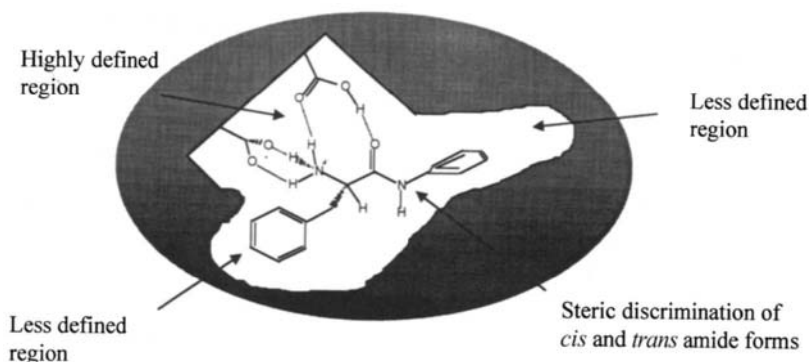


Fig. 5.24. Model of the L-PA binding site based on NMR and chromatographic data and the relation between structure and retention.

interactions between butyric acid and nucleotide bases [100]. By measuring the  $^1\text{H}$ -NMR chemical shifts of 9EA upon addition of butyric acid and comparing with the results for alkylated model compounds, the complexation constants and site of interactions can be determined. Thus 9EA interacts by a Watson–Crick type interaction ( $K_1 \approx 114/\text{M}$ ), a weaker Hoogsteen interaction ( $K_2 \approx 41/\text{M}$ ) and a single hydrogen bond interaction at the 3-position ( $K_3 \approx 5/\text{M}$ ) (Table 5.12). Downfield shifts were observed for 9EA when MAA was added. The studies by Lancelot were carried out at a concentration interval ( $[\text{9EA}] = 14 \text{ mM}$ ,  $[\text{butyric acid } [\text{BA}]] = 30 \text{ mM}$ ) and at a temperature ( $30^\circ\text{C}$ ) where only 1:1 complexes were formed. At higher acid concentrations and at lower temperatures, the propensity for 2:1 complexes will increase. It should be mentioned that a two-fold increase in the association constant in the binding of 2-aminopyrimidine to a carboxylic acid containing host was observed when the temperature was lowered from  $20^\circ\text{C}$  to  $10^\circ\text{C}$  [123]. Based on Lancelot's results, the complex distribution in  $\text{CHCl}_3$  at  $30^\circ\text{C}$  and at the concentrations present during polymerisation can be estimated. Assuming that ligand association to the 1:1 complex is similar to the association to free 9EA, i.e. binding of the first ligand does not affect the association constant for the second ligand, and accounting only for the two strongest complexes, the overall association constant  $K_{12}$  for the 1:2 complex is  $K_1K_2$ . Entering as total concentrations:  $[\text{9EA}]_0 = 25 \text{ mM}$  and  $[\text{BA}]_0 = 300 \text{ mM}$  (the latter corresponding to the concentration of MAA prior to polymerisation), and neglecting monomer dimerisation we have:

$$K_1 = [\text{BA-9EA}]_{\text{wc}}/([\text{BA}][\text{9EA}]) = 114/\text{M} \Rightarrow [\text{BA-9EA}]_{\text{wc}} \approx 34[\text{9EA}] \quad (15)$$

$$K_2 = [\text{BA-9EA}]_{\text{h}}/([\text{BA}][\text{9EA}]) = 41/\text{M} \Rightarrow [\text{BA-9EA}]_{\text{h}} \approx 12[\text{9EA}] \quad (16)$$

$$K_{12} = K_1K_2 = [\text{BA}_2\text{-9EA}]/([\text{BA}]^2[\text{9EA}]) = 4674 \text{ M}^2 \Rightarrow [\text{BA}_2\text{-9EA}] \approx 421[\text{9EA}] \quad (17)$$

where wc and h represent the Watson–Crick and Hoogsteen binding modes respectively. It thus appears as if a major part of 9EA is present as the 1:2 complex in

$\text{CHCl}_3$  at the concentrations used in this study. However, the presence of the other components in the monomer mixture, i.e. EDMA and the initiator, may affect the equilibria and prevent any definite conclusions from this estimate. Other studies indicate that estimates of the extent of pre-polymerisation complex formation may allow predictions of recognition properties of the resulting MIPs [124].

## **5.6. POST-TREATMENTS AFFECTING AFFINITY, SELECTIVITY AND MASS TRANSFER PROPERTIES**

Despite the fact that molecular imprinting allows materials to be prepared with high affinity and selectivity for a given target molecule, a number of limitations of the materials prevent their use in real applications. As mentioned in previous chapters, some of these limitations are:

- (1) Binding site heterogeneity
- (2) Extensive non-specific binding
- (3) Slow mass transfer
- (4) Bleeding of template
- (5) Low sample load capacity
- (6) Impractical manufacturing procedure
- (7) Poor recognition in aqueous systems
- (8) Swelling and shrinkage, which may prevent solvent changes
- (9) Lack of recognition of a number of important compound classes
- (10) Preparative amounts of template required

It is clear that improvements aimed at increasing the yield of high energy binding sites or modifying the site distribution in other ways will have a large impact on the performance of the materials (affecting limitations 1, 2, 4 and 5). The strategies adopted to achieve this have focused either on pre-polymerisation measures, aimed at stabilisation of the monomer–template assemblies prior to polymerisation, or on post-polymerisation measures aimed at modifying the distribution of binding sites by either chemical or physical means.

### **5.6.1. Thermal annealing or curing**

It has been shown that the selectivity, the kinetic properties and the sample load capacity of imprinted stationary phases can be affected by thermal post-treatments [7,14,59]. L-PA imprinted polymers were therefore investigated. The post-treatment can be either a curing step, achieved by heating the polymerisation tubes (photo-chemically or thermochemically initiated polymerisations) at elevated temperatures before work-up, or a thermal annealing step, consisting in heating the polymer in the dry state after removal of unreacted monomer and initiator [14]. The former treatment results in the consumption of remaining initiator and conversion of remaining monomer and unreacted pendant double bonds. Both treatments are expected to cause conformational changes in the materials.

The response to thermal annealing depended on the dry state morphology of the

materials. A material classified as gel-like, with a low porosity and a small internal surface area but with a high swelling factor, was more stable than a less swellable material with a mesoporous morphology [7]. This was true with respect to both the onset temperature for mass loss and the level of enantioselectivity (Table 5.9). Compared with untreated materials, a heat-treated gel-like material exhibits a lower selectivity, mainly at low concentrations, and a somewhat improved column efficiency, whereas porous materials lose most of their recognition properties.

The chromatographic properties of the L-PA imprinted polymers were determined before and after the thermal annealing step (Fig. 5.25) [14]. The mobile phase was acetonitrile, with acetic acid and water as modifiers. Drying the polymers at 50°C overnight resulted in a reduced peak splitting effect without significant changes in the retention factors. This contrasted with the results of heat treatments performed at higher temperatures. The most significant effects of the treatments at 120 and 140°C were a reduced retention of L-PA and a flattening out of the plots of selectivity versus sample size, which was of comparable importance at both temperatures. Treatment at 120°C led to a sharpening of the peaks and no peak splitting for D-PA. The material treated at 140°C gave a column exhibiting poor efficiency, while treatment at 160°C led to an apparent complete loss of selectivity. The increase in retention of D-PA with increasing sample load is probably associated with the use of acetic acid as a mobile phase modifier. Acetic acid interacts with the solutes and the retention process becomes endothermic [6,59]. The peak splitting effect, on the other hand, is probably related to the polymer porosity, i.e. the extent of micropores and the mobility of its chain segments. This is seen when comparing the peak profiles for materials treated at 50 and 120°C. Due to the abnormal chromatographic behaviour with acetic acid as modifier, the remaining chromatographic investigations were carried out with a buffered aqueous mobile phase. Adsorption isotherms obtained by frontal analysis showed that the heat treatment imparted higher sample load capacities to the stationary phase and slightly faster mass transfer kinetics, indicating that this treatment may be beneficial for the preparative applications of these materials [14]. Moreover, the thermal treatment improved markedly the long term thermal stability of the stationary phase.

In a previous study of the thermal post-treatment of suspension polymerised trimethylolpropane trimethacrylate, it was observed that a large decrease in the swelling and a slight decrease in the average pore size took place in materials treated at 130°C [107]. Since the original swelling observed prior to the treatment could be restored upon heating the material in a swelling solvent, the reduced swelling was attributed to a thermally induced relaxation process rather than to additional chemical cross-linking. Possibly, the temperature of the treatment was above the glass transition temperature of the interconnecting segments. In this context, it should be noted that atactic PMMA has a glass transition temperature of 105°C [3].

The thermal annealing of the MIP was accompanied by a significant reduction in the swelling and an increase in the apparent dry density of the material. This results in a higher density of the enantioselective binding sites, although they may be less accessible than prior to the thermal treatment. The nitrogen sorption data showed

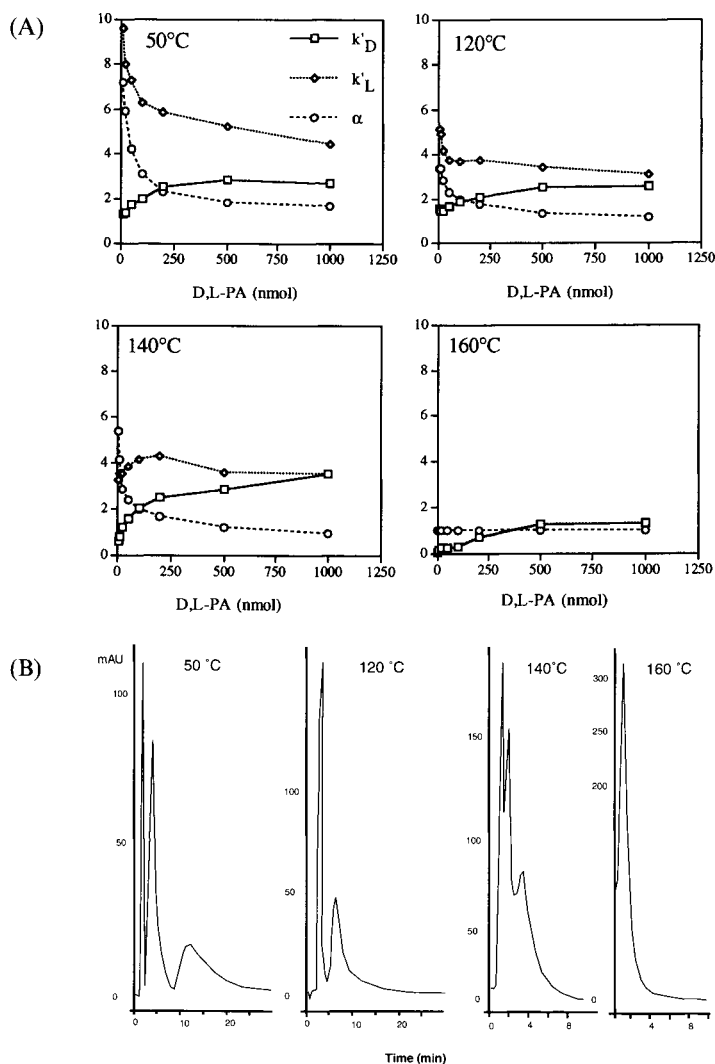


Fig. 5.25. (A) Separation factor ( $\alpha$ ) and capacity factors ( $k'$ ) for D- and L-PA versus amount injected D,L-PA on columns packed with heat-treated L-PA imprinted stationary phases prepared using dichloromethane as porogen. (B) Corresponding elution profiles at a sample load of 50 nmol D,L-PA. Mobile phase: acetonitrile/water/acetic acid: 92.5/2.5/5 (v/v/v). Note that the columns with the materials treated at 140 and 160°C were only of 5 cm length. From Chen *et al.* [14].

that all materials, whether before or after the thermal treatment, exhibited little or no porosity and only a small specific surface area. The IR spectra of the polymers showed a slight decrease of the intensity of the C=C stretch band at  $1638/\text{cm}^{-1}$  assigned to unreacted double bonds. This indicates that the heat treatment resulted



in a slight increase in the conversion of the pendant double bonds remaining in the materials. However, heating up to 140°C led to the apparent destruction of mainly high energy binding sites. Treatment at 160°C led to the total loss of the enantioselectivity. Apparently, this temperature exceeds the glass transition temperature of the more highly cross-linked regions of the matrix hosting the binding sites.

A curing step (120°C) applied to the L-PA imprinted polymers led to an apparent increase in sample load capacity [7]. As seen in Table 5.9 this treatment does not result in any significant differences in the dry state porosity and swelling of the material. However, it is likely that the number of unreacted double bonds is lower in these materials in view of the higher conversions observed in thermally versus photochemically polymerised materials (see Chapter 2).

### 5.6.2. Esterification

Photoinitiated L-PA imprinted and blank polymers prepared using acetonitrile as diluent were treated with a large excess of diazomethane [7]. This should lead to esterification of the carboxylic acid groups (Fig. 5.26). The modification was followed by a reinvestigation of swelling, solvent uptake, FTIR, differential scanning calorimetry (DSC), thermal gravimetric analysis (TGA) and chromatographic performance (Table 5.13). A somewhat lower swelling and solvent uptake was observed. More notable was the large decrease in the enantiomeric separation factor after the treatment. This shows the importance of the ion pair and hydrogen bonding interactions for recognition. In the IR spectrum only part of the OH band disappeared, mostly the absorbances at higher wave numbers. This is to be expected since the free carboxylic acid groups are likely to be more reactive than the hydrogen bonded groups. Also a large decrease in the vinyl band at 1639/cm<sup>-1</sup> was seen, probably due to a 1,3-addition of diazomethane to the double bond. Thus a large proportion of the double bonds seem to be accessible. The DSC and TGA traces for both polymers were almost identical. The only difference was the observation of an endotherm at low temperature for the treated polymers, corresponding to a mass loss which could be attributed to the weight of a methylester group. This was not observed in the untreated polymer.

Methylation of the polymer-bound carboxylic acid groups has also been attempted in the presence of the template molecule [125]. This experiment aimed at selectively blocking the non-specific binding sites, using the template to protect the acid groups of the templated sites during the treatment with methyl iodide. A significant increase in selectivity was observed using this approach.

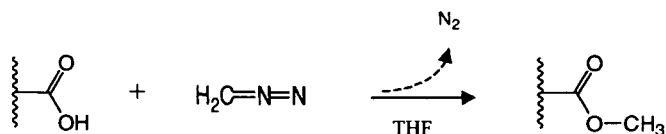


Fig. 5.26. Esterification of carboxylic acid groups of the L-PA MIPs with diazomethane.

TABLE 5.13

## CHEMICAL POST-REACTIONS OF MIPs IMPRINTED WITH L-PA

| Treatment                      | State        | Swelling | Solvent uptake (ml/ml) | Retention $k'_L$ | Separation factor $\alpha (= k'_L/k'_D)$ |
|--------------------------------|--------------|----------|------------------------|------------------|--|
| CH <sub>2</sub> N <sub>2</sub> | –COOH        | 1.36     | 0.78                   | 7.5              | 5.8                                      |
|                                | –COOMe       | 1.20     | 0.68                   | 1.7              | 1.4                                      |
| MeOH/10% NaOH:<br>4/1 (v/v %)  | Unhydrolysed | 1.55     | —                      | 2.0              | 5.6                                      |
|                                | Hydrolysed   | 1.70     | —                      | 1.2              | 2.3                                      |

The diazomethane and base treatment was performed on polymer prepared using acetonitrile and benzene as diluents respectively. The mobile phase was acetonitrile/acetic acid/water: 92.5/5/2.5 (v/v/v) and the sample load was 10 nmol D,L-PA. Data from [7].

### 5.6.3. Hydrolysis

In another experiment, the polymers were stirred at room temperature in MeOH/10% NaOH (80/20 (v/v)) overnight [7]. This gave rise to a higher swelling and to a substantial release of MAA, the latter probably due to hydrolysis of methacrylate ester bonds either from pendant groups or from remaining EDMA. The treatment resulted in a partial loss of selectivity and binding (Table 5.13). The increase in swelling has been attributed to hydrolysis of cross-links in the polymer [126], which may also explain the partial loss of selectivity (Fig. 5.27).

## 5.7. MEDIUM DEPENDENCE IN THE REBINDING TO MIPs

The rebinding to MIPs is strongly dependent on the medium. To predict the optimum medium for rebinding, factors related to template structure, as well as to polymer structure and morphology, have to be considered. In method development involving MIPs, the medium used in the rebinding step therefore has to be carefully optimised in order to fully exploit the MIPs ability to recognise the target template. Based on the increasing data available on the dependence of retention and selectivity in various media on the structure of the template, some general rules can be formulated. In the imprinting protocol using MAA as the functional monomer, the molecular recognition can be driven by hydrogen bonding, ion exchange and/or the hydrophobic effect, depending on the template and the medium (Fig. 5.28). Examples of the corresponding three categories of templates and how they behave in different chromatographic mobile phases will be given in this section.

### 5.7.1. Effect of swelling and porosity in different media

As mentioned in Chapter 2, the extent of swelling of cross-linked polymers prepared using the same monomer composition depends on their morphology and

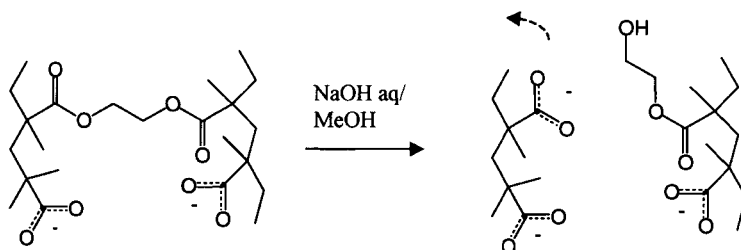


Fig. 5.27. Hydrolysis of cross-links in poly(MAA-co-EDMA).

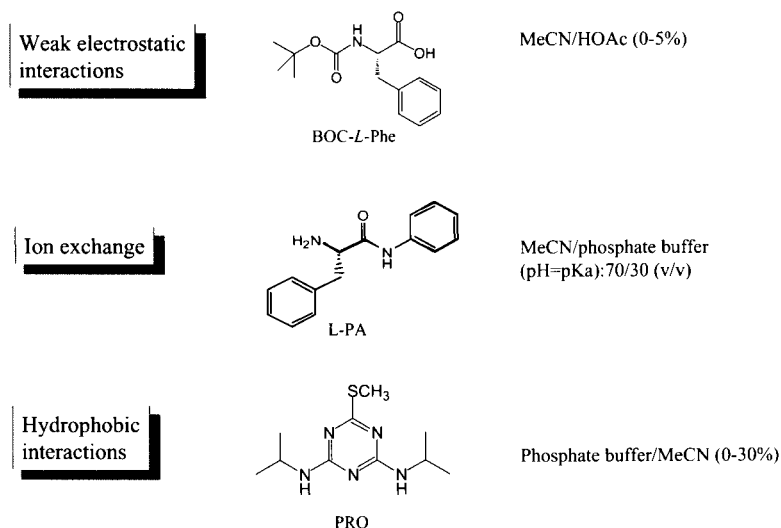


Fig. 5.28. Retention modes in chromatography using MIP-phases and examples of templates and typical mobile phases.

the extent of solvation of the polymer chains in the particular solvent used [127]. For the standard protocol using MAA as functional monomer these effects are well illustrated in a comparison of materials imprinted with L-PA in the presence of different solvents as diluents (Table 5.9) [7].

From this study it was seen that materials could be prepared which were gel-like and non-porous in the dry state, but swelled to twice their volume in a solvent. Other materials exhibited permanent porosity and swelled less in the same solvent. By studying the swelling of the gel-like materials in different solvents, good and bad solvents for this copolymer can be identified. It is seen that toluene, water and cyclohexane give lower swelling factors than acetonitrile, methanol and tetrahydrofuran (THF), the lowest swelling being seen with cyclohexane (Table 5.14). In view of the large differences in swelling of the gel-like

TABLE 5.14

## SWELLING FACTORS OF L-PA IMPRINTED AND BLANK NON-IMPRINTED POLYMERS (BL) IN DIFFERENT SOLVENTS

| <i>Solvent</i>   | Polymer   |             |           |           |             |           |
|------------------|-----------|-------------|-----------|-----------|-------------|-----------|
|                  | <i>T1</i> | <i>T1BL</i> | <i>T2</i> | <i>P1</i> | <i>P1BL</i> | <i>P2</i> |
| MeCN             | 1.19      | 1.19        | 1.31      | 1.36      | 1.31        | 1.84      |
| MeOH             | 1.17      | 1.19        | 1.30      | 1.37      | 1.29        | 1.83      |
| Toluene          | 1.13      | 1.12        | 1.30      | 1.30      | 1.25        | 1.71      |
| THF              | 1.19      | 1.17        | 1.30      | 1.35      | 1.31        | 1.79      |
| H <sub>2</sub> O | 1.19      | 1.13        | 1.28      | 1.30      | 1.28        | 1.77      |
| Cyclohexane      | 0.98      | 1.06        | 1.05      | 1.10      | 1.09        | 1.40      |

Swelling in ml/ml was determined in the various solvents. T and P refer to polymers prepared by thermochemical and photochemical initiation respectively. The porogens were acetonitrile (1) or THF (2). Data from [7].

materials, switching of solvents during an experiment will cause large differences in porosity and surface area, which may impair their life-time [128] and general use in analytical methods or in separations. One example of these effects comes from the L-PA model system [59,129]. In a mobile phase consisting of MeCN/potassium phosphate buffer (70:30 (v/v)), the column efficiency and resolution were considerably higher while the sample load capacity was lower than when evaluating the same polymer in an organic system of acetonitrile/acetic acid/water (92.5/5/2.5 (v/v/v)) (Fig. 5.29). In the latter system peak splitting and a particularly slow mass transfer were observed. This was interpreted as being due to a slight contraction of the polymer in the aqueous mobile phase. This leads to a more compact structure and closing of smaller pores, leaving the remaining accessible sites confined mainly to macropores. Since the macropores are more accessible than the micropores the mass transfer is more rapid but, on the other hand, less sample can now be loaded onto the column due to the lower amount of accessible binding sites. The change in mass transfer characteristics is reflected in a strong dependence of the selectivity, retention and resolution on flow rate and temperature of the organic mobile phases [6,59], whereas in the aqueous mobile phase the flow rate has less influence on the selectivity, resolution, plate number and asymmetry [59].

### 5.7.2. Chromatographic retention modes

#### 5.7.2.1. Electrostatic interactions – Organic mobile phases

For low to moderately polar templates, good recognition is generally seen using organic solvents as rebinding media, where the template interacts mainly electrostatically with the binding sites. In fact, most rebinding experiments to MIPs demonstrating high affinity and selectivity have been performed using organic solvents

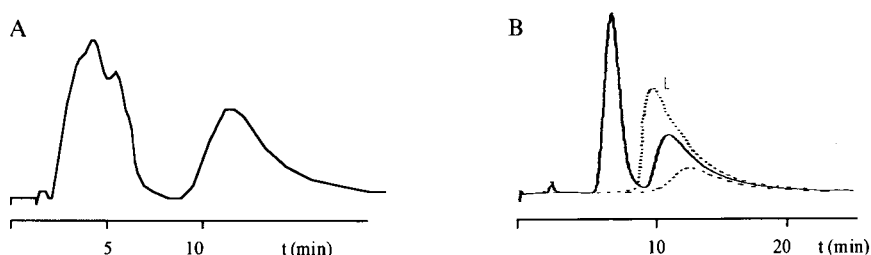


Fig. 5.29. Elution profiles of D,L-PA (100 nmol) injected on L-PA MIP stationary phases using two different mobile phases. (A) Mobile phase: acetonitrile/water/acetic acid: 92.5/2.5/5 (v/v/v). (B) Acetonitrile/potassium phosphate buffer 0.05 M, pH 7: 70/30 (v/v). The MIPs were prepared using dichloromethane as porogen. In (B) increasing loads of D,L-PA were applied. The sample loads were from right to left in the chromatogram 50, 100 and 200 nmol. The D-enantiomer is shown only at the 100 nmol sample load. From Sellergren and Shea [59].

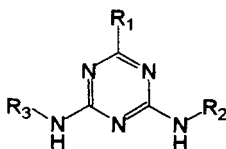
and, for most templates, the first chromatographic rebinding evaluation is carried out in organic mobile phase systems [130]. Model systems using L-PA [6], *N*-protected amino acids [17,18,47,131–133], triazines [32,134–136] and 9EA [24,69,137] as templates have been extensively studied in chromatography using this type of mobile phase. Acetonitrile has been found to be a suitable mobile phase solvent since it is classified as poorly hydrogen bonding and thus has little ability to compete for the hydrogen bonding sites of the template or the polymer binding sites [7]. Furthermore, it solvates the methacrylate polymer backbone well [111] and is polar enough to dissolve a large number of compounds. The initial evaluation is thus often performed in acetonitrile, eventually with the addition of a polar modifier in order to achieve a retention within a practical time window. In the L-PA model system, acetic acid and water are commonly used as modifiers [6]. Due to the strong interactions between the solute and the modifier in this case, an endothermic retention behaviour is seen, i.e. retention increases with temperature [6,59]. These modifiers, also commonly cause the retention to increase with increasing sample load (Fig. 5.25).

### Triazines

Triazines belong to a group of widely used herbicides that have become major pollutants of soil and environmental waters [138,139]. Therefore, analytical methods are needed to allow them to be monitored at concentrations below the  $\mu\text{g/L}$  level. The triazines are available in large numbers with small structural differences and with different known basicity and hydrophobicity (Table 5.15). This class of compounds is therefore well suited as a model system in molecular imprinting [32]. Their conformers and their interactions with small ligands are known [101]. More recently they have also been imprinted and the resulting materials have been successfully incorporated in analytical methods based on competitive assays or selective sample pre-treatments (see chapter 15) [135,140,141].

TABLE 5.15

## HYDROPHOBICITY AND BRÖNSTED BASICITY VALUES FOR TRIAZINES



|                 | R1   | R2                      | R3         | log P <sub>ow</sub> | pK <sub>a</sub> |
|-----------------|------|-------------------------|------------|---------------------|-----------------|
| Prometryn (PRO) | -SMe | iso-propyl              | iso-propyl | 3.4                 | 4.1             |
| Ametryn (AME)   | -SMe | iso-propyl              | ethyl      | 3.07                | 4.1             |
| Terbutylazine   | Cl   | t-butyl                 | ethyl      | 3.04                | 2.0             |
| Atrazine (ATR)  | Cl   | iso-propyl              | ethyl      | 2.6                 | 1.7             |
| Cyanazine (CYA) | Cl   | -2-(2-cyano)-<br>propyl | ethyl      | 1.7                 | 1.0             |

Data from [146].

A comparison of imprinted materials prepared against five structurally related triazines was anticipated to be informative of the structural and functional criteria important for the molecular recognition process [32]. In Fig. 5.30 the capacity factors of the compounds injected separately on all the triazine-selective columns are given. Despite the small structural differences between the templates, most of the materials showed pronounced selectivity for their template. However, the level of selectivity is not the same on all polymers. Whereas the polymer imprinted with cyanazine (P-CYA) showed essentially no selectivity for cyanazine, the polymers imprinted with the more basic and less polar triazines strongly and selectively retained their templates. The strongest interactions are expected to be a cooperative hydrogen bond between the nitrogen *para* to the chlorine (or thiomethyl) substituent and an exocyclic amino group of the triazine and the carboxylic acid group of MAA, as indicated in Fig. 5.31 [101]. As concluded by Albrecht and Zundel [64], the association between substituted pyridines and carboxylic acids in acetonitrile becomes stronger with increasing Brönsted basicity of the base. The strength of the monomer-template interaction is therefore expected to be strongly influenced by the basicity of the triazine. This means that more basic templates will interact more strongly with MAA, promoting a larger population of sites, along with sites with an optimal predisposition of carboxylic acid groups for binding of the template. However, in this case, since cyclic hydrogen bonds can form between MAA and the template, the hydrogen bond donor and acceptor properties for both the template and the monomer must be taken into account. This is clearly shown by the results published by the group of Takeuchi. In their study it was found that ATR was best recognised by polymers prepared using MAA as functional monomer, while AME was better recognised by polymers prepared using trifluoromethyl acrylic acid

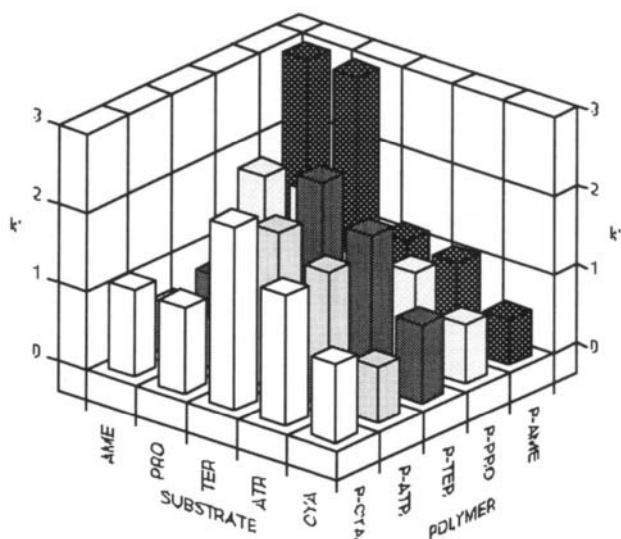


Fig. 5.30. 3D-representation of the capacity factors measured after separate injection of 10 nmol of different triazines on triazine selective columns using acetonitrile/acetic acid/water: 92.5/5/2.5 (v/v/v) as mobile phase. The  $pK_a$  values increase from front to back. From Dauwe and Sellergren [32].

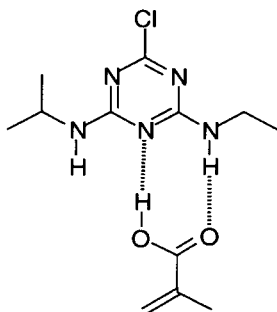


Fig. 5.31. Preferred site of interaction between carboxylic acids and ATR [101].

(TFM) as functional monomer [142]. These polymers exhibit group selectivity, i.e. the ATR MIP preferentially rebinds chlorotriazines while the AME MIP rebinds S-triazines.

#### *N-protected amino acids*

A large number of polymers imprinted with *N*-protected amino acids have been prepared and studied for their chromatographic behaviour in organic mobile phases [17,18,47,72,131–133]. In most cases they have been prepared using a poorly hydrogen bonding diluent, such as chloroform [47,131] or acetonitrile [18,72], and

MAA and/or VPY [132] or AAM [133] as functional monomers. They are then commonly evaluated in media consisting of the same solvent used as diluent together with a polar modifier.

The role of the mobile phase composition using a MIP for BOC-L-phenylalanine was studied by Allender *et al.* in order to gain a better understanding of the retention mechanism [47]. Firstly chloroform, the same solvent used as diluent, was chosen as the base solvent in the mobile phase. In addition to chloroform, non-polar solvents such as hexane and 2,2,4-trimethylpentane were studied as base solvents. However, despite longer retention times, little or no selectivity was observed in these phases. In agreement with the swelling data discussed in Chapter 2, the low swelling in such solvents should lead to pore closing and a lower accessibility to the imprinted sites. The chloroform mobile phase was then modified by the addition of different amounts of polar modifiers. The effect of the modifiers on the retention and selectivity in the separation of both enantiomers on the phase was discussed in terms of the physical properties of the modifier. It was observed that the retention of the enantiomer corresponding to the imprinted enantiomer correlated linearly with the hydrogen bond donor parameter taken from the literature (Fig. 5.32), with THF giving the highest selectivities. Since THF has no hydrogen bond donor capacity, this may indicate that modifier interactions involving the hydrogen bond accepting sites of the template or the polymer functional groups are likely to negatively affect the recognition. This should also be noted in the context of the solvent memory effect, where the best recognition is often seen in the same solvent used in imprinting [69,114]. An explanation for this effect is that the sites are complementary for the template solvated in the same solvent used as diluent. Since chloroform is a hydrogen bond donor, it is likely to interact mainly with the

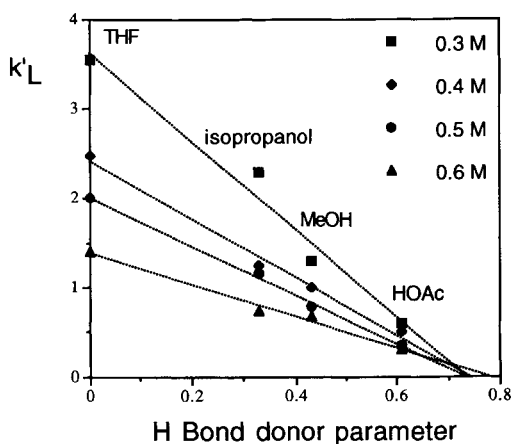


Fig. 5.32. Influence of hydrogen bond donor number of the mobile phase modifier on the capacity factor ( $k'_L$ ) of BOC-L-phenylalanine injected (10  $\mu$ g) on a MIP imprinted with the L-enantiomer. Mobile phase: dichloromethane containing different amounts of the polar modifiers. Reproduced from Allender *et al.* [47].



hydrogen bond accepting sites of the template or the sites and, therefore, a decreasing tendency of the modifier to compete for these sites will lead to better recognition.

### 9-Ethyladenine (9EA)

Polymers imprinted with 9EA were prepared using either chloroform or acetonitrile as diluents [69]. They were then evaluated in mobile phases based on either acetonitrile or chloroform. When the same solvent was used in the rebinding as in the polymerisation step, the strength and selectivity of the template rebinding increased with decreasing polarity and hydrogen bond capacity of the solvent. For instance, a polymer imprinted with 9EA using chloroform as diluent exhibited higher affinity for the template in a chloroform medium than that of a polymer prepared using acetonitrile as diluent evaluated in an acetonitrile medium (Table 5.16) [69]. Interestingly, when evaluating the latter polymer in the less polar chloroform medium a much lower affinity was observed. Likewise, the polymer prepared in chloroform showed a lower rebinding affinity in acetonitrile. Similar solvent dependence has been observed in a number of other systems. Reference should be made to the porogen imprinting effects observed by Hosoya *et al.* [114]. This indicates that the binding sites are complementary to the template, including part of the solvation shell, in the solvent used as diluent and/or that the polymer chains need to be solvated by the same solvent used in the synthesis in order to adopt a conformation for optimum rebinding of the template.

### Other examples

For templates interacting only weakly with the functional monomer, recognition is often only seen when using the same solvent used as diluent. Often, however, no selectivity is observed even then. The most common reasons for the lack of selectivity in these cases are sample overloading and/or slow mass transfer [59]. Decreasing the sample load leads to an increase in both retention and selectivity. Furthermore,

TABLE 5.16

CAPACITY FACTORS OF 9EA IMPRINTED POLYMERS PREPARED AND EVALUATED USING ACETONITRILE OR CHLOROFORM AS DILUENT AND MOBILE PHASE

| Diluent      | Mobile phase                           |  |
|--------------|--|--|
|              | Chloroform/acetic acid: 85/15<br>(v/v) | Acetonitrile/acetic acid: 85/15<br>(v/v) |
| Chloroform   | 17                                     | 2.7                                      |
| Acetonitrile | 2.0                                    | 7.5                                      |

Data from [69].

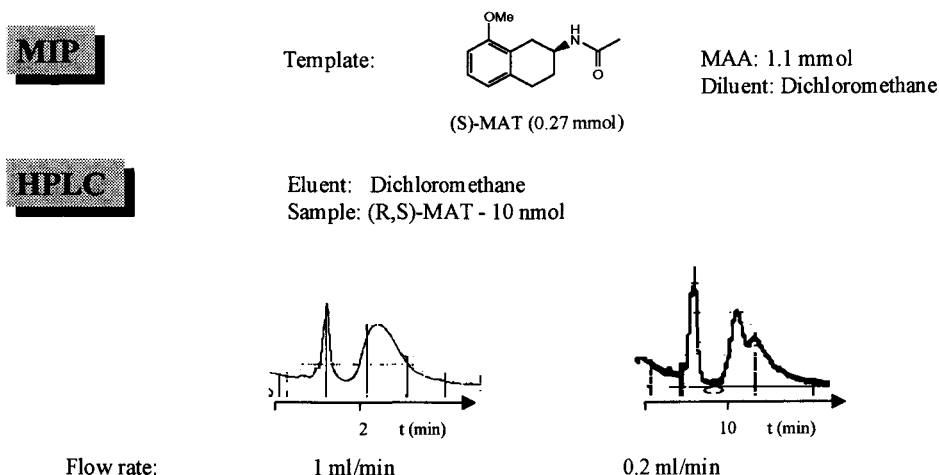


Fig. 5.33. Elution profiles of (R,S)-methoxyamidotetralin (MAT) applied on an (S)-amido-tetralin imprinted stationary phase. Mobile phase: dichloromethane. Sample: (R,S)-MAT, 10 nmol. Flow rate 1 mL/min or 0.2 mL/min. The polymer was prepared using 0.27 mmol template and 1.1 mmol MAA and otherwise as shown in Fig. 5.2.

as previously mentioned, the mass transfer kinetics are particularly slow in organic mobile phases. This problem is often overcome by decreasing the flow rate (see Fig. 5.33).

#### 5.7.2.2. Ion exchange retention mode

This mode is seen for templates with protolytic functional groups, i.e. Brönsted-basic or acidic groups. In the case where, respectively, an acidic (i.e. MAA) or basic (i.e. VPY) functional monomer is used in the preparation of the corresponding MIPs, the polymeric phases often show good chromatographic performance and excellent selectivity in aqueous mobile phases, where the retention is driven by ion exchange [129].

This was observed in the mobile phase optimisation for the resolution of D,L-PA on an L-PA imprinted polymer [129]. Using polymers imprinted with L-PA and a control polymer imprinted with benzylamine as stationary phases, Fig. 5.34A,B shows that each polymer bound preferentially the compound used as template. The selectivity, reflected in the separation factor  $\alpha$ , was high and constant at low pHs, whereas when  $\text{pH}_{\text{app}}$  exceeded the  $\text{p}K_{\text{a}}$  value of the solute  $\alpha$  dropped off to approximately 1 at  $\text{pH}_{\text{app}} = 9.5$ . The selectivity factor for BA on the BA MIP was estimated as an  $\alpha$  value calculated from the ratio of the capacity factor,  $k'$ , on the BA MIP to  $k'$  on the L-PA MIP. Also, this graph (Fig. 5.34D) shows a trend of decreasing  $\alpha$  with increasing pH, although here the decrease is observed over a larger pH range. The fact that maximum retention was observed at a  $\text{pH}_{\text{app}}$  corresponding to the apparent  $\text{p}K_{\text{a}}$  of the solute suggested that the retention was

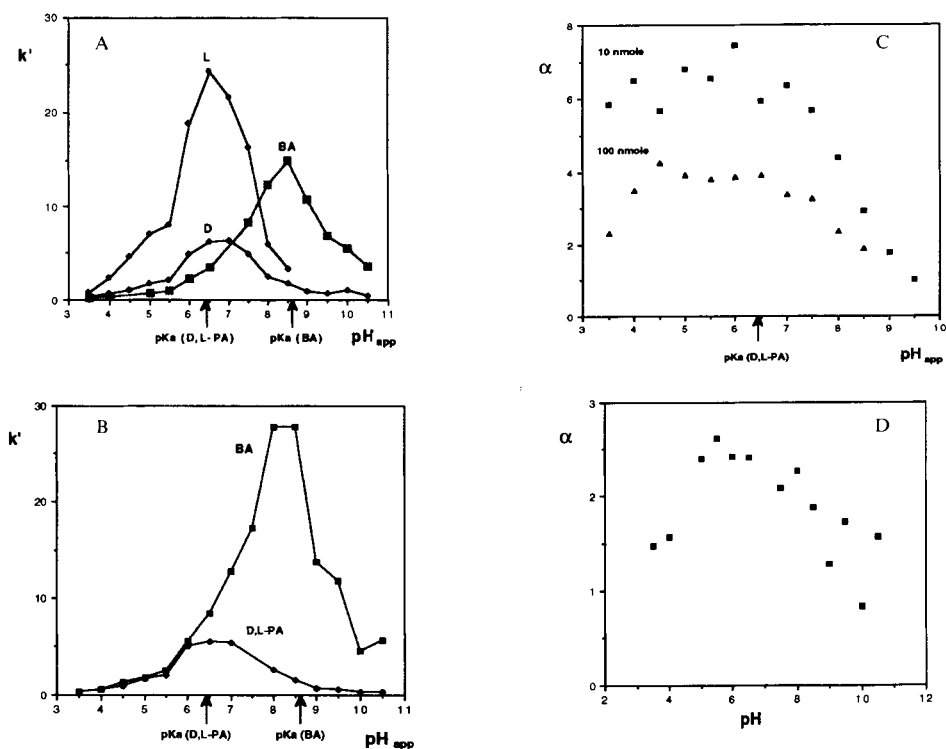


Fig. 5.34. Retention ( $k'$ ) of D- and L-PA and BA on (A) an L-PA MIP: PLPA and (B) a MIP imprinted with BA: PBA, injecting 100 nmol solute versus mobile phase apparent pH ( $pH_{app}$ ). (C) and (D) show the corresponding separation factors ( $\alpha$ ) obtained at two different sample loads. The separation factor of D,L-PA (C) was calculated as  $\alpha = k'_L/k'_D$  and of BA (100 nmol) (D) as  $\alpha = k'_{BA}(\text{on PBA})/k'_{BA}(\text{on PLPA})$ . From Sellergren and Shea [129].

controlled by a simple ion exchange process. Thus the amino group containing solute B (D,L-PA or BA) is bound to the polymer containing carboxylic acid groups (HA) forming ion pairs  $BH^+A^-$ . Assuming that ion exchange is the predominant retention mechanism, the capacity factor can be expressed as [143]:

$$k'_B = K \alpha^*_B \alpha^*_A \quad (18)$$

where  $\alpha^*_A$  and  $\alpha^*_B$  are the degree of ionisation of the acid (A) and the base (B) respectively and  $K$  is a constant for a given column and ionic strength (see also Chapter 2). In order to test the validity of this model,  $\alpha^*_A$  and  $\alpha^*_B$  need to be determined as a function of  $pH_{app}$ . These are obtained from the potentiometric titration data shown in Chapter 2 using the Henderson–Hasselbach equation. In Fig. 5.35A,  $\alpha^*$  for L-PA, BA and the polymer have been plotted versus  $pH_{app}$  and in Fig. 5.35B the product,  $\alpha^*_B \alpha^*_A$ . The agreement with the experimental chromatographic data, both in the pH where the maxima are found and in the relative retention of

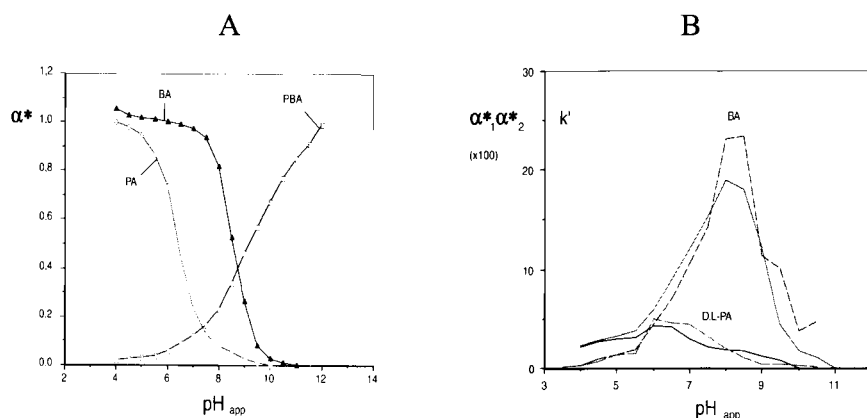


Fig. 5.35. (A) Degree of ionisation ( $\alpha^*$  as a function of mobile phase  $\text{pH}_{\text{app}}$  for the solutes BA and D,L-PA and for PBA.  $\alpha^*$  was calculated from the corresponding potentiometric titration data (see Fig. 2.14, in Chapter 2). (B) Product of the degree of ionisation of the solute ( $\alpha^*_B$ ) and the polymer PBA ( $\alpha^*_A$ ) ( $\times 100$ ) versus mobile phase  $\text{pH}_{\text{app}}$  (solid line). Overlaid are the experimental data from Fig. 5.34 (dashed line). From Sellergren and Shea [129].

the solutes at these maxima, is quite striking. A similar behaviour is often observed for weak bases on weak cation exchangers [143]. It can therefore be concluded that cation exchange is the dominating process controlling the retention in this system. What about the selectivity?

The decrease in enantioselectivity with increasing pH is probably related to: (a) deprotonation of a second group in the site, leading to a loss of an enantioselective hydrogen bond interaction, or (b) deprotonation of additional non-selective sites leading to increased non-specific binding. If  $K_{\text{ns}}$  in case (b) represents the average ion exchange equilibrium constant for the non-selective sites (ns),  $\alpha$  can be expressed as:

$$\alpha = \frac{K_L \alpha^*_L \alpha^*_s + K_{\text{ns}} \alpha^*_L \alpha^*_{\text{ns}}}{K_D \alpha^*_D \alpha^*_s + K_{\text{ns}} \alpha^*_D \alpha^*_{\text{ns}}} \quad (19)$$

Since the second term in both the numerator and the denominator are identical, an increase in  $\alpha^*_{\text{ns}}$  will obviously lead to a decrease in  $\alpha$ . In support of this explanation, the non-specific binding increases above  $\text{pH}_{\text{app}} = 6$ . This is clearly seen in the plot of  $k'$  versus  $\text{pH}_{\text{app}}$  for BA on the L-PA MIP (Fig. 5.34) and in the parallel increase in  $\alpha^*$  for the latter (Fig. 5.35). This can also be seen from the plot of the estimated separation factor of BA ( $\alpha_{\text{BA}}$ ) versus  $\text{pH}_{\text{app}}$  (Fig. 5.34), where  $\alpha$  is highest at low pH values (below  $\text{pK}_a(\text{BA})$ ) and decreases over a large pH interval. Furthermore, the potentiometric titrations showed that the LPA MIP had a lower average  $\text{pK}_a$  than a non-imprinted blank polymer (see Chapter 2). This strongly suggests that the carboxylic acid groups of the selective sites are more acidic than those of the non-selective sites.

In Fig. 5.36 a model is presented showing how the protonation states of

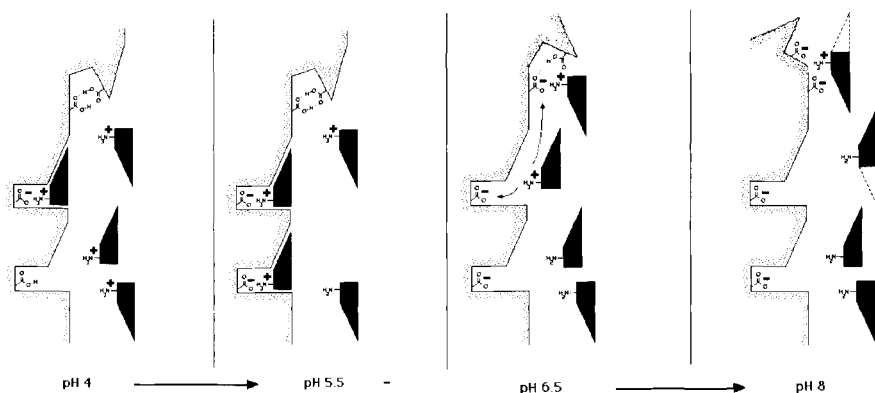


Fig. 5.36. Model showing how the protonation states of D,L-PA and the polymer (PLPA) can account for the change in retention and selectivity with pH as observed in Figs 5.34 and 5.35. From Sellergren and Shea [129].

D,L-PA and the L-PA MIP can account for the observed retention and selectivity. At  $\text{pH}_{\text{app}} = 4$  the solutes D- and L-PA (2-dimensional representation) are protonated and bind differentially to enantioselective sites. At  $\text{pH}_{\text{app}} = 5.5$  the solutes are partially deprotonated, while a larger amount of selective sites are available. This will result in an increase in  $k'$  while  $\alpha$  remains constant. At  $\text{pH}_{\text{app}} = 6.5$  (ca.  $\text{p}K_{\text{a}}$  for D,L-PA), half of the solutes are protonated and non-selective sites become deprotonated, resulting in stronger non-selective interactions and a net increase in binding. At  $\text{pH}_{\text{app}} = 8$ , the solute is only partially protonated, while the negative charge of the polymer increases, mainly as non-selective sites are deprotonated. Thus, the non-selective binding increases while retention as a whole decreases.

As noted in the first proposed explanation (a) for the change in enantioselectivity, an increase in pH may *per se* lead to a decrease in the enantioselectivity of the imprinted sites. One way to separate these effects is to measure the complete isotherms at several pH values and evaluate how the relative population of non-specific and specific sites, as well as their affinity for the template, change with respect to the mobile phase pH [40,50].

A number of other studies using uncharged templates or acids imprinted using VPY as functional monomer show pH dependent selectivities that can be rationalised considering this type of ion exchange model [144].

#### 5.7.2.3. Hydrophobic interactions – Aqueous mobile phases

When increasing the aqueous content in the mobile phase polar templates usually become less retained on MIPs, whereas templates of moderate to low polarity become more retained. The latter increase in retention is due to the hydrophobic effect [32, 145]. Thus, in contrast to the behaviour of other types of

affinity phases with biological recognition elements, such as immunoaffinity phases [138], the imprinted phases behave more like reversed phases when the aqueous content is high [26,32,34,141]. This leads to pronounced non-specific binding, often in the form of a total retention of all hydrophobic compounds. However, to some extent, this non-specific binding can be reduced by the addition of an organic modifier or a detergent [34]. This has been used in the development of a number of competitive aqueous assays using MIPs, often with detection limits and selectivities similar to those reported using corresponding immunoassays (see Chapter 14) [33,34].

In order to gain more insight into the influence of the hydrophobic effect on the chromatographic retention on MIPs the triazine model system was studied [32]. Considering the different hydrophobicities of the triazines (see Table 5.15), it was expected that an increase in the aqueous content of the mobile phase would reveal whether the hydrophobic effect contributed specifically or non-specifically to the observed retention. Three materials were therefore compared, one imprinted with the relatively hydrophobic triazine prometryn (PRO) ( $\log P_{ow} = 3.4$ ), one with the less hydrophobic triazine atrazine (ATR) ( $\log P_{ow} = 2.6$ ) and one reference material imprinted with nicotine (REF). Although the retention of all triazines increased when increasing the aqueous content from 2.5 to 70% (v/v), a marked difference between the columns was observed (Fig. 5.37). Considering first the reference column, the retention of the triazines increased with increasing  $\log P_{ow}$  values (Fig. 5.38), in agreement with observations on reversed-phase columns [146]. Typically, when the hydrophobic effect is the dominating retention mechanism, a linear dependence is seen between  $\log k'$  and  $\log P_{ow}$ , as well as between  $\log k'$  and the aqueous content in the mobile phase. The order of retention and the regular displacement of the curves with increasing aqueous content are evidence that the hydrophobic effect is the dominating retention mechanism of the triazines on the reference column. If we now consider the ATR selective column, in an aqueous poor mobile phase, ATR is clearly more retained on the ATR selective column than on the reference column. The structurally similar terbutylazine (TER) is also selectively retained on this column. As the aqueous content increases, the CI-triazines ATR and TER are more retained on this column than on the reference column, although the selectivity over the S-triazines decreases due to the increasing non-specific hydrophobic contribution to retention (Fig. 5.38). At 70% water only ATR and TER are more retained on this column than on the reference column. Comparison of Fig. 5.38A and Fig. 5.38B shows that the retention at this aqueous content is controlled by a non-specific hydrophobic driving force. Finally, considering the PRO selective column, the selectivity for PRO in the aqueous poor mobile phase is in the same order as that for ATR using the ATR selective column in the same medium. Increasing the aqueous content, it is observed that all triazines are more retained on this column than on the reference column. The retention pattern among the triazines is different from that observed using the ATR selective column. Thus, a pronounced preference for the S-triazines is seen. This appears most clearly at 70% water, where a  $k'$  of 150 was measured for PRO. Obviously, depending on

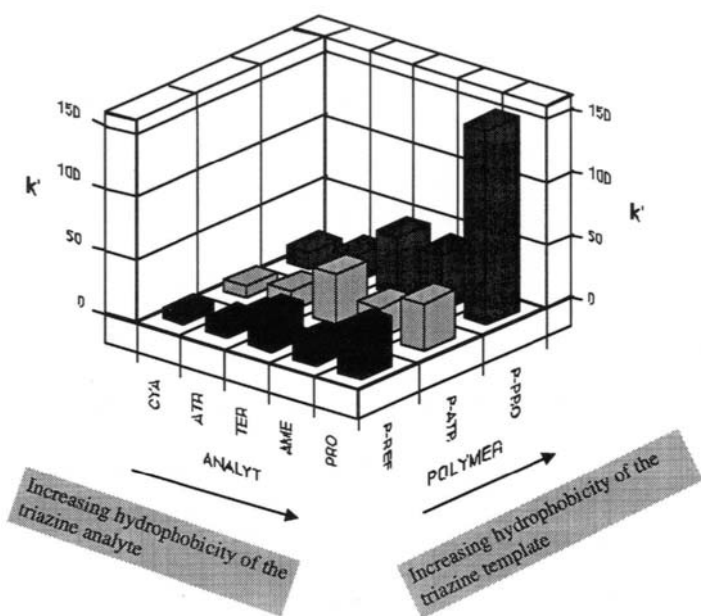


Fig. 5.37. 3D-representation of the capacity factors of five different triazines injected separately (10 nmol) on a reference column (REF), an ATR imprinted column and a PRO imprinted column in the mobile phase: acetonitrile/potassium phosphate buffer, 0.05 M, pH 4: 30/70 (v/v). The amount of CYA injected on the reference column was 100 nmol. The hydrophobicity of the triazines decrease from front to back of the graph. From Dauwe and Sellergren [32].

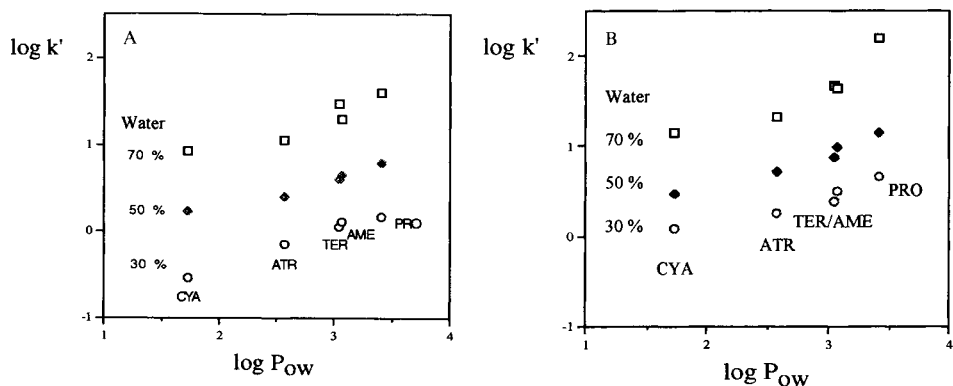


Fig. 5.38. Logarithmic plot of the capacity factors ( $k'$ ) versus the hydrophobicity values ( $\log P_{ow}$ ) of the different triazines measured on (A) a reference column and (B) a PRO imprinted column, using mobile phases with different aqueous contents. From Dauwe and Sellergren [32].

the hydrophobicity of the template, the hydrophobic effect can either enhance or attenuate the selectivity in the molecular recognition of imprinted polymers. This effect is analogous to the hydrophobic binding exhibited by enzymes and antibodies [97] and has been independently observed in several other systems [26,34,147].

### 5.7.3. Mobile phase optimisation

The development of separation methods using imprinted polymers is, of course, dependent on the associated requirements. The goal may simply be to find a method allowing maximum resolution of the analyte from structural analogues or matrix components, regardless of the type of mobile phase. Alternatively, requirements may be associated with mobile phase compatibility, considering the solvent used in the sample preparation or in a subsequent analytical separation step. In view of the many factors that come into play in this optimisation, be they related to polymer structural properties or to properties of the template, there is a need for systematic experimental design, where factors such as template properties, i.e. basicity/acidity, hydrophobicity, polarity, molecular weight, hydrogen bond properties, functionality, and polymer structural properties are related to observable responses, such as chromatographic retention and selectivity. Based on the existing data described in the previous sections a general decision tree can readily be constructed (Fig. 5.39). This assumes an evaluation involving two columns, one packed with the MIP and one packed with the reference, and injection of standards of the template or main analyte and structurally related compounds at several concentrations and at different flow rates and column temperatures. As a measure of the column efficiency and dead volume, the number of theoretical plates and the retention time of a non-interacting void marker is also routinely measured.

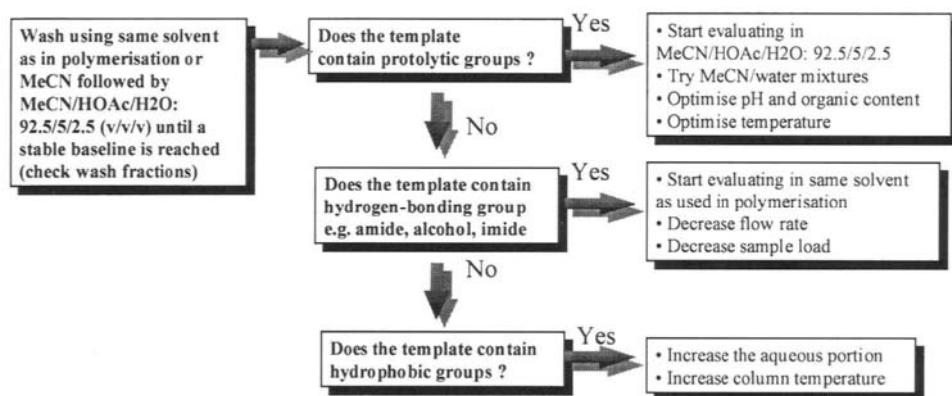


Fig. 5.39. Possible decision tree to apply in the optimisation of mobile phases for MIPs.



## 5.8. CONCLUSIONS

A number of conditions will directly influence the synthesis of new MIPs. Above all, the technique relies on the successful stabilisation of individually weak interactions between the template and the functional monomers. Stable monomer–template assemblies will in turn lead to a useful concentration of high affinity binding sites in the resulting polymer. The availability of the template in preparative amounts will determine whether it will have to be recycled or if a template analogue will have to be used. The latter alternative should also be considered in cases where the template is unstable, highly toxic or poorly soluble in the monomer mixture. Depending on the application, the polymer must meet certain requirements. If the material is going to be used as an HPLC stationary phase, monodisperse spherical particles are desirable and rapid adsorption–desorption of the template to and from the sites is necessary for high performance separations. However, broad and asymmetric band shapes and low saturation capacities, due to the heterogeneous distribution of binding sites and slow mass transfer processes are important problems that strongly limit the possible applications of these phases. Nevertheless, with designed functional monomers, new polymerisation techniques and combinatorial synthesis and screening techniques, MIPs that meet the above criteria may soon be a reality.

## REFERENCES

- 1 G. Wulff, *Angew. Chem., Int. Ed. Engl.*, **34**, 1812 (1995).
- 2 K. Mosbach, *Trends Biochem. Sci.*, **19**, 9 (1994).
- 3(A) G. Moad, D.H. Solomon (Eds.) *The Chemistry of free radical polymerization*, Elsevier Science Ltd., Oxford (1995).
- 3(B) J.M.G. Cowie, *Polymers: chemistry and physics of modern materials*, Blackie and Son, Glasgow (1991).
- 4 R. Arshady and K. Mosbach, *Macromol. Chem.*, **182**, 687 (1981).
- 5 O. Norrlöw, M. Glad and K. Mosbach, *J. Chromatogr.*, **299**, 29 (1984).
- 6 B. Sellergren, M. Lepistö and K. Mosbach, *J. Am. Chem. Soc.*, **110**, 5853 (1988).
- 7 B. Sellergren and K.J. Shea, *J. Chromatogr.*, **635**, 31 (1993).
- 8 D.J. O'Shannessy, B. Ekberg and K. Mosbach, *Anal. Biochem.*, **177**, 144 (1989).
- 9 B. Sellergren, *Makromol. Chem.*, **190**, 2703 (1989).
- 10 L.R. Snyder and J.J. Kirkland, *Introduction to modern liquid chromatography*, Wiley (1979).
- 11 G. Subramanian (Ed.) *A practical approach to chiral separation by liquid chromatography*, VCH, Weinheim (1994).
- 12 K. Nilsson, J. Lindell, O. Norrlöw and B. Sellergren, *J. Chromatogr.*, **680**, 57 (1994).
- 13 S. Nilsson, L. Schweitz and M. Petersson, *Electrophoresis*, **18**, 884 (1997).
- 14 Y. Chen, M. Kele, P. Sajonz, B. Sellergren and G. Guiochon, *Anal. Chem.*, **71**, 928 (1999).
- 15 M. Lepistö and B. Sellergren, *J. Org. Chem.*, **54**, 6010 (1989).
- 16 L.I. Andersson, D.J. O'Shannessy and K. Mosbach, *J. Chromatogr.*, **513**, 167 (1990).
- 17 L.I. Andersson and K. Mosbach, *J. Chromatogr.*, **516**, 313 (1990).
- 18 C. Yu and K. Mosbach, *J. Org. Chem.*, **62**, 4057 (1997).
- 19 O. Ramström, C. Yu and K. Mosbach, *J. Mol. Recognit.*, **9**, 691 (1996).

- 20 A.G. Mayes, L.I. Andersson and K. Mosbach, *Anal. Biochem.*, **222**, 483 (1994).
- 21 O. Ramström, I.A. Nicholls and K. Mosbach, *Tetrahedr. Asymm.*, **5**, 649 (1994).
- 22 D.J. O'Shannessy, B. Ekberg, L.I. Andersson and K. Mosbach, *J. Chromatogr.*, **470**, 391 (1989).
- 23 J.-M. Lin, T. Nakagama, K. Uchiyama and T. Hobo, *J. Pharm. Biomed. Anal.*, **15**, 1351 (1997).
- 24 K.J. Shea, D.A. Spivak and B. Sellergren, *J. Am. Chem. Soc.*, **115**, 3368 (1993).
- 25 G. Vlatakis, L.I. Andersson, R. Müller and K. Mosbach, *Nature* **361**, 645 (1993).
- 26 L.I. Andersson, R. Müller, G. Vlatakis and K. Mosbach, *Proc. Natl. Acad. Sci. USA*, **92**, 4788 (1995).
- 27 L. Stryer, *Biochemistry*, W.H. Freeman and Company, New York (1988).
- 28 J.O. Nelson, A.E. Karu and R.B. Wong (Eds) *Immunoanalysis of agrochemicals*, ACS Symposium Series, Vol. 586, American Chemical Society, Washington (1995).
- 29 L. Pauling, *J. Am. Chem. Soc.*, **62**, 2643 (1940).
- 30 M.J. Whitcombe, M.E. Rodriguez, P. Villar and E.N. Vulfson, *J. Am. Chem. Soc.*, **117**, 7105 (1995).
- 31 G. Wulff, T. Gross and R. Schönfeld, *Angew. Chem. Int. Ed. Engl.*, **36**, 1962 (1997).
- 32 C. Dauwe and B. Sellergren, *J. Chromatogr. A*, **753**, 191 (1996).
- 33 K. Haupt, A. Dzgoev and K. Mosbach, *Anal. Chem.*, **70**, 628 (1998).
- 34 L.I. Andersson, *Anal. Chem.*, **68**, 111 (1996).
- 35 D. Kriz and K. Mosbach, *Anal. Chim. Acta*, **300**, 71 (1995).
- 36 C. Still et al., *J. Am. Chem. Soc.*, **120**, 9112 (1998).
- 37 J.C. Hogan, *Nature*, **384**, 17 (1996).
- 38 K.A. Connors, *Binding constants. The measurement of molecular complex stability*, John Wiley & Sons, New York (1987).
- 39 A.M. Katti, M. Diack, M.Z. El Fallah, S. Golshan-Shirazi, S.C. Jacobson, A. Seidel-Morgenstern and G. Guiochon, *Acc. Chem. Res.*, **25**, 366 (1992).
- 40 P. Sajonz, M. Kele, G. Zhong, B. Sellergren and G. Guiochon, *J. Chromatogr.*, **810**, 1 (1998).
- 41 G. Wulff, R. Grobe-Einsler, W. Vesper and A. Sarhan, *Makromol. Chem.*, **178**, 2817 (1977).
- 42 M.J. Whitcombe, M.E. Rodriguez and E.N. Vulfson, *Spec. Publ. R. Soc. Chem.*, **158**, 565 (1994).
- 43 K.J. Shea and D.Y. Sasaki, *J. Am. Chem. Soc.*, **113**, 4109 (1991).
- 44 G. Wulff, W. Vesper, R. Grobe-Einsler and A. Sarhan, *Makromol. Chem.*, **178**, 2799 (1977).
- 45 K.J. Shea and T.K. Dougherty, *J. Am. Chem. Soc.*, **108**, 1091 (1986).
- 46 M. Kempe and K. Mosbach, *Anal. Lett.*, **24**, 1137 (1991).
- 47 C.J. Allender, C.M. Heard and K.R. Brain, *Chirality*, **9**, 238 (1997).
- 48 J. Matsui, A. Kaneko, Y. Miyoshi, K. Yokoyama, E. Tamiya and T. Takeuchi, *Anal. Lett.*, **29**, 2071 (1996).
- 49 B. Sellergren, *J. Chromatogr. A*, **673**, 133 (1994).
- 50 G. Guiochon, S. Golshan-Shirazi and A. Katti, *Fundamentals of preparative and nonlinear chromatography*, Academic Press, New York (1994).
- 51 T.E. Mallouk and D.J. Harrison (Eds) *Interfacial design and chemical sensing*, ACS Symposium Series 561, American Chemical Society, Washington DC (1994).
- 52 P. Tijssen, In: *Laboratory techniques in biochemistry and molecular biology*, Vol. 15, R.H. Burdon and P.H. van Knippenberg Eds, Elsevier, Amsterdam (1985).
- 53 R. Karlsson, A. Michaelsson and A.J. Mattson, *J. Immunol. Meth.*, **145**, 229 (1991).
- 54 T. Takeuchi, D. Fukuma and J. Matsui, *Anal. Chem.*, **71**, 285 (1999).
- 55 J. Å. Jönsson (Ed.) *Chromatographic theory and basic principles*, Marcel Dekker Inc., New York (1987).
- 56 C. Horvath and H.-J. Lin, *J. Chromatogr.*, **149**, 43 (1978).
- 57 J.C. Giddings, *Anal. Chem.* **13**, 1999 (1963).

- 58 J.R. Condor, *J. High Res. Chrom. & CC*, **5**, 341 (1982).
- 59 B. Sellergren and K.J. Shea, *J. Chromatogr. A*, **690**, 29 (1995).
- 60 A. Jardy and R. Rosset, *J. Chromatogr.*, **83**, 195 (1973).
- 61 R. Eksteen, J.C. Kraak and P. Linssen, *J. Chromatogr.*, **148**, 413 (1978).
- 62 T.P. O'Brien, N.H. Snow, N. Grinberg and L. Crocker, *J. Liq. Chromatogr. & Rel. Technol.*, **22**, 183 (1999).
- 63 M.H. Abraham, P.P. Duce, D.V. Prior, D.G. Barrat, J.J. Morris and P.J. Taylor, *J. Chem. Soc. Perkin Trans. II*, 1355 (1989).
- 64 G. Albrecht and G. Zundel, *Z. Naturforsch.*, **39a**, 986 (1984).
- 65 E. Fan, S.A. Van Arman, S. Kincaid and A.D. Hamilton, *J. Am. Chem. Soc.*, **115**, 369 (1993).
- 66 G. Wulff and R. Schönfeld, *Adv. Mater.*, **10**, 957 (1998).
- 67 B. Sellergren, *Anal. Chem.*, **66**, 1578 (1994).
- 68 S.H. Cheong, S. McNiven, A. Rachkov, R. Levi, K. Yano and I. Karube, *Macromolecules*, **30**, 1317 (1997).
- 69 D. Spivak, M.A. Gilmore and K.J. Shea, *J. Am. Chem. Soc.*, **119**, 4388 (1997).
- 70 W.H. Pirkle and T.C. Pochapsky, *J. Am. Chem. Soc.*, **108**, 352 (1986).
- 71 M. Kempe, L. Fischer and K. Mosbach, *J. Mol. Recognit.*, **6**, 25 (1993).
- 72 O. Ramström, L.I. Andersson and K. Mosbach, *J. Org. Chem.*, **58**, 7562 (1993).
- 73 R. Levi, S. McNiven, S.A. Piletsky, S.-H. Cheong, K. Yano and I. Karube, *Anal. Chem.*, **69**, 2017 (1997).
- 74 S.A. Piletsky, E.V. Piletskaya, T.L. Panasyuk, A.V. El'skaya, R. Levi, I. Karube and G. Wulff, *Macromolecules*, **31**, 2137 (1998).
- 75 S.A. Piletsky, Y.P. Parhometz, N.V. Lavryk, T.L. Panasyuk and A.V. El'skaya, *Sens. Actuators B*, **19**, 629 (1994).
- 76 A. Kugimiya, J. Matsui, T. Takeuchi, K. Yano, H. Muguruma, A.V. Elgersma and I. Karube, *Anal. Lett.*, **28**, 2317 (1995).
- 77 A. Kugimiya, T. Takeuchi, J. Matsui, K. Ikebukuro, K. Yano and I. Karube, *Anal. Lett.*, **29**, 1099 (1996).
- 78 S.A. Piletsky, E.V. Piletskaya, K. Yano, A. Kugimiya, A.V. Elgersma, R. Levi, U. Kahlow, T. Takeuchi, I. Karube et al., *Anal. Lett.*, **29**, 157 (1996).
- 79 J.V. Beach and K.J. Shea, *J. Am. Chem. Soc.*, **116**, 379 (1994).
- 80 K. Sreenivasan, *Talanta*, **44**, 1137 (1997).
- 81 K. Sreenivasan, *Angew. Makromol. Chem.*, **246**, 65 (1997).
- 82 K. Sreenivasan, *J. Appl. Polym. Sci.*, **71**, 1819 (1999).
- 83 K. Sreenivasan and R. Sivakumar, *J. Appl. Polym. Sci.*, **66**, 2539 (1997).
- 84 K. Sreenivasan and R. Sivakumar, *J. Appl. Polym. Sci.*, **71**, 1823 (1999).
- 85 P. Turkewitsch, B. Wandelt, G.D. Darling and W.S. Powell, *Anal. Chem.*, **70**, 2025 (1998).
- 86 K. Hosoya, Y. Shirasu, K. Kimata and N. Tanaka, *Anal. Chem.*, **70**, 943 (1998).
- 87 J. Matsui, Y. Miyoshi and T. Takeuchi, *Chem. Lett.*, **11**, 1007 (1995).
- 88 M. Zihui, Z. Liangmo, W. Jinfang, W. Quinghai and Z. Daoquian, *Biomed. Chromatogr.*, **13**, 1 (1999).
- 89 S.K. Chang, D. Van Engen, E. Fan and A.D. Hamilton, *J. Am. Chem. Soc.*, **113**, 7640 (1991).
- 90 K. Tanabe, T. Takeuchi, J. Matsui, K. Ikebukuro, K. Yano and I. Karube, *J. Chem. Soc., Chem. Commun.*, **22**, 2303 (1995).
- 91 H. Asanuma, M. Kakazu, M. Shibata, T. Hishiya and M. Komiyama, *Chem. Commun.*, **20**, 1971 (1997).
- 92 S.A. Piletsky, H.S. Andersson and I.A. Nicholls, *Macromolecules*, **32**, 633 (1999).
- 93 B. Sellergren, J. Wieschemeyer, K.-S. Boos and D. Seidel, *Chem. Mat.*, **10**, 4037 (1998).
- 94 K. Yano, T. Nakagiri, T. Takeuchi, J. Matsui, K. Ikebukuro and I. Karube, *Anal. Chim. Acta.*, **357**, 91 (1997).
- 95 C. Kirsten and T. Schrader, *J. Am. Chem. Soc.*, **119**, 12,061 (1997).
- 96 C.J. Welch, *J. Chromatogr. A*, **689**, 189 (1995).

- 97 A. Fersht, *Enzyme structure and mechanism*, W.H. Freeman and Company, New York (1985).
- 98 B. Sellergren and K.G.I. Nilsson, *Methods Mol. Cell. Biol.*, **1**, 59 (1989).
- 99 H.S. Andersson, A.-C. Koch-Schmidt, S. Ohlson and K. Mosbach, *J. Mol. Recognit.*, **9**, 675 (1996).
- 100 G. Lancelot, *J. Am. Chem. Soc.*, **99**, 7037 (1977).
- 101 G.J. Welhouse and W.F. Bleam, *Environ. Sci. Technol.*, **27**, 500 (1993).
- 102 J. Rebek, *Angew. Chem. Int. Ed. Engl.*, **29**, 245 (1990).
- 103 I.A. Nicholls, *Chem. Lett.*, **11**, 1035 (1995).
- 104 G. Wulff, R. Kemmerer and J. Vietmeier, *Nouv. J. Chim.*, **6**, 681 (1982).
- 105 H.S. Andersson and I.A. Nicholls, *Bioorg. Chem.*, **25**, 203 (1997).
- 106 A.G. Mayes and C.R. Lowe, *Methodol. Surv. Bioanal. Drugs*, **25**, 28 (1998).
- 107 P. Reinholdsson, T. Hargitai, R. Isaksson and B. Törnell, *Angew. Makromol. Chem.*, **192**, 113 (1991).
- 108 H.W. Offen, In: *Molecular complexes I*, R. Foster Ed., Elek Science, London, p. 117 (1973).
- 109 K.E. Weale, In: *Reactivity, mechanism and structure in polymer chemistry*, A. Jenkins Ed., Wiley, Belfast, p. 158 (1974).
- 110 B. Sellergren, C. Dauwe and T. Schneider, *Macromolecules*, **30**, 2454 (1997).
- 111 J. Bandrup and E.H. Immergut, *Polymer handbook*, Wiley, New York (1989).
- 112 J. Berglund, I.A. Nicholls, C. Lindbladh and K. Mosbach, *Bioorg. Med. Chem. Lett.*, **6**, 2237 (1996).
- 113 K.J. Shea and D.Y. Sasaki, *J. Am. Chem. Soc.*, **111**, 3442 (1989).
- 114 K. Hosoya, K. Yoshizako, K. Kimata, N. Tanaka and J. Haginaka, *J. Chromatogr.*, **18**, 232 (1997).
- 115 A.C. Beach and R. Gupta, *Carcinogenesis*, **13**, 1053 (1992).
- 116 G. Wulff and J. Gimpel, *Makromol. Chem.*, **183**, 2469 (1982).
- 117 D.J. Cram, *Angew. Chem. Int. Ed. Engl.*, **27**, 1009 (1988).
- 118 J. Matsui, Y. Miyoshi, O. Doblhoff-Dier and T. Takeuchi, *Anal. Chem.*, **67**, 4404 (1995).
- 119 G. Wulff and S. Schauhoff, *J. Org. Chem.*, **56**, 395 (1991).
- 120 J.L. Morrison, M. Worsley, D.R. Shaw and G.W. Hodgson, *Can. J. Chem.*, **37**, 1986 (1959).
- 121 A. Katz and M.E. Davis, *Macromolecules*, **32**, 4113 (1999).
- 122 B. Sellergren and K.J. Shea, *Tetrahedr. Assymm.*, **5**, 1403 (1994).
- 123 J.C.J. Adrian and C.S. Wilcox, *J. Am. Chem. Soc.*, **113**, 678 (1991).
- 124 M.J. Whitcombe, L. Martin and E.N. Vulfson, *Chromatographia*, **47**, 457 (1998).
- 125 S. McNiven, Y. Yokobayashi, S.H. Cheong and I. Karube, *Chem. Lett.*, **12**, 1297 (1997).
- 126 M. Jelinkova, L.K. Shataeva, G.A. Tischenko and F. Svec, *Reactive Polymers*, **11**, 252 (1989).
- 127 A. Guyot, In: *Synthesis and separations using functional polymers*, D.C. Sherrington and P. Hodge Eds, John Wiley & Sons Ltd, Tiptree, p. 1 (1988).
- 128 D.W. Armstrong, J.M. Schneiderheinze, Y.S. Hwang and B. Sellergren, *Anal. Chem.*, **70**, 3717 (1998).
- 129 B. Sellergren and K.J. Shea, *J. Chromatogr. A*, **654**, 17 (1993).
- 130 B. Sellergren, *Trends Anal. Chem.*, **18**, 164 (1999).
- 131 M. Kempe, *Anal. Chem.*, **68**, 1948 (1996).
- 132 T.P. O'Brien, N.H. Snow, N. Grinberg and L. Crocker, *J. Liq. Chrom. & Rel. Technol.*, **22**, 183 (1999).
- 133 M. Zihui, Z. Liangmo, W. Jinfang, W. Quinghai and Z. Daoqian, *Biomed. Chromatogr.*, **13**, 1 (1999).
- 134 J. Matsui, O. Doblhoff-Dier and T. Takeuchi, *Chem. Lett.*, **6**, 489 (1995).
- 135 M.T. Muldoon and L.H. Stanker, *Anal. Chem.*, **69**, 803 (1997).

- 136 R.J. Ansell, D. Kriz and K. Mosbach, *Curr. Opin. Biotechnol.*, **7**, 89 (1996).
- 137 D.A. Spivak and K.J. Shea, *Macromolecules*, **31**, 2160 (1998).
- 138 V. Pichon, L. Chen, N. Durand, F. Le Goffic and M.-C. Hennion, *J. Chromatogr. A*, **725**, 107 (1996).
- 139 D. Barceló, S. Lacorte and J. L. Marty, *Trends Anal. Chem.*, **14**, 334 (1995).
- 140 M.T. Muldoon and L.H. Stanker, *J. Agric. Food Chem.*, **43**, 1424 (1995).
- 141 J. Matsui, M. Okada, M. Tsuruoka and T. Takeuchi, *Anal. Commun.*, **34**, 85 (1997).
- 142 T. Takeuchi, D. Fukuma and J. Matsui, *Anal. Chem.*, **71**, 285 (1999).
- 143 D.J. Pietrzyk, In: *Packings and stationary phases in chromatographic techniques*, Vol. 47, K.K. Unger Ed., Marcel Dekker Inc., New York, p. 585 (1990).
- 144 C. Baggiani, F. Trotta, G. Giraudi, G. Moraglio and A. Vanni, *J. Chromatogr. A*, **786**, 23 (1997).
- 145 I.A. Nicholls, O. Ramström and K. Mosbach, *J. Chromatogr. A*, **691**, 349 (1995).
- 146 G. Sacchero, S. Apone, C. Sarzanini and E. Mentasti, *J. Chromatogr.*, **668**, 365 (1994).
- 147 O. Ramström, L. Ye and P.E. Gustavsson, *Chromatographia*, **48**, 197 (1998).
- 148 C. Milstein, *Sci. Amer.*, **243**, 66 (1980).
- 149 B. Sellergren and L. Andersson, *J. Org. Chem.*, **55**, 3381 (1990).
- 150 J.U. Klein, M.J. Whitcombe, F. Mulholland and E.N. Vulfson, *Angew. Chem. Int. Ed.*, **38**, 2057 (1999).
- 151 P.K. Dahl and F.H. Arnold, *J. Am. Chem. Soc.*, **113**, 7417 (1991).
- 152 L. Fischer, R. Müller, B. Ekberg and K. Mosbach, *J. Am. Chem. Soc.*, **113**, 9358 (1991).
- 153 L. Andersson, B. Sellergren and K. Mosbach, *Tetrahedr. Lett.*, **25**, 5211 (1984).
- 154 I.R. Dunkin, J. Lenfeld and D.C. Sherrington, *Polymer*, **34**, 77 (1993).
- 155 M. Kempe and K. Mosbach, *Tetrahedr. Lett.*, **36**, 3563 (1995).
- 156 O. Norrlöw, PhD Thesis, University of Lund (1986).
- 157 K. Hosoya, K. Yoshizako, Y. Shirasu, K. Kimata, T. Araki, N. Tanaka and J. Haginaka, *J. Chromatogr. A*, **728**, 139 (1996).
- 158 K. Yoshizako, K. Hosoya, Y. Iwakoshi, K. Kimata and N. Tanaka, *Anal. Chem.*, **70**, 386 (1998).

## **Metal-ion coordination in designing molecularly imprinted polymeric receptors**

PRADEEP K. DHAL

### **6.1. INTRODUCTION**

Research in the area of “nanotechnology” has generated a great deal of interest in recent years [1]. Realisation of such nanoscale level, structurally ordered materials might have far-reaching implications for electrooptic and biomimetic engineering. Thus design, synthesis and investigation of complex molecular structures and assemblies would lead to novel materials, which could be used in subtle technologies such as: sensors, computer memory elements, catalysis, medical diagnostics, and in other biomedical and biotechnological applications mimicking biological functions. Since molecular recognition is central to the development of these supramolecular systems, there has always been great interest in designing molecular recognition materials with a high degree of precision and sophistication [2]. Current strategies for the preparation of these materials involves directed pre-organisation of functional groups in the host systems (receptors), corresponding to the complementary functional groups of the guest molecules (substrates) [3]. Complementarity between the host–guest binding sites dictates the placement of functional groups in the synthetic receptor, while the multiple interactions and molecular rigidity contribute to the stability and specificity of the system.

Several strategies involving template-mediated chemical synthesis and molecular self-assembly processes have been developed for preparing these molecular and supramolecular systems with functional groups precisely positioned on the scale of nanometres or less [4]. “Molecular imprinting” technology is a facile method to prepare polymer based synthetic receptors [5]. Specific advantages associated with these polymeric molecular recognition materials include their robustness and the vast potential for materials engineering for specific applications, as well as their generality and relative simplicity. Key to the success of the polymeric systems is the specific positioning of binding sites that interact with the guest molecules reversibly in a solid phase. Towards this end, various intermolecular interactions (both covalent and non-covalent) have been investigated [6]. The aim of this article is to review the role of “metal–ligand coordination” interaction in designing novel molecularly imprinted polymeric receptors. The article summarises the state-of-the-art of the use of metal-coordination interaction to synthesise these polymeric receptors and their use for various applications.

## 6.2. BINDING SITE INTERACTIONS IN MOLECULARLY IMPRINTED POLYMERS

Selective recognition of substrates by molecularly imprinted polymers is critically dependent upon the nature of the binding interactions operating in the system. The kinetics and thermodynamics of substrate recognition and rebinding by imprinted polymers depend on the nature of the interaction involved, in addition to the physical and chemical nature of the material (*viz.* flexibility, accessibility of the binding sites, materials shapes, etc.) [7]. In order for the molecularly imprinted polymer to be useful, fast desorption and rebinding kinetics under mild conditions are as important as the substrate selectivity. This implies that the selection of appropriate binding interactions is very critical while designing molecularly imprinted materials. In addition to having more than one binding site, the best recognition is obtained when the interactions between the binding sites of the monomers and the templates have some directionality. Thus, both covalent and non-covalent interactions between the monomers and templates have been utilised in the preparation of these receptors. Different molecular interactions offer varying levels of specificity and reversibility. Thus covalent bonding is highly functional group specific and directional, yet it is notoriously slow in rebinding kinetics. On the other hand, hydrophobic interactions can be applicable to a vast array of compounds and thus is less specific, although extremely rapid. In general, non-covalent interactions are more appealing due to their versatility, faster kinetics and the requirement of milder conditions for their formation and breakage. Furthermore, certain non-covalent interactions like  $\pi$ - $\pi$  interactions, hydrogen bonding and metal-coordination interactions are quite directional and offer promising opportunities to design novel molecularly imprinted functional polymers.

## 6.3. ADVANTAGES OF METAL-COORDINATION INTERACTIONS IN MOLECULAR RECOGNITION

Analysis of different kinds of interactions involved in biological recognition processes reveals that metal ions play a very important role in some of the vital biological processes [8]. Interactions between metal ions and biological ligands are highly specific. Formation and breakage of these interactions take place under mild conditions in an aqueous environment [9]. There are several advantages associated with metal-coordination interaction, thus making this interaction a viable binding mode to prepare molecularly imprinted polymers. Metal ions offer a high degree of versatility in targeting different functional groups in many biologically relevant molecules as well as tailoring the kinetics and strength of individual interactions. For example, to target the imidazole groups of histidine residues in proteins,  $\text{Cu}^{2+}$  and  $\text{Fe}^{2+}$  can be used. On the other hand,  $\text{Ni}^{2+}$  and  $\text{Zn}^{2+}$  can be used to target phosphoryl groups. The availability of a vast array of ligands allows one to control and define the coordinating properties of metal centres towards different substrates [10]. The possibility of replacing metal ions in a given polymer matrix with other

metal ions to alter selectivities and binding kinetics further expands the scope of this approach. While electrostatic and hydrogen bonding interactions perform poorly in aqueous media, metal-coordination interaction is not affected by the solvent environment. Since, unlike other non-covalent interactions, definite interaction between the substrates and metal centres occurs, use of excess binding groups is not necessary, thereby minimising the formation of non-specific binding sites. Thus the flexibility, combined with the strength and specificity of metal-coordination interactions in various solvents, makes metal-coordination interaction an attractive binding mechanism for recognition of delicate substrates, in particular those of biological origin.

In separation science, “ligand-exchange chromatography” indeed exploits the rapid and reversible formation of metal complexes to separate compounds, which can donate electrons and coordinate to complexed metal ions immobilised on a solid support [11]. Retention of a given species is directly related to the stability of the mixed ligand complex it forms with the immobilised metal complex. Utilisation of this principle for the separation of chiral molecules, as well as large biological macromolecules such as proteins, has been successfully demonstrated.

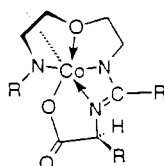
## 6.4. DESIGN OF MOLECULARLY IMPRINTED POLYMERS BASED ON METAL-COORDINATION INTERACTION

### 6.4.1. Bulk polymerised metal-coordinating polymeric receptors

Positioning of metal ions to match the arrangement of ligands on a substrate molecule through preorganisation of the said substrate with a metal-complexing monomer and its subsequent cross-linking polymerisation offers an attractive route to prepare novel polymeric receptors. Since the strength and specificity of metal–ligand coordination are amenable to regulation through the choice of appropriate metal ions and the ligands, the approach allows one to tailor-make imprinted polymers for substrates containing different kinds of functional groups. Furthermore, since the metal–ligand coordination complexes are stable in aqueous media, this offers the possibility to design receptors for complex biological macromolecules such as enzymes, hormones, DNA and RNA. Surprisingly, despite the potential advantages offered by metal-coordination interaction, relatively few efforts have been made to use this binding mode to design molecularly imprinted polymers.

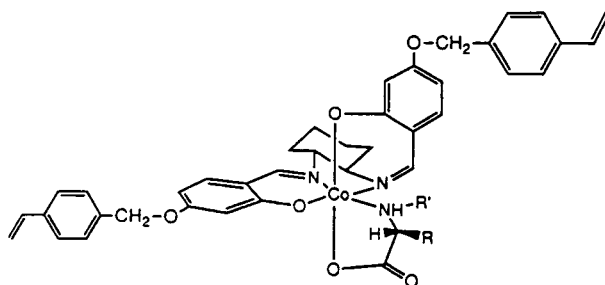
The first attempt to use metal-coordination interaction for preparing molecularly imprinted polymers was made by Belokon and co-workers [12]. Using *A* and *Δ*-bis[N-(5-methacryloylamino)salicylidene-*S*-norsalinate] Co(III) complexes (e.g. **1**) as the metal-complexing monomers, cross-linking template polymerisation was carried out using *N,N'*-methylenebisacrylamide as the cross-linking agent. This produced rigid polymer matrices with stabilised octahedral Co<sup>3+</sup> chiral complexes. Deuterium exchange studies with the polymeric complex proceeded with full retention of the configuration of the amino acid, thus suggesting that the initial conformation of the complex was retained in the polymer matrix.





1

Fujii *et al.* reported the use of metal-coordination interaction based imprinted polymers for specific recognition and binding of chiral amino acids [13]. In fact, this polymer exhibited the highest enantioselectivity for substrate recognition amongst all the imprinted polymers reported so far. A chiral Schiff base ligand of (1*R*,2*R*)-1,2-diaminocyclohexane and 4-(4-vinylbenzyloxy)salicylaldehyde, to which amino acids were bound through a  $\text{Co}^{3+}$  complex (2), was used as the template monomer. Copolymerisation of the monomer–template assembly with styrene and divinylbenzene produced the desired functional polymer network. After removal of the template amino acid from the polymer, the imprinted polymer was allowed to equilibrate with a racemate of the amino acid template. A remarkably high enantioselectivity (optical purity  $\sim 99.5\%$ ) in the optical resolution of the racemate was observed. This exceptionally high selectivity was attributed to a chiral cavity effect. Unfortunately, the slow mass transfer rate in the case of  $\text{Co}^{3+}$  complexes limits the practical application of this imprinted polymer as an adsorbent for chiral chromatography.



2

Using  $\text{Co}^{2+}$  as the metal centre, 1-vinyl imidazole as the functional monomer and amino acids as the templates, Leonhardt and Mosbach prepared imprinted metal-complexing polymers [14]. These polymers were aimed at being used as enzyme-like substrate specific catalysts (for more details, see Section 6.5.3.).

Systematic investigation towards using template polymerisation to control the spatial distribution of binding sites based on metal-coordination interaction has been carried out by Arnold and co-workers [15]. The objective of this endeavour has been to evaluate the scope and limitations of molecularly imprinted polymers containing metal coordinating sites in designing new generations of molecular recognition materials. The mild conditions required for the formation and breakage of this interaction have motivated this group to develop novel adsorbents for the recognition and separation of proteins and other biomolecules.

As the first attempt to demonstrate the advantage of this binding interaction, the strong coordination between the iminodiacetic acid (IDA)- $\text{Cu}^{2+}$  complex and imidazole was utilised to prepare molecularly imprinted polymers [16]. Using the compound (3) as the functional monomer and various bis-imidazole derivatives (e.g. 4–6) as the templates, cross-linking polymerisation of the template–monomer assemblies was carried out using ethylene glycol dimethacrylate as the cross-linking agent. Complexation of the monomer with the templates during polymerisation directed the positioning of metal ions in the polymer matrices, while a high degree of cross-linking stabilised these spatial arrangements of the metal-coordinating sites. Near quantitative desorption and reloading of the metal ions and substrates with these polymers suggested the high accessibility of the binding sites in these polymers. This imprinting polymerisation process is illustrated in Fig. 6.1. The fidelity of these polymers was tested by evaluating their abilities to distinguish between various *bis*-imidazole substrates.

The paramagnetic nature of  $\text{Cu}^{2+}$  ion was utilised to characterise these polymeric receptors by studying the interaction between the  $\text{Cu}^{2+}$  centres and imidazole groups using ESR spectroscopy [17]. Results from the ESR experiments indicate that  $\text{Cu}^{2+}$ -imidazole coordination bonds formed during the assembly of the monomer and template are conserved upon polymerisation. Furthermore, analysis of the ESR data obtained for different polymers suggested a defined arrangement of metal ion sites in the templated materials, which is absent in the non-templated control polymers.

In competitive substrate binding experiments, the polymers showed selectivity for the templates with which they were made. On the other hand, non-templated control polymers showed statistical preference for both substrates. Some results on the substrate selectivities of these polymers are presented in Table 6.1. It is particularly notable from this study that these imprinted polymers could distinguish positional isomers (4 and 5), which differ in their imidazole spacing by only  $\sim 4 \text{ \AA}$ .

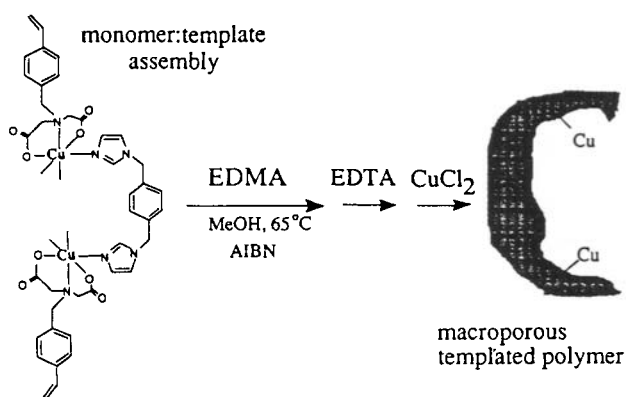
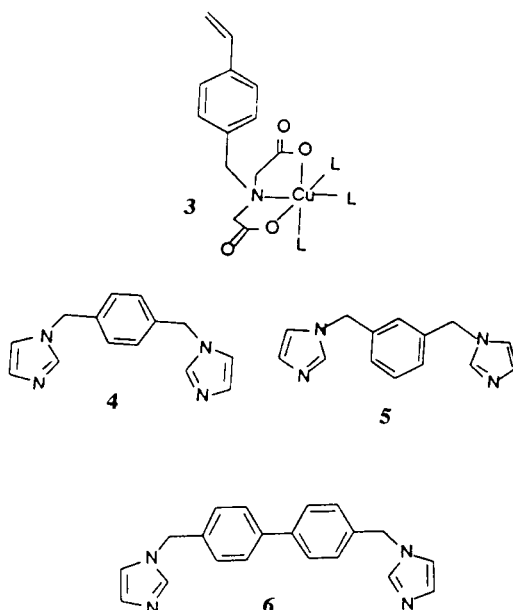


Fig. 6.1. Preparation of molecular imprinted metal-coordinating polymers for *bis*-imidazole substrates.



Maximum binding capacities of these polymers towards different substrates and their apparent binding constant values were determined. These results indicate that the substrate selectivity exhibited by these imprinted polymers may involve a combination of cooperative two-site coordination of the *bis*-imidazoles to the metal centres, as well as steric interaction with the cavity containing the binding sites.

Since the strength of the metal-coordination interaction between the metal complexes and the ligands depends on the nature of the metal ions and the coordinating ligands, the synthesis of newer monomer structures based on different kinds of complexing groups was attempted [18]. Furthermore, molecular variations included differential molecular rigidities in the monomer structures. The primary goal of these molecular design exercises was to use tight metal–ligand interactions to improve the binding strengths to a level as close to covalent bonding as possible. This is expected to minimise non-specific incorporation of monomer units in the polymer chain, which is prevalent with non-covalent interaction (*viz.* hydrogen bonding) based imprinted polymers. Towards this end, metal-complexing monomers containing cyclic polyamine (7) and bipyridine (8) ligands were synthesised. The monomer (8), in addition to a bipyridine group, contains three polymerisable groups, which would provide additional structural rigidity to the resulting imprinted polymer. Imprinted polymers for *bis*-imidazole substrates were prepared using this monomer. For the similar pair of *bis*-imidazole substrates, these polymeric receptors showed enhanced substrate selectivity compared to the corresponding polymeric receptors based on IDA monomer (see Table 6.1).

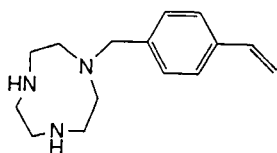
TABLE 6.1

SUBSTRATE SELECTIVITIES OF MOLECULARLY IMPRINTED METAL-COORDINATING POLYMERS TOWARDS VARIOUS *BIS*-IMIDAZOLE SUBSTRATES<sup>a, b</sup>

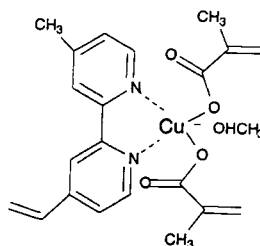
| Entry | Monomer used | Template used | Substrate pairs used | Relative selectivity ( $\alpha$ ) |
|-------|--------------|---------------|----------------------|-----------------------------------|
| 1     | 3            | None          | 4 + 5                | $\alpha_{4/5} = 1.02$             |
| 2     | 3            | 4             | 4 + 5                | $\alpha_{4/5} = 1.17$             |
| 3     | 3            | 4             | 4 + 6                | $\alpha_{4/6} = 1.35$             |
| 4     | 3            | 5             | 4 + 5                | $\alpha_{5/4} = 1.15$             |
| 5     | 8            | 4             | 4 + 5                | $\alpha_{4/5} = 1.38$             |
| 6     | 8            | 4             | 4 + 6                | $\alpha_{4/6} = 1.72$             |

<sup>a</sup>Reproduced from [17] and [18].

<sup>b</sup>These polymers were prepared by using ethylene glycol dimethacrylate as the cross-linker.



7



8

#### 6.4.2. Surface modified metal-coordinating imprinted polymers

Although metal-coordination interaction based imprinted polymers present many favourable characteristics, efforts to optimise the fidelity of the templating process can conflict with the overall properties of the materials, which are necessary for designing robust and efficient devices. For example, for chromatographic applications, the imprinted polymers prepared using relatively high concentration of cross-linking agents to capture the specific arrangement of the binding sites, can hinder the diffusion of the substrates inside the particles. This leads to band spreading and poor peak resolution. Accessibility of larger substrates to binding sites can also be severely impeded. Furthermore, bulk polymerised template polymers, which are ground and sieved to carry out the binding studies, may not possess the mechanical stability and uniformity required for rapid binding, which are mandatory for chromatographic and sensor applications.

One of the approaches to alleviate these problems is to produce a thin film of the imprinted polymers on the surface of an appropriate reactive solid support

possessing the desired physico-mechanical properties (see also Chapter 4 and 12). Two chemical approaches have been adopted to prepare such surface modified metal-coordinating imprinted polymers.

In one method Arnold and co-workers prepared a durable reactive polymer support using trimethylolpropane trimethacrylate (TRIM) as the precursor monomer [19]. Under controlled conditions, polymerisation of this trifunctional monomer yields macroporous polymer networks bearing surface-accessible unpolymerised methacrylate residues. The high mechanical stability of the poly(TRIM) matrix and its relatively low tendency to swell in different solvents suggested that functionalisation of this reactive support would be confined to the pore structures and would not affect the bulk properties or structure. This prompted them to evaluate the utility of the poly(TRIM) particles as reactive supports for molecular imprinting polymerisation. Reactivities of the polymer bound methacrylate residues were evaluated by grafting various functional polymer chains to this polymer support. Spectroscopic and surface analytical techniques were employed to characterise these surface grafted polymers. Thus,  $^{13}\text{C}$  NMR and FTIR spectroscopic analysis revealed the disappearance of the surface bound methacrylate residues and incorporation of new functional polymer chains. X-ray photoelectron spectroscopy and scanning electron microscopy analyses of the polymers suggested that the grafted functional polymer chains covered the surface of poly(TRIM) particles.

Molecular imprinting polymerisation of  $\text{Cu}^{2+}$ -IDA monomer (4)-*bis*-imidazole template assemblies on this reactive polymer surface enabled the creation of surface confined metal-complexing polymeric receptors. Faster kinetics for substrate and metal ion removal and reloading were observed with these imprinted polymers when compared to their bulk polymerised counterparts. The substrate recognition capabilities of both kinds of polymers were found to be comparable. This surface imprinting procedure is illustrated in Fig. 6.2.

In another approach, surface imprinted metal-coordinating sites were created by utilising modified porous silica particles as reactive solid supports [20]. Silica particles containing surface bound polymerisable groups were obtained by reacting porous silica particles with 3-(trimethoxysilyl)propyl methacrylate. The resulting methacrylate functionalised silica particles were used to prepare surface confined metal coordinating imprinted sites in a manner similar to that adopted for poly(TRIM) particles. These surface modified imprinted polymers were evaluated as chromatographic sorbents for the separation of different substrates (see Section 6.5.1.).

## **6.5. APPLICATIONS OF METAL-COORDINATED IMPRINTED POLYMERS**

The many beneficial features of metal-coordination interaction, combined with the attractiveness of template polymerisation, make these metal-complexing polymeric receptors a class of potentially useful materials. These functional polymers have been investigated for their usefulness in different analytical applications.

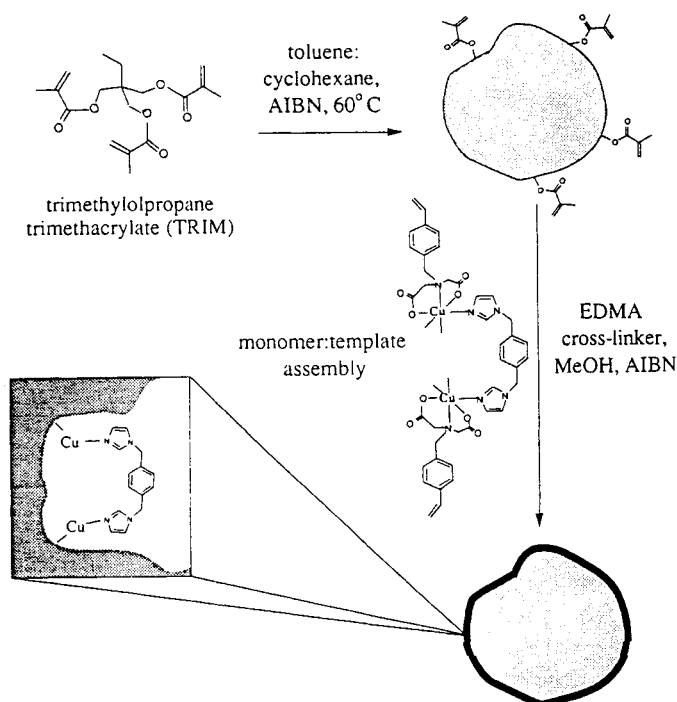


Fig. 6.2. Synthetic strategy for the preparation of surface imprinted metal-coordinating polymers using poly(TRIM) particles.

These applications include: (i) sorbents for chemo- and enantioselective separation; (ii) highly selective catalysts for chemical transformations; (iii) chemical and biological sensors.

### 6.5.1. Sorbents for separation media

The demonstrated benefits offered by ligand-exchange chromatography have been the motivation behind the development of metal-coordinating imprinted polymers as novel adsorbents for separation media. However, in spite of the potential attractive features of imprinted polymers to prepare substrate selective chromatographic adsorbents, successful demonstration of chromatographic separation using these polymers are still relatively few [21]. One problem has been that efforts to optimise the imprinting process can conflict with chromatographic performance. For example, the relatively high cross-linking density necessary to restore the specific arrangement of functional groups in the polymer matrix can hinder the diffusion of substrates in the particles. This results in band spreading and poor peak resolution. One of the approaches to overcome this diffusion problem is to graft copolymerise the monomer–template assemblies on the surface of a reactive solid support possessing desirable chromatographic properties.

In the case of metal-coordination interaction, it is reasoned that a monomer–template assembly held together by strong metal-to-ligand interaction would also minimise the dissociation during polymerisation. As a result, very strong interaction between the template and polymer would lead to very long retention time and hence excessive band broadening. Fortunately, since the strength and kinetics of metal-coordination interactions can be tailored, by replacing the metal ions used during imprinting with other ions better suited for chromatographic conditions, novel separation media can be envisioned. This “bait-and-switch” approach would truly enhance the opportunities for imprinted polymers.

Thus, by exploiting the ability to substitute the metal centres in imprinted polymers and the surface grafting methodology described above, Plunkett and Arnold demonstrated efficient chromatographic separation on metal-coordinated imprinted polymers [22]. Using the strong  $\text{Cu}^{2+}$ -imidazole interaction, they created imprinted metal-coordination sites on the surface of methacrylate functionalised silica particles. The copper ions were subsequently removed and were replaced by weakly coordinating  $\text{Zn}^{2+}$  ions. The resulting materials, when used as chromatographic packing materials, could separate closely similar *bis*-imidazole substrates (4) and (5) (see Fig. 6.3). Near baseline resolution of substrates was achieved. This result suggests that the “bait-and-switch” approach could significantly enhance the scope of the chromatographic performance of molecularly imprinted polymers.

In a subsequent study, the Arnold group developed molecularly imprinted metal-coordinating adsorbents for the racemic resolution of underivatised amino acids and other functional amines [23]. By utilising the  $\text{Cu}^{2+}$  containing monomer (3) as the functional monomer and an optically active amino acid as the template, the monomer–template assembly was polymerised on the surface of functionalised silica particles. The resulting polymers, after removal of the template, were used to resolve racemic mixtures of  $\alpha$ -amino acids. Adsorbents prepared using amino acids with larger aromatic side chains as templates exhibited the highest selectivity (a separation factor ( $\alpha$ ) = 1.65 for the enantioresolution of D,L-phenylalanine was

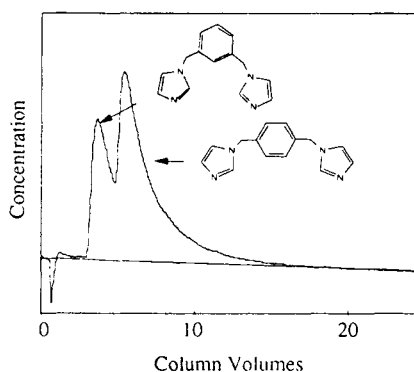


Fig. 6.3. Elution profile for *bis*-imidazole substrates on a column packed with surface imprinted metal-coordinating silica particles prepared by using *bis*-imidazole (4) as the template.

observed). More interestingly, the polymers showed cross-selectivity for amino acids similar to their templates. Thus, the imprinted polymer prepared using L- or D-phenylalanine as the template exhibited good enantioselectivity for resolving racemic tyrosine. Furthermore, it was possible to use the amino acid imprinted polymers for the resolution of amines, thus attesting to the versatility of the technique. Figure 6.4 shows the chromatogram of the resolution of an amine using such a polymer. The mechanisms underlying the observed enantioselectivity were discussed in the light of a 3-point interaction model (see Fig. 6.5).

### 6.5.2. Recognition and binding of proteins

Developing molecularly imprinted polymers as receptors for recognising and binding proteins has practical applications (see also Chapter 10). Such polymers can be used as attractive materials for down stream processing of important

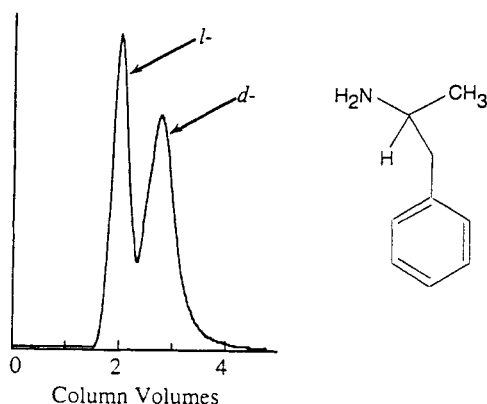


Fig. 6.4. Chromatographic separation of *d,l*  $\alpha$ -methylphenethylamine on a column packed with surface imprinted silica particles prepared by using L-phenylalanine as the template.

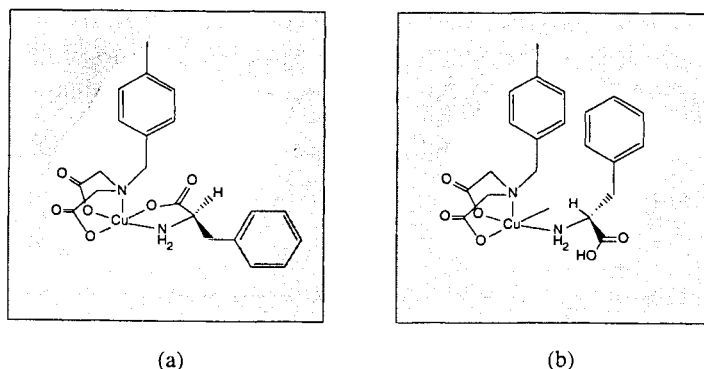


Fig. 6.5. Possible different interactions of enantiomers to the chiral cavity containing metal-coordinating sites obtained by molecular imprinting polymerisation.



proteins, as well as acting as sensors for binding proteins. Proteins are highly delicate substrates and contain large and complex arrangements of functional groups [24]. As a result, the design of molecularly imprinted polymers for this class of substrates is particularly challenging. The mildness of metal-coordination interaction and its affinity for specific functional groups present on protein surfaces (e.g. imidazole groups from histidine residues) makes it an attractive binding mode to prepare protein recognising polymeric receptors.

Arnold and co-workers attempted to prepare imprinted metal-coordinating polymers for proteins [25]. For this purpose, efforts were made to prepare metal-coordinating molecularly patterned surfaces in mixed monolayers spread at the air–water interface or liposomes. This approach was termed as “molecular printing” and is illustrated in Fig. 6.6. In this process, a protein template is introduced into the aqueous phase, which imposes a pattern of functional amphiphiles in the surfactant monolayer *via* strong interactions with metal-chelating surfactant head groups. The pattern is then “fixed” by polymerising the surfactant tails. The technique has also been employed for two dimensional crystallisation of proteins [26].

Mosbach *et al.* also attempted to use metal-coordination interaction to prepare polymeric adsorbents for selective recognition of proteins [27]. Using the monomer (3), they polymerised the protein–monomer complex on methacrylate-derived silica particles in the presence of ribonuclease A as the template protein. After removing the template, the imprinted functionalised silica particles were used as packing

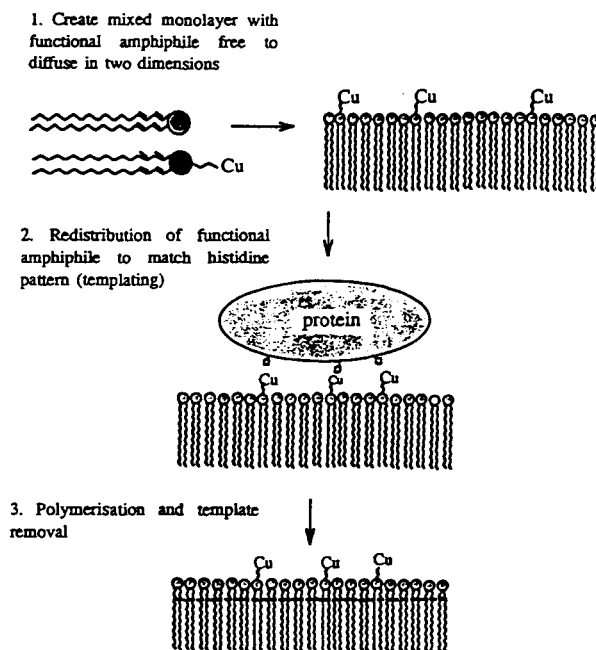


Fig. 6.6. Schematic illustration of molecular imprinting of proteins on the surface of a metal-coordinating bilayer assembly.

adsorbents in an HPLC column and the separation of lysozyme and ribonuclease A was performed using this column. An enhanced affinity for the ribonuclease A was observed.

### 6.5.3. Catalysis

The selectivity of molecularly imprinted materials and the versatility of metal–ligand coordination offer an attractive tool for the design and synthesis of novel catalytic systems.

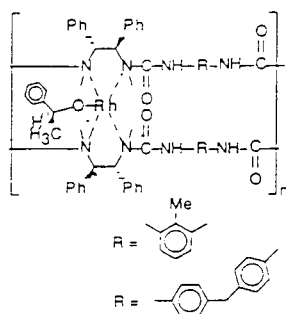
Leonhardt and Mosbach prepared metal-complexing imprinted polymers by polymerising  $\text{Co}^{2+}$  complexes of *N*-vinyl imidazole and *N*-protected amino acids [14]. After work-up of the polymer and removal of the amino acid templates, the catalytic activities of the resulting imprinted metal-complexing polymers were evaluated by following the hydrolysis of the *p*-nitrophenyl esters of various amino acids. Assessment of the rate of hydrolysis revealed a clear preference for the substrates used as the templates. The polymers could be used several times without any deterioration of the catalytic activities and true turnover was observed.

In an effort to prepare imprinted metal-complexing polymer gels exhibiting enzyme-like selective catalytic behaviour, Karmalkar *et al.* employed a metal-mediated approach to position imidazole, carboxyl and hydroxyl groups in a hydrogel matrix [28]. These three functional groups constitute the catalytic triad in the serine protease class of enzymes and their strategic positioning in the protein structure is the key to their catalytic properties. Thus, complexation of methacrylic acid, *N*-methacryloylhistidine and the print molecule, 2-[[[(isobutyrylamino)caproyl]-L-phenylalanyl]2-aminopyridine, with  $\text{CoCl}_2$  and its subsequent polymerisation with 2-hydroxyethyl methacrylate and ethylene glycol dimethacrylate produced the appropriate imprinted hydrogel. After removal of the print molecule and metal ions, the catalytic behaviour of the polymer was studied by monitoring the hydrolysis of *p*-nitrophenyl esters. The imprinted polymer catalysed the hydrolysis at a rate comparable to  $\alpha$ -chymotrypsin. On the other hand, a control polymer containing similar functional groups distributed in a random fashion showed only modest catalytic activity.

Development of molecularly imprinted enantioselective hydrogenation catalysts based on immobilised rhodium complexes was reported by Gamez *et al.* [29]. The imprinted catalysts were prepared by polymerising  $\text{Rh(I)}-(N,N'\text{-dimethyl-1,2-diphenylethanediamine})$  with di- and tri-isocyanates, using a chiral alkoxide as the template (9). The imprinted polymer, after removal of the template, was tested for the reduction of ketones to alcohols. An enhanced enantioselectivity was observed in the presence of the imprinted polymeric catalyst, in comparison to the control polymer.

### 6.5.4. Sensors

The ability of molecular imprinting technology to offer a generic synthetic strategy to prepare robust molecular recognition materials has been exploited to

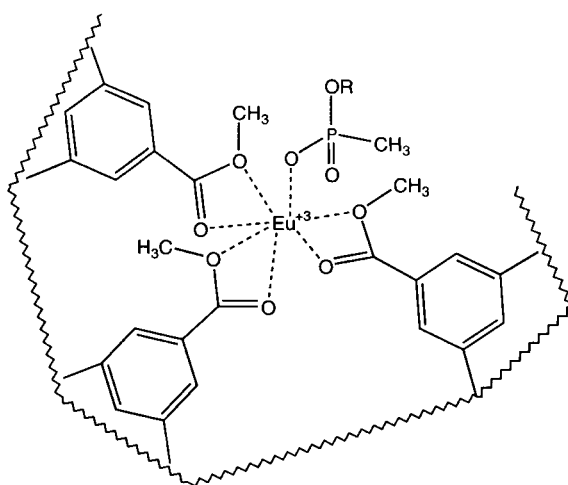


9

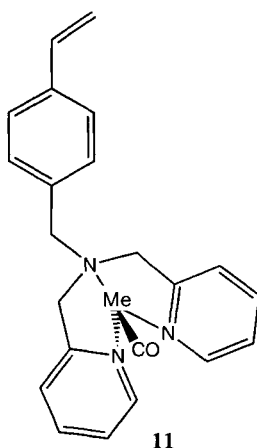
prepare novel molecular sensors and assay systems (see chapters 18–21). The additional feature of metal-coordination interaction in tailoring the strength and specificity of the host–guest binding in both organic and aqueous media is well suited to the use of these metal-complexing polymeric receptors as sensor elements.

Using europium ( $\text{Eu}^{3+}$ ) ion based metal-complexing imprinted polymers, Murray and co-workers have developed sensor devices for the detection of the nerve gases sarin and soman [30]. The luminescent characteristics of the  $\text{Eu}^{3+}$  ion, whose characteristic emission wavelength depends on the nature and position of the coordinating ligands, has been utilised for this purpose. The imprinted  $\text{Eu}^{3+}$ -complexed cavity (**10**) changes its shape when complexed to a nerve gas. This change is manifested in the change in its luminescent wavelength.

Application of metal-complexing imprinted polymers as sensors for small gas molecules has been demonstrated by Borovik and co-workers [31]. Thus, a sensor



10



for carbon monoxide (CO) was prepared by imprinting Cu(I) and Ag(I) complexes of a polymerisable pyridyl monomer (**11**). The imprinted cavities in the polymer matrices were precisely sized to the appropriate gas molecules used as the template. Changes in the colour and infrared stretching frequencies of the binding sites upon complexation with gas molecules have been used as the detection mode in this sensor device. In addition to detecting CO, imprinted polymers were developed for sensing other gas molecules such as nitric oxide (NO) and oxygen. The complexation process is reversible and, as a result, these polymeric sensors could have multiple uses.

Arnold and co-workers have developed a metal-complexing imprinted polymer as a sensor for glucose [32]. Since this polymer enables the detection and measurement of glucose concentrations in complex biological media, it was suggested that this imprinted polymer could be used as an inexpensive sensing device for monitoring the glucose levels in people suffering from diabetes mellitus. The chemical principle underlying this sensor is based on the fact that, at alkaline pH, the metal-complexing polymer binds glucose and instantly releases protons in proportion to glucose concentration. The sugar binding abilities of these polymers were found to depend on the type of template used for making the polymers (see Fig. 6.7).

## 6.6. CONCLUSIONS AND OUTLOOK

Molecular imprinting technology utilising metal-coordination interaction to assemble monomers and templates is a versatile strategy for the creation of novel abiotic receptors. In terms of strength, specificity and directionality, metal-coordination is closer to the covalent bond than non-covalent interactions, yet its formation and breakage can occur rapidly and under relatively mild conditions. These favourable features make metal-coordination a promising binding mode for preparing highly specific molecularly imprinted polymers. The applications of these materials include sorbents for rapid chemo- and stereo-selective chromatography,

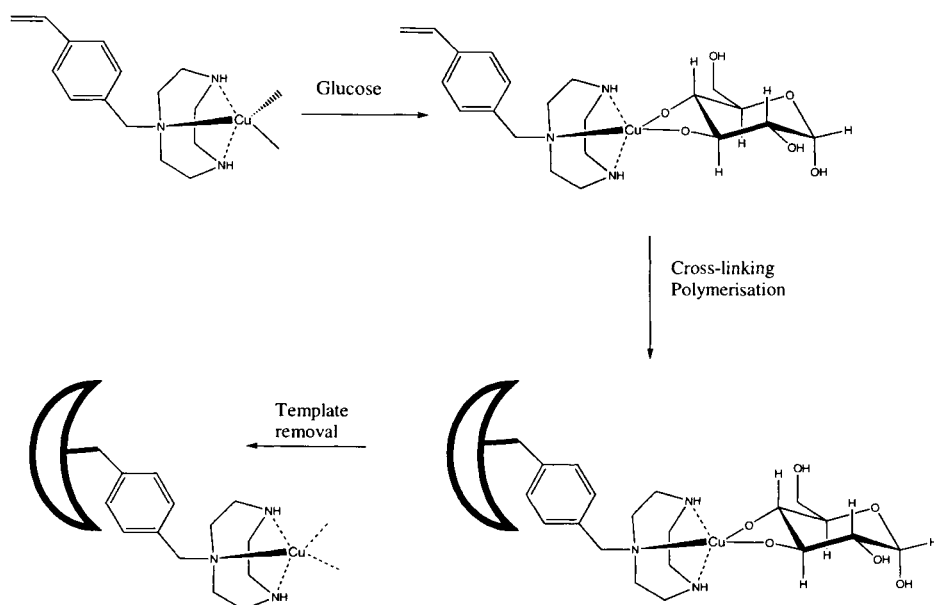


Fig. 6.7. Molecularly imprinted metal-complexing polymer as a glucose sensor.

enzyme-like catalysis, recognition of delicate biological macromolecules and as recognition elements in sensor devices.

Despite the above beneficial features of metal-coordination interaction and the ease and flexibility of template polymerisation, implementation of these strategies to prepare materials showing substrate selectivity comparable to low molecular weight receptors has not been achieved so far. For example, low molecular weight metal-complexing receptors designed to match the metal ion spacing to the spacing between the ligands of the substrates show orders of magnitude higher selectivity than the imprinted polymers [33]. This suggests that there remains significant room to fine tune and improve the performance of these polymeric receptors. The poor substrate selectivity of these imprinted polymers is probably due the presence of a heterogeneous population of binding sites (polyclonal) created in these polymeric receptors. While use of strong metal–ligand interaction minimises the formation of non-specific binding sites, the kinetics of rebinding and desorption are disappointingly slow. On the other hand, improvement of kinetics using weaker interactions leads to the formation of low affinity sites. In this regard, the “bait-and-switch” strategy is a conceptual advancement and more work needs to be done in this direction to gauge its full potential. While metal-coordinating imprinted polymers have been reasonably successful for small organic molecules, several chemical constraints are imposed in the context of delicate and complex substrates such as proteins. Although biological agents like antibodies are used as molecular recognition elements in bioseparations and diagnostics, their high cost and low stability provide a definitive impetus to develop abiotic polymeric receptors for these applications.

Among the different parameters that could be optimised to achieve viable metal-coordinating polymeric receptors are the nature of the chelating function, the metal ions, polymerisation conditions and cross-linking agents.

## REFERENCES

- 1 G.M. Whitesides, *Sci. Am.*, **273**, 114 (1995).
- 2 J.-M. Lehn, *Supramolecular chemistry*, VCH, Weinheim, Germany (1995).
- 3 J.S. Lindsay, *New J. Chem.*, **15**, 153 (1991).
- 4 D. Philip and J.F. Stoddart, *Angew. Chem., Int. Ed. Engl.*, **35**, 1154 (1996).
- 5 G. Wulff, *Angew. Chem., Int. Ed. Engl.*, **34**, 1812 (1995).
- 6 G. Wulff, *Trends Biotechnol.*, **11**, 85 (1993).
- 7 J. Steinke, D.C. Sherrington and I.R. Dunkin, *Adv. Polym. Sci.*, **123**, 81 (1995).
- 8 H. Siegel, *Metal ions in biological systems*, Dekker, New York (1976).
- 9 R.J. Sundberg and R.B. Martin, *Chem. Rev.*, **74**, 471 (1974).
- 10 R.D. Hancock and A.E. Martell, *Chem. Rev.*, **89**, 1875 (1989).
- 11 V.A. Davankov, In: *Complexation chromatography (Chromatographic science series)*, vol. 57, D. Caignant (Ed.), Dekker, New York, p. 197 (1992).
- 12 Y.N. Belokon, V.I. Tararov, T.F. Savel'eva, M.M. Vorob'ev, S.V. Vitt, V.F. Sizoy, N.A. Sukhacheva, G.V. Vasil'ev and V.M. Belikov, *Makromol. Chem.*, **184**, 2213 (1983).
- 13 Y. Fujii, K. Matsutani and K. Kikuchi, *J. Chem. Soc. Chem. Commun.*, 415 (1985).
- 14 A. Leonhardt and K. Mosbach, *React. Polym.*, **6**, 285 (1987).
- 15 S. Vidyasankar, P.K. Dhal, S.D. Plunkett and F.H. Arnold, *Biotech. Bioeng.*, **48**, 431 (1995).
- 16 P.K. Dhal and F.H. Arnold, *J. Am. Chem. Soc.*, **113**, 7417 (1991).
- 17 P.K. Dhal and F.H. Arnold, *Macromolecules*, **25**, 7051 (1992).
- 18 P.K. Dhal and F.H. Arnold, *New J. Chem.*, **20**, 695 (1996).
- 19 P.K. Dhal, S. Vidyasankar and F.H. Arnold, *Chem. Mater.*, **7**, 154 (1995).
- 20 S.D. Plunkett, PhD Thesis, California Institute of Technology (1994).
- 21 B. Sellergren and K.J. Shea, *J. Chromatogr. A*, **635**, 31 (1993).
- 22 S.D. Plunkett and F.H. Arnold, *J. Chromatogr. A*, **708**, 19 (1995).
- 23 S. Vidyasankar, M. Ru and F.H. Arnold, *J. Chromatogr. A*, **775**, 51 (1995).
- 24 A. Fersht, *Enzyme structure and mechanism*, 2nd ed., W.H. Freeman, San Francisco (1985).
- 25 S. Mallik, S.D. Plunkett, P.K. Dhal, R.D. Johnson, D. Pack, D. Shnek and F.H. Arnold, *New J. Chem.*, **18**, 299 (1994).
- 26 D.W. Pack, G. Chen, K. Maloney, C.T. Chen and F.H. Arnold, *J. Am. Chem. Soc.*, **119**, 2479 (1997).
- 27 M. Kempe, M. Glad and K. Mosbach, *J. Mol. Recogn.*, **8**, 35 (1995).
- 28 R.N. Karmalkar, M.G. Kulkarni and R.A. Mashelkar, *Macromolecules*, **29**, 1366 (1996).
- 29 P. Gamez, B. Dunjic, C. Pinel and M. Lemaire, *Tetrahedron Lett.*, **36**, 8779 (1995).
- 30 G.M. Murray, A.L. Jenkins, A. Bzhelyansky and O.M. Uy, *Johns Hopkins Apl. Tech. Dig.*, **18**, 464 (1997).
- 31 J.F. Krebs and A.S. Borovik, *J. Am. Chem. Soc.*, **117**, 10,593 (1995).
- 32 G.H. Chen, Z.B. Guan, C.T. Chen, L.T. Fu, S. Vidyasankar and F.H. Arnold, *Nature Biotechnol.*, **15**, 354 (1997).
- 33 S. Mallik, R.D. Johnson and F.H. Arnold, *J. Am. Chem. Soc.*, **116**, 8902 (1994).

This Page Intentionally Left Blank

## Covalent imprinting using sacrificial spacers

MICHAEL J. WHITCOMBE AND EVGENY N. VULFSON

### 7.1. INTRODUCTION

The idea of template-mediated assembly in biological systems was first postulated by Linus Pauling to explain the workings of the immune system [1]. We now know this elegant hypothesis to be incorrect, but the principle of using a target molecule to create its own recognition site was finally realised in the laboratory when artificial polymeric receptors were first prepared by the technique known as molecular imprinting. This involves the formation of a highly cross-linked polymeric matrix around a *template*, which can be the target molecule itself or a close structural analogue. The key to this procedure is to ensure that, during the polymerisation, functional groups of the template molecule are fully engaged in interactions with “complementary functionality” of polymer-forming components.

Inevitably the outcome of any imprinted polymer synthesis depends critically on the selection of functional groups which will be involved in the recognition process and how they are introduced into the binding site. The latter is usually achieved by either covalent modification of the template molecule with suitable polymerisable species or through the *in situ* formation of a non-covalent complex between the template molecule and functional monomers. These two basic strategies are known as *covalent* [2] and *non-covalent* [3] imprinting respectively. A detailed analysis of the relative merits of the two traditional imprinting methodologies is clearly outside the scope of this paper as they are discussed in detail in Chapters 4 and 5, but the major advantages and disadvantages are still worth mentioning.

The great attraction of the non-covalent method is its simplicity. As the formation of the template monomer complex is accomplished *via* self-assembly, there is virtually no requirement for organic synthesis. However, the drawback is an unavoidable inhomogeneity of the binding sites obtained. This is due to the formation of a multitude of complexes between the functional monomers and template during the initial stages of polymerisation (see [4] for a recent thermodynamic analysis of template–monomer complex formation in relation to the polymer's binding properties). Also, the necessity to shift the equilibrium towards the formation of higher stoichiometry complexes between template and monomers somewhat limits the choice of solvents that can be employed when making imprinted polymers by the non-covalent method. This, in turn, can impose restrictions on the choice of a manufacturing method, in particular the ability to produce beads, films and other structures that may be required for certain practical applications.



However, most of these difficulties should not arise in the case of template-monomer complexes formed with very high association constants. Consequently a number of laboratories, including our own, are currently involved in the design of new polymerisable monomers which can form strong complexes with some of the common structural motifs possessed by many template molecules [5–8]. (See also Chapter 4 for further examples.) The use of transition metal co-ordination complexes as templates in imprinting is another particularly promising approach (see Chapter 6 for more detail).

Generally, the strength of interactions is irrelevant to covalent imprinting, which, in principle, should allow the precise positioning of functional groups in the active site under widely different polymerisation conditions and hence improve compatibility with a range of polymer synthesis methods. However, the limited stock of functional groups for which covalent bond formation and cleavage are readily reversible under mild conditions has proven to be a serious obstacle to the development of practical applications employing this approach. In this chapter we shall describe an alternative strategy for the preparation of imprinted polymers. This is the so-called “sacrificial spacer” methodology which, in the authors’ opinion, combines certain attractive features of both the classical covalent and non-covalent methods.

## 7.2. SACRIFICIAL SPACER METHOD

The sacrificial spacer approach was first introduced by Whitcombe *et al.* [9] who used the 4-vinylphenyl carbonate ester of cholesterol (**1**) as a model template. As illustrated schematically in Fig. 7.1, the carbonate ester (**1**) functions as a covalently bound template monomer but, at the same time, is easily and efficiently cleaved hydrolytically with the loss of CO<sub>2</sub> to give a non-covalent recognition site bearing a phenolic residue. It was proposed that the binding of cholesterol (**2**) to these polymers is driven by the formation of a hydrogen bond in non-polar solvents as illustrated in Fig. 7.1. Indeed, chemical modification of the phenolic residue with acetyl or benzoyl chloride led to virtually complete inhibition of binding. It is clear that a very similar approach can be used to introduce a wide range of alternative functionalities such as amino-, carboxyl-, hydroxyl- and amido groups in the polymer’s recognition site. This has recently been accomplished in our laboratory and the results are currently being prepared for publication [10].

Polymers synthesised by the sacrificial spacer method were also shown to bind cholesterol from hexane solution with a single dissociation constant [9]. As with other imprinted materials we had expected to see a range of affinities but this did not appear to be the case as judged by the Scatchard plot, which revealed remarkably uniform binding over a large proportion of theoretical sites. From these data  $K_d$  was determined as  $0.59 \pm 0.12$  mM at a capacity of  $114 \pm 6$   $\mu$ mol/g. However, the most attractive feature of these polymers was the high specificity towards cholesterol over its close structural analogues (Fig. 7.2). Thus, in accordance with the proposed hydrogen-bonding mechanism, cholestane (**3**) and cholesteryl acetate

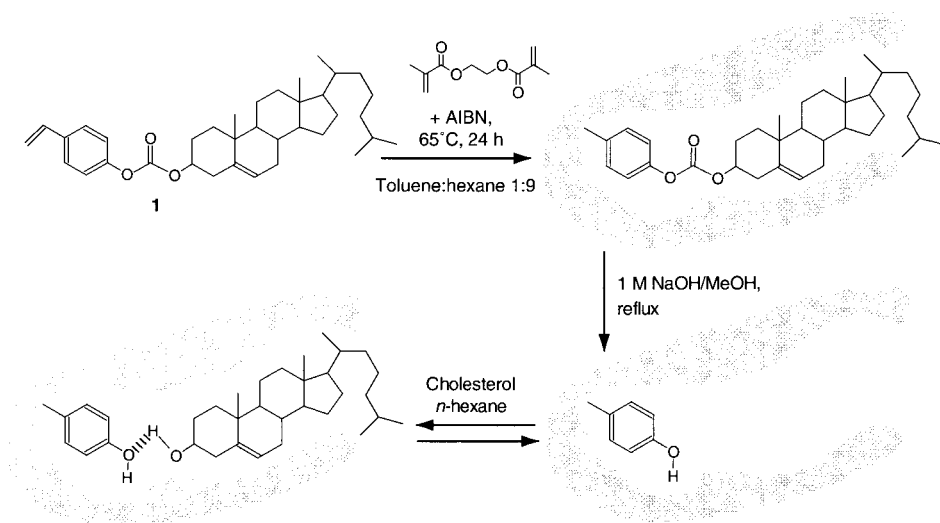


Fig. 7.1. The “sacrificial spacer” methodology. Imprinting of cholesterol via the 4-vinylphenyl carbonate ester (**1**). AIBN = 2,2'-azobisisobutyronitrile. Adapted from [9].

(**4**) did not bind to the imprinted polymer to an appreciable extent. When an oxygen atom at C3 was present, i.e. epicholesterol (**5**) and cholest-5-en-3-one (**6**), some binding was observed, albeit lower than that of (**2**) (Fig. 7.2). This observation demonstrates that ligand discrimination in the polymer recognition site was possible on the basis of the inversion of configuration of a single hydroxyl group.

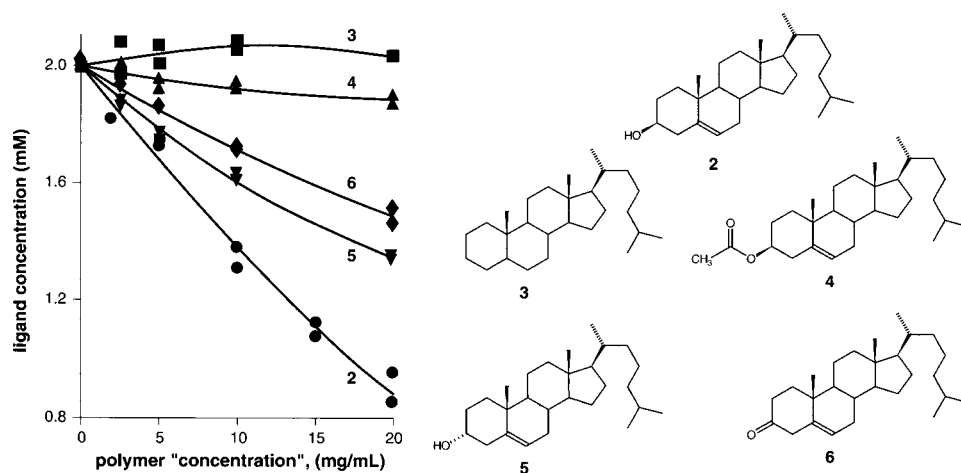


Fig. 7.2. Binding of structural analogues to cholesterol-imprinted polymer. Cholesterol (**2**), cholestane (**3**), cholesteryl acetate (**4**), epicholesterol (cholest-5-ene-3 $\alpha$ -ol) (**5**) and cholest-5-ene-3-one (**6**), all 2 mM in hexane. Adapted from [9].

It is of interest to compare these results with those obtained by Ramström *et al.* [11] who studied the specificity of methacrylic acid-based polymers non-covalently imprinted with the more heavily functionalised cortisol and corticosterone. These polymers also showed good discrimination between close structural analogues such as 11- and 21-deoxycortisol, prednisolone and cortisone. Although the results are not directly comparable, due to differences in experimental techniques and conditions used (solvents, ligand concentrations etc.), some parallels can be drawn. Non-covalent imprinting of these polyfunctional steroids gave non-linear Scatchard plots, which were adequately fitted to a two-site binding model. A small number of sites,  $<0.5 \mu\text{mol/g}$ , showed a high affinity for the template, with a  $K_d$  of the order of  $10^{-6}$  M, presumably due to sites in which at least two, and possibly more, methacrylic acid residues were involved in binding the template. The remaining sites,  $\approx 100\text{--}200 \mu\text{mol/g}$ , were characterised by a  $K_d$  in the millimolar range. Similar studies using testosterone as the template gave polymers with  $K_d$  in the range  $10^{-3}\text{--}10^{-4}$  M but with a total site population of only  $2\text{--}4 \mu\text{mol/g}$  [12,13].

The relative success of these two investigations could be due to the higher density of similar functional groups present in the corticosteroids relative to testosterone, resulting in more efficient complexation with methacrylic acid during the polymerisation step for the former templates. Covalent methods eliminate such differences by effectively holding all of the template in a single "complex" with the recognition site functionality; consequently a homogeneous binding site architecture is possible. In principle, it would be rather attractive to conduct a comparative investigation with steroid templates using a combination of non-covalent and sacrificial spacer methods to see whether the selectivity of polymers can be further improved. As we shall demonstrate below, the two methodologies are perfectly compatible and, in fact, it is the combination of the two approaches which we believe will be the key to the preparation of highly selective materials in many cases.

### 7.3. COMBINATION OF NON-COVALENT AND SACRIFICIAL SPACER METHODOLOGIES

The majority of imprinted polymers prepared so far have been made with relatively highly functionalised templates, typically containing multiple carboxy-, amino-, amido- and keto-groups [14]. Although there are several examples where successful imprints were obtained with poorly functionalised targets (e.g. monocarboxylic acids [15–17] and even aromatic hydrocarbons [18,19]), most of these reports still exploit strong hydrogen bonding and/or charge interactions. We therefore felt that the scope of molecular imprinting could be widened significantly if it was possible to exploit other chemical features of the template molecule. In particular the ability to form very weak hydrogen bonds, which are unlikely to be formed spontaneously by self-association with conventional monomers, and/or to engage in interactions involving aromatic  $\pi$  electrons were considered. In order to achieve this, novel functional monomers had to be designed and an appropriate method for their introduction into the polymer's recognition sites developed. Polychlorinated

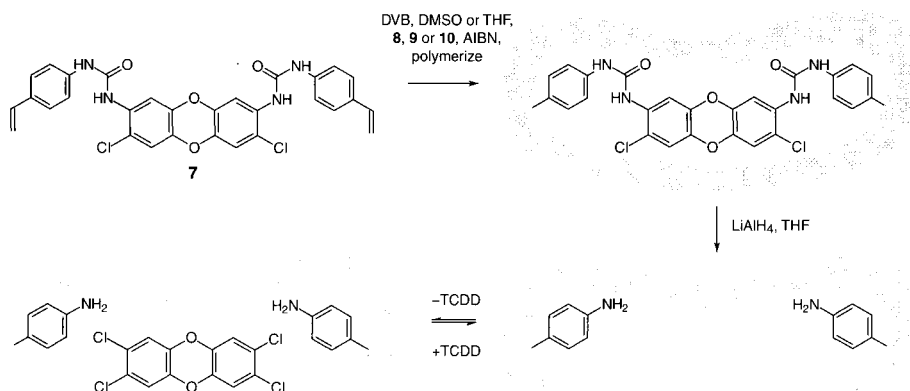


Fig. 7.3. Synthesis of polymeric receptors for TCDD by a modified “sacrificial spacer” approach using the urea monomer (7). DVB = divinylbenzene. Adapted from [23].

aromatics were particularly attractive model compounds for the purposes of this investigation on account of two structural features, namely the presence of aromatic chlorine atoms, which are known to form exceedingly weak hydrogen bonds in non-polar solvents [20], and an aromatic  $\pi$ -electron system which can interact with that of other aromatic molecules [21,22]. In our work, 2,3,7,8-tetrachlorodibenzodioxin (TCDD) was chosen as a representative target compound [23], because it is the most prominent member of a large family of polychlorinated dibenzodioxins that are currently the cause of serious environmental concern in most developed countries.

In order to achieve specific recognition of TCDD, we employed a modification of the sacrificial spacer methodology using diurea (7) as a template, where the two urea bridges were designed to act as sacrificial spacers (Fig. 7.3). The template was prepared by reacting 2,8-diamino-3,7-dichlorodibenzodioxin with 2 mole equivalents of 4-vinylphenylisocyanate. Hydride reduction of (7) after its incorporation into the polymer released the parent 2,8-diamino-3,7-dichlorodibenzodioxin, leaving two aromatic amines in the recognition site, positioned in such a way as to form hydrogen bonds with the chlorine atoms of TCDD subsequently bound to the polymer (Fig. 7.3). Typically, the template removal was about 50% as determined by the chlorine content of the polymers before and after reduction.

The aromatic  $\pi$ -electron system of TCDD was targeted through non-covalent interactions with several aromatic comonomers capable of forming  $\pi$ - $\pi$  interactions with the template at the stage of polymerisation. In particular, the electron deficient 2,3,4,5,6-pentafluorostyrene (8) and the electron rich 1,4-bis-(3/4-vinylbenzyloxy)-benzene (9) and 1-methoxy-3,5-bis-(4-vinylbenzyloxy)-benzene (10) were used (Fig. 7.4). As a consequence of the template structure and the expected  $\pi$ - $\pi$  complex between the diurea template and the monomer, the designed recognition site should be “equipped” with two aromatic amino groups situated on both sides of the

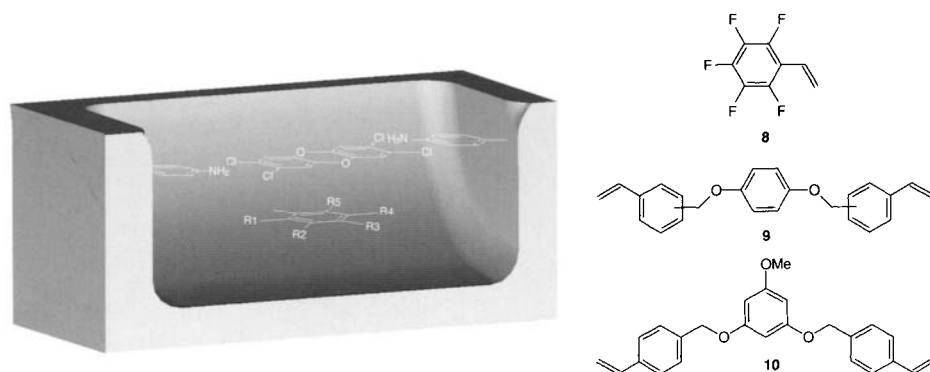


Fig. 7.4. (Left) Schematic representation of the proposed TCDD recognition site showing the covalently derived amine groups at the edge of the cavity and the non-covalently positioned  $\pi$ -complexing comonomer residue co-planar with the ligand. (Right) Structures of aromatic comonomers used in this study: pentafluorostyrene (**8**), 1,4-bis-(3/4-vinylbenzyloxy)-benzene (**9**) and 1-methoxy-3,5-bis-(4-vinylbenzyloxy)-benzene (**10**). Adapted from [23].

cavity, coplanar with the bound TCDD with the charge transfer monomer forming the “floor” of the imprint, as illustrated schematically in Fig. 7.4. Although the individual interactions between these functional groups and TCDD were weak, in combination they led to the formation of specific recognition sites as was confirmed in binding experiments with radioactively labelled TCDD at concentrations as low as 2 nM [23]. Under these conditions imprinted polymers bound up to 25% more ligand than non-imprinted controls made to contain exactly the same functionality. Unfortunately the high non-specific binding observed in these experiments (attributed to the relatively high proportion of charge transfer monomers used) made the detailed analysis of these polymers rather difficult. Nevertheless, the feasibility of engaging hydrogen bond interactions which are probably too weak to enable efficient complexation with monomers typically used for non-covalent imprinting (e.g methacrylic acid, acrylamide and others) was demonstrated. Furthermore, it was shown that non-covalent methods and sacrificial spacers can be employed jointly for the preparation of molecularly imprinted polymers.

#### 7.4. AMINO ACID SEQUENCE SPECIFIC POLYMERS

Several authors have compared imprinted polymers to biological receptors and even the term “plastic antibodies” has been coined to describe these remarkable materials. To a large extent, this comparison rests on a spectacular work of Mosbach and co-workers [24], who showed that theophylline- and diazepam-imprinted polymers displayed a specificity rather similar to that of polyclonal antibodies in binding studies with the template and its close structural analogues. However, it is the recognition of nucleotide or oligopeptide sequences which is

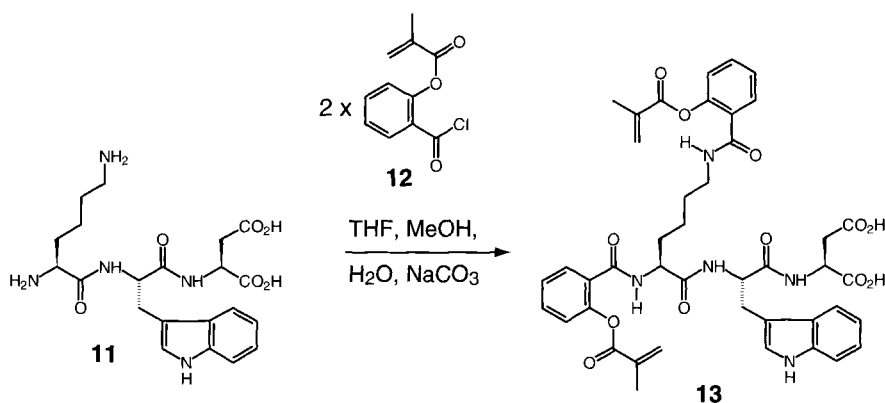


Fig. 7.5. Covalent modification of H-Lys-Trp-Asp-OH (**11**) with 2-methacryloyloxybenzoyl chloride (**12**) to form the template (**13**).

often seen by biologists as the real test of the ability of polymers to compete with their natural counterparts. Is the preparation of such materials possible and, if so, how would one go about it?

In our laboratory, we once again employed a combination of sacrificial spacer and non-covalent methodologies [25]. Carboxylic acids were the natural choice of functionality to interact with free amino groups of an oligopeptide in the polymer's binding sites. Hence, the target tripeptide, H-Lys-Trp-Asp-OH (**11**) was reacted with 2-methacryloyloxybenzoyl chloride (**12**) to obtain the template (**13**) as illustrated in Fig. 7.5. The key feature of this approach is the presence of a relatively labile ester bond between the methacrylic acid residue and the hydroxybenzamide moiety, the cleavage of which would leave the carboxyl group in the precise spatial arrangement to bind the target tripeptide, as well as a small "void" in the polymer to facilitate the template removal and re-binding of the ligand. This simple approach also enabled us to position carboxyl groups exclusively in the recognition sites, thus minimising non-specific interactions between ligands and the polymeric matrix itself.

The carboxylic acid group(s) of the template can be targeted *via* non-covalent complexation with, for example, 2-vinylpyridine. This monomer and the isomeric 4-vinylpyridine have been successfully used by other groups for non-covalent imprinting of amino acid derivatives [26], aryl carboxylic acids [15,17,27] and dipeptides [28]. A relatively short, highly functionalised template containing lysine and a dicarboxylic amino acid (aspartic acid) in the N- and C-terminal positions was judged to be a suitable target in order to simplify the synthesis of the peptide and its subsequent chemical modification. Also, the presence of multiple functional groups and a net charge of zero at neutral pH were perceived as advantageous, in terms of the subsequent characterisation of the polymer's recognition properties.

The polymer was prepared using conventional procedures and an initial analysis showed that it was capable of binding the tripeptide (**11**) in aqueous acetonitrile at

concentrations of  $10^{-5}$  M and above [25]. Significant binding to the imprinted but not to the control polymer was also observed in pure water, although at slightly higher ligand concentrations. In 80% acetonitrile/water the binding characteristics of the polymer were estimated to be  $K_d = 113 \pm 47 \mu\text{M}$  at a capacity of  $4.1 \pm 1.3 \mu\text{mol/g}$  dry polymer from curve-fitting to the isotherm.

The polymer selectivity was further probed with structural analogues of the tripeptide (**11**). For example, the replacement of lysine in the N-terminal position with arginine (**14**) or leucine (**15**) to disrupt and eliminate the interaction with one of the carboxyl groups in the polymer's recognition site respectively, led to the binding being reduced by 44% and >95% respectively (Table 7.1). It is interesting to note that many enzymes and antibodies also do not discriminate well between peptides containing lysine and arginine residues.

Similarly, substituting the C-terminus aspartic acid with the slightly bulkier glutamic acid, (**16**), or removing the aspartate residue from the sequence altogether (dipeptide, **17**) resulted in substantially reduced binding. This result clearly shows that the non-covalent aspects of the imprinting were equally important for recognition. Somewhat more surprising for us was to discover that the substitution of the central amino acid residue (tryptophan) with a smaller phenylalanine also led to a deterioration in binding (compare the uptake of **11** with that of **18** and **19** in Table 7.1). While we did not expect the side-chain of tryptophan to be strongly involved in any functional group interactions, binding between the N-H group of indole templates and 4-vinylpyridine residues has recently been reported in polymers prepared as catalysts for the benzisoxazole isomerisation reaction [29] and such an interaction cannot be ruled out in the case of our imprints.

Overall these data clearly demonstrate that polymers prepared by the combina-

TABLE 7.1

BINDING OF ANALOGOUS PEPTIDES TO LYS-TRP-ASP-  
IMPRINTED POLYMER

| Peptide   | Sequence         | Percentage bound to polymer <sup>a</sup> |         |
|-----------|------------------|--|---------|
|           |                  | Imprint                                  | Control |
| <b>11</b> | H-Lys-Trp-Asp-OH | 43                                       | 11      |
| <b>14</b> | H-Arg-Trp-Asp-OH | 24                                       | 9       |
| <b>15</b> | H-Leu-Trp-Asp-OH | <2                                       | 6       |
| <b>16</b> | H-Lys-Trp-Glu-OH | 5  | 3       |
| <b>17</b> | H-Lys-Trp-OH     | 35                                       | 17      |
| <b>18</b> | H-Lys-Phe-Asp-OH | 4  | <2      |
| <b>19</b> | H-Lys-Phe-OH     | 9  | 5       |

<sup>a</sup>Adapted from [25]. Binding determined by HPLC after incubating polymer (30 mg/mL) with peptide solutions (1 mM in 80% acetonitrile/water) at room temperature overnight.

tion of sacrificial spacer and non-covalent imprinting can discriminate between very similar amino acid sequences with a specificity approaching that of antibodies and other biological receptors. We believe that the success of our approach was, at least in part, due to the fact that the amino and carboxyl groups of the template oligopeptide were targeted separately by the combined approach described. It should be noted that although the requirement for covalent modification of the template may, to a certain extent, complicate the synthesis of polymers, it should not be regarded as a disadvantage. Indeed, it enables the polymer's functionality to be positioned precisely in the recognition site and at the same time increases the solubility of the template in solvents commonly used in the preparation of polymers.

## 7.5. CONCLUSIONS

The sacrificial spacer approach offers a versatile alternative to traditional methods of imprinting and can be used in conjunction with other approaches to prepare polymers with excellent recognition properties. The advantage of this approach is that all of the functional groups incorporated into the polymer by the imprinting step are only located in the template-derived cavities, which can significantly reduce problems associated with high non-specific binding in non-covalently imprinted polymers. As the covalent template monomers are not sensitive to the presence of water, it is possible to synthesise imprinted polymers by the industry-favoured techniques of aqueous-based emulsion and suspension polymerisation [30,31], without the need for expensive fluorocarbon solvents commonly used to prepare traditional non-covalently imprinted polymers [32–34]. A possible drawback is the need for chemical modification of the template, but this often has the advantage of rendering the resultant template more soluble in solvent and monomer mixtures. Unless this approach is made obsolete by the development of a battery of new, strongly complexing functional monomers, it will remain a valuable addition to the molecular imprinting toolkit.

## ACKNOWLEDGEMENTS

The authors wish to thank the BBSRC and MAFF for supporting the experimental work which formed the basis of this mini-review.

## REFERENCES

- 1 L. Pauling, *J. Am. Chem. Soc.*, **62**, 2643 (1940).
- 2 G. Wulff, *Pure and Appl. Chem.*, **54**, 2093 (1982).
- 3 K. Mosbach, *Trends Biochem. Sci.*, **19**, 9 (1994).
- 4 M.J. Whitcombe, L. Martin and E.N. Vulfson, *Chromatographia*, **47**, 457 (1998).
- 5 G. Wulff, T. Gross and R. Schonfeld, *Angew. Chem., Intl. Ed. Engl.*, **36**, 1962 (1997).
- 6 G. Wulff and R. Schonfeld, *Adv. Mater.*, **10**, 957 (1998).



- 7 K. Yano, K. Tanabe, T. Takeuchi, J. Matsui, K. Ikebukuro and I. Karube, *Anal. Chim. Acta*, **363**, 111 (1998).
- 8 C. Lübke, M. Lübke, M.J. Whitcombe and E.N. Vulfson, *Macromolecules*, **33**, 5098 (2000).
- 9 M.J. Whitcombe, M.E. Rodriguez, P. Villar and E.N. Vulfson, *J. Am. Chem. Soc.*, **117**, 7105 (1995).
- 10 P. Villar, M.J. Whitcombe and E.N. Vulfson, in preparation.
- 11 O. Ramström, L. Ye and K. Mosbach, *Chem. Biol.*, **3**, 471 (1996).
- 12 A.E. Rachkov, S.H. Cheong, A.V. Elskaya, K. Yano and I. Karube, *Polym. Advanc. Technol.*, **9**, 511 (1998).
- 13 S.H. Cheong, A.E. Rachkov, J.K. Park, K. Yano and I. Karube, *J. Polym. Sci. A, Polym. Chem.*, **36**, 1725 (1998).
- 14 K. Mosbach and O. Ramström, *BioTechnology*, **14**, 163 (1996).
- 15 K. Haupt, A. Dzgoev and K. Mosbach, *Anal. Chem.*, **70**, 628 (1998).
- 16 Y. Nomura, H. Muguruma, K. Yano, A. Kugimiya, S. McNiven, K. Ikebukuro and I. Karube, *Anal. Lett.*, **31**, 973 (1998).
- 17 M. Kempe and K. Mosbach, *J. Chromatogr. A*, **664**, 276 (1994).
- 18 F.L. Dickert, H. Besenbock and M. Tortschanoff, *Adv. Mater.*, **10**, 149 (1998).
- 19 F.L. Dickert, P. Forth, P. Lieberzeit and M. Tortschanoff, *Fresenius J. Analyt. Chem.*, **360**, 759 (1998).
- 20 J.W. Smith, In: *The chemistry of the carbon-halogen bond*, S. Patai, Ed., Wiley Interscience, London, Chapt. 5 (1973).
- 21 U. Pyell, P. Garrigues, G. Felix, M.T. Rayez, A. Thienpont and P. Dentraygues, *J. Chromatogr.*, **634**, 169 (1993).
- 22 K. Kimata, K. Hosoya, T. Araki, N. Tanaka, E.R. Barnhart, L.R. Alexander, S. Sirimanne, P.C. McClure, J. Grainger and D.G. Patterson, *Anal. Chem.*, **65**, 2502 (1993).
- 23 M. Lübke, M.J. Whitcombe and E.N. Vulfson, *J. Am. Chem. Soc.*, **120**, 13,342 (1998).
- 24 G. Vlatakis, L.I. Andersson, R. Müller and K. Mosbach, *Nature*, **361**, 645 (1993).
- 25 J.-U. Klein, M.J. Whitcombe, F. Mulholland and E.N. Vulfson, *Angew. Chem., Int. Ed. Engl.*, **38**, 2057 (1999).
- 26 O. Ramström, L.I. Andersson and K. Mosbach, *J. Org. Chem.*, **58**, 7562 (1993).
- 27 J. Haginaka, H. Takehira, K. Hosoya and N. Tanaka, *J. Chromatogr. A*, **816**, 113 (1998).
- 28 L. Ye, O. Ramström and K. Mosbach, *Anal. Chem.*, **70**, 2789 (1998).
- 29 X.C. Liu and K. Mosbach, *Macromol. Rapid Commun.*, **19**, 671 (1998).
- 30 A. Flores, D. Cunliffe, M. J. Whitcombe and E.N. Vulfson, *J. Appl. Polym. Sci.*, **77**, 1841 (2000).
- 31 N. Perez, M.J. Whitcombe and E.N. Vulfson, *J. Appl. Polym. Sci.*, **77**, 1851 (2000).
- 32 A.G. Mayes and K. Mosbach, *Anal. Chem.*, **68**, 3769 (1996).
- 33 R.J. Ansell and K. Mosbach, *J. Chromatogr. A*, **787**, 55 (1997).
- 34 R.J. Ansell and K. Mosbach, *Analyst*, **123**, 1611 (1998).

## Molecular imprinting approaches using inorganic matrices

DARRYL Y. SASAKI

### 8.1. INTRODUCTION

Inorganic matrices have played a key role in the initial discovery and early development of molecular imprinting. Many have cited the initial reports by Frank Dickey that describe the imprinting of molecular memory, or selective affinity, in silica sol-gel materials. However, little is known or discussed of the important body of work that followed over the next 25 years, where researchers throughout the world employed inorganic materials in an effort to understand this new phenomenon. In those early years, inorganic matrices, in particular the metal oxides, were found to have remarkable recognition properties for organic dyes, stereoisomers of drugs and various aromatic heterocycles. The duplication of Dickey's original work by other laboratories and their own extensions into more complex systems not only furthered the field but also aided in quietening the critics of that time. Today, the field has become dominated by the use of organic polymeric materials, which offer their own special materials and processing conditions. But, as the field of sol-gel chemistry has grown and some of the advantages of using metal oxide materials have become more apparent, the use of inorganic matrices as materials for molecular imprinting has begun to experience a revitalisation.

Inorganic matrices, in particular the metal and semi-metal oxides (both of which will be loosely referred to as metal oxides), are typically prepared as amorphous materials using sol-gel techniques. The sol-gel technique offers an extremely wide range of processing conditions to yield an even wider range of materials that can be produced. Typically, gelation conditions are at or near room temperature, which is ideal for template-functionalised monomer interactions that use weak short-range interactions such as hydrogen bonding and van der Waals' forces. In the organic polymer preparations the activation of a radical initiator typically requires elevated temperature and prolonged reaction times, which is of concern where important, but weak, interactions need to be preserved. Surface functionalisation of metal oxides, especially silica, is a mature field with the extensive research invested in chromatographic supports and self-assembled monolayers (SAM). Post-functionalisation of metal oxide gels has been reduced to a simple and reproducible procedure that can yield tailorable, surface-functionalised materials. A large number of commercially available functionalised metal oxide monomers make possible the rapid development of new materials.

Structurally, the metal oxides are extremely rigid materials offering very high

surface area and porosity. For a typical silica gel the extent of condensation, as determined spectroscopically via  $^{29}\text{Si}$  solid state NMR (*vide infra*), can be as high as 90%. The high cross-link density leads to negligible swelling in all solvents even at elevated temperatures. This structural integrity is a desirable feature in imprinted materials, allowing the structural features of the receptor cavity and spatial distribution of the functional groups to be maintained. Additionally, the stability at higher temperatures, well known with zeolitic materials, makes catalytic reactions with imprinted materials feasible. Metal oxide materials are also very stable with regard to ageing and oxidation effects. Organic materials, on the other hand, are prone to more damage due to ageing.

One of the most unique features of metal oxide materials is the highly compatible nature with aqueous based systems, allowing the incorporation of biologically based guests. Imprinted receptor sites for hydrophilic materials such as saccharides, phosphates, phosphonates, sulphonate dyes, drugs and proteins have been prepared. Imprinting techniques have been successfully employed either in the bulk phase or on the material surface. Typically, water competes strongly for binding sites in small molecule host-guest systems and imprinted organic polymers. However, in rebinding experiments performed with metal oxides in aqueous solutions, good affinities and enhancement of binding for imprinted sites have been observed. The metal oxide materials appear to present an accommodating environment for host-guest complexation in aqueous solutions.

This chapter will take a somewhat historical look at the development of molecular imprinting with metal oxide gels through those early decades and review the recent developments within the field. Interesting pieces of information from various literature sources will be highlighted and relevant connections discussed to form insights into the strengths and current inadequacies of metal oxides as imprinting materials. First, a quick look into the chemistry of metal oxide sol-gel materials will be taken to acquaint the reader with the various conditions that can be altered for improved material performance. Because of the vast scope of molecular imprinting in inorganic materials over the past 50 years, the body of literature has been broken down into three areas: two-dimensional materials, three-dimensional materials, and supramolecular templates and zeolites. The first two areas concern the imprinting of molecular species to achieve selective affinity materials for specific molecules. Within the discussion of the development of these two systems, highlights will be made of their applications towards sensors, separations, and catalysis. The section concerning supramolecular templates and zeolites has been included to point out the wide range of possibilities that exist with metal oxide matrices in the development of unique and tailorable structures directed by molecular species in various aggregated phases.

### 8.1.1 Sol-gel chemistry

The method of choice in the preparation of inorganic matrices for molecular imprinting has been the sol-gel technique. A number of excellent reviews and books are available for those interested in a more detailed understanding of the method

and the material properties [1–3]. Only some brief aspects of the sol-gel method, regarding preparation conditions, gel formation, gel structure and surface chemistry, will be described here to acquaint the reader with the process and material properties encountered within this chapter.

The sol-gel technique uses mild conditions to prepare a cross-linked, robust metal oxide gel. Gelation of silanes, such as tetraethoxysilane (TEOS) or sodium silicate, involves the use of aqueous solutions, sometimes containing alcohol, with a slight adjustment of pH to catalyse the condensation polymerisation. The cross-link density, material porosity and homogeneity of functionalised sites, are dependent on the solution pH, extent of ageing, method of solvent evaporation, water content in solution and type of catalyst, all of which provide a number of handles to modify the material of interest.

The gel structure from metal oxide sol-gels is highly dependent on the solution pH and catalyst used. The solution pH determines whether the rate limiting step for the reaction of silanes in the sol is hydrolysis or condensation (Fig. 8.1). At low pH, silane hydrolysis is slow and condensation is fast so polymer growth is favoured over cross-linking. At high pH the opposite occurs, where silane condensation is slow but hydrolysis is fast, so the growing polymer chains tend to cross-link rapidly and form particulates that aggregate, forming heterogeneous structures. Subsequently, gelation times are much faster with base catalysed sol-gel materials compared to acid catalysis. The acid catalysed gel is usually an optically transparent material that has a relatively homogeneous structure with small pores and high surface area. Conversely, base catalysed materials are optically translucent to opaque with lower surface area, large porous structure and lower density. Figure 8.2 shows scanning electron micrographs (SEM) of acid (HCl) and base (NH<sub>4</sub>OH) catalysed sol-gel matrices.

The sol, which is a fluid mixture of water (sometimes containing organic solvent), catalyst and oligomerised silanes, turns into a solid, wet gel after some period of reaction time. The wet gel contains open channels, which are precursors to pores in the dried material. The resultant porosity of the dried gel is directly affected by the drying conditions, gel-solvent interfacial tension, and reactivity of

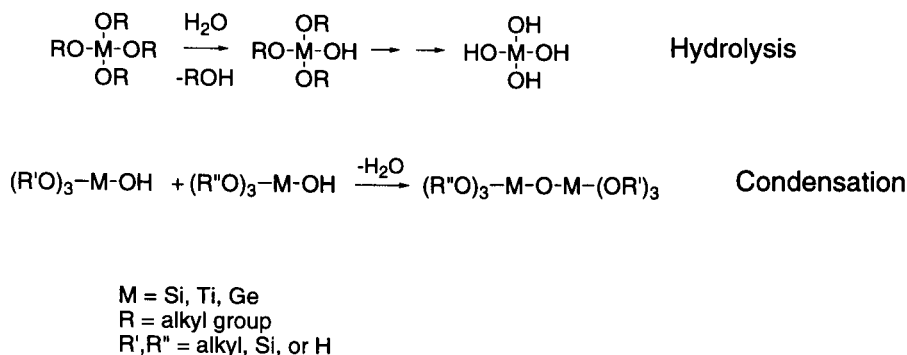


Fig. 8.1. Chemistry of silane hydrolysis and condensation.

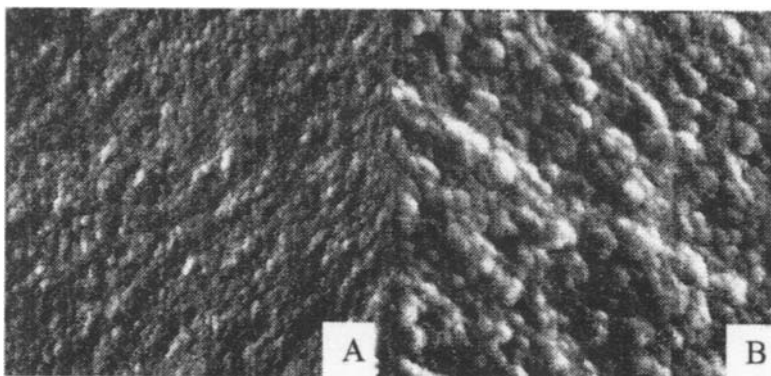


Fig. 8.2. SEMs of acid (A) and base (B) catalysed silica xerogels. The composition for acid catalysed gel is (in mole %) 18.4% *n*-propanol, 75.5% H<sub>2</sub>O, 6.1% TEOS, and 0.005% HCl. Composition for the base catalysed gel is 39.2% *n*-propanol, 47.9% H<sub>2</sub>O, 12.9% TEOS, 0.010% HCl, and 0.016% NH<sub>4</sub>OH.

the gel surface. In the case where the solvent and gel have high interfacial surface tension, removal of solvent by evaporation will cause the gel to shrink and the open channels to collapse creating a xerogel. If silanols (Si-OH) across an open channel react forming siloxane bonds (Si-O-Si) they will permanently close a potential pore, reducing the surface area and pore volume. However, if the silanols are capped by trimethylsilyl groups, condensation is prevented and the channel can re-open after removal of solvent to form a pore (*ambient pressure aerogels*) [4]. In the other case, where the solvent and gel have low interfacial surface tension, such as with the use of supercritical CO<sub>2</sub>, solvent removal induces very little shrinkage of the gel and the channel structure of the wet gel is preserved as open pores in the dry gel [5]. The end result is an *aerogel* which has extremely high surface area, large pore volume and exposed silanols that could be reacted with functionalised silane monomers at some later time.

Much like the organic polymers, the extent of cross-linking of the metal oxide gel can be adjusted by changing solvent systems, cross-linking agents or reaction time. However, what is unique to the metal oxides is that the surface chemistry can be tailored long after the gel structure has been set. Exposed silanol groups on the gel surface can react with neighbouring silanols to form siloxane bonds or conversely siloxane bonds can react with water to form silanols. A siloxane covered surface is hydrophobic whereas a silanol covered surface is hydrophilic. By varying the silanol to siloxane coverage on the material surface hydrophilicity can be readily adjusted. Figure 8.3 shows an extreme example of the reversible interchange of the silica surface between hydrophobic siloxanes and hydrophilic silanols. The siloxane surface can be converted to silanols by exposure to water and some acid or base catalyst, whereas silanol to siloxane conversion is effected by sintering of the gel.

Characterisation of metal oxide materials is similar to that of organic polymers, which includes surface area analyses and electron micrograph images. In addition

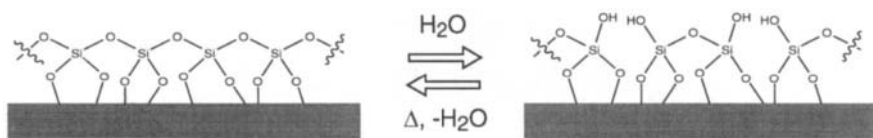


Fig. 8.3. Silica gel surface can consist of siloxane (Si-O-Si) bonds or silanol (Si-OH) groups, which are hydrophobic or hydrophilic respectively. Depending on material treatment, either chemical or thermal, the surface can have hydrophobic (left) or hydrophilic (right) properties.

to these tools, spectroscopic techniques have been developed for metal oxide materials to measure the extent of cross-linking, exposed silanols and derivatisation of the surface. For example, solid state  $^{29}\text{Si}$  NMR has been used to quantitatively determine the connectivity of silicon existing in the gel, which relates to extent of cross-linking [3]. Deconvolution of quaternary ( $\text{Si}(\text{OR})_4$ , where  $\text{R} = \text{H}$ , alkyl, or Si), or Q, silicon peaks finds that a large percentage of the silicons are in the complete or partially cross-linked states. Extents of cross-linking greater than 90% have been observed. Additionally, this technique can also be used to quantitatively measure the incorporation of functionalised monomers to the gel and their connectivity. An example of this will be given in the section covering imprinting in three-dimensional matrices.

Among the many desirable properties that are obtained with sol-gel formed metal oxide materials, it is perhaps the hydrophilic/hydrophobic duality of the matrix that allows the successful imprinting of molecular species. In the formation of the gel, templates will direct the placement of siloxane and silanol groups to complementarily interact with various hydrophobic and hydrophilic sites on the template. Figure 8.4 shows a possible form of an imprinted site for propyl orange in a silica matrix. Various aspects of molecular imprinting, such as these concepts, will be explored in the following sections.

## 8.2. TWO-DIMENSIONAL MATRICES

Langmuir-Blodgett (LB) films, SAM and films formed by chemical vapour deposition (CVD) have been used as two-dimensional matrices for molecular imprinting. These molecularly flat films offer a greater level of control over material structure, compared to three-dimensional matrices, due to the high orientation of the film structure [6]. LB and SAM films are composed of amphiphilic molecules that have hydrophilic, sometimes reactive, headgroups and hydrophobic tails. For LB films the molecules are spread on an aqueous surface and compressed to a particular surface pressure to build an organised monolayer. The monolayer is then transferred onto a solid substrate by vertically dipping a solid substrate through the monolayer. SAM films, on the other hand, spontaneously assemble *in situ* by soaking a solid substrate in a solution containing a reactive amphiphile. Using the selective reactivity of the headgroup for the substrate's surface, along

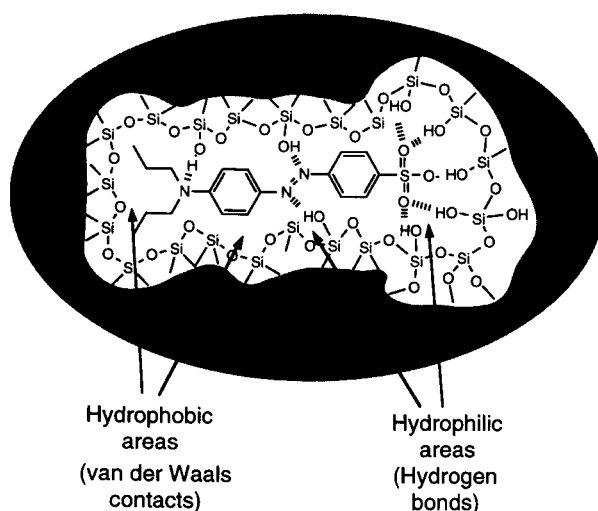


Fig. 8.4. Schematic of an imprinted site in a silica gel matrix using propyl orange as the template. The flexible hydrophobic/hydrophilic nature of the metal oxide gel matrix provides for appropriate siloxane/silanol formation to accommodate the functionality and structure of the imprinting molecule.

with favourable interactions between the assembling molecules, a highly organised film can be obtained. In a similar vein, CVD films can be formed on solid substrates using reactive molecules in the gas phase. In all these cases the films are highly ordered and asymmetric, with the hydrophilic headgroups oriented in one direction and the hydrophobic tails pointing in the opposite direction.

Siloxane based monolayer films prepared using both LB and SAM techniques have been studied as novel matrices for molecular imprinting and molecular recognition. The first attempt at employing a SAM technique for imprinting was performed in Tabushi's group in 1987 [7]. Using octadecyltrichlorosilane (ODS) as the matrix monomer and hexadecane as the template they created mixed monolayer films on  $\text{SnO}_2$  surfaces. Covalent attachment of the ODS portion of the mixed monolayer to the metal oxide surface allowed the removal of hexadecane template by solvent washing. What were left behind were hydrophobic pockets defined by the ODS alkyl chains (Fig. 8.5). Recognition studies were performed amperometrically using cyclic voltammetry (CV) to detect the binding of substrates in a methanol/water solution with phosphate buffer (pH 7.0). Vitamin  $\text{K}_1$ , containing a long hydrophobic alkyl chain, selectively bound to the film compared to vitamin  $\text{K}_2$  and vitamin E, and almost no binding was observed for vitamin  $\text{K}_3$ , which has no hydrophobic chain. The limit of detection of vitamin  $\text{K}_1$  in this amperometric "sensor" was found to be at micromolar concentrations. Binding of vitamin  $\text{K}_1$  could be inhibited by addition of hexadecane to solution.

Tabushi's group continued work in this field and showed that these simple thin film systems could be imprinted with more complex structures than just straight

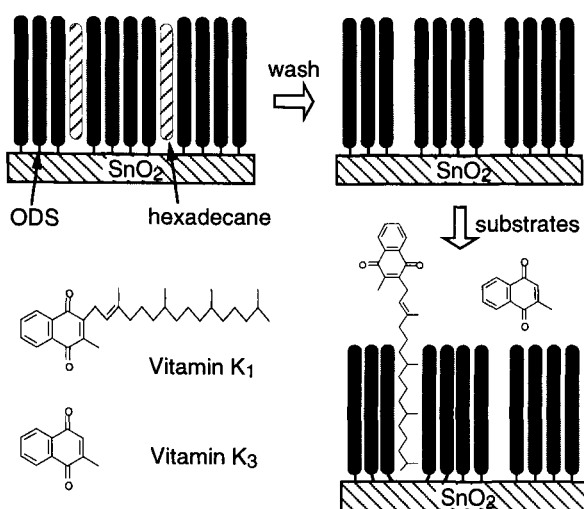


Fig. 8.5. Two-dimensional imprinting using hexadecane (hatched rods) as a template in an ODS (filled rods) matrix covalently attached to a  $\text{SnO}_2$  substrate. Removal of the template by washing leaves behind sites in the film that can bind vitamin K<sub>1</sub>, which has an isoprenyl appendage, but not vitamin K<sub>3</sub>.

alkane chains [8]. With ODS films as the matrix they prepared recognition sites using hexadecane, 2-cholesteryl-3,6-dioxadecylcarbonate and decyladamantane-1-carboxylate as templates on separate films. While the first two templates produced films with recognition properties for substrates with long, hydrophobic structures and excluded the binding of sterically bulky adamantane, the last template produced a film with recognition properties with exactly the opposite results. These results show that in spite of the simplicity of the octadecyl matrix, molecular imprinting for complex structures can be obtained.

Other research groups soon followed this work with versions of their own molecular imprinting in two-dimensional siloxane films. Using ellipsometry to measure changes in film thickness upon guest substrate binding on imprinted films Mosbach's group, in 1988, confirmed Tabushi's earlier work [9]. In the same year Cotton and co-workers used similar ODS SAMs to prepare imprinted films with porphyrin templates [10]. Selective binding for porphyrins was confirmed using surface enhanced Raman scattering and electrochemical analysis. A few years later, Kallury *et al.* also used ODS SAM films imprinted with hexadecane to bind stearic acid and octadecylamine [11]. Using X-ray photoelectron spectroscopy and contact angle measurements it was concluded that the substrates bound with the hydrophobic tails incorporated in the film and the polar headgroups oriented away from the surface. In 1993, Starodub *et al.* reported the use of imprinted electrode surfaces with trimethylsilane monolayers for the selective binding of amino acids, nucleotides and cholesterol [12]. The following year, Binnes *et al.* were successful in the preparation of ODS films with chiral recognition properties for 1,2-epoxydodecane [13].



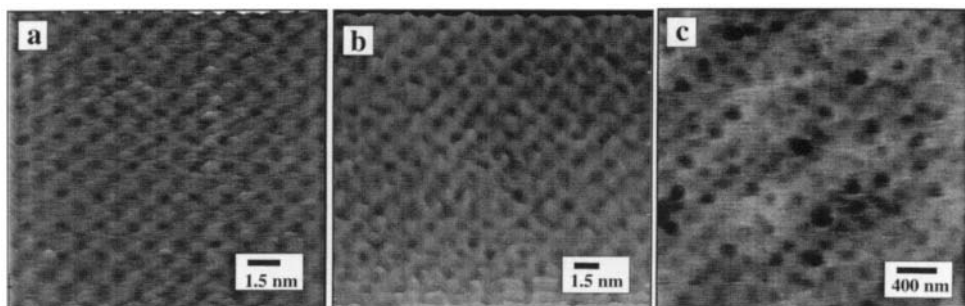


Fig. 8.6. Atomic force microscope images of a calcined octadecyltrimethoxysilane monolayer on silicon (a) and similar monolayers incorporating octadecylsulphonate as a template at 11 mole % (b) and 25 mole % (c) in the film. The pure film gave atomically flat surfaces within micron sized areas. The octadecylsulphonate templated films gave molecular level pores with 11% template but much larger pores at 25% template.

Imprinted metal oxide two-dimensional films have also been prepared using a CVD technique developed by Kodakari *et al.* [14,15]. They demonstrated that molecular imprints of aromatic aldehydes could be prepared in monolayer films of silica deposited by CVD on  $\text{SnO}_2$  surfaces. Taking advantage of the specific adsorption of aldehydes to  $\text{SnO}_2$ , templates such as benzaldehyde were dispersed and bound to the surface, followed by tetramethoxysilane deposition. The templates were removed from the surface by gas phase reaction with ammonia, converting the aldehydes to nitriles. Gas phase binding studies performed on the calcined films of imprinted and non-imprinted systems showed that size selective memory for the benzaldehyde template existed.

Although binding experiments allude to the existence of receptor sites in imprinted materials, direct physical evidence of these sites has been difficult to obtain in either two- or three-dimensional systems. Recently, we have been able to image, at the atomic level, cavities created in siloxane monolayer films *via* a molecular templating approach [16]. Mixed monolayers of octadecyltrimethoxysilane and sodium octadecylsulphonate were prepared as LB films on atomically flat silicon surfaces. Using the sulphonate amphiphile as a template and the silane amphiphile as a silica precursor, it was possible to create atomically flat silica films with a tailorable porous structure *via* calcination of the films. The pore size was dependent upon the mole fraction of template in the film. At concentrations near and below 11 mole % template, pores of the order of 3–4 Å in diameter could be created, while at 25% much larger pores, 20–25 Å in diameter, were observed (Fig. 8.6). These results address the issue of the generation of receptor sites formed *via* the aggregation of template molecules due to phase separation from the matrix. This is an important issue, which will be revisited at the end of this chapter, concerning the concentration and mole fraction of template in the forming matrix at what threshold is *molecular* imprinting achievable and what is the limit beyond which *aggregation*, or supramolecular assembly, becomes a factor.

### 8.3. THREE-DIMENSIONAL MATRICES

The sol-gel method offers a wide range of processing techniques that can produce thin films, bulk structures and coatings on porous materials for use as separation materials, sensors, and catalysts. This section will look at how research groups have cleverly used different sol-gel processing techniques to prepare a variety of materials with molecular memory. The section is broken down into several smaller sub-sections. The first topic will be molecular imprinting in thin films. Here we will look at dip-coating and spin-casting techniques that produce flat gel structures. The next topic will look at imprinting in bulk structures that will include imprinting in the gel matrix and imprinting localised at the gel surface. Characterisation of host-guest interactions *via* solid-state NMR techniques will also be covered. The last two topics will cover the applications of imprinted metal oxide materials in separations and catalysis.

#### 8.3.1. Thin films

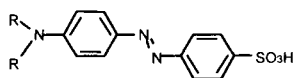
Recently, Lee *et al.* have employed a dip-coating technique to prepare nanometre thick  $\text{TiO}_2$  films doped with an azobenzene template [17]. The authors found that the best imprinting conditions were achieved when the template, 4-(4-propyloxyphenylazo) benzoic acid, was allowed to react with the metal oxide monomer, titanium tetrabutoxide, prior to gelation. The sol contained a high ratio of template to matrix monomer (1:4 or 1:2). Coating thickness, template removal from the film and substrate uptake were monitored using a combination of quartz crystal microbalance measurements and UV absorption data. Sol-gel coatings on treated quartz surfaces were found to have a thickness of 1.8–2.7 nm per dip cycle. Template removal was achieved with aqueous ammonia. In binding experiments conducted in tetrahydrofuran at a 0.25 mM substrate concentration, the imprinted gels were found to have recognition properties for the original template. Considering the high template to monomer ratio it is surprising that recognition properties were achieved, since the formation of isolated receptor sites would be impossible to attain for the majority of the occluded templates. However, the receptor sites are reportedly stable in the film and can be recycled over multiple experiments. These results perhaps indicate that the formation of isolated receptor sites is not a requisite for molecular memory.

Spin-casting techniques have also been used to prepare imprinted thin films. Makote and Collinson recently prepared metal oxide thin films imprinted with recognition sites for dopamine [18]. The dopamine template was loaded at 4 mole % in a sol with a 10:1 ratio of tetramethoxysilane and phenyltrimethoxysilane. The prepared film had a thickness of *ca.* 450 nm. CV analysis found that 90% of the templates could be removed by washing the films with pH 7 phosphate buffer. The opened receptor sites offered selective binding for related molecules containing catechol amines, such as dopamine, epinephrine and norepinephrine, as determined by CV. The use of phenyltrimethoxysilane turns out to be an essential ingredient for the gel matrix and is believed to provide some complementary affinity for the catechol amines *via* hydrophobic and/or  $\pi$ -stacking interactions.

### 8.3.2. Bulk structures

Probably the most well known work on molecular imprinting was the first publication on imprinting by Frank Dickey in Linus Pauling's laboratory at Caltech (see also Chapter 1). In 1949, Dickey showed that purely synthetic materials could be prepared with a memory for an imprint molecule [19]. The matrix he chose to use was prepared by sol-gel chemistry. In a silica gel matrix he found that it was possible to imprint memory that was shape selective. Soon others confirmed these observations and a new area in chemistry was born.

Dickey's sol-gel method was a bulk phase reaction that entrapped the imprinting dye throughout the gel matrix [20]. Acidification of an aqueous solution of sodium silicate in the presence of 5 mM concentration of azobenzene dyes produced a coloured silica gel. The gel was then aged and dried, crushed and sieved and, finally, the template extracted from the gel with methanol. Greater than 90% of the dye molecules could be extracted from the gel, the precise amounts being dependent upon the type of acid catalyst used. Imprinted materials were produced using methyl, ethyl, propyl and butyl orange dyes as templates and in each material the molecular recognition properties was greatest for the original template.



R = methyl, ethyl, propyl, butyl

Orange dyes

In his work, Dickey uncovered many of the important issues involved in imprinting in sol-gel materials with which researchers are still grappling today. In the gelation of the silica, a small but significant portion of dye molecules were completely immobilised. Interestingly, similar procedures are used today to entrap chemically sensitive chromophores for sensor materials. Attempts to remove the remaining dyes, such as ageing, heat treatment and neutral pH buffers, ended up degrading the gel and its recognition properties. Dickey considered these tightly bound dyes to reside in recognition sites with very high binding constants. It is also possible that the dyes are physically entrapped in the gel matrix, suffering extremely slow transport rates through the gel. In light of this work several groups, including ourselves, have used surface imprinting techniques to localise the imprinted sites to the gel surface for faster binding kinetics (*vide infra*).

Although the binding isotherms for the alkyl orange dyes in the imprinted silica gel indicated a complex system, Dickey was able to estimate binding constants by assuming a gel with two types of adsorbing sites, one strongly attracting (specific) and the other weakly attracting (non-specific). Using equation (1), where  $v$  is the

$$v = \frac{\alpha_1[S]}{K_1 + [S]} + \frac{\alpha_2[S]}{K_2 + [S]} \quad (1)$$

TABLE 8.1

BINDING PARAMETERS OF ALKYL ORANGE DYES TO IMPRINTED GELS<sup>a</sup>

| Gels             |               |                               |                              |                               |                              |
|------------------|---------------|-------------------------------|------------------------------|-------------------------------|------------------------------|
| Imprint molecule | Substrates    | $1/K_1$<br>(M <sup>-1</sup> ) | $\alpha_1$<br>( $\mu$ mol/g) | $1/K_1$<br>(M <sup>-1</sup> ) | $\alpha_2$<br>( $\mu$ mol/g) |
| Control          | Methyl orange | 700                           | 8.00                         | 670 000                       | 0.010                        |
|                  | Ethyl orange  | 555                           | 8.00                         | 670 000                       | 0.011                        |
| Methyl orange    | Methyl orange | 1250                          | 8.00                         | 670 000                       | 0.270                        |
|                  | Ethyl orange  | 910                           | 8.00                         | 670 000                       | 0.080                        |
| Ethyl orange     | Methyl orange | 1600                          | 8.00                         | 670 000                       | 0.190                        |
|                  | Ethyl orange  | 1910                          | 8.00                         | 670 000                       | 0.250                        |

All binding studies were performed in aqueous 5% acetic acid solution.

<sup>a</sup>Data from [20].

amount of substrate bound to the gel,  $\alpha_1$  and  $\alpha_2$  are the binding capacities of the weakly and strongly attracting sites respectively,  $K_1$  and  $K_2$  are their associated dissociation constants and  $[S]$  is the substrate concentration, reasonably good fits were obtained. The binding parameters for some of the investigated gels are listed in Table 8.1. All binding studies were performed in aqueous 5% acetic acid solutions. The imprinted materials exhibited an improvement in binding affinity and capacity over the control materials. It was also found that molecules that strongly interact with silica produce imprinted sites with better recognition properties compared to molecules with weak attraction to silica gel.

As in any materials, the recognition properties are dictated by the gel structure and surface chemistry. However, in metal oxide sol-gel materials the gel formation is influenced by a multitude of factors, such as solvents, water, catalysts, solvent evaporation and ageing. Furthermore, the surface chemistry of silica gels is heavily influenced by the solution pH. In his experiments Dickey discovered that condensation of the gel must be near completion for molecular imprinting to work. If the template were to be extracted from the wet gel before final shrinkage to the xerogel state the finished material would have no recognition properties. Dickey also suggested that the gelation rate is also important, in that a rapid gelation would not preserve "favourable configuration of the unreacted gel components". However, very slow gelation "will not suppress reactions that destroy favourable configurations that are already formed". In considering surface chemistry, adsorption experiments performed in aqueous solutions were most pronounced at low pH values, but did not improve below pH 3, which is coincidentally near the isoelectronic point of silica gel [2]. Increasing pH increases the anionic surface charge of the gel and decreases specific adsorption of azobenzene dyes. At pH 8, affinity of the azobenzene dyes is completely lost. Since the degradation of the silica gel is not appreciable at this pH, other mechanisms, such as

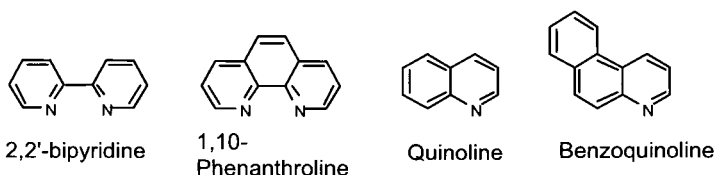
ionic repulsion between the gel surface and sulphonate guest, may play a role. Similar effects were also observed in other systems which will be discussed subsequently.

Research on imprinted materials continued in Pauling's laboratory, resulting in another paper by Bernhard, who repeated some of Dickey's work but used a non-ionic template molecule in place of the alkyl orange dyes [21]. Bernhard determined that by using a sulphonamide version (4-(*N,N*-dimethylamino)-4'-sulphonamidoazobenzene) of methyl orange (MO) as a template, receptor sites with even higher affinity for sulphonate and sulphonamide molecules could be prepared. Apparently, the polar sulphonamide headgroup stabilises the template in the forming gel matrix such that improved fidelity of the molecular imprint was achieved. An interesting side note is that Bernhard also observed a pH effect on MO binding to all gels and that at pH 7 the adsorption drops to near zero.

The fascinating discovery that simple amorphous silicates could be imprinted with molecular memory was not without its critics. In 1959, Morrison *et al.* published their results on molecular imprinting using Dickey's procedure [22]. Their results were, in general, the same as that of Dickey's. However, they claimed that the selective adsorption observed was an artefact of the entrapped dye in the gel having some affinity for similar dyes. Their claim was not substantiated by any spectroscopic or other analytical data and could not be proven, since removal of the entrapped dye compromised the gel.

In the following years a number of papers appeared in the literature that reaffirmed and enhanced the concept of molecular imprinting in silica gels. In 1955, Haldeman and Emmett repeated some adsorption experiments with Dickey's original gels and found them to still be selective after a year of ageing, although with some loss of adsorptivity [23]. Ten years later, Reed and Rogers repeated Dickey's work, obtaining nearly identical results, and looked into the dynamics of imprinting with structural isomers of azobenzene dyes [24]. During this decade Snyder published some theoretical studies concerning the structure of specifically absorbing sites existing on silica gels [25]. Then, Erlenmeyer and Bartels published results on imprinted silica gels using *N*-heterocycle aromatics as templates, such as 2,2'-bipyridine and 1,10-phenanthroline [26]. Good selective affinity was observed in these materials for their original templates. These gels imprinted with bis-nitrogen aromatics also exhibited selectivity for aromatics containing only one nitrogen, such as quinoline and isomers of benzoquinoline. Cross-over experiments were also conducted on gels imprinted with *bis*- and *mono*-nitrogen heterocycles. The results showed a general trend of size specific recognition.

During the time of Dickey's original publications Curti and Colombo prepared the first stereoselective adsorbents *via* molecular imprinting [27,28]. In this work,



which will be revisited in the next sub-section (on separation), the authors imprinted silica gels with an enantiomer of camphorsulphonic acid using the original sol-gel techniques of Dickey. Several years later, publications from the labs of Bartels, Prijs, and Erlenmeyer [29] and from Beckett and Anderson [30] reaffirmed the stereoselective adsorption capabilities of molecularly imprinted materials. Again, using the same sol-gel techniques, silica gels were prepared with molecular memory for stereoisomers of *N*-methyl-3-methoxymorphine, nicotine, quinine, quinidine, cinchonine and cinchonidine. The authors found that enantio-specific recognition could be obtained *via* molecular imprinting, although the effect was small. Larger effects were obtained with the imprinting of diastereoisomers. A sample of some of the work involving adsorption studies of quinine and quinidine imprinted gels equilibrated with quinine, quinidine, cinchonine and cinchonidine are shown in Table 8.2. As with the alkyl orange studies the results from the cross-over experiment are impressive.

In 1969, Majors and Rogers examined in further detail the conditions for imprinted gel formation that affect reproducibility in selective adsorption [31]. In their paper, the authors found that the ageing time, drying method and gelation rate all affect the binding capacity and selectivity much as Dickey had hypothesised

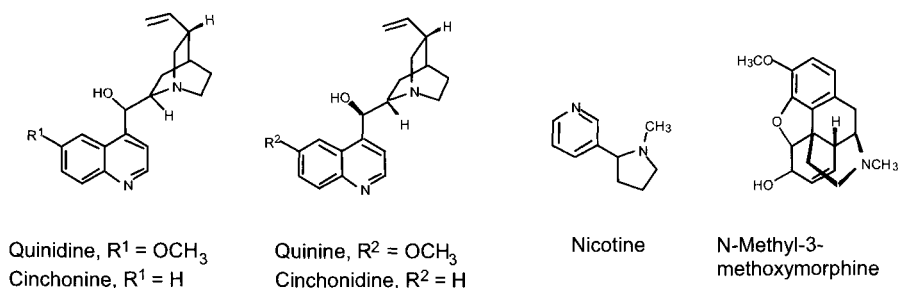


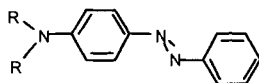
TABLE 8.2

#### ADSORPTION OF STEREOISOMERS ON QUININE AND QUINIDINE IMPRINTED GELS<sup>a</sup>

| Imprint molecule | Uptake expressed as moles $\times 10^5$ mole/kg of substrate of |            |            |            |              |
|------------------|---|------------|------------|------------|--------------|
|                  | Batch no.   | Quinine    | Quinidine  | Cinchonine | Cinchonidine |
| Quinine          | 1   | <b>217</b> | 160        | 163        | 207          |
|                  | 2   | <b>210</b> | 161        | 167        | 200          |
| Quinidine        | 1   | 194        | <b>224</b> | <b>218</b> | 190          |
|                  | 2   | 196        | <b>228</b> | <b>215</b> | 193          |

<sup>a</sup>Uptake of substrate at an equilibrium concentration of 25 mmole substrate/kg of gel in 5% aqueous acetic acid. Data from [30].

years earlier. The authors used *N,N*-dimethyl-*p*-phenylazoaniline and *N,N*-diethyl-*p*-phenylazoaniline as templates to structurally mimic MO and ethyl orange (EO) respectively, but would have better release from the gel compared to the orange dyes. Slower gelation times yielded materials with enhanced affinity for MO and EO and reduced affinity on the control gels. It was reasoned that the slower rate of gelation and xerogel formation creates materials with lower surface areas but better registry of the template with the forming gel, resulting in higher affinity receptor sites. In the control gel, however, lower surface area translated into reduced non-specific binding interactions at the surface and thus lower binding capacity.



*N,N*-Dialkyl-*p*-phenylazoaniline

In a subsequent paper, Majors and Rogers went on to examine structural characteristics of the imprinting molecule and their effects on the strength of adsorption of various substrates [32]. They found that recognition properties for large molecules could be achieved by gels imprinted with templates equivalent to just parts of the large molecules' structures. For example, simple *N,N*-dialkylanilines templates were found to imprint recognition sites for alkyl orange dyes with the recognition properties governed by the dialkyl amine moieties. Other structural changes in the template molecule, involving polar, non-polar, acidic and molecularly bulky groups, were examined and the affinities for various substrates tabulated. In summary, they found that the overall molecular geometry most heavily influenced the imprinted site, not the functionality of the template. The authors also performed a cross-over experiment looking at different alkyl substituted *p*-aminoazobenzene (*N,N*-dialkyl-*p*-phenylazoanilines) templates. Table 8.3 shows the data and alludes to the remarkable selectivity that can be achieved with molecular imprinting. In no case is the affinity of closely related substrates higher than the original template molecule.

Other recent works involving the use of metal oxide materials for imprinting includes that of Pinel *et al.*, who revisited the use of imprinted metal oxide sol-gels to resolve enantiomers [33]. The TEOS sol-gel materials imprinted with (–)-menthol were catalysed with acid, base or fluoride and aged for 2 weeks prior to removal of template. Although the resultant gels gave no enantioselectivity in the binding of menthol, regioselectivity was observed, with *o*-cresol having enhanced affinity over *p*-cresol, which was the opposite order of affinity on a control gel. Dai *et al.* have used an imprinting technique to prepare materials with selective adsorption for uranyl dioxide [34]. Fluorescence spectroscopic studies have allowed them to probe the imprinted site of these gels. Fluorescence has also been used by Lulka *et al.* [35] to determine binding constants for silica imprinted with recognition sites for fluorescein and *N*-acetyltryptophanamide.

The first use of functionalised silane monomers in the preparation of metal oxide imprinted gels came in the mid 1980s with the work from Glad *et al.* [36] and from

TABLE 8.3

NORMALISED RELATIVE ADSORPTION POWER RATIOS FOR  
*p*-AMINOAZOBENZENE DYES ON *p*-AMINOAZOBENZENE IMPRINTED GELS<sup>a</sup>

| Substrate <sup>b</sup> |                   |             |             |                    |             |                    |
|------------------------|-------------------|-------------|-------------|--------------------|-------------|--------------------|
| Imprint molecule       | R-NH <sub>2</sub> | R-NMeH      | R-NEtH      | R-NMe <sub>2</sub> | R-NMeEt     | R-NEt <sub>2</sub> |
| R-NH <sub>2</sub>      | <b>1.00</b>       | 0.79        | 0.72        | 0.69               | 0.69        | 0.75               |
| R-NMeH                 | 0.73              | <b>1.00</b> | 0.59        | 0.50               | 0.38        | 0.44               |
| R-NEtH                 | 0.76              | 0.93        | <b>1.00</b> | 0.66               | 0.53        | 0.60               |
| R-NMe <sub>2</sub>     | 0.56              | 1.00        | 0.75        | <b>1.00</b>        | 0.53        | 0.67               |
| R-NMeEt                | 0.57              | 0.65        | 0.65        | 0.7                | <b>1.00</b> | 0.92               |
| R-NEt <sub>2</sub>     | 0.43              | 0.63        | 0.63        | 0.6                | 0.87        | <b>1.00</b>        |

<sup>a</sup>Relative adsorption power is generally defined as: (amount of adsorbed dye on imprinted gel)/(amount of adsorbed dye on control gel) at 20  $\mu$ M equilibrium concentration. For further details of the equation see reference [32].

<sup>b</sup>Substrates equilibrated in 2 N aqueous HCl solution.

Adapted from [32].

Wulff *et al.* [37]. In both their methods to prepare receptor sites in metal oxide gels the researchers used a surface imprinting technique on silica gel. In 1985, Glad *et al.* used a unique mixture of phenyltriethoxysilane, *N*-2-aminoethyl-3-aminopropyltrimethoxysilane, and *bis*(2-hydroxy-ethyl)aminopropyltriethoxysilane monomers to heavily functionalise a silica surface. The gelation was performed at high temperature (85°C) and with low pH (2.5–3.0). Gels were imprinted with the dye molecules Rhodanile blue or Safranin O and the resultant materials exhibited good recognition properties for their original templates in liquid chromatography studies. Table 8.4 shows the selectivity factors for the dye imprinted gels.

In the same paper the researchers reported the preparation of metal oxide gels imprinted with recognition sites for proteins. The sol-gel procedure was similar to the one mentioned above, but carried out at low temperature (4°C) and with an additional boronate-silane monomer. The template protein, transferrin, contains two identical carbohydrate moieties that the boronate can react with to form cyclic boronate esters. Gels imprinted with transferrin gave good recognition properties for transferrin but relatively poor affinity for another protein bovine serum albumin (BSA), as measured by chromatographic retention times. Gels imprinted with BSA, which does not express carbohydrate moieties, had no measurable enhanced affinity for BSA or transferrin when compared to a control gel. The relative retention data are shown in Table 8.5.

Surface-functionalised gels were also prepared by Wulff *et al.* using diimine silane monomers [37]. The researchers were interested in isolating the effect of functional group positioning in molecularly imprinted materials. By using a



TABLE 8.4

SELECTIVITY FACTORS<sup>a</sup> OF IMPRINTED SILICA GELS

| Imprint molecule | Substrate      |             |
|------------------|----------------|-------------|
|                  | Rhodanile blue | Safranin O  |
| Rhodanile blue   | <b>1.00</b>    | 0.83        |
| Safranin O       | 0.81           | <b>1.00</b> |

<sup>a</sup>Selectivity factor =  $[r_1/r_1(\text{control})]/[r_2/r_2(\text{control})]$ , where  $r_1$  = retention volume for applied substrate,  $r_2$  = retention volume for printed substrate and  $r$  (control) = retention volume on control polymer. Data from [36].

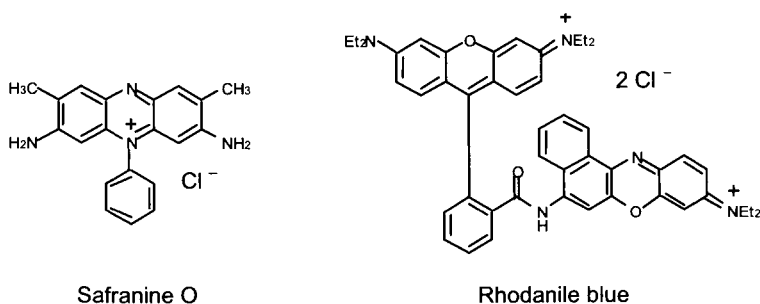


TABLE 8.5

RELATIVE RETENTION<sup>a</sup> OF TRANSFERRIN/BSA ON IMPRINTED GELS<sup>b</sup>

| Imprint molecule | Boronate-silane used? | Elution volume (mL) |             | Relative retention |
|------------------|-----------------------|---------------------|-------------|--------------------|
|                  |                       | Transferrin         | BSA         |                    |
| Transferrin      | Yes                   | <b>1.32</b>         | 0.61        | 2.16               |
|                  | No                    | 0.64                | 0.50        | 1.28               |
| BSA              | Yes                   | 0.71                | <b>0.58</b> | 1.22               |
|                  | No                    | 0.59                | 0.51        | 1.16               |
| None             | Yes                   | 0.73                | 0.60        | 1.22               |
|                  | No                    | 0.51                | 0.44        | 1.16               |

<sup>a</sup>Relative retention = elution volume (transferrin)/elution volume (BSA).

<sup>b</sup>Data from [36].

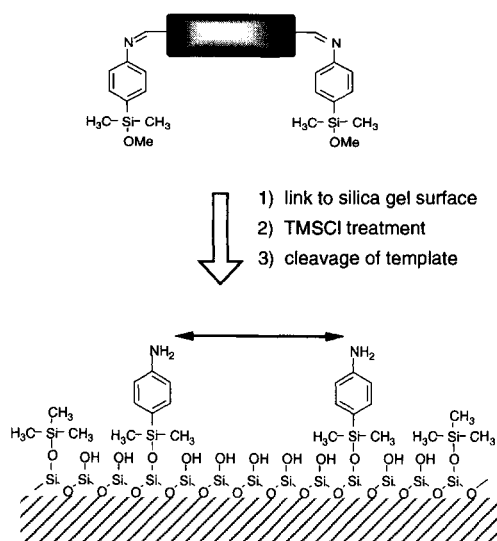


Fig. 8.7. Surface imprinting with a covalently coupled diimine template has been used to position two amines onto a “flat” silica surface in an effort to isolate the effect of functional group placement in molecular imprinting. The rectangular spacer between the imines represents either a phenyl or diphenylmethane. Adapted from [37].

surface-imprinting technique, linking the silane template assembly to a “flat” silica surface, the researchers believed they could eliminate the “footprint” impression (van der Waals’ and polar interactions) of the template but maintain functional group positioning in the matrix. Hydrolytic cleavage of the template creates a receptor site composed of two aromatic amines spaced at a specific distance determined by the geometry of the dialdehyde template (Fig. 8.7). Gels imprinted with diimines of isophthalaldehyde and (4,4'-dibenzaldehyde)methane were selective for their respective template molecules.

Surface imprinting has recently been used in our laboratory to prepare phosphate and phosphonate receptors in silica xerogels [38]. In an effort to obtain faster on/off binding kinetics and gain thermodynamic control of the host–guest interaction, we positioned the receptor sites as close as possible to the gel surface. This resulted in observed equilibration binding times of less than a minute.

Preparation of the imprinted gel was conducted using a non-covalent template assembly approach. The silane monomer, 1-trimethoxysilylpropyl-3-guanidinium chloride, was mixed with half an equivalent of an appropriate phosphonate template and the mixture exposed to freshly prepared porous silica xerogels. Near quantitative covalent attachment of the guanidine-silane monomers to the gel surface was confirmed using cross-polarisation magic angle spinning  $^{29}\text{Si}$  solid state NMR measuring the silicon  $T_n$  ( $(\text{RO})_3\text{SiR}'$ , where  $\text{R} = \text{Si}$ , methyl, or  $\text{H}$  and  $\text{R}' = \text{propylguanidine}$ ) ratios. Rebinding studies performed in aqueous solutions at  $\text{pH} \sim 5$  produced binding curves similar to those found for the imprinted gels in

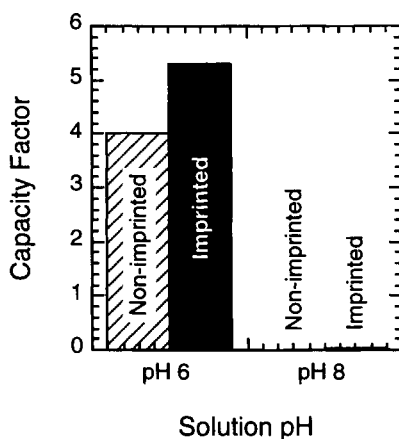


Fig. 8.8. A comparison of capacity factors from HPLC studies of guanidine-functionalised silica xerogels imprinted (dark bars) and non-imprinted (hatched bars) with PPA template, measured at pH 6 and pH 8.

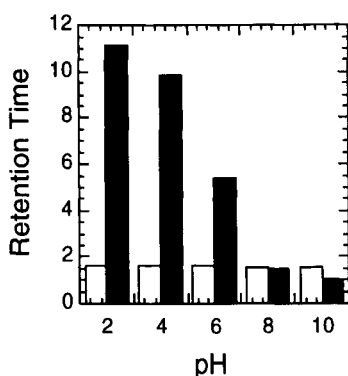


Fig. 8.9. A study of pH effect on HPLC retention times of PPA (dark bar) and acetone (white bar), a non-interacting substrate, on non-imprinted guanidine-functionalised xerogels.

Dickey's original papers. The binding curves could be estimated using a Langmuir isotherm composed of two adsorption sites, one having a strong specific interaction with a large association constant ( $K_a$ ) and the other a weak non-specific interaction with a small  $K_a$ . For the specific interaction,  $K_a$ s of imprinted gels were on the order of  $10^3/\text{M}$  in aqueous solutions. Binding constants for imprinted materials were typically 2–3 times higher than randomly functionalised gels. Non-functionalised gels had no measurable affinity for either phosphates or phosphonates.

In HPLC studies, a pH effect on substrate binding was observed with these materials. Figure 8.8 graphically illustrates the effect of pH on substrate affinity on imprinted and non-imprinted gels. At pH 6, the imprinted gel shows a molecular

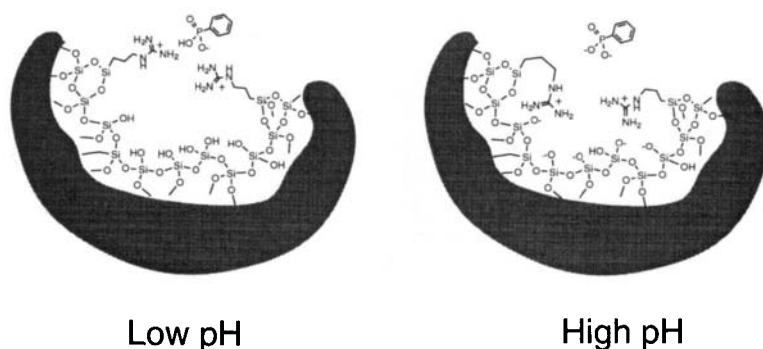


Fig. 8.10. PPA interacting with a guanidine-functionalised silica surface encounters different scenarios at low and high pH. At low pH the surface silanols are protonated and the guanidines are free to interact with PPA, whereas at high pH the surface becomes anionically charged and inhibits binding.

memory effect for phenylphosphonic acid (PPA), exhibiting a larger capacity factor compared to the non-imprinted gel. At pH 8, however, the affinity for both gels to PPA is abolished. A more global effect of pH on guanidine-functionalised gels is shown in Fig. 8.9. Increasing the solution pH reduces the affinity of PPA to the gel. Although mentioned only briefly in their papers, Dickey and Bernhard observed similar results with the adsorption of alkyl orange dyes to imprinted silicates. Dickey mentions, and we concur, that at pH 8 the material is not degraded and can resume a high level of binding by returning it to lower pHs. The silica surface can become highly charged at pHs increasingly higher than 2. At pH 2 and below the gel surface is at its isoelectric point with silanols fully protonated. Increasing the pH builds anionic charge on the gel surface and also on the phosphates and phosphonates, as well as sulphonate containing substrates. A possible scenario of the ionic repulsion involved between the host and guest at low and high pH is illustrated in Fig. 8.10.

These results illustrate an important effect on host-guest interaction in imprinted materials, in particular the metal oxides, i.e. that solution conditions can dramatically alter surface chemistry. It may be possible to minimise these effects by neutralising the surface or modifying the gel with organically modified silanes (ormosils), or perhaps the change in host-guest affinity at different pHs could be used advantageously in some applications. Further investigations to more fully understand this phenomenon and how to control surface chemistry effects are needed.

Characterisation of the receptor site in these surface imprinted xerogels has been made possible through solid state NMR techniques [39]. The PPA substrate, when bound to the guanidine-functionalised xerogel, can bind in a two-point, one-point or non-specific mode (Fig. 8.11). Phosphorous solid state NMR studies of these imprinted xerogels were performed and assignments could be made for the non-specific (21.0 ppm), one-point (15.5 ppm) and two-point (6.5 ppm) host-guest interactions. Figure 8.12 shows that, by increasing the concentration of PPA on the gel,

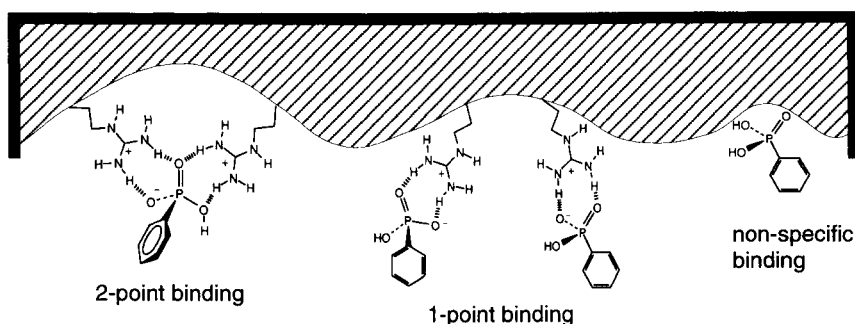


Fig. 8.11. Various modes of binding of PPA to the imprinted guanidine-functionalised gel.

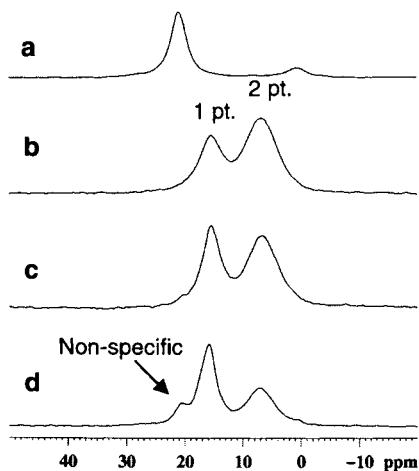


Fig. 8.12. Solid state  $^{31}\text{P}$  NMR of imprinted, guanidine-functionalised xerogels bound with varying amounts of PPA showing the binding mode with the associated peak resonance. The spectra are as follows: (a) pure PPA, (b) 2:1 guanidine/PPA, (c) 1:1 guanidine/PPA, and (d) 1:3 guanidine/PPA.

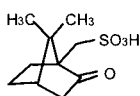
two-point binding modes are converted to one-point binding modes and that at high concentrations of PPA, the guanidine-PPA interactions become fully saturated and excess PPA sits non-specifically on the gel surface. NMR spectra of materials that have been washed with 1 N HCl, to remove template, and subsequent rebinding of PPA guest in aqueous solutions at pH 5 yield peaks at 12 and 5 ppm. Apparently, the bound PPA was able to detect a change in the environment at the receptor site from the initially formed material. One of the probable changes that have occurred is the formation of a highly polar silanol surface from the hydrolysis of remaining ethoxy groups from TEOS gel formation and the possibility of reorientation of the functional groups to act at neighbouring receptor sites.

Very recently, other groups have begun efforts in using functionalised silanes to

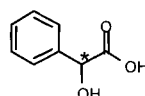
prepare molecularly imprinted sol-gels with unique properties. In a study that extends Wulff's original work in two-dimensions [37], Katz and Davis [40] prepared imprinted receptor sites with amino groups positioned in a three-dimensional architecture using an aromatic tricarbamate template. By utilising molecular probes coupled with solid state NMR and infrared and fluorescence spectroscopies, the researchers were able to define the spatial positioning of the functional groups about the imprinted site, as well as the geometry of the imprinted cavity. Dai *et al.* [41] have taken advantage of the regular three-dimensional structure of a mesoporous silica gel and shown significant improvement in the preparation of selective adsorption sites for transition metal ions compared to flat silica surfaces. Diamino silane ligands coordinated with  $\text{Cu}^{2+}$  were grafted into the cylindrical pores of the surfactant templated silica. The imprinting step not only improved the  $\text{Cu}^{2+}$   $K_d$  by six-fold, but simultaneously decreased affinity for  $\text{Zn}^{2+}$  by the same amount. And, in a study of the reorganisational process of the silica matrix following template removal, Boury *et al.* [42], employing numerous analyses, including  $^{29}\text{Si}$  solid state NMR,  $\text{N}_2$  adsorption porosimetry and small angle X-ray scattering, found that significant structural changes do occur, indicating a need for further developments in matrix modification for successful molecular imprinting.

### 8.3.3. Separations

Soon after the initial report of molecular imprinting by Dickey, Curti and Colombo published their own results on imprinted silica gels using chiral molecules as templates [27]. In chromatography experiments the imprinted gels were able to resolve racemic mixtures of the template molecules. The imprinted gels were prepared using the same sol-gel technique as Dickey with acetic acid as catalyst at a solution pH of 4. Gels imprinted with *d*-camphorsulphonic acid were washed free



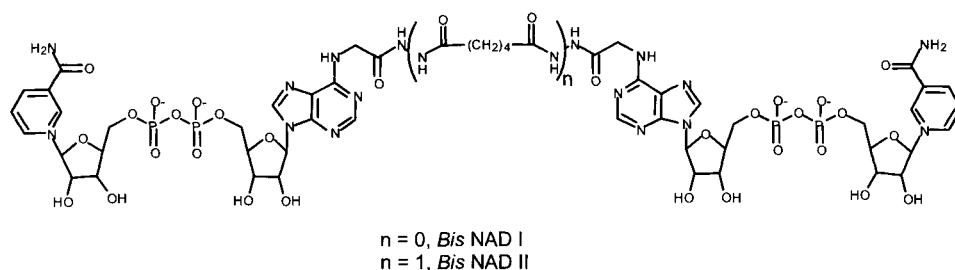
*d*-Camphorsulphonic acid



Mandelic acid

of template molecules with methanol and loaded into a column. A racemic mixture of *dl*-camphorsulphonic acid passed through the column produced fractions enriched in *l*-camphorsulphonic acid with 30% ee on a single pass. The authors also completed experiments with mandelic acid imprinted gels, although the chiral resolution was not as efficient as with camphorsulphonic acid.

Other results involving liquid chromatography separations with imprinted metal oxides have been published in recent years. Norrlöw *et al.* prepared surface imprinted silica gels functionalised with boronic acids that could form covalent linkages with riboses *via* boronate ester formation [43]. The gels were imprinted with templates containing two (nicotinamide adenine dinucleotide (NAD)) or four ribose units (bis-NAD I, bis-NAD II). Columns were packed with the imprinted



gels and HPLC studies performed in aqueous buffered solutions. Table 8.6 shows the HPLC retention volumes of the nucleotide substrates to the imprinted gels. Remarkable recognition properties that discriminated between *bis*-NAD I and *bis*-NAD II substrates, differing only by 10 Å in their separation of the two NAD residues, were observed. Also, the NAD substrate, containing just two riboses, exhibited highest affinity to NAD imprinted gels. The *bis*-NAD substrates gave overall higher affinities to the boronate-functionalised gels compared to NAD, owing to the larger number of ribose units.

Selective chromatography materials were, however, unsuccessfully prepared in a report where phenanthrene and dibenzamide were used as templates. Kaiser and Andersson prepared gels following the procedures of Morihara to create molecular “footprints” in alumina thin films on silica particles or using azomethane to form a thin carbon film surrounding adsorbed template on the silica surface [44]. On either anhydrous or wet surfaces the imprinted gels did not exhibit any preferential affinity for the template molecule. A number of possible reasons could be given for the unsuccessful imprinting. Some examples include poor affinity of the polyaromatic compound for silica gel, making it a poor template for the matrix to form around [20,25], distinct differences between adsorption sites on silica and alumina surfaces that may complicate comparisons and the gel drying procedures, which may have been inadequate for efficient molecular imprinting.

TABLE 8.6

RETENTION VOLUMES OF NUCLEOTIDE SUBSTRATES TO IMPRINTED METAL OXIDE GELS<sup>a</sup>

| Imprint molecule | Substrate   |             |                |                 |
|------------------|-------------|-------------|----------------|-----------------|
|                  | dATP (mL)   | NAD (mL)    | bis-NAD I (mL) | bis-NAD II (mL) |
| dATP             | <b>0.58</b> | 1.05        | 4.10           | 4.45            |
| NAD              | 0.58        | <b>1.40</b> | 4.38           | 5.15            |
| bis-NAD I        | 0.58        | 0.77        | <b>4.03</b>    | 1.93            |
| bis-NAD II       | 0.58        | 0.77        | 1.82           | <b>4.27</b>     |

<sup>a</sup>Data from [43].

Imprinted metal oxides can also be effective as gas separation membranes. Raman and Brinker, in an effort to find alternatives to perm-selective organic polymer gas separation membranes, looked to metal oxide sol-gel materials with their tailorable porosity [45]. These chemically robust materials should improve performance by minimising effects from membrane swelling and material degradation. A template approach appeared promising since porosity could be simply controlled by varying the concentration of template in the gel or by altering the template structure. The membranes were prepared by dip-coating an alumina mesh in a sol containing a mixture of methyltriethoxysilane (MTES) and TEOS. Drying and heating of the membranes collapses the gel structure and further calcination at 550°C pyrolyses the methyl template, creating pores in the gel (Fig. 8.13). The resultant network of pores produces a highly selective gas membrane that can achieve  $\text{CO}_2/\text{CH}_4$  separation factors as high as 12.2, with  $\text{CO}_2$  permeance several orders of magnitude higher than the best organic polymer membranes.

#### 8.3.4. Catalysis

With the addition of a catalytic centre, an imprinted recognition site can be transformed into an enzyme mimetic material offering substrate selective catalysis. Over the past decade a few research groups have studied catalytic effects of imprinted metal oxides in esterification reactions. In this section a brief overview will be given on their efforts to understand the catalytic selectivity and structure of the active site. For additional reading an excellent review can be found by Davis *et al.* [46].

The first use of imprinted metal oxides for catalysis was performed by Morihara *et al.* in the late 1980s [47,48]. Substrate selective catalytic sites for the esterification of anhydrides were prepared using an alumina sol-gel technique formed on silica gel. Template molecules, present during the final stages of alumina gel formation, are thought to leave footprint-like impressions on the gel surface after subsequent

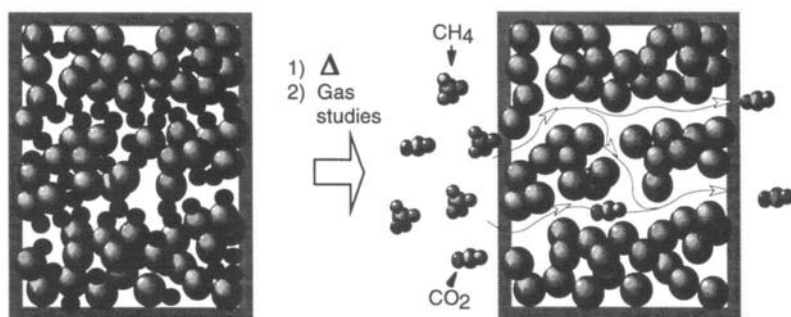


Fig. 8.13. Tailored porosity in MTES/TEOS sol-gel materials using the methyl group as a template. Calcination of the gel removes the methyl groups (black balls on left side of figure) generating porosity for selective permeation of  $\text{CO}_2$  from a  $\text{CO}_2/\text{CH}_4$  gas mixture. Adapted from [45].



removal. The materials are aptly termed “footprint” catalysts. The alumina serves as the imprintable matrix as well as providing the Lewis acid centres for catalysis. Benzenesulphonamide templates were initially used to create receptors with tetrahedral geometry at the active site to efficiently activate the transition state intermediate for nucleophilic reaction.

Catalytic behaviour of the footprint materials followed Michaelis–Menten kinetics, yielding a Michaelis constant  $K_m$  and catalytic rate constant  $k_{cat}$  for each imprinted matrix. The value of  $K_m$  characterises the interaction of the enzyme with the substrate, similar to but not equal to dissociation constants. The constant  $k_{cat}$  is the rate at which the active site converts the substrate to product. Together, the ratio  $k_{cat}/K_m$  is the *enzyme selectivity*, which describes the active site’s efficiency in catalysing a reaction on a particular substrate.

Morihara’s work with benzenesulphonamide templates produced significant improvements in selectivity in catalysing the esterification of benzoic anhydride with various alcohols compared to control materials. The original template and analogues of it also served as competitive inhibitors to the catalytic reaction [49,50]. These experiments showed conclusively that the active site is the sulphonamide imprinted site. Additionally, active sites could be prepared with various analogues of the benzene sulphonamide templates showing various catalytic properties in the esterification reaction. Inhibition studies with these materials clearly display the molecular imprinting effect, i.e. the best inhibitors with the highest inhibition constant  $K_i$  were the original template molecules. Table 8.7 shows a sample of these inhibition studies with the data expressed as the free energy of binding  $RT\ln(1/K_i)$ .

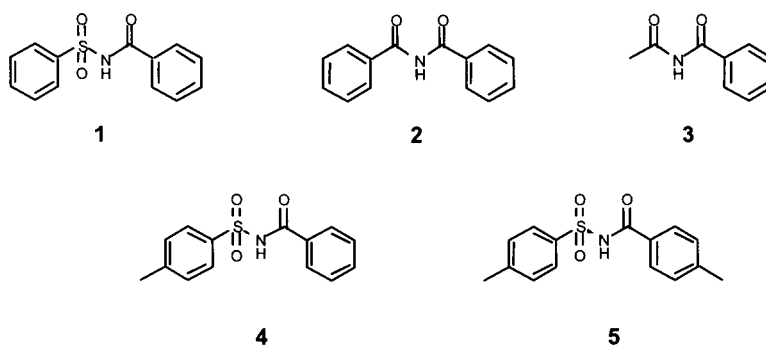
Subsequent studies by Morihara’s group established that it was possible to obtain chiral selective catalysts as well [51,52]. Enantioselective esterification was observed for amino acid derivatives and chiral amines.

TABLE 8.7

SUBSTRATE INHIBITION OF FOOTPRINT GELS IN ESTERIFICATION OF BENZOIC ANHYDRIDE<sup>a</sup>

| $-AG = RT\ln(1/K_i)/kJ$ |             |             |             |     |             |
|-------------------------|-------------|-------------|-------------|-----|-------------|
| Footprint molecule      | 1           | 2           | 3           | 4   | 5           |
| <b>1</b>                | <b>23.9</b> | 20.5        | 8.0         |     |             |
| <b>2</b>                | 22.6        | <b>22.6</b> | 8.4         |     |             |
| <b>3</b>                | 9.2         | 8.4         | <b>13.0</b> |     |             |
| <b>4</b>                | 2.9         | 2.9         | <b>21.3</b> | 4.6 |             |
| <b>5</b>                | 4.2         | 0.0         | 4.2         |     | <b>18.8</b> |

<sup>a</sup>1-Butanolysis reaction performed with benzoic anhydride at 55°C in 1-butanol/benzene (3:7 v/v) mixture. Kinetic parameters of  $k_{cat}$ ,  $K_m$ , and  $K_i$  were obtained from Lineweaver–Burke plots. Data from [50].



The footprint catalysts' improvement in enzymatic selectivity ( $k_{\text{cat}}/K_{\text{m}}$ ) were typically two to four times greater than the controls. However,  $k_{\text{cat}}$  was considerably lower in the imprinted materials compared to the controls. The source of the enhancement in catalytic selectivity was from  $K_{\text{m}}$ , the affinity of the imprinted site for specific substrates. Through a series of studies, Morihara's group found that the Lewis acid centre at the benzenesulphonamide imprinted site was located over a  $\text{sp}^2$  carbonyl group, not at the  $\text{sp}^3$  sulphonamide as expected [53]. This allowed the imprinted site to bind early on in the reaction pathway and have high affinity for reactant molecules. The group was able to achieve higher  $k_{\text{cat}}$  values using a phosphonamide derivative as a template that centres the Lewis acid over the  $\text{sp}^3$  site. By pushing the activated imprinted site to favourably bind the transition state,  $k_{\text{cat}}$  increases of an order of magnitude were realised, together with improvement of  $k_{\text{cat}}/K_{\text{m}}$  of almost 30-fold. Figure 8.14 illustrates the differences in the imprinted sites using sulphonamide and phosphonamide templates.

A similar approach was later used by Heilmann and Maier in their effort to prepare active sites for transesterifications and lactonisations in silica gels [54,55]. The researchers prepared phosphonate-silane templates and used them as transition state analogues (TSA) to imprint tetrahedral geometry at the active centre in the imprinted receptor. The templates were mixed in a sol containing a 100-fold excess of TEOS and the gelation catalysed with HCl. Following drying for several days at room temperature the gel was heated to 250°C to remove the template. Transesterification studies, at 130–140°C, on materials imprinted with (6) exhibited selective reactivity for ethyl-2-phenylethanoate with sterically smaller alcohols, octanol or hexanol, compared to the bulkier phenylethanol. Furthermore, competition studies that compared reactivity of naphthyl to phenyl carboxylates showed a higher selectivity for the phenyl compound. Control materials showed no catalytic activity.

In a continuation of their work, however, Heilmann and Maier found that their "imprinted" silica gels exhibited selective transesterification and lactonisation that was no better than control materials containing phosphoric acid [55]. In fact, the catalytic activity could be removed by rinsing the gel in water. The TSA apparently turns into phosphoric acid during the high temperature treatment and then remains on the gel as a Brönsted acid catalyst (Fig. 8.15). The enhancement of selectivity

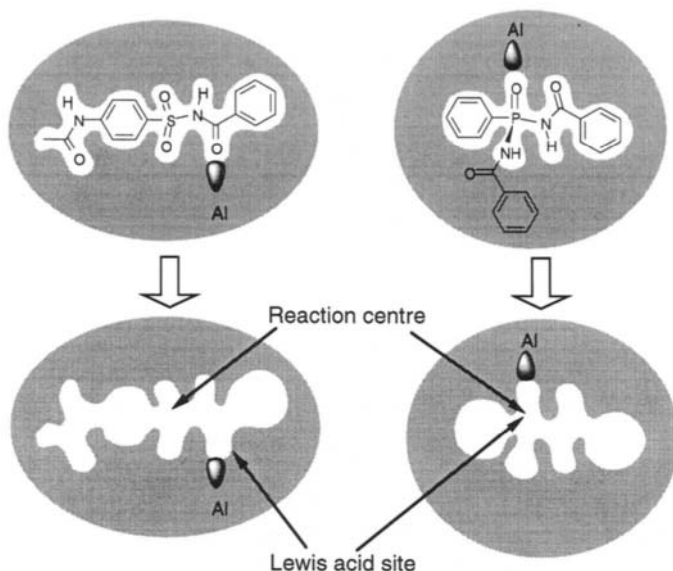


Fig. 8.14. Footprint catalysts prepared with sulphonamide and phosphonamide templates. Both generate tetrahedral reactions centres but differ in the placement of the Lewis acid reactive centre resulting in large differences in catalytic rate. Adapted from [49].

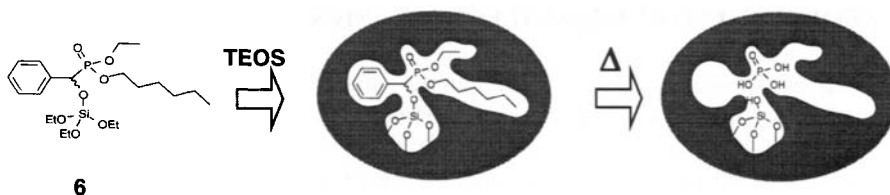


Fig. 8.15. Heilmann and Maier attempted to generate tetrahedral reactive centres for catalytic reaction, however, calcination of the material left behind phosphoric acid that complicated results. Parts adapted from [54].

observed with certain reactions was attributed to the presence of the micropores in the sol-gel materials.

Soon after publication of these reports, Ahmad and Davis attempted to reproduce Heilmann and Maier's initial transesterifications and found that their imprinted materials were considerably weaker in catalytic activity than originally reported [56]. Additionally, selectivities between phenyl and naphthyl carboxylates, as discussed earlier, were not observed. Solid state  $^{31}\text{P}$  NMR detected phosphate in the gel at different bound states to the matrix. The phosphoric acid, which slowly leaches out of the gel, was identified as the catalyst and the existence of an activated imprinted site was discounted.

These careful studies that identify advances and inadequacies in imprinted materials all help to define the rules for the preparation of effective receptor sites. For Morihara, the alumina matrix provides Lewis acid centres at the imprinted sites, yielding selective catalytic receptors. Thoughtful design of the template molecule can greatly improve enzyme-mimetic performance. For Heilmann and Maier, although the TSA is adequately designed, the phosphoric acid needed for catalytic activity most probably occupies the tetrahedral active site rendering the receptor useless. Improved design of template molecules should yield faster rates and higher selectivity.

A unique method to imprint catalytic sites on the surface of silica particles has recently been introduced by Markowitz *et al.* [57], where trypsin-like selectivity for amide linkages was observed. The researchers used an inverse micellar system as the imprinting medium incorporating a surfactant functionalised with a phenylalanine-2-aminopyridine template at the headgroup position. Gelation of TEOS with amino-, carboxyl-, and imidazole-functionalised silanes in the presence of the micellar solution produced 400–600 nm silica beads that exhibited hydrolytic activity for arginine containing substrates. Three to ten-fold rate enhancements were observed over randomly functionalised gels. The imprinted gels, however, showed an unexpectedly higher selectivity and activity for the substrate having the opposite chirality to the template, revealing some unique host–guest interactions with these micellar imprinted gels.

## 8.4. ZEOLITES AND SUPRAMOLECULAR IMPRINTING

Some important metal oxide materials that have used molecular and supramolecular templates to direct structure formation are the zeolites and related semi-crystalline aluminosilicates. In this section we shall discuss the use of ammonium cations that direct formation of microporous zeolites and finish with some of the possibilities that exist with the use of surfactant systems and molecular aggregates to create mesoporous structure. Excellent books and reviews are suggested for additional reading into the detailed description of the art [58–60]. The intention of this section is to briefly introduce this area and describe the types of materials being produced using various imprinting techniques in metal oxide materials.

Zeolites are crystalline aluminosilicates found in nature and have been prepared synthetically since the 1800s. Their robust structure, porous architecture and internal acidic sites make them excellent sorption materials, ionic exchange materials and catalysts for industrial processes. There are numerous known zeolite structures that have been obtained naturally or prepared synthetically through various routes. In the simplest cases the porous architecture can be altered by exchanging different sized cations into the pores to vary pore diameter or volume.

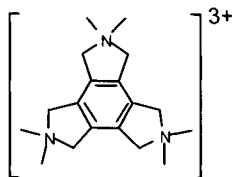
In the search for zeolites with new pore dimensions and channel structure, researchers employed the use of templating molecules to direct the growth of the aluminosilicates. Tetramethylammonium was the first of these templates used to prepare sodalite and others soon followed [61]. Recently, spectroscopic studies have

revealed the intimate contact between the template molecule with the forming aluminosilicate matrix. Cross-polarisation NMR studies by Burkett and Davis showed that the template, at least initially, imprints structural information from itself into the nucleation site of zeolite crystal growth [62,63].

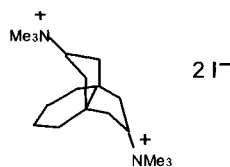
In most cases these molecular templates serve as structure forming guides for the zeolite, but rarely do the materials have molecularly imprinted sites as mentioned in the previous sections. An example of such a rare case is with the triquat cation template 2,3,4,5,6,7,8,9-octahydro-2,2,5,5,8,8-hexamethyl-1H-benzo[1,2-c:3,4-c':5,6-c'']tripyrrylium [64]. The unique crystal structure of the resultant zeolite ZSM-18 contains internal voids that neatly fit the triquat, suggesting that the matrix forms in perfect registry with the template. In a way one could call it molecular imprinting at the highest level. Another example of a unique zeolite with properties tailored through the design of a template is that of SSZ-26 [65,66]. The diammonium-propellane structure of *N,N,N,N',N',N'*-hexamethyl-8,11-[4.3.3.0]dodecane diammonium diiodide templates the formation of multichannel zeolites with intersecting 10- and 12-ring pores.

Supramolecular imprinting involves the use of surfactant aggregates to template the growth of metal oxide materials [67–69]. An important discovery in the zeolite arena was the facile preparation of mesoporous (2–50 nm diameter range) metal oxides called MCM-41 and their various analogues [70,71]. These materials have a highly regular porous structure that looks much like a honeycomb under the transmission electron microscope. The one-dimensional channels are believed to be templated by the hexagonal packed structure of rod-like micelles. Figure 8.16 shows schematically how the supramolecular templating process works for this system. The uniform pore dimensions can be tailored from ~15 Å to greater than 100 Å by altering the length of the trimethylammonium surfactant or by co-addition of small organic molecules that can swell the micelles.

In addition to the one-dimensional templated structure of the MCM-41 materials, two- and three-dimensional systems have also been prepared. A number of papers have used the lamellar structures of amphiphile assemblies to prepare flat, striated metal oxide materials [72,73]. These materials often exhibit enhanced properties over materials that have uncontrolled three-dimensional growth. Vesicles have also been used to engineer spherical imprints into silicates [74,75]. Even more elaborate supramolecular surfactant systems, that yield toroidal and other unusually shaped metal oxides, have also been reported [76,77].



Triquat cation



*N,N,N,N',N',N'*-Hexamethyl-8,11-[4.3.3.0]  
dodecane diammonium

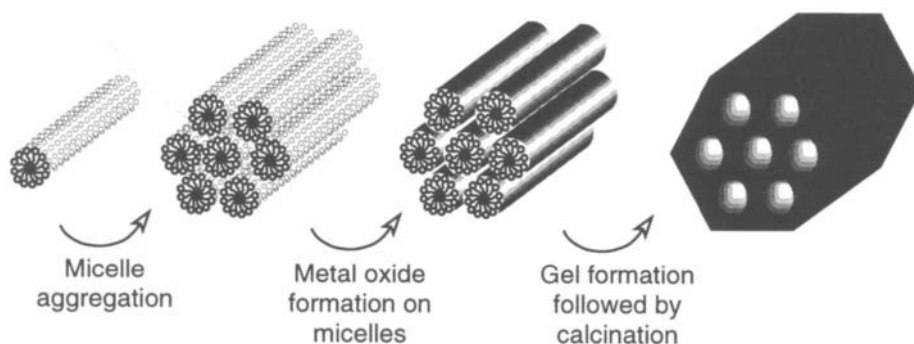


Fig. 8.16. Supramolecular assembly of surfactants to create organised rod-like micelles can template the formation of metal oxides with well defined mesoporous structure, i.e. MCM-41 materials. Adapted from [66].

The zeolite processing temperature of  $\sim 100\text{--}150^\circ\text{C}$  can be contrasted against the room temperature conditions used for typical molecular imprinting in amorphous metal oxide materials. However, in either case, molecules and molecular assemblies are able to influence the formation of the inorganic matrix, creating fascinating structures and, sometimes, with surprisingly accurate registry with the template.

## 8.5. CONCLUSION

Imprinting in metal oxides, whether it be molecular or supramolecular, creates a wide range of materials having numerous potential applications. Over the past 50 years, scientific inquiry into molecular imprinting has generated materials with selective adsorption powers that can readily discriminate between molecules with different structure, chemistry and even stereoisomerism. Imprinted metal oxide materials have demonstrated highly selective molecular affinity in sensors, separations and catalysis experiments. The numerous investigations reviewed in this chapter have each added some insight into the phenomenon of molecular imprinting. Collectively, they have established a foundation of understanding concerning the formation of the molecularly imprinted site, binding of guest molecules to the imprinted receptors and the creation of unusual structures and surface chemistries only possible with metal oxide gels. By coupling into the recent growth of interest in inorganic sol-gel chemistry a new growth of interest in molecular imprinting in inorganic systems can be looked forward to.

## ACKNOWLEDGEMENTS

The author would like to thank Ms Carol Ashley for her helpful discussions and for providing Fig. 8.2, Dr Frere MacNamara for translations and interpretations of

literature and Professor Ken Shea and Dr Todd Alam for their helpful advice in the preparation of this manuscript. Sandia is a multiprogram laboratory operated by Sandia Corporation, a Lockheed Martin Company, for the United States Department of Energy under Contract DE-AC04-94AL85000.

## REFERENCES

- 1 C.J. Brinker, K.D. Keefer, D.W. Schaeffer and C.S. Ashley, *J. Non-Cryst. Solids*, **48**, 47 (1982).
- 2 R.K. Iler (Ed.), *The chemistry of silica*, Wiley, New York (1979).
- 3 C.J. Brinker and G.W. Scherer (Eds), *Sol-gel science*, Academic Press, Inc., San Diego (1990).
- 4 S.S. Prakash, C.J. Brinker, A.J. Hurd and S.M. Rao, *Nature*, **374**, 439 (1995).
- 5 S.T. Reed, C.S. Ashley, C.J. Brinker, R.J. Walko, In: *Sol-gel optics*, R. Ellefson and J. Gill Eds, SPIE Vol. 1328, p. 220 (1990).
- 6 A. Ulman (Ed.), *An introduction to ultrathin organic films. From Langmuir-Blodgett to self-assembly*, Academic Press, Inc., San Diego (1991).
- 7 I. Tabushi, K. Kurihara, K. Naka, K. Yamamura and H. Hatakeyama, *Tet. Lett.*, **28**, 4299 (1987).
- 8 K. Yamamura, H. Hatakeyama, K. Naka, I. Tabushi and K. Kurihara, *J. Chem. Soc. Chem. Comm.*, 79 (1988).
- 9 L.I. Andersson, C.F. Mandenius and K. Mosbach, *Tet. Lett.*, **29**, 5437 (1988).
- 10 J.-H. Kim, T.M. Cotton and R.A. Uphaus, *J. Phys. Chem.*, **92**, 5575 (1988).
- 11 K.M.R. Kallury, M. Thompson, C.P. Tripp and M.L. Hair, *Langmuir*, **8**, 947 (1992).
- 12 N.F. Starodub, S.A. Piletsky, N.V. Lavryk and A.V. El'skaya, *Sens. Actuator. B*, **13-14**, 708 (1993).
- 13 R. Binnes, A. Gedanken and S. Margel, *Tet. Lett.*, **35**, 1285 (1994).
- 14 N. Kodakari, N. Katada and M. Niwa, *J. Chem. Soc., Chem. Commun.*, 623 (1995).
- 15 N. Kodakari, N. Katada and M. Niwa, *Chem. Vap. Deposition*, **3**, 59 (1997).
- 16 S. Singh, D.Y. Sasaki, J. Cesarano III and A.J. Hurd, *Thin Solid Films*, **339**, 209 (1999).
- 17 S.-W. Lee, I. Ichinose and T. Kunitake, *Langmuir*, **14**, 2857 (1998).
- 18 R. Makote and M.M. Collinson, *Chem. Comm.*, 425 (1998).
- 19 F.H. Dickey, *Proc. Nat. Acad. Sci.*, **35**, 227 (1949).
- 20 F.H. Dickey, *J. Phys. Chem.*, **59**, 695 (1955).
- 21 S.A. Bernhard, *J. Am. Chem. Soc.*, **74**, 4946 (1952).
- 22 J.L. Morrison, M. Worsley, D.R. Shaw and G.W. Hodgson, *Can. J. Chem.*, **37**, 1986 (1959).
- 23 R.G. Haldeman and P.H. Emmett, *J. Phys. Chem.*, **59**, 1034 (1955).
- 24 G.H. Reed and L.B. Rogers, *Anal. Chem.*, **37**, 861 (1965).
- 25 L.R. Snyder, *J. Phys. Chem.*, **67**, 2622 (1963).
- 26 H. Erlenmeyer and H. Bartels, *Helv. Chim. Acta*, **47**, 1285 (1964).
- 27 R. Curti and U. Colombo, *J. Am. Chem. Soc.*, **74**, 3961 (1952).
- 28 R. Curti and U. Colombo, *Gazz. Chim. Ital.*, **82**, 491 (1952).
- 29 H. Bartels, B. Prijs and H. Erlenmeyer, *Helv. Chim. Acta*, **49**, 1621 (1966).
- 30 A.H. Beckett and P. Anderson, *Nature*, **179**, 1074 (1957).
- 31 R.E. Majors and L.B. Rogers, *Anal. Chem.*, **41**, 1052 (1969).
- 32 R.E. Majors and L.B. Rogers, *Anal. Chem.*, **41**, 1058 (1969).
- 33 C. Pinel, P. Loislil and P. Gallezot, *Adv. Mater.*, **9**, 582 (1997).
- 34 S. Dai, Y.S. Shin, L.M. Toth and C.E. Barnes, *J. Phys. Chem.*, **101**, 5521 (1997).
- 35 M.F. Lulka, J.P. Chambers, E.R. Valdes, R.G. Thompson and J.J. Valdes, *Anal. Lett.*, **30**, 2301 (1997).

- 36 M. Glad, O. Norrlöw, B. Sellergren, N. Siegbahn and K. Mosbach, *J. Chromatogr.*, **347**, 11 (1985).
- 37 G. Wulff, B. Heide and G. Helfmeier, *J. Am. Chem. Soc.*, **108**, 1089 (1986).
- 38 D.Y. Sasaki, D.J. Rush, C.E. Daitch, T.M. Alam, R.A. Assink, C.S. Ashley, C.J. Brinker and K.J. Shea, In: *Molecular and ionic recognition with imprinted polymers*, R.A. Bartsch and M. Maeda Eds, American Chemical Society, Washington DC, p. 314 (1998).
- 39 D.Y. Sasaki, T.M. Alam and R.A. Assink, *Chem. Mater.*, **12**, 1400 (2000).
- 40 A. Katz and M.E. Davis, *Nature*, **403**, 286 (2000).
- 41 S. Dai, M.C. Burleigh, Y. Shin, C.C. Morrow, C.E. Barnes and Z. Xue, *Angew. Chem. Int. Ed.*, **38**, 1235 (1999).
- 42 B. Boury, R.J.P. Corriu, V.L. Strat and P. Delord, *New J. Chem.*, **23**, 531 (1999).
- 43 O. Norrlöw, M.-O. Månsson and K. Mosbach, *J. Chromatogr.*, **396**, 374 (1987).
- 44 G.G. Kaiser and J.T. Andersson, *Fresenius J. Anal. Chem.*, **342**, 834 (1992).
- 45 N.K. Raman and C.J. Brinker, *J. Membr. Sci.*, **105**, 273 (1995).
- 46 M.E. Davis, A. Katz and W.R. Ahmad, *Chem. Mater.*, **8**, 1820 (1996).
- 47 K. Morihara, S. Kurihara and J. Suzuki, *Bull. Chem. Soc. Jpn.*, **61**, 3991 (1988).
- 48 K. Morihara, E. Tanaka, Y. Takeuchi, K. Miyazaki and N. Yamamoto, *Bull. Chem. Soc. Jpn.*, **62**, 499 (1989).
- 49 K. Morihara, E. Nishihata, M. Kojima and S. Miyake, *Bull. Chem. Soc. Jpn.*, **61**, 3999 (1988).
- 50 T. Shimada, K. Nakanishi and K. Morihara, *Bull. Chem. Soc. Jpn.*, **65**, 954 (1992).
- 51 K. Morihara, M. Kurokawa, Y. Kamata and T. Shimada, *J. Chem. Soc., Chem. Comm.*, 358 (1992).
- 52 K. Morihara, M. Takiguchi and T. Shimada, *Bull. Chem. Soc. Jpn.*, **67**, 1078 (1994).
- 53 T. Shimada, R. Kurazono and K. Morihara, *Bull. Chem. Soc. Jpn.*, **66**, 836 (1993).
- 54 J. Heilmann and W.F. Maier, *Angew. Chem. Int. Ed. Engl.*, **33**, 471 (1994).
- 55 J. Heilmann and W.F. Maier, *Zeit. Natur. B Chem. Sci.*, **50**, 460 (1995).
- 56 W.R. Ahmad and M.E. Davis, *Cat. Lett.*, **40**, 109 (1996).
- 57 M.A. Markowitz, P.R. Kust, G. Deng, P.E. Schoen, J.S. Dordick, D.S. Clark and B.P. Gaber, *Langmuir*, **16**, 1759 (2000).
- 58 R.M. Barrer (Ed.), *Zeolites and clay minerals as sorbents and molecular sieves*, Academic Press Inc., New York (1978).
- 59 M.E. Davis and R.F. Lobo, *Chem. Mater.*, **4**, 756 (1992).
- 60 D.W. Breck (Ed.), *Zeolite molecular sieves: structure, chemistry, and use*, Wiley and Sons, New York (1974).
- 61 R.M. Barrer and P.J. Denny, *J. Chem. Soc.*, 971 (1961).
- 62 S.L. Burkett and M.E. Davis, *Chem. Mater.*, **7**, 920 (1995).
- 63 S.L. Burkett and M.E. Davis, *Chem. Mater.*, **7**, 1453 (1995).
- 64 S.L. Lawton and W.J. Rohrbaugh, *Science*, **247**, 1319 (1990).
- 65 S.I. Zones, M.M. Olmstead and D.S. Santilli, *J. Am. Chem. Soc.*, **114**, 4195 (1992).
- 66 R.F. Lobo, M. Pan, I. Chan, H.-X. Li, R.C. Medrud, S.I. Zones, P.A. Crozier and M.E. Davis, *Science*, **262**, 1543 (1993).
- 67 N.K. Raman, M.T. Anderson and C.J. Brinker, *Chem. Mater.*, **8**, 1682 (1996).
- 68 J.S. Beck, J.C. Vartuli, G.J. Kennedy, C.T. Kresge, W.J. Roth and S.E. Schramm, *Chem. Mater.*, **6**, 1816 (1994).
- 69 Q. Huo, D.I. Margolese and G.D. Stucky, *Chem. Mater.*, **8**, 1147 (1996).
- 70 C.T. Kresge, M.E. Leonowicz, W.J. Roth, J.C. Vartuli and J.S. Beck, *Nature*, **359**, 710 (1992).
- 71 J.S. Beck, J.C. Vartuli, W.J. Roth, M.E. Leonowicz, C.T. Kresge, K.D. Schmitt, C.T.-W. Chu, D.H. Olson, E.W. Sheppard, S.B. McCullen, J.B. Higgins and J.L. Schlenker, *J. Am. Chem. Soc.*, **114**, 10,834 (1992).
- 72 K. Sakata and T. Kunitake, *J. Chem. Soc., Chem. Commun.*, 504 (1990).
- 73 A. Sellinger, P.M. Weiss, A. Nguyen, Y. Lu, R.A. Assink, W. Gong and C.J. Brinker, *Nature*, **394**, 256 (1998).



- 74 S. Oliver, A. Kuperman, N. Coombs, A. Lough and G.A. Ozin, *Nature*, **378**, 47 (1995).
- 75 P.T. Tanev and T.J. Pinnavaia, *Science*, **271**, 1267 (1996).
- 76 H. Yang, N. Coombs and G.A. Ozin, *Nature*, **386**, 692 (1997).
- 77 I.A. Aksay, M. Trau, S. Manne, I. Honma, N. Yao, L. Zhou, P. Fenter, P.M. Eisenberger and S.M. Gruner, *Science*, **273**, 892 (1996).

## Imprinting polymerisation for recognition and separation of metal ions

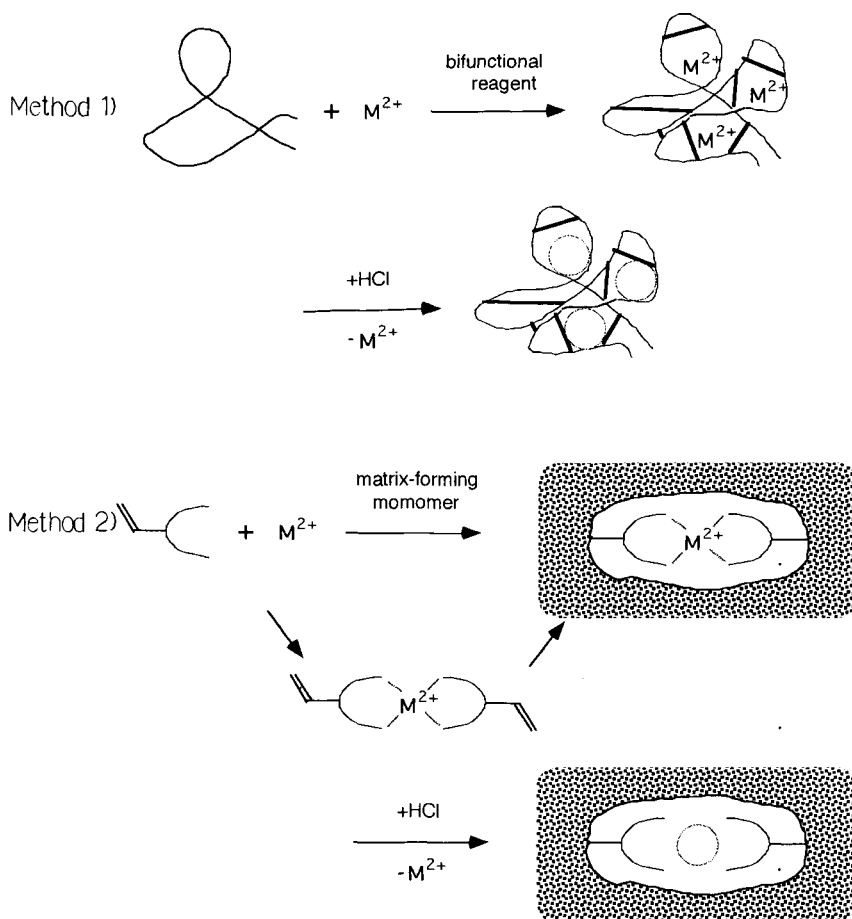
KAZUHIKO TSUKAGOSHI, MASA HARU MURATA AND MIZUO MAEDA

### 9.1. INTRODUCTION

The technique of molecular imprinting [1] has attracted much attention as a method to prepare highly-selective host polymers. The technique basically consists of three steps; (i) synthesis of functional vinyl monomers that can interact with a target template, (ii) free radical polymerisation of the vinyl monomers with cross-linking reagents in the presence of the template and (iii) removal of the template from the cross-linked copolymer resin. This method has been demonstrated to be effective for metal ions, saccharides, amino acid derivatives and other organic compounds of low molecular weight. Nishide *et al.* reported the first example of metal ion-imprinted resins [2,3], which could adsorb the guest metal ion selectively from a weakly acidic solution. This feature is in remarkable contrast with that of conventional metal-chelating resins, which are usually designed for use in more acidic solutions [4]. Kabanov *et al.* also developed adsorbents selective to metal ions by the imprinting polymerisation and characterised them by spectrometric analysis [5]. Since their successful work, various metal ions have been examined as imprinted guests, including Cu(II), Zn(II), Ni(II), Co(II), Cd(II), Fe(III), Hg(II), Ca(II), *etc.* The imprinted resins can readily and efficiently achieve the separation, recovery and purification of valuable metal ions in a variety of matrices. In this chapter, we will review imprinting polymerisation for the recognition and separation of metal ions.

### 9.2. SURVEY OF PREPARATION METHODS OF METAL ION-IMPRINTED RESINS

Early metal ion-imprinted resins may be roughly classified into the following two types, depending on their preparation procedures (Scheme 9.1). Method 1: linear chain polymers carrying metal-binding groups are cross-linked with a bifunctional reagent in the presence of metal ions. Method 2: metal ion-complexing monomers are prepared and polymerised with matrix-forming monomers in the presence of the metal ion. As a more sophisticated way of carrying out Method 2, specific metal ion complexes from ligands having vinyl groups were prepared, isolated and then polymerised with matrix-forming monomers.



Scheme 9.1. Techniques for the preparation of metal ion-imprinted resin.

Although both of these imprinting techniques were certainly successful ways to prepare metal ion-selective adsorbents, they have some fundamental problems in common. The preparations were mainly based on solution polymerisation or bulk polymerisation techniques, so that the imprinted structures were usually formed in the resultant bulk resins. This raised some problems such as (i) grinding and sieving is necessary before use, (ii) partial destruction of the imprinted structures is inevitable in the grinding process, (iii) residual guest in the resin is possible and (iv) handling of water-soluble organic molecules of biological importance as guests (target molecules) is difficult.

A drastic improvement in the imprinting technique was thus demanded to solve these problems. A third category of metal ion imprinting was recently proposed. The imprinting was conducted on an aqueous-organic interface (surface imprinting). Surface imprinting has been achieved using several approaches: seed emulsion

polymerisation, oil/water (O/W) emulsion polymerisation and water/oil (W/O) emulsion polymerisation.

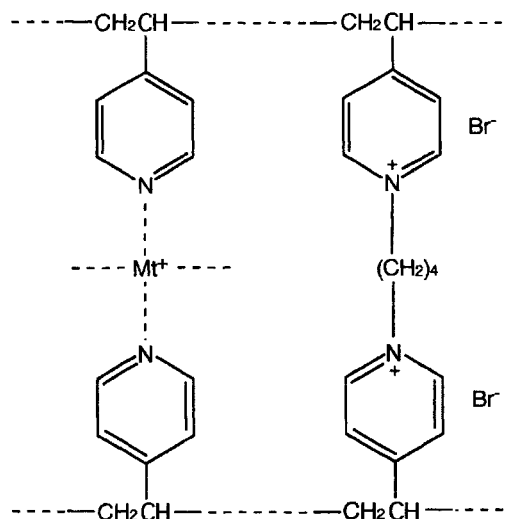
### 9.3. EARLY STUDIES ON METAL ION-IMPRINTING

#### 9.3.1. Method 1 in Scheme 9.1

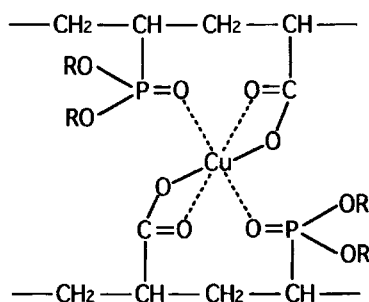
As a typical example of Method 1, Nishide *et al.* cross-linked poly(4-vinylpyridine) (PVP) with 1,4-dibromobutane (DB) in the presence of metal ions as templates [2-4]. The adsorption behaviour of Cu(II), Co(II), Zn(II), Ni(II), Hg(II) and Cd(II) on the obtained resins was studied. The resins preferentially adsorbed the metal ion which had been used as template. PVP was cross-linked by alkylation of pyridine groups in PVP with DB to yield insoluble PVP resins, of which free pyridines were utilised to coordinate metal ions (Scheme 9.2). The stability constant of the Cu(II) complex of the resin was largest for the resin prepared with Cu(II) as template, being due to its large entropy change for the complexation.

Kabanov *et al.* cross-linked a copolymer of diethyl vinylphosphonate and acrylic acid with *N,N'*-methylene diacrylamide in the presence of metal ions [5,6]. Scheme 9.3 illustrates the possible coordination of Cu(II) with the functional groups of the adsorbent. The obtained resins were characterised by IR and  $^1\text{H}$ -NMR spectroscopy, in addition to the metal adsorption test.

Ohga *et al.* cross-linked chitosan with epichlorohydrin to give an imprinted resin [7]. The obtained resin was utilised in column chromatography for separating metal ions. The column packed with a Cd(II)-imprinted resin could separate Cd(II),



Scheme 9.2. Interaction between metal ions and PVP.



Scheme 9.3. Interaction between Cu(II) and a polymer of diethyl vinylphosphonate and acrylic acid.

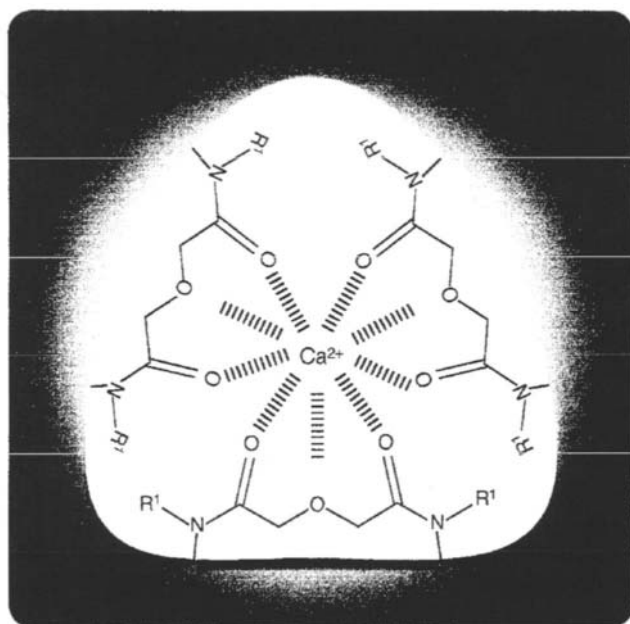
Cu(II) and Hg(II). This separation was achieved with 95–100% recovery by using a small column ( $8.0 \times 0.4$  cm i.d.). In addition, almost identical chromatograms were obtained when the metal ions were loaded into the column again after complete washing with deionised water, indicating an effective durability in repeated use.

### 9.3.2. Method 2 in Scheme 9.1

The first example for Method 2 was reported by Nishide and co-workers, who polymerised a metal complex of 1-vinylimidazole with 1-vinyl-2-pyrrolidone and divinylbenzene [8]. The metal–vinylimidazole complex was copolymerised, cross-linked with 1-vinyl-2-pyrrolidone by  $\gamma$ -ray irradiation and the template metal ion was removed by treating the polymer complex with an acid. These poly(vinylimidazole) (PVI) resins adsorbed metal ions more effectively than the PVI resin prepared without the template. The number of adsorption sites and the stability constant of the Ni(II) complex were larger for the PVI resin prepared with the Ni(II) template, as seen by the smaller dissociation rate constant of Ni(II) from the resin.

Poly(4-methyl-4'-vinyl-2,2'-bipyridine) has been prepared by Gupta *et al.*, as have various copolymers with divinylbenzene [9]. When polymerisation was carried out in the presence of metal ions, a metal-containing copolymer was obtained which, when the metal ion was removed with acid, retained some memory of the original metal ion.

Rosatzin *et al.* copolymerised *N,N'*-dimethyl-*N,N'*-bis(4-vinylphenyl)-3-oxapentanediamide (a metal ionophore), divinylbenzene and styrene in a chloroform solution in the presence of Ca(II) or Mg(II) [10]. The Ca(II) ionophore resin is illustrated in Scheme 9.4. The metal ion added to the matrix mixture, was expected to act as a template for the ionophore during the polymerisation. The resulting polymers were analysed for their ability to extract ions from aqueous methanol. The polymers prepared against Ca(II) and Mg(II) were found to bind Ca(II) with 6- and 1.7-times lower dissociation constants, respectively, when

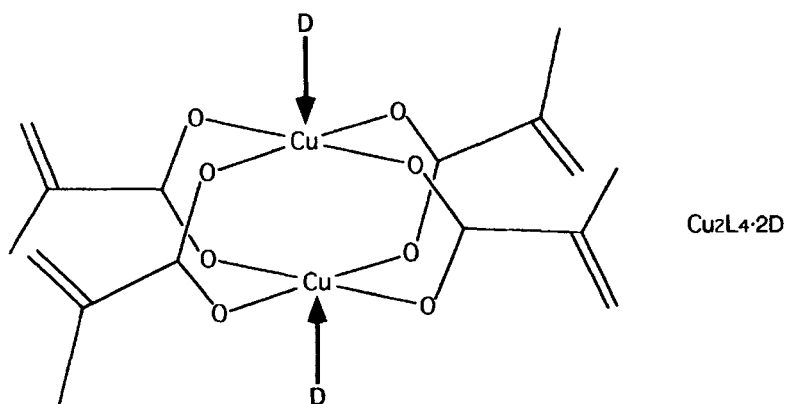


Scheme 9.4. Ca(II) ionophore prepared in resin matrix.

compared with reference polymers prepared in the absence of metal ions. The increased binding strength was attributed to the spatial arrangement of ionophore units in the resulting polymers by the template ions during the polymerisation. In addition, the number of binding sites for Ca(II) which was determined for the respective polymer preparation agreed well with theoretical values calculated based on the stoichiometry of complexation of the ionophore with Ca(II) and Mg(II), respectively.

In the above resin preparations, polymerisation was carried out without previously isolating the relevant monomer complexes. As a more sophisticated way of carrying out Method 2, specific metal ion complexes were prepared from ligands having vinyl groups and polymerised with matrix-forming monomers. For example, Kuchen *et al.* synthesised and isolated a metal ion-methacrylic acid complex and polymerised it with ethylene glycol dimethacrylate in a benzene/methanol solution [11]. The Cu(II)-methacrylic acid complex is shown in Scheme 9.5; D = H<sub>2</sub>O, pyridine or 4-vinylpyridine. The Cu(II)-imprinted resins exhibit an increased effective capacity for Cu(II) about 4-times larger than that of non-imprinted resins. The addition of 4-vinylpyridine made the stereospecific configuration more rigid through axial coordination to the Cu(II)-complex. The rigid configuration may lead to the improved adsorption capacity.

The following researchers also reported metal ion imprinting. Fujii *et al.* prepared a metal ion complex of 2-acetyl-5-(*p*-vinylbenzyloxy)phenol, and



Scheme 9.5. Cu(II)-acrylic acid complex. D = H<sub>2</sub>O, pyridine, or 4-vinylpyridine.

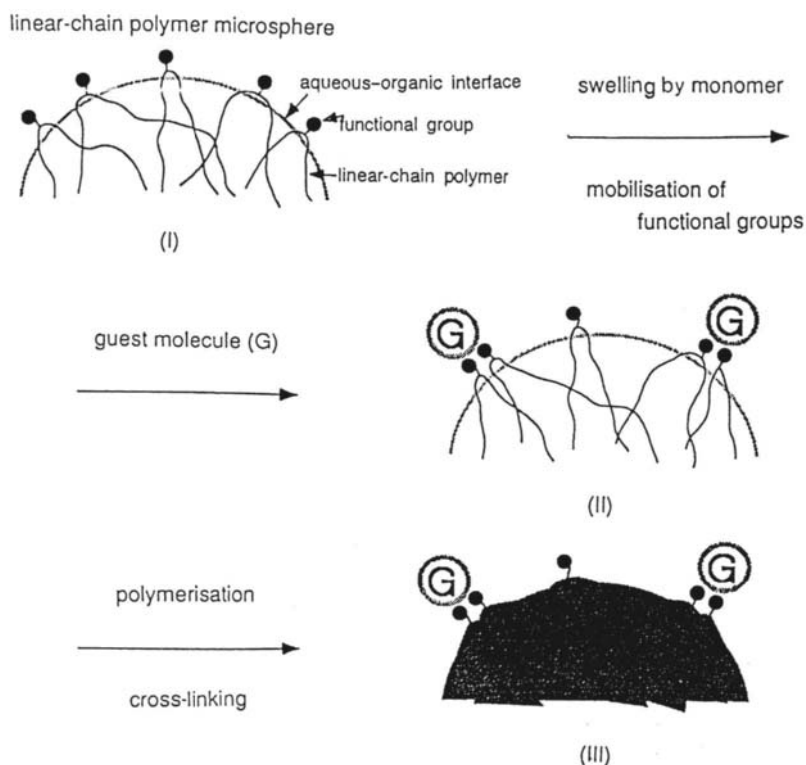
polymerised it with acrylamide and ethylene glycol dimethacrylate [12]. Isobe and co-workers used Amberlite XAD-2 as a matrix resin and a 4-vinylpyridine-metal ion complex was introduced to the resin through polymerisation [13].

#### 9.4. METAL ION-IMPRINTED MICROSPHERES PREPARED BY REORGANISATION OF COORDINATING GROUPS ON A SURFACE

##### 9.4.1. The concept of surface imprinting by the use of seed emulsion polymerisation

In 1992, Takagi's group proposed a new imprinting technique, 'surface imprinting', to solve the problems associated with conventional imprinting techniques. In this technique, an aqueous-organic interface in an emulsified resin suspension (latex) was used as a guest-recognition matrix in imprinting polymerisation. In this section, surface imprinting by the use of seed emulsion polymerisation will be described, i.e. an imprinted structure is introduced on the surface of a microsphere prepared by seed emulsion polymerisation [14–18].

The concept of this technique is shown in Scheme 9.6. First, a seed microsphere emulsion is prepared. The microspheres consist of linear-chain polymers carrying the functional groups which can interact with the target molecule (I). Divinyl-type monomers are then added to the emulsion, so that the seed microspheres become swollen and the polymer chains are provided with substantial mobility. When guest molecules are introduced into the emulsion, the functional groups interact with the guest molecules at the aqueous-organic interface to form complexes (II). The structures thus obtained are immobilised by the subsequent cross-linking polymerisation of the divinyl-type monomers (III). This is followed by removal of guest molecules from the microspheres to give imprinted host structures. The concept of this technique was embodied in 1992 for metal ion guests as described below.



Scheme 9.6. Concept of surface imprinting by use of seed emulsion polymerisation.

#### 9.4.2. Preparation and physicochemical characterisation of the microspheres

Metal ion-imprinted microspheres were prepared as follows [14,15]. Seed emulsion was obtained by the polymerisation of styrene, butyl acrylate and methacrylic acid in water. Divinylbenzene, butyl acrylate and water were further added to the polymerisation mixture (seed emulsion) and the emulsion was left for a defined time so that the seed microspheres became swollen. The emulsion was combined with a metal ion solution to achieve complexation between the metal ion and the carboxyl group on the surface. Then the divinylbenzene-containing emulsion was polymerised by the use of  $\gamma$ -rays at room temperature. The microspheres obtained by centrifugation were washed with a hydrochloric acid solution to remove the metal ion. The microspheres obtained were then dried under vacuum. Non-imprinted microspheres (as a reference) were synthesised similarly, but without a metal ion.

Cu(II)-, Ni(II)-, Co(II)-imprinted microspheres and the non-imprinted microspheres were obtained in 85–90% yield. Analysis was made for their chemical composition and particle size distributions. The elemental analyses were in good



agreement with the chemical composition of the feed mixture. Particle form and size distribution were measured by FE-SEM. The microspheres had submicron dimensions and assumed a neat spherical shape. These results were consistent with those of the particle grading analyses.

#### 9.4.3. Metal adsorption behaviour of the microspheres

The metal adsorption behaviour of the non-imprinted and Cu(II)-, Ni(II)- and Co(II)-imprinted microspheres was examined at pH 5.6 [15]. The adsorption was expressed as the percentage of metal ions adsorbed on the resin with respect to the total amount of metal ions originally added to the solution (Table 9.1).

First of all, Cu(II) was most effectively adsorbed by Cu(II)-imprinted microspheres, followed by non-imprinted, Ni(II)-imprinted and Co(II)-imprinted microspheres. This sequence clearly verified the effect of Cu(II) imprinting; the carboxylate groups and the polymer chains that carry them are placed on the Cu(II)-imprinted microsphere surface in such a way that they match the square planar coordination around the Cu(II) ion.

As for Ni(II) adsorption, only Cu(II)- and Ni(II)-imprinted microspheres exhibited a binding affinity under the described adsorption conditions; the adsorption was higher for Ni(II)-imprinted microspheres (17%) than for Cu(II)-imprinted microspheres (7%). This, again, clearly indicated the effect of imprinting.

The Ni(II)-imprinted microspheres were characterised by the Ni(II) binding affinity, which exceeded the affinity to the Cu(II)-imprinted microsphere. This was in contrast to the Irving–Williams series. In order to confirm this surprising result, a Ni(II)-imprinted microsphere was prepared in duplicate and it was found that the two preparations gave almost identical results; preparation 1, 14% for Cu(II) and 17% for Ni(II); preparation 2, 13% for Cu(II) and 18% for Ni(II). It is emphasised that the results all came from the difference in the spatial disposition of the

TABLE 9.1

PERCENTAGE ADSORPTION OF SINGLE METAL ION SPECIES ONTO NON-IMPRINTED AND METAL ION-IMPRINTED MICROSPHERES<sup>a,b</sup>

| Imprinted ion | Adsorption (%) |        |        |
|---------------|----------------|--------|--------|
|               | Cu(II)         | Ni(II) | Co(II) |
| None          | 24             | 0      | 0      |
| Cu(II)        | 40             | 7      | 0      |
| Ni(II)        | 14             | 17     | 0      |
| Co(I)         | 5              | 0      | 0      |

<sup>a</sup>Conditions: pH 5.6; 0.050 g of microspheres; 1.0 mL of  $5.0 \times 10^{-4}$  M metal ion solution; shaking time, 18 h.

<sup>b</sup>For 3–5 samples, the standard deviation was  $\pm 2\%$ .

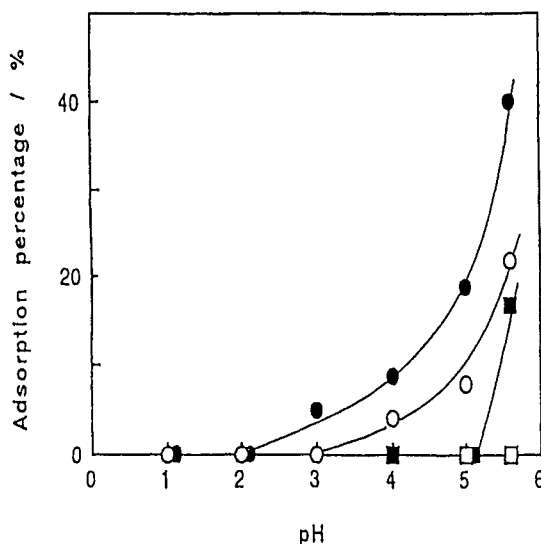


Fig. 9.1. Metal ion adsorption onto non-imprinted and metal ion-imprinted microspheres. Effect of the pH. Solid circles: adsorption of Cu(II) onto Cu(II)-imprinted microsphere, open circles: adsorption of Cu(II) onto non-imprinted microsphere, solid squares adsorption of Ni(II) onto Ni(II)-imprinted microsphere, open squares: adsorption of Ni(II) onto non-imprinted microsphere. Conditions: 0.05 g microspheres, 0.1 cm<sup>3</sup> metal ion solution ( $5.0 \times 10^{-4}$  mol/dm<sup>3</sup> metal ion) and 12–18 h shaking time.

carboxylato groups, which are fixed on the microsphere surface by cross-linked divinylbenzene.

Figure 9.1 shows the pH dependence of the metal-ion adsorption onto Cu(II)- and Ni(II)-imprinted microspheres and non-imprinted microspheres. Imprinted microspheres adsorbed the corresponding imprinted metal ions more effectively than did the non-imprinted microspheres over the entire pH range where metal ion adsorption took place. In all cases, the adsorption percentages increased with increasing pH. This means that the carboxyl groups on the microsphere surface participated in the metal-ion binding in their ionised carboxylate forms.

#### 9.4.4. FT-IR and ESR studies on Cu(II)-loaded microspheres

Takagi's group also examined the origin of the imprinting effect through FT-IR and ESR [17]. Three types of Cu(II)-loaded microspheres were prepared and named Sample 1, 2, and 3 in the following way. Non-imprinted, as well as Cu(II)-imprinted microspheres (0.15 g) were added to a Cu(II) solution to make the Cu(II)-loaded microspheres. They were named Sample 1 and 2, respectively. In addition, Cu(II)-loaded microspheres, II in Scheme 9.6, were separated from the second-step polymerisation mixture by simple centrifugation. The obtained microspheres were dried under vacuum and named Sample 3.

First, the amount of Cu(II) carried by the microsphere samples was estimated for Samples 1–3. This was determined by measuring the concentration of free Cu(II) in the aqueous solution at adsorption equilibrium: Sample 1,  $1.5 \times 10^{-6}$  mol g<sup>-1</sup>; Sample 2,  $5.7 \times 10^{-6}$  mol g<sup>-1</sup>; Sample 3,  $1.4 \times 10^{-4}$  mol g<sup>-1</sup>.

The preparation of the microspheres followed the recipe by Okubo *et al.* [19]. Therefore, the amount of carboxyl groups in the microspheres was expected to be similar to that of Okubo's microspheres. It was assumed that the total amount of surface carboxyl groups in the microspheres would be  $2.2 \times 10^{-4}$  mol g<sup>-1</sup>, according to Okubo's report, and that each Cu(II) ion would be coordinated by two carboxylate groups. Then, the mole fraction of carboxyl groups bound to Cu(II) with respect to the total surface carboxyl groups in the Cu(II)-loaded microspheres was to be as follows: Sample 1, 1/70; Sample 2, 1/20; Sample 3, 1/1. It is noted that all the carboxyl groups on the surface of Sample 3 seem to be complexed with Cu(II).

The FT-IR spectrum of Sample 3 is shown in Fig. 9.2 as an example. When the absorption band intensity of acrylic butyl ester at 1730 cm<sup>-1</sup> was taken as standard (normalised intensity, 1.0), then the absorption band intensities for dimeric carboxyl group at 1705 cm<sup>-1</sup> and carboxylate anion at 1601 cm<sup>-1</sup> were, respectively, found to be as follows: Sample 1, 0.41 and 0.52; Sample 2, 0.41 and 0.54; Sample 3, 0.31 and 0.62. The values for Sample 1 and 2 were very similar to those of microspheres which were not loaded with Cu(II) (0.41 and 0.52). In fact, for Samples 1 and 2, the fraction of Cu(II)-bound carboxylate groups with respect to the total number of carboxyl groups in the microspheres was calculated to be about 1/120 and 1/30, respectively. This small value could be the reason why the change in absorption intensity at 1705 and 1601 cm<sup>-1</sup> was not observed for Sample 1 and 2. On the other hand, almost all of the surface carboxyl groups in Sample 3 were proposed to engage in Cu(II) adsorption; the band intensity for dimeric carboxyl decreased and that of carboxylate increased. This means that carboxyl groups on the microsphere surface participate in Cu(II) binding in their ionised carboxylate forms [17].

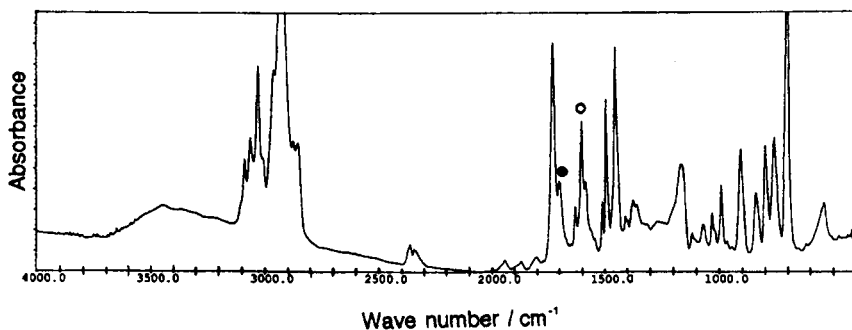


Fig. 9.2. FT-IR spectra of Cu(II)-loaded microsphere. The open circle mark is for absorption of carboxylate group and the solid circle for dimeric carboxyl group. Sample 3.

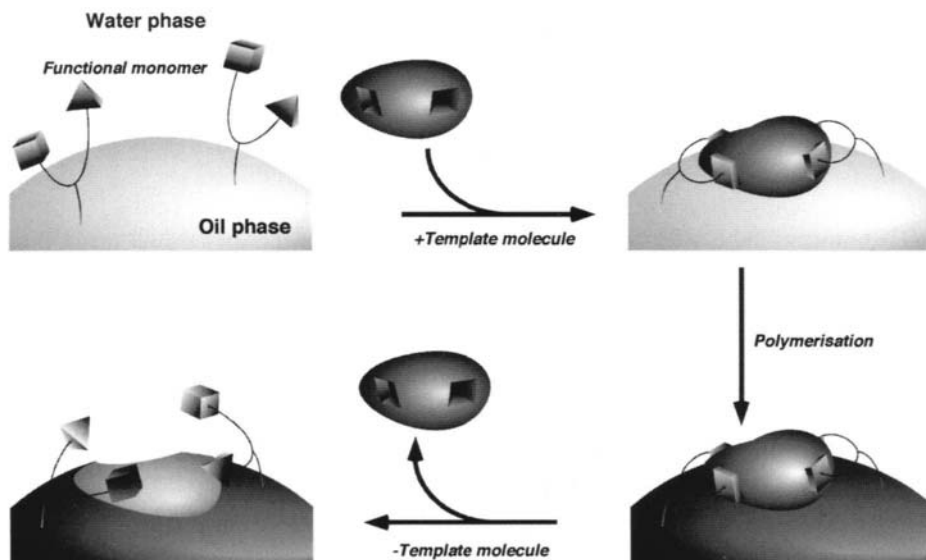
ESR spectra were examined for Samples 1–3 [17]. As these spectra suffer from considerable noise due to the small sample volume of Cu(II),  $g//$  and  $A//$  values could not be determined clearly. However, all spectra indicated a pattern characteristic for a square-planar Cu(II) complex carrying four coordinating oxygen atoms [20,21].

Cu(II) spectral intensities for Samples 1–3 were in the order of Sample 3 > Sample 2 > Sample 1. Although ESR spectrometry in general is semi-quantitative in nature, the order of the spectral intensity was consistent with the amount of Cu(II) on the microspheres as determined by the Cu(II) adsorption study. The imprinting effect or an enhanced Cu(II) adsorption behaviour as indicated by the metal adsorption test is in a sense indirect, because it only shows the decrease in Cu(II) concentration in a test solution. Meanwhile, the presented ESR spectra directly indicated such an enhanced Cu(II) adsorption and complex chemical structure of the adsorbed Cu(II) species in the Cu(II)-imprinted microspheres.

## 9.5. METAL ION-IMPRINTED RESINS PREPARED BY O/W EMULSION POLYMERISATION

### 9.5.1. Surface imprinting by use of O/W emulsion

In this section, surface imprinting which is carried out in O/W emulsion will be reviewed [22–26]. Maeda *et al.* presented the concept of the technique as illustrated in Scheme 9.7. This technique relies on a cooperative interaction of multiple func-



Scheme 9.7. Concept of surface imprinting by use of O/W emulsion polymerisation.

tional groups with a target: the approach involves the pre-organisation of functional surfactants (amphiphilic host monomers) on an O/W emulsion surface by cooperative interactions with the target (template guest) in the aqueous phase. The organised structure involving the template and the functional surfactants is then immobilised by polymerisation of the oil phase, which is made up of a vinyl monomer. Removal of the template results in polymeric resins which carry the functional groups spatially arranged on their surface, giving recognition sites with preferential rebinding ability for the template molecule.

### **9.5.2. Potassium oleate and dioleoyl hydrogen phosphate as functional monomers**

The preliminary example of the surface imprinting by an O/W emulsion polymerisation was carried out using potassium oleate as an amphiphilic coordinating monomer, divinylbenzene as a resin matrix-forming monomer and Cu(II) as a target metal [22,23]. The template effect was demonstrated by the highly-effective binding of the Cu(II)-imprinted resin to Cu(II) as compared with that of a reference (non-imprinted) one. This novel imprinting method was extended to the preparation of organophosphate-carrying resins by using dioleoyl hydrogen phosphate as an amphiphilic host, in the presence of, or in the absence of, Cu(II) or Zn(II) [21]. As a result, the Cu(II)-imprinted resin adsorbed Cu(II) much more effectively than did the non-imprinted one, while the Zn(II)-imprinted one showed an adsorption ability for Cu(II) as small as the non-imprinted one, indicating the dependence of selectivity on the template.

### **9.5.3. Metal ion-imprinted resins by O/W emulsion polymerisation**

Surface imprinting in O/W emulsion was carried out with three different metal ions, Cu(II), Zn(II) and Cd(II), as the template guests [25,26]. The host surfactant employed was oleyl phenyl hydrogen phosphate, while sodium dodecyl sulphate (SDS) was used as a co-surfactant to stabilise the emulsion during the imprinting polymerisation.

Table 9.2 shows the preparation conditions for the imprinted resins. First, the Cu(II)-binding behaviour of the resins was examined. The resins of Cu(II)-imprinted (0.5) and Cu(II)-imprinted (1.0) adsorbed their own template ion (i.e. Cu(II)) much more effectively than did the other resins, i.e. Zn(II)-imprinted, Cd(II)-imprinted or non-imprinted. In particular, the Cu(II)-imprinted (1.0) resin, which was prepared using 1 g of SDS as a co-surfactant, showed a pronounced rebinding of Cu(II) in the entire concentration range investigated. In addition, adsorptivity of Cu(II) to the Cu(II)-imprinted (1.0) resin was much better than that to the Cu(II)-imprinted (0.5) resin. Conversely, Cu(II)-imprinted (2.0), which was prepared using 2 g of SDS, showed a much lower binding ability to Cu(II). The reason for this bell-shaped dependency on the amount of SDS is not clear. However, these results suggest that the surface structure of the resin was influenced by the addition of SDS during the polymerisation. A more quantitative way to evaluate the complexation abilities of these chelating resins is to plot the average

TABLE 9.2

PREPARATION CONDITIONS OF THE TEMPLATED RESINS<sup>a</sup>

| Polymer code        | Template | SDS/g (mmol) |
|---------------------|----------|--------------|
| Non-imprinted (0.5) | none     | 0.5 (1.7)    |
| Cu-imprinted (0.5)  | Cu(II)   | 0.5 (1.7)    |
| Zn-imprinted (0.5)  | Zn(II)   | 0.5 (1.7)    |
| Cd-imprinted (0.5)  | Cd(II)   | 0.5 (1.7)    |
| Non-imprinted (1.0) | none     | 1.0 (3.5)    |
| Cu-imprinted (1.0)  | Cu(II)   | 1.0 (3.5)    |
| Zn-imprinted (1.0)  | Zn(II)   | 1.0 (3.5)    |
| Cd-imprinted (1.0)  | Cd(II)   | 1.0 (3.5)    |
| Non-imprinted (2.0) | none     | 2.0 (6.9)    |
| Cu-imprinted (2.0)  | Cu(II)   | 2.0 (6.9)    |
| Zn-imprinted (2.0)  | Zn(II)   | 2.0 (6.9)    |
| Cd-imprinted (2.0)  | Cd(II)   | 2.0 (6.9)    |

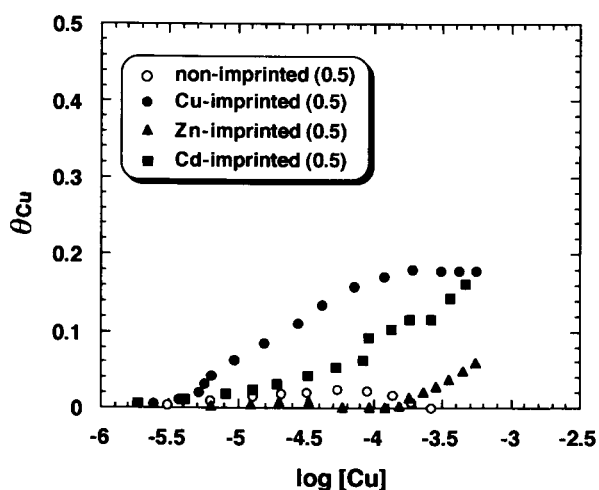
<sup>a</sup>Total aqueous solution, 40 cm<sup>3</sup>; divinylbenzene, 20 cm<sup>3</sup>; functional monomer, 0.4 g (1.0 mmol).

number of bound metal ions per phosphate group ( $\theta_M$ ), which is calculated using the equation

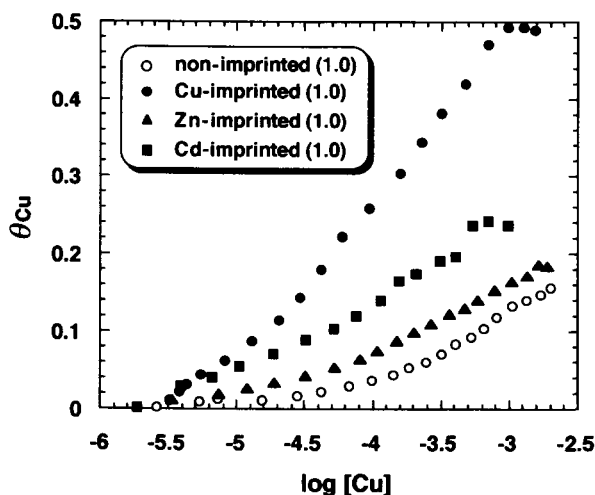
$$\theta_M = (n_M)_{\text{bound}}/n_{\text{ex}} = (C_M - [M]) \times V/n_{\text{ex}}$$

M means Cu(II) or Cd(II) and  $(n_M)_{\text{bound}}$  indicates the amount of bound metal ions (calculated by  $(C_M - [M])$  multiplied by the total solution volume ( $V$ ; dm<sup>3</sup>);  $C_M$ , initial metal ion concentration and  $[M]$ , metal ion concentration at adsorption equilibrium) and  $n_{\text{ex}}$  is the amount of phosphate groups in the resin (mol) as calculated from the amount originally fed to the emulsion. Figure 9.3 shows the Cu(II)-binding isotherms obtained using Cu(II)-imprinted (0.5) and Cu(II)(1.0) resins. The two Cu(II)-imprinted resins (Cu-imprinted(0.5) and Cu-imprinted(1.0)) showed maximum preferential Cu(II) binding compared to the other resins over the entire [Cu-(II)] region. In both resins, the maximum value of  $\theta_M$  is in the order Cu(II)-imprinted > Cd(II)-imprinted > Zn(II)-imprinted > non-imprinted resins. In particular, the maximum  $\theta_M$  value for Cu-imprinted (1.0) reached almost 0.5. Assuming that the binding mode was due to a 2:1 complex (phosphate: Cu(II)), almost all the phosphate groups used in the polymerisation functioned as preferential Cu(II)-binding sites on the resin surface.

The Cd(II)-binding isotherms for the Cd(II)-imprinted(0.5) and Cd(II)-imprinted(1.0) resins are shown in Fig. 9.4. As expected, Cd(II)-imprinted(0.5) and Cd-imprinted(1.0) resins prepared in the presence of Cd(II) were clearly shown to



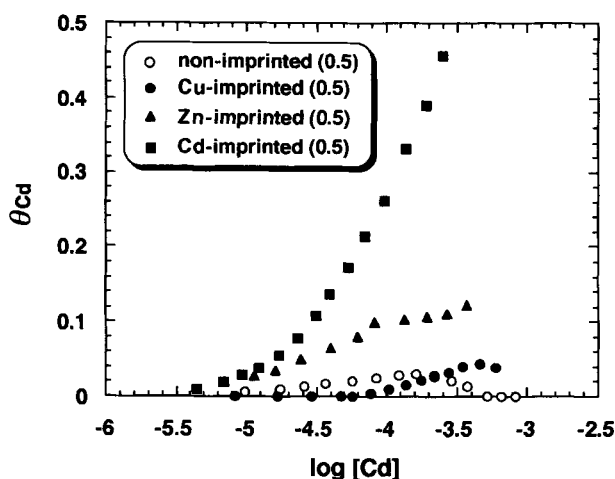
a) SDS 0.5g



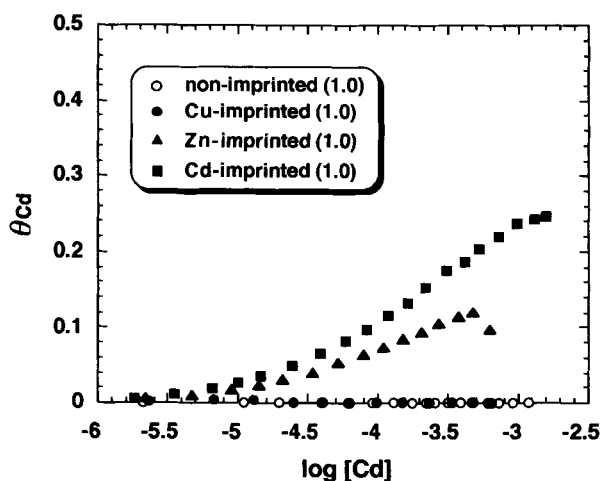
b) SDS 1.0 g

Fig. 9.3. Cu(II)-binding isotherms for the resins: (a) SDS as a co-surfactant, 0.5 g. (b) SDS, 1.0 g. Open circles, non-imprinted resin; solid circles, Cu(II)-imprinted resin; solid triangles, Zn(II)-imprinted resin; solid squares, Cd(II)-imprinted resin. Conditions; 0.5 g of resin and  $C_{\text{KNO}_3} = 0.1 \text{ mM}$ , at  $25^\circ\text{C}$  for a potentiometric titration.

adsorb Cd(II) much more effectively than did the other resins. In contrast to this, Cu(II)-imprinted(0.5) and Cu(II)-imprinted(1.0) did not adsorb any significant amount of Cd(II). These results clearly indicated that the metal-binding sites were formed differently on each resin. The oleyl phenyl hydrogen phosphate moieties are



a) SDS 0.5g



b) SDS 1.0 g

Fig. 9.4. Cd(II)-binding isotherms for the resins: (a) SDS as a co-surfactant, 0.5 g. (b) SDS, 1.0 g. Open circles, non-imprinted resin; solid circles, Cu(II)-imprinted resin; solid triangles, Zn(II)-imprinted resin; solid squares, Cd(II)-imprinted resin. Conditions; 0.5 g of resin and  $C_{\text{KNO}_3} = 0.1 \text{ mM}$ , at  $25^\circ\text{C}$  for a potentiometric titration.

implanted on the resin surface in such a way that they can match a desirable coordination around the template ion when they interact with the ion. The Cu(II)-, Cd(II)- and Zn(II)-imprinting probably serves to place the phosphate groups in the square planar, tetrahedral and tetrahedral configurations, respectively. From this



viewpoint, it should be noted that the Zn(II)-imprinted resins adsorbed moderate amounts of Cd(II), which has the same coordination configuration as Zn(II) (Fig. 9.4). On the non-imprinted resins, in contrast, oleyl phenyl hydrogen phosphate moieties are randomly distributed on their surface as determined by such conditions as pH, counter ion ( $\text{Na}^+$ ) and co-surfactant (SDS) concentrations. Thus, the non-imprinted resins showed only a small metal-binding ability in all the cases.

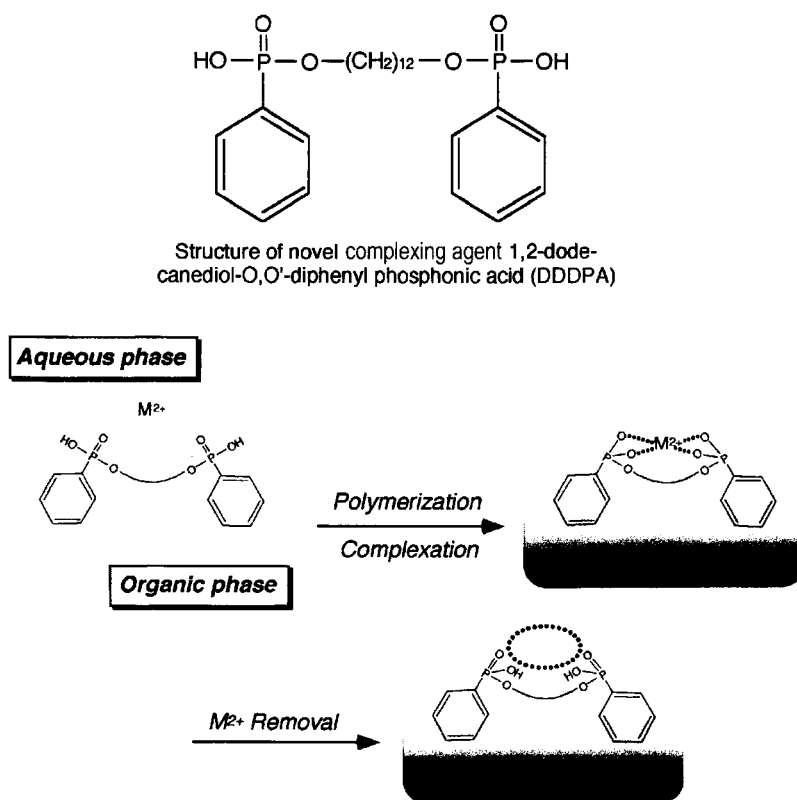
Interestingly, the optimal amount of SDS differed between the Cu(II)- and Cd(II)-imprinted resins with respect to the selectivity: the superior resins were Cu(II)-imprinted(1.0) and Cd(II)-imprinted(0.5), which were prepared using 1 g and 0.5 g of SDS, respectively. This is probably related to the surface activity of oleyl phenyl hydrogen phosphate in the presence of template ions: the addition of a suitable amount of co-surfactant gives a stable emulsion, while an excessive addition would result in the exclusion of the template ion-phosphate complex from the resin surface. In fact, the templated resins which were prepared using 2 g of SDS showed low recovery of template ions after polymerisation when compared with the resins prepared with using 0.5 or 1 g of SDS. For instance, Cu(II) was removed quantitatively (99% recovery) from Cu(II)-imprinted(0.5) resin by washing with a hydrochloric acid solution, whereas the similarly treated Cu(II)-imprinted(2.0) resin gave only 45% of Cu(II) added before polymerisation. This may suggest that the population of accessible phosphate groups on the Cu(II)-imprinted(2.0) resin is smaller than on other resins. Apart from these considerations, the use of SDS as co-surfactant obviously offers a new technical advantage in the preparation of surface imprinting by O/W emulsion.

## **9.6. METAL ION-IMPRINTED RESINS PREPARED BY W/O EMULSION POLYMERISATION**

### **9.6.1. Imprinting polymerisation in W/O emulsion**

1,12-Dodecanediol-*O,O'*-diphenyl phosphonic acid (DDDPA) having two functional groups in the molecular structure was designed as a complexing agent by Nakashio's group for surface imprinting in a W/O emulsion [27–29]. The separation of Zn(II) and Cu(II) with the resins was conducted and the imprinting effect was characterised by comparison of the results from ordinary solvent extraction of the metal ions.

Zn(II) was employed as a print molecule because of its strong interaction with the bifunctional monomer, DDDPA. Divinylbenzene, L-glutamic acid dioleylester ribitol and toluene were used as matrix-forming monomer, emulsion stabiliser and diluent, respectively. After polymerisation, the print molecules were removed from the resin, upon which selective recognition sites were formed. The schematic illustration of surface template polymerisation with DDDPA is shown in Scheme 9.8. The Zn(II)-imprinted resins were ground into particles, whose volume-averaged diameters were *ca.* 40  $\mu\text{m}$ . The yield was *ca.* 80%.



Schematic illustration of surface template polymerization with DDDPA

Scheme 9.8. Concept of surface imprinting by use of W/O emulsion polymerisation and structure of DDDPA.

Figure 9.5 shows the pH dependence of the adsorption of Zn(II) and Cu(II) on the Zn(II)-imprinted resins with DDDPA. The adsorption percentage increased with increasing pH for both ions. The ability of the Zn(II)-imprinted resins to adsorb Zn(II) was high, due to the interfacial activity of DDDPA and the strong interaction between Zn(II) and DDDPA. The Zn(II)-imprinted resins adsorbed Zn(II) much more effectively than Cu(II) over the entire pH range. It was surprising that Zn(II) and Cu(II) were completely separated in the vicinity of pH 3. The high selectivity was considered to be produced by the Zn(II)-memorised cavity on the surface of the resins.

The pH dependence in liquid-liquid extraction for Zn(II) and Cu(II) using the same extractant DDDPA is shown in Fig. 9.6. In the solvent extraction system, an effective selectivity was not observed compared with that of the imprinted resins. Because the functional monomers (extractants) in the solvent extraction are conformationally mobile, they can take both the tetrahedral configuration for

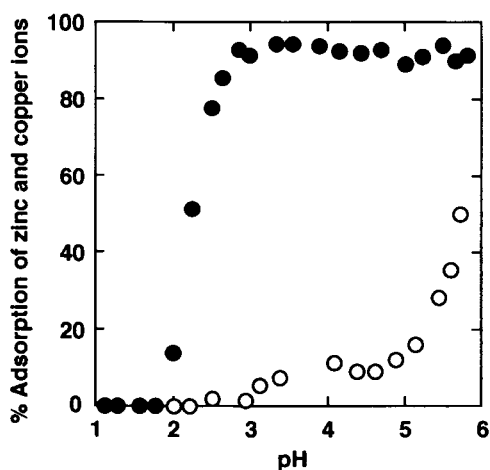


Fig. 9.5. pH dependence of the adsorption of Zn(II) (solid circles) and Cu(II) (open circles) on the Zn(II)-imprinted resin using DDDPA as a functional monomer.

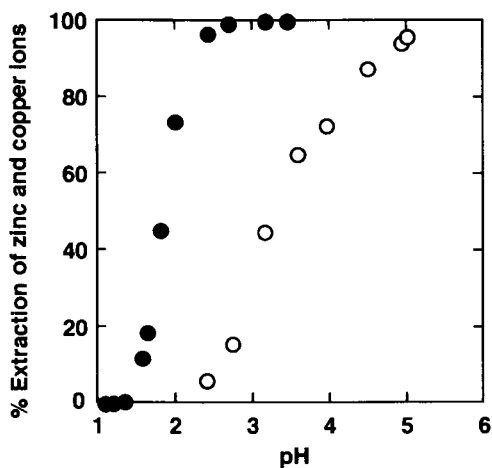


Fig. 9.6. pH dependence in liquid-liquid extraction of Zn(II) (solid circles) and Cu(II) (open circles) using DDDPA.

complexation of Zn(II) and the square planar configuration for complexation of Cu(II). Thus, the selectivity towards the ions only depends on the stability of the complex between the extractants and the ions. In contrast, the functional monomers on the Zn(II)-imprinted resins are fixed in the tetrahedral configuration and therefore the ability to recognise Zn(II) is extremely high.

### 9.6.2. Dioleoyl phosphate (DOLPA) as functional monomer with $\gamma$ -ray irradiation

$\gamma$ -rays were used to make the polymer matrices rigid and to allow the functional monomer to attach firmly to the matrices [29].

Figure 9.7 shows the pH dependence of the competitive adsorption of Zn(II) and Cu(II) on Zn(II)-imprinted resins which were irradiated with  $\gamma$ -rays. DOLPA was used as a functional monomer. No difference was observed between non-irradiated and irradiated polymers with respect to their ability for Zn(II) binding. An irradiated blank polymer, which did not include DOLPA, adsorbed no metal ions. These results clearly showed that irradiation with  $\gamma$ -rays did not destroy the Zn(II)-

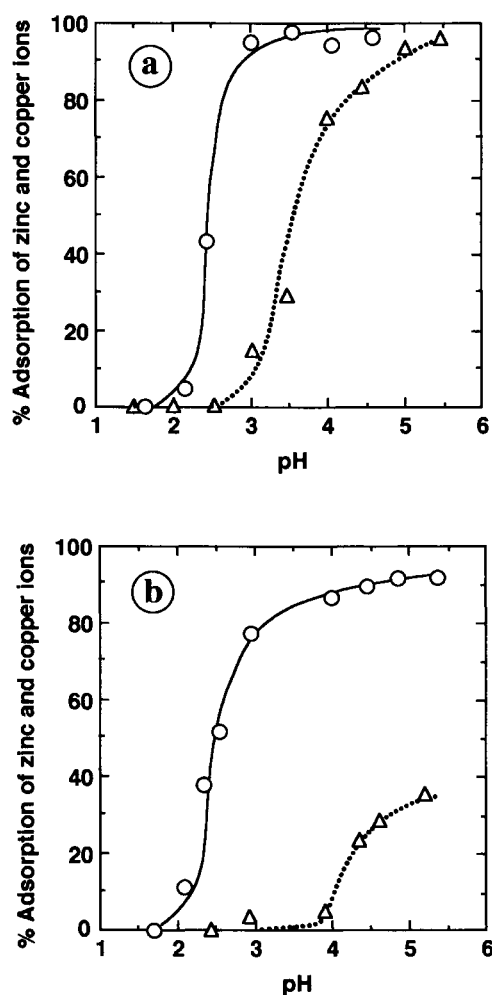


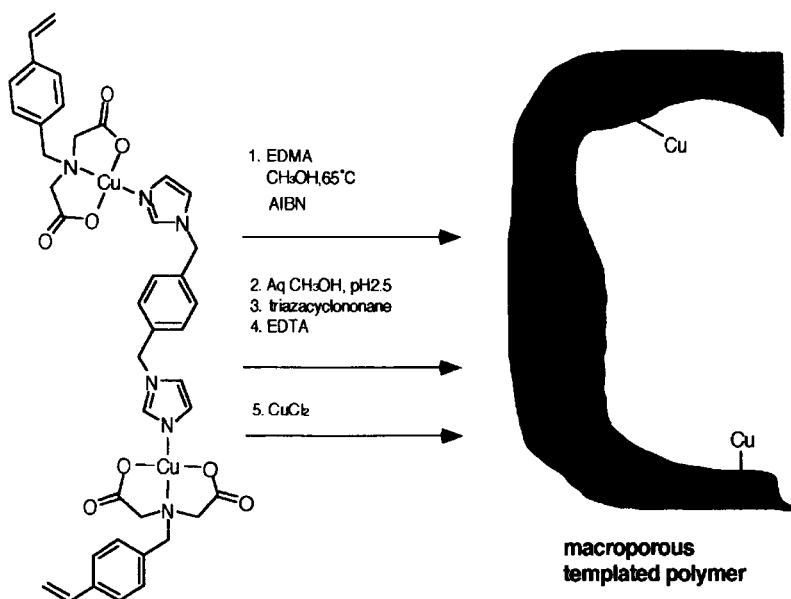
Fig. 9.7. pH dependence of the adsorption of Zn(II) (open circles) and Cu(II) (open triangles) with Zn(II)-imprinted resin (a) before and (b) after  $\gamma$ -ray irradiation.

DOLPA complex and produces few functional groups, such as carbonyl groups, within the range used. In contrast with Zn(II) binding, the Cu(II)-binding ability of irradiated polymers was drastically reduced; irradiated polymers can distinguish the coordination of Zn(II) from that of Cu(II). The improvement in the selectivity was attributed to the induced cross-linking in the polymer matrices by irradiation with  $\gamma$ -rays, which renders the polymer matrices rigid, consequently making the binding sites stable enough to recognise Zn(II). Furthermore, the double bond in the oleyl chains of DOLPA was reduced and DOLPA combined rigidly with the polymer matrices. Therefore,  $\gamma$ -ray irradiation is considered to be a very convenient way for fixing the binding sites for target metal ions.

## 9.7. APPLICATIONS OF METAL ION-IMPRINTED RESINS AND FUTURE ASPECTS

### 9.7.1. Biomimetic applications

Arnold *et al.* reported a novel variation of the metal ion-imprinting technique to synthesise rigid macroporous polymers containing strategically distributed Cu(II)-iminodiacetate complexes (Scheme 9.9) (see also Chapter 6). The resulting polymers exhibited selectivity for bisimidazole ‘protein analogues’ that are not distinguishable by reversed-phase HPLC. They proposed that a very high affinity and selectivity could be achieved in polymer matrices containing metal ions strategically posi-



Scheme 9.9. Cu(II)-iminodiacetate complex in macroporous polymer.

tioned to match the distribution of metal-coordinating groups on the surface of the molecule of interest [30–32].

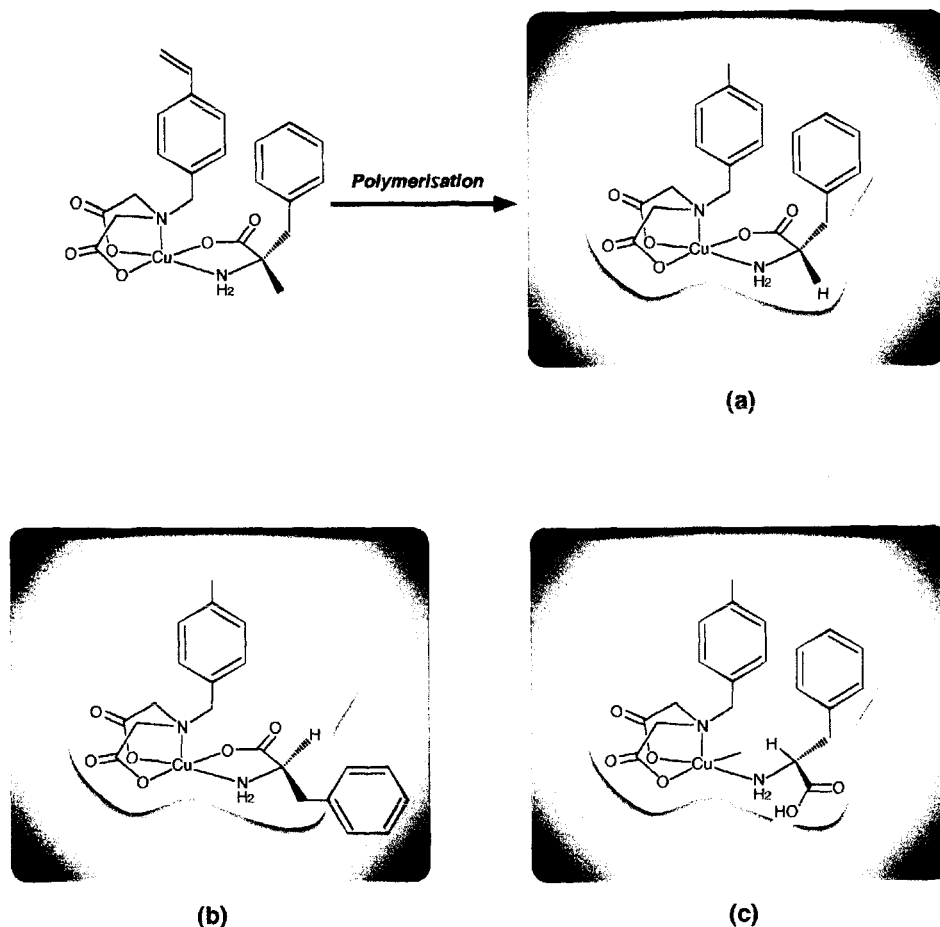
Furthermore, they combined molecular imprinting with the ability of amino acids to chelate metal ions to create ligand-exchange chromatography supports suitable for chiral separations of non-derivatised amino acids [33]. They investigated several aliphatic and aromatic amino acids in order to evaluate the role of the side group in imprinting enantioselectivity. By working with an achiral monomer bearing an iminodiacetate function, they showed that the enantioselectivity of the adsorbent arises from the chirality of the recognition sites created during polymerisation.

Molecular imprinting thus led to chiral recognition through the formation of chirally-selective binding sites. In light of the three-point interaction model, this implies that the polymer stabilised the binding of the template enantiomer and/or destabilised (sterically hindered) binding of the opposite enantiomer. As illustrated in Scheme 9.10, for a polymer templated with L-phenylalanine, rebinding of the L-enantiomer proceeds through chelation of the metal ion, in addition to which the aromatic side chain fits into a cavity that selects for both the size and shape of this group. In contrast, metal chelation by of the D-enantiomer would be sterically hindered. Alternatively, if the side group of the D-amino acid fits into the cavity, only monodentate binding to the metal would be possible.

### 9.7.2. Chemical sensors

Murray and co-workers reported imprinted resins for the selective sequestering and sensing of metal ions [34,35] (see also Chapter 19). This research explored the utilisation of metal ion-imprinted resins as selective sequestering agents and as components of electrochemical and optical sensors. Results from the characterisation of the metal ion templated electrodes for Pb(II) and UO<sub>2</sub>(II) demonstrated a broad linear range of measurement with a near-Nernstian response and a strong preference for the imprinted metal ion over the other metal ions tested. The selectivity coefficients of the Pb(II) selective electrode were systematically evaluated by the separate solution method, the fixed interference method and the matched potential method under various conditions. The life-time of the electrode was relatively long; this was one of the advantages rendered by imprinted resins in which the functional groups were covalently attached to the polymer matrix. An optical sensor based on imprinted resins was employed to determine Pb(II) in the parts per billion range. Rosatzin *et al.* have also reported an ion selective electrode based on metal ion-imprinted resins; details have been described in the above section.

Fish reported that a Zn(II)-imprinted resin, containing a sandwich arrangement of the well known 1,4,7-triazacyclononane (TACN) ligand, was found to be highly selective toward reintroduced Cu(II) in the presence of Fe(III), Co(II), Ni(II), Zn(II) and Mn(II), after the removal of the Zn(II) template with 6 N HCl [36]. The following parameters were addressed: structures of the monomers of the *N*-(4-vinylbenzyl)TACN-Zn(II) complexes, polymerisation parameters, structure of the polymer TACN-template metal ion complex and selectivity to reintroduced metal

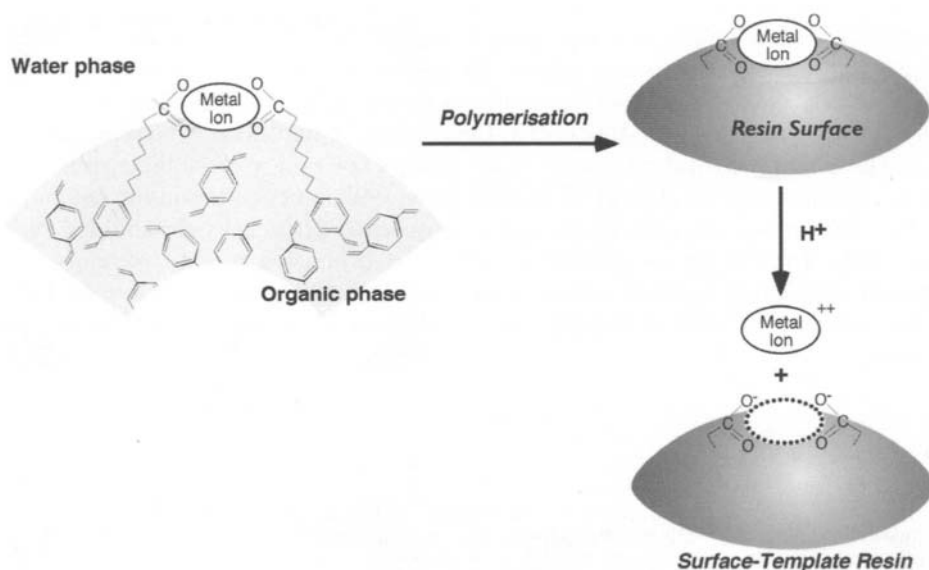


Scheme 9.10. Source of enantioselectivity in imprinted ligand-exchange materials. Molecular imprinting with L-Phe gives a cavity that is selective for L-Phe. (a) The L-isomer can simultaneously chelate to metal ion and fit into the shape-selective cavity. (b) Rebinding of the D-isomer is hindered because chelation of the metal ion by the D-isomer is sterically unfavourable. (c) Alternatively, if the molecule fits into the cavity, it cannot chelate Cu(II).

ions as a function of the thermodynamic stability and the metal ion templating parameters for the polymer TACN–metal ion complexes that were formed.

### 9.7.3. Other techniques using metal ion-imprinting

Another technique was proposed as an efficient method for the preparation of surface-template resins. In surface imprinting, a functional surfactant (emulsifier) that is capable of binding metal ions and functions as a vinyl monomer must orient at the interface between the matrix monomers and water and emulsify the mixture.



Scheme 9.11. Concept of surface imprinting using monomer-type surfactants.

The surfactant should be polymerised with the matrix monomers in the form of a metal complex. In order to make surface imprinting easy and reliable, the monomer-type surfactant 10-(*p*-vinylphenyl)decanoic acid has been prepared and applied to an emulsifier for the preparation of surface-template resins [37]. The preparation of metal-imprinted resins is illustrated in Scheme 9.11.

It was proposed that a polymer bearing functional groups can be quickly 'frozen' as a thin film in the presence of template molecules. Because of the wide surface area in the thin film system, template molecules can be easily extracted from the film surface and the structure of the binding site constructed in the thin film can be easily characterised by various spectroscopic methods. Kobayashi *et al.* reported their idea for the recognition of theophylline [38]. Shinkai *et al.* succeeded in the preparation of porous thin films by casting a specific water-THF solution of poly-(vinyl chloride-co-acrylic acid) and in the spectrophotometric characterisation of the metal ion imprinting and rebinding processes [39]. The results clearly disclosed how the memory is imprinted and how the rebinding takes place on the film surface.

## 9.8. CONCLUSION

Molecular recognition has drawn much attention with regard to separation chemistry. One of the promising approaches to create molecular-recognising materials is the 'molecular imprinting' method, the concept of which was proposed by Wulff *et al.* about 20 years ago. The new methodology does not require a precise



molecular design and multi-step procedures to construct highly-selective resins. Metal-ion imprinted resins can achieve the separation, recovery and purification of valuable metal ions in a variety of matrices readily and efficiently. However, there may be some fundamental drawbacks; for example, complexation between imprint molecules and functional monomers is not always fast and water-soluble substances cannot be employed as imprint molecules. Since 1992, a novel imprinting technique, surface imprinting, has been proposed to conquer the drawbacks of metal ion-selective resins. Imprinting polymerisation will be a promising way to recognise and separate metal ions, together with organic ions like amino acids and proteins. Interesting research is now underway for application to chemical and biomimetic sensors.

## REFERENCES

- 1 G. Wulff, "Polymeric Reagents and Catalysis" (ACS Symp. Ser. 308), W.T. Ford Ed., American Chemical Society, Washington DC, p. 186 (1986).
- 2 H. Nishide, J. Deguchi and E. Tsuchida, *Chem. Lett.*, 169 (1976).
- 3 H. Nishide and E. Tsuchida, *Makromol. Chem.*, **177**, 2295 (1976).
- 4 H. Nishide, J. Deguchi and E. Tsuchida, *J. Polym. Sci., Polym. Chem. Ed.*, **15**, 3023 (1977).
- 5 V.A. Kabanov, A.A. Efendiev and D.D. Orujev, *J. Appl. Polym. Sci.*, **24**, 259 (1979).
- 6 A.A. Efendiev and V.A. Kabanov, *Pure and Appl. Chem.*, **54**, 2077 (1982).
- 7 K. Ohga, Y. Kurauchi and H. Yanase, *Bull. Chem. Soc. Jpn.*, **60**, 444 (1987).
- 8 M. Kato, H. Nishide and E. Tsuchida, *J. Polym. Sci., Polym. Chem. Ed.*, **19**, 1803 (1981).
- 9 S.N. Gupta and D.C. Neckers, *J. Polym. Sci., Polym. Chem. Ed.*, **20**, 1609 (1982).
- 10 T. Rosatzin, L.I. Andersson, W. Simon and K. Mosbach, *J. Chem. Soc. Perkin Trans.*, **2**, 1261 (1991).
- 11 W. Kuchen and J. Schram, *Angew. Chem. Int. Ed. Engl.*, **27**, 1695 (1988).
- 12 Y. Fujii, H. Maie, S. Kumagai and T. Sugai, *Chem. Lett.*, 995 (1992).
- 13 A. Nakashima and T. Isobe, *Memoirs of the Faculty of Science, Kyushu University*, **16**, 33 (1987).
- 14 K.Y. Yu, K. Tsukagoshi, M. Maeda and M. Takagi, *Anal. Sci.*, **8**, 701 (1992).
- 15 K. Tsukagoshi, K.Y. Yu, M. Maeda and M. Takagi, *Bull. Chem. Soc. Jpn.*, **66**, 114 (1993).
- 16 K. Tsukagoshi, K.Y. Yu, M. Maeda and M. Takagi, *Kobunshi Ronbunshu (Japanese Journal of Polymer Science and Technology)*, **50**, 455 (1993).
- 17 K. Tsukagoshi, K.Y. Yu, M. Maeda, M. Takagi and Tohru Miyajima, *Bull. Chem. Soc. Jpn.*, **68**, 3095 (1995).
- 18 K. Tsukagoshi, M. Maeda and M. Takagi, *Bunseki Kagaku*, **45**, 975 (1996).
- 19 M. Okubo, K. Kanada and T. Matsumoto, *J. Appl. Polym. Sci.*, **33**, 1511 (1987).
- 20 T. Watanabe, *Bunseki*, **11**, 742 (1977).
- 21 H. Yokoi, S. Kawata and M. Iwaizumi, *J. Am. Chem. Soc.*, **108**, 3361 (1986).
- 22 H. Kido, K. Tsukagoshi, M. Maeda, M. Takagi and T. Miyajima, *Anal. Sci.*, **8**, 749 (1992).
- 23 H. Kido, H. Sonoda, K. Tsukagoshi, M. Maeda, M. Takagi, H. Maki and T. Miyajima, *Kobunshi Ronbunshu (Japanese Journal of Polymer Science and Technology)*, **50**, 403 (1993).
- 24 M. Maeda, M. Murata, K. Tsukagoshi and M. Takagi, *Anal. Sci.*, **10**, 113 (1994).
- 25 M. Murata, S. Hijiya, M. Maeda and M. Takagi, *Bull. Chem. Soc. Jpn.*, **69**, 637 (1996).

- 26 M. Murata, M. Maeda and M. Takagi, *Anal. Sci. Technol.*, **8**, 529 (1995).
- 27 M. Yoshida, K. Uezu, M. Goto and F. Nakashio, *J. Chem. Eng. Jpn.*, **29**, 174 (1996).
- 28 K. Uezu, H. Nakamura, J. Kanno, T. Sugo, M. Goto and F. Nakashio, *Macromolecules*, **30**, 3888 (1997).
- 29 K. Uezu, H. Nakamura, M. Goto, M. Murata, M. Maeda, M. Takagi and F. Nakashio, *J. Chem. Eng. Jpn.*, **27**, 436 (1994).
- 30 P.K. Dhal and F.H. Arnold, *J. Am. Chem. Soc.*, **113**, 7417 (1991).
- 31 P.K. Dhal and F.H. Arnold, *Macromolecules*, **25**, 7051 (1992).
- 32 S.D. Plunkett and F.H. Arnold, *J. Chromatogr. A.*, **708**, 19 (1997).
- 33 S. Vidyasabkar, M. Ru and F.H. Arnold, *J. Chromatogr. A.*, **775**, 51 (1997).
- 34 X. Zeng, A. Bzhelyansky, S.Y. Bae, A.L. Jenkins and G.M. Murray, In: *Recognition with imprinted polymers*, R.A. Bartsch and M. Maeda Eds, American Chemical Society, Washington DC, Chapt. 15 (1998).
- 35 X. Zeng and G.M. Murray, *Separation Sci. Technol.*, **31**, 2403 (1996).
- 36 R.H. Fish, In: *Recognition with imprinted polymers*, R.A. Bartsch and M. Maeda Eds, American Chemical Society, Washington DC, Chapt. 20 (1998).
- 37 K. Koide, H. Senba, H. Shosenji, M. Maeda and M. Takagi, *Bull. Chem. Soc. Jpn.*, **69**, 125 (1996).
- 38 T. Kobayashi, Y. Wang and N. Fujii, *Chem. Lett.*, 927, (1995).
- 39 Y. Kanekiyo, K. Inoue, Y. Ono, M. Sano, S. Shinkai and D.N. Reinhoudt, *J. Chem. Soc., Perkin Trans. 12*, 719 (1999).

This Page Intentionally Left Blank

## **Bio-imprinting: polymeric receptors with and for biological macromolecules**

PRADEEP K. DHAL, MOHAN G. KULKARNI AND RAGHUNATH A. MASHELKAR

### **10.1. INTRODUCTION**

Controlling both the molecular scale order in materials and the propagation of this molecular order up to the meso- and macroscopic scale constitutes one of the significant advancements in materials research. This field of research, which has garnered several names, including “molecular recognition” and “nanotechnology”, has rapidly evolved into an exciting and fast-moving branch of science [1]. Its broad ranging applications, ranging from biomedicine to biomimetics to information technology, has attracted the attention of a large number of researchers in recent years. Thus, miniaturisation capabilities afforded by this technique can lead to a new generation of information storage and processing devices, novel diagnostics and drug discovery processes [2]. In the area of biotechnology and biomedicine, the significant applications of molecular recognition technology include chemo-, enantio- and bio-selective separation of small molecular and macromolecular drugs and drug intermediates, targeted and site-specific drug delivery, chemical and biological sensors, catalysis, etc. [3].

The key to this field of research is the design of highly specific, functional materials called synthetic receptors. The underlying basis for the preparation of these synthetic receptors is template mediated molecular level assembly of functional groups in specific geometry [4]. “Molecular imprinting technology” is one of such approaches, which enables one to prepare robust synthetic receptors by carrying out polymerisation reactions in the presence of a target molecular substrate (guest or template) [5]. Sometimes this is also referred to as “template polymerisation”. In the past 25 years, this novel approach to prepare molecular receptors has attracted a great deal of attention. Different aspects of molecular imprinting technology and their current status have been dealt with in the accompanying chapters of this book. The uniqueness of this approach to produce molecular recognition materials lies in its generic nature and relative simplicity.

Most of the efforts in the area of molecular imprinting have been directed towards preparing polymeric receptors for small organic molecules by cross-linking polymerisation of vinyl and related monomers. The technique certainly appears to be attractive for preparing receptors to recognise large biomolecular species like proteins, carbohydrates and even biomolecular assemblies such as whole cells. Furthermore, preparation of receptors using these biological macromolecules as the

matrix forming precursors appears conceptually very attractive. Review of the current status of the research in these areas constitutes the scope of this chapter. The article is accordingly divided into three sections: (i) preparation of materials by preorganisation of biopolymers for applications in separation and catalysis; (ii) design and synthesis of synthetic receptors for biopolymers; (iii) design and synthesis of biomimetic, responsive gels showing enzyme-like recognition and catalytic behaviour.

## **10.2. MOLECULAR IMPRINTING USING BIOLOGICAL MACROMOLECULES AS MATRIX FORMING MATERIALS**

The general principle of molecular imprinting technology involves cross-linking polymerisation of functional monomers around a substrate molecule (guest) bearing complementary functional groups. This results in imparting a “molecular memory” for the substrate in the matrix after removal of the former. Rigidity of the polymer network achieved through cross-linking is responsible for retaining the specific arrangement of the functional groups in these receptors [6]. Although most of the efforts in this direction have focused on polymerisation chemistry using functional monomers, there have been certain reports in the literature dealing with preparation of imprinted polymers by cross-linking of preformed soluble polymers [7] (see also Chapter 9). Biological macromolecules such as proteins and polysaccharides are unique in terms of their well-defined molecular and supramolecular structure [8]. In addition to carrying an array of functional groups along their macromolecular chain (which can be utilised for both covalent and non-covalent interactions), these biopolymers possess higher order structural organisations, such as helices,  $\beta$ -sheets, etc. The inherent chirality of these macromolecules results in the creation of chiral environments around their vicinity. Therefore, these attractive features of biopolymers, along with their ready availability from renewable natural resources, make them an interesting class of precursors to prepare molecularly imprinted functional matrices, which can be used for specific recognition and separation of substrates and for carrying out chemo- and stereo-selective catalysis.

### **10.2.1. Molecularly imprinted matrices using proteins as the precursors**

Preparation of protein-based molecularly imprinted receptors has been conceptually derived from non-aqueous enzymology research, pioneered in particular by Klibanov and co-workers [9]. Systematic studies by Klibanov's group and other researchers reveals that enzymes function efficiently in anhydrous organic solvents, in a manner similar to more conventional aqueous media [10]. A striking feature of proteins in anhydrous media is their high conformational rigidity, which has given rise to enhanced thermal stability and ligand memory. These characteristics of the proteins in anhydrous solvents have been the driving force for developing molecularly imprinted protein-based systems as a class of novel molecular receptors. These

materials have been reported to exhibit interesting substrate recognition and catalytic properties.

#### 10.2.1.1. Molecularly imprinted protein matrices for recognition and separation

Russell and Klivanov demonstrated the first example of the viability of realising molecularly imprinted protein-based molecular receptors [11]. They allowed the enzyme subtilisin (a protease) to interact with a competitive inhibitor in aqueous solution. The role of the competitive inhibitor is to act as the template that freezes the defined tertiary structure of the enzyme. Following freeze drying, the inhibitor was removed by washing with an anhydrous organic solvent. The resulting templated enzyme was found to be several times more active than the native enzyme in anhydrous media. The key to the success of this design principle has been considered to be the formation of an array of hydrogen bonding patterns leading to a “frozen in” tertiary structure. As long as the templated protein is kept away from hydrogen bond donating solvents, this structural integrity is preserved. With increasing water concentration in the surrounding media, the fidelity of the imprinted protein is lost. The imprinting procedure is schematically illustrated in Fig. 10.1.

Followed by this initial success, Klivanov *et al.* carried out further systematic and in-depth studies in this direction using a large variety of proteins. By utilising bovine serum albumin (BSA) as the matrix forming protein, they prepared several such artificial receptors exhibiting shape-selective and enantioselective molecular recognition characteristics [12,13]. Thus, BSA imprinted with L-malic acid was

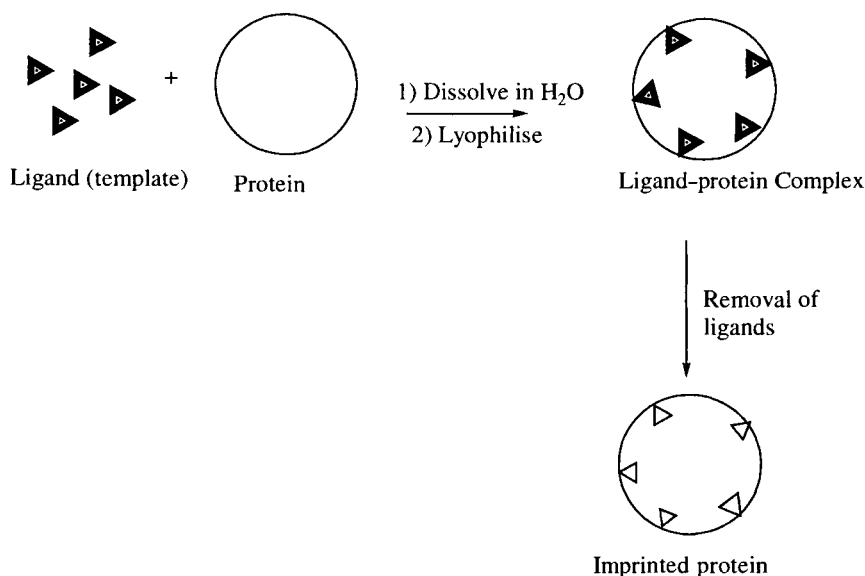


Fig. 10.1. Preparation of molecularly imprinted proteins by template mediated freeze drying.

TABLE 10.1

BINDING BEHAVIOUR OF L-MALIC ACID TOWARDS VARIOUS IMPRINTED GLOBULAR PROTEINS IN ETHYL ACETATE OBTAINED IN THE PRESENCE OF THIS TEMPLATE<sup>a</sup>

| Protein                            | Net ligand binding <sup>b</sup> |                |
|------------------------------------|---------------------------------|----------------|
|                                    | Mole equivalent                 | mg/g protein   |
| BSA                                | 24.2 $\pm$ 1.8                  | 48.4 $\pm$ 3.6 |
| Bovine erythrocyte haemoglobin     | 24.4 $\pm$ 1.7                  | 50.7 $\pm$ 3.5 |
| Chicken egg ovalbumin              | 16.2 $\pm$ 1.2                  | 48.2 $\pm$ 3.6 |
| Bovine pancreatic chymotrypsinogen | 9.1 $\pm$ 0.5                   | 48.8 $\pm$ 2.7 |

<sup>a</sup>Reproduced from [13].

<sup>b</sup>Defined as the difference between the ligand bound to imprinted protein and that bound to non-imprinted protein.

capable of binding greater than 26 mole equivalent of the ligand, while the non-imprinted BSA bound one-tenth of that amount under identical conditions. Subsequently, a number of proteins were imprinted using this ligand as the template. Substrate selectivities of these imprinted protein matrices reveal parallel behaviours, thus attesting to a general pattern of this approach. Some of these results are summarised in Table 10.1. The nature of the solvents (such as their polarity) is of paramount importance for these receptors to retain their "ligand memory" properties. Thus, the imprinted BSA obtained by using malic acid template was found to lose its substrate binding capacity significantly with increasing solvent polarity (see Table 10.2).

Further investigations were carried out by this group to establish the scope and limitations of this technique. Other globular proteins like haemoglobin, ovalbumin, lysozyme, as well as some homopolypeptides like poly(L-aspartic acid), were utilised as the matrix forming elements [13]. The study revealed that a sufficiently large polymer chain is a critical requirement to achieve the memory effect. The underlying mechanism for substrate recognition has been ascribed to multi-point hydrogen bonding interaction between the substrates and the proteins, which results in the formation of cavities of defined shape inside the protein matrices. Furthermore, imprinted BSA using malic acid as the template has exhibited affinity for other structurally analogous dicarboxylic acids, thereby attesting to the versatility of these receptors for molecular recognition. Chromatographic columns have been prepared using the malic acid imprinted BSA particles as the adsorbents and separation of maleic acid and acrylic acid has been shown to be possible by using ethyl acetate as the mobile phase.

In addition to the freeze drying technique to prepare protein-based molecularly imprinted materials, chemical cross-linking has also been employed to prepare

TABLE 10.2

EFFECT OF SOLVENT ON BINDING OF L-MALIC ACID TO BSA IMPRINTED WITH THIS LIGAND<sup>a</sup>

| Solvent                 | Net amount of L-malic acid bound <sup>b</sup><br>(mole equivalent) |
|-------------------------|--|
| Ethyl acetate           | 24.2 ± 1.8   |
| Hexyl acetate           | 21.3 ± 1.4   |
| Butyl acetate           | 17.6 ± 2.4   |
| 3-Octanone              | 15.0 ± 1.7   |
| 2-Butenone              | 14.5 ± 1.4   |
| 2-Ethoxyethyl acetate   | 11.1 ± 1.8   |
| tert-Butyl methyl ether | 11.0 ± 1.3   |
| Acetone                 | 10.6 ± 2.5   |
| Dioxane                 | 4.8 ± 1.2  |
| Dimethylformamide       | 3.2 ± 3.7  |

<sup>a</sup>Reproduced from [13].<sup>b</sup>Defined as the difference between the ligand bound to imprinted protein and that bound to non-imprinted protein.

protein-based receptors. The cross-linking reduces the conformational flexibility of the biopolymer, thereby retaining the memory. Kriegel *et al.* investigated substrate imprinted conformational changes in the regulatory properties of octameric yeast phospho-fructokinase [14]. Cross-linking of the enzyme was carried out in the presence of fructose-6-phosphate as the template. After removal of the template, the resulting imprinted enzyme exhibited significantly higher affinity for this substrate compared to the native enzyme. More detailed study suggested that although the imprinted enzyme did not show any cooperativity with respect to the template, it is activated by adenosine monophosphate (AMP). This AMP-induced activation increases the affinity of the imprinted enzyme towards the template. Furthermore, interaction of the enzyme with adenosine triphosphate at the substrate binding site was not affected by this covalent cross-linking.

In order to shed some light on the structural features of these molecularly imprinted protein-based matrices (exhibiting memory in anhydrous media), Klibanov and co-workers carried out Fourier-transform infrared (FTIR) spectroscopic investigations with these materials [15]. Quantitative structural analyses of the FTIR spectra of L-malic acid imprinted BSA, lysozyme and chymotrypsinogen were carried out. Comparison of the spectra of the imprinted and non-imprinted enzymes revealed significant changes in their secondary structures. While a rise in  $\beta$ -sheet content was invariably observed in the case of lyophilised enzymes, its content was substantially lower in the case of imprinted proteins. Furthermore, an alteration in the  $\alpha$ -helix contents of the imprinted proteins was observed. Based on these findings they concluded that the presence of template molecules during



lyophilisation of the proteins creates multi-site hydrogen bonding-based receptor sites, which are primarily responsible for the substrate-selective characteristics of these imprinted proteins.

Yennawar and co-workers employed high resolution X-ray crystallographic methods to investigate the structural explanation for this kind of enzyme memory in non-aqueous solvents [16]. Lyophilised  $\alpha$ -chymotrypsin containing the inhibitor *N*-acetyl-D-tryptophan was used for X-ray crystallography study. The enzyme inhibitor complex was soaked with water–isopropanol and hexane–isopropanol mixtures separately. In the non-aqueous environment, the indole ring of the inhibitor was found to be bound in the specificity pocket of the enzyme for L-amino acid. No inhibitor binding was observed in the aqueous structure, although the inhibitor concentration was identical in both cases. In the non-aqueous structure, five hexane and three isopropanol molecules were located. On the other hand, one isopropanol was observed in the aqueous structure. No significant conformational rearrangement was observed in the active site upon binding to this ligand. This is contrary to the suggestion of Klibanov *et al.*, who suggested that a new binding site was created during the non-aqueous imprinting of the enzymes.

#### 10.2.1.2. *Molecularly imprinted protein matrices for catalysis*

Substrate selectivity and stereoselectivity of enzyme catalysis are known to be influenced by the reaction media. As has been mentioned in the preceding section, a profound feature of the behaviour of enzymes in an anhydrous organic medium is the conformational stability, which leads to enhanced thermal stability and the ligand “memory” property. These features of enzymes have been exploited to impart novel catalytic characteristics that are absent in the native biopolymers.

Initial efforts in this direction were made in the laboratory of Klibanov. As has been mentioned in the preceding section, competitive inhibitor imprinted subtilisin, after lyophilisation and removal of the template, exhibited 100 times more catalytic activity in octane compared to the same enzyme lyophilised in the absence of the template [11]. Using a number of other enzymes, they subsequently expanded these bio-imprinting experiments. Thus, Dabulis and Klibanov utilised different hydrolytic enzymes (four proteases and three lipases) [17]. Aqueous solutions of these enzymes were lyophilised in the presence of *N*-acetyl-L-phenylalanine amide as the template. After removal of the template, the catalytic activities of these imprinted enzymes were tested by their abilities to catalyse transesterification reactions in anhydrous media. The catalytic properties of the imprinted enzymes were found to be far greater than the corresponding non-imprinted, lyophilised enzymes. Interestingly, the ligand-induced activation was expressed regardless of whether the substrate employed for the transesterification reaction structurally resembled the template. Furthermore, when the enzymes were lyophilised in the presence of lyoprotectants like sorbitol, other sugars and poly(ethylene glycol), a dramatic enhancement in the enzymatic activity in anhydrous media was observed. Some representative examples of this study are summarised in Table 10.3. Based on these observations, the mechanism of such template excipient-induced enzyme activation

TABLE 10.3

TRANSESTERIFICATION REACTION OF VINYL BUTYRATE WITH BENZYL ALCOHOL IN ANHYDROUS CARBON TETRACHLORIDE CATALYSED BY DIFFERENT HYDROLYTIC ENZYMES IMPRINTED WITH THE SUBSTRATE ANALOGUE *N*-ACETYL-L-PHENYLALANINE AMIDE<sup>a</sup>

| Enzyme                             | Initial reaction rate, $v$<br>( $\mu\text{M}/\text{h}/\text{mg}$ ) <sup>b</sup> |                      | $v_{\text{imprinted}}/$<br>$v_{\text{non-imprinted}}$ |
|------------------------------------|---|----------------------|---|
|                                    | Imprinted enzyme  | Non-imprinted enzyme |   |
| <i>Aspergillus oryzae</i> protease | 1500  | 42                   | 36  |
| Subtilisin Carlsberg               | 12,400  | 34                   | 365   |
| $\alpha$ -Chymotrypsin             | 2300  | 8.7                  | 264   |

<sup>a</sup>Reproduced from [17].

<sup>b</sup>Enzyme activities were measured after washing off the templates.

was considered to arise from the ability of the excipients to alleviate reversible denaturation of enzymes upon lyophilisation.

Interesting results on designing catalytically active bio-imprinted proteins have also been reported by Mosbach and co-workers [18]. After equilibrating  $\alpha$ -chymotrypsin with *N*-acetyl-D-tryptophan (an inhibitor) in an aqueous buffer, they rapidly precipitated the resulting enzyme–substrate complex in propanol. The precipitated enzyme–substrate complex was dried and the template was removed carefully from it under anhydrous conditions. The catalytic activity of the imprinted enzyme was investigated by carrying out the synthesis of the ethyl ester of the template. The imprinted enzyme exhibited a high degree of substrate selectivity and unnatural (D) enantioselectivity in propanol and acetone. On the other hand, the enzyme precipitated in the absence of the inhibitor did not catalyse this esterification reaction. An active site titration study of this imprinted  $\alpha$ -chymotrypsin with *trans*-cinnamoyl imidazole revealed that 68% of the active sites were accessible. These researchers also observed that incremental addition of water to the reaction media led to the loss of the selective catalytic properties of these imprinted enzymes. This parallels the observation of Klibanov *et al.* Furthermore, they found that  $\alpha$ -chymotrypsin could not be imprinted using the L-enantiomer (the substrate) as the template, thereby suggesting that it is an active site related effect.

A systematic and in-depth study involving bio-imprinted subtilisin using nucleophilic substrates as the templates has been reported by Rich and Dordrick [19]. They allowed subtilisin Carlsberg to interact with thymidine (the template) in an aqueous buffer solution and the resulting complex was lyophilised. After removing the template, catalytic activity of the imprinted enzyme was studied by the acylation reaction of thymidine. Compared to the control (enzyme lyophilised from the aqueous solution in the absence of the nucleotide template), the imprinted enzyme

showed up to 50 fold enhanced catalytic activity in anhydrous tetrahydrofuran. Although the use of several other substrates (e.g. thymine and ribose) as the template produced enzymes with enhanced catalytic properties for thymidine acylation, the thymidine imprinted enzyme was the most efficient catalyst for this purpose. Furthermore, by lyophilising the enzyme in the presence of different nucleophilic substrates, a library of imprinted enzymes with altered substrate selectivities was produced. This approach enabled the production of receptors which could discriminate between structurally different (e.g. sucrose vs. thymidine) and structurally similar (e.g. thymidine vs. deoxyadenosine) nucleophiles. A molecular modelling study suggested that the interaction of thymidine (or the unrelated substrate sucrose) with subtilisin during the imprinting procedure led to structural changes in the catalytic triad. A molecular dynamics study indicated that the structural changes in the catalytic triad occurred during imprinting. These changes have been considered to be the major factors that contribute to the imprinting-induced substrate selectivity.

Another novel approach to prepare catalytically active bio-imprinted enzymes has been reported by Braco and co-workers [20]. This approach, known as “interfacial activation”, involves lyophilisation of lipolytic enzymes in the presence of phospholipid-based liposomes as the template. The efficacy of this imprinting process is controlled by the interface between the liposomes and the enzymes. This strategy to prepare bio-imprinted enzymes is illustrated in Fig. 10.2. It was found that the amphiphiles do not provide mere lyoprotection, rather they are responsible for generating imprinting-induced conformationally rigid active sites. This technique was tested with a number of lipases and the resulting imprinted enzymes showed enhanced catalytic activity in anhydrous media [21].

An industrially significant application of the tailored enzymatic activity was reported by Gonzalez and Braco [22]. A bio-imprinted lipase was employed for the

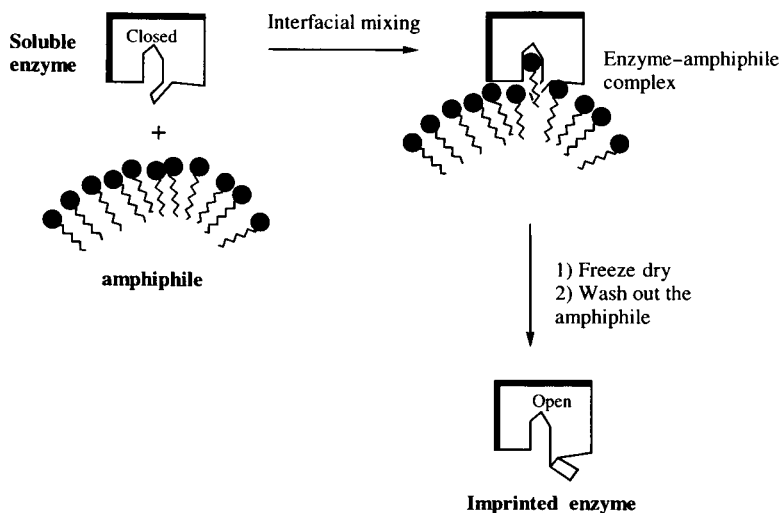


Fig. 10.2. Preparation of bio-imprinted enzymes by interfacial activation technique.

synthesis of flavour esters from fatty acids such as oleic acid and terpenyl alcohols such as geraniol and menthol. *Candida rugosa* lipase and *Geotrichum candidum* lipase were employed as the enzymes. For the specific alcohol under consideration (*viz.* geranyl alcohol), the rate of esterification depended upon the fatty acid used. The highest enhancement was achieved for C<sub>14</sub> fatty acid, which was attributed to the balance between substrate size and the stabilising hydrophobic interaction at the catalytic site. The methodology thus not only enabled enhanced reaction rates, but also broadened the chain length of fatty acid for which the specificity could be realised. The method has been found to be superior to conventional methods to enhance enzymatic activity in organic solvents.

Mechanistic evaluation of the catalytic activities of these bio-imprinted enzymes was carried out by Kaplan and co-workers to study the role of the template molecules on the shapes of the active sites [23]. The study was carried out with  $\alpha$ -chymotrypsin using iodomethane mediated deactivation as the mechanistic probe. Iodomethane (which is known to dimethylate the imidazole ring of the histidine moieties of enzymes) was found to deactivate the native lyophilised enzyme. On the other hand, the enzyme lyophilised in the presence of a competitive inhibitor, *N*-acetyl-D-tryptophan, was fully protected from such deactivation. Using indole as the template, the iodomethane-induced deactivation was enhanced. These findings suggest that the appropriate template molecules occupy the active sites of the enzymes leading to generation of an enhanced catalytically active conformation during lyophilisation. Fig. 10.3 illustrates the schematic representation of the role of such ligand binding on the reactivity of the catalytic triads.

Bio-imprinting of enzymes to enhance their enantioselectivity is thus fairly established. This is particularly useful for enzymes which inherently offer low enantioselectivity, e.g. lipases. Okahata and co-workers established that lipid coating of lipases enhances the solubility of the enzymes in organic media [24]. Subsequently, the technique was extended to phospholipase D for transphosphatidylolation of water insoluble phospholipids in organic solvents and to  $\beta$ -D-galactosidase for the

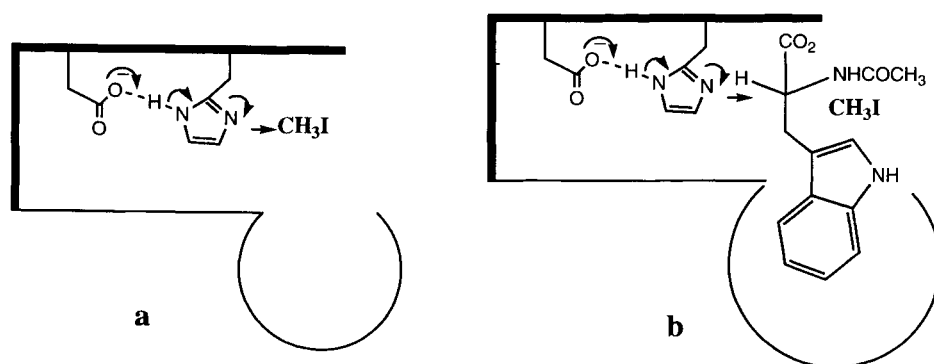


Fig. 10.3. Schematic illustration of the reactivity of the imidazole moiety of the catalytic triad of  $\alpha$ -chymotrypsin towards methyl iodide: (a) ligand free and (b) ligand bound enzyme.

transgalactosylation reactions in two-phase systems. While the lipid coating enhanced the catalytic activity, it did not improve the enantioselectivity of lipases, which depends upon the origin of the lipase. By combining the lipid coating with imprinting methodology, significant enhancement in both the reaction rates and the enantioselectivity of the enzyme catalysed reactions was achieved.

Thus, an aqueous solution of lipase from *Candida cylindracea* was imprinted with (*R*)-1-phenyl ethanol in aqueous solution and the enzyme–substrate assembly was coated with the synthetic glycolipid dicetadecyl-*N*-D-glucono-L-glutamate (by mixing the latter as an acetone solution with the imprinted enzyme and precipitating the coated imprinted lipase at low temperature). This enzyme resulted in the highest enantioselectivity and reaction rates for the esterification of lauric acid with 1-phenyl-ethanol. Some of the representative examples from this study are summarised in Table 10.4. However, the enantioselectivity was lost at temperatures greater than 60°C, and upon storage in iso-octane for more than a day at room temperature. The fact that the enantioselectivity of these coated, imprinted enzymes could be retained at higher levels by storing them in the solvent in the presence of the print molecules suggested that the loss in enantioselectivity, as well as catalytic activity, during storage at room temperature in solvent was due to the deterioration of the imprinting effect.

Photostimulation of the catalytic activities of bio-imprinted enzymes was studied by Willner and co-workers [25]. The goal of this study was to control the enzymatic activity with light. They linked a photoactive group such as nitropyran to  $\alpha$ -chymotrypsin. The resulting conjugated enzyme was allowed to interact with *N*-acetyl-L-phenylalanine (as template) in an aqueous medium. After precipitating the enzyme–template complex, the template was carefully eluted from the enzyme. The catalytic activities of the non-imprinted and imprinted photoactive enzymes were

TABLE 10.4

RESULTS ON ENANTIOSELECTIVE ESTER SYNTHESIS USING LIPID COATED BIO-IMPRINTED LIPASE 'OF' IN ANHYDROUS ISO-OCTANE<sup>a,b</sup>

| Enzymes                             | Initial rates<br>(mM/s/mg protein) |         | Enantio-<br>selectivity |
|-------------------------------------|------------------------------------|---------|-------------------------|
|                                     | $v_R$                              | $v_S$   | $v_R/v_S$               |
| Native lipase (not imprinted)       | 0.071                              | 0.013   | 5.5                     |
| Imprinted native lipase             | 0.0027                             | 0.00046 | 5.9                     |
| Lipid-coated lipase (not imprinted) | 0.44                               | 0.026   | 16                      |
| Imprinted, then lipid coated lipase | 1.1                                | 0.014   | <u>77</u>               |
| Lipid coated, then imprinted lipase | 0.93                               | 0.043   | 22                      |

<sup>a</sup>Reproduced from [24].

<sup>b</sup>Ester syntheses were carried out at 40°C using (*R*)- or (*S*)-1-phenylethanol (50 mM) and lauric acid (500 mM) in the presence of 1.0 mg of the enzyme.

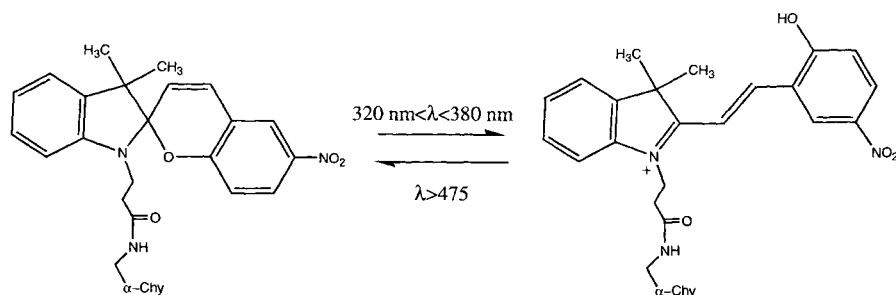


Fig. 10.4. Photostimulated spiropyran–merocyanine interconversion of photoactivatable enzyme.

studied under anhydrous conditions by light irradiation. Since the photoactive nitropyran moiety undergoes light mediated spiropyran–merocyanine isomerisation (see Fig. 10.4), this leads to changes in the conformation of the enzyme, thereby affecting its catalytic activity. A clear distinction in the catalytic activities of the imprinted and control photoactive enzymes was observed. Application of this approach to design novel biosensors and drug delivery systems has been envisaged by these authors.

Most of the studies to develop catalytically useful enzymes through molecular imprinting have involved use of inherently catalytically active enzymes. It would be interesting to incorporate catalytic properties to other non-catalytic proteins. In a parallel research area, very elegant studies have been successfully carried out to prepare catalytic antibodies [26]. Antibodies, which are known to bind specific molecules (antigens) with very high affinity and specificity, normally lack catalytic properties. By raising antibodies against transition state analogues (haptens), a number of catalytic antibodies have been developed for performing important organic transformations. On the other hand, examples of the incorporation of catalytic properties into non-enzymatic proteins are relatively scarce. Keyes *et al.* made the first attempt in this direction [27]. They set out to transform proteins to semi-synthetic enzymes by an imprinting procedure. The process involved partial denaturation of a protein and its subsequent contact with a substrate, which may be an inhibitor for the enzyme to be modelled. The protein was subsequently subjected to cross-linking, followed by removal of the template. This led to induction of enzymatic activity in the modified protein, while the precursor protein was either non-catalytic or had different catalytic activity. Proteins like albumin, concanavalin A etc., were used to produce these synthetic enzymes.

Another example in this direction has been reported by Ohya and co-workers [28]. By using a method analogous to that of Keyes *et al.*, they have induced catalytic activity in BSA by molecular imprinting. However, unlike the cross-linking reaction employed by Keyes *et al.* to stabilise the conformation of the imprinted protein, these authors resorted to lyophilisation to “lock-in” the conformation. The enzymatic activity of this synthetic enzyme was demonstrated with a dehydrofluorination reaction.

Hollfelder *et al.* have independently established that a wide range of albumins exhibited catalytic activities similar to the catalytic antibodies in the eliminative ring opening of a benzisoxazole [29]. The efficacy of the catalytic antibody was attributed to result from the activation of carboxylate by the polar environment of the active site, which was mimicked by albumins.

Slade and Vulfson have shown that the catalytic activity of native BSA in the dehydrofluorination reaction in aqueous media is greater than that reported for catalytic antibodies and molecularly imprinted polymers [30]. These authors therefore imprinted  $\beta$ -lactoglobulin and papain using *N*-isopropyl-4-nitrobenzyl amine as the transition state analogue. The catalytic activity of the imprinted proteins was evaluated in the dehydrofluorination reaction using acetonitrile as the reaction medium. A three fold rate enhancement in the  $K_{\text{cat}}$  value *vis-à-vis* non-imprinted proteins was observed.

### 10.2.2. Molecularly imprinted matrices using carbohydrates as the precursors

Carbohydrate-based macromolecules (*viz.* polysaccharides) constitute another class of biological macromolecules which exhibit interesting functional properties. These biopolymers, like proteins, are chiral and possess helical conformations. Polysaccharides like starch and cellulose are based on simple sugar derivatives and thus contain hydroxyl groups. On the other hand, complex carbohydrates like glycoproteins and glycolipids are a class of biopolymers which contain protein or lipid moieties in addition to polysaccharide segments. These complex biopolymers play very significant roles in important biological processes. Chitosan is a multi-functional polysaccharide based on amino glycoside repeat units and thus possesses amino and hydroxyl groups. This biopolymer is obtained by the hydrolysis of a naturally occurring polysaccharide, *N*-acetyl polyglucosamine. The presence of multiple functional groups in carbohydrates makes them a useful class of materials for preparing molecularly imprinted polymeric receptors. However, despite their attractiveness, relatively little work has been carried out to prepare carbohydrate derived molecularly imprinted matrices.

The first example on the use of carbohydrates to prepare abiotic receptors for molecular recognition was reported by Shinkai and co-workers [31]. Their motivation for this study was based on the substrate selectivity behaviour of cyclodextrins. Cyclodextrins are cyclic oligomers of glucose (6, 7 or 8 repeat units) which exhibit very interesting molecular recognition properties [32]. To prepare robust and modular cyclodextrin type materials, they attempted to cross-link starch in the presence of different template molecules. Removal of the template molecules from the cross-linked starch produced functional matrices showing affinities for their templates. Thus, cyanuric chloride cross-linked amylose using methylene blue as the template showed excellent binding behaviour for this template (see Fig. 10.5).

In subsequent years, Wulff and Kubik carried out a more elaborate study in this direction. They prepared inclusion complexes of amylose with different substrates [33]. Intra- and intermolecular cross-linking of these complexes was carried out using both cyanuric chloride and epichlorohydrin as the cross-linking agents. These

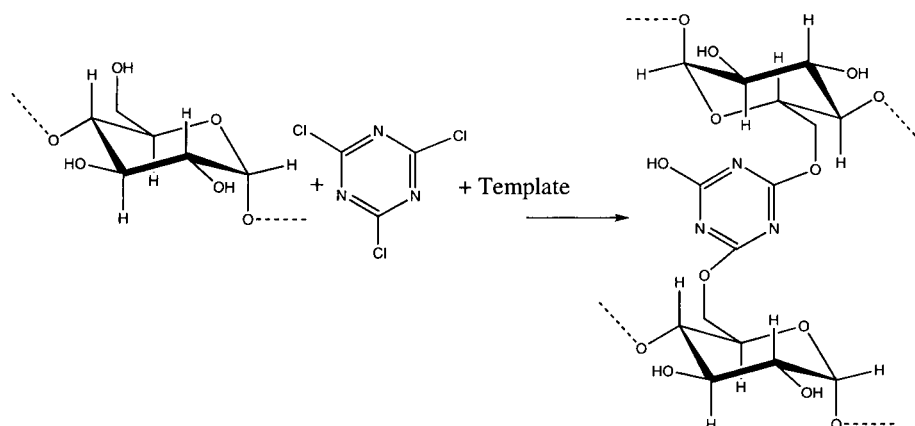


Fig. 10.5. Preparation of molecular receptors by template mediated cross-linking of poly-saccharides.

modified amylose derivatives, after removal of the templates, showed interesting substrate selectivity behaviour.

Recently, Komiyama and co-workers have reported the preparation of novel cyclodextrin derived imprinted carbohydrates for the efficient recognition of cholesterol [34].  $\beta$ -Cyclodextrin was cross-linked in the presence of cholesterol using different diisocyanates as the cross-linking agents. These cyclodextrin matrices, after removal of the template, exhibited selective preference towards cholesterol compared to the non-templated cross-linked cyclodextrin.

Ohga *et al.* prepared selective cation exchange resins using chitosan as the matrix forming precursor [35]. Chitosan was cross-linked in the presence of different metal ions like Cu(II), Cd(II), Zn(II), Ni(II), etc., using epichlorohydrin as the cross-linking agent. The metal ions were subsequently removed from these imprinted matrices. The resin prepared using Cu(II) as the template showed higher affinity for this metal ion. On the other hand, Cd(II) templated resin showed higher affinity for Hg(II). The Langmuir adsorption behaviour of these metal ion receptors was found to be dependent upon the amount of cross-linking agent used, thus suggesting the role of the rigidity of the matrix for substrate selectivity.

### 10.3. MOLECULAR IMPRINTING OF BIOLOGICAL MACROMOLECULES AND ASSEMBLIES

Design and synthesis of novel materials which are capable of recognising proteins and other biological assemblies, such as whole cells and viruses, have potential fundamental and practical applications [36]. Specific applications of such materials would encompass down-stream bioprocessing for the purification of biopharmaceuticals, drug delivery, diagnostics, sensors, etc. Currently, biologically derived recognition agents, like antibodies, enzymes, receptors, etc., are being used

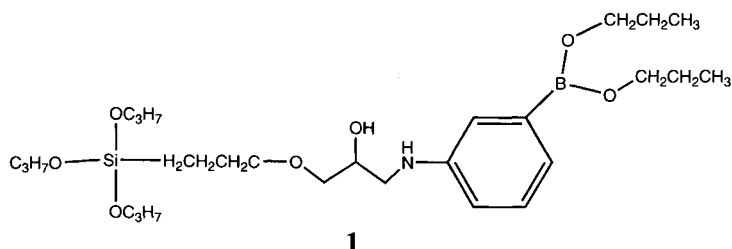


for some of these applications [37]. In the area of bioseparation, much of the cost of producing an enzyme or hormone occurs in product recovery. Extremely high selectivity for a specific biological macromolecule can be obtained through interactions such as antigen–antibody reactions, enzyme–substrate/inhibitor binding and hormone–receptor binding. Unfortunately, these methods tend to be very expensive and involve labile systems. Hence there is an incentive to develop inexpensive, robust and reusable replacements for these expensive and labile recognition agents.

Molecular imprinting technology, which is based on matching spatial distribution of complementary functional groups on the surface of receptor polymers to those of target molecules, has been largely confined to small organic molecules as the substrates. On the other hand, literature on the development of imprinted polymers for the recognition of proteins and other biological species is relatively scarce. This is due to the fact that the problem of designing imprinted polymers for biopolymers is a difficult mission compared to small molecules. Some of the limitations include the relative complexities of protein and cell surfaces, which carry large numbers of competing binding sites. Furthermore, their sensitivity to temperature, pH, the nature of the solvent, biocompatibility and large molecular sizes are some of the major factors which need consideration while designing molecular imprinting polymerisation processes for these substrates. This implies that there is an incentive to develop very innovative chemistries to prepare imprinted polymers as receptors to selectively recognise and bind biological macromolecules and assemblies.

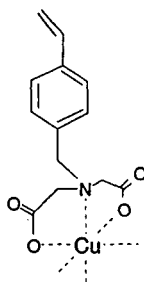
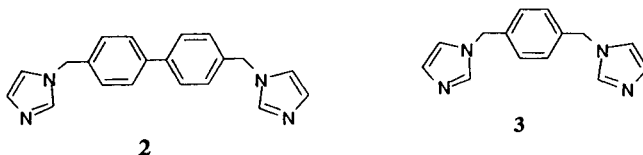
In spite of the above limitations, efforts have been made in recent years to prepare imprinted polymers for the recognition of proteins. The first example in this direction was reported by Mosbach and co-workers [38]. They were able to prepare a thin layer of polymer coating on the surface of porous silica beads, which was selective for the glycoprotein transferrin. Transferrin contains two identical carbohydrate moieties, each with two branches ending in a sialic acid group. Since boronic acid is known to interact covalently with *cis*-diol groups (e.g. those in carbohydrate moieties of glycoproteins) [39], the boronic acid–diol interaction was used as the binding site for preparing said polymer. They prepared a boronate silane functional monomer, *N*-[2-hydroxy-3-(tripropoxy silyl)propoxy]propyl-3-amino-benzene boronic acid (**1**), which was allowed to equilibrate with the protein. Subsequently a mixture of several other organic silanes was added and the mixture was polymerised. Polysiloxanes were prepared with both transferrin and BSA as the template. A control polymer was prepared in the absence of a protein. The selectivity of the polymers for transferrin was tested in chromatographic experiments and was reported as the relative retention (relative retention = elution volume for the transferrin/elution volume of BSA). The relative retention of transferrin imprinted polymer was found to be 2.16. In contrast, the relative retention for both control and BSA imprinted polymers was found to be 1.22. This suggests that the transferrin imprinted polymer showed a higher affinity for transferrin when compared to BSA.

Arnold and co-workers proposed a novel and generic approach to prepare molecularly imprinted matrices for the selective recognition and binding of proteins [40]. They used metal coordination interaction to induce complementary binding



between the matrix bound metal chelates, with the coordinating ligands present on the surface of proteins. The rationale to this approach was derived from the fact that, due to the complexities of protein surfaces, an effective and general recognition would depend on the strategic placement of as few specific functional groups as possible. Thus, incorporation of strong and specific binding interactions is crucial for distinguishing proteins from one another when in contact with the receptor. Metal coordination interaction has been considered to meet most of these needs. Surface exposed metal coordinating residues such as histidines exhibit high affinity for different metal ions (*viz.* Cu(II), Zn(II), Hg(II), etc.). This affinity between metal chelates and proteins has been the basis for protein purification using immobilised metal affinity chromatography [41].

In order to address this problem in a systematic manner, they set out to prove this concept using structural analogues of proteins at the beginning [42]. Towards this end, they synthesised a number of small molecule bisimidazole derivatives (e.g. **2** and **3**) as protein analogues. Metal coordinating functional monomers (e.g. **4**) were prepared and cross-linking polymerisation reactions were carried out in the presence of these bisimidazole derivatives as the templates. After removal of the



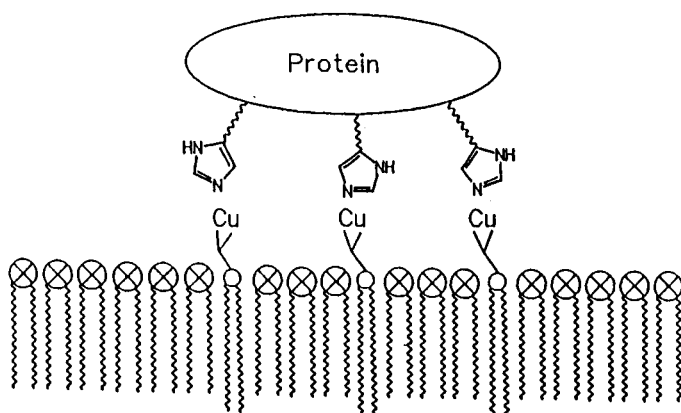


Fig. 10.6. Schematic illustration of metal coordination mediated two-dimensional assemblies for protein recognition.

templates, substrate selectivities of these polymers were tested under batch and chromatographic conditions [43]. Another approach devised by this group to design synthetic receptors for proteins was the synthesis of two-dimensional matrices such as liposomes and bilayers [44]. By using metal coordination mediated vesicle formation (Fig. 10.6) they prepared two-dimensional receptors. A good deal of effort was made to understand the properties of these interfacial functional matrices with metal coordination sites, with an aim towards the rational design of polymeric receptors for selective recognition of proteins.

Mosbach and co-workers also attempted to use metal coordination interactions to prepare polymeric adsorbents for selective recognition of proteins [45]. Using the monomer **4**, they polymerised the protein–monomer complex on methacrylate derivatised silica particles in the presence of ribonuclease A as the template protein. After removing the template, the imprinted functional silica particles were used as packing adsorbents in an HPLC column and the separation of lysozyme and ribonuclease A was carried out using this column. An enhanced affinity for the ribonuclease A was observed.

Venton and co-workers carried out the synthesis of functional sol-gel matrices in the presence of protein-based templates to prepare imprinted polysiloxanes for protein recognition [46]. They proposed that organic functional side chains on silanol monomers tended to associate with complementary functional groups on the protein surface during polymerisation (see Fig. 10.7). This phenomenon would lead to complementary binding pockets for the proteins inside the polymer matrices. 3-aminopropyl triethoxysilane was used as the functional monomer and tetraethyl-orthosilicate as the cross-linker. Sol-gel synthesis was carried out using urease and BSA as the template proteins. After formation of the matrices, removal of the templates was accomplished by pronase digestion. The template free silica prepared in the presence of urease as the template showed preferential binding affinity towards its template over the non-templated protein, BSA. However, using the closely

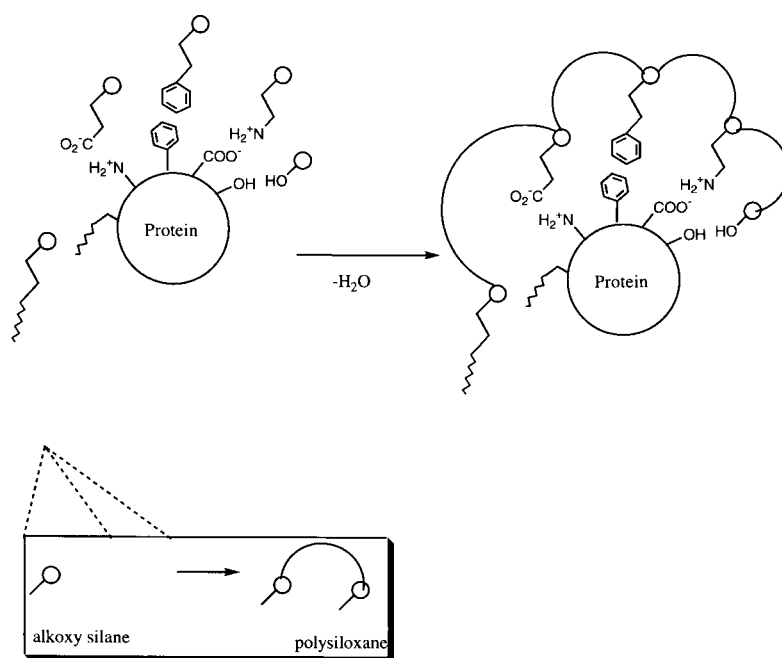


Fig. 10.7. Schematic illustration of the role of proteins in directing positioning of the binding sites in imprinted polymer matrix.

analogous proteins haemoglobin and myoglobin as templates, the resulting polymers were unable to distinguish the template from non-templates. This further reinforces the need to devise matrices based on highly specific binding interactions.

Hjerten and co-workers prepared substrate-specific polyacrylamide gels by carrying out cross-linking polymerisation in the presence of proteins [47]. Polymerisation of acrylamide and *N,N'*-methylenebisacrylamide was carried out in the presence of cytochrome C and haemoglobin as the templates. After removal of the templates using surfactants and acetic acid, substrate selectivities of the polymer gels were tested by chromatography. The imprinted polymers reportedly showed preferential affinities for their templates.

Burow and Minoura performed a similar kind of investigation to prepare protein imprinted polymers [48]. They used methacrylate modified silica particles as the carrier matrix on which imprinted sites were created. Using acrylic acid as the functional monomer and *N,N'*-1,2-diethylene bisacrylamide as the cross-linker, template polymerisation was carried out in the presence of glucose oxidase. This approach led to formation of a thin layer of cross-linked polymer film on the silica surface. After removing the template protein, substrate selectivity of the polymer was tested. Preferential affinity of the polymer for its template suggests the formation of substrate-selective binding sites in the polymer matrix.

In the approaches mentioned above, the capacity of receptors to bind enzymes

was low, probably because only the weak non-covalent interactions between the enzyme and monomers were exploited to create the receptor sites. Another reason for this low uptake could be that, while the tertiary structure of enzyme is three dimensional, the imprinting was restricted to the two-dimensional surface of the silica-based support, which can recognise only the superficial surface topography of an enzyme. Thus, there is a need to develop a methodology which will provide a stronger interaction between the receptor and the enzyme.

Inhibitors contain functional groups which possess strong affinity for the active site of enzymes. These interactions have been exploited in affinity precipitation and affinity ultrafiltration techniques for selective recovery of enzymes [39]. Thus, utilising this principle of biospecific inhibitor–enzyme interaction, Vaidya *et al.* have developed an elegant imprinting methodology for the recognition of enzymes [49]. By using this “affinity-imprinting” (which is a combination of molecular imprinting and affinity chromatography), novel protein receptors were designed. For this purpose, *N*-acryloyl-*para*-aminobenzamidine was used as the affinity monomer and the monomer was allowed to form a complex with the active site of trypsin. The optimal ratio of the affinity monomer to trypsin was arrived at from active site titration. This complex was polymerised with the comonomer acrylamide and the cross-linker *N,N'*-methylenebisacrylamide to form gels. After polymerisation trypsin was removed. This created a polymer matrix possessing cavities with shapes specific for trypsin. The trypsin imprinted gel behaved as a true receptor, as evidenced by the fact that it exhibited a linear Scatchard plot for the uptake of trypsin. The corresponding plot for the non-imprinted gel was non-linear, manifesting simple affinity chromatographic behaviour. In a batch experiment, the trypsin imprinted gel exhibited exclusive uptake of trypsin, while a closely related enzyme, chymotrypsin, was not taken up. In competitive binding experiments using a mixture containing trypsin and chymotrypsin, the trypsin imprinted gel took up trypsin exclusively. In terms of capacity, this gel had an uptake capacity of 0.62 mg trypsin/g of polymer, which is much higher than the capacity of the imprinted silica gel for glucose oxidase (5.6  $\mu\text{g/g}$ ) reported by Burow and Minoura [48].

An elegant approach to prepare imprinted polymer surfaces using whole cells such as bacteria as the templates has been pioneered by Vulfson and co-workers [50] (see also Chapter 11). The process employed is analogous to lithographic technology, which has been used in the microelectronics industry to pattern semiconductor chips [51]. These polymer particles bearing functional groups have patterns exactly matching the shape and size of the template microorganisms. Since the templates used are whole cells, very careful and mild chemistries were adopted to maintain the biocompatibility of the system. Thus, this cell mediated lithographic process to prepare spatially functionalised polymer surfaces is a multi-step procedure. In the first stage, an interfacial polycondensation reaction between a polyamine and a diacid chloride was carried out in the presence of a suspension of the bacterium, *Listeria monocytogenes*. The microorganism readily partitioned at the interface and was held in place by a covalent bond *via* its surface nucleophilic groups with the acid chloride moieties in the polyamide network. This polymerised assembly was photopolymerised with diacrylates to produce polymer beads. The

unreacted amino groups of the polyamine-based polyamide–bacteria network were blocked by cyanate-terminated perfluoropolyether, followed by removal of the bacteria by hydrolysis. This process created lithographic patterns complementary to the bacterial template. These anisotropic patches on the surface of the polymer matrices, having dimensions defined by the template microorganisms, can be further modified to adjust the chemistry in the sites such that they could be used for various biotechnological applications.

#### **10.4. PROTEIN MIMETIC IMPRINTED GELS: RESPONSIVE HYDROGELS EXHIBITING BIOMOLECULAR RECOGNITION PROPERTIES**

The key objective of molecularly imprinted polymer research has been to prepare abiotic materials exhibiting enzyme-like recognition and catalysis behaviour (see also Chapter 4). These polymers, which are prepared by extensive cross-linking polymerisation in the presence of template molecules, are obtained as rigid, insoluble, solid materials with frozen complementary binding sites corresponding to the template molecules. On the other hand, enzymes are protein-based biopolymers that are inherently soluble in aqueous media. Enzymes possess defined globular conformations that are preserved in solution and they undergo reversible structural changes in response to certain changes in their surrounding environment (*viz.* allosteric effect and induced fit). These characteristics are attributed to their capabilities for retaining conformational memory, which manifests molecular recognition and highly selective catalytic properties [52]. Understanding the physical basis of such functions of enzymes and the use of that knowledge to prepare synthetic materials is of great interest to synthetic chemists. A solution towards this end would provide an opportunity to obtain novel biomimetic functional materials.

In general, polymers in solution or as swollen gels do not exhibit such kinds of supramolecular properties. However, in recent years, a class of novel, aqueous swellable polymers (hydrogels) has been synthesised which can respond to environmental changes and amplify them in the form of phase transitions [53]. These hydrogels have been found to undergo a volume transition between the swollen and collapsed phases, either continuously or discontinuously. The transition is reversible and can be triggered by external stimuli like temperature, solvent composition, pH, ionic strength and light, as well as by specific molecules. These gels are called “responsive” or “smart” gels. They have been used to prepare artificial muscles, actuators, controlled release systems, sensors, optical shutters, etc.

Attempts have been made to utilise the molecular imprinting technique to this class of smart gels to prepare hydrogel substances showing enzyme-like behaviour in molecular recognition and catalysis. One such attempt has been made by Tanaka and co-workers, who have developed a theoretical model to the structures of such polymer gels [54]. Based on computer simulation, they proposed that imprinting polymerisation of a dense solution of monomers would control the monomer sequence of an artificial heteropolymer during its synthesis. This would lead to a polymer chain exhibiting quick and reliable renaturability to some unique spatial

fold capable of certain functional properties. In order to test their proposition, they prepared a polymeric gel that could selectively recognise, absorb and release a specific molecule in response to phase transition conditions [55]. The building blocks for such polymers consist of two groups of monomers each having different roles. One of the groups forms a complex with the target substrate and the other allows the polymer chain to expand and collapse reversibly in response to environmental changes. The active site develops an affinity for the target agent only when they are in proximity. The proximity is controlled by the reversible phase transition of the hydrogel. The idea was tested with a polymer gel made to selectively recognise, absorb and release heavy metal ions. Thus, a copolymer of acrylic acid (metal ion binding component) and *N*-isopropylacrylamide (phase transition component) was prepared in the presence of Cu(II) ions. The resulting gels exhibited interesting phase transition behaviours that are not evident in the absence of metal ions, thus showing the importance of the presence of strategic recognition epitopes in their architectures.

In an effort to prepare polymer gels exhibiting enzyme-like selective catalysis behaviour, Karmalkar *et al.* employed a metal mediated approach to position imidazole, carboxyl and hydroxyl groups in a hydrogel matrix [56]. These three functional groups constitute the catalytic triad in the serine protease class of enzymes and their strategic positioning in the protein structure is the key to their catalytic properties. Thus, complexation of methacrylic acid (MAA) with *N*-methacryloylhistidine and the print molecule, 2-[[[(isobutyrylamino)caproyl]-L-phenylalanyl]2-aminopyridine, by CoCl<sub>2</sub> and its subsequent polymerisation with 2-hydroxyethyl methacrylate and ethylene glycol dimethacrylate offered the desired hydrogel. After removal of the print molecule and metal ions, the catalytic behaviour of the polymer was studied by monitoring the hydrolysis of *p*-nitrophenyl esters. The imprinted polymer catalysed the hydrolysis at a rate comparable to  $\alpha$ -chymotrypsin. On the other hand, a control polymer containing similar functional groups distributed in a random fashion showed only modest catalytic activity.

In a subsequent study, the Co<sup>2+</sup> coordinated assembly was grafted onto a cross-linked poly(glycidoxypromethylmethacrylate) (GMA)-ethylene glycol dimethacrylate (EDMA) support surface. The template and Co<sup>2+</sup> ions were then leached out from the matrix. This surface grafted polymer exhibited turnover, Michaelis–Menten kinetics and mechanisms such as inhibition by tosyl phenyl alanyl chloromethyl ketone and inhibition on acetylation of hydroxyl group of 2-hydroxyethylmethacrylate (HEMA), similar to native chymotrypsin.

It was earlier reported that copolymerisation of HEMA, MAA and methacrylate-histidine coordinated with Co<sup>2+</sup> resulted in a copolymer in which the three monomers are so placed along the polymer chain that they could be again brought close to each other to form a complex with Co<sup>2+</sup>. Due to the different monomer reactivity ratios of the three monomers, such placement of monomers was not observed when copolymerisation was carried out in the absence of Co<sup>2+</sup>. This suggests that monomers bearing hydroxyl, carboxyl and imidazole groups, when coordinated with Co<sup>2+</sup>, undergo polymerisation as a monomeric Co(II) complex and do not form a random copolymer of the three monomers.

Encouraged by the above finding, Lele *et al.* set out to explore if a generalised methodology to synthesise the polymeric mimics of chymotrypsin could be established [57,58]. Mimics of chymotrypsin were synthesised by grafting  $\text{Co}^{2+}$  coordinated monomer-template assemblies of various hydroxyl, carboxyl and imidazole bearing monomers and a template molecule on the cross-linked poly(GMA-EDMA) support. Chymotrypsin-specific substrate *N*-cbz-Tyr-PNP was selected to evaluate the efficacy of these surface imprinted enzyme mimetic gels. In order to induce specificity for this substrate, a template molecule, structurally similar to *N*-CBZ-Tyr-PNP (*viz.* *N*-nicotinoyl-tyrosyl benzyl ester) was used. The cooperative effect within the triad, substrate recognition and saturation kinetics exhibited by the triad were established using these polymers.

Watanabe *et al.* prepared a thermoresponsive hydrogel that showed substrate recognition behaviour in the shrunken state due to specific volume changes in response to the concentration of guest molecules [59]. This observation indicates that it is possible to impart structurally stable molecule-specific phases in a polymer gel that are reversible, similar to the molecular recognition abilities of proteins. The technique involved the polymerisation of *N*-isopropylacrylamide, acrylic acid and *N,N'*-methylene-bisacrylamide in the presence of *dl*-norephedrine.HCl or *dl*-adrenaline.HCl as the guest molecules. The resulting gels, after removal of the templates, were tested for their swelling behaviour in the presence of the guest molecules. While in the swollen state, the swelling ratio of the imprinted thermoresponsive gel was independent of any external agent; in the shrunken state, the swelling ratio increased with increasing concentration of the guest molecule such as norephedrine. This result suggests the creation of molecular recognition phases in the polymer conformations.

## 10.5. CONCLUSIONS AND OUTLOOK

The bio-imprinting aspect of molecular imprinting research offers an exciting avenue to design promising functional materials. Preparation of imprinted matrices using biological macromolecules as the precursors is a facile and straightforward method to transform common proteins into useful receptors showing recognition and catalytic properties. Being an interdisciplinary area of research, bio-imprinting may stimulate chemists as well as biologists to come up with novel strategies to modify and enhance the molecular recognition abilities of these bio-imprinted materials. The outcome can be exploited to design efficient and selective analytical devices, such as biosensors for diagnostics, support materials for chemoselective and enantioselective separations and site-specific biodegradable drug delivery devices. Preparation of such functional materials may require incorporation of additional functional sites (e.g. the photoactive groups of Willner and co-workers [25]) into the imprinted biopolymer matrices. Research efforts in this direction seem to be a worthwhile proposition. Elaborating on their enzyme-mimetic imprinted hydrogel [56], Karmalkar *et al.* have succeeded in incorporating photosensitive groups into hydrogels [60]. The catalytic activity of these gels could be reversibly



switched on and off as a result of photochemically induced swelling and de-swelling of the gel by restricting the diffusion of the substrates to the active site of the enzyme mimics. The activity could also be reversibly switched off in acidic media by protonating the imidazole group. Development of biological signal responsive imprinted materials would further open up biomedical applications. Further research efforts in this direction seem to be worthwhile proposition.

Bio-imprinting procedures have enabled the transformation of native enzymes to give more efficient and selective catalysts, as well as the conversion of non-catalytic proteins to enzyme-like catalysts. The methodology complements other approaches, like protein engineering, catalyst engineering, solvent engineering, etc., to prepare novel biocatalysis systems [61]. In particular, transformation of non-catalytic proteins to enzyme-like catalysts parallels the research efforts in the area of catalytic antibodies [26]. It appears that this approach will be a rewarding endeavour and more efforts should be made in this direction. Easy access to numerous proteins may enable a high throughput screening procedure for quick evaluation of the scope and limitation of this method. Attempts should be made to stabilise the imprinted superstructures in these imprinted protein matrices so that the novel recognition and catalytic properties are retained for extended periods of time under various environmental conditions. This is particularly significant to the preparation of any practical materials.

Another class of biopolymers that show sophisticated biological recognition are DNA and RNA and they play key roles in life processes. Any attempts to prepare imprinted matrices using these biopolymers would be very rewarding. In addition to being scientifically exciting, it may offer a novel approach to diagnose and treat diseases at genetic level (e.g. gene therapy). Thoughtful efforts in this direction would certainly take molecular imprinting research to a more respectable level.

Preparation of imprinted polymers for the recognition of proteins and other biomacromolecules and assemblies may open the door to the preparation of polymer-based biosensors and other diagnostics, which may present the currently dominant enzymes and antibodies with their first serious challengers as biomedical analytical tools. Such methodologies for small molecules have already been reported [62]. However, unlike small molecule imprinting, implementation of template polymerisation techniques to delicate and large biopolymers, possessing complex surface epitopes, does present significant challenges. Surface imprinting appears to be one promising way around this problem. Towards this end, a recent report by Ratner and co-workers on preparation of template imprinted nano-structured surfaces for protein recognition is quite promising [63]. By using a radio-frequency glow-discharge plasma deposition technique, they could deposit a thin polymer film around disaccharide coated proteins on a mica surface. The disaccharide became covalently attached to the polymer film, creating polysaccharide-like cavities on the surface that exhibited highly selective recognition for a variety of template proteins. Further developments in the area of designed surfaces, monolayers and vesicle-based materials, cell mediated lithography, as well as surface polymerisation using reactive matrices, appear to be very promising in this respect.

The use of molecular imprinting methodology to prepare functional, responsive hydrogels is a conceptual advancement. This approach, which uses biological information, may enable *de novo* design of novel protein-like polymers from non-proteinaceous precursors, with capabilities of shape memorisation, molecular recognition and catalysis, without using biological systems.

## REFERENCES

- 1 G.M. Whitesides, J.P. Mathias and C.T. Seto, *Science*, **254**, 1312 (1991).
- 2 J.S. Lindsay, *New J. Chem.*, **15**, 153 (1991).
- 3 J.M. Lehn, *Angew. Chem. Int. Ed. Engl.*, **29**, 1304 (1990).
- 4 R. Hoss and F. Vögtle, *Angew. Chem. Int. Ed. Engl.*, **33**, 389 (1994).
- 5 G. Wulff, *Angew. Chem. Int. Ed. Engl.*, **34**, 1812 (1995).
- 6 K.J. Shea, *Trends Polym. Sci.*, **2**, 166 (1994).
- 7 H. Nishide, J. Deguchi and E. Tsuchida, *Chem. Lett.*, 169 (1976).
- 8 T.E. Creighton, *Proteins: structure and molecular properties*, 2nd ed., W.H. Freeman, New York (1993).
- 9 A. Zaks and A.M. Klibanov, *Science*, **224**, 1249 (1984).
- 10 A.M. Klibanov, *Trends Biochem. Sci.*, **14**, 141 (1989).
- 11 A.J. Russell and A.M. Klibanov, *J. Biol. Chem.*, **263**, 1624 (1988).
- 12 L. Braco, K. Dabulis and A.M. Klibanov, *Proc. Natl. Acad. Sci. USA*, **87**, 274 (1990).
- 13 K. Dabulis and A.M. Klibanov, *Biotech. Bioeng.*, **39**, 176 (1992).
- 14 T. Kriegl, W. Schellenberger, G. Kopperschlager and E. Hoffman, *Biomed. Biochim. Acta*, **50**, 1159 (1991).
- 15 P. Mishra, K. Griebenow and A.M. Klibanov, *Biotech. Bioeng.*, **52**, 609 (1996).
- 16 H.P. Yennawar, N.H. Yennawar and G.K. Farber, *J. Am. Chem. Soc.*, **117**, 577 (1995).
- 17 K. Dabulis and A.M. Klibanov, *Biotech. Bioeng.*, **41**, 566 (1993).
- 18 M. Ståhl, U. Jeppsson-Wistrand, M.-O. Mansson and K. Mosbach, *J. Am. Chem. Soc.*, **113**, 9366 (1991).
- 19 J.O. Rich and J.S. Dordick, *J. Am. Chem. Soc.* **119**, 3245 (1997).
- 20 I. Mingarro, C. Abad and L. Braco, *Proc. Natl. Acad. Sci. USA*, **92**, 3308 (1995).
- 21 H.N. Gonzalez and L. Braco, *J. Mol. Catal.*, **B3**, 111 (1997).
- 22 H.N. Gonzalez and L. Braco, *Biotech. Bioeng.*, **59**, 122 (1998).
- 23 N.A.S. Stewart, A. Taralp and H. Kaplan, *Biochem. Biophys. Res. Commun.*, **240**, 27 (1997).
- 24 Y. Okahata, A. Hatano and K. Ijro, *Tetrahedron Asym.*, **6**, 1311 (1995).
- 25 M. Lion-Dagan and I. Willner, *J. Photochem. Photobiol. A: Chemistry*, **108**, 247 (1997).
- 26 L.C. Hsieh-Wilson, X.-D. Xiang and P.G. Schultz, *Acc. Chem. Res.*, **29**, 164 (1996).
- 27 M.H. Keyes, D.E. Albert and S. Saraswathi, *Ann. N. Y. Acad. Sci.*, **501**, 201 (1987).
- 28 Y. Ohya, J. Miyaoka and T. Ouchi, *Macromol. Rapid Commun.*, **17**, 871 (1996).
- 29 F. Hollfelder, J.A. Kirby and D.S. Tawfik, *Nature*, **383**, 60 (1996).
- 30 C. Slade and E.N. Vulfson, *Biotech. Bioeng.*, **57**, 211 (1998).
- 31 S. Shinkai, M. Yamada, T. Sone and O. Manabe, *Tetrahedron Lett.*, **24**, 3501 (1983).
- 32 M.L. Bender and M. Komiyama, *Cyclodextrin chemistry*, Springer-Verlag, Berlin (1978).
- 33 G. Wulff and S. Kubik, *Carbohydr. Res.*, **237**, 1 (1992).
- 34 H. Asanuma, M. Kakazu, M. Shibata, T. Hishiya and M. Komiyama, *Chem. Commun.*, 1971 (1997).
- 35 K. Ohga, Y. Kurauchi and H. Yanase, *Bull. Chem. Soc. Jpn.*, **60**, 444 (1987).
- 36 J.W. Jacobs and S.P.A. Fodors, *Trends Biotechnol.*, **12**, 19 (1994).
- 37 I. Chaiken (Ed.), *Affinity chromatography and biological recognition*, Academic Press, San Diego (1983).

- 38 M. Glad, O. Norrlöw, B. Sellergren, N. Siegbahn and K. Mosbach, *J. Chromatogr.*, **347**, 11 (1985).
- 39 M.J. Benes, A. Stambergova and W.H. Scouten, In: *Molecular interactions in bioseparations*, T.T. Ngo Ed., Plenum, New York, p. 313 (1993).
- 40 S. Mallik, S.D. Plunkett, P.K. Dhal, R.D. Johnson, D. Pack, D. Shnek and F.H. Arnold, *New J. Chem.*, **18**, 299 (1994).
- 41 F.H. Arnold, *Bio/Technology*, **9**, 151 (1991).
- 42 P.K. Dhal and F.H. Arnold, *Macromolecules*, **25**, 7051 (1992).
- 43 S.D. Plunkett and F.H. Arnold, *J. Chromatogr. A.*, **708**, 19 (1995).
- 44 D.R. Shnek, D.W. Pack, D.Y. Sasaki and F.H. Arnold, *Langmuir*, **10**, 2382 (1994).
- 45 M. Kempe, M. Glad and K. Mosbach, *J. Mol. Recogn.*, **8**, 35 (1995).
- 46 D.L. Venton and E. Gudipati, *Biochim. Biophys. Acta*, **1250**, 126 (1995).
- 47 J.L. Liao, Y. Wang and S. Hjerten, *Chromatographia*, **42**, 259 (1996).
- 48 M. Burow and N. Minoura, *Biochem. Biophys. Res. Commun.*, **227**, 419 (1996).
- 49 A.A. Vaidya, B.S. Lele, M.G. Kulkarni and R.A. Mashelkar, *J. Appl. Polym. Sci.* **64**, 418 (1999).
- 50 C. Alexander and E.N. Vulfon, *Adv. Mater.*, **9**, 751 (1997).
- 51 S.A. MacDonald, C.G. Willson and J.M.J. Frechet, *Acc. Chem. Res.*, **27**, 151 (1994).
- 52 A. Fresht, *Enzyme structure and mechanism*, 2nd ed., W.H. Freeman, San Francisco (1985).
- 53 A.R. Khare and N.A. Peppas, *Polymer News*, **16**, 230 (1991).
- 54 V.S. Pande, A.Y. Grosberg and T. Tanaka, *Proc. Natl. Acad. Sci. USA*, **91**, 12,976 (1994).
- 55 T. Tanaka, C. Wang, V.S. Pande, A.Y. Grosberg, A. English, S. Masamune, H. Gold, R. Levy and K. King, *Faraday Discuss.*, **102**, 201 (1996).
- 56 R.N. Karmalkar, M.G. Kulkarni and R.A. Mashelkar, *Macromolecules*, **29**, 1366 (1996).
- 57 B.S. Lele, M.G. Kulkarni and R.A. Mashelkar, *React. Funct. Polym.*, **39**, 37 (1999).
- 58 B.S. Lele, M.G. Kulkarni and R.A. Mashelkar, *Polymer*, **40**, 215 (1999).
- 59 M. Watanabe, T. Akahoshi, Y. Tabata and D. Nakayama, *J. Am. Chem. Soc.*, **120**, 5577 (1998).
- 60 R.N. Karmalkar, V. Premnath, M.G. Kulkarni and R.A. Mashelkar, *Proc. Roy. Soc.*, (in press).
- 61 F.H. Arnold, *Protein. Eng.*, **2**, 21 (1988).
- 62 G. Vlatakis, L.I. Andersson, R. Muller and K. Mosbach, *Nature*, **361**, 645 (1993).
- 63 H. Shi, W. Tsai, M.D. Garrison, S. Ferrari and B.D. Ratner, *Nature*, **398**, 593 (1999).

## **Surface imprinting of microorganisms**

NATALIA PEREZ, CAMERON ALEXANDER AND EVGENY N. VULFSON

### **11.1 INTRODUCTION**

Over the past few years imprinting has been successfully applied to the preparation of polymers which have exhibited selectivity for a wide range of natural products, such as amino acids [1] and short peptides [2,3], monosaccharides and their derivatives [4,5], nucleotides [6,7], steroids [8,9], as well as numerous drugs [10–13] and pollutants [14,15]. Most of the research has focused on the synthesis of polymers capable of resolving racemic mixtures [16,17], but other applications, e.g. in solid phase extraction [18–21], synthetic chemistry [22], catalysis [23–25], sensors [26,27], removal of undesirable components from complex mixtures [28] and separation of proteins [29,30], have also been reported. For a number of years now we have been interested in extending the concept of molecular imprinting to encompass much larger moieties such as, for example, whole cells. The aim of this mini-review is to describe the progress made in the last few years and discuss possible implications of this emerging technology.

### **11.2 IMPRINTING OF MICROORGANISMS**

As discussed in detail in other chapters of this book, molecular imprinting relies on the pre-arrangement of complementary functionality in polymer binding sites in a precise spatial arrangement to recognise the target selectively. The principal difficulty in imprinting macromolecular aggregates or cells in comparison to relatively simple organic molecules, is the need to ensure that such complementary functionality is incorporated into the polymer as a defined array or at a surface, rather than as individual groups. This clearly requires the development of appropriate methods or techniques and, in some cases, special polymerisable monomers. For example, to imprint a microorganism it is necessary to resolve three immediate issues: (i) to decide on appropriate functionality in the sites, (ii) to find a way of reproducing the size and shape of a microorganism in the polymer matrix, (iii) to position the functionality within the defined sites. It is also important to render the rest of the surface non-functional or inert and to ensure that any recognition sites are easily accessible. To date, there have been few published accounts of surface imprinting, although a number of authors have indicated that such a technique would be highly desirable. It would also seem beneficial to employ reagents and conditions

compatible with normal cell environments, at least during the initial stages of polymer synthesis.

### 11.3 METHODOLOGY

Initially we felt that the method of polymer formation was the key issue and attempted to imprint microorganisms by interfacial polycondensation, as this procedure is well established for encapsulating cells and bioactive molecules. We decided to prepare a soluble pre-polymer with suitable pendent antibody or lectin moieties to form the recognition component in nascent binding sites. Polyamines and polyethyleneglycols seemed to be a good starting point because the chemistry of protein attachment to these water-soluble polymers is well developed. We reasoned that microorganisms would complex with water-soluble ligand-modified polymers and, if the amount of attached polyamine/polyethylene glycol was high enough, the resultant polymer-coated aggregate would partition to an aqueous-organic interface as illustrated in Fig. 11.1.

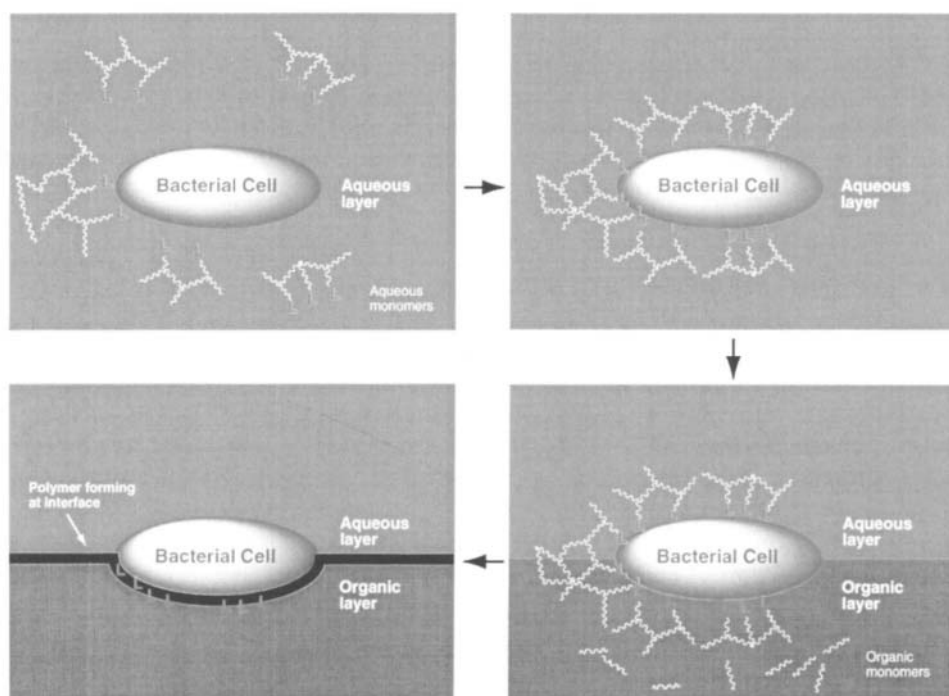


Fig. 11.1 Imprinting of bacterial cells. Aqueous pre-polymers with attached affinity ligands (L) bind to bacteria. Introduction of an organic phase containing a diacid chloride and partitioning of the pre-polymer/cell complex to the interface results in polymerisation at and around the surface of bacteria.

The inclusion of a suitable cross-linking agent, such as a diacid chloride, in the organic phase would generate a polymeric film on reaction with the aggregate, such that microorganisms would be captured at the interface. Relatively hydrophobic diacid chlorides (e.g. adipoyl chloride) were chosen as cross-linkers due to their high reactivity and low solubility in water.

However, we made several observations in the course of preliminary experiments which necessitated changing the above protocol. Firstly, it was found that removal of the template bacteria was difficult to accomplish under conditions which were sufficiently mild to preserve the native conformation of the underlying protein ligands. This was presumably due to covalent attachment of the microorganisms to the polymer. With hindsight this is perhaps not too surprising, given that there are numerous nucleophilic groups on the outer surface of bacterial cells capable of reacting with pendent acid chloride functionality on the forming polymer chains. Secondly, the resulting polymeric microcapsules were fragile and rather thin-walled (Fig. 11.2) and tended to burst on handling. Clearly, an alteration of the preparation procedure was necessary to achieve satisfactory mechanical stability of the materials.

Thirdly, it appeared that microorganisms partitioned to the aqueous-organic interface regardless of the presence of ligand-modified pre-polymer. This observation opened up the interesting possibility of imprinting microorganisms first by "fixing" the size and shape of the sites and introducing affinity ligands at a later stage. The overall process, which we have described as bacteria-mediated lithography [31], is schematically illustrated in Fig. 11.3.

By using the tendency of cells to assemble at the interface between organic and aqueous layers, we were able to carry out polymerisation at or around the surface of bacteria under physiological conditions of pH and temperature (Fig. 11.3a). The resultant polymer microcapsules (Fig. 11.3b), bearing imprinted sites complementary in size and shape to the bacterial templates, were reinforced in a second stage by photochemically polymerising cross-linking vinylic monomers in the organic core (Fig. 11.3c). The beads were then reacted with a perfluoropolyether capped with diisocyanate end groups to block residual amine functionality at the surface and to ensure that the imprinted sites became chemically distinct from the bulk (Fig. 11.3d). The penultimate stage involved hydrolysis to remove the templates and thus re-expose the sites, previously occupied by cells, for further modification (Fig. 11.3e). Finally a fluorescent-labelled biological ligand was introduced specifically into these sites using conventional carbodiimide chemistry (Fig. 11.3f).

Each step of this synthetic procedure was followed by confocal laser and/or scanning electron microscopy (SEM) and the corresponding photomicrographs are shown in Fig. 11.4.

Figure 11.4a,b show the microcapsules as initially formed with *Listeria monocytogenes* and *Staphylococcus aureus* attached to the forming polyamide capsule wall. The bacteria, respectively rod and coccoid shaped, were clearly visible on the outside surface of the capsules when labelled with ethidium bromide, as evidenced by confocal optical sections. Variation of the initial bacterial concentration and

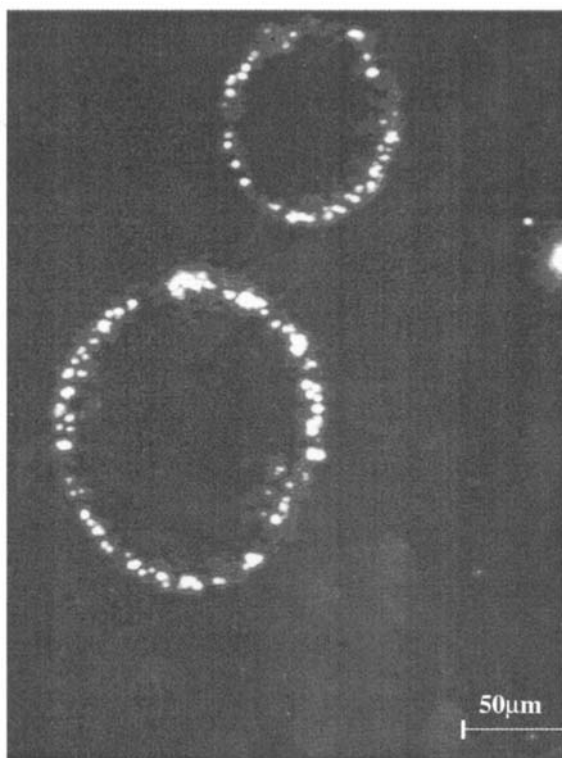


Fig. 11.2. Polymeric microcapsules imprinted with *Listeria monocytogenes*. The image was obtained using laser confocal microscopy. Photograph shows an optical cross-section through capsules. *Listeria* cells were labelled with a fluorescent dye and therefore appear as bright 'dots'.

the polymerisation conditions enabled control of surface coverage by the cells. Polymerisation of the inner core of the capsules by irradiation generated solid beads, as shown in Fig. 11.4c,d. SEM micrographs of the beads showed some variation in the positions of the bacteria, with some cells deeply buried in the outer shell of the polyamide surface whilst the majority appeared to lie only slightly embedded in the polymer wall. However, the presence of deep (100–200 nm) indentations became readily apparent in SEM micrographs after removal of the bacterial templates (Fig. 11.4e,f). Although these “prints” were much less numerous than the more “shallow” functionalised sites, exact size and shape complementarity of these areas to the imprinting microorganisms was clearly observed (Fig. 11.4e shows a *Listeria monocytogenes* bacterium in an imprint site). The lithographic nature of this imprinting process was demonstrated by “developing” the difference in chemical functionality at the newly exposed sites and the bulk of the perfluoropolymer-grafted bead surfaces. Accordingly, free amine and

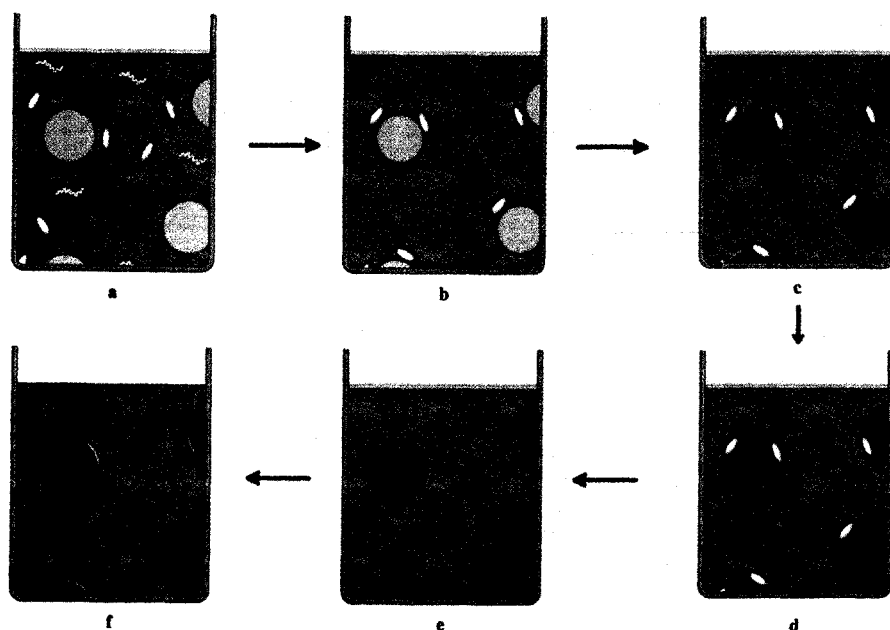


Fig. 11.3. Schematic presentation of the bacteria-mediated lithographic process. A suspension of bacteria (green ovoids) is stirred with water-soluble monomers (shown in white) in a two-phase system (a): the organic solvent is depicted in light grey. Cells partition to the aqueous-organic interface as polyamide microcapsule walls (dark blue) form (b). Acrylic monomers in the organic phase are cross-linked photochemically to give beads with a solid core (dark grey) (c). The polymer beads are reacted with an isocyanate-functional per-fluoropolyether (red); only those areas which are not covered by bacteria are blocked by the reagent (d). The cells are removed to expose imprint sites (e), and the functionality in the sites is developed by reaction with a fluorescent label or affinity ligand (yellow) as the final stage of the lithographic process (f).

carboxyl groups arising from the unmodified polyamide surfaces at the imprint sites were reacted with a fluorescent-labelled lectin (FITC-Concanavalin A) *via* 1-ethyl-3-(3-dimethylaminopropyl)carbodiimide coupling. In this way, the functionality in the imprinted areas was chemically amplified, i.e. the lithographic image of the cells on the polymer surface was enhanced and developed *via* use of the fluorescent label (Fig. 11.4g,h). Although in this case a broad specificity lectin was introduced at the sites, the same procedure could be used for the introduction of more particular affinity ligands (for example antibodies) for selective recognition of the template microorganism.

Even a brief examination of these figures shows that we have successfully reproduced the size and the shape of the cells (in this case *Listeria*



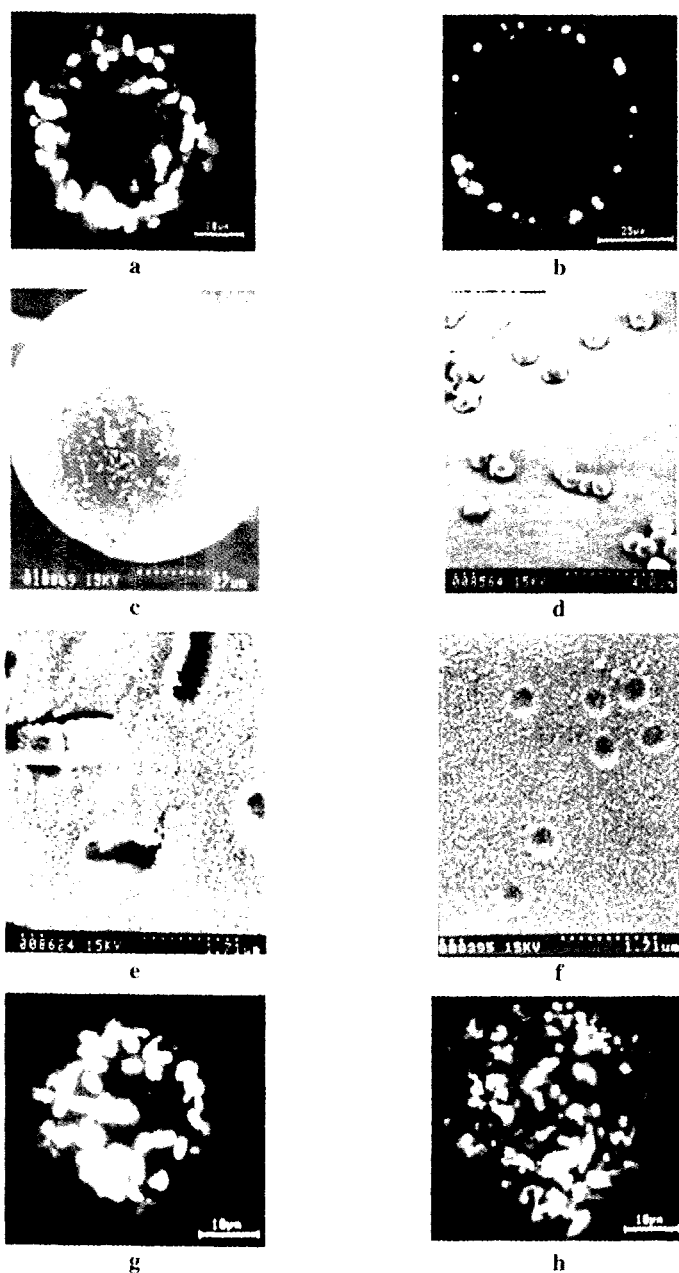


Fig.11.4. Laser confocal and SEM of the materials prepared according to the process depicted in Fig. 11.3. Photographs show individual stages in the cell-mediated lithography of polymer surfaces using *Listeria monocytogenes* (left column: a, c, e, g) and *Staphylococcus aureus* (right column: b, d, f, h) as templates. Imprinted microcapsules (a, b) and solid polymer beads before (c, d) and after (e, f) the removal of template cells. (g, h) Show the imprint sites after reacting the beads with fluorescent-labelled Concanavalin A.

*monocytogenes*) and, most importantly, differentiated the functionality within the sites from that of the rest of the surface. The areas of brightness in Fig. 11.4g,h correspond to the sites previously occupied by bacteria and hence retaining amine functionality and reactivity to the fluorescent lectin FITC-Concanavalin A, whilst the non-imprinted areas were unreactive. It is therefore perfectly feasible to produce anisotropic polymers functionalised with affinity ligands in well defined clusters and, at the same time, suppress any non-specific interactions of microorganisms with the rest of the surface by chemical means. It is also apparent, from a more careful examination of the synthetic protocol described in Fig. 11.3, that the microorganism templates are, in effect, used as protecting groups in a manner analogous to those in conventional organic chemistry, in this case to mask the functionality of the underlying surface. This is why in our original publications [32] we called this process "bacteria-mediated lithography".

An obvious question which arises from this work is how useful these materials can be in practice. We have performed a brief assessment of the beads in microbiological assays and found that there was some discrimination between microorganisms on the basis of their size and shape. Thus, the beads imprinted with *Listeria monocytogenes* showed better adsorption of this microorganism than materials prepared with *Staphylococcus aureus* by a factor of two. Conversely, the latter showed about an eight-fold preference for *Staphylococcus* over *Listeria*. This relative "bias" toward *Staphylococcus* is not too surprising, as this microorganism is smaller than *Listeria* and is round rather than rod shaped. However, the selectivity observed was clearly insufficient for practical usage in microbiology where the enrichment of cultures (i.e. the selectivity of the method) is often expressed in orders of magnitude. Nevertheless, this result confirmed that it is possible to obtain polymeric materials of identical composition which do discriminate between bacteria on the basis of size and shape.

## 11.4 POTENTIAL APPLICATIONS

It should be stressed that from the very beginning we were aiming to produce materials which would bear biological ligands in the imprinted sites to achieve a reasonable degree of specificity. As the feasibility of introducing proteins into the sites has been established, the incorporation of specific affinity ligands such as antibodies can easily be accomplished using the same chemistry. Of immediate interest of course, is the production of highly selective adsorbents for cell separation and for biomedical, environmental and food analysis of microorganisms. At present this is achieved by using antibodies immobilised on the surface of polymer beads (which usually contain a paramagnetic core to facilitate recovery) [33]. The selectivity of this assay is dominated by two main factors: the specificity of antibodies (or other biological ligands employed) and the non-specific interactions between microorganisms present in the sample and the surface of the beads. The use of a population of target cells as template for the preparation of affinity adsorbents offers several distinct advantages. Firstly, as illustrated in Fig. 11.5 relatively

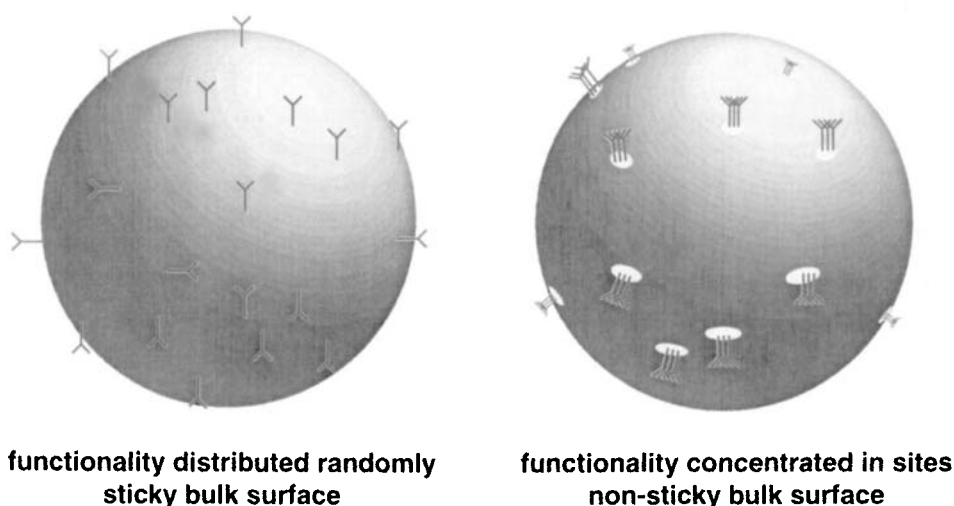


Fig. 11.5. Distribution of functionality in cell-lithographed polymer beads. Anisotropic distribution of chemical functionality in the beads enables affinity ligands (e.g. antibodies) to be placed in 'patches', rather than randomly on the surface.

expensive biological ligands can be directed to where they are most needed, i.e. in discrete binding sites, and concentrated there rather than spread out across the surface.

This should enhance the selectivity of recognition. Secondly, non-specific cell adhesion can be suppressed by rendering the remaining surface chemically inert, in this case by treatment with the diisocyanatoperfluoropolyether. As a result the selectivity of the separation and analysis should be considerably improved compared to more conventional supports. The relative inertness of the bulk of the surface should also prevent aggregation of the beads, thus speeding up and facilitating microbiological analyses in multiphasic matrices, such as food samples or complex biological fluids. In addition, the synthetic methodology allows for magnetite to be incorporated easily into the beads to make them paramagnetic if necessary.

Another potential application of the cell-imprinted polymers is the manufacture of tailor-made substrata for the cultivation of animal cells. These can be prepared either in the form of beads or planar surfaces, analogous perhaps to Petri dishes but containing discrete cell "nests", separated by a layer of non-adhesive polymer to prevent contact between the cells (Fig. 11.6).

It has been shown [34,35] that the prevention of intercellular communication can lead to synchronisation of whole cultures, thus facilitating the production of cell-cycle specific metabolites of pharmaceutical importance. Perhaps a similar approach could be used in pharmacological analysis of drugs and their effects on individual cells rather than on whole tissue.

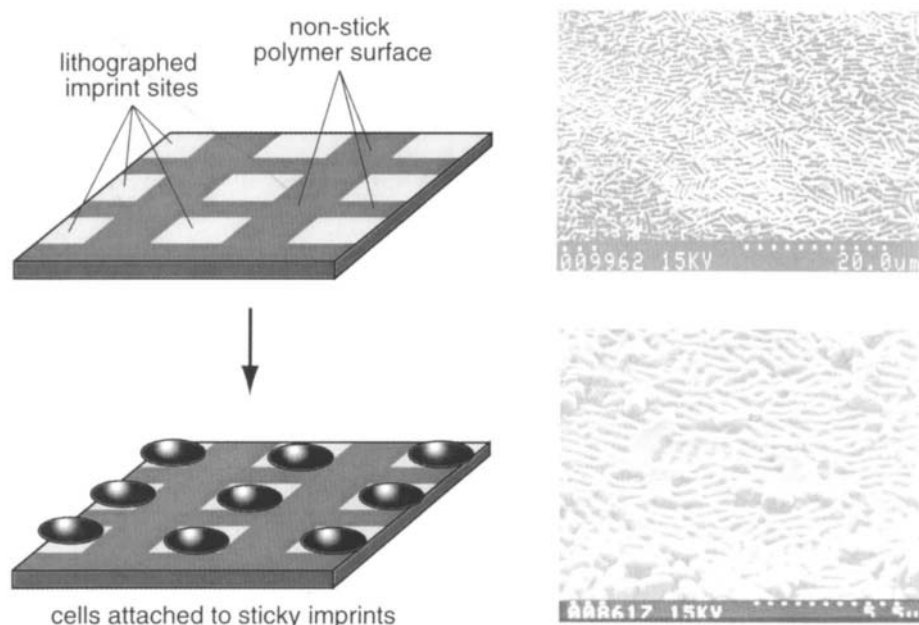


Fig. 11.6. Cell-mediated lithography of planar surfaces. SEM of *Listeria monocytogenes* imprint sites on the surface of a thick polymer film (right). See text for further details.

## 11.5 CONCLUSIONS

In conclusion, a new imprinting methodology has been developed to deal with whole microorganisms by positioning the templates at the loci of interfacial polymerisation and using the cells as protecting groups or lithographic masks for subsequent functionalisation. The obtained anisotropic polymers can be further functionalised with affinity ligands combined in well defined clusters, whilst at the same time suppressing non-specific interactions of microorganisms with the rest of the surface. The polymers can be produced in a range of morphologies to suit particular applications, although it should be stressed that much more effort is still required to bring these or similar materials to the marketplace.

## REFERENCES

- 1 C. Yu and K. Mosbach, *J. Org. Chem.*, **62**, 4057 (1997).
- 2 L.I. Andersson, R. Müller, G. Vlatakis and K. Mosbach, *Proc. Natl. Acad. Sci. USA*, **92**, 4788 (1995).
- 3 O. Ramström, I.A. Nicholls and K. Mosbach, *Tetrahedron: Asymmetry*, **5**, 649 (1994).
- 4 G. Wulff and H.G. Poll, *Makromol. Chem.*, **188**, 741 (1987).
- 5 G.H. Chen, Z.B. Guan, C.T. Chen, T.L. Fu, V. Sundaresan and F.H. Arnold, *Nature Biotechnol.*, **15**, 354 (1997).

- 6 K.J. Shea and D.A. Spivak, *Macromolecules*, **31**, 2160 (1998).
- 7 J. Mathew and O. Buchardt, *Bioconjugate Chem.*, **6**, 524 (1995).
- 8 O. Ramström, L. Ye and K. Mosbach, *Chem. Biol.*, **3**, 471 (1996).
- 9 S.H. Cheong, S. McNiven, A. Rachkov, R. Levi, K. Yano and I. Karube, *Macromolecules*, **30**, 1317 (1997).
- 10 G. Vlatakis, L.I. Andersson, R. Müller and K. Mosbach, *Nature*, **361**, 645 (1993).
- 11 M. Senholdt, M. Siemann, K. Mosbach and L.I. Andersson, *Anal. Lett.*, **30**, 1809 (1997).
- 12 Y. Tomioka, Y. Kudo, T. Hayashi, H. Nakamura, M. Niizeki, T. Hishinuma and M. Mizugaki, *Biol. Pharm. Bull.*, **20**, 397 (1997).
- 13 J. Matsui and T. Takeuchi, *Anal. Commun.*, **34**, 199 (1997).
- 14 F.L. Dickert, H. Besenböck and M. Tortschanoff, *Adv. Mater.*, **10**, 149 (1998).
- 15 M.T. Muldoon and L.H. Stanker, *J. Agric. Food Chem.*, **43**, 1424 (1995).
- 16 M. Kempe and K. Mosbach, *J. Chromatogr. A*, **664**, 276 (1994).
- 17 M. Kempe and K. Mosbach, *J. Chromatogr. A*, **694**, 3 (1995).
- 18 M.T. Muldoon and L.H. Stanker, *Anal. Chem.*, **69**, 803 (1997).
- 19 L.I. Andersson, A. Paprica and T. Arvidsson, *Chromatographia*, **46**, 57 (1997).
- 20 B.A. Rashid, R.J. Briggs, J.N. Hay and D. Stevenson, *Anal. Commun.*, **34**, 303 (1997).
- 21 M. Walshe, J. Howarth, M.T. Kelly, R. O'Kennedy and M.R. Smyth, *J. Pharm. Biomed. Anal.*, **16**, 319 (1997).
- 22 S.E. Byström, A. Börje and B. Åkermark, *J. Am. Chem. Soc.*, **115**, 2081 (1993).
- 23 G. Wulff, T. Gross and R. Schonfeld, *Angew. Chem. Int. Ed. Engl.*, **36**, 1962 (1997).
- 24 J. Matsui, I.A. Nicholls, I. Karube and K. Mosbach, *J. Org. Chem.*, **61**, 5414 (1996).
- 25 X.-C. Liu and K. Mosbach, *Macromol. Rapid Commun.*, **18**, 609 (1997).
- 26 S. Starodub, S.A. Piletsky, N.V. Lavryk and A.V. Elskaya, *Sens. Actuators B*, **18-19**, 629 (1994).
- 27 D. Kriz, O. Ramström and K. Mosbach, *Anal. Chem.*, **69**, A345 (1997).
- 28 M.J. Whitcombe, C. Alexander and E.N. Vulfson, *Trends Food Sci. Technol.*, **8**, 140 (1997).
- 29 D.R. Shnek, D.W. Pack, D.Y. Sasaki and F.H. Arnold, *Langmuir*, **10**, 2382 (1994).
- 30 S. Hjerten, J.L. Liao, K. Nakazato, Y. Wang, G. Zamaratskaia and H.X. Zhang, *Chromatographia*, **44**, 227 (1997).
- 31 C. Alexander, A. Aherne, M.J. Payne, N. Perez and E.N. Vulfson, *J. Am. Chem. Soc.*, **118**, 8771 (1996).
- 32 C. Alexander and E.N. Vulfson, *Adv. Mat.*, **9**, 751 (1997).
- 33 J. Ugelstad, A. Berge, T. Ellingsen, R. Schmid, T.N. Nilsen, P.C. Mork, P. Stenstad, E. Hornes and O. Olsvik, *Prog. Polym. Sci.*, **17**, 87 (1992).
- 34 R. Singhvi, A. Kumar, G.P. Lopez, G.N. Stephanopoulos, D.I.C. Wang, G.M. Whitesides and D.E. Ingber, *Science*, **264**, 696 (1994).
- 35 B.J. Spargo, M.A. Testoff, T.B. Nielson, D.A. Stenger, J.J. Hickman and A.S. Rudolph, *Proc. Natl. Acad. Sci. USA*, **91**, 11070 (1994).

## **Polymerisation techniques for the formation of imprinted beads**

ANDREW G. MAYES

### **12.1 INTRODUCTION**

As the molecular imprinting technique has developed, much effort has been directed towards understanding the nature of the imprinting process and optimising parameters that affect the quality of the final imprinted receptor sites. Relatively little effort has been expended in developing polymerisation methods that would be amenable to mass-production, or in producing polymer particles with improved characteristics for particular end-uses such as chromatography or solid-phase extraction. Since most of the research has originated from academic research groups, the need to optimise the polymer production process and the yields obtained has been of secondary importance compared with developing greater understanding of the mechanism of the imprinting process and exploring new concepts and opportunities offered by this rapidly developing research area. As practical applications emerge, however, this balance will begin to change and convenient production methods will become more important.

The majority of work in the molecular imprinting field has relied on production of blocks of imprinted polymer in some type of mould (usually a glass tube). The block of polymer is subsequently crushed, ground and sieved, either manually or mechanically, before being used for evaluation of the imprinted receptors obtained. While this has proved adequate for academic study, it is inappropriate for larger scale production and has probably compromised the quality of many of the results obtained, particularly in chromatographic evaluation. Grinding and sieving is slow and produces irregular particles with rather limited control over particle size and shape. This depends on the nature of the polymer and the method used for grinding/crushing. Very small particles are subsequently removed by differential sedimentation after suspension in a solvent. This is wasteful and relatively slow, although on a larger scale it could no doubt be improved by an air-flow fractionation technique. The resulting fractionated particles pack poorly in columns and have rather low efficiency and high back pressures when used in chromatography. Direct production of imprinted polymer beads, in contrast, is rapid and gives an almost quantitative yield of useable particles. Beaded particles pack much more efficiently in columns and give better flow properties and low back pressures. Beads are also much more physically robust and are less prone to fragmentation and fines production during handling than sharp-edged crushed fragments. Finally,

production of beads offers some operational advantages, such as the ability to scale up UV initiated polymerisations, and to recover valuable template molecules for recycling due to the ease of particle recovery and washing.

Since molecular imprinting is now maturing towards the point where it can be usefully integrated into real-world applications, the need to produce materials cheaply, efficiently and reproducibly in beaded form is becoming much more pressing. This chapter reviews progress in this direction, critically discussing the methods available with reference to published work, and offering some pointers to probable future development.

## **12.2 SPECIAL CONSIDERATIONS RELEVANT TO MOLECULARLY IMPRINTED BEADS**

When considering the suitability of a bead production technique for imprinting, it is essential to evaluate the compatibility of the conditions used for polymerisation with those required for complex formation between functional monomers and templates. Where covalent imprinting methods are used, the covalent adducts are often highly stable and need quite harsh conditions to disrupt them. Such adducts could be used in most of the procedures described below with reasonable expectation of success. The same can be said for many metal-chelate complexes, which have stabilities approaching covalently bonded structures. The use of cyclic boronate esters is an exception. This adduct is unstable in water and hence cannot be combined efficiently with aqueous suspension polymerisation.

Where non-covalent approaches are used, much more care needs to be taken. If the interaction between template and monomers is predominantly through hydrogen bonding, methods involving the use of water or other strongly hydrogen bonding solvents are probably best avoided. In this case, competition between solvent and monomers will, at best, compromise the imprinting effect and, at worst, eliminate it entirely. Where ion-pairing is involved the situation is less clear-cut. In general it is still best to avoid highly polar environments, but these can be tolerated in some cases and satisfactory results have been achieved. In practice, many templates rely on a balance of hydrogen bonding, ion-pairing and also hydrophobic interactions to define the receptor sites. In such cases the solvent environment will clearly alter the contributions made by the different types of interactions and it is not always easy to predict the effect that changing solvent environments will have. For instance, imprinting of the herbicide 2,4-D gave surprisingly good results when carried out in a methanol/water mixture [1].

Another issue that must be addressed with suspension methods is that of partitioning of the various components in the two phases. Where all components of the imprinting mixture are very hydrophobic this should cause little problem, but for many templates and functional monomers a significant fraction of material could partition into the aqueous phase. This can be minimised by judicious choice of pH and ionic strength, but some compromises may be necessary due to the number of different components present. In theory, any partition effect can be predicted and

allowed for when calculating the amounts of each component to add, but this assumes the availability of all the necessary partition coefficients and neglects possible synergistic effects. In practice it is an additional parameter that will probably need to be optimised experimentally.

### **12.3 TECHNIQUES THAT HAVE BEEN USED TO MAKE MOLECULARLY IMPRINTED BEADS**

A wide range of techniques is emerging for making imprinted polymer beads. Some of the techniques are very general in their application, while others are only applicable to certain situations, mostly for reasons related to the issues discussed in the previous section. The approaches tested to date are summarised in Table 12.1, together with some of the advantages and disadvantages of each method. Each method is discussed in much greater detail in a subsequent section, where references to the primary literature can also be found.

### **12.4 IMPRINTED BEAD PRODUCTION METHODS**

#### **12.4.1 Utilising the pores in preformed beads (method I in Table 12.1)**

In this technique preformed porous beads are used as 'micro-vessels' in which to carry out small scale bulk polymerisations. Both inorganic (silica) [2–4] and organic (trimethylol propane trimethacrylate (TRIM) [5] beads have been used. Since bead formation is separated from the imprinting procedure in this case, the beads can be synthesised under any appropriate conditions to give the desired size, porosity and surface properties. Silica and controlled pore glass beads with a wide range of sizes and porosities are available commercially. Methods for synthesising suitable TRIM beads are described in the literature [6,7]. The porosity of these beads could probably be further improved by optimising the porogenic solvent mixture, as has been done for styrene-based polymers. Monodisperse beads made by aqueous two-step swelling procedures would give better uniformity and methods for this are available in the literature.

Cross-linked beads made by vinylic polymerisations usually have some residual polymerisable functionalities [8], which allows the secondary imprinting polymerisation to covalently attach to the bead structure giving very stable particles. Where glass or silica is used a pretreatment with vinyl [9] or methacryloxy [2] silane derivatives ensures stable covalent attachment, while at the same time blocking surface silanol groups which might otherwise interfere with imprinting.

In a typical procedure, the beads are mixed with an imprinting mixture (containing somewhat more solvent than usual) and mixed for some time with application of mild vacuum and/or sonication to ensure penetration of the mixture into the pore structure. The slurry is then heated to initiate polymerisation. After completion the beads are extensively washed and treated as for ground particles.



TABLE 12.1

## TECHNIQUES FOR MAKING IMPRINTED POLYMER BEADS

| Polymerisation method   | Complexity | Product                          | Advantages   | Disadvantages   |
|---|------------|----------------------------------|--|---|
| I<br>Bulk — in bead pores<br>(may fill the pores or just coat<br>the surfaces of the pores) | Medium     | Depends on<br>original beads     | Much better particle shape<br>than ground bulk polymer<br>Direct transfer of bulk<br>polymer recipes<br>Better chromatographic<br>packings | Careful preparation required<br>Volume of bead reduces<br>volume of<br>imprinted polymer per unit<br>column<br>Expense of original beads  |
| IIa<br>Suspension — in water  | Medium     | Spherical beads,<br>polydisperse | Highly developed technology<br>with huge literature base<br>Highly reproducible results<br>Large scale possible<br>High quality beads      | Water is incompatible with<br>most non-covalent imprinting<br>procedures<br>Only possible for some<br>covalent and metal chelate-<br>based processes<br>Phase partitioning of<br>monomers complicates<br>system |
| IIb<br>Suspension — in<br>perfluorocarbon   | Medium     | Spherical beads,<br>polydisperse | Dispersant does not interfere<br>with imprinting<br>All methods possible<br>Good quality beads produced                                    | Expense of liquid<br>fluorocarbons (can be reused)<br>Specialist surfactant polymers<br>required<br>Little literature or<br>optimisation to date  |

|  |        |  |  |  |
|--|--------|--|--|--|
| III.<br>Non-aqueous dispersion   | Low    | Random aggregates or precipitates (could be monodisperse beads if stabilisers are present) | Simple<br>Amenable to many types of columns and tubes<br>No processing necessary   | Random aggregates produced<br>Outcome very dependent on solvents used<br>Only charged Ts gave good results<br>Little literature for imprinting |
| IV.<br>Two-stage swelling  | High   | Monodisperse beads   | Monodisperse beads<br>Excellent packing for HPLC<br>Well established method  | Need for aqueous emulsions compromises many imprinting processes and templates<br>Little literature for imprinting                             |
| V.<br>Aerosol polymerisation   | Medium | Spherical beads, polydisperse  | Inexpensive dispersant<br>No interfering interactions from dispersant or surfactants   | Only demonstrated for a very atypical imprinting system to date  |
| VI.<br>Surface rearrangement of latex (latex obtained from seeded emulsion polymerisation) | High   | Near-monodisperse beads  | Monodisperse product<br>Special opportunities offered by the surface imprinting process (rapid kinetics, site accessibility) | Mechanism used rules out most templates<br>Only demonstrated for metal ions<br>Few examples to date  |

The main benefit of this technique lies in the fact that it is, in chemical terms, essentially identical to bulk polymerisation. Any recipe which has been optimised by grinding and sieving of bulk materials could be transferred directly to the pores of preformed beads. The main drawback is that quite careful experimental technique is required when filling the pores and carrying out the polymerisation to avoid undue aggregation of beads. The final volume of imprinted polymer is also obviously limited by the space occupied by the original bead structure. This could range from about 5% to 40% or more. Suitable beads with low polydispersity can also be quite expensive, which makes the technique unattractive for some applications.

When packed into chromatography columns, TRIM beads imprinted with Boc-L-Phe were shown to have column efficiencies and separation abilities superior to ground and sieved bulk material [5]. The theoretical plate number was approximately double that obtained with conventional crushed polymer under the same conditions and the resolution of a racemate was also slightly enhanced. The difference, however, was not that great considering the additional preparation time and effort involved.

Plunkett and Arnold [3] reported imprinted supports based on metal-chelate interactions made in the pores of 10  $\mu\text{m}$  Lichrosphere beads. These were highly stable, even after prolonged use for several hundred hours, and achieved reasonable separations of related *bis*-imidazole model compounds. Unfortunately no direct comparison with the performance of bulk-imprinted material was presented. A photograph of part of a silica bead containing imprinted polymer is shown in Fig. 12.1.

This technique undoubtedly produces beaded materials with reasonable separation abilities and better packing and flow properties than ground and sieved bulk

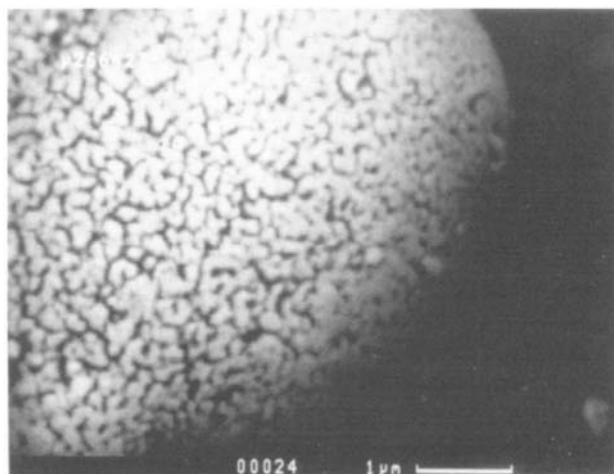


Fig. 12.1. Electron micrograph of part of a 10  $\mu\text{m}$  Lichrosphere bead containing imprinted polymer in its pores (from [3]).

material. The improvement, however, is marginal considering the additional effort and expense involved and this technique will probably be superseded as other techniques are developed further.

#### 12.4.2 Suspension polymerisation in water (method IIa in Table 12.1)

Suspension polymerisation methods for producing beaded polymers from acrylic and styrene-based monomers are very well established processes [10,11]. They are typically used in the production of ion exchange resins and supports for solid-phase synthesis. Methods have been extensively optimised over the years, but unfortunately such optimisations tend to be more art than science, since there are so many operational variables. Factors such as reactor geometry and impeller design must be set alongside the physical conditions used and the chemical composition of the monomer mixture and colloidal stabilisers. In practice, however, reasonable results can be obtained using a wide range of conditions, although the polydispersity of the product will probably be higher when using small scale reactors and sub-optimal conditions. The process is relatively easy to perform and many suitable recipes can be found in the literature. Indeed, this method was used to make imprinted beads in a number of the early studies into molecular imprinting when rather stable covalently bonded adducts, such as carboxylate esters [12,13] or metal chelates [14], were used as templates. With such templates there is no problem with interference by water and a conventional suspension polymerisation works well. This is also true of the 'sacrificial monomer' approach recently introduced by Whitcombe *et al.* [15] and they have reported cholesterol-imprinted beaded polymers made using aqueous suspension polymerisation [16], although no comparative binding studies have been published to date. A photograph of cholesterol-imprinted beads made by conventional suspension polymerisation is shown in Fig. 12.2.

In a typical procedure the organic-based imprinting mixture is mixed with 4–10 volumes of water containing a suitable suspension stabiliser. This is most often a polymer such as poly(vinyl alcohol) or poly(vinylpyrrolidone). The two phases are then vigorously mixed by stirring or homogenising to produce a suspension of small organic droplets in the aqueous dispersant. The final bead size is largely determined by the size of these droplets, which in turn is determined by the shear force used during mixing, together with the nature and volumes of the phases and the type and amount of stabiliser used. In practice results are very dependent on reactor design and geometry and external factors such as temperature, as well as the above parameters, so most systems are optimised empirically to give the desired outcome.

As well as the more common oil in water suspension methods, it is also possible to make stable water in oil suspensions by choosing alternative surfactants with much lower hydrophilic/lipophilic balance values, combined with solvents such as hydrocarbons as the dispersing phase. These can be used to make beaded polymers from water-soluble monomers such as acrylamide. Although little work has been done to date with imprinting in aqueous conditions (using hydrophobic interactions

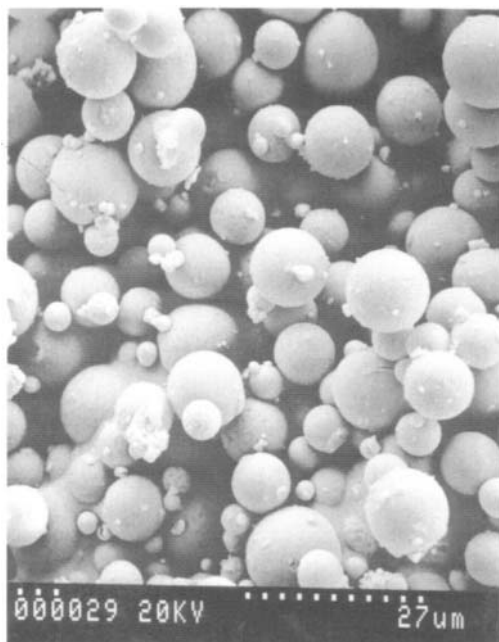


Fig. 12.2. Electron micrograph of EDMA beads covalently imprinted with cholesterol made by conventional suspension polymerisation in water using poly(vinyl alcohol) as stabiliser and a dioctyl phthalate/decane mixture as porogen (M.J. Whitcombe, unpublished).

or metal chelates for example), it may well be a useful method in the future and it is convenient that technology already exists for bead production.

#### **12.4.3. Suspension polymerisation in fluorocarbon liquids (method IIb in Table 12.1)**

When non-covalent imprinting is to be used, the nature of the suspension medium becomes much more critical, as discussed in the introductory comments. In order to try to overcome the problem posed by the presence of water, the author proposed a novel approach based on the use of a liquid fluorocarbon phase to disperse the droplets of imprinting mixture [17]. A similar approach was independently adopted by another worker [18] but was not applied to molecular imprinting. Liquid fluorocarbons are immiscible with most other organic compounds (with the exception of some highly halogenated molecules that have significant solubility). They are also non-toxic and chemically inert and thus do not interfere with the interactions used in non-covalent imprinting. These liquids appeared ideal as suspension media for all types of imprinting and the process seemed to offer a universal solution. A number of hurdles needed to be overcome, however, before the concept could be realised.

The main problem encountered was the stabilisation of the suspension of the

imprinting mixture in the fluorocarbon liquid. This was hindered by the high density of the fluorocarbon, which caused 'creaming' and favoured droplet coalescence. No literature existed on making such suspensions and this necessitated the design, synthesis and testing of a range of novel polymeric surfactants, the most successful of which were graft copolymers with a perfluorosulphonamidoethyl acrylate backbone and methoxypolyethylene glycol grafts of medium length (MW  $\sim 2000$ ) [17]. These worked very well for UV initiated polymerisations in chlorinated solvents such as chloroform or dichloroethane. When other solvents were used, however, the beads were of poorer quality, and the suspension broke down at higher temperatures. Further optimisation of the surfactants [19], changing the length and ratio of the polyethylene glycol (PEG) grafts and the substitution of a stearyl ether terminal group on the PEG produced superior results in solvents such as toluene and also enabled thermal polymerisations at 45°C to be achieved reliably.

In recent work (A.G. Mayes, in preparation) it has been found that the suspension stabilisation problem can be largely overcome by speeding up the polymerisation procedure, so that gelling has taken place before the suspension has time to break down. By introducing efficient photoinitiators designed specifically for UV photopolymerisation (e.g. dimethoxyphenyl acetophenone) and higher intensity UV sources, the polymerisation can be completed in less than 5 min. In this time frame, even suspensions made using acetonitrile as porogenic solvent are stable enough to produce beads using the originally described surfactant [17]. Beads of imprinted ethylene glylate (EDMA)/methacrylic acid (MAA) polymers, produced by this method using toluene, chloroform and acetonitrile as porogenic solvents, are shown in Fig. 12.3.

An advantage of UV initiated suspension polymerisation is that since the droplets are small and vigorously mixed they all come close to the reactor wall and the UV source as polymerisation proceeds. Thus, although the suspension is white and not transmissive, initiation is still efficient and polymerisation is rapidly

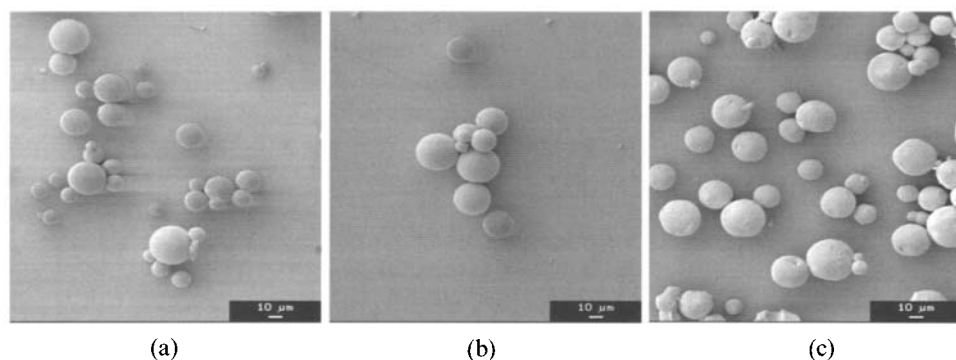


Fig. 12.3. Electron micrographs of imprinted beads produced by suspension polymerisation of typical EDMA/MAA imprinting mixtures in a liquid fluorocarbon. The porogenic solvents were (a) toluene, (b) chloroform and (c) acetonitrile.

completed. This is in sharp contrast to UV initiated bulk polymerisations where polymerisation is efficient near the tube walls but much less efficient in the centre. This is often manifested as different textures and hardnesses when the polymers are crushed. It is not clear what effect this has on material performance. If the benefits of low temperature UV initiation are to be realised on a larger scale, however, suspension polymerisation offers a viable option.

Beads made using the perfluorocarbon suspension method have been shown to have good chromatographic properties in model studies using Boc-Phe as template [17]. Particularly good flow properties were achieved for both EDMA- and TRIM-based polymers, with low back pressures compared with crushed bulk polymers. Separations were comparable with conventional crushed bulk materials at low flow rates and gave almost identical  $\alpha$ -values and resolution factors. The beaded polymers also gave satisfactory results at much higher flow rates where conventional materials cannot operate. Typical chromatograms showing the chiral resolution of Boc-Phe by 5.7  $\mu\text{m}$  TRIM beads imprinted with Boc-L-Phe are shown in Fig. 12.4.

Beads made in a similar way were also assessed for their performance in radioligand binding assays. Initial work used imprinting of diazepam as a model system (A.G. Mayes, unpublished), but the performance was disappointing due to the high level of non-specific binding to the beaded reference polymer. In subsequent work developing the perfluorocarbon suspension polymerisation system, Ansell and Mosbach achieved improved results for radioligand binding assays by imprinting of propranolol in a TRIM-based polymer, using toluene as porogenic solvent together with a modified surfactant and thermal initiation [20]. Magnetic imprinted beads were also produced by including finely divided magnetite particles in the polymeri-

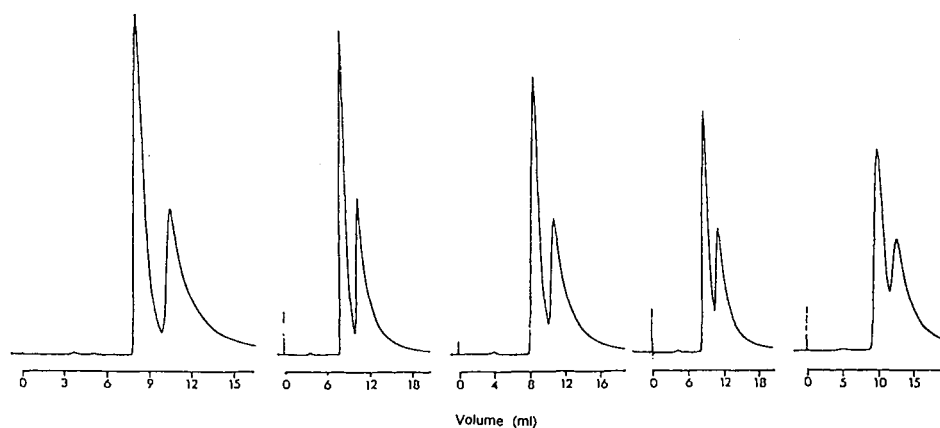


Fig. 12.4. HPLC traces showing separation of 1 mg tert-butoxycarbonyl D,L-phenylalanine on a 25 cm  $\times$  4.6 mm diameter column of 5.7  $\mu\text{m}$  TRIM beads. The flow rates were (left to right) 0.5, 1, 2, 3 and 5 ml/min. Good separation was achieved even at high flow rates where ground and sieved material performs poorly (from [17]).

sation mixture. Levels of non-specific binding were still high relative to ground material, but it was demonstrated that a useable assay could be achieved with both magnetic and non-magnetic beads. Magnetic beads should be useful in solid-phase extraction and binding assays where they can be mixed and recovered using electromagnetic devices, such as those manufactured and marketed by Dynal for this purpose.

The reason for the high levels of non-specific binding has not been reported to date, but is believed to be due to covalent grafting of a layer of fluorinated surfactant onto the bead surface during the polymerisation procedure. This phenomenon is currently being investigated and new surfactants designed and synthesised, where the fluorocarbon components can be removed after polymerisation to leave a much cleaner bead surface with lower non-specific binding characteristics.

Using a similar philosophy to the perfluorocarbon liquid approach, Piletsky carried out suspension polymerisations in silicone oil. This liquid is also immiscible with some organic liquids, although the range of immiscible combinations is much smaller than for perfluorocarbons. Beads were successfully produced containing imprints of ATP and poly-A in an EDMA/*N,N*-diethyl-2-aminoethylmethacrylate system with DMF as solvent and an excess of silicone oil as dispersant [21].

#### 12.4.4 Dispersion polymerisation methods (method III in Table 12.1)

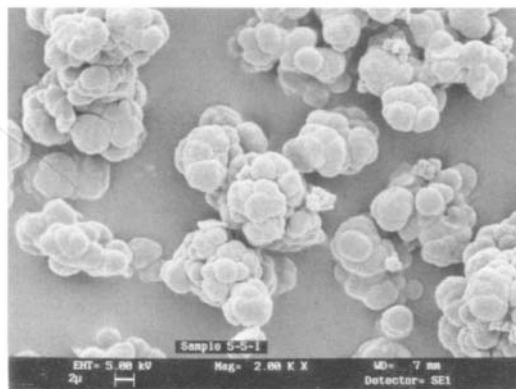
Many dispersion polymerisation methods have been described in the literature for production of beaded polymer particles made from styrene- and acrylate-based monomers [22]. The solvents used range from highly polar alcohols [23,24] to very apolar hydrocarbons [25] so it might be supposed that this methodology could be adapted readily to the synthesis of molecularly imprinted beads. The methods used usually include a colloidal stabiliser, which protects the growing particles from coalescence. The resulting particles are spherical and near monodisperse. The size range varies depending on the exact conditions and recipe used but typically falls in the 2–6  $\mu\text{m}$  range. Even larger beads have been achieved in some cases.

In a typical procedure monomers and initiator are dissolved in the appropriate solvent or solvent mixture together with a colloidal stabiliser, which is usually a polymer. The mixture is purged with inert gas to remove oxygen, then heated to initiate polymerisation, usually with gentle agitation or stirring. After completion of polymerisation the particles are recovered by filtration, sedimentation or centrifugation and washed.

Unfortunately, to date, this technique has received little attention from the molecular imprinting community and only one report of a dispersion polymerisation method had appeared until very recently [26]. This is probably better classified as a precipitation polymerisation, since random aggregates were produced rather than beads. No colloidal stabilisers were included in this procedure. The aggregates were made *in situ* in chromatography columns, which avoided the need to grind and sieve the polymer and pack the columns. Due to the rather polar nature of the solvent mixtures used (cyclohexanol, dodecanol, isopropanol), good imprints were only achieved for compounds which interact strongly with functional monomer



A.



B.

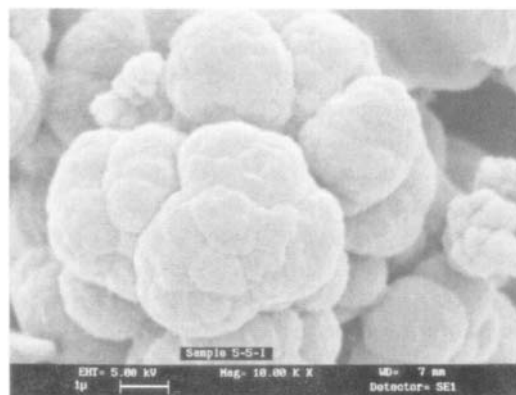


Fig. 12.5. Electron micrographs of dispersion/precipitation polymers imprinted with pentamidine in isopropanol–water. Magnification in (A)  $2000\times$  and in (B)  $10,000\times$ . (From [26])

(MAA in this case), such as pentamidine and atrazine. In this respect the method is limited in the range of templates which can be used, but the preparation is very convenient and avoids grinding and sieving, although some adjustment of column lengths was required as the material compacted under flow. Photographs of typical particles produced by this techniques are shown in Fig. 12.5.

In an attempt to realise imprinted polymers using the dispersion method, the author has made beaded particles using normal imprinting mixtures containing two different templates, Boc-L-Phe and morphine, polymerised in a 1:1 mixture of chloroform and heptane. In the presence of appropriate surfactants, near monodisperse beads of about  $2\text{ }\mu\text{m}$  diameter were produced. The Boc-L-Phe beads were packed into chromatography columns and showed excellent flow properties, but unfortunately no imprinting effect could be measured. Similar negative result were recorded for the morphine beads when assayed by radioligand binding.

Greater success has been achieved, however, using propranolol and theophylline as templates in EDMA/MAA or divinylbenzene (DVB)/MAA polymers using

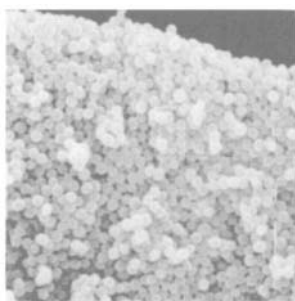


Fig. 12.6. Electron micrograph of  $17\beta$ -estradiol-imprinted TRIM/MAA latex made by dispersion polymerisation in acetonitrile (from [27])

heptane as the dispersion solvent (K. Haupt, personal communication). Bead quality was quite poor, with many aggregates present, but the material gave similar results to bulk polymers in radioligand binding assays.

Recently, sub-micron polymer lattices imprinted with theophylline and  $17\beta$ -estradiol have been successfully synthesised by precipitation polymerisation in acetonitrile [27]. The particles were both spherical and monodisperse and were obtained in high yield. Binding properties of the beads were shown to be similar to conventionally imprinted materials, although the capacity was higher and equilibration times lower, presumably due to better accessibility of the binding sites in these very small particles. A photograph of the  $17\beta$ -estradiol-imprinted latex is shown in Fig. 12.6.

Overall, the dispersion polymerisation approach might offer an effective solution to bead production in many situations if the precise balance of solvent composition, imprinting recipe and synthetic conditions can be appropriately matched to produce particles with the desired size, morphology, porosity and binding characteristics.

#### 12.4.5 Aqueous two-step swelling method (method IV in Table 12.1)

Aqueous two-step swelling is a technique for producing monodisperse polymer particles over a size range much greater than that achievable by direct dispersion polymerisation. The properties of the particles, such as porosity, can also be controlled. The concept was first introduced by Ugelstad and Mørk [28] and has since been adopted by many workers. It is used to produce a number of commercial products for chromatography and bioseparations, such as 'Mono-beads' by Pharmacia and 'Dynabeads' by Dynal.

The technique involves first producing a 'seed' latex by emulsifier-free emulsion polymerisation. A polystyrene latex of about  $1\ \mu\text{m}$  diameter is usually used. The seed particles are initially swollen using a microemulsion of a free radical initiator and a low molecular weight 'activating solvent', such as dibutyl phthalate, emulsified in water by sonication using sodium dodecyl sulphate as stabiliser. The seed

particles are stirred gently with the emulsion for a number of hours until the emulsion droplets are absorbed into the seed particles.

The swollen particle dispersion is then added to a second dispersion containing monomers, cross-linkers, porogenic solvents and templates dispersed in water using a polymeric stabiliser such as polyvinyl alcohol containing about 10% residual acetate groups. The mixture is again stirred for several hours until the monomer containing droplets have been absorbed into the seed particles. The dispersion is then purged with inert gas to remove dissolved oxygen and raised to polymerisation temperature where it is held for 24 h. The beaded polymer particles are finally washed with a range of solvents prior to use. For HPLC application beads of about 5  $\mu\text{m}$  are typically produced, but the technique is capable of yielding particles up to 100  $\mu\text{m}$  or more by changing the levels of activating solvent and the volume ratios of the various dispersion phases.

The first report of aqueous two-step swelling applied to molecular imprinting was by Hosoya *et al.* in 1994 [29]. In this report diaminonaphthalenes were imprinted. The beaded polymers produced had separation abilities comparable with those previously reported for the same templates imprinted by bulk polymerisation in rods [30], but with much better column efficiencies and peak shapes. The templates used are very hydrophobic and interact strongly with the MAA monomer used, hence the system seems to imprint effectively even in the presence of water saturated droplets (since the monomer phase must be in equilibrium with the dispersing phase after 12 h mixing). A more detailed methodological description of the two-step swelling process as applied to imprinting is given in [31], where a novel chiral monomer is also introduced. This chiral monomer was further evaluated with respect to its ability to achieve enantioseparations when imprinted with a racemic template [32], again using the two-step swelling procedure to produce beads for chromatographic evaluation. A photograph of the near-monodisperse imprinted beads produced by this technique is shown in Fig. 12.7.

The same group has also reported the imprinting of naproxen using vinyl pyridine as functional monomer [33,34]. This is a more interesting result in the

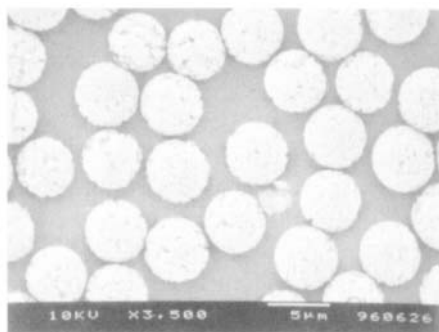


Fig. 12.7. Electron micrograph showing near-monodisperse imprinted beads made using the aqueous two-step swelling procedure (K. Hosoya, unpublished).

sense that the template is more typical of the types of template most often imprinted. Again, the imprinting effect was comparable with that achieved using conventional bulk polymerisation [35]. As with the diaminonaphthalenes discussed above, a strong ion-pair interaction is important in the recognition process, together with hydrophobic interactions. This is also true for another example [36] where propranolol was imprinted, although in this case the base is presented by the template and the acid by the functional monomer. It would be interesting to see whether templates relying purely on hydrogen bonding could still be imprinted in this system where the monomer phase is water saturated. The imprinting of  $17\beta$ -estradiol using two-phase swelling comes close to this, using a mixture of hydrophobic interaction and hydrogen bonding [37]. It could also be anticipated that highly water-soluble templates would be problematic in this system, although the partitioning could theoretically be overcome by adding a sufficient excess (providing this was economically feasible and did not destabilise the dispersion).

The two-step swelling technique provides a useful route to high quality chromatographic packings and appears to be applicable to a range of relatively hydrophobic compounds containing at least one ion-pairing functionality. Fortunately a large number of drugs fall into this category. Based on chromatographic  $\alpha$ -values, the recognition achieved by these beaded polymers is very similar to those for equivalent crushed bulk polymers. Disappointingly, the plate numbers and peak shapes are not greatly improved, despite the highly uniform packing. This is probably due to more complex factors such as diffusion and kinetic limitations, coupled with low binding site density and heterogeneity [38].

#### 12.4.6 Aerosol polymerisation methods (method V in Table 12.4)

Polymerisation of droplets of imprinting mixtures as aerosols rather than as suspensions in a liquid offers some very significant advantages. The need for large volumes of dispersant liquid is removed and there is no problem with interference from the dispersing fluid. Inert gases such as nitrogen or carbon dioxide are inexpensive and would allow radical polymerisations to proceed. Also, no surfactants are required so the particles produced would have very clean surfaces. To date, however, no reports linking this technique with conventional molecular imprinting using methacrylate or styrene systems have appeared, although related monomers have been polymerised successfully by this approach [39].

The use of cationically initiated aerosol polymerisation has been applied to a novel monomer system for molecular imprinting. The polymerisation of a *bis*-epoxysilicone monomer using 4-(octyloxy)phenylphenyliodonium hexafluoroantimonate as a UV activated initiator was studied with thebaine (a morphine derivative) used as template [40]. This system polymerises very rapidly (only a few seconds are required) and is not inhibited by oxygen, hence aerosols can be generated in air. Beaded polymers with a size range from 10 to 70  $\mu\text{m}$  were produced, templated with thebaine. The size distribution could probably be improved by using more sophisticated aerosol generation (a simple spray gun was used in this case). Template extraction was rather inefficient relative to conventional materials, with

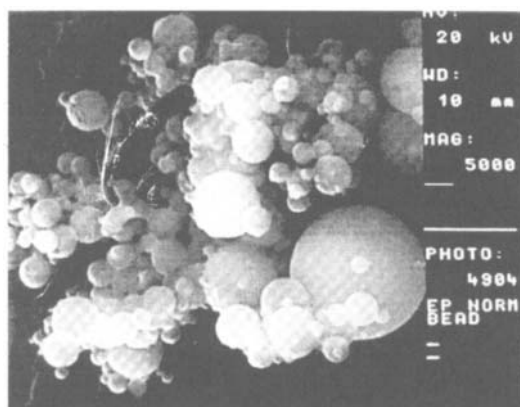


Fig. 12.8. Electron micrograph of epoxysilicone beads imprinted with thebaine made by aerosol polymerisation in air (from [39]).

only 32% recovered, but in rebinding studies the templated polymers had a capacity slightly higher than conventional materials imprinted with morphine [41]. Typical beads produced by this novel approach are shown in Fig. 12.8.

Unfortunately, a variety of chemical functionalities, including carboxylic acids and nitrogenous bases, inhibited the cationic polymerisation mechanism and were thus incompatible since they slowed down the polymerisation too much. The technique is, therefore, somewhat limited in the range of functional monomers and templates which could be used, but the technique points the way towards a broader-minded approach to both the chemistry and technology of molecular imprinting.

#### **12.4.7 Surface rearrangement of latex particles (method VI in Table 12.1)**

Imprinting by surface rearrangement of latex particles was first introduced in 1992 [42] and has since been the subject of a series of studies [43–49] (see also Chapter 9). The technique is very attractive, in that it is the only technique discussed in this chapter which specifically addresses the issue of accessibility of the imprinted binding sites. In this case the binding sites are formed at the surface of latex particles by rearrangement of polymer chains at the latex/water interface, followed by a secondary polymerisation to fix the conformations in place. Originally, surface carboxylate functionalities were used, but this has subsequently been extended to phosphonate groups using an interfacially active polymerisable phosphonate ester. The beads produced are uniform, since they originated from a seeded emulsion polymerisation, which produces near-monodisperse particles.

By optimising conditions, a range of transition metal cations have been imprinted using the surface rearrangement approach. The capacity is reasonable, since the small size of the latex (typically 0.5  $\mu\text{m}$  diameter) gives a high overall surface area. Detailed methodology and results will not be discussed here since they

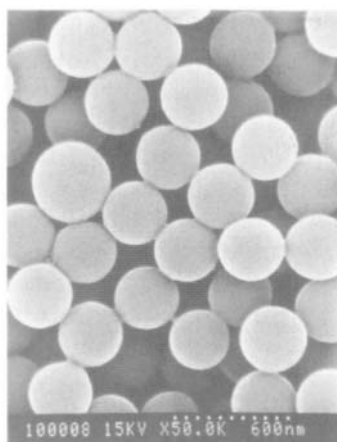


Fig. 12.9. Electron micrograph of a polymer latex surface imprinted with copper (II) ions by the surface rearrangement method (from [44]).

are presented elsewhere in this book (Chapter 9). Fig. 12.9 shows a photograph of a typical surface-imprinted latex.

While this approach to surface imprinting is attractive, it has only been demonstrated for metal ion imprinting to date. If the technique could be extended to encompass small organic molecules then it would have far greater impact, and would have particular relevance to agglutination type assays, and use with tagged macromolecules, where access to surface-localised binding sites is crucial.

## 12.5 CONCLUSIONS AND FUTURE PERSPECTIVE

From the preceding discussion, it is evident that a range of possible solutions is available for synthesis of molecularly imprinted polymer beads. None of the techniques discussed are perfect, however, and few are being used routinely in the laboratory as tools for synthesis of imprinted materials. Ground and sieved bulk material is still favoured for studies involving development of new imprinting strategies and for mechanistic studies of the imprinting process. More practical applications for imprinted polymers are beginning to emerge, however, and this should fuel the search for more convenient routine production methods. As well as further development of established techniques, some new strategies will no doubt be developed, either specifically for molecular imprinting or by adaptation of techniques developed for other purposes. A few possible developments are outlined below.

Polymerisation in supercritical carbon dioxide has generated great interest in recent years for a number of reasons, including its environmentally benign nature as a solvent and the ease of removing it from products at the end of a reaction, as well as more subtle issues such as the tuneability of its density and solvation

properties. Both polyacrylates [50] and polystyrene [51] have been successfully polymerised in supercritical carbon dioxide to give spherical dispersion particles of linear polymer. Recently it has been shown that highly cross-linked particles can be produced in supercritical carbon dioxide [52] and it seems only a relatively small step from this to molecularly imprinted particles produced in this way. Such an approach will doubtless be reported in the near future.

The synthesis of highly porous monodisperse DVB spheres by precipitation polymerisation has recently been reported [53]. This is of particular interest since good porosity was achieved, in contrast to most of the results discussed above for attempts to make imprinted polymers by dispersion methods. It is clear that high porosity can be achieved with the right combination of conditions. The reported method used rather low concentrations of monomers and continued the reaction to only a small degree of total conversion. For some imprinting situations, such as those using scarce templates, this might be unacceptable. In other cases no such restrictions pertain, so a more comprehensive evaluation of imprinting using this method seems timely.

An ideal solution to the problem of finding a universal method for making monodisperse imprinted beads would be a combination of the inertness of fluorinated liquids with the quality of beads produced by the two-step swelling process. Unfortunately, to date it has not proved possible to make a microemulsion of the organic phase in a liquid fluorocarbon. It might be possible to get some control of particle size, however, by swelling a seed latex with the smallest droplet-size suspension which can be made. Work is in progress to evaluate this possibility. Other methods are available to achieve better particle size control in suspension polymerisation and these should also be evaluated [54].

In summary, no perfect and universally applicable solution to making beaded imprinted polymers has yet been invented, but a number of promising techniques have been introduced during the last few years which will doubtless be further developed and refined alongside a range of novel approaches. Only time will tell whether any of these techniques will displace crushed bulk polymer as the production method of choice, either in the laboratory or on a production scale.

## ACKNOWLEDGEMENTS

The author would like to thank the following people for supplying photographs of imprinted polymers for reproduction in this chapter: Prof. F. Arnold, Dr M.J. Whitcombe, Mr. L. Ye, Prof. K. Hosoya, Prof. C.M. Breneman and Prof. K. Tsukagoshi.

## REFERENCES

- 1 K. Haupt, A. Dzgoev and K. Mosbach, *Anal. Chem.*, **70**, 628 (1998).
- 2 G. Wulff, D. Oberkobusch and M. Minarik, *React. Polym.*, **3**, 261 (1985).
- 3 S. Plunkett and F. Arnold, *J. Chromatogr. A*, **708**, 19 (1995).

- 4 S. Vidyasankar, M. Ru and F. Arnold, *J. Chromatogr. A*, **775**, 51 (1997).
- 5 M. Glad, P. Reinholdsson and K. Mosbach, *React. Polym.*, **25**, 47 (1995).
- 6 A. Schmid, L.-I. Kulin and P. Flodin, *Makromol. Chem.*, **192**, 1223 (1991).
- 7 P. Reinholdsson, T. Hargitai, R. Isaksson and B. Törnelli, *Angew. Macromol. Chem.*, **192**, 113 (1991).
- 8 J.-E. Rosenberg and P. Flodin, *Macromolecules*, **20**, 1522 (1987).
- 9 J.M. Lin, T. Nakagama, K. Uchiyama and T. Hobo, *J. Liq. Chromatogr.*, **20**, 1489 (1997).
- 10 A. Guyot, In: *Synthesis and separations using functional polymers*, D.C. Sherington and P. Hodge Eds, John Wiley and Sons, London, p. 1 (1988).
- 11 M. Munger and E. Tromsdorf, In: *Polymerization processes*, C.E Schildknecht and I. Skeist Eds, Wiley Interscience, New York (1977).
- 12 J. Damen and D. Neckers, *Tetrahed. Lett.*, **21**, 1913 (1980).
- 13 J. Damen and D. Neckers, *J. Org. Chem.*, **45**, 1382 (1980).
- 14 V. Braun and W. Kuchen, *Chem. Ztg.*, **108**, 255 (1984).
- 15 M. Whitcombe, M. Rodriguez, P. Villar and E. Vulfson, *J. Am. Chem. Soc.*, **117**, 7105 (1995).
- 16 M. Whitcombe, C. Alexander and E. Vulfson, *Trends Fd. Sci. Technol.*, **8**, 140 (1997).
- 17 A. Mayes and K. Mosbach, *Anal. Chem.*, **68**, 3769 (1996).
- 18 O.-W. Zhu, *Macromolecules*, **29**, 2813 (1996).
- 19 R. Ansell and K. Mosbach, *J. Chromatogr. A*, **787**, 55 (1997).
- 20 R. Ansell and K. Mosbach, *Analyst*, **123**, 1611 (1998).
- 21 S.A. Piletsky, PhD Thesis, Institute of Bioorganic Chemistry, Kiev (1991).
- 22 K.E.J. Barrett, *Dispersion polymerization in organic media*, John Wiley and Sons, London (1975).
- 23 C.K. Ober and K.P. Lok, *Macromolecules*, **20**, 268 (1987).
- 24 A.J. Paine, *J. Pol. Sci: Pol. Chem.*, **28**, 2485 (1990).
- 25 B. Williamson, R. Lukas, M.A. Winnik and M.D. Croucher, *J. Colloid Int. Sci.*, **119**, 559 (1987).
- 26 B. Sellergren, *J. Chromatogr. A*, **673**, 133 (1994).
- 27 L. Ye, P.A.G. Cormack and K. Mosbach, *Anal. Commun.*, **36**, 35 (1999).
- 28 J. Ugelstad and P.C. Mørk, *Adv. Coll. Interfacial Sci.*, **13**, 101 (1980).
- 29 K. Hosoya, K. Yoshikazo, N. Tanaka, K. Kimata, T. Araki and J. Haginaka, *Chem. Lett.*, 1437 (1994).
- 30 J. Matsui, T. Kato, T. Takeuchi, M. Suzuki, K. Yokoyama, E. Tamiya and I. Karube, *Anal. Chem.*, **65**, 2223 (1993).
- 31 K. Hosoya, K. Yoshihako, Y. Shirasu, K. Kimata, T. Araki, N. Tanaka and J. Haginaka, *J. Chromatogr. A*, **728**, 139 (1996).
- 32 K. Hosoya, Y. Shirasu, K. Kimata and N. Tanaka, *Anal. Chem.*, **70**, 943 (1998).
- 33 J. Haginaka, H. Takehira, K. Hosoya and N. Tanaka, *Chem. Lett.*, 555 (1997).
- 34 J. Haginaka, H. Takehira, K. Hosoya and N. Tanaka, *J. Chromatogr. A*, **816**, 113 (1998).
- 35 M. Kempe and K. Mosbach, *J. Chromatogr.*, **664**, 276 (1994).
- 36 J. Haginaka, Y. Sakai and S. Narimatsu, *Anal. Sci.*, **14**, 823 (1998).
- 37 J. Haginaka and H. Sanbe, *Chem. Lett.*, 1089 (1998).
- 38 B. Sellergren and K. Shea, *J. Chromatogr. A*, **690**, (1995).
- 39 J.F. Widmann and E.J. Davis, *Colloid Polym. Sci.*, **274**, 525 (1996).
- 40 M.A. Vorderbruggen, K. Wu and C.M. Breneman, *Chem. Mater.*, **8** 1106 (1996).
- 41 L. Andersson, R. Müller, G. Vlatakis and K. Mosbach, *Proc. Natl. Acad. Sci. USA*, **92**, 4788 (1995).
- 42 K. Yu, K. Tsukagoshi, M. Maeda and M. Takagi, *Anal. Sci.*, **8**, 701 (1992).
- 43 K. Tsukagoshi, K. Yu, M. Maeda and M. Takagi, *Bull. Chem. Soc. Jpn.*, **66**, 114 (1993).
- 44 M. Maeda, M. Murata, K. Tsukagoshi and M. Takagi, *Anal. Sci.*, **10**, 113 (1994).
- 45 K. Tsukagoshi, K. Yu, M. Maeda, M. Takagi and T. Miyajima, *Bull. Chem. Soc. Jpn.*, **68**, 3095 (1995).



- 46 M. Murata, S. Hijiya, M. Maeda and M. Takagi, *Bull. Chem. Soc. Jpn.*, **69**, 637 (1996).
- 47 Y. Koide, H. Senba, H. Shosenji, M. Maeda and M. Takagi, *Bull. Chem. Soc. Jpn.*, **69**, 125 (1996).
- 48 I. Fujiwara, M. Maeda and M. Takagi, *Anal. Sci.*, **12**, 545 (1996).
- 49 Y. Koide, K. Tsujimoto, H. Shosenji and M. Maeda, *Bull. Chem. Soc. Jpn.*, **71**, 789 (1998).
- 50 J.M. DeSimone, E.E. Maury, Y.Z. Menceloglu, J.B. McClain, T.R. Romack and J.R. Coombes, *Science*, **257**, 945 (1994).
- 51 D.A. Canelas, D.E. Betts and J.M. DeSimone, *Macromol.*, **29**, 2818 (1996).
- 52 A.I. Cooper, W.P. Hems and A.B. Holmes, *Macromol. Rapid. Comm.*, **19**, 353 (1998).
- 53 W.-H. Li and H.D.H. Stöver, *J. Pol. Sci. Pol. Chem.*, **36**, 1543 (1998).
- 54 S. Omi, K. Katame, A. Yamamoto and M. Iso, *J. Appl. Pol. Sci.*, **51**, 1 (1994).

## Techniques for the *in situ* preparation of imprinted polymers

JUN MATSUI AND TOSHIFUMI TAKEUCHI

### 13.1 INTRODUCTION

Molecularly imprinted polymers have come to be recognised as antibody mimics since Mosbach and co-workers demonstrated the use of imprinted polymers for the sorbent assay of drugs [1]. Not only in applications, but also in preparation principle, imprinted polymers can be regarded as antibody mimics; the synthesis proceeds in a “tailor-made” fashion and the resultant polymers show specific binding for a given guest molecule. Also, imprinted polymers have many characteristic features as synthetic antibody mimics that contrast with natural antibodies.

#### 13.1.1 Molecular-level design

Molecular-level design can be made by establishing “tailor-made” binding sites. Such design of imprinted polymers can mostly be done by selection of functional monomers [2–4]. Basically, the functional monomers are selected according to the functionality of a template molecule, so that the functional monomers are bound with the template during the polymerisation process and a complementary binding site can be formed in the resultant polymer. Imprinted polymers can also be designed according to the environments of their use; a functional monomer providing electrostatic interaction can be used in non-polar environments and one with hydrophobic interaction in aqueous environments. Due to the flexible molecular-level design, imprinted polymers can be applied in a wide range of chemical and analytical fields. Such molecular-level design can hardly be performed in natural antibody preparations. Although modification of antibodies for higher environmental tolerance have been reported [5], antibodies generally mainly work in aqueous solution.

#### 13.1.2 Morphology design

Another notable difference between imprinted artificial antibodies and natural antibodies lies in the fact that imprinted polymers are classified as cross-linked organic polymers, generally insoluble in common solvents. This characteristic feature makes them attractive and advantageous for application in analytical and separation technology, because imprinted polymers can be used as affinity materials

without any immobilisation procedure after the preparation. For practical use, however, polymers need to be prepared in a desirable form for the application. Here, a macro-morphology design appears to be an important matter. For the use of imprinted polymers as stationary phases in chromatography, polymers need to be synthesised as beads or to be modified as particles after bulk polymerisation (Fig. 13.1) (see Chapter 12). This chapter describes a new molecular imprinting technique in which further improvement of preparation procedure and operation is involved, namely *in situ* molecular imprinting.

*In situ* molecular imprinting can be defined as a technique for preparing imprinted polymers in a place where the polymers are subsequently utilised. Imprinted polymers prepared by an *in situ* technique, therefore, require no subse-

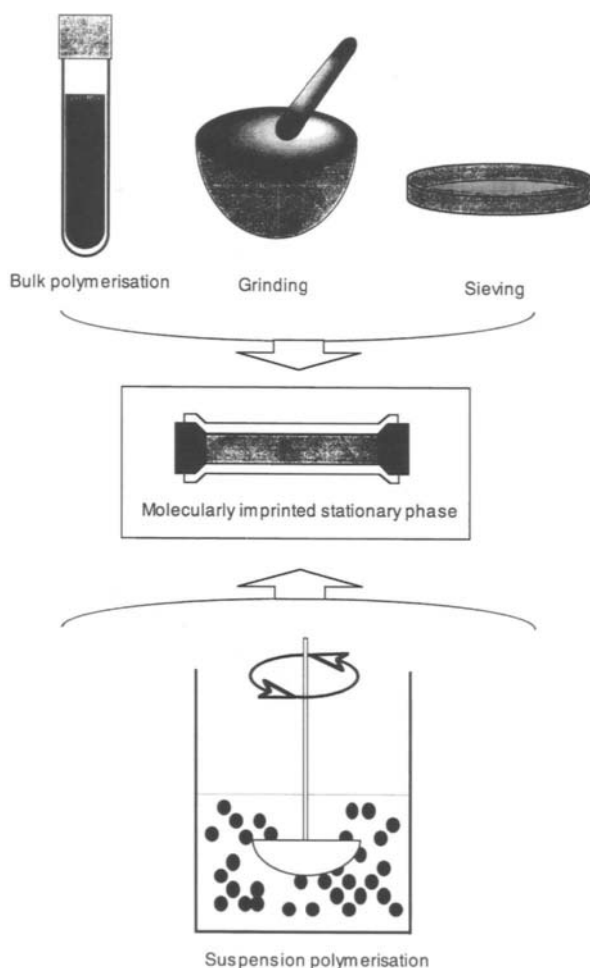


Fig. 13.1. Two examples of approaches to molecularly imprinted stationary phases.

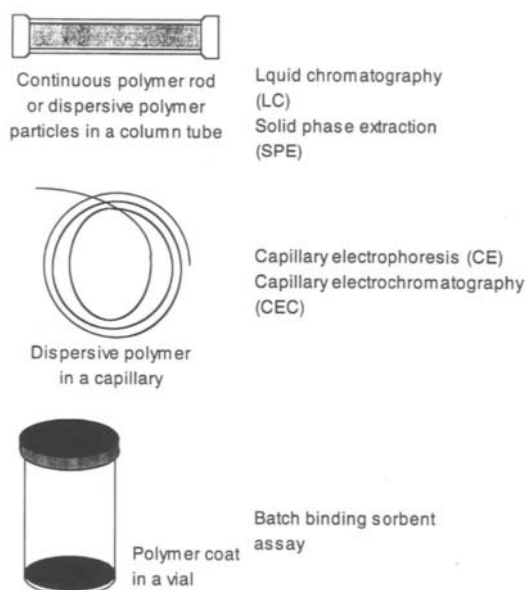


Fig. 13.2. *In situ* imprinted polymers and their applications.

quent treatment of the resultant polymer, except washing to extract the template, and can be directly used for subsequent analyses or applications. In this chapter, three major examples are introduced, (i) preparation in a column tube for chromatographic use, (ii) preparation in a capillary for capillary electrophoresis (CE) or capillary electrochromatography (CEC) and (iii) preparation in a vial for batch use. These *in situ* approaches utilise polymer rods, dispersion polymers and polymer coats, respectively (Fig. 13.2).

## 13.2 *IN SITU* IMPRINTED POLYMER RODS

### 13.2.1 Polymer rods as chromatographic stationary phases

Because molecularly imprinted polymers can be compared to antibodies, many of the applications of antibodies are also potential applications of imprinted polymers; for instance, imprinted polymers can be used as affinity media in liquid chromatography, like antibodies in affinity chromatography. For conventional chromatographic use of imprinted polymers, block polymers are broken to pieces, ground, sieved and packed in a column. These experimental steps, however, make the whole procedure, from polymer preparation to chromatographic use, extremely tedious and time-consuming. The procedure also results in polymer particles of irregular size and shape, which may have a negative influence on column efficiency.

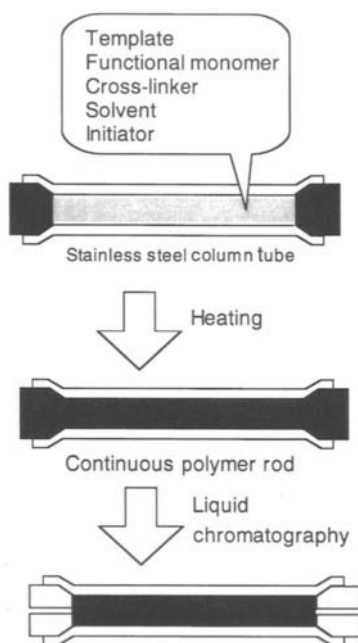


Fig. 13.3. *In situ* procedure for preparing molecularly imprinted polymer rods.

To overcome these problems, the first *in situ* molecular imprinting was reported by Matsui *et al.* for the preparation of a molecularly imprinted chromatographic stationary phase [6]. Polymerisation was carried out in a stainless-steel column (Fig. 13.3) by following the procedure of Fréchet and co-workers [7]. A column filled with all the reagents necessary for molecular imprinting was heated in a water bath, resulting in a ready-to-use column filled with a continuous imprinted polymer rod, through which the eluent flows due to the porosity of the imprinted polymer. An enantioselective polymer rod was obtained by *in situ* molecular imprinting using L-phenylalanine anilide as the template. When applied as the stationary phase in chromatography this rod was capable of separating the enantiomers with a separation factor of 1.7. When the antipode was imprinted, the resultant polymer rod showed an inverted selectivity. Theophylline was also used as a model template molecule for preparing an imprinted polymer rod and the selectivity was examined among xanthine derivatives [8]. As seen in Table 13.1, the imprinted polymer rod exhibited a higher selectivity for the original template theophylline in comparison with the results using a non-imprinted polymer rod. This suggests that molecular imprinting also works in the *in situ* polymerisation and that a template-selective polymer rod can be obtained by the technique. Figure 13.4 shows a typical chromatogram obtained on the polymer rod imprinted with theophylline.

Thus, the *in situ* method afforded a simple and fast preparation of molecularly

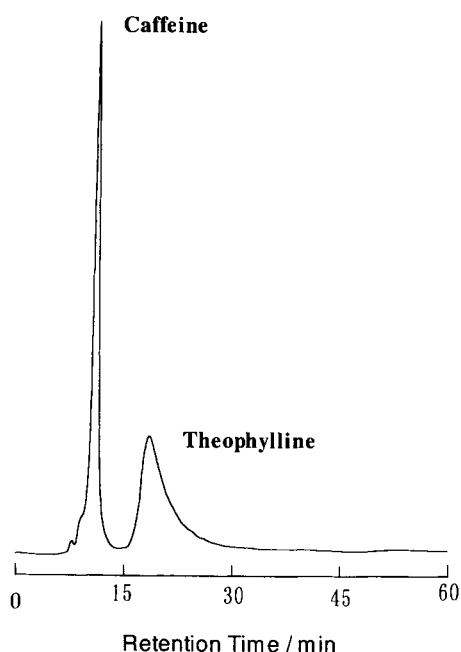


Fig. 13.4. Typical chromatogram using a molecularly imprinted polymer rod imprinted with theophylline.

TABLE 13.1

CAPACITY FACTOR OF XANTHINE DERIVATIVES ON A THEOPHYLLINE-IMPRINTED POLYMER ROD COLUMN

| Entry | Template     | Polymer | Capacity factors |             |          |
|-------|--------------|---------|------------------|-------------|----------|
|       |              |         | Theophylline     | Theobromine | Caffeine |
| A     | Theophylline | EDMA    | 1.2              | 1.0         | 0.16     |
| B     | None         | EDMA    | 0.47             | 0.61        | 0.12     |
| C     | Theophylline | ST-DVB  | 1.9              | 1.3         | 0.37     |
| D     | None         | ST-DVB  | 1.4              | 1.3         | 0.36     |

Column space size, 50 × 4.6 mm i.d.; flow rate, 0.35 ml/min; eluent, acetonitrile. ST-DVB, styrene-divinylbenzene.

imprinted chromatographic media. Continuous polymer rods, however, usually exhibit higher back-pressure than conventional stationary phases and sometimes face a problem caused by excessive back-pressure. Therefore, the polymerisation solvents, known to play important roles as pore formers, have to be carefully

chosen so that the resultant polymers are porous enough to give good eluent-flow properties. This restricts the selection of polymerisation solvents and sometimes makes it difficult to meet the requirement that the solvents should not interfere with interaction between a template and functional monomers. To date, the most successful pore formers in imprinted rod preparation have been reported to be cyclohexanol–dodecanol, though these solvents may be less favourable for hydrogen bonding and ionic interaction between a template and functional monomers. Probably for this reason, the polymer rod imprinted against a phenylalanine anilide gave a smaller separation factor as compared to a bulk polymer [9].

Although the effectiveness of molecularly imprinted stationary phases prepared by conventional method have been demonstrated [10], peak broadening is a problem in attaining high resolution. Therefore, the use of polymer rods was also expected to improve column efficiency because it does not involve a procedure of polymer crushing and grinding. Unfortunately, significant improvements of peak shapes were not observed by using polymer rods. Further accurate control of pore size might be necessary for this sake. For the purpose of obtaining imprinted stationary phases with high column efficiency, several other attempts have been reported, e.g. suspension polymerisation [11] and two-step polymerisation [12,13], for the synthesis of imprinted polymer beads (see Chapter 12).

### 13.2.2 Tool for selecting functional monomer

The *in situ* preparation of imprinted columns can be used for optimising the conditions of molecular imprinting. Although some basic studies have been reported to be helpful for anticipating a molecular imprinting mechanism and recipe [14], it is hard to perform the best-condition synthesis without trial-and-error efforts. A simple and fast *in situ* method is expected to be available to find the conditions. Here, an example is shown where the *in situ* method was used for selecting appropriate functional monomers. Selection of functional monomers is crucial in non-covalent molecular imprinting, because the principle is based upon the template–functional monomer complexation and functional monomers play an important role in recognising a substrate as residues in resultant polymers.

Imprinting of cinchona alkaloids was examined as a model imprinting system and the effectiveness was compared using methacrylic acid (MAA) and 2-(trifluoromethyl)acrylic acid (TFM) as functional monomers [15]. Cinchonidine (1) and its antipode cinchonine (2) were used as templates to prepare four imprinted polymer rods; MAA-based cinchonidine-imprinted polymer rod (M1), MAA-based cinchonine-imprinted polymer rod (M2), TFM-based cinchonidine-imprinted polymer rod (F1) and TFM-based cinchonine-imprinted polymer rod (F2) (Table 13.2). When comparing the separation factors of the two sets of imprinted polymers, it was found that the two template species have different tastes in selecting functional monomers. For cinchonidine imprinting, MAA appeared to be a superior functional monomer; the separation factor of M1 is larger than that of F1. On the contrary, TFM gave a polymer F2 showing a better diastereoselectivity to

TABLE 13.2

## DIASTEREOSELECTIVITY OF CINCHONIDINE(1)-IMPRINTED AND CINCHONINE(2)-IMPRINTED POLYMER RODS

| Analyte | TFM-based polymer rods |          |      |          | MAA-based polymer rods |          |      |          |
|---------|------------------------|----------|------|----------|------------------------|----------|------|----------|
|         | F1                     |          | F2   |          | M1                     |          | M2   |          |
|         | $k'$                   | $\alpha$ | $k'$ | $\alpha$ | $k'$                   | $\alpha$ | $k'$ | $\alpha$ |
| 1       | 11.5                   | 2.0      | 6.6  | —        | 3.9                    | 2.6      | 1.5  | —        |
| 2       | 5.8                    | —        | 34.7 | 5.3      | 1.5                    | —        | 4.7  | 3.1      |

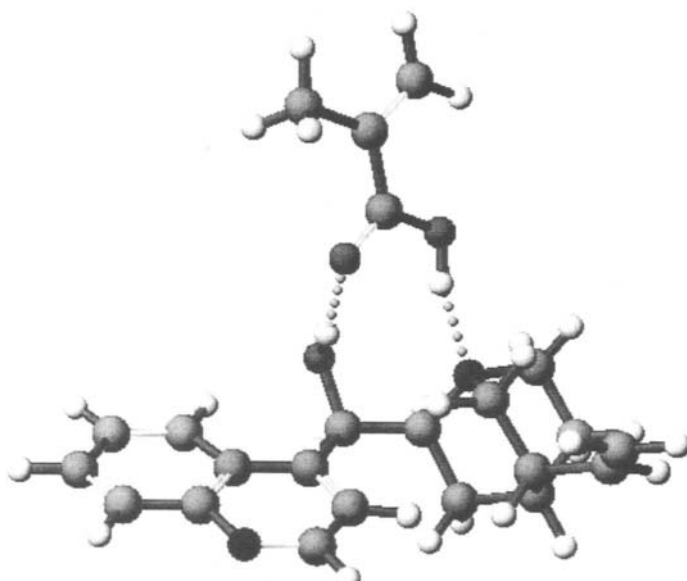


Fig. 13.5. Possible structure of a complex of cinchonidine and MAA.

cinchonine. These differences are assumed to be derived from the structural difference between cinchonidine and cinchonine. It would be possible for cinchonidine to form a double hydrogen bond with a functional monomer MAA at a quinuclidine nitrogen and a hydroxyl group (Fig. 13.5). This could be a reason why cinchonidine-imprinting favours MAA over TFM, which is a stronger acid but may be less prone to form cyclic hydrogen bonds due to its lower proton accepting capacity. On the other hand, cinchonine does not form a complex based on such double hydrogen bonding, where the functional monomer approaches too close to a quino-line ring. Therefore, cinchonine was not imprinted so effectively as cinchonidine using MAA as functional monomer.



### 13.3 *IN SITU* DISPERSION POLYMERS

Another *in situ* preparation of molecularly imprinted columns employs dispersion polymerisation, whereby agglomerated polymer particles are obtained [16]. The procedure is similar to the rod preparation; a mixture of the chemicals for the polymer preparation, such as a template, a functional monomer, a cross-linker, a porogen and an initiator is put in a column and heated to effect polymerisation. This method also requires polar solvents, such as cyclohexanol–dodecanol and isopropanol–water, to obtain aggregated polymer particles of well-defined microsises. A crucial difference with the rod preparation lies in the volume of the porogen used; larger volumes of porogens are used in dispersion polymerisation.

Pentamidine (PAM), a drug used for AIDS-related disorders, was imprinted by *in situ* dispersion polymerisation to prepare a PAM-selective stationary phase, using MAA as the functional monomer, ethylene glycol dimethacrylate (EDMA) as the cross-linker and isopropanol/water as the porogen. The obtained columns can be used directly for liquid chromatography and showed an enhanced selectivity for PAM, as compared to a benzamidine-imprinted column. Photo-irradiation at lower temperature was also adopted for the polymerisation, using a glass tube in place of a stainless-steel column, which could be advantageous for shifting the equilibrium toward complex formation of the template and the functional monomer during the polymerisation process.

The *in situ* molecular imprinting protocol employing dispersion polymerisation has some advantageous features. The dispersion polymer can be removed from a column and re-packed when a column is damaged after repeated use. Back-pressure of agglomerated polymer particles is less problematic; therefore, this *in situ* method can be applied to a wider range of analytical techniques. Here, two applications of *in situ* dispersion polymer, solid phase extraction (SPE) and CE are described.

#### 13.3.1. Use of imprinted affinity media in SPE

Sorbents for SPE need to work only in “on” or “off” modes, strongly adsorbing and easily releasing a sample, while moderate strength of retention with good resolution factors is required for chromatographic stationary phases. Furthermore, the column efficiency, negatively affected by peak broadening and tailing, is much less significant in SPE applications. SPE is thus regarded as an application suitable for imprinted polymers. SPE was performed using a dispersion polymer for enrichment of a specific sample [17]. Some other examples of imprinted polymer-based SPE are also reported [18,19], though these non-*in situ* works are not discussed here (see instead Chapter 15).

The dispersion polymer was applied for the specific enrichment of PAM in urine samples. After being conditioned with pH 5 or pH 7 mobile phase, the sample solution (100 mL) spiked with PAM was loaded with the mobile phase at a flow rate of 2 mL/min. PAM was then desorbed by a pH 2 mobile phase at flow rate of 0.1 mL/min. The elution was monitored by UV absorption. A low concentration (30 nM) of PAM in urine sample was enriched (enrichment factor = 54) and

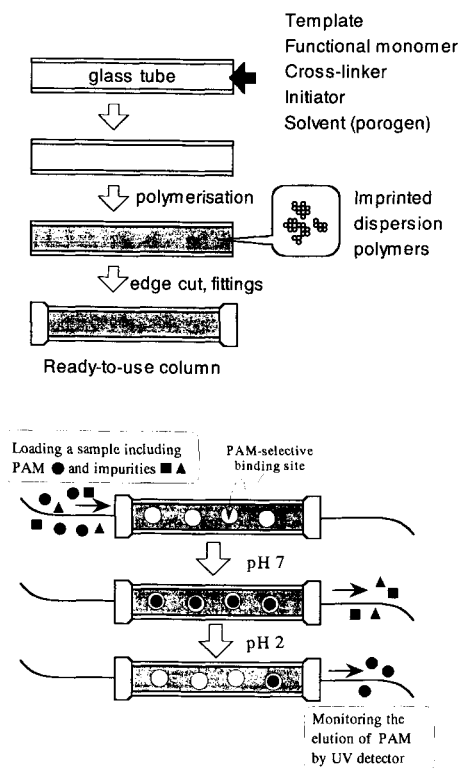


Fig. 13.6. *In situ* preparation of imprinted dispersion polymers and their application in SPE.

successively analysed by HPLC (Fig. 13.6). Here, the pH of the mobile phase was the factor to control the adsorption strength of the imprinted polymer sorbent based on an ion exchange mechanism; the SPE sorbent is “on” at a higher pH and “off” at a lower pH.

Thus, the selective enrichment of the target analyte was successfully demonstrated using the imprinted polymer. Conventional SPE sometimes needs to be combined with a different type of SPE or other separation steps to complete pre-purification, because compounds with similar chemical properties may accompany the analyte as impurities. On the other hand, imprinted polymer is an affinity-type SPE sorbent that exhibits specificity for an analyte; therefore, the imprinted polymer-based SPE is able to streamline the whole procedure of analysis. Although aqueous conditions were employed here, it is also notable that the utility in organic solvents is one of the useful characteristics of imprinted polymers as SPE sorbents [18,19].

### 13.3.2. Use of imprinted affinity media in electrophoresis

*In situ* molecular imprinting was applied to prepare imprinted polymer-filled or modified capillaries usable in CE and CEC (see also Chapter 16). To date, attempts

have been eagerly made to control the selectivity in CE and CEC analyses, especially to achieve chiral separations, employing antibodies and modified cyclodextrins as chiral selectors. The use of antibodies, however, sometimes presents the serious problem of air bubble formation. Although artificial receptors such as cyclodextrins are free from such problems, the design and synthesis of such artificial receptors with desired selectivity are not easy and the resultant selectivity can rarely be predicted. Furthermore, a process is required for immobilising these artificial receptors to support materials. Therefore, imprinted polymers were expected to be alternative chiral selectors exhibiting predetermined selectivity. Nilsson *et al.* showed the first example of molecularly imprinted polymer CE, employing PAM and BAM as template molecules [20]. Capillaries filled with a polymerisation mixture including the template PAM or BAM, a functional monomer MAA, a cross-linker EDMA, an initiator 2,2'-azo-bisobutyronitrile and a porogen isopropanol/water, were heated to effect the polymerisation. The porogen was carefully selected so as to make the *in situ* imprinted polymer sufficiently porous. The PAM-imprinted capillary showed an enhanced retention ability for PAM over a BAM-imprinted capillary. The electrolyte used for CE showed the influence on the retention ability and selectivity of the imprinted polymer, suggesting a retention mechanism based upon ionic interaction between PAM and carboxylate residues. Although resolution of racemic phenylalanine anilide was also examined using the L-isomer as the template, resolution was not observed. This is supposedly due to the porogen used for polymerisation, cyclohexanol-dodecanol, which may be too polar to allow sufficient template-functional monomer complexation during the polymerisation process.

Thus, it appeared that molecular imprinting could be used to achieve CE with desired selectivity. However, it was also shown that the protocol to fill imprinted polymer gels in a capillary *in toto* is problematic because the solvent selection has to simultaneously satisfy the high imprinting efficiency and the porous morphology of the resultant polymers. Other problems, such as formation of bubbles, difficulties in pumping and slow transportation of samples could also occur. Therefore, a refined *in situ* method was introduced, whereby the inner surface of the capillary is modified by imprinted polymers [21,22]. It is crucial in this technique to optimise the conditions for preparing the polymer coating with an appropriate thickness to allow the three-dimensional cross-linked structure to recognise a template. Therefore, pre-modification was conducted to introduce polymerisable functional groups on the inner surface of the capillaries before coating with imprinted polymers. The pre-modification of capillaries was carried out by treatment with aqueous NaOH, followed by reaction with 3-methacryloxypropyltrimethoxysilane. The silane-activated capillary was filled with a reaction mixture after rinsing with the same solvent as used in the reaction mixture. Subsequently, the capillary was heated at 65°C for 48 h to complete the polymerisation. Investigation was made concerning the concentration of cross-linkers and the selection of porogen in the reaction mixtures. It appeared that the resultant polymer coatings were significantly affected by these factors. Polymer coatings of appropriate thickness demonstrated template-directed enantioselectivity for (+)-2-phenylpropionic acid.

CEC was demonstrated in the analysis of  $\beta$ -adrenergic antagonists using capillaries modified with propranolol-imprinted polymer. *In situ* molecular imprinting was performed *via* photo-polymerisation at  $-20^{\circ}\text{C}$  within a capillary that was pre-modified with 3-methacryloxypropyltrimethoxysilane. The time for UV irradiation was carefully determined so as to obtain a polymer coating of appropriate thickness. Enantioseparation of the racemate of propranolol was successfully demonstrated with a separation factor of 1.12 and a resolution factor of 1.26.

### 13.4 *IN SITU* MOLECULAR IMPRINTING FOR BATCH APPLICATIONS

Batch use of imprinted polymers has been applied in the evaluation of polymers by saturation binding tests and in the applications of molecularly imprinted sorbent assays [1,23,24]. In a common procedure, imprinted polymers obtained as blocks were crushed, ground and sieved to prepare sized polymer particles. The resultant particles were then distributed into each vial and recovered by filtration after use. Recently, a new batch-type *in situ* procedure has been reported. It utilises a polymer coating prepared on an inner surface at the bottom of a vial and allows direct assessment of the polymers. In this section, this type of *in situ* preparation of imprinted polymers and an application to combinatorial chemistry are described.

#### 13.4.1 Batch-type *in situ* polymer preparation

A typical preparation procedure can be described as follows: the reagents for molecular imprinting, such as template species, functional monomers, cross-linking agents, solvent and initiator are dispensed into a glass vial; after being purged with nitrogen gas, the vial is heated in an aluminium rack or placed under UV light in a thermostatic water bath to allow the polymerisation to be initiated; the resultant polymer coat in the vial can be directly used for subsequent procedures. This *in situ* protocol enables us to employ a robot easily for automating the synthesis and evaluation of polymers. Liquid handling equipment was programmed to automatically perform (i) dispensing of the reagents, (ii) washing of the resultant polymers, (iii) dispensing of sample solutions and (iv) injection of the supernatant to an HPLC or a FIA system (Fig. 13.7). This automated procedure is capable of preparing and evaluating a number of imprinted polymers in a short time. Also, the liquid handler can be programmed to dispense orderly or randomly varied quantities of the reagents to prepare a combinatorial library of imprinted polymers.

#### 13.4.2 Combinatorial method for molecular imprinting

The molecular imprinting technique, based upon a self-association of molecules to build up a binding site structure, requires an appropriate choice of the building blocks, e.g. functional monomers. Construction and screening of imprinted

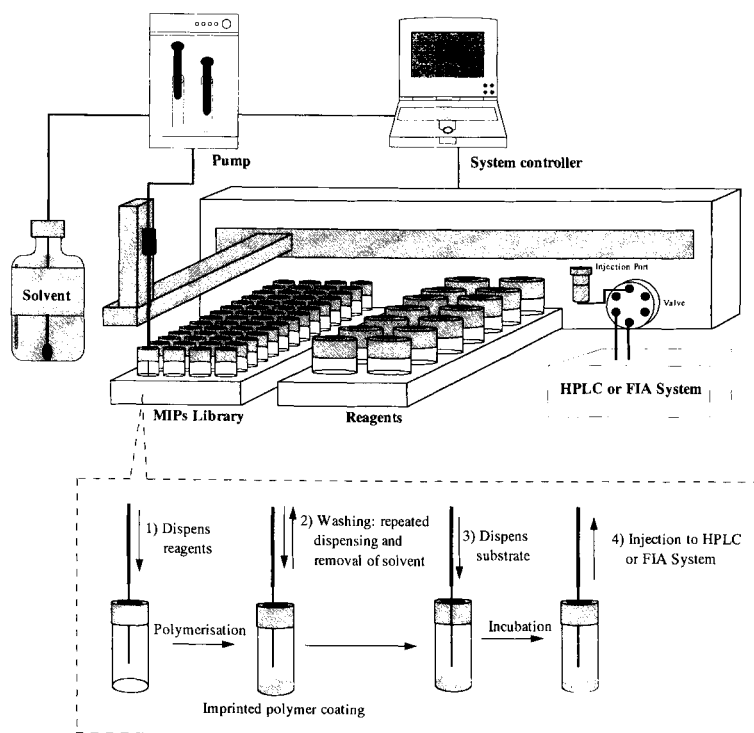


Fig. 13.7. Batch-type *in situ* molecularly imprinted procedure for preparing a library of artificial antibody polymers.

polymer libraries is one of the best ways to determine the suitable components and conditions for a given molecular imprinting system. Here, we show an example of the combinatorial chemistry approach to obtain molecularly imprinted artificial antibodies for triazine herbicides [25]. Using atrazine and ametryn, both triazine herbicides, as model template molecules, combinatorial libraries of molecularly imprinted artificial receptors were prepared (Fig. 13.8). The functional monomers examined were MAA and TFM. Ethylene glycol dimethacrylate, chloroform and 2,2'-azobis(dimethylvaleronitrile) were used as cross-linker, solvent and initiator, respectively, in fixed amounts. Using a ratio of zero to six equivalents of MAA and TFM to the template, a library consisting of 49 imprinted polymer members was prepared for each template. Each member of the atrazine-imprinted polymer library is named P(ATRx<sub>y</sub>), where *x* is a molar equivalent of MAA and *y* is that of TFM to the template. An abbreviation, AME, is used for the ametryn imprinted polymers instead of ATR.

The polymers were incubated with atrazine or ametryn solution after being washed repeatedly to remove the template. Free substrate in the supernatant was quantified to evaluate the affinity to the template species (Fig. 13.9). In both polymer libraries, it can be roughly stated that more functional monomer resulted

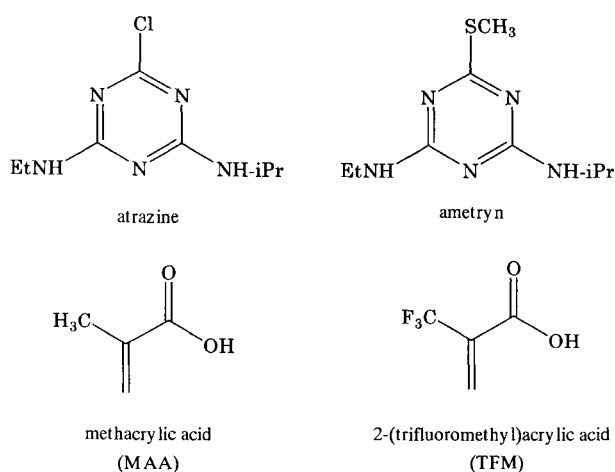


Fig. 13.8. Structure of the template species and the functional monomers used for preparing combinatorial libraries of imprinted polymers.

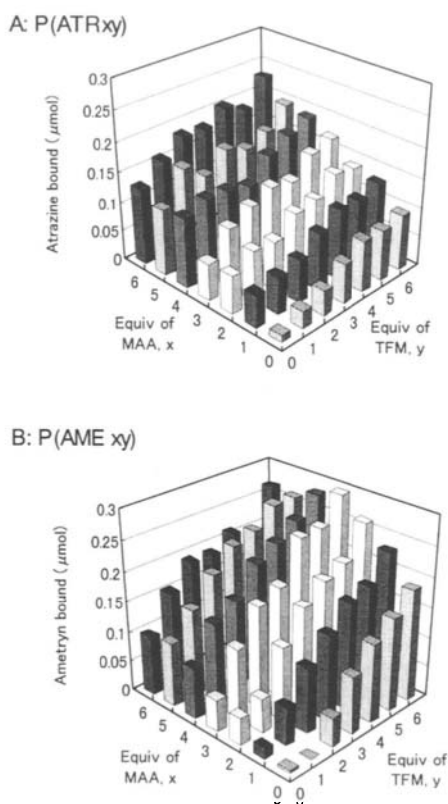


Fig.13.9. Binding of the original template species in atrazine-imprinted (A) and ametryn-imprinted (B) polymers.

in more adsorption of the template, showing that both MAA and TFM are effective for adsorbing the template species. After careful comparison, however, some differences can be found between the two functional monomers. MAA seems more effective for developing the affinity in the atrazine-imprinted polymer library, according to the result that P(ATR60) gave a larger amount of atrazine bound as compared to P(ATR06). In contrast, P(AME06) showed a higher adsorbing performance over P(AME60), suggesting that TFM is a more effective functional monomer in ametryn imprinting.

Selectivity was examined by investigating the adsorption of the other herbicide; the atrazine-imprinted polymers were tested using ametryn as a substrate and *vice versa*. The ratio of the adsorption of the original template versus that of the reference substrate, defined as a selectivity factor, is shown in Fig. 13.10. Library members showing a larger selectivity factor can be regarded as being more selective for the original template. Here again, each of the atrazine- and ametryn-imprinted polymer libraries showed a different preference; MAA is effective for a larger selectivity factor in the atrazine-imprinted library and TFM in the ametryn-imprinted polymers. Considering the affinity and the selectivity to the original template, it

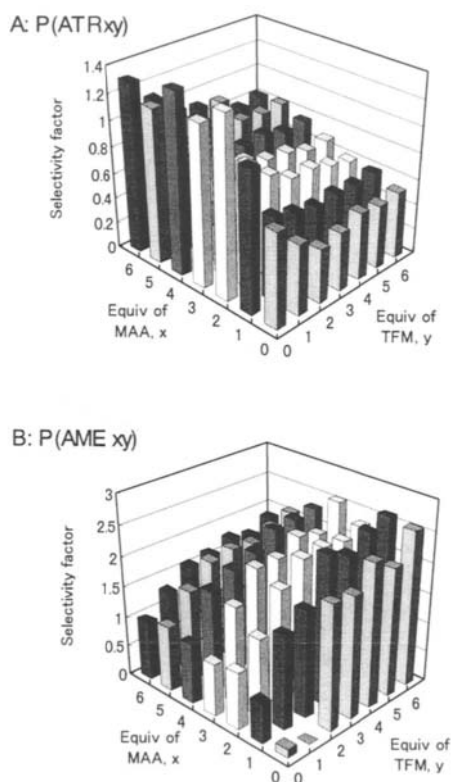


Fig. 13.10. Selectivity of atrazine-imprinted (A) and ametryn-imprinted (B) polymers.

appeared that, in the atrazine-imprinted polymer library, MAA-rich polymers are favourable because TFM made a smaller contribution in increasing the affinity to atrazine and even gave negative influences on the selectivity. In the ametryn-imprinted library, however, TFM turned out to be a very useful functional monomer for developing both affinity and selectivity and TFM-rich members are better artificial antibodies against ametryn. Thus, the preferable functional monomer system was established and good artificial antibodies were selected by the combinatorial method.

Accordingly, it was found that atrazine and ametryn show the different tastes in selection of functional monomers; atrazine was suitably imprinted with MAA and ametryn with TFM, although atrazine and ametryn are of a similar structure and differ only in one functional group. Ametryn has a methylthio group instead of a chloro group in atrazine. Basic spectroscopic studies, e.g. UV and NMR titrations, would be helpful for choosing appropriate functional monomers by preliminary investigation of species and the stability and population of the complexes of a template and functional monomers, which governs the efficiency in molecular imprinting. Currently, however, it is more promising to determine empirically which and how much functional monomer should be used for a given template molecule to be imprinted. Combinatorial molecular imprinting employing the batch-type *in situ* protocol can be utilised not only to find the most effective functional monomer, but also for determining their best mixing ratios when different functional monomers are simultaneously engaged [26]. Also, it is helpful in optimising other conditions concerning cross-linkers, solvents and initiators. Thus, combinatorial chemistry, as applied in molecular imprinting, appears to be a promising approach to molecularly imprinted artificial antibodies exhibiting predictable molecular recognition performance.

The availability of various functional monomers is essential to operate molecular imprinting by a combinatorial method. Therefore, efforts to design and synthesise novel functional monomers have been made for developing a desired specificity and functions [2,3, 27]. With a wide selection of functional monomers, further functionalised polymers, such as catalysts and sensor materials, will also be developed by the combinatorial chemistry-based molecular imprinting.

### 13.5 CONCLUSIONS

A molecularly imprinted polymer is an artificial antibody that is tailored for a specific molecule. The *in situ* technique introduces another attractive feature, in that the imprinted polymer is tailor-made for a specific application with a minimum of experimental steps, emphasising the original statement that imprinted polymers can be easily and simply prepared and applied. It is also shown that the *in situ* method is useful for designing a molecular imprinting system and would be helpful for mechanistic studies of molecular imprinting and recognition. Thus, advances in the basics and applications of molecular imprinting can be expected by this technique.



## REFERENCES

- 1 G. Vlatakis, L.I. Andersson, R. Müller and K. Mosbach, *Nature*, **361**, 645 (1993).
- 2 K. Tanabe, T. Takeuchi, J. Matsui, K. Ikebukuro, K. Yano and I. Karube, *J. Chem. Soc., Chem. Commun.*, **1995**, 2303 (1995).
- 3 K. Yano, T. Nakagiri, T. Takeuchi, J. Matsui, K. Ikebukuro and I. Karube, *Anal. Chim. Acta*, **357**, 91 (1997).
- 4 J. Matsui, H. Kubo and T. Takeuchi, *Anal. Sci.*, **14**, 699 (1998).
- 5 W. Stöcklein, A. Gebbert and R.D. Schmid, *Anal. Lett.*, **23**, 1465 (1990).
- 6 J. Matsui, T. Kato, T. Takeuchi, M. Suzuki, K. Yokoyama, E. Tamiya and I. Karube, *Anal. Chem.*, **65**, 2223 (1993).
- 7 F. Svec and J.M.J. Fréchet, *Anal. Chem.*, **64**, 820 (1992).
- 8 J. Matsui, Y. Miyoshi, R. Matsui and T. Takeuchi, *Anal. Sci.*, **11**, 1017 (1995).
- 9 L.I. Andersson, D.J. O'Shannessy and K. Mosbach, *J. Chromatogr.*, **513**, 167 (1990).
- 10 M. Kempe, L. Fischer and K. Mosbach, *J. Mol. Recogn.*, **6**, 25 (1993).
- 11 A.G. Mayes and K. Mosbach, *Anal. Chem.*, **68**, 3769 (1996).
- 12 K. Hosoya, K. Yoshizako, N. Tanaka, K. Kimata, T. Araki and J. Haginaka, *Chem. Lett.*, **1994**, 1437 (1994).
- 13 K. Hosoya, K. Yoshizako, Y. Shirasu, K. Kimata, T. Araki, N. Tanaka and J. Haginaka, *J. Chromatogr. A*, **728**, 139 (1996).
- 14 B. Sellergren, M. Lepistö and K. Mosbach, *J. Am. Chem. Soc.*, **110**, 5853 (1988).
- 15 J. Matsui, I.A. Nicholls and T. Takeuchi, *Anal. Chim. Acta*, **365**, 89 (1998).
- 16 B. Sellergren, *J. Chromatogr. A*, **673**, 133 (1994).
- 17 B. Sellergren, *Anal. Chem.*, **66**, 1578 (1994).
- 18 M.T. Muldoon and L.H. Stanker, *Anal. Chem.*, **69**, 803 (1997).
- 19 J. Matsui, M. Okada, M. Tsuruoka and T. Takeuchi, *Anal. Commun.*, **34**, 85 (1997).
- 20 K. Nilsson, J. Lindell, O. Norrölow and B. Sellergren, *J. Chromatogr. A*, **680**, 57 (1994).
- 21 L. Schweitz, L.I. Andersson and S. Nilsson, *Anal. Chem.*, **69**, 1179 (1997).
- 22 O. Brüggemann, R. Freitag, M.J. Whitcombe and E.N. Vulfson, *J. Chromatogr. A*, **781**, 43 (1997).
- 23 M. Siemann, L.I. Andersson and K. Mosbach, *J. Agric. Food Chem.*, **44**, 141 (1996).
- 24 M.T. Muldoon and L.H. Stanker, *J. Agric. Food Chem.*, **43**, 1424 (1995).
- 25 T. Takeuchi, D. Fukuma and J. Matsui, *Anal. Chem.*, **71**, 285 (1999).
- 26 J. Matsui, Y. Miyoshi and T. Takeuchi, *Chem. Lett.*, 1007 (1995).
- 27 J. Matsui, Y. Tachibana and T. Takeuchi, *Anal. Commun.*, **35**, 225 (1998).

## **Application of molecularly imprinted polymers in competitive ligand binding assays for analysis of biological samples**

LARS I. ANDERSSON

### **14.1 INTRODUCTION**

Immunoassay is an analytical technique which depends on the binding reaction between the molecule of interest, the antigen, and a complementary molecule, the antibody [1,2]. The antigen is so called because it is a molecule capable of eliciting an immune response when injected into an animal, in which it is treated as a foreign species. Immunoassay technology is widely employed in clinical medicine, where it is successfully used for the analysis of protein, peptide and steroid hormones, a wide range of biochemical markers and also for the therapeutic monitoring of drugs. Although specific antibodies are the most familiar, and also by far the most commonly used binding species in quantitative binding assays (immunoassays), other biological binding molecules are also available. These include circulating binding proteins (referred to as protein binding assays), enzymes, cellular receptors (receptor assays) and even whole cells. However, the latter complementary molecules can only provide reagents for a limited range of molecules. Furthermore, in many instances, they do not offer the unique specificity that can be attained with an antibody and also possess relatively low affinity constants. Several non-biological binding systems can be envisaged, such as molecules designed and synthesised with the desired binding properties and synthetic polymers made by molecular imprinting techniques.

With reference to the detection principle and the format of the antigen-antibody reaction, immunoassays come in many different designs [1]. One division is in excess reagent (non-competitive) methods, in which the optimal concentration of antibody is high, and limited reagent (competitive) methods, in which the optimal concentration of antibody is low (Fig. 14.1). Briefly, the principal design of a competitive immunoassay is based on the analyte ligand and a labelled ligand being presented to a limited number of antibody binding sites. The label can be a radioactive isotope, an enzyme or a fluorescent compound. The two ligands compete for binding to the same sites. Hence, the amount of labelled ligand bound to the antibodies, as well as the amount free in solution, is quantitatively related to the amount of analyte added to the incubation mixture. The unique complementarity between antigen and antibody may enable the selective binding of an antigen in a complex biological matrix such as whole blood, plasma, serum or urine. Therefore, characteristic for many immunoassays is their ability to detect minute

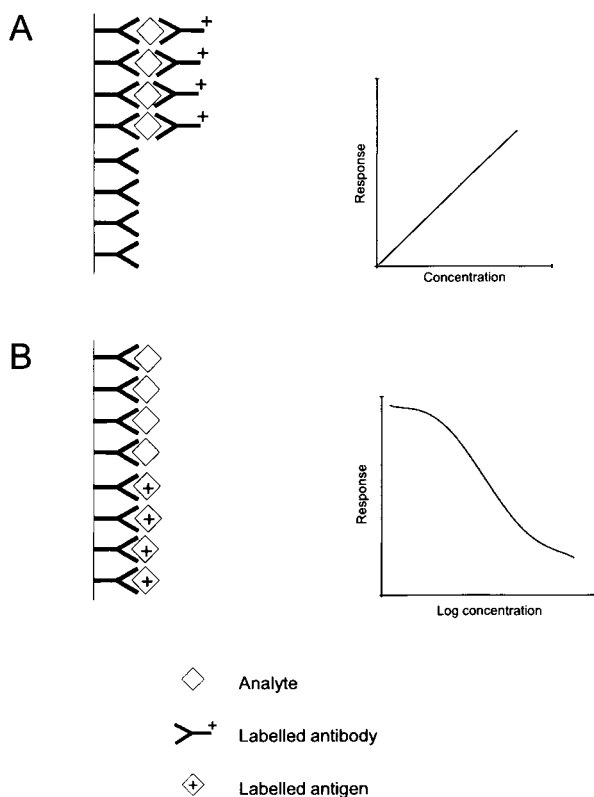


Fig. 14.1. Basic competitive and non-competitive immunoassay designs. (A) Non-competitive immunoassays use paired antibodies directed against different parts of the analyte molecule. The first antibody is used to capture the analyte from the sample and the second, labelled antibody to measure the amount of analyte bound, resulting in a response directly related to the concentration of analyte in the sample. (B) Competitive immunoassays use labelled antigen to measure unoccupied sites, resulting in a sigmoidal dose-response curve where the signal is inversely related to the concentration of analyte in the sample.

amounts of analyte in small sample volumes without prior extensive sample pre-treatment.

## 14.2 USE OF MOLECULARLY IMPRINTED POLYMERS (MIPs) AS ANTIBODY MIMICS

In recent years, an increasing number of MIPs offering comparable affinities and cross-reactivity profiles to those of antibodies have been synthesised. Indeed, in 1993 it was demonstrated that imprinted polymers can be substituted for antibodies in immunoassay protocols [3]. The imprint-based assay was referred to as MIA (for

molecularly imprinted sorbent assay). In this first paper, assays for the determination of theophylline and diazepam in human serum were presented. The actual assay was performed using organic solvents as the incubation medium and a prior extraction of the analyte from the serum sample had to be included. Later, analyte-MIP systems that can be employed equally well for organic solvent or aqueous buffer-based assays were developed [4,5]. Also, the direct assay of plasma samples has been demonstrated [6].

In order to become a viable alternative, MIP-based assays need to offer an added value to the conventional antibody-based immunoassays. Some characteristics of the MIP-based assays are summarised in Table 14.1. Superior characteristics of MIPs in comparison to antibodies are observed with respect to chemical, mechanical and thermal stability. The MIPs are compatible with autoclave conditions (120°C, 20 min) and are unaffected by acid and base treatment [7]. In fact, to achieve as complete removal of imprint molecules as possible, in the author's laboratory it is routine to include a wash step with 5 M sodium hydroxide in the MIP synthesis work-up protocol. The possibility of using a wider range of assay solvents, namely both aqueous and organic solvents, enables the solubility of the analyte to be assured and problems with non-specific adsorption minimised. Furthermore, high polymer stability leads to improved shelf life, where the MIP can be stored for several years in the dry state at ambient temperatures.

For biomacromolecules, antibody technology is, and will remain so in the foreseeable future, the obvious alternative. Molecular imprinting may, however, offer an alternative for small molecules that can be dissolved together with the monomers in an organic solvent. Antibody preparation against low-molecular weight compounds, so-called haptens, requires conjugation of the hapten to a carrier protein before injection into the animal [1,2]. Conjugation may present a

TABLE 14.1

## SOME CHARACTERISTICS OF MIP-DERIVED ANTIBODY MIMICS

|   |  |
|---|--|
| Permits assay development based on both organic solvent and aqueous buffer        | Young technology: further research focusing on the analytical performance is warranted     |
| Simple preparation of MIPs  | Poor sensitivity   |
| High tolerance to mechanical and thermal stress                                   | Further studies into detection modes other than measurement of radioactivity are warranted |
| Excellent storage stability: ambient temperature and humidity are not problematic |  |
| Non-biological origin may lead to reduction in the number of laboratory animals   |  |

synthetic challenge and often changes the structural properties of the antigen exposed to the immune system. Therefore, the antibodies elicited may be directed against a structure subtly different to the intended one. Provided the molecule is soluble in the polymerisation mixture, MIP preparation does not include derivatisation of haptenic molecules. The synthesis of MIPs is simple, which contrasts with the often time-consuming generation of antibodies against small molecules. Production of polyclonal antibodies suffers from the fact that different individuals elicit antibodies with different properties and to generate an antiserum with the desired selectivity immunisation of several animals is strongly recommended [1,2]. MIP preparation can be reproduced, with each batch having close to identical properties. In our experience, the batch to batch variation of parameters, such as avidity, binding site density and selectivity, are small and can be considered negligible. The preparation of monoclonal antibodies, however, offers scale-up possibilities and long-term production of antibodies of consistent quality [1,2]. Furthermore, emerging antibody technologies, such as the use of naive libraries and antibody engineering, provide access to antibodies against non-immunogenic substances and predictable selectivity patterns [1,8].

### 14.3 ORGANIC SOLVENT-BASED ASSAYS

Until recent years, a majority of studies on molecular imprinting have been conducted using organic solvents as the rebinding medium. Likewise, work on MIA initially employed organic solvent-based rebinding conditions. In the first study, molecular imprints against theophylline and diazepam were used to develop an assay for the determination of these drugs in human serum [3]. Theophylline is a bronchodilating drug commonly used in the prevention and treatment of asthma and diazepam is a member of the benzodiazepine group of drugs widely used as antidepressants, tranquillisers and muscle relaxants. Prior to the actual assay, performed using organic solvents as the incubation medium, the analyte was extracted from the serum using liquid-liquid extraction. Such extractions have long been standard in bioanalysis for cleaning up biological samples. Briefly, an organic solvent, such as heptane, diethyl ether, methylene chloride, etc., is added to the sample, which can be serum or any other biological matrix. The pH of the sample is adjusted to acidic, basic or neutral pH, depending on which is most favourable for a quantitative extraction of the analyte of interest into the organic phase. Using MIA, both theophylline and diazepam could be determined in clinically significant concentrations satisfactory for therapeutic monitoring of the drugs (Table 14.2). For theophylline, a comparison of the results obtained using a commercial immunoassay technique and the MIA competitive binding assay for the determination of theophylline in patient samples showed good correlation between the two methods [3].

In situations where the analyte is poorly soluble in aqueous buffers, the use of organic solvents may even be beneficial. One such example is determination of cyclosporin, which is a potent immunosuppressive drug used in transplant surgery

TABLE 14.2

## SUMMARY OF STUDIES ON COMPETITIVE LIGAND BINDING EXPERIMENTS EMPLOYING MIPS

| Analyte                                  | Incubation medium                                     | Concentration of MIP (mg/ml) | Limit of detection (nM) | Reference |
|--|---|------------------------------|-------------------------|-----------|
| <i>Measurement of radioactivity</i>      |   |                              |                         |           |
| Atrazine                                 | Acetonitrile  | 50                           | 4600                    | [10]      |
|  | Toluene-acetonitrile (19:1)                           | 1                            | 250                     | [11]      |
| Corticosterone                           | Tetrahydrofuran-heptane                               | 1                            | 100                     | [12]      |
| Cortisol                                 | Tetrahydrofuran-heptane                               | 1                            | 100                     | [12]      |
| Cyclosporin                              | Diisopropylether                                      | 0.0375                       | 4                       | [9]       |
| Diazepam                                 | Toluene-heptane (3:1)                                 | 5                            | 200                     | [3]       |
| 2,4-D                                    | 20 mM phosphate buffer pH 7.0 + 0.1% Triton X-100     | 0.15                         | 135                     | [16]      |
| 17 $\beta$ -Estradiol                    | Acetonitrile  | 30                           | 4000                    | [20]      |
| Methyl- $\alpha$ -D-glucoside            | Acetonitrile-acetic acid (199:1)                      | 10                           |                         | [21]      |
| Morphine                                 | 20 mM citrate buffer pH 6 + 10% ethanol               | 1                            | 790                     | [4]       |
|  | Toluene-acetic acid (49:1)                            | 0.1                          | 150                     | [4]       |
|  | Toluene-acetic acid (49:1)                            | 0.1                          | 100                     | [22]      |
| Leu-enkephalin                           | Acetonitrile-acetic acid (19:1)                       | 8                            |                         | [4]       |
| (S)-Propranolol                          | Plasma-270 mM phosphate buffer pH 7.4-ethanol (6:3:1) | 0.05                         | 20                      | [6]       |
|  | 25 mM citrate buffer pH 6 + 2% ethanol                | 0.05                         | 6                       | [5]       |
|  | 25 mM citrate buffer pH 6 + 2% ethanol                | 0.02                         | 10                      | [14]      |
|  | Toluene-acetic acid (199:1)                           | 0.05                         | 5.5                     | [5]       |
| Theophylline                             | Acetonitrile-acetic acid (99:1)                       | 12.5                         | 3500                    | [3]       |
|  | Acetonitrile  | 5                            | 500                     | [20]      |
|  | Toluene-tetrahydrofuran (9:1; v/v)                    | 0.2                          | Not analysed            | [23]      |
| <i>Measurement of fluorescence</i>       |   |                              |                         |           |
| Chloramphenicol                          | Acetonitrile  | NA <sup>a</sup>              | 9000                    | [24,25]   |
| 2,4-D                                    | 20 mM phosphate buffer pH 7.0 + 0.1% Triton X-100     | 0.5                          | 100                     | [17]      |
|  | Acetonitrile  | 0.2                          | 100                     | [17]      |
| Triazine                                 | Ethanol   | 10                           | 10,000                  | [26]      |
| <i>Measurement of UV-absorbance</i>      |   |                              |                         |           |
| Phenylalanine                            | Methanol  | NA                           | 5000                    | [27]      |
| <i>Electrochemical detection</i>         |   |                              |                         |           |
| 2,4-D                                    | 20 mM phosphate buffer pH 7 containing 10% methanol   | 0.25                         | 1000                    | [18]      |
| <i>Measurement of enzymatic activity</i> |   |                              |                         |           |
| 2,4-D                                    | 0.1 M phosphate buffer pH 7.0 + 0.1% Triton X-100     | 6 <sup>b</sup>               | 180,000 <sup>b</sup>    | [19]      |
|  |   | 0.5 <sup>c</sup>             | 4500 <sup>c</sup>       | [19]      |

<sup>a</sup> Not applicable<sup>b</sup> Colorimetric detection of the label 2,4-D-tobacco peroxidase.<sup>c</sup> Chemiluminescence detection of the label 2,4-D-tobacco peroxidase.

to prevent organ rejection. Due to the narrow therapeutic range of cyclosporin between adequate immunosuppression and toxicity, therapy requires periodic monitoring of the whole blood concentration of the drug. Most laboratories rely on immunoassay methods. Often, an organic solvent, such as methanol, is added to the whole blood sample to release the analyte from red blood cells and to keep the hydrophobic analyte soluble in the incubation mixture. Hence, although not necessarily being the major component in the incubation mixture, organic solvent compatibility of the antibody is an issue. A model MIP-based assay, which could be performed in organic solvents directly after solubilisation and extraction has been developed [9]. Due to their close structural resemblance, the cyclosporin MIP was found to bind the parent drug and four first generation metabolites with equal strength. This led to these four metabolites showing 100% cross-reactivity in the cyclosporin assay. Thus, the assay could be used for determination of the total concentration of cyclosporin A and its major metabolites. A potential application of this assay may be in the determination of the total level of parent drug and metabolites in human whole blood, which in conjunction with any of the specific assays available permits the determination of the total concentration of metabolites.

Several groups have investigated the molecular imprinting of (*S*)-triazine herbicides, such as atrazine, of which two studies on the development of atrazine MIAs have been reported [10,11]. Atrazine is not considered to be highly toxic. However, due to its persistence and previous widespread use, residue analysis of this herbicide is a significant parameter in environmental testing programmes. Both MIA methods were performed in organic solvents, acetonitrile and a mixture of 5% acetonitrile in toluene, respectively. An advantage of the MIP approach in contrast to immunoassays, it was argued, was that the MIA would allow for the analysis of crude organic solvent extracts and alleviate the need for solvent exchange into aqueous-based systems [10].

In a study not primarily focusing on assay development, MIPs mimicking natural steroid binding sites were made through molecular imprinting of corticosterone and cortisol [12]. The MIA technique was employed to investigate their ligand selectivities and binding characteristics. Optimal binding performance was claimed to be achieved with tetrahydrofuran–heptane mixtures which contained small amounts of acetic acid. The MIPs were found to be highly selective for the ligands used in their preparation and the cross-reactivities with compounds of related structure resembled those obtained in studies with the corresponding biological natural antibodies. In a later study, steroid MIPs were used as stationary phases for chromatographic screening of a combinatorial steroid library consisting of 12 closely related  $\Delta^4$ -androstene-3-one structures [13].

#### 14.4 AQUEOUS BUFFER-BASED ASSAYS

As mentioned above, most studies published thus far have dealt with organic solvent-based samples or used liquid–liquid extraction prior to analysis. To become a true alternative to conventional immunoassay techniques which use antibodies,

however, MIPs have to be fully compatible with biological samples. Some of the analyte-MIP systems developed more recently may be utilised equally well using an aqueous buffer or an organic solvent. This was demonstrated for a morphine MIP [4] and studied in detail using an (*S*)-propranolol MIP [5]. Investigations into the influence of pH, the concentrations of ethanol and citrate buffer and ionic strength on efficiency of (*S*)-propranolol binding were undertaken. These optimisations led to improvements of several orders of magnitude in the limit of quantification and reductions of the amount of imprinted polymer used. The binding increased with increasing pH, as did the non-specific binding to a non-imprinted polymer, and maximum difference occurred at pH 6. The workable region was, however, established to be in the range of pH 5–8. Addition of ethanol reduced the non-specific binding, while the specific binding was constant between 2% and 16% ethanol. Similarly, while the specific binding was unaffected at buffer concentrations above 5 mM, increased ionic strength and buffer concentration reduced the non-specific binding. Equally high sensitivity was obtained with the aqueous assay as with the solvent-based assay, with limits of determination for pure systems as low as 6 nM. The work has been pursued to the development of a model assay for direct determination of (*S*)-propranolol in biological samples [6]. A typical assay uses only 50 µg of polymer and can be used for measuring (*S*)-propranolol plasma and urine concentrations in the range of 20 to 1000 nM with acceptable accuracy and precision. This demonstrates that molecular imprint-based assays of biological samples without prior sample clean-up are possible.

To facilitate separation of bound and free radioligand, composite beads composed of magnetic iron oxide and a methacrylic acid-trimethylol propane trimethacrylate copolymer have been prepared [14]. Molecular imprinting of (*R,S*)-propranolol in such composite beads was done through inclusion of iron oxide in a suspension polymerisation protocol utilising a perfluorocarbon as the dispersing phase [15]. A competitive radioligand binding assay, which uses a magnet to separate polymer from solution was set up. Although it was argued a more efficient separation would result from higher content of iron oxide in the beads, by optimisation of the preparation method, these beads could easily be withdrawn from a solution by the applied magnetic field. Using tritiated (*S*)-propranolol as the radioligand, the magnetic (*R,S*)-propranolol MIP was found to exhibit very similar cross-reactivity for (*R*)-propranolol and (*R,S*)-metoprolol to the non-magnetic bulk polymer described above.

Molecular imprinting of the herbicide 2,4-dichlorophenoxyacetic acid (2,4-D) was undertaken using a mixture of methanol–water as the solvent of polymerisation [16,17]. 4-Vinylpyridine was used as the functional monomer and complex formation in the pre-polymerisation mixture was suggested to rely on hydrophobic and ionic interactions. This contrasts with other MIPs used for ligand binding assays, which have been made employing apolar solvents for polymerisation and methacrylic acid as the functional monomer. Using apolar solvents, complex formation in the pre-polymerisation mixture is mainly due to hydrogen bonding. In sodium phosphate buffer pH 7.0, containing 0.1% of the detergent Triton X-100, this MIP showed excellent selectivity for 2,4-D over several close structural



analogues. In contrast to the situation for methacrylic acid type MIPs binding analytes containing amino groups, it was found that the non-specific binding was high at low pH and was insignificant at pH 6 and above.

## 14.5 SELECTIVITY

In most studies, the selectivities of the MIPs have been estimated by measuring the amount of each ligand required to displace 50% of the binding of radiolabelled imprint species to the MIP ( $IC_{50}$ ). The first MIA study reported excellent selectivity of the theophylline method for theophylline (1,3-dimethylxanthine) in the presence of the structurally related compound caffeine (1,3,7-trimethylxanthine) [3]. Despite their close resemblance (they differ by only one methyl group), caffeine showed less than 1% cross-reactivity. A similar level of specificity was recorded for cortisol and corticosterone MIPs, which were able to detect the absence and presence of single hydroxyl groups and double bonds in the steroid structure [13].

In some instances, the absence of a requirement for derivatisation has been shown to result in specificities of the MIP system comparable to those reported for antibodies [4,5,12,17]. The selectivity recorded for morphine MIPs is an illustrative example. The very closely related structure codeine interferes to a lesser extent with morphine binding to the MIP than to most of the anti-morphine antibodies reported to date [4]. This finding is significant in the context of codeine being a notoriously difficult cross-reactant for biological anti-morphine antibodies. Conjugation of morphine to a carrier protein can be accomplished through reaction at any of three positions (Fig. 14.2), of which the phenol is the one most commonly used. Then the presence of an alkyl spacer leads to the antigen being structurally more similar to codeine than to morphine and, consequently, the resulting antibodies will bind codeine more strongly than morphine.

An interesting point is the differing selectivities obtained for the organic solvent and aqueous buffer-based assays. This was first demonstrated for (*S*)-propranolol

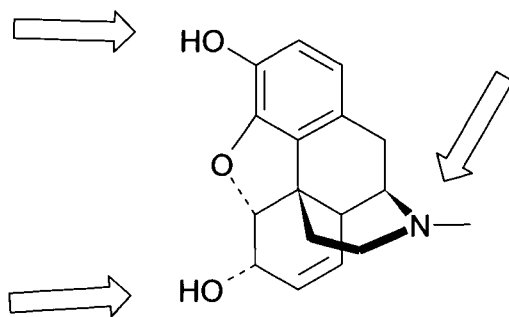


Fig. 14.2. Available positions for linking morphine to a carrier protein. Depending on which position is used for conjugation different sides of the morphine molecule are exposed to the immune system.

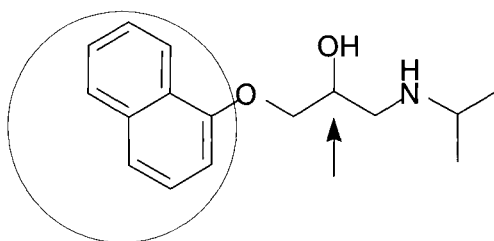


Fig. 14.3. Structure of propranolol. The chiral carbon is indicated by the arrow and the hydrophobic naphthyl group is encircled.

MIPs [5] and later for other MIPs [17, L.I. Andersson, unpublished results]. Using aqueous buffers as the incubation medium, the (*S*)-propranolol MIP showed high substrate-selectivity for propranolol in the presence of structurally similar  $\beta$ -blockers. When toluene was used as the solvent instead, the MIP showed excellent enantio-selectivity, the cross-reactivity of the (*R*)-enantiomer being only 1%. These different selectivity profiles are due to a different balance between hydrophobic and polar interactions in toluene and water, since polar interactions, such as hydrogen bonds, are strong in apolar solvents and hydrophobic interactions are strong in water. The aminopropanediol part of the structure is identical for all  $\beta$ -blockers and the individual drugs differ by their ether substituent, which for propranolol is a hydrophobic naphthyl ring system (Fig. 14.3). Enantio-recognition requires recognition through hydrogen bonding of the configuration of the polar functionalities surrounding the chiral carbon. This indicates that, depending on the type of specificity required, the conditions for the assay can be chosen so as to obtain the selectivity pattern most relevant to the particular analysis problem.

## 14.6 SENSITIVITY

Like polyclonal antibodies, the polymers contain a heterogeneous population of binding sites with a range of affinities for the imprint molecule. Thus, multiple apparent equilibrium dissociation constants ( $K_D$ ), varying from high to low affinity, are obtained on analysis of binding data. Apparent  $K_D$  values down to  $10^{-9}$  M have been obtained, as compared to the  $10^{-6}$ – $10^{-14}$  M range typical for antibodies. Due to the binding site heterogeneity, the apparent affinity (and hence the sensitivity) of the assay system is partly determined by the concentrations of polymer and labelled compound in the incubation mixture. At low polymer and radioligand concentrations, only the high-affinity sites are able to bind the radioligand and in the competitive assay format the displacement events occur predominantly at these saturated high-affinity sites. Furthermore, under these conditions the non-specific binding can be greatly reduced or eliminated.

Initially, the sensitivities reported for imprint-based assays were in the  $\mu\text{mol/L}$  range, but recent publications report detection limits in the  $\text{nmol/L}$  range (Table

14.2), therefore allowing MIP-based assays at clinically relevant concentrations. Another one to two orders of magnitude lower limits of detection may in theory be achieved, and is desirable, with the present detection system which uses tritium-labelled tracers. The improvement of the previously poor sensitivities has been obtained through refinements of the MIP preparation and optimisation of the rebinding conditions. Further lowering of the detection limits requires improved washing protocols of the MIP prior to use. While being of less significance in many other applications, for MIA near-quantitative removal of the imprint species is critically important, since a more thorough extraction yields a MIP where more of the high-avidity sites are free. Complete extraction requires extensive washing using solvents with strong elution power, such as aqueous ethanol containing acid or base. In our experience, alternating acid and base washes have proven beneficial, and such very thorough extraction protocols do improve assay sensitivity [L.I. Andersson, unpublished results]. Further investigations into the washing procedure are, however, warranted. A second means of improving assay sensitivity is to increase the inherent affinity of the MIP through the preparation of imprints with a more precise complementarity to the imprint molecule. Here, ongoing developments of the various imprinting technologies (see other chapters in this book) are hoped not only to increase affinity, but also to improve homogeneity of the imprint population.

## 14.7 NON-RADIOACTIVE ASSAYS

Based on the 2,4-D MIP described above, a fluorescent ligand displacement assay for this herbicide has been developed [17]. The tracer used was a non-related fluorescent coumarin derivative, however, having some structural elements in common with 2,4-D. It was found that the 2,4-D MIP did bind the coumarin tracer and that this binding could indeed be displaced by the imprint species. In pure acetonitrile the displacement curve was near-identical to that obtained using radiolabelled 2,4-D, while in aqueous buffer the displacement curve for the fluorescent tracer was shifted to higher concentrations of analyte relative to that for the radioligand. The radiolabelled and the fluorescent assays showed similar levels of specificity and sensitivity. The fluorescent assay was claimed to be useful both in aqueous buffer and in organic solvents, in both instances with a limit of detection of 100 nM. In another study, the electrochemically active non-related structure homogentisic acid was used as a tracer in a competitive assay for detection of 2,4-D [18]. Quantification of unbound tracer was done by voltammetry. Also, an integrated sensor could be developed by coating the MIP particles directly onto the working electrode [18]. Although not being universally applicable, it was concluded that the approach proposed may be useful in many instances.

Recently, an enzyme-labelled assay for 2,4-D has been presented [19]. The label was 2,4-D conjugated to the enzyme tobacco peroxidase, which allowed for both colorimetric and chemiluminescence detection. In this instance, the 2,4-D MIP was synthesised in the form of microspheres [20]. In contrast, despite its higher binding

capacity for radiolabelled 2,4-D, a conventional MIP, prepared by bulk polymerisation, showed only weak binding of the 2,4-D–tobacco peroxidase conjugate. Imprinted microspheres are believed to have a higher proportion of their binding sites at or close to their surface, and the imprints are more accessible to bind bulky enzyme-labelled 2,4-D reporter molecules. Added analyte displaced binding of the label and calibration curves for 2,4-D could be established. Although, at present, the sensitivity of the enzyme-labelled assay is poorer than that recorded for the corresponding assays based on the use of fluorescent and radiolabelled tracers, the development represents an important extension of MIA to detection systems widely used in immunoassay technology.

Further investigations into the use of fluorescent and enzymatic labels in MIP-based assays are highly warranted. A general concern is that the bulkiness of such labels may affect their binding to the MIP, which in turn may compromise assay sensitivity. While a wealth of data is available, though often fragmented and unstructured, systematic studies on structure–binding affinity relationships would aid the structural design of tracers based on non-radioactive labels. As the general trend towards increased use of non-radioactive techniques of immunoassay seems stable, the successful introduction of usable alternatives to radioactive tracers is crucial to a wider acceptance of MIA.

## **14.8 CONCLUSIONS AND FUTURE OUTLOOK**

Several studies into the use of MIPs in the bioanalysis of drugs and other compounds have already been presented (Table 14.3). As discussed in this chapter, an area with great interest is the use of MIPs as substitutes for antibodies in immunoassay. Whereas for proteins and other biomacromolecules MIPs still have to prove their utility, molecular imprinting complements antibody technology in the context of assay development for low molecular weight compounds. In this area, MIPs provide a combination of polymer mechanical and chemical robustness with highly selective molecular recognition, in many instances comparable to biological systems. For instance, poorly water soluble analytes can be assayed using organic solvents. The relative lack of sensitivity of MIA methods needs attention. At present, sensitivity is limited due to leakage of imprint molecules and the use of appropriate washing protocols in the MIP preparation is imperative. From a practical standpoint, the extension of the utility of MIP-based assays to the direct assay of biosamples, without any requirements for transfer of the analyte into an organic solvent, is essential. Recently it was demonstrated that MIPs have the capacity to bind in a specific manner analytes from plasma and urine samples [6,30,33,35,37]. These findings are promising for the development of general approaches to the use of imprint-based assays in combination with biological samples.

An application of molecular imprinting in drug bioanalysis closer to practical realisation is probably that of solid phase extraction (SPE). This application does not suffer to the same extent from the drawbacks generally associated with MIPs, such as peak broadening in liquid chromatography and leakage of imprint mole-

TABLE 14.3

## SUMMARY OF BIOANALYTICAL APPLICATIONS EMPLOYING MIPS

|  |   |         |
|--|---|---------|
| <b>SPE</b>                             |   |         |
| Atrazine                               | Chloroform extract of beef liver homogenate   | [28]    |
| Darifenacin                            | Plasma–acetonitrile (1:1; v/v)  | [29]    |
| Hydroxycoumarin                        | Urine   | [30]    |
| Nicotine                               | Ethyl acetate extract of chewing gum  | [31]    |
|  | Methanol–0.1 M NaOH extract of cigarette tobacco  | [32]    |
| Propranolol                            | Dog plasma, rat bile and human urine  | [33,34] |
| Pentamidine                            | Diluted urine   | [35]    |
| Sameridine                             | Heptane–ethanol (9:1; v/v) after extraction of human plasma                               | [36]    |
| Tamoxifen                              | Human plasma and urine  | [37]    |
| Theophylline                           | Chloroform extract of human serum   | [38,39] |
| Triazine herbicides                    | Acetonitrile after C18-extraction of urine, apple extract and water containing humic acid | [40]    |
| <b>MIA</b>                             |   |         |
| Cyclosporin                            | Diisopropyl extract of human whole blood  | [9]     |
| Diazepam                               | Toluene–heptane (3:1; v/v) after extraction of human serum                                | [3]     |
| (S)-Propranolol                        | Human plasma and urine  | [6]     |
| Theophylline                           | Acetonitrile–acetic acid (99:1; v/v) after extraction of human serum                      | [3]     |
| <b>Competitive displacement sensor</b> |   |         |
| Chloramphenicol                        | Acetonitrile after extraction of bovine serum   | [41]    |
| <b>Sensor</b>                          |   |         |
| Caffeine                               | Serum and urine diluted with borate buffer pH 8   | [42]    |
| Flavonol                               | Olive oil–hexane–chloroform (5:14:6; v/v/v)   | [43]    |
| Glucose                                | Porcine plasma  | [44]    |
| <b>Liquid chromatography</b>           |   |         |
| Naproxen                               | Serum   | [45]    |

cules in MIA. The on–off type chromatography employed is less sensitive to poor chromatographic performance of MIP sorbents. A strategy to circumvent problems with leakage of imprint molecules during elution, leading to uncertainties in the concentration determination, is the alternative imprint molecule approach. A close structural analogue of the analyte(s) of interest is used as the imprint molecule. Provided the imprint species and the analyte(s) can be separated by the subsequent liquid or gas chromatography, which in most instances is a valid assumption, the leakage will appear as a separate peak and present no problem. Analogous to MIA, non-specific adsorption to the polymer can be reduced by the use of small amounts of MIP and proper washing schemes prior to elution. Due to the strong affinity of the MIP for the analyte, a potential problem may be the harsh conditions required to effect quantitative elution of the analyte. Several groups have

already applied MIP-based SPE to biological samples (Table 14.3) and this technique may well be established generally in the not-too-distant future.

## REFERENCES

- 1 C.P. Price and D.J. Newman (Eds), *Principles and practice of immunoassay*, 2nd edn, Macmillan Reference Ltd, London (1997).
- 2 B. Law (Ed.), *Immunoassay, a practical guide*, Taylor & Francis Ltd, London (1996).
- 3 G. Vlatakis, L.I. Andersson, R. Müller and K. Mosbach, *Nature*, **361**, 645 (1993).
- 4 L.I. Andersson, R. Müller, G. Vlatakis and K. Mosbach, *Proc. Natl. Acad. Sci. USA*, **92**, 4788 (1995).
- 5 L.I. Andersson, *Anal. Chem.*, **68**, 111 (1996).
- 6 H. Bengtsson, U. Roos and L.I. Andersson, *Anal. Commun.*, **34**, 233 (1997).
- 7 D. Kriz and K. Mosbach, *Anal. Chim. Acta*, **300**, 71 (1995).
- 8 C.A.K. Borrebäck (Ed.), *Antibody engineering*, 2nd edn, Oxford University Press, New York (1995).
- 9 M. Senholdt, M. Siemann, K. Mosbach and L.I. Andersson, *Anal. Lett.*, **30**, 1809 (1997).
- 10 M.T. Muldoon and L.H. Stanker, *J. Agric. Food Chem.*, **43**, 1424 (1995).
- 11 M. Siemann, L.I. Andersson and K. Mosbach, *J. Agric. Food Chem.*, **44**, 141 (1996).
- 12 O. Ramström, L. Ye and K. Mosbach, *Chem. Biol.*, **3**, 471 (1996).
- 13 O. Ramström, L. Ye, M. Krook and K. Mosbach, *Anal. Commun.*, **35**, 9 (1998).
- 14 R.J. Ansell and K. Mosbach, *Analyst*, **123**, 1611 (1998).
- 15 A.G. Mayes and K. Mosbach, *Anal. Chem.*, **68**, 3769 (1996).
- 16 K. Haupt, A. Dzgoev and K. Mosbach, *Anal. Chem.*, **70**, 628 (1998).
- 17 K. Haupt, A.G. Mayes and K. Mosbach, *Anal. Chem.*, **70**, 3936 (1998).
- 18 S. Kröger, A.P.F. Turner, K. Mosbach and K. Haupt, *Anal. Chem.*, **71**, 3698 (1999).
- 19 I. Surugiu, L. Ye, E. Yilmaz, A. Dzgoev, B. Danielsson, K. Mosbach and K. Haupt, *Analyst*, **125**, 13 (2000).
- 20 L. Ye, P.A.G. Cormack and K. Mosbach, *Anal. Commun.*, **36**, 35 (1999).
- 21 A. Mayes, L.I. Andersson and K. Mosbach, *Anal. Biochem.*, **222**, 483 (1994).
- 22 A.G. Mayes and C.R. Lowe, In: *Methodological surveys in bioanalysis of drugs*, vol. 25. *Drug development assay approaches including molecular imprinting and biomarkers*, E. Reid, H.M. Hill and I.D. Wilson Eds, p. 28 (1998).
- 23 E. Yilmaz, K. Mosbach and K. Haupt, *Anal. Commun.*, **36**, 167 (1999).
- 24 R. Levi, S. McNiven, S.A. Piletsky, S.-H. Cheong, K. Yano and I. Karube, *Anal. Chem.*, **69**, 2017 (1997).
- 25 S. McNiven, M. Kato, R. Levi, K. Yano and I. Karube, *Anal. Chim. Acta*, **365**, 69 (1998).
- 26 S.A. Piletsky, E.V. Piletskaya, A.V. Elaskaya, R. Levi, K. Yano and I. Karube, *Anal. Lett.*, **30**, 445 (1997).
- 27 S.A. Piletsky, E. Terpetschnig, H.S. Andersson, I.A. Nicholls and O.S. Wolfbeis, *Fresenius J. Anal. Chem.*, **363**, 512 (1999).
- 28 M.T. Muldon and L.H. Stanker, *Anal. Chem.*, **69**, 803 (1997).
- 29 R.F. Venn and R.J. Goody, In: *Methodological surveys in bioanalysis of drugs*, vol. 25. *Drug development assay approaches including molecular imprinting and biomarkers*, E. Reid, H.M. Hill and I.D. Wilson Eds, p. 13 (1998).
- 30 M. Walshe, J. Howarth, M.T. Kelly, R.O'Kennedy and M.R. Smyth, *J. Pharm. Biomed. Anal.*, **16**, 319 (1997).
- 31 Å. Zander, P. Findlay, T. Renner, B. Sellergren and A. Swietlow, *Anal. Chem.*, **70**, 3304 (1998).
- 32 W.M. Mullett, E.P.C. Lai and B. Sellergren, *Anal. Commun.*, **36**, 217 (1999).

- 33 P. Martin, I.D. Wilson, D.E. Morgan, G.R. Jones and K. Jones, *Anal. Commun.*, **34**, 45 (1997).
- 34 P. Martin, I.D. Wilson, G.R. Jones and K. Jones, In: *Methodological surveys in bioanalysis of drugs, vol. 25. Drug development assay approaches including molecular imprinting and biomarkers*, E. Reid, H.M. Hill and I.D. Wilson Eds, p. 21 (1998).
- 35 B. Sellaergren, *Anal. Chem.*, **66**, 1578 (1994).
- 36 L.I. Andersson, A. Paprica and T. Arvidsson, *Chromatographia*, **46**, 57 (1997).
- 37 B.A. Rashid, R.J. Briggs, J.N. Hay and D. Stevenson, *Anal. Comm.*, **34**, 303 (1997).
- 38 W.M. Mullett and E.P.C. Lai, *Anal. Chem.*, **70**, 3636 (1998).
- 39 W.M. Mullett and E.P.C. Lai, *J. Pharm. Biomed. Anal.*, **21**, 835 (1999).
- 40 B. Bjarnason, L. Chimuka and O. Ramström, *Anal. Chem.*, **71**, 2152 (1999).
- 41 R. Levi, S. McNiven, S.A. Piletsky, S.-H. Cheong, K. Yano and I. Karube, *Anal. Chem.*, **69**, 2017 (1997).
- 42 C. Liang, H. Peng, X. Bao, L. Nie and S. Yao, *Analyst*, **124**, 1781 (1999).
- 43 J.L. Suárez-Rodríguez and M.E. Díaz-García, *Anal. Chim. Acta*, **405**, 67 (2000).
- 44 G. Chen, Z. Guan, C.-T. Chen, L. Fu, V. Sundaresan and F.H. Arnold, *Nature Biotechnol.*, **15**, 354 (1997).
- 45 J. Haginaka, H. Takehira, K. Hosoya and N. Tanaka, *J. Chromatogr. A*, **849**, 331 (1999).

## Molecularly imprinted polymers in solid phase extractions

BÖRJE SELLERGREN AND FRANCESCA LANZA

### 15.1. INTRODUCTION

Analytical methods for rapid determination of chemicals, biomolecules or cells are of growing interest in various fields such as environmental control, drug development, health protection, forensics and biotechnology [1–4]. The steadily increasing number of organic environmental pollutants (pesticides, industrial waste and degradation products) is a major health hazard and has therefore created a need for efficient environmental monitoring relying on low-cost, rapid and automated methods of analysis. The analytical challenge associated herewith is obvious from the large number of EU-sponsored projects on this subject. An equally important challenge is the rapid analysis of low levels of drugs, narcotics and their metabolites in humans, as well as the quality control of food, foodstuffs and pharmaceuticals. The development of efficient analytical methods in these fields will have a direct impact on the quality and efficiency of health care, forensic activities and the food industry.

The analysis of target molecules in complex mixtures often requires pretreatment steps [5]. First, if the analyte is present in low concentration, it needs to be concentrated in order to be detected by standard analytical techniques. Secondly, if it is present in a complex mixture of similar compounds, a clean-up step is required. Solid phase extraction (SPE) has become a widely used technique for sample

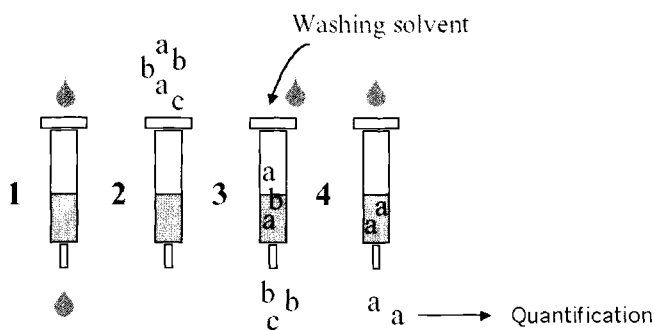


Fig. 15.1. SPE for enrichment and clean-up of complex samples prior to analyte (a) quantification. Steps: (1) conditioning of the sorbent, (2) percolation of the water sample, (3) washing step and (4) elution step.



pretreatment as it is easily automated, flexible and environmentally friendly (Fig. 15.1) [6–8]. It consists of percolating a known volume of a liquid sample through a solid sorbent (in the format of a cartridge, column or a disk) under carefully chosen conditions favouring the preferential absorption of the analyte over the matrix components. In the most common technique uncharged analytes are adsorbed on a hydrophobic sorbent. The analyte of interest is then recovered from the sorbent by elution in a small volume (smaller than the applied sample volume) of an appropriate solvent mixture. High enrichments as well as efficient sample clean-up can thus be obtained in one step.

## 15.2. MULTI-PURPOSE SPE PHASES

The attainable enrichment and clean-up in SPE depend primarily on the selectivity and affinity of the sorbent for the selected target analyte or analytes, the sample load capacity for the analytes and the rate of mass transfer to and from the binding sites, the latter affecting the minimum desorption volume and thus the enrichment that can be obtained. Other factors of importance are the reproducibility of the recovery yields and the stability and reusability of the sorbent when on-line procedures are desired. For hydrophobic analytes satisfactory results are usually obtained using standard reversed phase sorbents. Thus hydrophobised silica (C8, C18), styrene-divinylbenzene copolymers (PS-DVB) and graphitised carbon black (GCB) are the conventional sorbent materials used in SPE (Fig. 15.2)

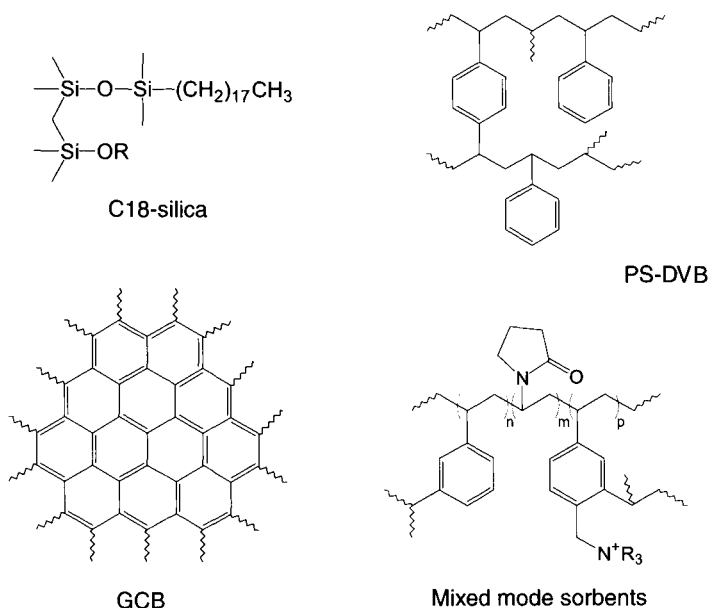


Fig. 15.2. Common multi-purpose sorbents used in SPE.

[8]. A high sample load capacity, together with the wide range of trapped analytes, are the interesting features of reversed phase materials (mainly C18), whereas their poor selectivity, the narrow pH stability range and the limited breakthrough volumes for hydrophilic analytes are their main disadvantages. In the case of hydrophilic analytes enrichment and clean-up are usually more difficult to obtain. This leads to disturbances in the subsequent chromatographic analysis. Therefore sorbents that can be tailor-made to bind hydrophilic analytes have been developed. For instance, highly porous mixed mode sorbents containing both hydrophobic and hydrophilic polar moieties have been designed (see Fig. 15.2) [9]. These have been shown to retain highly polar pesticides and metabolites, such as glyphosate and hydroxylated atrazine metabolites, that are not well retained on high capacity reversed-phase materials. The mixed mode sorbents also exhibited high selectivity and sensitivity for extracting a wide range of acidic, basic and neutral drugs from complex matrices such as blood, urine and human plasma. These phases are, however, not suited for on-line operation. In these cases restricted access materials (RAM) have found widespread use allowing direct repeat injections of untreated blood plasma or urine samples [10–12]. Through pore-size selective surface modification techniques the outer surface of the support particles can be made hydrophilic and non-sticky to plasma proteins whereas the inner surface, non-accessible to plasma proteins, is made hydrophobic or equipped with other functional groups (Fig. 15.3). Thus these phases are able to efficiently remove the high molecular weight matrix components and quantitatively retain the drugs of interest and have therefore been used for the on-line enrichment and sample clean-up of biofluids. In this field, liquid–liquid extraction is often still the recommended method for sample preparation, although the need for high throughput screening in the drug monitoring step has made SPE, often in the 96-well plate format, the method of choice [13].

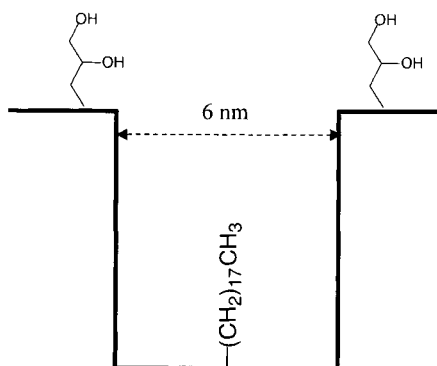


Fig.15.3. RAM developed for direct injection of biological fluids.

### **15.3 HIGH AFFINITY SPE PHASES**

The complex sample matrixes, in combination with the need for lower detection limits, has increased the demand for phases that can strongly and selectively bind an analyte or a group of analytes. Biological molecular recognition elements (enzymes, antibodies or cells) can be used for this purpose. For instance immunoaffinity based enrichment techniques can be used for specific determination of a particular analyte or a class of analytes [2,8]. As with most affinity techniques relying on biological recognition elements, method robustness and reproducibility, receptor immobilisation technique and the time and cost involved in providing the receptor for a new target analyte are factors that may be associated with problems.

Therefore the development of synthetic phases that can offer similar recognition properties seems desirable. One promising way to introduce selectivity in chemical analysis is the use of molecularly imprinted polymers (MIPs) [14–16]. These can in favourable cases recognise small molecules with affinities and selectivities exceeding that of antibody–antigen and have, due to their robustness, capacity and reproducibility, potential as reusable adsorbents in assays or sample pretreatment.

### **15.4 MOLECULARLY IMPRINTED SPE (MISPE)**

Highly selective sorbents towards a large number of analytes of environmental and pharmaceutical interest can be prepared by molecular imprinting [17]. The most versatile approach to the synthesis of molecularly imprinted sorbents is based on self-assembly of the template and a complementary functionalised monomer (e.g. methacrylic acid (MAA)) prior to polymerisation (see Chapter 5). Several examples of the successful application of MIPs to SPE have been described in the literature (Table 15.1). In most cases MIPs have been used in a cartridge format in the off-line mode to clean-up and enrich samples prior to various detection techniques. In some cases the protocols have only been preliminarily tested to show the feasibility of the approach [18–21], in others they have been fully validated [22–24]. The retentivity and selectivity of the sorbents are generally first assessed by HPLC–UV. The results of these studies reveal whether aqueous samples can be directly applied to the column, as in the extraction of hydrophobic analytes from aqueous media, e.g. biological or environmental samples, or whether the analyte has to be transferred to an organic solvent of lower polarity prior to the MISPE, as for analytes that are not sufficiently retained in aqueous mobile phases. In the former case the adsorption step often occurs in the liquid chromatography (LC) reversed phase mode of operation and is usually non-selective (Fig. 15.4). Here the selectivity is introduced by selective wash procedures which serve to remove non-selectively bound matrix components [19,25–27,30]. The analyte is then recovered eluting with solvents of increasing eluotropic strength. In the latter case, however, the adsorption occurs similarly to the LC normal phase mode of operation and can be highly selective [22–24,28].

TABLE 15.1

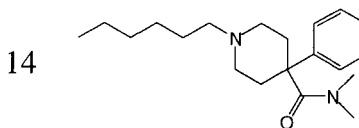
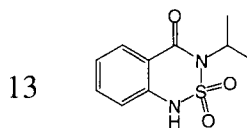
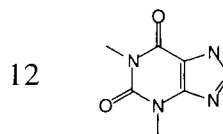
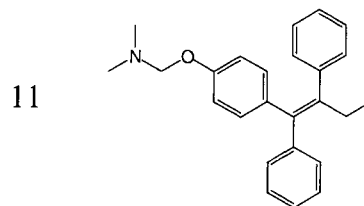
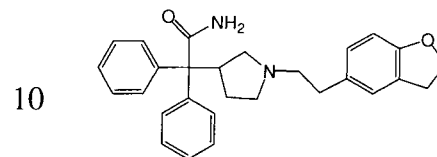
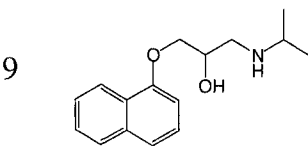
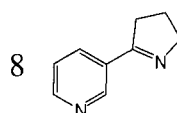
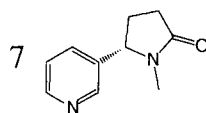
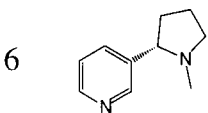
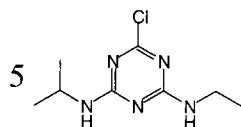
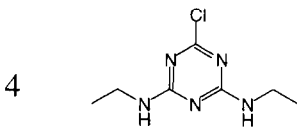
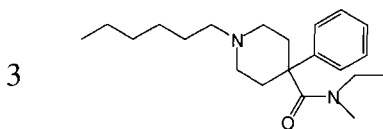
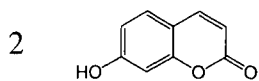
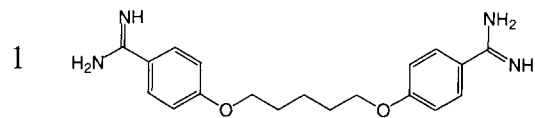
SAMPLE APPLICATION, WASHING AND ELUTION CONDITIONS IN PREVIOUS MISPE PROTOCOLS. For structures of the analytes see page 361

| Analyte   | MIP format | Recognition assessment         | Protocol    | Sample                 | Sample modification prior to application                    | Washing step                                       | Elution Mep                              | Detection technique               | Reference |
|---|------------|--------------------------------|-------------|------------------------|---|--|--|-----------------------------------|-----------|
| A Pentamidine <b>1</b>  | Column     | HPLC                           | Off-line SD | Urine                  | Dilution with buffer pH 5 (1/1) then dilute with MeCN (3/7) | MeCN/buffer pH 9 (1), pH 5 (2); 7/3                | MeCN/buffer pH 3: 7/3                    | UV                                | [18]      |
| B 7-Hydroxy-coumarin <b>2</b>                                   | Cartridge  | —                              | Off-line SD | Urine                  | pH adjustment (6.0)   | Water  | MeOH                                     | CZE                               | [26]      |
| C Sameridine <b>3</b>   | Batch      | Radioligand binding experiment | Off-line SA | Plasma                 | Extraction in heptane                                       | Heptane-EtOH (1/1)                                 | Heptane/EtOH/NaOH (5 N) 170/13/17        | GC-FID                            | [23]      |
| D Simazine <b>4</b>   | Cartridge  | HPLC                           | Off-line SD | Water                  | None  | Dichloromethane (previous drying of the cartridge) | MeOH                                     | HPLC-UV                           | [19]      |
| E Atrazine <b>5</b>   | Cartridge  | Batch rebinding                | Off-line SA | Beef liver extracts    | Extraction in chloroform                                    | Chloroform   | MeCN/HOAc: 9/1 (v/v)                     | HPLC-UV ELISA                     | [24]      |
| F Nicotine <b>6</b> ,<br>Cotinine <b>7</b><br>Myosmine <b>8</b> | Cartridge  | HPLC                           | Off-line SA | Chewing gum            | Dissolution in ethyl acetate/25% ammonia                    | Acetonitrile (previous drying of the cartridge)    | MeCN/H <sub>2</sub> O/TFA (97.3/2.5/0.2) | HPLC-UV                           | [22]      |
| G Propranolol <b>9</b>  | Cartridge  | Cumulative recovery curves     | Off-line SD | Plasma, bile and urine | None  |  | MeOH/H <sub>2</sub> O 1% TFA or TEA      | Scintillation counting<br>HPLC-UV | [27]      |

| Analyte                                | MIP format              | Recognition assessment | Protocol    | Sample                           | Sample modification prior to application              | Washing step                                | Elution step                      | Detection technique            | Reference |
|--|-------------------------|------------------------|-------------|----------------------------------|---|---|-----------------------------------|--------------------------------|-----------|
| H Darifenacin <b>10</b>                | Cartridge               | HPLC                   | Off-line SA | Plasma                           | Addition of CH <sub>3</sub> CN 50% (deproteinisation) | 50% and then 70% CH <sub>3</sub> CN         | CH <sub>3</sub> CN with 0.1 % TFA | HPLC-UV Scintillation counting | [20]      |
| I Tamoxifen <b>11</b>                  | Cartridge               |                        | Off-line SD | Plasma and urine                 | None  | (1)H <sub>2</sub> O, (2) MeCN               | MeCN/HOAc 4/1 (v/v)               | HPLC-UV                        | [25]      |
| J Theophylline <b>12</b> and analogues | Column and micro-column | Batch rebinding        | On-line SA  | Serum                            | Extraction in chloroform                              | Pulses of MeCN                              | Pulse of MeOH                     | UV                             | [28]      |
| K Triazines                            | Column                  | HPLC                   | On-line     | Humic acid, apple extract, urine | Adsorption on C18, Desorption with MeCN               | MeCN  | Water plug                        | HPLC-UV                        | [32]      |
| L Bentazone <b>13</b>                  | Cartridge               | HPLC                   | Off-line SD | Water                            | pH adjustment (5.0)                                   | (1)Buffer (50 mM, pH 5, 50mM NaCl) (2) MeCN | MeOH/HOAc 99/1 (v/v)              | HPLC-UV                        | [21]      |

SD = selective desorption; SA = selective adsorption; CZE = capillary zone electrophoresis; ELISA = enzyme linked sorbent assay.

Refer to page 359



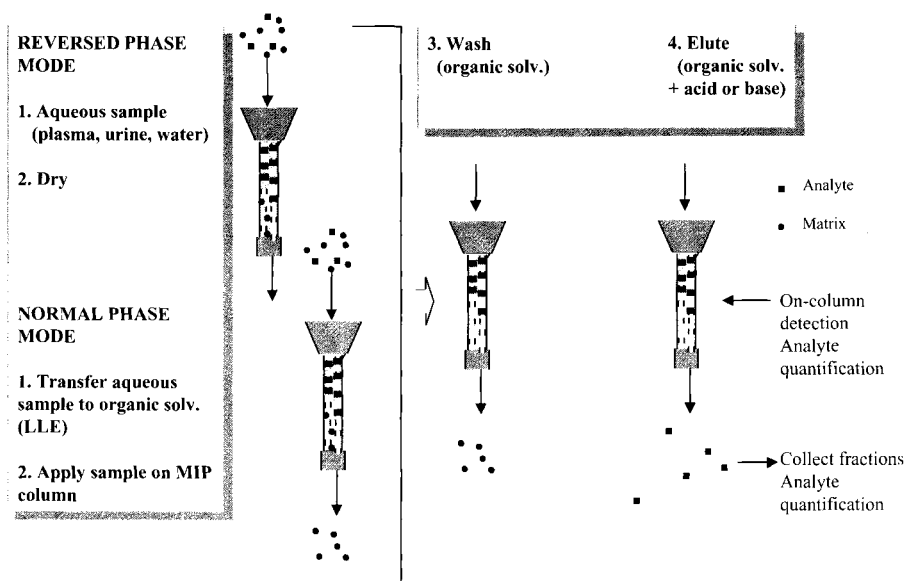


Fig. 15.4. Reversed phase and normal phase mode of operation in the off-line application of MIPs in SPE.

In MISPE the washing and elution conditions need to be carefully optimised in terms of pH, ionic strength and solvent composition in order to fully exploit the MIPs' ability to recognise the template. In cases where recognition is driven by electrostatic interactions best results are often seen when using the porogenic solvent as wash solvent (solvent memory effect) [29]. This causes compatibility problems since many of the porogens are not miscible with water. This problem can be solved by drying of the MIP cartridges prior to the washing step [19,30]. Unfortunately the drying step is difficult to combine with on-line procedures which instead rely on the use of water miscible solvents in the wash step. Alternatively a coupled column system may be adopted where the analytes are first non-specifically adsorbed on a multi-purpose SPE column, e.g. a hydrophobic sorbent (C18 reversed phase or restricted access sorbent) and then transferred to a dedicated MIP sorbent in organic media. This approach is suitable for on-line applications, as recently demonstrated by Boos and co-workers [31] and Bjarnason *et al.* [32], and has the advantage of allowing the direct injection of biological samples (Fig. 15.5).

In addition it leaves the imprinted sorbent wetted by organic solvents, minimising swelling and shrinking of the material, conditioning times and bleeding effects. Swelling–shrinkage of the polymers leads to changes in site accessibility and can cause entrapment of the analytes, which in turn leads to low recoveries. In this context the pulsed elution method recently described by Mullet and Lai also does not require solvent switching and would thus allow a higher sample throughput [28].

Once a selective extraction has been achieved, the analyte needs to be efficiently

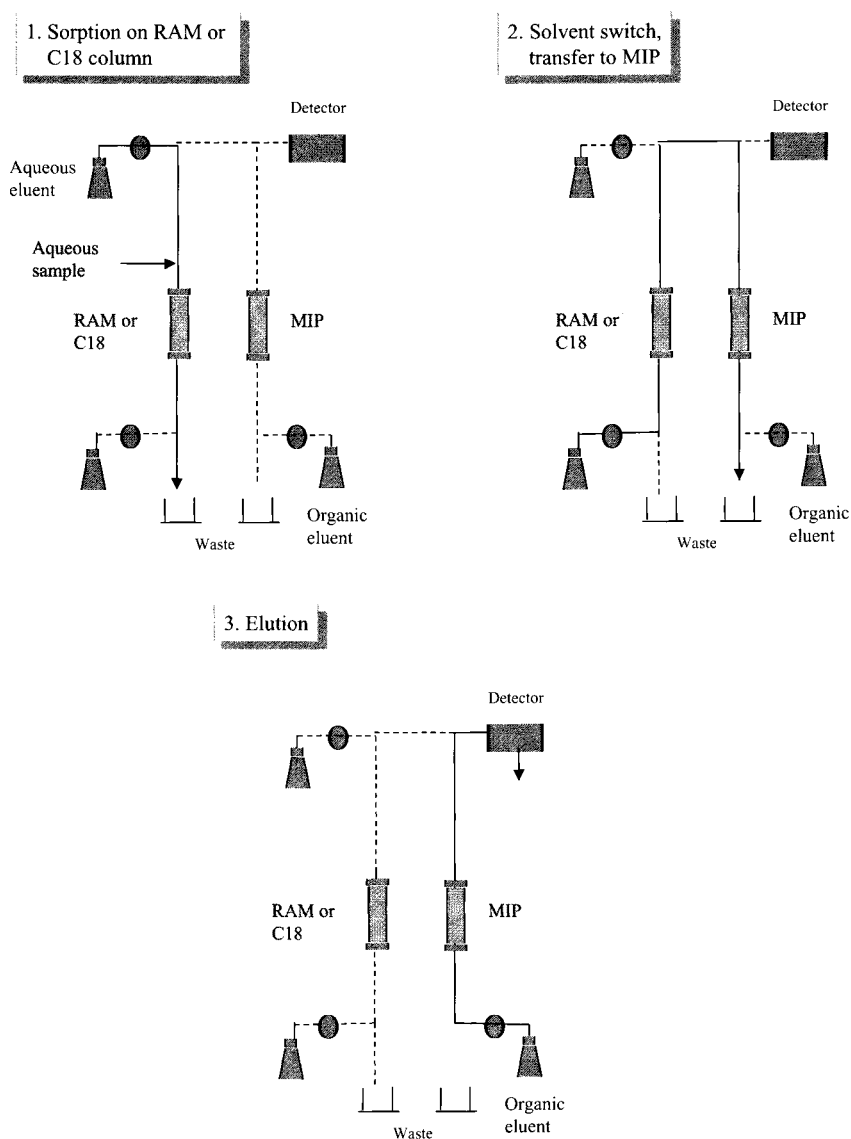


Fig. 15.5. RAM or C18-MIP coupled column system for prefractionation based on size and polarity and transfer of analyte to a solvent for enhanced recognition of the target analyte.

desorbed from the phase in the smallest volume. This will lead to a large enrichment and a high recovery of purified analyte. Ideally the purity and concentration is high enough to allow direct quantification in the eluate [18,28], possibly in combination with more specific detection techniques such as diode array detection (DAD) or MS.



Most of the imprinted sorbents used in MISPE were prepared using MAA and ethylene glycol dimethacrylate (EDMA) as monomers. In these cases elution of more weakly bound analytes such as triazines [19,30,32], 7-hydroxy-coumarin (**2**) [26] or theophylline (**12**) [28] can be achieved using methanol or water as elution solvent. For more strongly bound analytes such as stronger nitrogen Brønsted bases, efficient elution has been achieved using eluents of the same base solvent but with the addition of small amounts of acids (e.g. acetic acid, trifluoroacetic acid (TFA)) or base (e.g. triethylamine (TEA)) [20–22,25,33].

#### 15.4.1. Off-line protocols

##### 15.4.1.1. Sample clean-up of biological fluids

The first MISPE protocol reported in the literature [18] involved the use of an imprinted dispersion polymer in a column format, for the selective enrichment of pentamidine (**1**) in urine. In this case the high selectivity of the polymer allowed the analyte to be detected directly in the eluate without the need for any further chromatographic separation (entry A in Tables 15.1 and 15.2). In view of the high selectivity of MIPs, this is a viable approach that brings the benefits of shorter analysis times and simpler instrumentation. In most cases, however, MISPE has been used prior to a chromatographic separation step. The MIP has been applied in a batch-wise extraction [23] or in columns or cartridges [20–22,24–26,33].

The former format was used by Andersson *et al.* for the analysis of the analgesic drug sameridine (**3**) in human plasma (entry C in Tables 15.1 and 15.2) [23]. Quantification limits below nM concentrations were required here. In order to circumvent problems related to bleeding of non-extracted template (see below) this group used a compound (**14**), structurally related to the analyte, as template. The structural similarity is unlikely to seriously impair the binding of the analyte and thus the detection limit can be significantly lowered. The accuracy and intra-assay precision of the complete MISPE protocol based on the batchwise preconcentration of sameridine from human plasma were at least as good as those observed for the routine liquid–liquid extraction method. The advantage of the MISPE protocol was the high selectivity, resulting in less interferences in the subsequent GC analysis and potentially higher sensitivities by applying larger sample volumes.

The evaluation of an MIP for the SPE of propranolol (**9**) from biological fluids was addressed by Martin *et al.* [27,33,34] who compared the cumulative recovery curves obtained with different solvents of increasing eluotropic strength containing various modifiers (entry G in Tables 15.1 and 15.2). It appeared that the conditions chosen for the elution of the retained propranolol were extremely important to ensure a selective extraction. In fact the imprinted material non-specifically adsorbed a range of molecules structurally similar and dissimilar to propranolol. However, a careful choice of the eluent allowed the non-specifically bound analytes to be washed off first and propranolol to be quantitatively recovered in a second step. Interestingly comparing the strong modifiers TFA and TEA only the latter

TABLE 15.2

DETAILS OF THE MIP SYNTHESIS AND METHOD VALIDATION RESULTS FOR THE PROTOCOLS IN TABLE 15.1. For structures of the templates see page 361

| Template  | Porogen                         | Polym. <sup>a</sup><br>techn. | m <sub>MIP</sub> <sup>b</sup><br>(mg) | V <sub>sample</sub> <sup>c</sup><br>(mL) | Conc.<br>range <sup>d</sup> | Recovery <sup>e</sup><br>(%) |
|---|---------------------------------|-------------------------------|---------------------------------------|--|-----------------------------|------------------------------|
| A Pentamidine <b>1</b>  | <i>i</i> -propanol/<br>water    | 60°C <sup>f</sup>             | 2400                                  | 30 (urine)                               | 10–60 nM                    | 10 (90) <sup>j</sup>         |
| B 7-Hydroxy-<br>coumarin <b>2</b>                               | CHCl <sub>3</sub>               | 60°C                          | 400                                   | 0.25<br>(urine)                          | 60–300 μM                   | 90                           |
| C <b>14</b>   | Toluene                         | UV, RT                        | 5                                     | 600 mg<br>(plasma)                       | 8–120 nM                    | 100                          |
| D Simazine <b>4</b>   | CHCl <sub>3</sub>               | 50°C <sup>g</sup>             | 2000                                  | 500 (water)                              | 460 nM                      | 91                           |
| E Atrazine <b>5</b>   | CHCl <sub>3</sub>               | 60°C                          | 250                                   | 20 (CHCl <sub>3</sub><br>extract)        | 0.005–0.5<br>ppm            | 89 (93) <sup>k</sup>         |
| F Nicotine <b>6</b> ,<br>Cotinine <b>7</b><br>Myosmine <b>8</b> | CH <sub>2</sub> Cl <sub>2</sub> | UV, 10°C                      | 270                                   | 0.5<br>(EtOAc<br>extract)                | 250 μM                      | ca. 100                      |
| G Propranolol <b>9</b>  | Toluene                         |                               | 30                                    | 0.5<br>(plasma)                          | 0.040–10 μM                 | ca. 100                      |
| H Darifenacin <b>10</b>   | THF/<br>EtOAc                   | UV, 4°C                       | 100                                   | 1 (dil.<br>plasma)                       | 47–235 μM                   | ca. 100                      |
| I Tamoxifen <b>11</b>   | MeCN                            | 60°C                          | 500                                   | 0.5 (urine)                              | 1.3 μM                      | 102                          |
| J Theophylline <b>12</b><br>and analogues                       | CHCl <sub>3</sub>               | 60°C                          | — <sup>h</sup>                        | 0.020 (CHCl <sub>3</sub><br>ext)         | 13–5200 μM                  | —                            |
| K Simazine <b>4</b>   | CH <sub>2</sub> Cl <sub>2</sub> | UV, 4°C                       | — <sup>i</sup>                        | 200 (humic<br>acid water)                | 300 nM                      | —                            |
| L Bentazone <b>13</b>   | CHCl <sub>3</sub>               | 60°C                          | 500                                   | 50 (water)                               | 42 μM                       | 96                           |

Polymers were prepared using MAA (A–K) or 4-vinylpyridine/MAA (1/1) (L) as functional monomers and EDMA as cross-linking monomer in the presence of the template and various solvents (porogens) as shown schematically in Fig. 5.2. (Chapter 5). EtOAc = ethylacetate, THF = tetrahydrofuran, RT = room temperature.

<sup>a</sup>Polymerisation technique. Thermochemical initiation at elevated temperatures or UV-photochemical initiation at low temperature.

<sup>b</sup>Weight of dry MIP packed in the SPE cartridge or column.

<sup>c</sup>Volume and type of sample added to the MIP phase.

<sup>d</sup>Typical concentration range used in the extraction tests.

<sup>e</sup>Exact or approximate recoveries reported.

<sup>f</sup>Polymer obtained as dispersible agglomerates of micronized particles.

<sup>g</sup>Polymer prepared in water suspension.

<sup>h</sup>Column dimensions: 80 × 4 mm.

<sup>i</sup>Column dimensions: 150 × 4.6 mm.

<sup>j</sup>Recovery by loading and washing in pH 5 buffer. In parentheses the corresponding value after loading and washing in pH 7 buffer.

<sup>k</sup>Recovery obtained by HPLC quantification. In parentheses the corresponding value when quantification was done by ELISA.

resulted in selective clean-up. Also matching the wash solvent with the porogenic solvent seems to result in higher selectivity and recovery.

Stevenson *et al.* compared MISPE with immunoaffinity extraction for the quantification of tamoxifen (**11**) in urine and plasma (entry I in Tables 15.1 and 15.2) [25,35]. This group reported considerable problems with template bleeding, i.e. continuous release of small amounts of non-extracted template particularly upon solvent changes. A number of different wash procedures were tested but none gave satisfactory results that would allow reliable quantification of low levels of the drug. Although the materials could be used for the selective extraction at higher concentration levels and the manufacturing of the materials was simple, the immunoaffinity technique was favoured, since these phases allowed the drug to be selectively extracted from biological fluids at low concentration levels and with high accuracy.

Similar problems were reported by Venn and Goody in the application of MISPE in the quantification of the developmental drug darifenacin (**10**) in blood (entry H in Tables 15.1 and 15.2) [20,36]. A comparison of MIPs using different functional monomers and porogens with respect to chromatographic selectivity for the drug was first performed. Using MAA as the functional monomer, the resulting MIP could efficiently discriminate between the drug enantiomers and was therefore employed in an off-line SPE procedure. The blood was deproteinised by addition of acetonitrile (50%) and the sample directly applied to the MISPE cartridge. After washing of the cartridge with acetonitrile, the drug was efficiently retained on the MIP whereas early breakthrough was seen on the non-imprinted control cartridge. The selectivity was further investigated by comparing the extraction of a number of structurally related analogues and substructures. Thus the materials performed well in terms of selectivity, capacity and robustness. Nevertheless applications for trace or ultra trace level analysis were again precluded due to the excessive template bleeding.

#### 15.4.1.2. Extraction of analytes of environmental concern

Triazines belong to a group of widespread herbicides that have become major pollutants of soil and ground waters [37,38]. Therefore analytical methods are needed allowing them to be monitored at concentrations below  $\mu\text{g}/\text{levels}$ . The triazines are available in large number with small structural differences and with different known basicity and hydrophobicity (see Chapter 5.). This class of compounds is therefore well suited as a model system in molecular imprinting [39]. Previous results indicate that highly selective MIPs can be prepared against triazines [39–42]. The strongest interactions are expected to be a cooperative hydrogen bond between the nitrogen *para* to the chlorine (or thiomethyl) substituent and an exocyclic amino group of the triazine and the carboxylic acid group of MAA as indicated in Fig. 5.31 (Chapter 5) [43]. This interaction is also accompanied by secondary interactions that can be the association of a second acid group to the triazine ring system or shape complementarity arising from the polymer backbone. Thus the polymers effectively discriminate between chloro- and S-triazines. For the

chlorotriazines highest selectivity is seen using MAA as monomer, whereas for the S-triazines trifluoromethyl acrylic acid is the monomer of choice [44].

The use of MISPE for the clean-up of beef liver extracts before quantification of atrazine (**5**) by HPLC-UV or ELISA was evaluated by Muldoon and Stanker (entry E in Tables 15.1 and 15.2) [24]. In both cases the application of MISPE resulted in improvements in analyte quantification. In particular for the HPLC method the use of MISPE improved the accuracy and precision and lowered the limit of detection. In the case of ELISA a better accuracy was achieved in the determination although the precision was similar. With the analyte present at ppb levels, the reliability of either determination method would have been marginal without the MISPE step.

The application of MIPs prepared using triazines as templates to the SPE of water samples requires drying of the cartridge after the sample application in order to remove water traces, which would disrupt the interactions between the analytes and the sorbent. In the protocol described by Matsui *et al.* [19] the aqueous sample was applied to the MIP cartridge, which was then carefully dried prior to a selective dichloromethane wash (entry D in Tables 15.1 and 15.2). HPLC-UV analysis of wastes and extracts showed that all the impurities were washed off without significant elution of simazine (**4**) and that the analyte was quantitatively recovered in the eluate.

Recently the group of Barcelo performed a detailed investigation on the off-line application of chlorotriazine imprinted MIPs in the analysis of real environmental water samples [30]. Two imprinted polymers were synthesised, using either dichloromethane or toluene as porogen and terbutylazine as template, and were implemented to the SPE of six chlorotriazines in natural water and sediment samples. All extracted samples were analysed by LC/DAD. Several washing solvents, as well as different volumes, were tested to remove the matrix components non-specifically adsorbed on the sorbents. This clean-up step was shown to be of prime importance to the successful extraction of the pesticides from the aqueous samples. Interestingly the wash solvent giving the highest level of clean-up and recovery was the same as that used as porogen. Optimal analytical conditions were obtained using the MIP imprinted with dichloromethane as porogen, 2 mL of dichloromethane were used in the washing step and the preconcentrated analytes were eluted with 8 mL of methanol. The recoveries were higher than 80% for all the chlorotriazines except propazine (53%) when 50 or 100 mL groundwater samples, spiked at 1  $\mu\text{g/L}$  level, were analysed (Figure 15.6). The limits of detection varied from 0.05 to 0.2  $\mu\text{g/L}$  when preconcentrating a volume of 100 mL of groundwater sample. Natural sediment samples from the Ebre Delta area (Tarragona, Spain) containing atrazine and deethylatrazine were Soxhlet extracted and analysed by the methodology developed in this work. No significant interferences from the sample matrix were noticed, thus indicating good selectivity of the sorbents used.

The above studies show that the imprinted sorbents can be used in two modes: in the reversed phase mode (sample application) and in the affinity mode (dichloromethane washing). Otherwise there are only few reports on the use of MIPs for the pretreatment of samples of environmental concern. Recently an MIP imprinted using the herbicide bentazone as template was synthesised and evaluated by

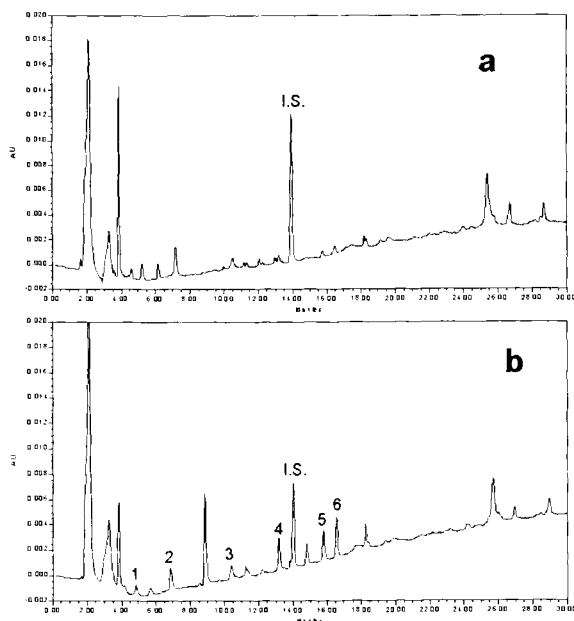


Fig. 15.6. LC/DAD chromatogram at 220 nm obtained after preconcentration of 100 mL of groundwater sample spiked at 1  $\mu\text{g/L}$  through (a) a blank cartridge prepared using a non-imprinted control polymer and (b) a cartridge prepared using a polymer imprinted with terbutylazine. Peaks: 1 = deisopropylatrazine, 2 = deethylatrazine, 3 = simazine, 4 = atrazine, 5 = propazine, 6 = terbutylazine and I.S. = diuron (internal standard).

Baggiani *et al.* [21] in frontal LC (entry L in Tables 15.1 and 15.2). The material was then used as sorbent for the SPE and a preliminary procedure for the enrichment of the analyte from water samples was tested. Good recoveries (91–96 %) and concentration factors of 3.2–15.2 were found.

#### 15.4.2. On-line protocols

##### 15.4.2.1. Extraction of nicotine

In the development of a clean-up step for nicotine and structurally related compounds in nicotine containing chewing gum, an on-line MISPE procedure was developed (Fig. 15.7) and the resulting method compared with an SPE run on a non-imprinted blank column (entry F in Tables 15.1 and 15.2) [22]. The sample pretreatment would in this case be particularly suited for MISPE since the analytes, together with matrix components, were present in a non-polar solvent used to dissolve the chewing gum matrix. Nicotine MIPs were prepared by the standard protocol using MAA as the functional monomer. The resulting polymers were crushed, sieved and packed into standard HPLC columns for evaluation. Using

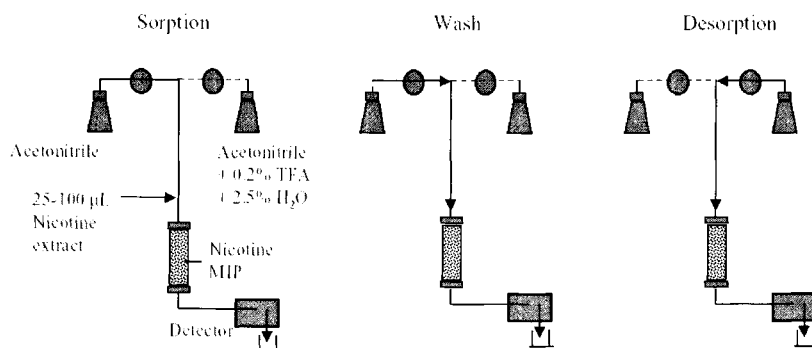


Fig. 15.7. On-line extraction of nicotine chewing gum extracts.

acetonitrile as wash solvent nicotine could be eluted as a sharp peak from the imprinted sorbent by adding 0.2% TFA. This led to quantitative recoveries in a large concentration interval. The elution conditions were then optimised on-line. The chewing gum extract was added to the column and the column was washed with acetonitrile followed by elution of the analytes. As seen there is a pronounced difference between the MIP and the blank column concerning breakthrough volumes and recovery of the analytes in the elution step. Whereas three of the four analytes broke through prior to the elution step on the blank column, only the most hydrophobic analyte, nicotyrine, broke through on the MIP (Fig. 15.8).

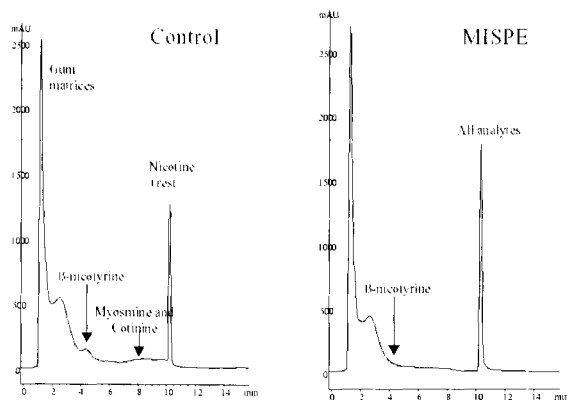


Fig. 15.8. Adsorption and elution of 100 µL of a placebo chewing gum extract spiked with nicotine (0.5 mg/mL) and β-nicotyrine, cotinine and myosmine (0.05 mg/mL). The step elution was as follows: MeCN: 0–8 min, MeCN + 0.2 % TFA + 2.5% H<sub>2</sub>O: 8–12 min, MeCN: 12–15 min. The peak identity was established by separate injections and spectral analysis using a diode array detector. Rest refers to still not eluted β-nicotyrine, cotinine and myosmine. In MISPE, only β-nicotyrine could be detected in the adsorption and wash steps.

Transferring the procedure to an off-line mode, quantification by reversed phase HPLC showed that all analytes except  $\beta$ -nicotyrine were quantitatively recovered. Due to the enhanced stability of the nicotine MIP, achieved by thermal annealing, and the reusability of the MIP, the procedure may be suited for automation.

#### 15.4.2.2. MISPE with pulsed elution

A method for the analysis of theophylline in blood serum based on MISPE with pulsed elution was developed by Mullett and Lai (entry J in Tables 15.1 and 15.2) [28]. The method made use of a MIP column for the on-line enrichment of theophylline and an injection of a small plug of methanol to produce a rapid pulsed desorption of the analyte. The sample was applied in chloroform since in this solvent a complete retention of the analyte was observed. The matrix constituents (e.g. lipids) and the potential interferences (e.g. other drugs) which were not recognised by the binding sites were rapidly eluted with chloroform. Then a rapid and quantitative recovery of theophylline was accomplished in a pulsed format through injection of 20  $\mu$ L of methanol. In this way the eluted analyte could be detected directly by UV. The pulsed elution approach was further applied to micro SPE columns (0.8 mm i.d., 80 mm long), which offer the advantage of lower consumption of solvents and faster analysis times [45]. With the application of 20  $\mu$ L solvent pulses it was demonstrated that the non-specifically bound analytes could be removed and nicotine could be quantitatively recovered over a linear dynamic range of 1–1000  $\mu$ g/L and with a detection limit of 1.8  $\mu$ g/mL.

#### 15.4.2.3. On-line coupled column approaches

The drying step required in many of the off-line procedures is not compatible with on-line operations. Moreover, if the MIP columns are to be reused, fouling caused by macromolecular matrix components precludes direct injection of biological fluids. In these cases an attractive alternative is to use a precolumn designed to transfer low molecular weight analytes into an organic solvent simultaneously excluding biological macromolecules. This is possible using a coupled column system where the analytes are first non-specifically adsorbed on a multi-purpose SPE column, e.g. a hydrophobic sorbent (C18 reversed phase or restricted access sorbent), and then transferred to a dedicated MIP sorbent in organic media. The approach is suitable for on-line applications as recently demonstrated by Boos and co-workers [31] and Bjarnason *et al.* [32] and has the advantage of allowing the direct injection of biological samples (Fig. 15.5). Furthermore the column switching allows the pretreatment step to be separated from the analysis so that a sample can be pretreated while another one is being analysed, leading to a higher sample throughput.

### 15.5. THE DEVELOPMENT OF NEW MISPE PROTOCOLS

Three different steps are involved in the development of a new SPE protocol based on molecular imprints: the synthesis of the material, the assessment of its

recognition properties, the development of the extraction protocol and the final validation of the protocol.

First of all a suitable combination of monomers and a porogenic solvent has to be found where the template can be successfully imprinted (see Chapter 5) [17]. The thermodynamic stability of the monomer–template assemblies is the key factor in this step. One or more functionalised vinyl monomers are sought which are capable of forming strong non-covalent interactions with the functional groups of the template. The monomer–template assemblies need to be stable enough for them to be transformed to specific binding sites during the polymerisation. The structure and morphology of the polymer matrix are strongly influenced by the type and amount of cross-linker and porogen [46]. These factors affect in turn the sorption–desorption kinetics and the stability of the material and therefore require careful optimisation. Recently developed techniques for rapid parallel synthesis and evaluation of large groups of materials are particularly promising in this respect (see Chapter 13) [44,47].

Once a suitable material has been found a chromatographic characterisation step is required where the recognition properties of the sorbent are evaluated in different mobile phases. In order to predict suitable extraction protocols, the sorbents should thus be characterised in terms of affinity, selectivity and sample load capacity (breakthrough volumes) for the analytes. Except for establishing recognition based on the retention times of the template and analogues at one or two different concentrations, frontal analysis or batch rebinding at several concentrations yield thermodynamic information in terms of binding energy and mass transfer kinetics [48–50].

The assessment can also be done by an off-line SPE procedure where the cumulative recovery curves of the sorbents are evaluated in different solvents and at different pHs. A suitability test for propranolol imprinted sorbents, to be used in SPE of plasma and urine samples, was developed by Olsen *et al.* [34]. This was based on the solvent composition required to give a recovery of either 20 or 50% of the extracted material (ES20 or ES50 values) on the blank and the imprinted cartridge. The method was developed in order to allow a rapid estimate of the specific and non-specific contributions to overall binding.

Finally a validation step for the overall MISPE procedure is mandatory to allow the use of the method itself in place of the regulatory methods. The issues to be considered here are the accuracy and precision of the method based on the MISPE protocol, its limit of quantification, selectivity and ruggedness. In particular the inter- and intra-assay precision need to be checked with real samples and certified reference materials and methods [23,24].

## 15.6. TEMPLATE BLEEDING: AN UNRESOLVED ISSUE IN MISPE PROTOCOLS

One problem in molecular imprinting concerns the small amount of template that remains strongly bound to the polymer after extraction. This usually



amounts to more than 1% of the amount of template given to the monomer mixture and remains bound even after careful washing of the polymer [23,25,51,52]. This may not constitute a problem in preparative separations or catalysis but when the materials are used for sample preparation prior to analytical quantification of low levels of analytes, bleeding of this fraction will cause false results [23,25]. In view of the previously determined concentrations (Table 15.2) this essentially limits the use of MISPE to samples with ppt or ppm as low concentrations [42]. In spite of careful washing, slow leakage of template often occurs upon exchange of solvents. This problem may be reduced by thermal posttreatment of the materials [22] or prevented by the use of a template analogue as template [23]. Obviously more effective wash procedures may also lead to less bleeding [25]. An often overlooked factor is the amount of sorbent that is required for high recovery (see Table 15.2). Previous examples have shown that the capacity of the sorbents often is far higher than required, i.e. only a fraction of the sites are actually used in the extraction step [42][20]. By adding just enough sorbent to give complete occupancy of the templated sites upon extraction, the effective bleeding will be reduced.

The question is then how the template is incorporated in the polymer. Some templates may react with free radicals and become covalently incorporated in the matrix. In order to establish whether this is occurring, model reactions between the template, the initiator and a small amount of monovinyl monomer should be carried out. By this mechanism, however, no leakage can occur since the template would be covalently bound to the polymer. Leakage is possible, however, if the template is physically entrapped in the densely cross-linked regions of the nuclei [22]. Swelling and shrinking of the polymer may then cause slow bleeding of this fraction. Here it seems that thermal treatments at temperatures exceeding the glass transition temperature [49], but below temperatures where the sites are deformed, alleviates some of these problems. In addition the problem is often reduced by avoiding solvent switches or drying of the sorbent.

It is important to carefully determine the recovery of the template and to verify the identity of the recovered template. The recovery can be estimated by determining either the amount of template in the extracts or the amount of template in the polymer [52,53]. For this purpose solution  $^1\text{H}$ -NMR, HPLC, GC, elemental analysis and scintillation counting have been used. By NMR the identity of the extracted fraction is easily verified as well as unreacted monomer remaining in the polymer. Quantification can here be done by comparing the integrals of the template with that of an internal standard. More accurate quantification of the amount of template in the extract can be obtained by chromatography [52]. Furthermore elemental analysis on a heteroatom unique for the template can be used to determine the recovery. Higher sensitivities are here obtained using trace analytical techniques. High sensitivities are also obtained using radioactively labelled templates. The amount of template in the polymer before and after extraction is then compared by scintillation counting on the polymer, or by total combustion of the polymer followed by counting of the isotopes [53].

## 15.7. CONCLUSIONS

MIP-related applications in analytical chemistry are currently experiencing a rapid growth. Most intensely studied are the use of MIPs as recognition elements in chemical sensors or in assays and MIPs as sorbents in MISPE to achieve a selective clean-up of biological samples with high analyte enrichment factors. The development of MIP based sensors, apart from the synthesis of the recognition element with adequate recognition and kinetic properties, are associated with a number of technical difficulties, i.e. the coupling of the binding event to a measurable signal and the type of signal transducer, the sensor stability, the sensor reusability. In this regard the MISPE applications are more straightforward in view of the more limited requirements. Thus for a new target analyte an MIP exhibiting adequate selectivity, affinity and mass transfer properties in the recognition of the analyte are the primary requirements. Eventual problems associated with template bleeding also need to be addressed. Furthermore the time needed to synthesise these phases will be decisive as to whether they will be successful in competing with alternative biological recognition elements such as antibodies.

However, when these requirements are fulfilled the MIPs can be directly used in extraction columns or cartridges in combination with existing instrumentation. High target affinity and selectivity translates to lower detection limits, shorter analysis times and cheaper instrumentation in the resulting method, factors that are likely to lead to a widespread use of these phases in the near future.

## ACKNOWLEDGEMENTS

The authors are grateful to the European Commission for financing part of the reported work herein within the program for Training and Mobility for Researchers (TMR), contract number FMRX CT 98-0173 with the following participants: Damia Barceló, CID-CSIC, Barcelona, Spain; Werner Blau, Trinity College Dublin, Ireland; Karl-Siegfried Boos, Maximilians-Universität München, Germany; Kees Ensing, University of Groningen, The Netherlands; George Horvai, Technical University of Budapest, Hungary; Lars Karlsson, Astra Hässle AB, Mölndal, Sweden; David Sherrington, University of Strathclyde, UK.

## REFERENCES

- 1 M. Vanderlaan, L.H. Stanker, B.E. Watkins and D.W. Roberts, (Eds.) *Immunoassays for trace chemical analysis; monitoring toxic chemicals in humans, food, and the environment*, American Chemical Society, Washington DC (1991).
- 2 J.O. Nelson, A.E. Karu and R.B. Wong, (Eds.) *Immunoanalysis of agrochemicals*, ACS Symposium Series, 586, American Chemical Society, Washington DC (1995).
- 3 T.E. Mallouk and D.J. Harrison, (Eds.) *Interfacial design and chemical sensing*, ACS Symposium Series, 561, American Chemical Society, Washington DC (1994).
- 4 E. Reid, H.M. Hill and I.D. Wilson, (Eds.) *Drug development assay approaches, including*

- molecular imprinting and biomarkers, *Methodol. Surv. Bioanal. Drugs*, 25, Royal Society of Chemistry, Cambridge, UK (1998).
- 5 C.F. Poole and S.K. Poole, *Chromatography today*, Elsevier, Amsterdam (1991).
  - 6 I. Liska, J. Krupcik and P.A. Leclercq, *J. High. Res. Chrom.*, **12**, 577 (1989).
  - 7 L.A. Berrueta, B. Gallo and F. Vicente, *Chromatographia*, **40**, 474 (1995).
  - 8 M.-C. Hennion, *J. Chromatogr. A*, **856**, 3 (1999).
  - 9 M.S. Mills, E.M. Thurman and M. J. Pedersen, *J. Chromatogr.*, **629**, 11 (1993).
  - 10 K.-S. Boos and A. Rudolphi, *LC•GC*, **15**, 602 (1997).
  - 11 J.A. Perry, *J. Liq. Chromatogr.*, **13**, 1047 (1990).
  - 12 A. Rudolphi and K.-S. Boos, *LC•GC*, **15**, 814 (1997).
  - 13 S. Pleasance and R.A. Biddlecombe, In: *Drug development assay approaches including molecular imprinting and biomarkers*, Vol. 25, E. Reid, H.M. Hill and I.D. Wilson Eds, Royal Society of Chemistry, Cambridge, UK, p. 205 (1998).
  - 14 R.A. Bartsch and M. Maeda, *Molecular and ionic recognition with imprinted polymers*, ACS Symposium Series, 703, Oxford University Press, Washington DC (1998).
  - 15 D. Kriz, O. Ramström and K. Mosbach, *Anal. Chem.*, **69**, 345A (1997).
  - 16 D. Barceló, Special issue on molecular imprints and related approaches for solid-phase extraction and sensors in chemical analysis, *Trends Anal. Chem.*, **18**, 1999.
  - 17 B. Sellergren, *Trends Anal. Chem.*, **18**, 164 (1999).
  - 18 B. Sellergren, *Anal. Chem.*, **66**, 1578 (1994).
  - 19 J. Matsui, M. Okada, M. Tsuruoka and T. Takeuchi, *Anal. Commun.*, **34**, 85 (1997).
  - 20 R.F. Venn and R.J. Goody, *Chromatographia*, **50**, 407 (1999).
  - 21 C. Baggiani, G. Giraudi, C. Giovannoli, A. Vanni and F. Trotta, *Anal. Commun.*, **36**, 263 (1999).
  - 22 Å. Zander, P. Findlay, T. Renner, B. Sellergren and A. Swietlow, *Anal. Chem.*, **70**, 3304 (1998).
  - 23 L.I. Andersson, A. Paprica and T. Arvidsson, *Chromatographia*, **46**, 57 (1997).
  - 24 M.T. Muldoon and L.H. Stanker, *Anal. Chem.*, **69**, 803 (1997).
  - 25 B.A. Rashid, R.J. Briggs, J.N. Hay and D. Stevenson, *Anal. Commun.*, **34**, 303 (1997).
  - 26 M. Walshe, J. Howarth, M.T. Kelly, R. O'Kennedy and M.R. Smyth, *J. Pharm. Biomed. Anal.*, **16**, 319 (1997).
  - 27 P. Martin, I.D. Wilson, D.E. Morgan, G.R. Jones and K. Jones, *Anal. Commun.*, **34**, 45 (1997).
  - 28 W.M. Mullett and E.P.C. Lai, *Anal. Chem.*, **70**, 3636 (1998).
  - 29 D. Spivak, M.A. Gilmore and K.J. Shea, *J. Am. Chem. Soc.*, **119**, 4388 (1997).
  - 30 I. Ferrer, F. Lanza, A. Tolokan, V. Horvath, B. Sellergren, G. Horvai and D. Barcelo, *Anal. Chem.* **72**, 3934 (2000).
  - 31 C.T. Fleischer, K.-S. Boos, F. Lanza and B. Sellergren, Poster at 23rd International symposium on high performance liquid phase separations and related techniques, Granada, Spain (1999).
  - 32 B. Bjarnason, L. Chimuka and O. Ramström, *Anal. Chem.*, **71**, 2152 (1999).
  - 33 See chapter by: P. Martin, I.D. Wilson, G.R. Jones and K. Jones, in ref. [4]. p.21.
  - 34 J. Olsen, P. Martin, I.D. Wilson and G.R. Jones, *Analyst*, **124**, 467 (1999).
  - 35 D. Stevenson, *Trends Anal. Chem.*, **18**, 154 (1999).
  - 36 See chapter by: R.F. Venn and R.J. Goody, in ref [4] p.13.
  - 37 V. Pichon, L. Chen, N. Durand, F. Le Goffic and M.-C. Hennion, *J. Chromatogr. A*, **725**, (1996).
  - 38 D. Barceló, S. Lacorte and J.L. Marty, *Trends Anal. Chem.*, **14**, 334 (1995).
  - 39 C. Dauwe and B. Sellergren, *J. Chromatogr. A*, **753**, 191 (1996).
  - 40 M. Siemann, L.I. Andersson and K. Mosbach, *J. Agric. Food Chem.*, **44**, 141 (1996).
  - 41 M.T. Muldoon and L.H. Stanker, *J. Agric. Food Chem.*, **43**, 1424 (1995).
  - 42 J. Matsui, Y. Miyoshi, O. Doblhoff-Dier and T. Takeuchi, *Anal. Chem.*, **67**, 4404 (1995).
  - 43 G.J. Welhouse and W.F. Bleam, *Environ. Sci. Technol.*, **27**, 500 (1993).

- 44 T. Takeuchi, D. Fukuma and J. Matsui, *Anal. Chem.*, **71**, 285 (1999).
- 45 W.M. Mullett, E.P.C. Lai and B. Sellergren, *Anal. Commun.*, **36**, 217 (1999).
- 46 B. Sellergren, *Makromol. Chem.*, **190**, 2703 (1989).
- 47 F. Lanza and B. Sellergren, *Anal. Chem.*, **71**, 2092 (1999).
- 48 P. Sajonz, M. Kele, G. Zhong, B. Sellergren and G. Guiochon, *J. Chromatogr.*, **810**, 1 (1998).
- 49 Y. Chen, M. Kele, P. Sajonz, B. Sellergren and G. Guiochon, *Anal. Chem.*, **71**, 928 (1999).
- 50 C. Baggiani, F. Trotta, G. Giraudi, G. Moraglio and A. Vanni, *J. Chromatogr. A*, **786**, 23 (1997).
- 51 K.J. Shea, D.A. Spivak and B. Sellergren, *J. Am. Chem. Soc.*, **115**, 3368 (1993).
- 52 B. Sellergren and K.J. Shea, *J. Chromatogr.*, **635**, 31 (1993).
- 53 B. Sellergren, B. Ekberg and K. Mosbach, *J. Chromatogr.*, **347**, 1 (1985).

This Page Intentionally Left Blank

## Capillary electrochromatography based on molecular imprinting

LEIF SCHWEITZ AND STAFFAN NILSSON

### 16.1 INTRODUCTION

The ever ongoing research into novel stationary phases for chromatographic separations of chemical entities has sparked interest in molecular imprinting [1–5] as a facile technique for the synthesis of phases with pre-determined selectivity. The imprinted polymers can be made selective for one of the enantiomers of a chiral compound, a specific compound or a class of compounds. Most molecularly imprinted polymer (MIP) studies have focused on chiral separation problems and many different racemic compounds have been successfully resolved, including drugs [6–8], amino acid derivatives [1–3] and sugars [1–3]. Often, good separations can be achieved and separation factors as high as 17.8 have been reported [9]. The often severe peak broadening and tailing of peaks observed, however, hamper a wider use of molecularly imprinted phases for chromatographic applications. This is in part due to the MIPs being prepared as bulk polymers, which are ground and sized into irregular particles of 25  $\mu\text{m}$  or less before packing into liquid chromatography (LC) columns. Another factor claimed to contribute to peak broadening is imprint heterogeneity, with a distribution of sites from high to low affinity for the ligand and variable association and dissociation kinetics [2]. The recent development of a novel suspension polymerisation technique by which uniformly shaped beads of defined size range can be made [10] has only partially overcome the problem of poor performance of imprinted columns. Also, separation systems based on continuous rods of imprinted polymer inside LC stainless steel columns have still to show any advantage over packed particle columns [11,12]. For a detailed description of these techniques see Chapter 13. Discussions on the use of MIPs in LC can be found in some recent reviews [1–3]. Being inherently more efficient chromatography techniques [13], it is believed that the use of capillary electrochromatography (CEC) and capillary electrophoresis (CE) would greatly improve the performance of imprinted polymer-based separations.

### 16.2 CEC

#### 16.2.1 Short introduction to CEC

CEC is often looked upon as a hybrid method of micro-bore LC and CE. The technique consists of the application of an electric field over a capillary column that

contains a stationary phase (Fig. 16.1). The mobile phase is driven through the capillary column by electroosmosis. Electroosmotic flow (EOF) was identified as a distinct physical phenomenon in 1852 [14]. EOF refers to the movement of a liquid relative to a charged stationary surface due to an applied electric field. In CEC, EOF arises from the fact that most surfaces, i.e. the capillary wall and the packing material, acquire a surface charge from ionisation and/or adsorption of charged species. In principle, the EOF causes all species, regardless of charge, to migrate in the same direction, provided the EOF velocity is of sufficient magnitude. This enables simultaneous analysis of positively, negatively, and neutrally charged analytes. It is assumed that a near plug-like flow velocity profile is achieved, since the flow originates from the surface of the capillary and/or the stationary phase. This will thus give rise to less band broadening than a pressure driven flow system such as in LC. The flow profiles have been investigated by means of microscope optics in capillaries. Flow profiles of a plug [15] or near a plug were observed [16]. In the latter case, a reversed parabolic flow profile was observed. It has been proposed that a plug-like flow profile will be achieved if the column diameter is

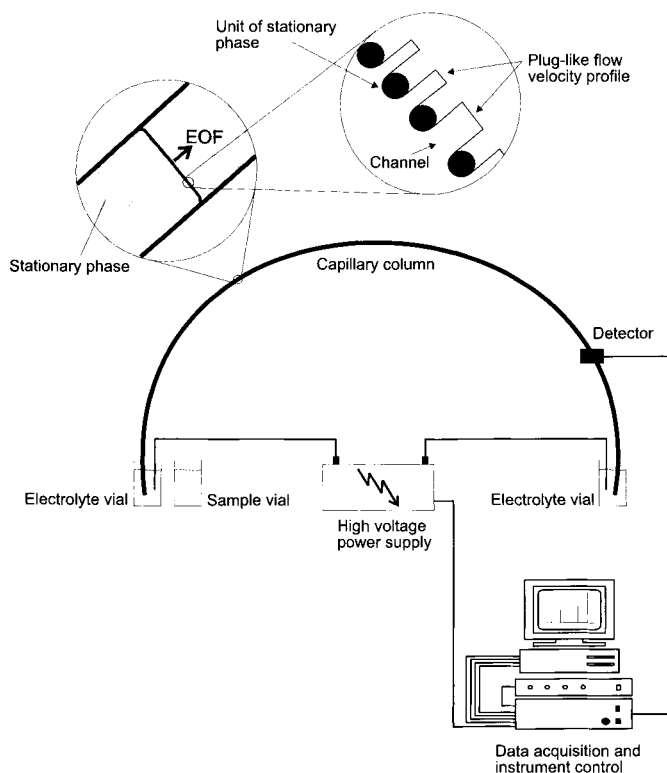


Fig. 16.1. Schematic of a CEC instrument. The capillary column is typically 20–50 cm long with an inner diameter of 50–100  $\mu\text{m}$ . The high voltage supply normally delivers 0–30 kV. About 1–10 nL of sample is usually injected electrokinetically.

much greater than the thickness of the so-called double layer of electric charge. As a rule of thumb the column diameter should be greater than ten times the double layer thickness. In the case where the diameter of the column approaches the thickness of the double layer, overlap may occur, which will eventually result in a parabolic flow velocity profile. In CE this is not a problem, but in the case of CEC, the mean channel diameter must be considered instead of the column diameter. EOF will not be affected in a CEC column packed with particles down to  $0.5\ \mu\text{m}$  [17]. When considering stationary phases prepared as porous monoliths, distorted flow profiles due to narrow pores must be considered.

Due to the plug-like flow velocity profile, which will reduce the eddy diffusion [18], CEC is predicted to be a more efficient separation technique than conventional LC. A band broadening effect that occurs in CEC, but not in LC, is caused by Joule heating, resulting in a temperature gradient from the centre of the column to its confines. If the column diameter is kept small (less than  $100\ \mu\text{m}$ ) and the ionic strength of the electrolyte is not too high (i.e. keeping buffer concentrations below  $0.01\ \text{M}$ ), this effect does not reduce chromatographic efficiency (plate number).

The stationary phase can be filled into the capillary, bonded as a film to the capillary walls (open tubular CEC) or introduced into the capillary as a suspension or solution of the mobile phase (pseudo-stationary phase). The separation is, in the case of neutrally charged analytes, based on partitioning between the stationary phase and the mobile phase or, in the case of charged analytes, based on both partitioning and electrophoretic mobility (charge to friction coefficient ratio).

Since first demonstrated by Pretorius *et al.* in 1974 [19], CEC has emerged as a separation technique. CEC has since been applied by Jorgenson and Lukacs [20] in 1981 and by Tsuda *et al.* [21] in 1982 to analyse neutral compounds that could not be separated by capillary zone electrophoresis. Several aspects of CEC including applications, column preparation, instrumentation and detection have been focused upon and have recently been thoroughly reviewed [18,22–28].

### 16.2.2 Equipment

A CEC instrument basically consists of a system for injection (pressure driven or electrokinetic), a column in which the separation takes place, a detector and a high voltage supply (Fig. 16.1). The most commonly used detector so far has been UV with transmission through the capillary outside of the packed bed. Laser induced fluorescence detection has been employed in several studies. Also, mass-spectrometry has been used. Normally, isocratic CEC is performed, but approaches to gradient CEC have been reported [29]. However, special equipment must be employed in most cases.

The most commonly used CEC columns have been packed with conventional chromatography stationary phases, sometimes as very small particles ( $0.5\ \mu\text{m}$ ), introduced by high-pressure packing methods. Ultrasonic treatment during the packing has also been reported. Electrokinetic migration of the packing material into the capillary column has also been employed. All packing methods involve the fabrication of frits that hold the packed bed. Frits are usually made by sintering



silica gel or pure silica. The preparation of frits is a rather laborious task and it has been argued that frits may play a role in bubble formation inside the column during CEC runs and may also be responsible for peak distortion and band broadening. Recently, stationary phases in the form of monoliths have been reported. *In situ* prepared monolithic silica columns [30] or polymer-based monolithic stationary phases have been reported [31–38], also in combination with molecular imprinting [39–41]. These approaches do not require any frits and also allow fine tuning of porosity, morphology and chemical functionality of the stationary phase.

### 16.3 MOLECULAR IMPRINTING — A BRIEF HISTORY: PREPARATION AND APPLICATION

Modern molecular imprinting technology appeared in the 1970s, when Takagishi and Klotz [42] and Wulff and Sarhan [43] reported that chemical memories could be prepared in synthetic polymers. The latter report showed enantiomer recognition. The group of Wulff then presented a series of papers dealing with what is called the covalent approach to molecular imprinting, since reversible covalent interactions are the basis for molecular recognition in these systems. In the early 1980s the Mosbach group developed the non-covalent approach to molecular imprinting [44]. This approach, in which the molecular recognition is based on non-covalent interactions, such as hydrogen bonding, ionic interactions, hydrophobic interactions, etc., has been recognised as a more general approach to molecular imprinting, since the number of compound classes that could be imprinted were dramatically increased. A third approach, which is based on metal-ion chelation between template and polymer, has also been reported [45]. Prior to the modern molecular imprinting technology development, reports as early as in the 1930s and 1940s dealing with template induced molecular recognition were published. The most important might be the paper by Dickey [46], which is frequently considered to be the first example of molecular imprinting.

As mentioned above, the non-covalent imprinting approach is somewhat more general than its cousin-techniques. It is also the technique which has been used exclusively for the preparation of molecularly imprint-based CEC separation systems so far.

The template, the functional monomers and the cross-linking monomers are dissolved in a non-polar solvent. The functional monomers and the template form complexes and the strength of these are reflected in the selectivity of the imprinted polymer. The choice of functional monomer is based on the template structure. Functional monomers are chosen for their ability to interact non-covalently with the template molecule. The most frequently used functional monomer so far is methacrylic acid (MAA). Also vinylpyridines have been frequently used. As cross-linking monomers, ethyleneglycol dimethacrylate (EDMA) or trimethylolpropane trimethacrylate (TRIM) are widely used. Several other types of functional and cross-linking monomers have been used in molecular imprinting experiments using the non-covalent approach. The choice of monomers is of course important to the

quality of the resultant imprints. The choice of solvent, the porogen, is also of significant importance. The porogen should not disturb the complex formation between template and functional monomers. The type of monomers, as well as the type of porogen, also plays an important role in the morphology and porosity of the resultant MIP.

The MIP is usually prepared as a highly cross-linked, rigid bulk polymer and the polymerisation reaction is initiated by photo- or thermo-labile free radical initiators such as 2,2'-azobis(isobutyronitrile). For molecular imprint-based CEC systems, the introduction of the imprinted polymer into the capillary column has been focused on and several approaches have been developed (see below). The polymerisation process can be performed in between 1 and 24 h. It has been shown that the temperature during the polymerisation process is important. A lower temperature leads to imprinted polymers with higher selectivity [47] or better chromatographic performance [39].

For a more comprehensive introduction to the preparation of various MIPs, consult other chapters of this book or the recent reviews covering the area of molecular imprinting, including preparation and applications [48–55].

## 16.4 CEC BASED ON MOLECULAR IMPRINTING

### 16.4.1 Adjustment of MIPs to columns of capillary format

Several approaches to adjust MIPs to capillary formats have been reported [56,57]. Interestingly, none have utilised the method of grinding bulk prepared imprinted polymers into smaller units that could subsequently be packed into a capillary column using ordinary packing procedures. This is the usual way to prepare MIP-based HPLC columns. The reason for avoiding this procedure when it comes to capillary columns is the difficulties associated with the packing procedure, especially the packing of the irregular particles which result from the grinding step in MIP preparation. The development of preparation procedures where effectively mono-disperse MIP spheres of adequate size, combined with effective packing procedures, might ignite interest in this approach in the future. Instead, researchers have tried alternative preparation procedures including the *in situ* preparation of MIP monoliths.

#### 16.4.1.1 *In situ* dispersion polymerisation

The first reported preparation of capillary columns containing MIPs utilised a thermally initiated dispersion polymerisation procedure [58]. The functional monomer MAA and the cross-linking monomer EDMA were used. Agglomerates of micrometre-sized globular polymer particles were claimed to be prepared *in situ* in the capillary. Molecular imprinting of L-phenylalanine anilide, pentamidine and benzamidine was undertaken. A pH-dependent retardation of pentamidine over benzamidine in the pentamidine capillary was observed, while the opposite,

retardation of benzamidine over pentamidine in a benzamidine imprinted capillary, was not. Enantiomer separation of racemic phenylalanine anilide could not be achieved using the L-phenylalanine anilide imprinted capillary. This lack of enantioselectivity may be a consequence of the polymerisation method requiring the use of a dispersion medium, such as cyclohexanol and 1-dodecanol. Protic solvents are known to interfere with the ionic and hydrogen bonds giving rise to complexation between the imprint molecule and the functional monomers. Hence, the formation of well-defined imprints with such a method is less efficient. Nevertheless, this study was the foundation of a patent application on the combination of molecular imprinting and CE [59].

#### 16.4.1.2 Gel-entrapped MIP particles

A different approach to MIP-based CEC involves immobilisation of MIP particles, of the same type as those that have been used for LC, inside capillaries [60–62]. The MIP was prepared in bulk from MAA and EDMA monomers in apolar porogens and subsequently crushed into small ( $<10\ \mu\text{m}$ ) irregular polymer particles. These particles were suspended in a solution of acrylamide/bis-acrylamide monomers and introduced into the capillary column where a poly(acrylamide) gel was formed [60]. A MIP particle slurry could also be contained within the capillary by closing each end of the capillary with a small plug of poly(acrylamide) gel (Fig. 16.2) [61,62]. The quality of the packing was not reported. An open, buffer-filled capillary with a detection window had to be connected to the MIP-filled capillary

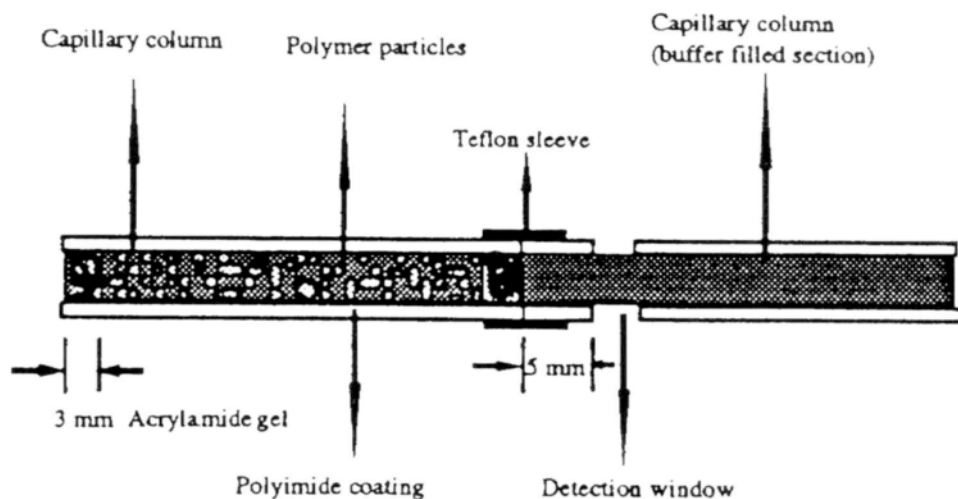


Fig. 16.2. Schematic of a capillary column, in which the MIP particles were held by closing the ends of the capillary with poly(acrylamide) plugs. The MIP containing part of the capillary was connected to an open, buffer-filled capillary via a teflon sleeve. Reprinted from Ref. [62]: Copyright (1997), with permission from Marcel Dekker, Inc.

by a piece of teflon tube to be able to perform detection. By this method, the resultant capillary column had to be equilibrated electrophoretically, since a high hydrodynamic pressure could not be applied.

#### 16.4.1.3 MIPs as pseudo-stationary phase

In a preliminary study [63], MIP particles made by the bulk preparation method were added to the background electrolyte as a pseudo-stationary phase. The optimum amount of MIP that could be added without causing excess turbidity was 0.05% (w/v). The use of a chiral functional monomer, *N*-acryloyl-L-alanine, proved to be more effective than MAA in terms of enantiomer separation ability. Polymers prepared without any templating ligand were extremely insoluble in the background electrolyte and no enantiomer separation using such polymers was found. This lack of reference polymer still raises the question of whether the enantiomer separation is based on a true imprinting effect or caused by the chiral character of the polymer matrix. In any case, good baseline separations were achieved.

#### 16.4.1.4 MIP coatings

Preparation of coatings of imprinted polymer inside capillaries has been reported [64]. An investigation into the effect of several parameters, including type of porogen, type and concentration of cross-linker and silanisation of the inner surface of the capillary, on the synthesis of MIP-coatings of controllable thickness from *trans*-3-(3-pyridyl)-acrylic acid as functional monomer and EDMA or divinylbenzene as cross-linking monomers was undertaken. Although preliminary, the results obtained may open up the interesting technique of open tubular CEC [65–68] for molecular imprinting. In a more recent study [69], the MIP coatings were prepared from MAA and 2-vinylpyridine (2VPy) as functional monomers and either EDMA or TRIM as cross-linking monomers. The effects of polymerisation conditions on column preparation and chromatographic performance were studied. Enantiomer separations of *rac*-dansyl phenylalanine were achieved with good selectivity and efficiency.

#### 16.4.1.5 *In situ* prepared MIP monoliths

Thus far, the most successful approach to MIP-based CEC utilises capillary columns filled with a monolithic, super-porous imprinted polymer [39–41]. The morphology of a certain MIP monolith is depicted in Fig. 16.3. Using this system enantiomer separations with baseline resolution have been carried out in less than 2 minutes. The MIP-filled capillaries are obtained by an *in situ* photo-initiated polymerisation process (Fig. 16.4). The capillary is filled with a pre-polymerisation mixture of imprint molecule, functional and cross-linking monomers (MAA and TRIM, respectively), radical initiator (2,2'-azobisisobutyronitrile) and solvent (toulene). Both ends of the capillary are sealed and the polymerisation is performed

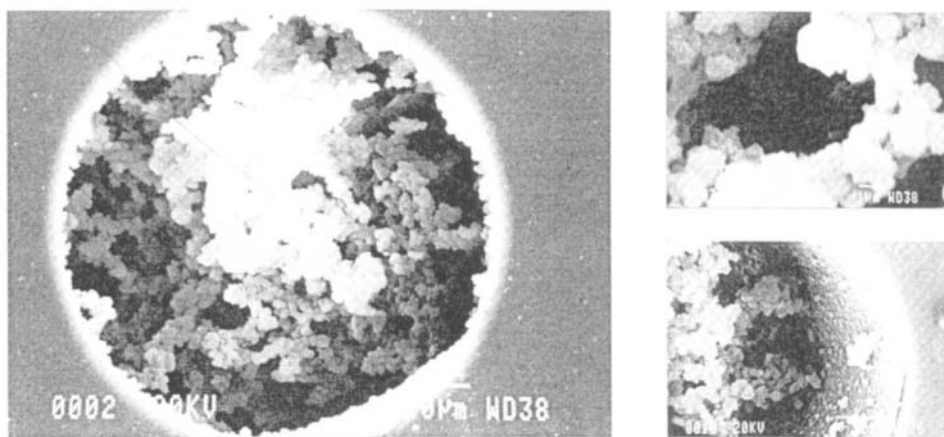


Fig. 16.3. Scanning electron micrographs of cross-sections of a MIP-filled capillary column. The super-porous morphology of the polymer monolith can be seen. Micrometre-sized globular units of macroporous MIP surrounded by interconnecting super-pores (left). A super-pore of about  $7\ \mu\text{m}$  in width (above, right). Covalent attachments of the MIP to the capillary wall (below, right). Reprinted from [39]: Copyright (1997), with permission from American Chemical Society.

by placing the capillary under a UV source (350 nm) at  $-20^\circ\text{C}$ . The polymerisation reaction is stopped by hydrodynamically flushing the remaining monomer, radical initiator and imprint molecule out of the capillary column. In the same way the solvent is exchanged for electrolyte. After a short time of equilibration the capillary column is ready for use. The inner surface of the capillary is derivatised with methacryloxy propyltrimethoxysilane, which participates in the polymerisation reaction. In this way the polymer monolith is covalently attached to the inner wall of the capillary (Fig. 16.3), thereby preventing elution of the polymer during electrochromatography. The technique is simple and quick, and enables imprint-based separation systems to be operational within 3 h from the start of capillary preparation. The success of this approach relies on the polymer-filled capillaries possessing good flow-through properties, since before use the organic solvent employed for polymerisation must be replaced by an electrically conducting electrolyte. This method requires, however, a careful timing of the polymerisation reaction to establish the optimal reaction time for the system used. If the reaction time is too long, the polymer will be dense and hydrodynamic flushing will be impossible. Too short a reaction time will result in a low amount of MIP in the capillary column. Once established, the success rate of producing capillary columns with a super-porous monolithic stationary phase is 100%.

In a slightly modified approach, the MIPs can be rendered super-porous by the use of 1–25% iso-octane as a porogenic agent [40,41]. The porogen is composed of a mixture of solvents in which the porogenic agent (iso-octane) acts as a bad solvent for the growing polymer chains, while the other solvent (toluene for

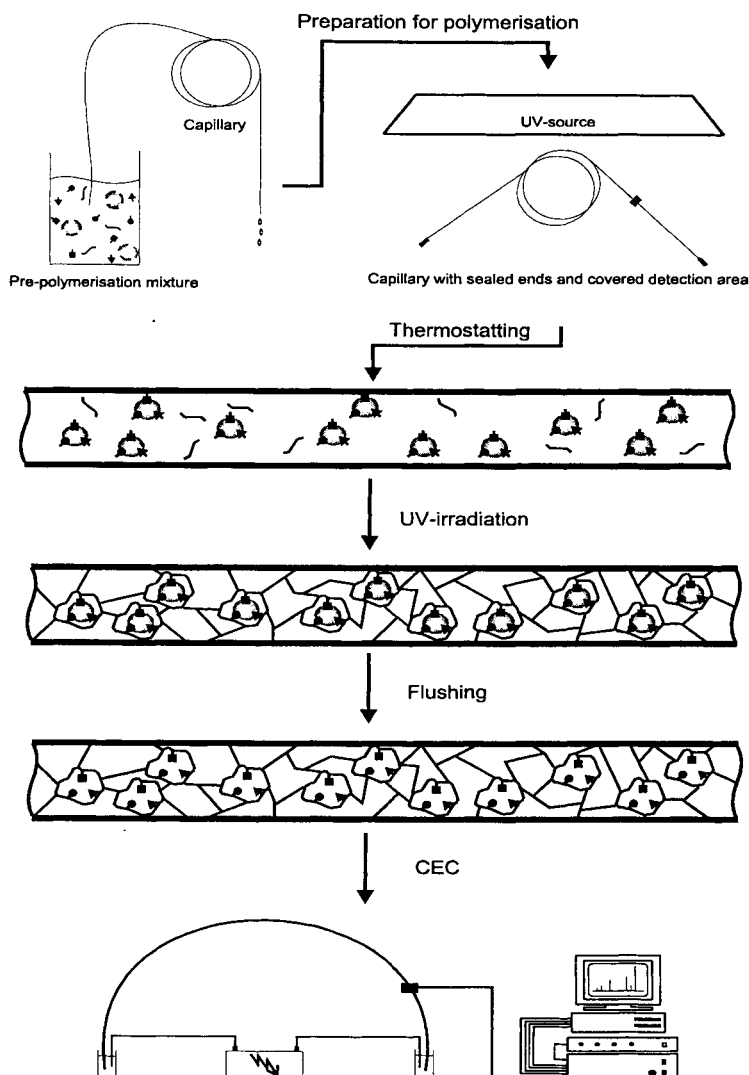


Fig. 16.4. Preparation of a capillary column with a super-porous MIP monolith. A mixture of imprint molecule, functional and cross-linking monomer, radical initiator and a solvent is prepared and introduced into the capillary. Both ends of the capillary are sealed and the polymerisation reaction is initiated by placing the capillary under a UV source. After completion of the polymerisation reaction, the solvent used for polymerisation is exchanged for electrolyte. The flushing also extracts imprint molecules and remaining traces of unreacted monomer and radical initiator out of the polymer. The capillary column is then ready for CEC. Reprinted from [57]; Copyright (1998), with permission from Elsevier Science.

example) acts as a good one. In the choice of porogen it is important that no or minimal disturbance of the imprinting procedure is caused by the solvent. Imprinted super-porous polymer monoliths can be prepared using several cross-linking monomers (TRIM, pentaerythritol triacrylate (PETRA), pentaerythritol tetraacrylate (PETEA), or EDMA) and functional monomers (MAA and 2VPy) using a porogen composed of 1–25% (v/v) iso-octane in toluene. It is important to optimise the volume ratio of iso-octane to toluene in the pre-polymerisation mixture to obtain capillary columns with optimal flow-through characteristics. If the iso-octane content is too low a dense polymer monolith is formed, precluding hydrodynamic pumping of liquid. However, too large an amount leads to the polymer having a soft gel-like appearance rather than being a rigid monolith. The amount of iso-octane in the porogen must also be correlated to the monomer to porogen ratio. It has also been found that the amount of templating ligand in the pre-polymerisation mixture affects the resultant morphology of the polymer monolith [40]. An increased flow resistance of the monoliths on increased molar ratio of templating ligand has been observed from otherwise identical pre-polymerisation mixtures.

Regarding the detection protocols used with capillary columns with molecularly imprinted stationary phases, on-column UV absorbance detection has been exclusively used. Some sort of open tubular area without imprinted polymer is normally prepared to perform detection. It has been shown, however, that UV detection can be performed through the imprinted polymer [39] in some cases. A nice feature with the photo-induced polymerisation procedure is that a part of the capillary column can be covered during the polymerisation reaction, thus preventing polymer being formed in that area. This is utilised to readily prepare detection windows on the MIP capillary columns. There is then no need for coupling of a second capillary to the imprinted polymer-filled capillary to be able to perform detection.

Another approach to monolithic imprinted polymer capillary columns has been reported. The polymerisation was performed at 60°C and thus thermally initiated [70,71]. The result is a dense polymer inside the whole capillary. The resulting MIP capillary then has to be connected to an electrolyte-filled open capillary *via* a teflon tube and a detection window is prepared on the open capillary to facilitate detection (as described above, Fig. 16.2). Also, ammonium acetate (1–2 mM) is added as a conducting agent to the pre-polymerisation mixture. This is done to allow exchange of the solvent of polymerisation for electrolyte, which can be achieved electrophoretically by stepwise increase of the electric field until a stable base-line is obtained.

It is very important that no gas bubbles are trapped in the polymer monolith or in the connected buffer-filled capillary, since the solvent–electrolyte exchange would then be impossible. It can also be speculated that the ammonium acetate present in the pre-polymerisation mixture might interfere with the imprinting process. Nonetheless, successful columns have been prepared using this approach. Since the monolith is very dense, it may intuitively be concluded that there is a larger amount of MIP in these capillaries than in the super-porous ones described above.

### 16.4.2 Electrochromatographic separations

As yet, research into the field of MIP-CEC has focused on the adaptation of imprinted polymers to electrochromatography and the preparation of MIP stationary phases within fused silica capillaries. The optimisation of separation parameters has been less addressed. Most often, the electrolyte is composed of 70–90% of an organic modifier, such as acetonitrile, and an aqueous buffer at low pH. In many instances, the aqueous component is merely a mixture of water and acid. In one study, using (*S*)-ropivacaine imprinted polymer-filled capillaries, it was found that an electrolyte composed of 80% acetonitrile and 20% aqueous buffer was suitable

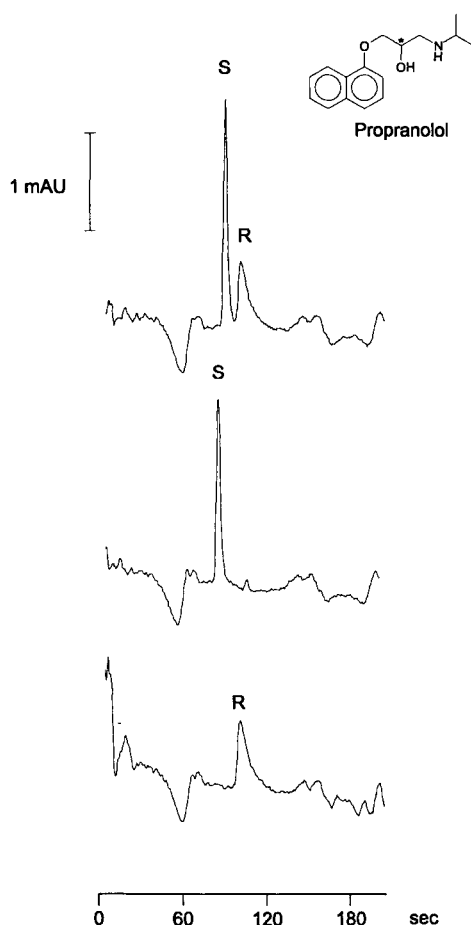


Fig. 16.5. CEC-separation of the enantiomers of propranolol using a capillary column with a stationary phase containing imprints of (*R*)-propranolol. Reprinted from [39]; Copyright (1997), with permission from American Chemical Society.



for CEC separation of the enantiomers of ropivacaine [40]. The enantiomer separation increased with increasing pH, at least in the pH range 2–6.5, as well as with increasing volume ratio of acetonitrile to aqueous buffer. In most cases, however, larger separations occurred at the expense of peak broadening. It was observed that the resolution could be improved by increasing the capillary temperature. Similar observations were made in a study on the separation of the enantiomers of amino acids in a capillary with L-phenylalanine anilide MIP [61,62]. The optimal composition of the electrolyte was found to be a mixture of 90% acetonitrile, 5% water and 5% acetic acid. Omitting the acetic acid resulted in a complete loss of enantiomer separation. Again, the resolution was found to be improved at elevated temperatures. Baseline separations of the enantiomers of propranolol (Fig. 16.5) and metoprolol were achieved using an electrolyte composed of 80% (v/v) acetonitrile and 20% (v/v) 4 M or 2 M acetate buffer (from ammonium acetate and acetic acid) pH

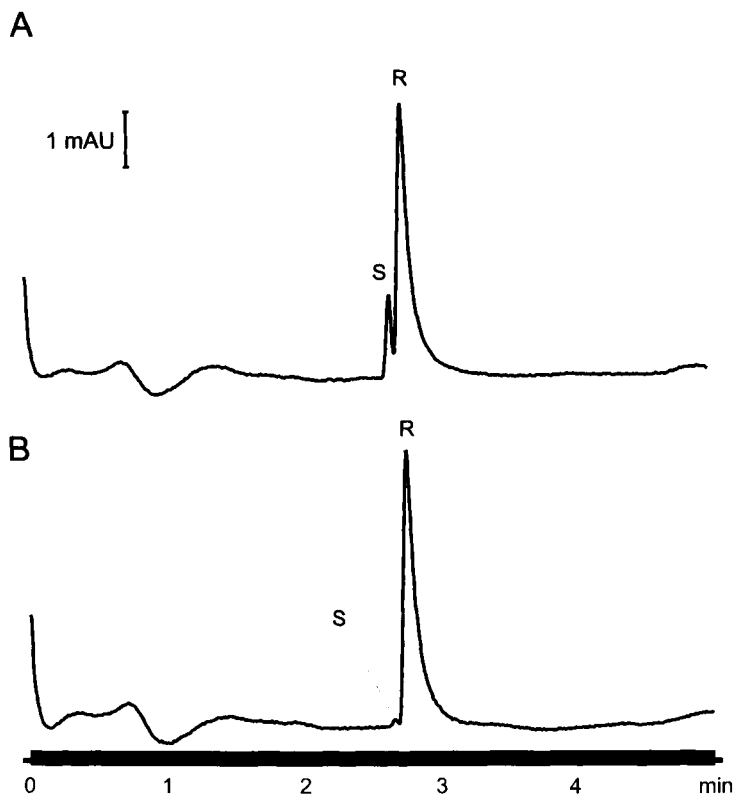


Fig. 16.6. CEC-separation of non-racemic mixtures of propranolol on a capillary column with imprints of (*R*)-propranolol. (A) 9 + 1 mixture of (*R*)- and (*S*)-propranolol; (B) 99 + 1 mixture of (*R*)- and (*S*)-propranolol. Reprinted from [39]; Copyright (1997), with permission from American Chemical Society.

3.0 respectively [39]. Also, the (*S*)-enantiomer of propranolol could be separated and detected using an (*R*)-propranolol imprinted column from a non-racemic sample containing only 1% (*S*)-propranolol (Fig. 16.6).

Pure enantiomer imprinting of L-phenylalanine anilide, (*R*)-propranolol, (*S*)-metoprolol and (*S*)-ropivacaine has been undertaken and these MIP capillaries have been used in the CEC mode for enantiomer separations [39–41,60–62,70,71] (Table 16.1). Baseline separations for the enantiomers of phenylalanine (Fig. 16.7) and for propranolol and metoprolol could be carried out in less than 2 min. (Fig. 16.5). A propranolol column was shown to be able to resolve several other  $\beta$ -blockers, including prenalterol, atenolol, pindolol, etc. (Fig. 16.8) [41] and the ropi-

TABLE 16.1

## TYPES OF MIPs USED IN CEC

| Type of column                        | Template molecule                   | Monomers used<br>(functional/cross-linking)                    | Separated species                             | Reference |
|---------------------------------------|-------------------------------------|--|---|-----------|
| Dispersion polymerised MIP            | Benzamidine                         | MAA/EDMA   | Selective retardation of imprint species [58] |           |
|                                       | Pentamidine                         |  | Selective retardation of imprint species [58] |           |
|                                       | L-Phenylalanine anilide             |  | No chiral separation                          |           |
| Super-porous MIP monolith             | ( <i>R</i> )-Propranolol            | MAA, 2VPy/TRIM, PETRA, PETEA, EDMA                             | Enantiomers of $\beta$ -blockers [39,41]      |           |
|                                       | ( <i>S</i> )-Metoprolol             |  | <i>rac</i> -Metoprolol [40]                   |           |
|                                       | ( <i>S</i> )-Ropivacaine            |  | Enantiomers of local anaesthetics             |           |
| MIP monolith                          | L-Phenylalanine anilide             | MAA, 2VPy/EDMA   | Enantiomers of amino acids [70, 71]           |           |
| MIP particles entrapped in acrylamide | L-Phenylalanine anilide             | MAA/EDMA   | Enantiomers of amino acids [60–62]            |           |
|                                       | L-Phenylalanine                     |  | Enantiomers of amino acids [62]               |           |
| MIP as electrolyte additive           | ( <i>S</i> )-Propranolol            | <i>N</i> -acryloyl-alanine/EDMA                                | <i>rac</i> -Propranolol [63]                  |           |
| MIP as film coating                   | ( <i>S</i> )-2-Phenylpropionic acid | <i>trans</i> -3-(3-pyridyl)-acrylic acid/EDMA, divinyl-benzene | <i>rac</i> -2-Phenylpropionic acid [64]       |           |
|                                       | ( <i>R</i> )-2-Phenylpropionic acid | MAA, 2VPy/TRIM, EDMA   | <i>rac</i> -2-Phenylpropionic acid [69]       |           |
|                                       | Dansyl-L-phenylalanine              |  | <i>rac</i> -Dansyl phenylalanine              |           |

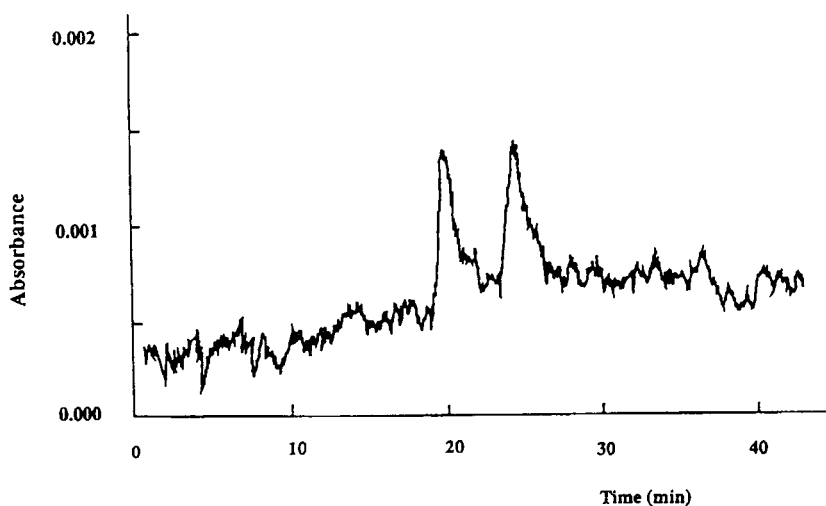


Fig. 16.7. CEC-separation of D,L-phenylalanine on a column containing imprints of L-phenylalanine anilide. This demonstrates the interesting strategy of using a structurally similar compound to the analyte as the imprint molecule for the MIP preparation. Due to their low solubility in the pre-polymerisation mixture, amino acids are normally not amenable to non-covalent imprinting. Reprinted from [69]: Copyright (1997), with permission from Elsevier Science.

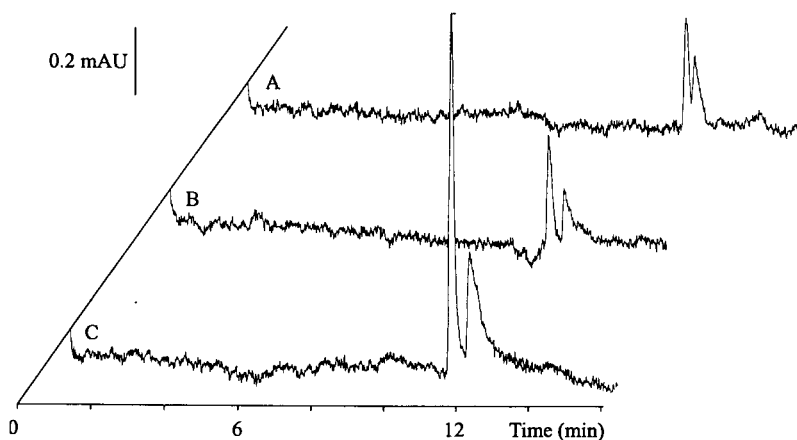


Fig. 16.8. Enantiomer separations of (A) *rac*-prenalterol, (B) *rac*-atenolol and (C) *rac*-pin-dolol on a capillary column containing imprints of (*R*)-propranolol. This demonstrates the ability of a MIP to recognise structural analogues of the template molecule used for the imprint preparation. Reprinted from [41]: Copyright (1997), with permission from Wiley-VCH.

vacaine column could separate the enantiomers of structurally similar local anaesthetics, including mepivacaine and bupivacaine [40]. All reported separated species using CEC with molecularly imprinted stationary phases are presented in Table 16.1.

In particular, a molecularly imprint-based CEC system was compared with an immobilised protein-based system and a cyclodextrin-based system for the enantiomer separation of  $\beta$ -adrenergic antagonists. It was shown that the MIP-based system could separate all the analytes tested without any change in the experimental conditions (i.e. electrolyte composition). This was not possible using the other systems. The chromatographic efficiency, however, was superior for the cyclodextrin-based system. The poor efficiency is a rather discouraging, yet common, feature of molecular imprint-based separation systems. Also, the protein-based systems showed poor efficiency in this study, but optimised conditions can improve this [72,73]. Nevertheless, the MIP-based and protein-based systems showed good selectivity.

The discouraging efficiency obtained so far using molecularly imprinted stationary phases in chromatography probably originates from the imprinting procedure itself. It is argued that this process yields a population of imprints with varying quality. Thus, an imprinted polymer matrix consists of imprints exhibiting different kinds of sites, ranging from high affinity to low affinity for the analyte. The result may be unfavourable kinetics for analyte association to and dissociation from the imprinted phase. The future research into the preparation of uniform imprints with the same affinity, or at least a narrow range of affinities, will improve the chromatographic efficiency. One can also argue that unfavourable non-specific interaction of the analyte to the polymer matrix may contribute to bad efficiency. New polymer matrices may in that case overcome such problems. As expected, however, the CEC-based separations show better efficiency when compared with the LC-based ones.

## 16.5 CONCLUSIONS AND FUTURE OUTLOOK

The combination of CEC, which provides a high degree of chromatographic efficiency and short separation times, and molecular imprinting, which provides a means for preparing stationary phases of pre-determined selectivity, may well lead to efficient and highly selective separation systems. Molecular imprinting technology represents a widely applicable strategy for producing stationary phases with selectivity for a predetermined ligand or class of compounds. Its utility has been shown repeatedly by the imprinting of a range of functionally distinct compounds. The chemical resistance of the polymer permits the use of organic solvents, of strong acidic and basic buffers and of high voltages, all attractive features for CEC usage. The micro-column format of CEC leads to a minimal consumption of chemicals, including the templating ligand used for imprinting. Since the concentration of imprint species in the pre-polymerisation mixture is high, the large scale production of MIP-based micro-columns may be more easily realised compared with

conventional LC columns. Typically, 10–100 nmol of imprint species are required for a polymer the size of a capillary column, which is about 1–10  $\mu\text{L}$ . Although the chromatographic performance is better than that obtained in MIP-based LC, separation efficiencies characteristic of CEC are still to be achieved. For MIP-based stationary phases to become a true complement to the selectors presently employed in CEC, further improvements in peak shape and efficiency are required. To achieve this, further research into both the methodology for the preparation of MIP-based columns and optimisation of the conditions for MIP-based electrochromatography is warranted.

## REFERENCES

- 1 G. Wulff, *Angew. Chem. Int. Ed. Engl.*, **34**, 1812 (1995).
- 2 K. Mosbach and O. Ramström, *BioTechnology*, **14**, 163 (1996).
- 3 I.A. Nicholls, L.I. Andersson, K. Mosbach and E.B., *Trends Biotechnol.*, **13**, 47 (1995).
- 4 J. Steinke, D.C. Sherrington and I.R. Dunkin, *Adv. Polym. Sci.*, **123**, 81 (1995).
- 5 S. Mallik, S.D. Plunkett, P.K. Dahl, R.D. Johnson, D. Pack, D. Schnek and F.H. Arnold, *New J. Chem.*, **18**, 299 (1994).
- 6 J. Matsui, I.A. Nicholls and T. Takeuchi, *Tetrahedron Asymmetry*, **7**, 1357 (1996).
- 7 M. Kempe and K. Mosbach, *J. Chromatogr. A*, **664**, 276 (1994).
- 8 L. Fischer, R. Müller, B. Ekberg and K. Mosbach, *J. Am. Chem. Soc.*, **113**, 9358 (1991).
- 9 O. Ramström, I.A. Nicholls and K. Mosbach, *Tetrahedron Asymmetry*, **5**, 649 (1994).
- 10 A.G. Mayes and K. Mosbach, *Anal. Chem.*, **68**, 3769 (1996).
- 11 J. Matsui, T. Kato, T. Takeuchi, K. Yokoyama and I. Tamiya, *Anal. Chem.*, **65**, 2223 (1993).
- 12 J. Matsui and T. Takeuchi, *Anal. Commun.*, **34**, 199 (1997).
- 13 J.H. Knox and I.H. Grant, *Chromatographia*, **32**, 317 (1991).
- 14 D. Burgreen and F.R. Nakache, *J. Phys. Chem.*, **68**, 1084 (1964).
- 15 J.A. Taylor and E.S. Yeung, *Anal. Chem.*, **65**, 2928 (1993).
- 16 T. Tsuda, S. Kitagawa, R. Dadoo and R.N. Zare, *Bunseki Kagaku*, **46**, 409 (1997).
- 17 J.H. Knox and I.H. Grant, *Chromatographia*, **24**, 135 (1987).
- 18 M.M. Robson, M.G. Cikalo, P. Myers, M.R. Euerby and K.D. Bartle, *J. Microcolumn Sep.*, **9**, 357 (1997).
- 19 V. Pretorius, B.J. Hopkins and J.D. Schieke, *J. Chromatogr.*, **99**, 23 (1974).
- 20 J.W. Jorgenson and K.D. Lukacs, *J. Chromatogr.*, **218**, 209 (1981).
- 21 T. Tsuda, K. Nomura and G. Nakagawa, *J. Chromatogr.*, **248**, 241 (1982).
- 22 K.A. Kelly and M.G. Khaledi, *Chem. Anal.*, **146**, 277 (1998).
- 23 K.D. Altria, N.W. Smith and C.H. Turnbull, *Chromatographia*, **46**, 664 (1997).
- 24 A.L. Crego, A. Gonzalez and M.L. Marina, *Crit. Rev. Anal. Chem.*, **26**, 261 (1996).
- 25 G. Ross, M. Dittmann, F. Bek and G. Rozing, *American Laboratory*, **28**, 34 (1996).
- 26 J.J. Pesek and M.T. Matyska, *Electrophoresis*, **18**, 2228 (1997).
- 27 A.S. Rathore and C. Horvath, *J. Chromatogr. A*, **781**, 185 (1997).
- 28 J.H. Miyawa and M.S. Alasandro, *LC GC Magazine of Sep. Sci.*, **16**, 36 (1998).
- 29 C. Yan, R. Dadoo, R.N. Zare, D.J. Rakestraw and D.S. Anex, *Anal. Chem.*, **68**, 2726 (1996).
- 30 S.M. Fields, *Anal. Chem.*, **68**, 2709 (1996).
- 31 E.C. Peters, M. Petro, F. Svec and J.M.J. Frechet, *Anal. Chem.*, **70**, 2288 (1998).
- 32 J.L. Liao, N. Chen, C. Ericson and S. Hjerten, *Anal. Chem.*, **68**, 3468 (1996).
- 33 E.C. Peters, K. Lewandowski, M. Petro, F. Svec and J.M.J. Frechet, *Anal. Commun.*, **35**, 83 (1998).
- 34 E.C. Peters, M. Petro, F. Svec and J.M.J. Frechet, *Anal. Chem.*, **70**, 2296 (1998).

- 35 E.C. Peters, M. Petro, F. Svec and J.M.J. Frechet, *Anal. Chem.*, **69**, 3646 (1997).
- 36 A. Palm and M.V. Novotny, *Anal. Chem.*, **69**, 4499 (1997).
- 37 C.P. Palmer, *J. Chromatogr. A*, **780**, 75 (1997).
- 38 C. Ericson, J.L. Liao, K. Nakazato and S. Hjerten, *J. Chromatogr. A*, **767**, 33 (1997).
- 39 L. Schweitz, L.I. Andersson and S. Nilsson, *Anal. Chem.*, **69**, 1179 (1997).
- 40 L. Schweitz, L.I. Andersson and S. Nilsson, *J. Chromatogr. A*, **792**, 401 (1997).
- 41 S. Nilsson, L. Schweitz and M. Petersson, *Electrophoresis*, **18**, 884 (1997).
- 42 T. Takagishi and I.M. Klotz, *Biopolymers*, **11**, 483 (1972).
- 43 G. Wulff and A. Sarhan, *Angew. Chem.*, **84**, 364 (1972).
- 44 R. Arshady and K. Mosbach, *Macromol. Chem.*, **182**, 687 (1981).
- 45 P.K. Dhal and F.H. Arnold, *J. Am. Chem. Soc.*, **113**, 7417 (1991).
- 46 F.H. Dickey, *Proc. Natl. Acad. Sci. USA*, **35**, 227 (1949).
- 47 D.J. O'Shannessy, B. Ekberg and K. Mosbach, *Anal. Biochem.*, **177**, 144 (1989).
- 48 R.J. Ansell, D. Kriz and K. Mosbach, *Curr. Opin. Biotechnol.*, **7**, 89 (1996).
- 49 D. Kriz, O. Ramstrom and K. Mosbach, *Anal. Chem.*, **69**, A345 (1997).
- 50 A.G. Mayes and K. Mosbach, *TRAC Trends in Anal. Chem.*, **16**, 321 (1997).
- 51 K. Mosbach, *TIBS*, **19**, 9 (1994).
- 52 B. Sellergren, *TRAC Trends in Anal. Chem.*, **16**, 310 (1997).
- 53 B. Sellergren, *International Laboratory*, 10A (1997).
- 54 T. Takeuchi and J. Matsui, *Acta Polymerica*, **47**, 471 (1996).
- 55 G. Wulff, *TIBTECH*, **11**, 85 (1993).
- 56 N.H.H. Heegard, S. Nilsson and N.A. Guzman, *J. Chromatogr. B*, **715**, 29 (1998).
- 57 L. Schweitz, L.I. Andersson and S. Nilsson, *J. Chromatogr. A*, **817**, 5 (1998).
- 58 K. Nilsson, J. Lindell, O. Norrlöw and B. Sellergren, *J. Chromatogr. A*, **680**, 57 (1994).
- 59 K. Nilsson and B. Sellergren, International application number PCT/SE94/00025.
- 60 J.-M. Lin, T. Nakagama, K. Uchiyama and T. Hobo, *Chromatographia*, **43**, 585 (1996).
- 61 J.-M. Lin, T. Nakagama, K. Uchiyama and T. Hobo, *Biomed. Chromatogr.*, **11**, 298 (1997).
- 62 J.-M. Lin, T. Nakagama, K. Uchiyama and T. Hobo, *J. Liq. Chromatogr. Relat. Technol.*, **20**, 1489 (1997).
- 63 M. Walshe, E. Garcia, J. Howarth, M.R. Smyth and M.T. Kelly, *Anal. Commun.*, **34**, 119 (1997).
- 64 O. Brüggemann, R. Freitag, M.J. Whitcombe and E.N. Vulfson, *J. Chromatogr. A*, **781**, 43 (1997).
- 65 R. Swart, J.C. Kraak and H. Poppe, *TRAC Trends in Anal. Chem.*, **16**, 332 (1997).
- 66 F. Li, H. Jin, J. Gu and R. Fu, *J. Beijing Inst. Technol.*, **5**, 122 (1996).
- 67 P. Narang and L.A. Colon, *J. Chromatogr. A*, **773**, 65 (1997).
- 68 Z.J. Tan and V.T. Remcho, *J. Microcolumn Sep.*, **10**, 99 (1998).
- 69 Z.J. Tan and V.T. Remcho, *Electrophoresis*, **19**, 2055 (1998).
- 70 J.-M. Lin, T. Nakagama, K. Uchiyama and T. Hobo, *J. Pharm. Biomed. Anal.*, **15**, 1351 (1997).
- 71 J.M. Lin, T. Nakagama, X.Z. Wu, K. Uchiyama and T. Hobo, *Fresenius J. Anal. Chem.*, **357**, 130 (1997).
- 72 S. Birnbaum and S. Nilsson, *Anal. Chem.*, **64**, 2872 (1992).
- 73 H. Ljungberg and S. Nilsson, *J. Liq. Chromatogr.*, **18**, 3685 (1995).

This Page Intentionally Left Blank

## Molecularly imprinted polymers in enantiomer separations

MARIA KEMPE

### 17.1 INTRODUCTION

More than half of all drugs on the market are asymmetric molecules. Many of these are administered as racemates. Since biological recognition systems are based on optically active molecules, the two enantiomers of a racemic drug may interact by different mechanisms with these systems. One of the enantiomers may exert pharmacologically different or unwanted side effects [1–3]. The same is true for racemic pesticides and herbicides; often only one of the enantiomers possesses the desired activity.

The demand for optically active compounds has spurred numerous research efforts in the areas of asymmetric synthesis and chiral separations. The impetus behind these chirotechnological activities often comes from regulatory authorities, e.g. the Food & Drug Administration. Both preparative methods for large-scale purification of optically active compounds [4] as well as analytical methods for pharmacological studies and for assaying the enantiomeric purity of chiral precursors and final products of asymmetric syntheses are needed [5].

Chiral separation by liquid chromatography can be divided into four approaches: (i) derivatisation with a chiral reagent and separation of the resulting diastereomers on a non-chiral stationary phase (non-CSP); (ii) direct separation on a non-CSP by the use of a chiral mobile phase additive; (iii) derivatisation with a non-chiral reagent and separation on a CSP; and (iv) direct separation on a CSP.

A CSP consists of a chiral selector, which either alone constitutes the stationary phase or which has been immobilised to a solid phase. The chiral selector is a low molecular weight compound or a polymer, either synthetic or natural. A broad range of CSPs has been developed. Examples of CSPs that have been used successfully include polysaccharides, such as cellulose and its derivatives [6] and cyclodextrins [7], and proteins, e.g. bovine serum albumin,  $\alpha_1$ -acid glycoprotein, cellulase, trypsin and  $\alpha$ -chymotrypsin [8]. Several different synthetic polymers have also proven to be useful CSPs, for example the 'Blaschke-type CSPs' (polyacrylamides and polymethacrylamides) [9] and the 'Pirkle-type CSPs' [10].

An alternative approach to effect chiral discrimination is to use the technique of *molecular imprinting*, the subject of this book. This technique, sometimes also referred to as *template polymerisation*, results in synthetic polymers of predetermined selectivity. Receptor-like binding sites are tailor-made *in situ* by the copolymerisation of cross-linkers and functional monomers, which are interacting with



*print molecules* (or *templates*). After polymerisation, the print molecules are removed from the polymer, either by extraction or by chemical cleavage, leaving recognition sites complementary to the print molecules in shape and the positioning of functional groups. The polymer is subsequently able to rebind the print molecules. If one of the enantiomers of a racemic compound is used as the template, the resulting polymer will be able to discriminate between the two enantiomers.

Molecularly imprinted polymers (MIPs) for chiral separations have been prepared mainly by two approaches: (i) covalent binding of the template to the functional monomer(s) and (ii) non-covalent binding (self-assembly) of the template and the functional monomer(s).

### 17.1.1 Covalent molecular imprinting

In the covalent approach, the print molecules are covalently coupled to polymerisable molecules prior to polymerisation (see Chapter 4). The covalent bonds have to be relatively easy to break to allow cleavage of the print molecules after polymerisation. Print molecules have been coupled to monomers through the formation of boronic, carboxylic and phosphonic ester bonds, amide bonds, imines and ketals. After copolymerisation with a high degree of cross-linker, the print molecules are cleaved from the polymer. A representative example of the covalent approach is shown in Fig. 17.1.

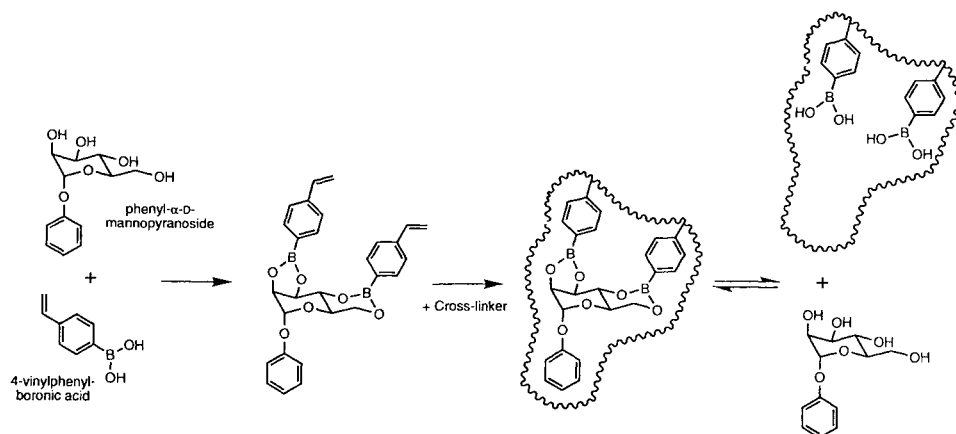


Fig. 17.1. Covalent molecular imprinting.

### 17.1.2 Non-covalent molecular imprinting

Non-covalent molecular imprinting relies on multiple non-covalent interactions between the print molecules and the monomers. The monomers are chosen to allow hydrogen bonds, ionic interactions,  $\pi$ - $\pi$  interactions and/or hydrophobic interactions with the print molecules. Before polymerisation, the monomers and the print

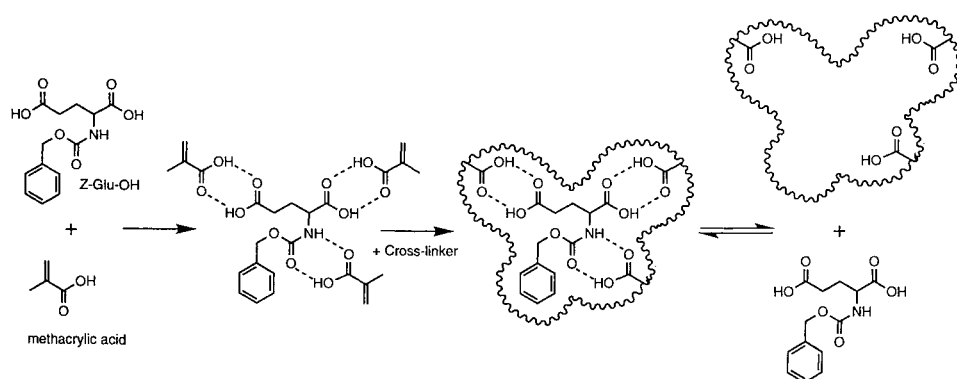


Fig. 17.2. Non-covalent molecular imprinting.

molecules are self-assembled simply by dissolving them in an appropriate solvent. Cross-linker is added and the polymerisation is initiated. The print molecules are subsequently extracted from the highly cross-linked polymeric network obtained (Fig. 17.2). The association/dissociation kinetics of non-covalent MIPs is in general faster than that observed on polymers prepared by the covalent approach. For this reason, the former polymers are more attractive as stationary phases for chromatography. Even if numerous examples of covalently imprinted stationary phases have been reported, it was not until the development of the non-covalent approach that the technique became competitive in the preparation of CSPs. This review will therefore focus mainly on non-covalent molecular imprinting. The covalent approach has been covered in several excellent reviews by Wulff [11,12] and is also discussed in more detail in Chapter 4.

## 17.2. POLYMER SYSTEMS

### 17.2.1 Monomers and cross-linkers

A broad range of functional monomers and cross-linkers has been used for the preparation of MIPs. The choice of the functional monomers depends on the nature and functionalities of the print molecule. The most widely used monomer is methacrylic acid, which has been shown to interact through ionic interactions and hydrogen bonds with amines, amides, carbamates and carboxylic acids [13–15]. The monomers and the print molecules self-assemble upon mixing and the strength of the complex is of importance for the selectivity of the polymer. For this reason, a considerable amount of research effort has focused on finding optimal monomers for various classes of print molecules and functionalities. For example, for some print molecules, polymers prepared with vinylpyridines [16,17], 2-(trifluoromethyl)acrylic acid [18] or acrylamide [19] resulted in higher selectivities and affinities than polymers made from methacrylic acid. Mixtures of functional monomers

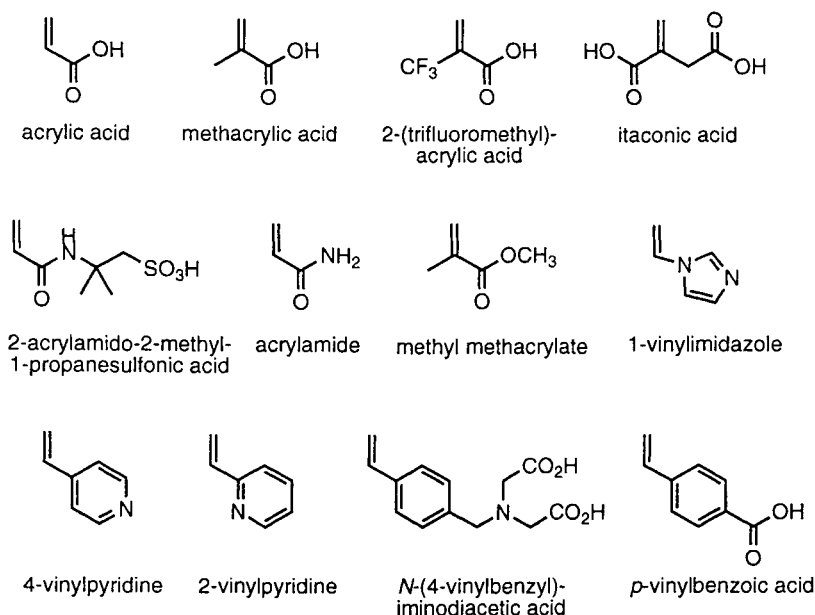


Fig. 17.3. Functional monomers used for the preparation of MIPs.

have, in some cases, been shown to give polymers with better recognition properties than polymers prepared from only one type of functional monomer [17]. A selection of functional monomers is shown in Fig. 17.3.

The geometry of the imprinted sites and the correct positioning of the functional groups will only be retained in a rigid polymer network. MIPs are therefore generally prepared with a high degree of cross-linker. This brings about an attractive feature of the polymers: high mechanical stability. Ethylene glycol dimethacrylate (EDMA) has been used extensively as the cross-linking agent. MIPs prepared from trifunctional cross-linkers, such as trimethylolpropane trimethacrylate (TRIM) and pentaerythritol triacrylate (PETRA), have been shown to be superior to EDMA-based polymers in terms of efficiency and load capacity [20]. The polymers prepared from these cross-linkers have a more porous character than those prepared from EDMA. A selection of cross-linkers is shown in Fig. 17.4.

### 17.2.2 Polymerisation solvents

Not only the *rigidity* is crucial to the efficiency of MIPs, but also the *accessibility*; as many recognition sites as possible should be accessible for rebinding. The material should therefore be porous. This is realised by dissolving monomers, cross-linkers and print molecules in a porogenic solvent prior to polymerisation. The effect of the solvent on the polymer morphology can be monitored by measuring physical parameters such as surface area, pore diameter and pore volume.

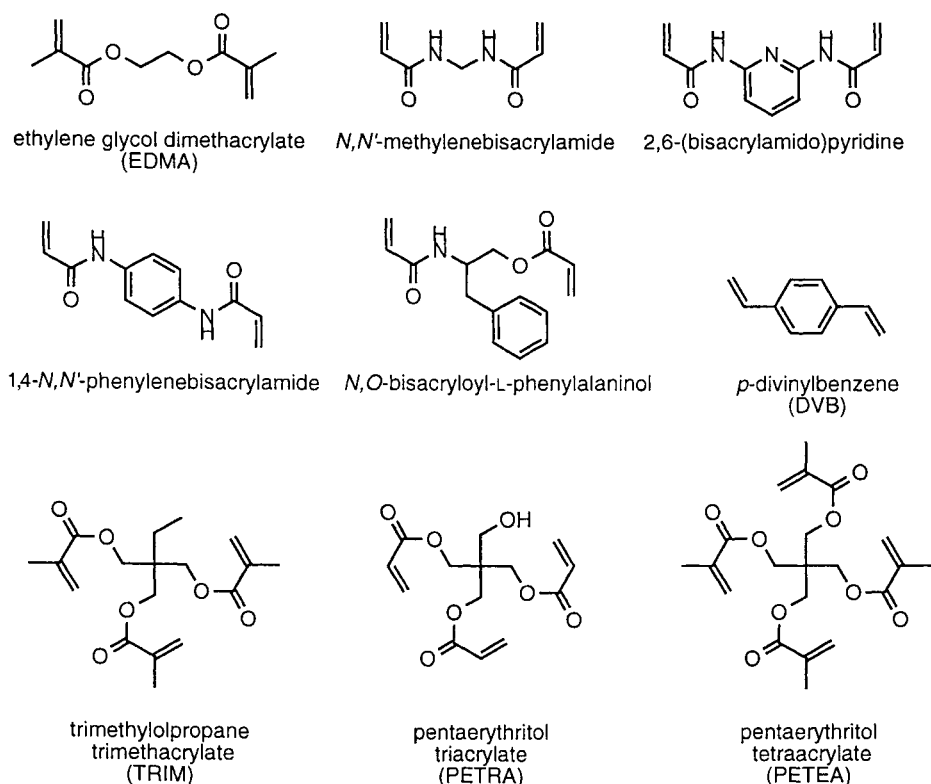


Fig. 17.4. Cross-linkers used for the preparation of MIPs.

The choice of solvent is in many cases critical. The solvent should preferably not interfere with the interactions between the monomers and the templates during the self-assembly. These interactions are often electrostatic and hydrogen bonding in nature. Aprotic organic solvents of low polarity and low hydrogen bonding capacity are therefore preferred. A correlation between the hydrogen bonding capacity of the porogen and the polymer selectivity has been demonstrated [21].

### 17.2.3 Polymerisation methods

MIPs can be prepared by various techniques (see also Chapters 12 and 13). Radical polymerisation, either thermolytically or photolytically initiated, is often employed [22]. The most common and straightforward method is bulk polymerisation to prepare polymer monoliths, followed by grinding and sieving to give particles of appropriate size. This method can be applied readily to the preparation of stationary phases for high-performance liquid chromatography (HPLC). The disadvantage, however, is that the grinding procedure usually creates particles with a broad size distribution and substantial amounts of very fine particles, which have

to be removed and discarded by repetitive sedimentations before packing the columns. Furthermore, the particles are of highly irregular shape. According to chromatographic theory this will hamper the performance.

To address these problems, techniques to prepare spherical composites and grafted polymers have been developed. MIPs were polymerised in the pores of spherical synthetic polymer beads and silica particles [23–25]. The selectivities of these materials were in the same range as those obtained on irregular particles prepared from bulk polymers, while the chromatographic efficiencies were improved.

Alternatively, the polymerisation can be done directly in the column, either by bulk polymerisation [26] or by a dispersion polymerisation technique [27]. In the case of bulk polymerisation, the solvent has to be an extremely good porogen to produce continuous pores that allow a flow through the polymer monolith. The solvents reported for this approach were fairly polar. Such solvents are detrimental to monomer–template assemblies relying on polar interactions, thereby reducing the versatility of the technique. Similar problems can be seen in the dispersion polymerisation approach, in which agglomerates of micron-sized globular particles are formed when the polymer precipitates in the dispersion medium. Polar solvents with high hydrogen bond capacities used as dispersion media will interfere with hydrogen bonds between the templates and the functional monomers. This was seen with molecularly imprinted CSPs selective for L-phenylalanine anilide. The column efficiency was higher for columns prepared by dispersion polymerisation than for columns packed with ground, irregular particles prepared by bulk polymerisation, whereas the selectivity was lower due to the use of a polar solvent as the dispersion medium [27].

Spherical beads can be prepared by suspension polymerisation. The classical approach, which involves suspension of the organic phase (monomers, cross-linkers, print molecules and porogen) in water, is problematic if one or more of the components is water-soluble. Furthermore, water will interfere with any polar interactions involved in the monomer–print molecule complex. A two-step swelling and polymerisation method with water as the suspension medium suffers from the same problem [28]. An alternative approach, in which a perfluorocarbon liquid is used instead of water as the suspension solvent, has been developed [29]. Perfluorocarbon liquids are immiscible with most organic solvents and do not interfere with polar interactions. Molecularly imprinted CSPs prepared by this method showed chromatographic performances comparable to those obtained on irregularly-beaded MIP CSPs, although higher flow rates could be applied.

### **17.3 CHIRAL CHROMATOGRAPHY**

Initial studies on non-covalent MIPs, pioneered by Mosbach and co-workers, focused mainly on the preparation of materials selective for amino acid derivatives [13–17,19–23,30–38]. The polymers did not only possess selectivity for the amino acid used as the print molecule, but were also found to be enantioselective; the

enantiomer present during the polymerisation was preferentially bound. These findings, together with observations that the polymers were mechanically and chemically stable, made them attractive as CSPs and spurred further research.

The imprinting effects of MIPs prepared with optically active compounds as the print molecules are readily demonstrated by chromatographic evaluations. For example, when the L-enantiomer of an amino acid derivative is used as the print species, a column packed with the resulting polymer will retain the L-enantiomer longer than the D-enantiomer and *vice versa* when the D-enantiomer is used as the print molecule. Reference polymers prepared with the racemate or without print molecule will not be able to resolve the racemate. A stereoselective memory is hence induced in the polymers by the print molecules and is in many cases very precise.

Molecularly imprinted CSPs have been prepared for applications in HPLC, TLC (thin-layer chromatography), CE (capillary electrophoresis) and CEC (capillary electrochromatography). CSPs for HPLC are by far the most studied.

### 17.3.1 HPLC

A large number of chiral amino acids and peptides has been imprinted. Several MIPs selective for pharmaceuticals have also been described. The most widely used method has been bulk polymerisation followed by grinding, sieving and packing into HPLC columns. Alternatively, the polymers can be prepared by any of the methods discussed above. Some examples of MIP CSPs are found in Table 17.1.

The specificity and selectivity of MIPs can be fine-tuned by careful choice of monomers and solvent and by optimising the molar ratios of the components in the polymerisation mixture. The recognition relies on multiple interaction points. The more functionalised the print molecule is, the more interactions are possible. The recognition sites produced show a distribution of binding strengths; the sites are heterogeneous or 'polyclonal'. This results in non-linear adsorption isotherms, which can be fitted to binary models corresponding to a small number of highly selective sites and a large number of less selective sites [48,49]. When the MIPs are used for chromatographic applications, the heterogeneity of the sites is reflected by asymmetric peaks [49].

The selectivities of MIPs are in many cases comparable to those of commercially available CSPs. For example, a separation factor ( $\alpha$ ) of 17.8 was found for the separation of the two enantiomers of a dipeptide on poly(methacrylic acid-*co*-EDMA) imprinted with one of the enantiomers (Fig. 17.5) [43].

In a study on  $\beta$ -adrenergic blockers, (*S*)-timolol was imprinted in EDMA-based polymers. When the functional monomer was methacrylic acid, the polymer was able to resolve not only racemic timolol (**1**), but also racemic propranolol (**2**). In

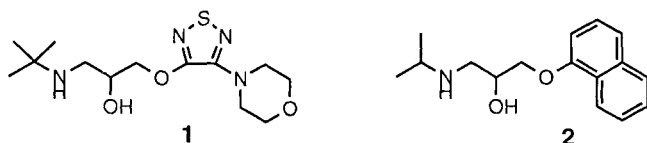


TABLE 17.1

A SELECTION OF MOLECULARLY IMPRINTED CSPs FOR HPLC<sup>a</sup>

| Print molecule                          | Polymer <sup>b</sup>      | $\alpha^c$ | $R_s^d$ | $f/g^e$ | Ref. |
|---|---------------------------|------------|---------|---------|------|
| <b>Amino acids</b>                      |                           |            |         |         |      |
| H-L-Phe-OH                              | poly(CuVBIDA-co-EDMA)     | 1.45       | n.d.    | n.d.    | [39] |
| H-L-Phe-NHPh                            | poly(MAA-co-EDMA)         | 13         | n.d.    | n.d.    | [40] |
| H-D- <i>p</i> -NH <sub>2</sub> Phe-NHPh | poly(MAA-co-EDMA)         | 15         | n.d.    | n.d.    | [41] |
| Ac-D-Trp-OMe                            | poly(MAA-co-EDMA)         | 3.92       | 2.2     | 1.0     | [17] |
| Ac-L-Trp-OH                             | poly(AAM-co-EDMA)         | 3.24       | 2.02    | n.d.    | [19] |
| Boc-L-Trp-OH                            | poly(MAA-co-2VPy-co-EDMA) | 4.35       | 1.9     | 1.0     | [17] |
| Fmoc-L-Phe-OH                           | poly(MAA-co-EDMA)         | 1.36       | n.d.    | n.d.    | [36] |
| Z-L-Asp-OH                              | poly(4VPy-co-EDMA)        | 2.81       | 1.22    | 0.81    | [16] |
| Z-L-Phe-OH                              | poly(MAA-co-TRIM)         | 2.29       | 3.14    | 1.00    | [20] |
| Z-L-Tyr-OH                              | poly(MAA-co-PETRA)        | 2.86       | 5.47    | 1.00    | [20] |
| Dansyl-L-Phe-OH                         | poly(MAA-co-2VPy-co-EDMA) | 3.15       | 1.6     | 0.96    | [17] |
| <b>Peptides</b>                         |                           |            |         |         |      |
| H-L-Phe-Gly-NHPh                        | poly(MAA-co-EDMA)         | 5.1        | n.d.    | n.d.    | [42] |
| Boc-L-Phe-Gly-OEt                       | poly(MAA-co-TRIM)         | 3.04       | 3.44    | 1.00    | [20] |
| Z-L-Ala-L-Ala-OMe                       | poly(MAA-co-TRIM)         | 3.19       | 4.50    | 1.00    | [20] |
| Ac-L-Phe-L-Trp-OMe                      | poly(MAA-co-EDMA)         | 17.8       | n.d.    | 1.00    | [43] |
| Z-L-Ala-Gly-L-Phe-OMe                   | poly(MAA-co-TRIM)         | 3.60       | 4.15    | 1.00    | [20] |
| <b>Pharmaceuticals</b>                  |                           |            |         |         |      |
| ( <i>S</i> )-Timolol                    | poly(MAA-co-EDMA)         | 2.9        | 2.0     | n.d.    | [44] |
| ( <i>S</i> )-Naproxen                   | poly(4VPy-co-EDMA)        | 1.65       | n.d.    | n.d.    | [45] |
| ( <i>S,R</i> )-Ephedrine                | poly(MAA-co-TRIM)         | 3.42       | 1.6     | n.d.    | [46] |
| ( <i>S,S</i> )-Pseudoephedrine          | poly(MAA-co-TRIM)         | 3.19       | 1.8     | n.d.    | [46] |
| ( <i>S</i> )-Benzyl benzodiazepine      | poly(MAA-co-EDMA)         | 3.03       | n.d.    | n.d.    | [47] |

<sup>a</sup>The print molecules and their optical antipodes were separated.

<sup>b</sup>AAM denotes acrylamide; CuVBIDA, Cu(II)[*N*-(4-vinylbenzyl)]iminodiacetate; MAA, methacrylic acid; 2VPy, 2-vinylpyridine; 4VPy, 4-vinylpyridine.

<sup>c</sup>The separation factors were calculated as  $\alpha = k'_{\text{print molecule}}/k'_{\text{optical antipode}}$ ;  $k' = (t - t_0)/t_0$ ;  $t$  is the retention time of the analyte and  $t_0$  is the retention time of unretained compound (the void).

<sup>d</sup>The resolution factors ( $R_s$ ) were calculated according to G. Wulff *et al.*, *J. Liq. Chromatogr.*, **9**, 385 (1986).

<sup>e</sup>The resolution factors ( $f/g$ ) were calculated according to V.R. Meyer, *Chromatographia*, **24**, 639 (1987).

contrast to this, a timolol-imprinted polymer prepared with itaconic acid as the functional monomer instead of methacrylic acid could only resolve racemic timolol out of a number of racemates of structurally related  $\beta$ -blockers (Fig. 17.6). This clearly demonstrates that the selectivity of MIPs can be highly dependent on the functional monomer used [44].

A comparison of six different CSPs, all imprinted with the same print molecule

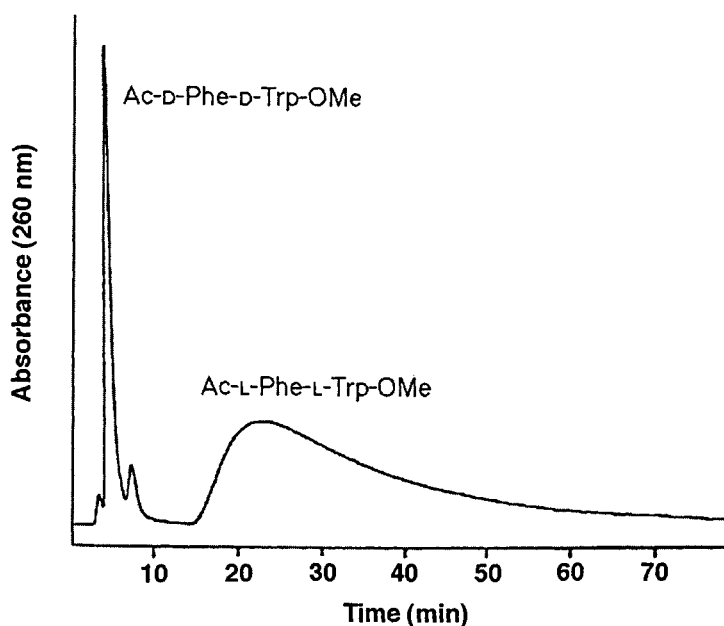


Fig. 17.5. Separation of 10  $\mu\text{g}$  of a mixture of Ac-L-Phe-L-Trp-OMe and Ac-D-Phe-D-Trp-OMe on a poly(methacrylic acid-*co*-EDMA) CSP ( $4.6 \times 200$  mm column) imprinted with Ac-L-Phe-L-Trp-OMe. Isocratic elution at 1 mL/min with  $\text{CHCl}_3$ -HOAc (99:1). Attenuation was increased 10-fold at 10 min. (Adapted from [43], with permission from Elsevier Science, UK.)

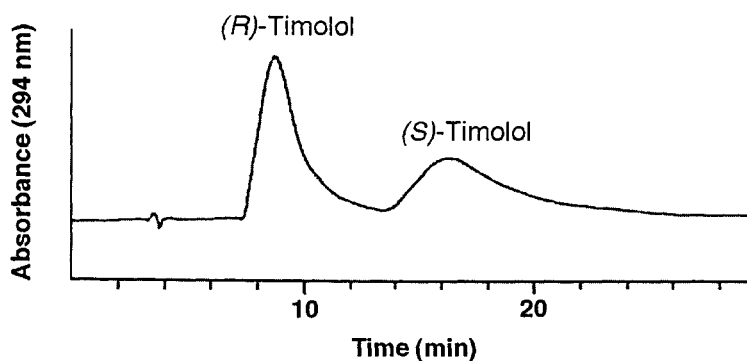


Fig. 17.6. Separation of 20  $\mu\text{g}$  of racemic timolol on a poly(itaconic acid-*co*-EDMA) CSP ( $4.6 \times 200$  mm column) imprinted with (*S*)-timolol. Isocratic elution at 1 mL/min with EtOH-THF-HOAc (5:4:1). (Adapted from [44], with permission from the American Chemical Society, USA.)



TABLE 17.2

## CHIRAL SEPARATION OF RACEMIC Z-TYR-OH ON MOLECULARLY IMPRINTED CSPs

| Polymer <sup>a</sup>      | Separated amount ( $\mu\text{g}$ ) | Column size (mm) | Eluent  | Flow (mL/min) | $\alpha^b$ | $R_s^c$ | $f/g^d$ | Ref. |
|---------------------------|------------------------------------|------------------|---|---------------|------------|---------|---------|------|
| poly(MAA-co-EDMA)         | 10                                 | $4.6 \times 250$ | 0.1% HOAc in $\text{CH}_3\text{CN}$                           | 1.0           | 1.82       | n.d.    | 0.50    | 17   |
| poly(4VPy-co-EDMA)        | 20                                 | $4.6 \times 200$ | 0.25% HOAc in THF   | 0.5           | 4.00       | 1.53    | 0.94    | 16   |
| poly(2VPy-co-EDMA)        | 10                                 | $4.6 \times 250$ | 1% HOAc in $\text{CH}_3\text{CN}$                             | 1.0           | 3.81       | 1.9     | 0.95    | 17   |
| poly(2VPy-co-EDMA)        |                                    | $4.6 \times 100$ | 75% 10mM Na phosphate buffer pH 4 in $\text{CH}_3\text{CN}$   | 0.5           | 1.70       | 2.47    | n.d.    | 50   |
| poly(MAA-co-2VPy-co-EDMA) | 10                                 | $4.6 \times 250$ | 1% HOAc in $\text{CH}_3\text{CN}$                             | 1.0           | 4.32       | 1.90    | 0.97    | 17   |
| poly(MAA-co-2VPy-co-EDMA) |                                    | $4.6 \times 100$ | 75% 10mM Na phosphate buffer pH 3.5 in $\text{CH}_3\text{CN}$ | 0.5           | 1.49       | 1.40    | n.d.    | 50   |
| poly(AAM-co-EDMA)         | 40                                 | $4.6 \times 250$ | $\text{CH}_3\text{CN}$  | 1.0           | 3.62       | 2.52    | n.d.    | 19   |
| poly(MAA-co-PETRA)        | 100                                | $4.6 \times 250$ | Gradient  | 1.0           | 2.86       | 5.47    | 1.00    | 20   |
| poly(MAA-co-PETRA)        | 1000                               | $4.6 \times 250$ | 1% HOAc in $\text{CHCl}_3$                                    | 1.0           | 2.06       | n.d.    | 0.93    | 20   |

<sup>a</sup>AAM denotes acrylamide; MAA, methacrylic acid; 2VPy, 2-vinylpyridine; 4VPy, 4-vinylpyridine.

<sup>b</sup>The separation factors were calculated as  $\alpha = k'_L/k'_D$ ;  $k' = (t - t_0)/t_0$ ;  $t$  is the retention time of the analyte and  $t_0$  is the retention time of unretained compound (the void).

<sup>c</sup>The resolution factors ( $R_s$ ) were calculated according to G. Wulff *et al.*, *J. Liq. Chromatogr.*, **9**, 385 (1986).

<sup>d</sup>The resolution factors ( $f/g$ ) were calculated according to V.R. Meyer, *Chromatographia*, **24**, 639 (1987).

(Z-L-tyrosine), confirms that the choice of monomers is important for the selectivity of the resulting polymers (Table 17.2). The selectivity of EDMA-based polymers was higher when vinylpyridines were used, either alone or together with methacrylic acid, than when methacrylic acid was used alone [16,17]. Methacrylic acid interacts with the print molecule through hydrogen bonds. The beneficial effect of vinylpyridine is attributed to strong ionic interactions between the carboxy groups of the print molecule and the pyridinyl groups. The enantioselectivity decreased when applying aqueous solvent mixtures instead of organic solvents as the eluents [50]. The selectivity was lost completely for polymers made from methacrylic acid as the sole functional monomer, while the decrease was less pronounced for polymers made from vinylpyridine.

A polymer prepared with acrylamide also showed a higher selectivity than the one prepared with methacrylic acid [19]. This was attributed to the formation of stronger hydrogen bonds of the amide groups (originating from acrylamide) than of the carboxyl groups (originating from methacrylic acid).

It is noteworthy that the load capacity and the resolving capability increased when the tri-functional cross-linker PETRA was used instead of EDMA [20]. The same features have been seen with polymers prepared from TRIM, another trifunctional cross-linker. Poly(methacrylic acid-*co*-TRIM) imprinted with a dipeptide was able to resolve 1 mg of the racemate with almost base-line separation (analytical column:  $4.6 \times 250$  mm) (Fig. 17.7).

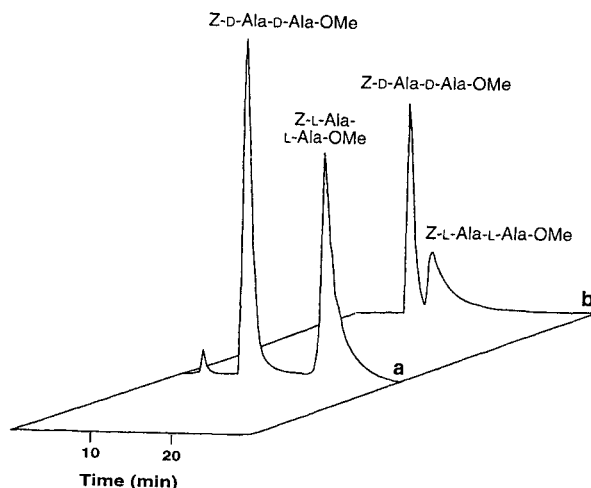
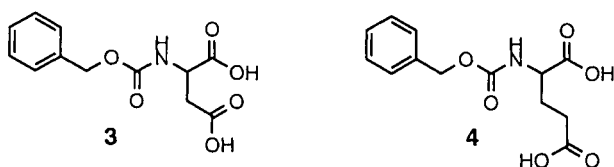


Fig. 17.7. Separation of mixtures of Z-L-Ala-L-Ala-OMe and Z-D-Ala-D-Ala-OMe on a poly(methacrylic acid-*co*-TRIM) CSP ( $4.6 \times 250$  mm column) imprinted with Z-L-Ala-L-Ala-OMe. (a)  $100 \mu\text{g}$  were applied. Gradient elution at 1 mL/min with  $\text{CHCl}_3$ -HOAc (99.75:0.25) and  $\text{CHCl}_3$ -HOAc (4:1) (= B). Gradient: 0–10 min, 0% B; 10–18 min, 0–5% B; 18–22 min, 5% B; 22–24 min 5–0% B. Detection at 260 nm. (b) 1 mg was applied. Isocratic elution at 1 mL/min with  $\text{CHCl}_3$ -HOAc (99.75:0.25). Detection at 260 nm. (Adapted from [20], with permission from the American Chemical Society, USA.)

In some cases, MIPs discriminate effectively between structurally related molecules. An example of this can be seen with poly(4-vinylpyridine-*co*-EDMA) imprinted with Z-L-aspartic acid (**3**) [16]. The chromatogram in Fig. 17.8a shows the resolution of racemic Z-aspartic acid on this CSP. Aspartic acid and glutamic acid differ by only one methylene unit, but despite this small difference, the Z-aspartic acid-imprinted CSP was unable to resolve racemic Z-glutamic acid (**4**) (Fig. 17.8b). The side-chain of Z-L-glutamic acid cannot be accommodated into the recognition site in a way that allows specific interaction between the carboxy functionality and the positioned pyridine group of the polymer. The same type of polymer, imprinted with Z-L-glutamic acid, was able to resolve racemic Z-glutamic acid, but not racemic Z-aspartic acid [16]. Similar observations have been seen with poly(methacrylic acid-*co*-EDMA) imprinted with these print molecules [15].



In other cases, the recognition sites accept structurally related molecules. Polymers imprinted with Z-L-phenylalanine (**5a**) were able to resolve racemic Z-phenylalanine efficiently (Table 17.3). Racemic Z-alanine (**5b**) could also be resolved on these CSPs, although lower separation factors were observed. When the amino group of the racemate was protected with Boc (*tert*-butoxycarbonyl)

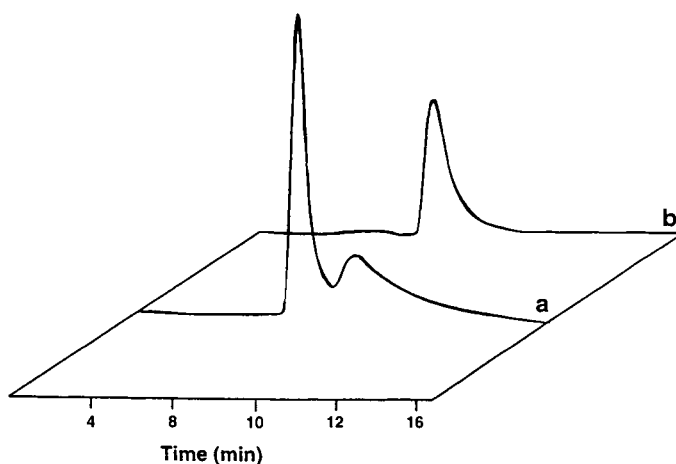
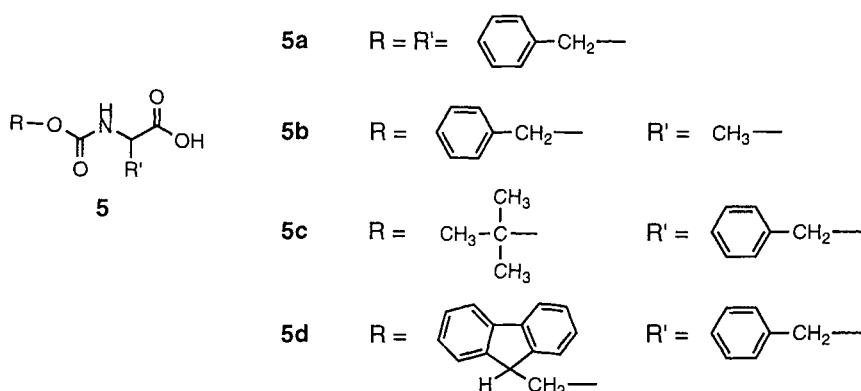


Fig. 17.8. Poly(4-vinylpyridine-*co*-EDMA) CSP ( $4.6 \times 200$  mm column) imprinted with Z-L-aspartic acid. (a)  $20 \mu\text{g}$  of racemic Z-aspartic acid were applied. Isocratic elution at  $0.5 \text{ mL/min}$  with THF–HOAc (24:1) and detection at  $260 \text{ nm}$ . (b)  $20 \mu\text{g}$  of racemic Z-glutamic acid were applied. Isocratic elution at  $0.5 \text{ mL/min}$  with THF–HOAc (199:1) and detection at  $260 \text{ nm}$ . (Adapted from [16], with permission from John Wiley & Sons, UK.)



(**5c**) or Fmoc (9-fluorenylmethyloxycarbonyl) (**5d**) the separations were poorer than with the racemate of the print molecule, which was protected with Z (benzyloxycarbonyl). In contrast to the CSPs described above, which were unable to resolve the racemate of a molecule which only differed from the print molecule by one methylene unit, these polymers were able to resolve all of the tested structurally related racemates, even if the separations were not as good as with the print molecule and its optical antipode. This shows that the polymer recognises both the amino-protecting group and the side-chain, but that some cross-reactivity exists and that an exact fit is not necessary for enantioseparation in these cases [36]. Similar effects were recently seen with polymers imprinted with dansylated amino acids [51]. Cross-reactivity of MIPs imprinted with *N*-protected amino acids has also been studied batch-wise [52].

TABLE 17.3

SEPARATION OF RACEMIC AMINO ACID DERIVATIVES ON Z-L-PHE-OH-IMPRINTED CSPs

| Racemate    | $\alpha$                           |                                    |
|-------------|------------------------------------|------------------------------------|
|             | poly(MAA-co-EDMA) <sup>a,b,c</sup> | poly(MAA-co-TRIM) <sup>a,b,d</sup> |
| Z-Phe-OH    | 1.84                               | 2.49                               |
| Boc-Phe-OH  | 1.31                               | 1.78                               |
| Fmoc-Phe-OH | 1.21                               | 1.66                               |
| Z-Ala-OH    | 1.28                               | 1.59                               |

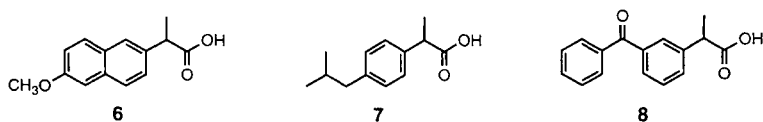
<sup>a</sup>MAA, methacrylic acid.

<sup>b</sup>The separation factors were calculated as  $\alpha = k'_L/k'_D$ ;  $k' = (t-t_0)/t_0$ ;  $t$  is the retention time of the analyte and  $t_0$  is the retention time of unretained compound (the void).

<sup>c</sup>Data from [36]. Isocratic elutions at 0.5 mL/min with chloroform. Column size: 4.5 × 100 mm.

<sup>d</sup>Data from [20]. Isocratic elutions at 1 mL/min with 0.1% HOAc in chloroform. Column size: 4.6 × 100 mm.

(*S*)-Naproxen (**6**), a non-steroidal anti-inflammatory drug, has been imprinted in poly(4-vinylpyridine-*co*-EDMA) by two different approaches. Bulk polymerisation followed by grinding and sieving of the monolith resulted in highly irregular particles [45] and a two-step swelling and polymerisation method gave uniformly sized beads [28]. Both materials, used in the chromatographic mode, were able to separate naproxen from the related molecules ibuprofen (**7**) and ketoprofen (**8**).



The polymers were also able to resolve racemic naproxen, but not the racemates of ibuprofen and ketoprofen (Fig. 17.9). Even though direct comparisons of the two chromatograms cannot be done because of differing flow rates, it is not obvious that the chromatographic efficiency was better with the uniformly sized beads (Fig. 17.9b) than with the irregular particles (Fig. 17.9a). This may be due to the detrimental influence of water on the stability of the monomer–print molecule complex

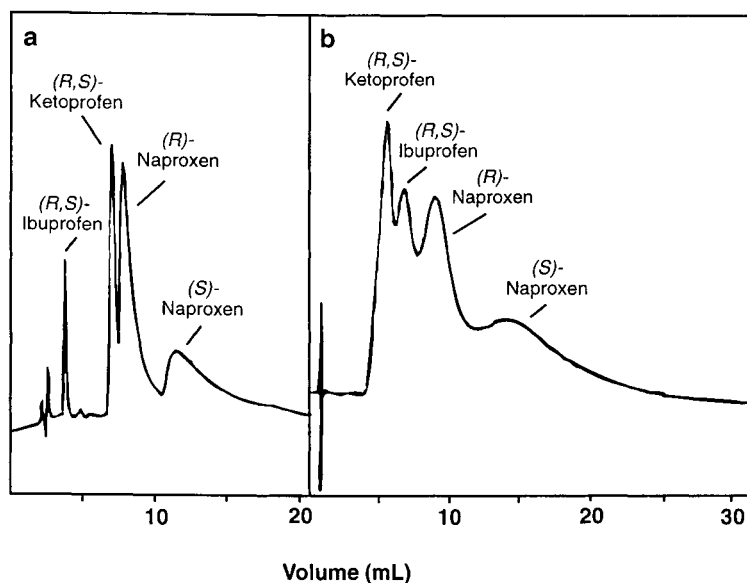


Fig. 17.9. Separation of racemic mixtures of naproxen, ibuprofen, and ketoprofen on poly(4-vinylpyridine-*co*-EDMA) CSPs (4.6 × 100 mm columns) imprinted with (*S*)-naproxen. (a) The column was packed with particles prepared by grinding and sieving a bulk polymer. Isocratic elution at 0.1 mL/min with THF–heptane–HOAc (250:250:1) and detection at 260 nm. (Adapted from [45], with permission from Elsevier Science, UK.) (b) The column was packed with beads prepared by a two-step swelling and polymerisation method. Isocratic elution at 1.0 mL/min with CH<sub>3</sub>CN–phosphate buffer (20 mM, pH 4.0) (1:1) and detection at 254 nm. (Adapted from [28], with permission from the Chemical Society of Japan.)

during the self-assembly and polymerisation, since water was used as the suspension medium in the two-step swelling and polymerisation method.

Uniformly sized beads prepared by the two-step swelling and polymerisation method have recently been modified with an external hydrophilic layer to allow direct serum injection assays of naproxen [53].

In general, the polymerisations of non-covalent MIPs, relying on hydrogen bonds and electrostatic interactions, are preferably done in non-aqueous solutions to prevent water molecules from interfering with the interactions between the monomers and the templates, as previously discussed. Several reports, however, show that chromatography can be performed efficiently with buffered aqueous eluents. For example, the column efficiency of a MIP imprinted against L-phenylalanine anilide improved when buffer-organic solvent mixtures were used instead of organic solvents containing acetic acid as the modifier [49]. In a study using acrylamide as the functional monomer, the selectivity and the resolving capability increased when the water content of the eluent increased (Fig. 17.10) [54].

Arnold and co-workers have developed an approach that allows both the imprinting and the subsequent chiral separation of free amino acids to be carried out in aqueous solutions [39]. The recognition was based on metal coordination-chelation interactions using *N*-(4-vinylbenzyl)iminodiacetic acid as the functional monomer. (For a further discussion of this system see Chapters 6 and 9.) The method worked best for aromatic amino acids (Fig. 17.11).

In most studies of chiral MIPs, non-chiral monomers were used together with optically active templates. By using a chiral functional monomer, Hosoya and co-

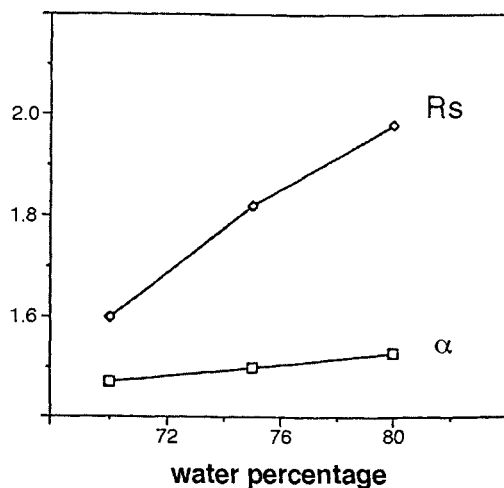


Fig. 17.10. Effect of the water content of the mobile phase on the separation factor ( $\alpha$ ) and the resolution factor ( $R_s$ ). 10  $\mu$ g of racemic Boc-L-Tyr-OH were injected on a poly(acrylamide-co-EDMA) CSP (4.6  $\times$  250 mm column) imprinted with Boc-L-Tyr-OH. Isocratic elution at 1.0 mL/min with 10 mM glycine in water-acetonitrile. (Adapted from [54], with permission from Marcel Dekker, USA.)

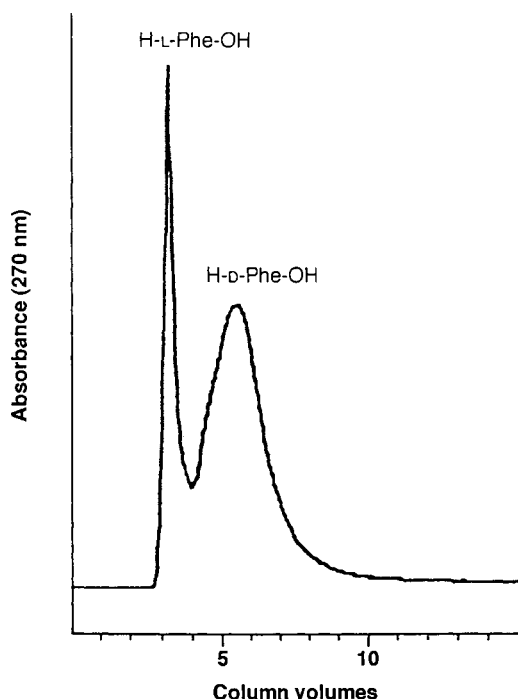


Fig. 17.11. Separation of 17  $\mu\text{g}$  of racemic phenylalanine on poly(Cu(II)[*N*-(4-vinylbenzyl)]iminodiacetate-*co*-EDMA) grafted to silica particles ( $4.6 \times 50$  mm column). The polymer was imprinted with D-phenylalanine. Isocratic elution at 1 mL/min, 50°C with 1.5 mM glycine in water. (Adapted from [39], with permission from Elsevier Science, UK.)

workers succeeded in preparing a molecularly imprinted CSP with a racemic template, *N*-(3,5-dinitrobenzoyl)- $\alpha$ -methylbenzylamine [55]. The CSP was then used to resolve the template (Fig. 17.12). Another chiral monomer, a polymerisable L-valine derivative, was used by Karube and co-workers to prepare MIPs for the separation of dipeptide diastereomers. The inherent diastereoselectivity of the polymer was enhanced by the imprinting procedure [56]. In another study, optically active sugar acrylates were used to prepare polymers capable of separating Z-aspartic acid [57].

### 17.3.2 TLC

MIPs selective for phenylalanine anilide have been evaluated as stationary phases in TLC [58]. Glass backing plates were coated with mixtures of finely ground MIP particles and binders. The plates showed a preferential retardation of the enantiomer used as the print molecule (Fig. 17.13). The  $R_f$  values of both enantiomers on non-imprinted polymers were higher than those observed on the

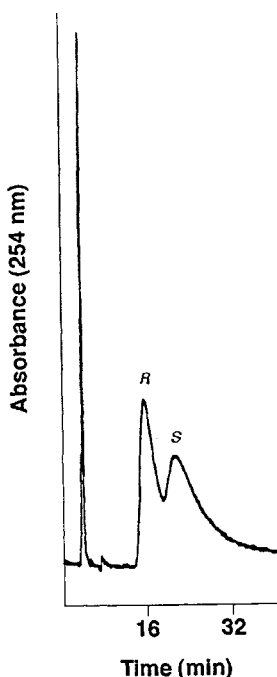


Fig. 17.12. Separation of 3.2 nmol of racemic *N*-(3,5-dinitrobenzoyl)- $\alpha$ -methylbenzylamine on poly((*S*)-(-)-methacryloyl-1-naphthylethylamine-*co*-EDMA) prepared by a two-step swelling and polymerisation method using racemic *N*-(3,5-dinitrobenzoyl)- $\alpha$ -methylbenzylamine as template. Isocratic elution at 1 mL/min with hexane–ethyl acetate (1:1). (Adapted from [55], with permission from the American Chemical Society, USA.)

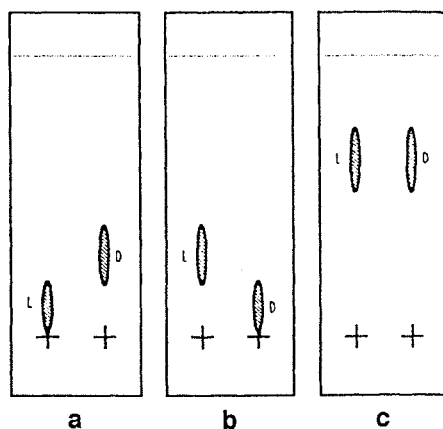


Fig. 17.13. Separation of L- and D-phenylalanine anilide on TLC plates covered with poly(methacrylic acid-*co*-EDMA) imprinted with (a) L-phenylalanine anilide, (b) D-phenylalanine anilide and (c) no print molecule. Elution with  $\text{CH}_3\text{CN}$ –HOAc (99:5). (Adapted from [58], with permission from the American Chemical Society, USA.)



imprinted polymers. The separations suffered from spot broadening, which was attributed to the heterogeneity of the recognition sites. TLC plates have also been prepared with MIPs imprinted with adrenergic drugs [59,60]. It was noted that the spot shape was improved when using eluents containing acetic acid. The MIP TLC technique is attractive because it is simple, fast and allows multiple analyses in the same run.

### 17.3.3 CE and CEC

Chiral separations by CE and CEC are achieved using a chiral selector which is either free in the mobile phase or immobilised to the stationary phase. MIPs can be used as the selector in both approaches. Molecularly imprinted capillary columns

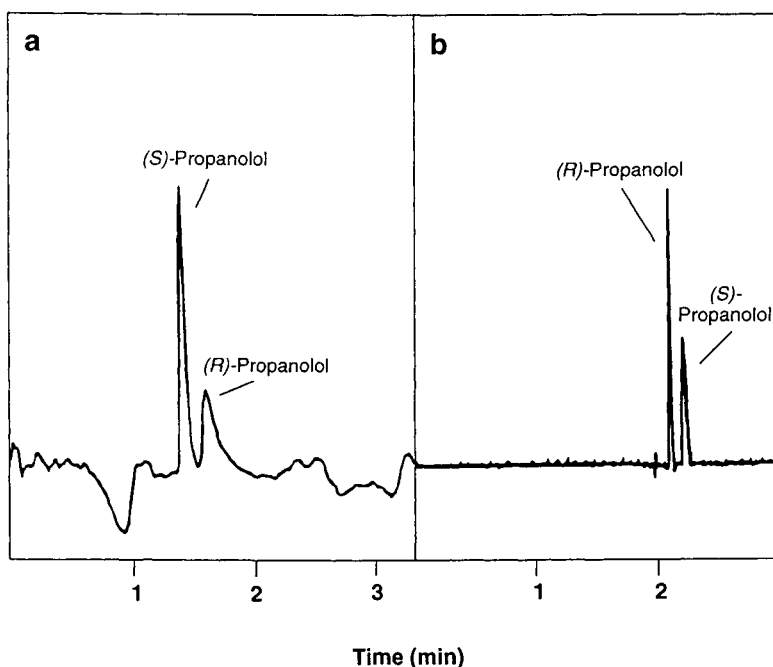


Fig. 17.14. (a) CEC. Separation of racemic propranolol on a poly(methacrylic acid-co-TRIM) CSP ( $75\ \mu\text{m} \times 350\ \text{mm}$  capillary column) imprinted with (*R*)-propranolol. The sample was injected electrokinetically (5 kV, 3 s) and was separated at a constant voltage of 30 kV. The electrolyte was  $\text{CH}_3\text{CN}$ -acetate buffer (4 M, pH 3.0) (8:2). Detection at 214 nm. The capillary was thermostatted to  $60^\circ\text{C}$  and an overpressure of 7 bar was applied. (Adapted from [61], with permission from the American Chemical Society, USA.) (b) CE. Separation of racemic propranolol using 0.05% (w/v) *poly*(*N*-acryloylalanine-co-EDMA) particles imprinted with (*S*)-propranolol as a chiral additive in the background electrolyte ( $100\ \mu\text{m} \times 470\ \text{mm}$  capillary column). The sample was injected by a 3 s pressure injection and was separated at a constant voltage of 15 kV. The electrolyte was 5 mM phosphate buffer, pH 7.0. Detection at 210 nm. Temperature:  $25^\circ\text{C}$ . (Adapted from [62], with permission from the Royal Society of Chemistry, UK.)

have been prepared by various approaches: (i) packing preformed MIP particles into the capillaries; (ii) dispersion polymerisation *in situ* in the capillaries; (iii) incorporating preformed MIP particles into poly(acrylamide) gels; (iv) *in situ* polymerisation on the inner walls of the capillaries; (v) filling the capillaries with a monolithic polymer with continuous pores by *in situ* polymerisation; and (vi) entrapment of MIP particles in silica.

Figure 17.14a shows the separation of racemic propranolol by CEC on a capillary column filled with poly(methacrylic acid-*co*-TRIM), polymerised *in situ* using (*R*)-propranolol as the print molecule [61]. Several attractive features make this system look promising for the future: very low consumption of the print molecule (in this case only 10  $\mu\text{g}$ ), fast preparation of the capillaries (3 h) and fast separation (less than 2 min). In Fig. 17.14b, MIP particles selective for (*S*)-propranolol were added to the mobile phase in a CE separation [62]. The application of MIPs in CE and CEC is described in more detailed in Chapter 16.

### 17.3.4 Other methods

Chiral separation using MIPs can also be achieved by bubble fractionation [63] and with MIP membranes [64–68]. MIP particles selective for an amino acid derivative were used as collectors for enantiomeric enrichment by bubble fractionation. The method is envisaged to be a potentially powerful approach to process-scale separations [63].

## 17.4 CONCLUSIONS

Molecular imprinting is a technique with great potential. MIPs have found many applications and many more are likely to be developed. One of the first applications investigated was their use as CSPs, the subject of this chapter. A number of polymer systems has been developed and these have been used for the imprinting of different classes of chiral compounds.

One of the advantages of MIP CSPs, in comparison with other CSPs, is that the material is designed directly for a specific molecule or class of molecules and that the elution order of the enantiomers is therefore known.

To be able to attribute the binding of an MIP to an imprinting effect it is of utmost importance to show that specific recognition sites have been formed due to the presence of the print molecules during the polymerisation. This is usually done by comparisons with appropriate reference polymers. Polymers prepared without print molecules are not always the best choice, since the physical properties (surface area, porosity, etc.) of these polymers often differ from those of imprinted polymers. Reference polymers prepared with the optical antipode or a racemic mixture as the print species are preferred. The selectivity will be reversed when using the optical antipode and a racemic mixture will give a polymer incapable of separating the two enantiomers (unless the monomer(s) is/are chiral).

The goal of any endeavour involving chromatographic separations is to achieve

the best possible performance with respect to selectivity, resolution, load capacity and analysis time. Many research efforts on MIPs have therefore focused on improving the chromatographic performance. The use of monodisperse spherical beads instead of irregular particles improves the efficiency, and investigations in this direction with MIPs have already given promising results. Another issue that needs to be further investigated is the heterogeneity of the binding sites. A more homogeneous population of sites would improve the chromatographic performance. The load capacity of MIPs has been improved by the use of trifunctional cross-linkers such as TRIM and PETRA instead of the bifunctional EDMA. These findings look promising for the future development of MIPs for semi-preparative and preparative purifications.

## REFERENCES

- 1 D.E. Drayer, In: *Drug stereochemistry. Analytical methods and pharmacology*, I.W. Wainer and D.E. Drayer Eds, Marcel Dekker, New York, p. 209 (1988).
- 2 W.E. Müller, In: *Drug stereochemistry. Analytical methods and pharmacology*, I.W. Wainer and D.E. Drayer Eds, Marcel Dekker, New York, p. 227 (1988).
- 3 J.R. Powell, J.J. Ambre and T.I. Ruo, In: *Drug stereochemistry. Analytical methods and pharmacology*, I.W. Wainer and D.E. Drayer Eds, Marcel Dekker, New York, p. 245 (1988).
- 4 E. Francotte and A. Junker-Buchheit, *J. Chromatogr., Biomed. Appl.*, **576**, 1 (1992).
- 5 M.R. Wright and F. Jamali, *J. Pharmacol. Toxicol. Meth.*, **29**, 1 (1993).
- 6 H.Y. Aboul-Enein, *Anal. Lett.*, **25**, 231 (1992).
- 7 F. Bressolle, M. Audran, T.-N. Pham and J.-J. Vallon, *J. Chromatogr. B*, **687**, 303 (1996).
- 8 S.G. Allenmark and S. Andersson, *J. Chromatogr. A*, **666**, 167 (1994).
- 9 G. Blaschke, *J. Liq. Chromatogr.*, **9**, 341 (1986).
- 10 W.H. Pirkle and J.E. McCune, *J. Chromatogr.*, **471**, 271 (1989).
- 11 G. Wulff, In: *Polymeric reagents and catalysts*, ACS Symp. Series, 308, W.T. Ford Ed., American Chemical Society, Washington DC, p. 186 (1986), and references therein.
- 12 G. Wulff, *Angew. Chem. Int. Ed. Engl.*, **34**, 1812 (1995), and references therein.
- 13 B. Sellergren, M. Lepistö and K. Mosbach, *J. Am. Chem. Soc.*, **110**, 5853 (1988).
- 14 D.J. O'Shannessy, L.I. Andersson and K. Mosbach, *J. Mol. Recogn.*, **2**, 1 (1989).
- 15 L.I. Andersson and K. Mosbach, *J. Chromatogr.*, **516**, 313 (1990).
- 16 M. Kempe, L. Fischer and K. Mosbach, *J. Mol. Recogn.*, **6**, 25 (1993).
- 17 O. Ramström, L.I. Andersson and K. Mosbach, *J. Org. Chem.*, **58**, 7562 (1993).
- 18 J. Matsui, O. Doblhoff-Dier and T. Takeuchi, *Anal. Chim. Acta*, **343**, 1 (1997).
- 19 C. Yu and K. Mosbach, *J. Org. Chem.*, **62**, 4057 (1997).
- 20 M. Kempe, *Anal. Chem.*, **68**, 1948 (1996).
- 21 B. Sellergren and K.J. Shea, *J. Chromatogr.*, **635**, 31 (1993).
- 22 D.J. O'Shannessy, B. Ekberg and K. Mosbach, *Anal. Biochem.*, **177**, 144 (1989).
- 23 M. Glad, P. Reinholdsson and K. Mosbach, *React. Polym.*, **25**, 47 (1995).
- 24 P.K. Dhal, S. Vidyasankar and F.H. Arnold, *Chem. Mater.*, **7**, 154 (1995).
- 25 S.D. Plunkett and F.H. Arnold, *J. Chromatogr. A*, **708**, 19 (1995).
- 26 J. Matsui, T. Kato, T. Takeuchi, M. Suzuki, K. Yokoyama, E. Tamiya and I. Karube, *Anal. Chem.*, **65**, 2223 (1993).
- 27 B. Sellergren, *J. Chromatogr. A*, **673**, 133 (1994).
- 28 J. Haginaka, H. Takehira, K. Hosoya and N. Tanaka, *Chem. Lett.*, 555 (1997).
- 29 A.G. Mayes and K. Mosbach, *Anal. Chem.*, **68**, 3769 (1996).

- 30 L. Andersson, B. Sellergren and K. Mosbach, *Tetrahedron Lett.*, **25**, 5211 (1984).
- 31 B. Sellergren, B. Ekberg and K. Mosbach, *J. Chromatogr.*, **347**, 1 (1985).
- 32 B. Sellergren, *Chirality*, **1**, 63 (1989).
- 33 M. Lepistö and B. Sellergren, *J. Org. Chem.*, **54**, 6010 (1989).
- 34 D.J. O'Shannessy, B. Ekberg, L.I. Andersson and K. Mosbach, *J. Chromatogr.*, **470**, 391 (1989).
- 35 M. Kempe and K. Mosbach, *Anal. Lett.*, **24**, 1137 (1991).
- 36 M. Kempe and K. Mosbach, *Int. J. Peptide Protein Res.*, **44**, 603 (1994).
- 37 M. Kempe and K. Mosbach, *J. Chromatogr. A*, **691**, 317 (1995).
- 38 M. Kempe and K. Mosbach, *J. Chromatogr. A*, **694**, 3 (1995).
- 39 S. Vidyasankar, M. Ru and F.H. Arnold, *J. Chromatogr. A*, **775**, 51 (1997).
- 40 B. Sellergren and K.J. Shea, *J. Chromatogr. A*, **654**, 17 (1993).
- 41 B. Sellergren and K. Nilsson, *Meth. Mol. Cell. Biol.*, **1**, 59 (1989).
- 42 L.I. Andersson, D.J. O'Shannessy and K. Mosbach, *J. Chromatogr.*, **513**, 167 (1990).
- 43 O. Ramström, I.A. Nicholls and K. Mosbach, *Tetrahedron: Asymmetry*, **5**, 649 (1994).
- 44 L. Fischer, R. Müller, B. Ekberg and K. Mosbach, *J. Am. Chem. Soc.*, **113**, 9358 (1991).
- 45 M. Kempe and K. Mosbach, *J. Chromatogr. A*, **664**, 276 (1994).
- 46 O. Ramström, C. Yu and K. Mosbach, *J. Mol. Recogn.*, **9**, 691 (1996).
- 47 B.R. Hart, D.J. Rush and K.J. Shea, *J. Am. Chem. Soc.*, **122**, 460 (2000).
- 48 L.I. Andersson, R. Müller, G. Vlatakis and K. Mosbach, *Proc. Natl. Acad. Sci. USA*, **92**, 4788 (1995).
- 49 B. Sellergren and K.J. Shea, *J. Chromatogr. A*, **690**, 29 (1995).
- 50 O. Ramström, L. Ye and P.-E. Gustavsson, *Chromatographia*, **48**, 197 (1998).
- 51 T.P. O'Brien, N.H. Snow, N. Grinberg and L. Crocker, *J. Liq. Chromatogr. Rel. Technol.*, **22**, 183 (1999).
- 52 C.J. Allender, K.R. Brain and C.M. Heard, *Chirality*, **9**, 233 (1997).
- 53 J. Haginaka, H. Takehira, K. Hosoya and N. Tanaka, *J. Chromatogr. A*, **849**, 331 (1999).
- 54 C. Yu, O. Ramström and K. Mosbach, *Anal. Lett.*, **30**, 2123 (1997).
- 55 K. Hosoya, Y. Shirasu, K. Kimata and N. Tanaka, *Anal. Chem.*, **70**, 943 (1998).
- 56 K. Yano, T. Nakagiri, T. Takeuchi, J. Matsui, K. Ikebukuro and I. Karube, *Anal. Chim. Acta*, **357**, 91 (1997).
- 57 X.-C. Liu and J.S. Dordrick, *J. Polym. Sci. A: Polym. Chem.*, **37**, 1665 (1999).
- 58 D. Kriz, C. Berggren Kriz, L.I. Andersson and K. Mosbach, *Anal. Chem.*, **66**, 2636 (1994).
- 59 R. Suedee, C. Songkram, A. Petmoreekul, S. Sangkunakup, S. Sankasa and N. Kongyari, *J. Pharm. Biomed. Anal.*, **19**, 519 (1999).
- 60 R. Suedee, T. Srichana, J. Saelim and T. Thavornpibulbut, *Analyst*, **124**, 1003 (1999).
- 61 L. Schweitz, L.I. Andersson and S. Nilsson, *Anal. Chem.*, **69**, 1179 (1997).
- 62 M. Walshe, E. Garcia, J. Howarth, M.R. Smyth and M.T. Kelly, *Anal. Commun.*, **34**, 119 (1997).
- 63 D.W. Armstrong, J.M. Schneiderheinze, Y.-S. Hwang and B. Sellergren, *Anal. Chem.*, **70**, 3717 (1998).
- 64 M. Yoshikawa, J. Izumi and T. Kitao, *Polym. J.*, **29**, 205 (1997).
- 65 M. Yoshikawa, J. Izumi, T. Kitao and S. Sakamoto, *Macromol. Rapid Commun.*, **18**, 761 (1997).
- 66 M. Yoshikawa, T. Fujisawa, J. Izumi, T. Kitao and S. Sakamoto, *Anal. Chim. Acta*, **365**, 59 (1998).
- 67 M. Yoshikawa, J. Izumi, T. Ooi, T. Kitao, M.D. Guiver and G.P. Robertson, *Polym. Bull.*, **40**, 517 (1998).
- 68 M. Yoshikawa, T. Fujisawa and J. Izumi, *Macromol. Chem. Phys.*, **200**, 1458 (1999).

This Page Intentionally Left Blank

## **Biomimetic electrochemical sensors based on molecular imprinting**

DARIO KRIZ AND RICHARD J. ANSELL

### **18.1 INTRODUCTION**

The explosive growth of interest in molecular imprinting in general during the last five years has also been apparent in the area of imprinted materials for chemical sensors. Whilst any estimate of the actual number of publications is approximate and subjective, we estimate that there were 15 publications specifically addressing sensors or sensing systems using molecularly imprinted material (MIM) sensors up until 1993, then 20 between 1994 and 1997 and 14 in 1998 alone. The combination of specific molecular recognition capabilities with stability and robustness are obviously especially attractive to those working in the sensor field. Additionally, workers in this multidisciplinary field may be comparatively open to adopting new technologies. The last few years have also produced several reviews dealing partly or wholly with the applications of MIMs in sensors [1–5].

A great diversity of approaches has been followed to develop MIM sensors. We have found it helpful to apply three complementary classifications to these approaches: (i) the nature of the transducer employed in the sensor; (ii) the nature of the MIM; (iii) what is measured: a property of the analyte (the MIM serving simply to concentrate the analyte near the transducer), a property of the MIM which changes upon interaction with the analyte, or a second messenger, whose concentration is dependent on the analyte interacting with the MIM. It is often difficult to assign a material as molecularly imprinted or not. Thus, we use the expression MIM here to refer to materials which are designed to rebind the template used in their preparation and refer to other materials where the template and the subsequent analyte differ as templated materials.

We will first provide an overview of the different transducers and recognition elements employed in chemical sensors and biosensors, then consider how these have been combined with different MIMs.

### **18.2 CHEMICAL SENSOR TECHNOLOGY**

#### **18.2.1 Chemical sensors**

Sensors are designed to provide quantitative information about our environment or inner state in real time. The demand for such devices to measure the levels of

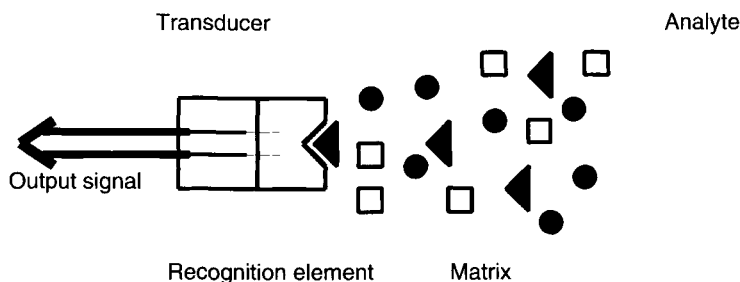


Fig. 18.1. The principle of a chemical sensor.

ever more chemical compounds at ever lower concentrations, in industry, medicine and agriculture, now fuels a vast research industry. A chemical sensor selectively recognises a target analyte molecule in a complex matrix and gives an output signal which correlates with the concentration of the analyte. It consists of a recognition element and a transducer in close contact to each other (Fig. 18.1). The recognition element is responsible for the selective binding of the analyte in a matrix containing both related and non-related compounds. Upon binding, the transducer is responsible for the translation of this chemical event into a quantifiable output signal. A huge variety of approaches has been reported [6,7].

The main parameters describing the performance of a sensor are: *selectivity*, *sensitivity*, *stability* and *reusability* and *response time*. Application areas include: *research*, *medicine* (clinical and home diagnostics, physician's office testing, surgical *in vivo* monitoring), *industry* (fermentation monitoring, food and drug processing and water and waste monitoring), *environmental monitoring* (detection of toxic chemicals in air, water and soil, measurements of biological oxygen demand), *agriculture* (diagnosis of plant and animal diseases, agricultural chemical monitoring, quality control of meat and plant products), *the military* (detection of chemical and biological agents including explosives, nerve gases and biological toxins).

## 18.2.2 The transducer

When the analyte interacts with the recognition element of a sensor, there is a change in one or more physicochemical parameters associated with the interaction. The transducer converts these parameters into an electrical output signal that can be amplified, processed and displayed in a suitable form.

### 18.2.2.1 Electrochemical transducers

Electrochemical transducers are classified as amperometric, potentiometric or conductometric [8]. In addition we will here consider field-effect transistor-based transducers separately. Potentiometric sensors make use of the development of an electrical potential at the surface of an electrode when it is placed in a solution containing ions that can exchange with the surface. The potential of the electrode is

measured under zero-current conditions against a reference electrode and is proportional to the logarithm of the analyte activity in the sample. Among these sensors are the ion-selective electrodes (ISEs) [9], perhaps the most commercially successful chemical sensors. Classical (symmetrical) ISEs are based on an ion-selective membrane that separates the sample from an inner electrolyte. Coated wire electrodes (CWEs) are ISEs in which the membrane is attached directly to the wire electrode [10]. Severinghaus-type electrodes are based on the diffusion of a gas through a gas-permeable membrane into an inner electrolyte compartment where it dissociates producing ions that are measured by an ISE [11]. In solid-state electrolyte potentiometric gas sensors the potential is measured across a solid electrolyte with one surface contacting the sample [12]. Potentiometric sensors are limited to the measurement of charged species or of gases that dissociate to give charged species in a liquid or solid electrolyte.

In amperometric sensors the current flowing between two electrodes, the working and counter electrodes, is measured as a function of the applied potential. A reference electrode is usually incorporated. Like potentiometric sensors, they require a conducting electrolyte. A current peak is measured due to the transfer of electrons to or from a species; the analyte if it is redox active, a second messenger formed by a catalyst acting on the analyte or a host which changes its redox properties in response to the analyte (e.g. the doping–undoping current of a conducting polymer). To increase selectivity the working electrode is coated with a selective layer and is termed a chemically modified electrode (CME) [13]. This layer selectively accumulates the analyte and/or rejects interferents and/or includes a redox-active host or electrocatalyst. The electrode itself is usually made of gold, carbon or a carbon paste incorporating the selective layer [14] (which can be deposited by screen-printing). The most popular amperometric method for chemical sensing is cyclic voltammetry, which provides additional selectivity, since every redox-active species has its own characteristic standard oxidation and reduction potentials and thus simultaneously present species give different oxidation and different reduction peaks. Amperometric gas sensors are either based on solid-state electrolytes [15] or comprise electrodes in a solvent electrolyte separated from the sample by a gas-permeable membrane (such as the Clark oxygen electrode [16]).

Conductometric sensors measure the change in conductivity of a selective layer, in contact with two electrodes, due to its interaction with the analyte. Thus, they function best in matrices which are themselves non-conducting, i.e. gases or non-conducting liquids. This diverse group includes chemiresistors, in which the selective layer is typically a conducting polymer [17], semiconducting oxide gas sensors, where the layer is the metal oxide surface [18], and conductometric gas-membrane sensors [19], all of which usually measure DC resistance. Dielectrometers measure the change in capacitance or dielectric constant of the selective layer [20] using an AC source. Conductometric semiconducting oxide gas sensors depend on the exchange of electrons between the oxide surface and adsorbed oxygen or hydrogen. The measurement of other gases often depends on oxygen or hydrogen produced in their catalytic breakdown. Other elements are included in the oxide as selective catalysts. While their selectivity is often limited, semiconducting oxide gas sensors



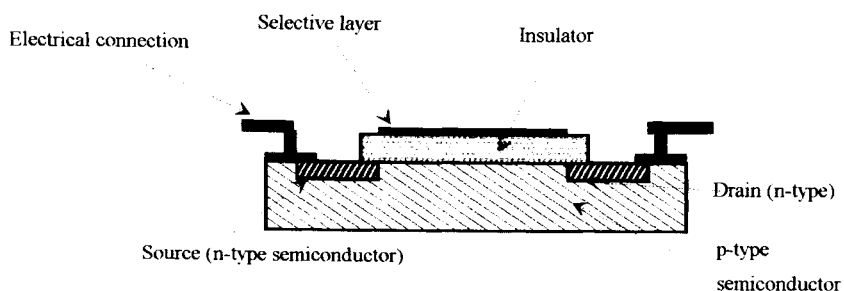


Fig. 18.2. Schematic of a simplified CHEMFET.

are of great commercial interest as they can be produced reproducibly, inexpensively and in chips integrated with their electronics *via* standard semiconductor processing techniques.

Chemically sensitive field effect transistors (CHEMFETs) are based on the change in resistance between the source and drain of a field-effect transistor due to the potential across the gate, which comprises a p-type semiconductor, an insulator and a selective layer (Fig. 18.2). Like semiconducting oxide gas sensors they may be produced *via* standard semiconductor processing techniques, but additional selectivity can be introduced *via* the selective layer. These devices include pH-sensitive ion-selective field effect transistors (pH-ISFETs [21], where there is no layer but protons interact directly with the insulator surface), membrane ISFETs [22] (where the selective layer comprises an ion-exchange polymer or plasticised hydrogel incorporating an ionophore as in membrane ISEs), enzyme field effect transistors [23] (where the selective layer incorporates an enzyme, for instance urease, which produces protons in response to urea) and gas-sensitive FETs [24], including work-function-based sensors where the selective layer is replaced by an electrode which responds to a gas.

#### 18.2.2.2 Other transducers

Mass-sensitive transducers are either piezoelectric crystals in which the resonant frequency of the bulk material is measured or surface acoustic wave devices which comprise a separate waveguide and piezoelectric transmitter and receiver [25]. In both cases the signal changes in response to mass changes due to the binding of an analyte to a recognition element on the surface. Optical transducers can measure changes in absorbance, reflectance, refractive index, luminescence or scattering. Many optical sensors have been developed based on indicators or fluorophores that change their absorbance or fluorescence characteristics selectively in the presence of different analytes [26]. Such systems have been miniaturised using optical fibre technology. Indirect optical biosensors are based on the products of enzymatic reactions, labelled competitors or labelled second antibodies [27]. The direct sensing of analytes binding to receptors on a surface can also be achieved using methods such

as ellipsometry, reflectometry or surface plasmon resonance [28,29]. Thermometric transducers are based on measurement of the generation or consumption of heat due to the interaction of the analyte and the recognition component in the chemical sensor [30]. The enzyme thermistor has been the most popular chemical sensor developed using this concept [31]. Magnetometric transducers have recently been introduced by our group [32,33]. For a detailed description of optical sensors see Chapter 20. Few naturally occurring magnetic substances exist in nature, so these devices are limited to immunosensors with paramagnetically labelled second messengers to quantify the analyte, but have the advantage that they suffer little from non-specific interference.

### 18.2.3 The recognition element

A classification of the recognition elements used in sensors can be made on the basis of their physicochemical/biological/biomimetic origin and catalytic/non-catalytic nature (see Table 18.1).

#### 18.2.3.1 Physicochemical recognition elements

Most ISEs are based on purely physicochemical and non-catalytic recognition elements: solid membranes with fixed ionic sites (e.g. the glass pH electrode), ion-exchange polymer membranes or plasticised hydrogel membranes incorporating ionophores [9]. Silicon oxide or metal oxides act as the recognition element in pH-ISFETs, gas-sensitive FETs, solid-state electrolyte, solid-state semiconductor and many conductometric gas sensors.

Ion-exchange polymers, redox polymers and especially electroconducting polymers have been utilised extensively in CMEs including CWEs, ISFETs, amperometric and conductometric sensors, both as selective accumulators and as

TABLE 18.1

EXAMPLES OF DIFFERENT TYPES OF RECOGNITION ELEMENTS USED IN ELECTROCHEMICAL SENSORS

|                 | Non-catalytic  | Catalytic   |
|-----------------|--|---|
| Physicochemical | Solid-state and ion-exchange membranes, metal oxides, solgels, zeolites, conducting polymers | Doped semiconducting oxides, immobilised metals       |
| Biological      | Lectins, antibodies, receptors, DNA  | Enzymes, micro-organisms, abzymes, organelles, tissue |
| Biomimetic      | Supramolecular receptors, synthetic ligands and inhibitors, MIMs                             | Porphyrins, artificial enzymes                        |

electrocatalysts [34]. Electroconducting polymers such as polypyrrole conduct *via* their highly delocalised electronic structure. They can themselves be switched between different redox states and may additionally be modified with electrocatalytic groups. Their conducting properties are modified by protonation and by the inclusion of anions. Polypyrrole has been employed as a pH- [35], gas- [36] and ion- [37,38] sensitive recognition element in different sensors.

Inorganic crystalline solids, especially zeolites, have been applied as selective adsorbents in mass-sensitive [39], amperometric [40] and conductometric [41] gas sensors.

### *18.2.3.2 Biological recognition elements*

Biological recognition systems offer exquisite selectivity and sensitivity. A vast range of approaches has been described [42,43].

Direct immunosensors are based on non-catalytic recognition elements, primarily antibodies but also DNA, lectins and ligand-bound receptors. Binding can be detected directly by mass-sensitive [44] or optical sensors such as surface plasmon resonance [29]. The design is less suited to electrochemical sensors. Although some examples based on potentiometric or conductometric changes due to binding of analyte to antibody have been reported [45,46], indirect techniques, which provide more opportunities for signal amplification have been favoured. Indirect immunosensors are based on the detection of a competitor or second antibody to the analyte. For optical sensors, this second messenger should itself be coloured or fluorescent or should be labelled with an indicator [27]. For magnetic sensors it must be paramagnetic [32,33]. For electrochemical sensors, it should be electroactive or labelled with an enzyme which produces ions or an electroactive species [47].

Enzyme sensors can measure analytes that are the substrates of enzymatic reactions. Thermometric sensors can measure the heat produced by the enzyme reaction [31], while optical or electrochemical transducers measure a product produced or cofactor consumed in the reaction. For example, several urea sensors are based on the hydrolysis of urea by urease producing ammonia, which can be detected by an ammonium ion-selective ISE or ISFET [48] or a conductometric device [49]. Amperometric enzyme sensors are based on the measurement of an electroactive product or cofactor [50]; an example is the glucose oxidase-based sensor for glucose, the most commercially successful biosensor. Enzymes are incorporated in amperometric sensors in functionalised monolayers [51], entrapped in polymers [52], carbon pastes [53] or zeolites [54]. Other catalytic biological systems such as micro-organisms, abzymes, organelles and tissue slices have also been combined with electrochemical transducers.

Despite their advantages of specificity and selectivity, biosensors suffer from a severe disadvantage, the instability of the biological recognition system, which makes storage and operation in harsh chemical environments problematic. This problem has been addressed using a newly developed sensor with injected recognition element biosensors (whose operational principle is based on the one time use

of the recognition element, which must be catalytic) [55]. An alternative approach is to develop new synthetic entities with similar recognition properties to biological systems, but with enhanced stability.

#### 18.2.3.3 Biomimetic recognition elements

Breslow has defined biomimetic chemistry as ‘the field in which chemists invent new substances and reactions that imitate biological chemistry’ [56]. Interpreted in a broad sense, this covers all recognition elements based on host–guest molecular recognition, including the neutral carrier ionophores used in liquid-membrane ISEs [57]. Host–guest chemistry has been used to develop receptors for simple or complex anions, such as ATP, for use in liquid-membrane potentiometric sensors and CHEMFETs [58]. Supramolecular ionophores have also been incorporated in monolayers for conductometric sensors [59] and in conducting polymers for amperometric sensors [60]. Host–guest chemistry has also been extensively used in the design of molecular fluorescent sensors [61].

Biomimetic ligands for macromolecules such as proteins, including enzyme inhibitors and short peptides, have been extensively investigated as affinity elements in surface plasmon resonance sensors and to a lesser extent in mass-sensitive affinity sensors [62,63]. A number of approaches has been described involving bilayer lipid membranes, between two solution phases or anchored on a solid support, containing biological or biomimetic recognition elements [64,65]. Mass-sensitive, optical and electrochemical transducers have been applied to such systems. Electrochemical methods have included measurement of membrane potentials due to ion binding to lipid-bound receptors and amperometric measurements on the current due to ion transport across a membrane *via* specific ion channels or promoted by analyte binding to a co-transporter.

Electrocatalytic groups such as porphyrins and phthalocyanines that act as supramolecular hosts for different metals and mimic the active sites of various proteins are commonly used in amperometric sensors [66,67]. A biomimetic sensor based on an artificial enzyme or ‘synzyme’ has been demonstrated [68]. The artificial enzyme used in this study was a synthetic polymer (quaternised polyethyleneimine containing 10% primary amines) which decarboxylated oxaloacetate. The product carbon dioxide was detected potentiometrically *via* a gas membrane electrode.

MIMs are also included in this group, as their development was inspired by the instructional theory of antibody formation, and they have often been referred to as ‘artificial antibodies’.

### 18.3 SENSORS UTILISING MOLECULARLY IMPRINTED RECOGNITION SITES

We now describe the different approaches to the combination of MIMs with some of the transducer types outlined above, emphasising especially electrochemical transducers for measurements in solution, since other sensor approaches will be dealt with elsewhere in this volume.

### **18.3.1 Approaches using imprinted macroporous methacrylate, acrylate or vinyl polymers**

Whilst macroporous methacrylate, acrylate, acrylamide and vinyl polymers have been the most widely applied matrices for molecular imprinting and have exhibited the best selectivities in batch binding and chromatographic studies, they are not easily combined with transducers. Since they are non-conducting, they cannot be used alone as electrode materials in electrochemical sensors. They are also difficult to prepare reproducibly in the form of thin films or membranes. However, they have been employed in optical sensors and sensing devices by exploiting the optical properties of the analyte [69] or by introducing an optical signalling component at the recognition site [70–74]. They have also been used in electrochemical sensors, where they serve only to selectively accumulate the analyte, and in indirect approaches as outlined below. They may also be incorporated in electrodes *via* composite materials with conducting polymers (Section 18.3.4.4.).

#### *18.3.1.1 Early approaches*

Potentiometric measurements on an imprinted methacrylate polymer were described in 1990. An HPLC column was packed with a phenylalanine anilide-imprinted methacrylic acid (MAA)-ethyleneglycol dimethacrylate (EDMA) copolymer [75] and the potential between the ends of the column was measured during the chromatographic separation of the print molecule from its optical antipode in acetone/nitrile/acetic acid. However, the device was non-specific and better described as a chromatography detector rather than a sensor. The origin of the signal is additionally rather unclear. The streaming potential measured as described across the entire column would be expected to respond in a stepwise square-wave manner to the presence of analyte on the column, rather than analogously to a post-column absorbance detector, as observed.

An early attempt to make a 'real' electrochemical sensor based on a molecularly imprinted methacrylate polymer utilised conductometric measurements on a field-effect capacitor [76]. A thin film of phenylalanine anilide-imprinted MAA-EDMA copolymer was deposited on the surface of semiconducting p-type silicon and covered with a perforated platinum electrode. An AC potential was applied between this electrode and an aluminium electrode on the back side of the semiconductor and the capacitance measured as a function of the potential when the device was exposed to the analyte in ethanol. The print molecule could be distinguished from phenylalanine but not from tyrosine anilide and the results were very variable between devices, which was attributed to difficulties in the film production. The mechanism by which analyte bound to the polymer might influence the capacitance is again rather unclear.

#### *18.3.1.2 Sensors based on accumulation in the polymer*

More impressive results were obtained with a competitive amperometric device in 1995 [77]. Morphine (for structure see Chapter 14) was imprinted in an

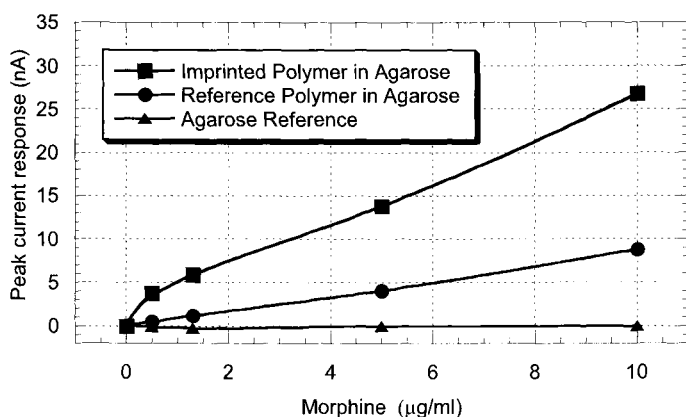


Fig. 18.3. The graph illustrates the competitive morphine sensor response as a function of the morphine concentration (0–10  $\mu\text{g/ml}$ ) present in the solution. Three sensor types were examined, incorporating the morphine-imprinted polymer in agarose, reference polymer in agarose and agarose-only covered platinum electrodes.

MAA-EDMA copolymer as a bulk monolith with acetonitrile as porogen [78]. Imprinted methacrylate polymer particles were trapped in agarose gel on the surface of a platinum electrode and used to accumulate the redox-active analyte morphine from an aqueous–ethanol solution. As the methacrylate polymer is non-conducting, amperometric measurement at this stage yielded only a weak and non-specific response. However, when the non-redox-active competitor codeine was added, some of the morphine was displaced from the polymer and oxidised at the electrode before it could diffuse into solution. The signal was related to the original morphine concentration. In a device with a non-imprinted polymer essentially no signal was observed on the addition of codeine. Although the indirect approach is cumbersome, the sensor was able to detect morphine within the concentration range 0.1–10  $\mu\text{g/ml}$  (Fig. 18.3) and showed autoclave compatibility, long-term stability and resistance to harsh chemical environments, significant advantages compared with biosensors. Although the response of the sensor was slow due to the time required for equilibration in the sample solution (2 h), this may be due only to the configuration, requiring diffusion of the analyte through the polyacrylamide matrix. More recent work has shown that the binding of morphine to the polymer in suspension occurs in minutes [79].

A conductometric device for measurement of benzyltriphenylphosphonium ions was developed next [80]. Particles of benzyltriphenylphosphonium chloride-imprinted MAA-EDMA copolymer were held in a layer between two platinum wires using a filter paper. The device was exposed to the analyte in acetonitrile, an AC potential applied and the conductance recorded. The direct measurement principle is based on the enrichment of the analyte, a charged species, close to the electrode. A semi-linear response was observed between 1 mg/l and 20 mg/l (Fig. 18.4). In the two latter sensors it was anticipated that the effect of non-specific

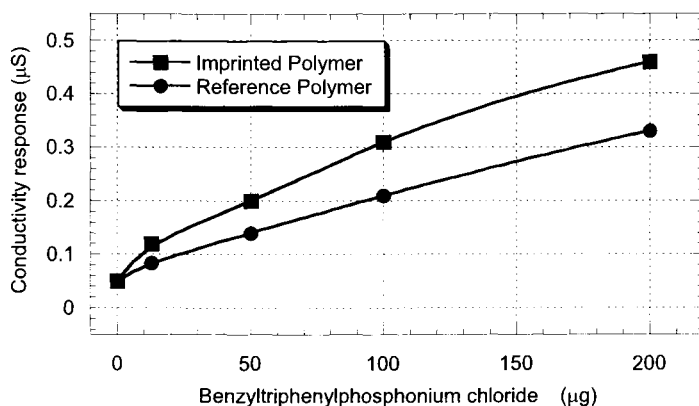


Fig. 18.4. Conductivity of benzyltriphenylphosphonium ion-imprinted and non-imprinted polymer-based sensors in the presence of increasing concentrations of benzyltriphenylphosphonium chloride in acetonitrile.

interfering compounds could be accounted for by subtracting the signal obtained from devices with non-imprinted polymers. For both devices, the morphology of irregular polymer particles is not ideal and faster kinetics and more reproducible results might be expected by the use of thin films of polymer (R.J. Ansell, A. Fiorovanti, M. Mecklenburg, E. Missongé, J.-F. Lipskier and K. Mosbach, unpublished results).

An approach similar to the amperometric morphine sensor has very recently been described by Kröger *et al.* [81]. Particles of poly(EDMA-co-4-vinylpyridine) imprinted with 2,4-dichlorophenoxyacetic acid were trapped in agarose on a screen-printed carbon electrode. The sensor was equilibrated in a solution of the template analyte species with a fixed amount of the electroactive competitor homogentisic acid, then the free homogentisic acid was quantified by differential pulse voltammetry. This approach has the advantage of being applicable to non-redox-active species, provided a suitable redox-active competitive probe can be found.

An interesting approach toward an indirect glucose sensor has been described by Chen *et al.* [82–84]. A ligand-exchanger polymer was prepared by copolymerising *N,N'*-methylenebisacrylamide in aqueous methanol with the complex 1-(4'-vinylbenzyl)-1,4,7-triazacyclononane Cu(II) methyl- $\beta$ -D-glucopyranoside (Fig. 18.5). When the glucopyranoside was extracted and the polymer placed in aqueous buffer, rebinding of glucose in the imprinted sites was accompanied by the release of a proton. This could in future be combined with a pH electrode to form a sensor, although the authors acknowledge that the buffering capacity of whole blood makes the design difficult to apply to such samples.

#### 18.3.1.3 Sensors based on permeation through the polymer

A number of approaches have been reported towards forming molecularly imprinted polymer membranes, which are intended to selectively transport the

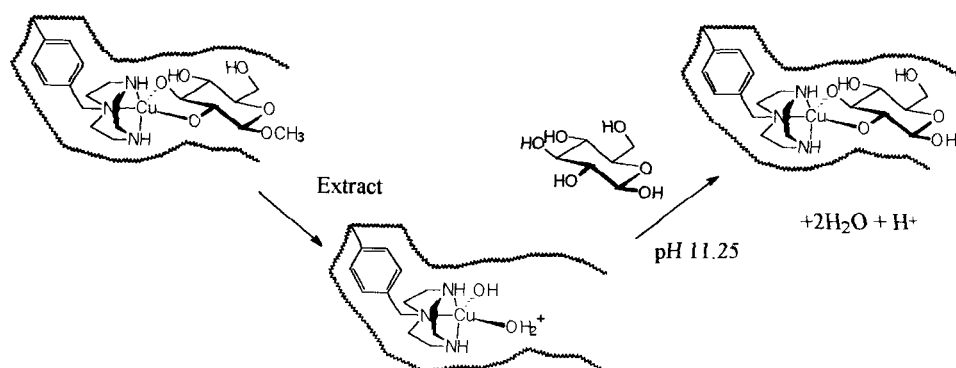


Fig. 18.5. The glucose-containing complex molecularly imprinted by Chen *et al.* (adapted from [83]).

analyte/template [85–89], though with mixed success. Such membranes could usefully be combined with, for instance, an amperometric detection method for an electroactive analyte. However, such an application has not yet, to our knowledge, been reported.

Piletsky *et al.* have adopted a different approach towards sensing using molecularly imprinted polymer membranes in a conductometric device [90–93]. Cross-linked acrylate copolymer membranes are prepared on glass filters, in the presence of templates which are subsequently extracted, and placed between two buffer-filled compartments containing electrodes (Fig. 18.6). A solution of analyte is added (whether to one or both compartments is unclear), an alternating voltage is applied between the electrodes and resistance is recorded. For poly(EDMA-co-(diethylamino)ethylmethacrylate) membranes non-covalently imprinted with atrazine or L-phenylalanine and poly(EDMA-co-MAA) membranes imprinted with atrazine the resistance falls when the original template is added, but much less with other

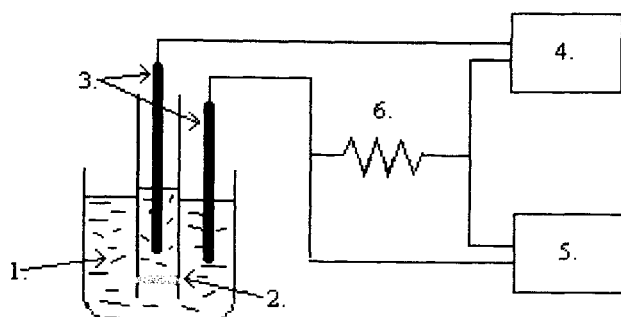


Fig. 18.6. AC resistometric sensing apparatus as described by Piletsky *et al.* [92]. 1. Electrochemical cell, 2. filter with polymer membrane, 3. platinum electrodes, 4. AC generator, 5. voltmeter, 6. 1 kOhm resistance.



species. This is explained in terms of a 'gate effect'; rebinding of the template causing shrinking of the polymer network and increasing its ion transport capability. No drop in resistance was observed for atrazine with a non-imprinted polymer. The detection limit (approximately 50  $\mu\text{M}$ ) and selectivity (approximately ten-fold lower response to simazine) obtained with the atrazine sensor are impressive [92]. For a membrane covalently imprinted with a sialic acid–boronic acid complex an increase in resistance is observed in the presence of the template [93]. Control studies are not presented in this case though, and the reason for the 'anti-gate' effect remains unclear.

In Piletsky's latest work, 'free-standing' membranes are formed by polymerisation between two glass slides, with oligourethane acrylate being incorporated in the polymer mixture to lend extra flexibility [94,95]. Using atrazine again as the imprinted species, a detection limit for atrazine of 5 nM and 20-fold selectivity over simazine are reported.

### **18.3.2 Templated inorganic materials**

There is a great interest at present in the use of supramolecular organic templates in the preparation of inorganic materials (see also Chapter 8). The mesoporous zeolite MCM-41, prepared in the presence of a surfactant template which is subsequently extracted, has been used for selective amperometric detection of copper (II) and mercury (II) [96]. Surfactants have also been used as templates in the preparation of metal oxides for application in gas sensors [97]. The molecular recognition properties of all these materials are due purely to size and shape selectivity, to the coordination properties of metal centres within the material or to functionalities introduced after the removal of the template, so they are not molecularly imprinted but are perhaps to be regarded as a complementary technology. The analogy between zeolites and macroporous cross-linked methacrylate polymers is especially relevant, as they are both rigid non-conducting materials and have been applied in sensors either as thin films or as particles.

The sol-gel technique is well-suited to producing thin layers of inorganic material, especially silanes, on electrodes and waveguides and this has led to its widespread use in the preparation of sensors [98,99]. Additionally, sol gels are often ionic conductors, which provides a means for electrochemical transduction. In view of the earlier use of silica in molecular imprinting (see Chapters 1 and 8), surprisingly few attempts have been reported to produce electrochemical sensors based on molecularly imprinted sol gels. Titanium oxide films containing 4-(4-propyloxyphenylazo)benzoic acid [100] or carbobenzyloxy-L-alanine [101] as a template, formed by gelation of tetrabutoxytitanium on quartz-crystal microbalances, have been used as mass sensors for different aromatic carboxylic acids and carbobenzyloxy amino acids in acetonitrile. No selectivity comparisons with non-templated films were presented however. This is a problem with many studies on imprinting in sol gels, and the existence of real selective imprinted sites in such materials remains controversial [102].

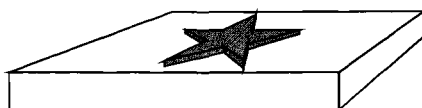
One limitation of traditional sol-gel MIMs is the limited possibility to introduce

functional groups into any templated recognition sites, and thus the limited selectivity which could be achieved. However, sol-gel technology has advanced and there are now many cases where organic components, and even biological macromolecules, have been incorporated in sol gels to provide recognition and/or transducing components [103,104]. An approach towards molecularly imprinted composite organosilicate films containing organic groups at the recognition sites has been reported recently by Makote and Collinson [105]. A sol comprising tetramethoxysilane and phenyltrimethoxysilane with dopamine as template was deposited at a glassy carbon electrode. The dopamine was leached out in buffer, leaving a silicate film with phenyl groups which might be arranged at recognition sites. In cyclic voltammetry, the electrode exhibited an enhanced amperometric response toward dopamine, compared with electrodes with non-templated films or templated films made only from tetramethoxysilane, so not containing phenyl functionalities, and decreased sensitivity to ascorbic acid. Although it is not yet clear if the selectivity in this composite material really arises from templated recognition sites, we believe that the technique warrants further investigation.

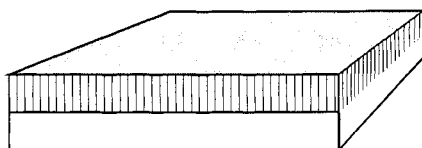
### 18.3.3 Gate sites in surface monolayers

Gate sites may be formed in self-assembled monolayers when the layers are prepared on surfaces in the presence of a template which is subsequently extracted (Fig. 18.7). The principle was first described by Sagiv using visible absorption spectroscopy to determine the uptake of cyanine dyes [106]. Yamamura and co-workers

1. Template associates with surface



2. Assemble surface monolayer



3. Extract template, leaving gate site

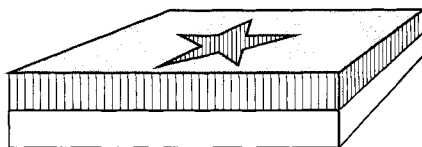


Fig. 18.7. Schematic of the formation of gate sites in surface-assembled monolayers and their use in sensing.

[107] first used the principle in a real sensor. Octadecylsilane (ODS) monolayers were assembled from solution on tin (IV) oxide electrodes in the presence of a template, n-hexadecane, which was subsequently washed out. The electrodes exhibited an enhanced amperometric response to hydrophobic electroactive guest molecules such as vitamin K<sub>1</sub>, vitamin K<sub>2</sub> and vitamin E, relative to uncoated electrodes or those prepared without template. Subsequently, a limited degree of selectivity was shown by using different templates and examining the amperometric response to vitamin K<sub>1</sub> in the presence of different competing ligands [108].

An optical sensor was described based on gate sites. Ellipsometric measurements were made by Andersson *et al.* [109] on ODS monolayers on silica surfaces containing gate sites formed using hexadecane as template. Vitamin K<sub>1</sub> was shown to bind more strongly to such surfaces than other species, including oleyl cholesterol. The level of selectivity obtainable with such a simple template is obviously limited; better results could be expected with more sophisticated templates, in particular rigid planar molecules. Thus, Kim *et al.* [110] used surface-enhanced resonance Raman spectroscopy to demonstrate the properties of gate sites templated with porphyrins in ODS monolayers on glass. A degree of selectivity was observed for rebinding the template porphyrin over other larger porphyrins.

More recently, a number of approaches have been followed to devise amperometric solution-phase sensors in which surface templated gate sites act as molecular sieving barriers, admitting only the electroactive analyte of interest to the electrode surface, while the protecting monolayer blocks the access of other molecules. Gate sites have been formed in self-assembled mixed thiol monolayers [111] or Langmuir–Blodgett mixed thiol/alcohol monolayers [112] on gold electrodes. In these cases the template is not extracted from the surface, but is nevertheless considered to form molecular-sieving defects within the otherwise passivating surface. Starodub *et al.* [113] described some preliminary results with indium–tin oxide electrodes modified with trimethylsilane by vapour deposition using amino acids as templates for gate sites. Morita *et al.* [114,115] used catechol as a template to form gate sites in an aminopropylsilane monolayer on a gold electrode. After washing, the amperometric response to the electroactive template catechol was enhanced relative to catecholamines and epinephrine, compared with electrodes treated with template only.

Very recently Lahav *et al.* [116] used a photochemically cleavable template to introduce gate sites into an alkanethiol self-assembled monolayer on a gold electrode. The electrode showed an enhanced amperometric response to the electroactive template, compared with an electrode with a monolayer without gate sites.

Gate sites in silane monolayers on tin (IV) oxide electrodes have also been studied for resistometric gas-phase sensing [117].

Common to many of these studies is that selectivity, where it has been examined at all, has only been reported between the template and species of quite different charge or polarity. It is difficult in such cases to attribute selectivity to the geometry of the gate sites rather than changes in the bulk properties of the electrode surface. Gate sites in self-assembled monolayers provide a simple method for the modification of sensor surfaces. However, the degree of selectivity obtainable in this way,

without the involvement of chemical functional groups, seems to be limited. Improved results for small molecules could perhaps be achieved with the templated positioning of functional groups on the surface to give an element of specificity within the 'gate sites' [118–120]. A related approach has recently been described by Mirsky *et al.* [121] using a 'molecular spreader bar', or a template which is not subsequently removed, to form recognition sites in a self-assembled monolayer of dodecanethiol on gold which selectively bind molecules of similar shape to the spreader bar.

### 18.3.4 Templating in conducting and redox polymers

Conducting polymers are of great interest for the construction of electrochemical sensors [122]. Chemically or electrically initiated polymerisation can be used to form thin films on electrode surfaces. These offer a considerable increase in surface area, and hence response, compared with monolayers, while maintaining fast kinetics as compared with bulk macroporous polymers. The polymer itself may act as a recognition element in combination with gas-phase resistometric sensing or solution-phase amperometric or potentiometric sensing. Further, catalytic or host groups may be covalently incorporated in the films [123] and enzymes may be physically entrapped [52], together with coenzymes and/or redox mediators for amperometric sensing.

#### 18.3.4.1 Ion sieving

It has been known for some time that polypyrrole, the most studied conducting polymer, exhibits a 'memory' for the anion of the electrolyte used in its preparation [124]. The selectivity of polypyrrole films towards anions is related to the size and

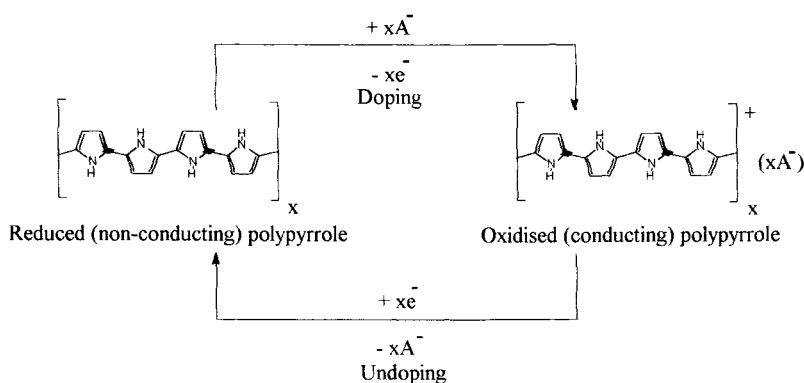


Fig. 18.8. Doping and undoping of a poly(pyrrole) film during oxidation and reduction cycles. When a poly(pyrrole) coated electrode is cycled between the reduction and oxidation potentials, the current observed at the oxidation potential is related to the ability of anions to enter the polymer film and 'dope' the polypyrrole.

charge of the anion. Films are prepared by electrochemical initiation either at a fixed oxidising potential or by cycling between oxidising and reducing potentials. Repeated doping and undoping of the film with the anion of interest during polymerisation may give rise to ion sieving channels (Fig. 18.8). Selective potentiometric sensors for chloride and nitrate have been prepared in this way, the response arising from the anion diffusing into the oxidised film [37,38]. Polypyrrole polymerised in the presence of a nitrate salt has also been used for sensing of  $\text{NO}_x$  gases, based on the  $\text{NO}_x$  crossing a gas-permeable membrane and forming nitrate in solution, which was detected potentiometrically [125]. Other conducting polymers also appear to exhibit ion-sieving properties dependent on the conditions used in their preparation [126].

#### 18.3.4.2 More complex systems

In an attempt to achieve higher selectivity in polypyrrole *via* the doping anion, we prepared films by potential cycling using L-glutamate and L-aspartate as electrolytes (D. Kriz and R.J. Ansell, unpublished work 1994). However, we were unable to demonstrate any selectivity in the resulting films using potentiometric or amperometric measurements. A slightly different approach was used by Spurlock *et al.* [127], who prepared films on glassy carbon at a fixed potential with ATP as electrolyte. Films were subsequently over-oxidised, which removes the conducting ability of the film and was shown to cause release of the ATP. The films exhibited an enhanced selectivity in their voltammetric response to adenine compared with films prepared using other electrolytes. However, conventional electrolytes with adenine or inosine as additives altered the selectivity of the prepared films in less predictable ways.

The rational preparation of selective recognition sites in polypyrrole by templating methods would seem to require the introduction of functional groups and cross-linking to preserve the sites. These requirements were elegantly combined by Bidan *et al.* [128] using metal-ligand complexes like that shown in Fig. 18.9. Polymerisation, demetallation with a competing chelate and reloading with different metals were followed by cyclic voltammetry. While selectivity between different metals was not shown, the demetallated films nonetheless took up more metal

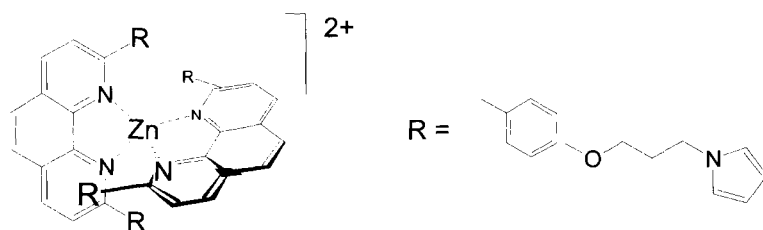


Fig. 18.9. Metal complex polymerised to give polypyrroles containing complexing cavities [128].

during reloading than films of polymerised ligand prepared in the absence of metal, suggesting that the ligand cavity is to some extent preserved.

Another conducting polymer, polyaniline, has been investigated as a sensor material by Pringsheim *et al.* [129]. Aniline and (3-aminophenyl)boronic acid were chemically polymerised. The resulting polymers exhibit optical and potential changes in the presence of sugars. However, films prepared using the analogous glucose–boronate complex, which is then hydrolysed to leave functional templated binding sites, exhibit no change in selectivity relative to the original films (E. Pringsheim and O. Wolfbeis, personal communication). *o*-Phenylenediamine has also been electropolymerised in the presence of glucose to give a thin, non-conducting film on the surface of a quartz-crystal microbalance [130]. The film exhibited an enhanced response to glucose relative to a film prepared without the template. In this case though a comparison of the selectivities of the two films was not presented.

#### 18.3.4.3 Redox polymers

Porphyrins are often employed in sensors on account of their ability to act as cation hosts and, with a suitable metal ion coordinated, as redox catalysts. Electropolymerised poly(metalloporphyrin)s have been used as potentiometric anion-selective electrodes [131] and as amperometric electrocatalytic sensors for many species including phenols [132], nitrous oxide [133] and oxygen [134]. Panasyuk *et al.* [135] have electropolymerised [nickel-(protoporphyrin IX)dimethylester] (Fig. 18.10) on glassy carbon in the presence of nitrobenzene in an attempt to prepare a nitrobenzene-selective amperometric sensor. Following extraction of the nitrobenzene the electrode was exposed to different species and cyclic voltammetric measurements made. A response was observed at the reduction potential of nitrobenzene (the polyporphyrin film acts only to accumulate the analyte and not in a catalytic fashion). Selectivity for nitrobenzene compared with *m*-nitroaniline and *o*-nitrotoluene was enhanced compared with an untreated electrode, while a glassy carbon-

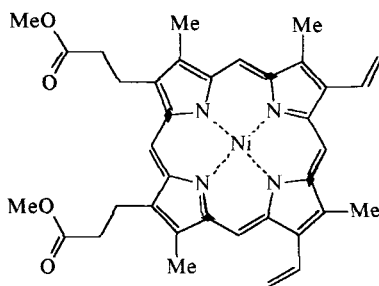


Fig. 18.10. [Nickel-(protoporphyrin IX)dimethylester], which was electropolymerised on glassy carbon with nitrobenzene as template to prepare a nitrobenzene-selective sensor [135].

poly[nickel-(protoporphyrin IX)] electrode prepared in the absence of nitrobenzene gave no response. This result appears to be the most convincing demonstration of molecular imprinting in an electroactive polymer, although the origin of the recognition has yet to be explained.

There are many other conducting and redox polymers which could be investigated for imprinting effects. We expect this to become something of a growth area in the field.

#### *18.3.4.4 Composite materials*

In view of the limited success thus far in preparing specific recognition sites in conducting polymers *via* templating, we have investigated the preparation of new materials comprising composites of polypyrrole with molecularly imprinted methacrylate polymers [136]. It was hoped that the resulting conducting composites would preserve the superior recognition properties of molecularly imprinted acrylate polymers and in addition exhibit greater stability compared with conducting polymers.

Pyrrole was adsorbed into the pores of ground and sieved particles of morphine-imprinted acrylate polymer particles (1–20  $\mu\text{m}$ ), then polymerised chemically. The morphine-specific molecular recognition properties were not significantly altered compared with pure MAA-EDMA polymer (as determined by competitive radioligand binding). In addition, the composite particles were shown to have electrical conductivity when examined as dry layers on an interdigitated finger array device. The conductivity was dependent on the packing of the particles and hence the contact area between particles.

Figure 18.11 illustrates atomic force microscopy (AFM) pictures of gold-covered silica substrates covered with composite particles. These particles were immobilised by the simultaneous electropolymerisation of pyrrole. Thus, even traditional MAA-EDMA copolymer particles can readily be electrically connected to an electrode, thereby obtaining close contact between the transducer and the recognition sites within the polymer. The device is being developed into an amperometric morphine sensor.

## **18.4 CONCLUSIONS AND OUTLOOK**

We have outlined several approaches which have been followed towards electrochemical sensing using MIMs. Macroporous cross-linked methacrylate, acrylamide and styrene-based polymers, which have been used most extensively in other applications of molecular imprinting, can only be used alone for indirect electrochemical sensors. Nevertheless, we believe there is a future for such devices, especially in combination with new techniques for developing thin films of such polymers, which will be better suited to deposition on electrodes. In addition, composite materials comprising conventional imprinted polymers and conducting polymers may offer both selective binding and simple signal transduction. One aspect which has yet to

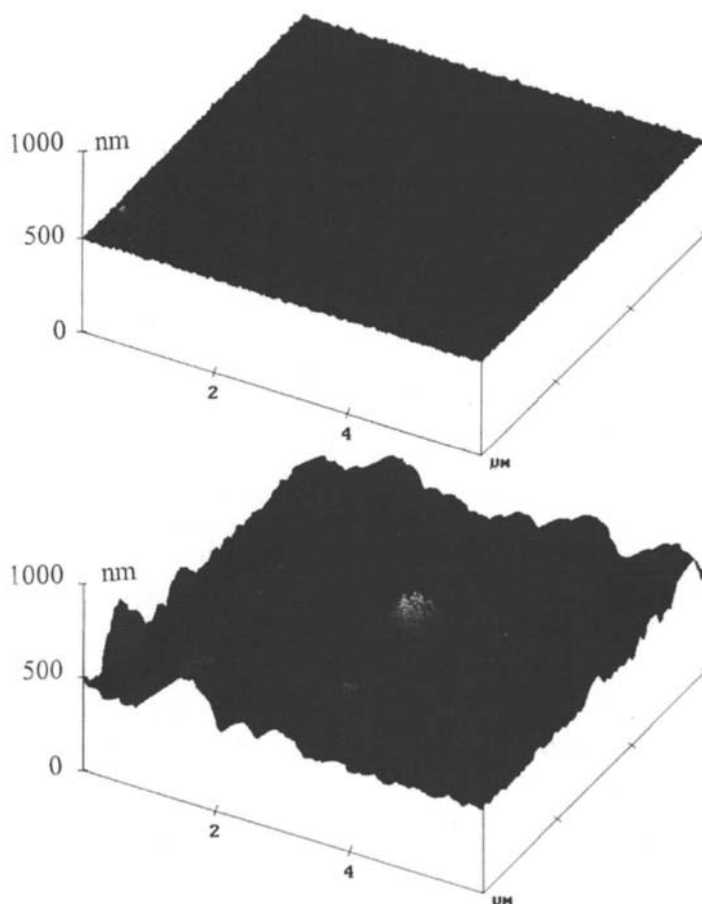


Fig. 18.11. AFM pictures of polypyrrole modified gold-covered silica substrates without (upper picture) and with (lower picture) a layer of composite particles.

be investigated is the combination of catalytic polymers with electrochemical detection of a product produced by the catalytic reaction. In this way interference from other electroactive compounds can often be avoided.

In attempts to circumvent the limitations of macroporous cross-linked methacrylate, acrylamide and styrene polymers as materials, other materials and morphologies have been investigated for the construction of sensors based on molecular imprinting; self-assembled monolayers, sol-gels and conducting polymers, as well as other materials so far applied only in mass-sensitive or optical sensors [137,138]. It is likely that many new materials will be investigated in the future. However, the principles underlying the construction of imprinted molecular recognition sites in all these materials are not yet well understood, and extensive basic studies of the



processes involved, as conducted over many years with macroporous methacrylate, acrylamide and styrene polymers, would be useful to aid the future development of practical sensors.

Thus, whilst many of the sensing systems we have described exhibit interesting selectivities and sensitivities, it is only conclusively shown in a few cases that this selectivity arises from specific imprinted molecular recognition sites. The best examples are those where the sensor can discriminate optical isomers; in these cases the observed selectivity cannot be due to any differences in the physical properties of the analytes. Where the analyte of interest is not chiral, it is of paramount importance, as in all research on molecular imprinting, to examine control sensors comprising non-templated materials and, ideally, materials templated with another compound, before attributing any observed selectivity to molecular imprinting. Only if the origin of selectivity is known can rational efforts be directed at improving selectivity. In addition, since 100% specificity for the analyte of interest is unlikely to be achieved, it will be useful for any practical device to include a control sensor based on a non-templated or differently-templated material, in order to subtract the non-specific signal from that obtained with the imprinted sensor.

A development which may be relevant to future work on imprinted sensors is the expanding research on electronic noses and tongues [139–141]. In these devices an array of sensors is used and the contents of a sample are deduced by pattern-recognition processing. Each individual sensor does not then need to be 100% specific for one species, so long as all the sensors exhibit differing patterns of selectivity. From a device incorporating both imprinted and control sensors as outlined above to an array of different imprinted sensors may not be a very great leap.

In conclusion, we believe molecular imprinting can be usefully combined with electrochemical transducers to produce new chemical sensors that exhibit selectivity, sensitivity and great stability and tolerance of harsh environments when compared with biosensors.

## REFERENCES

- 1 R.J. Ansell, D. Kriz and K. Mosbach, *Curr. Opin. Biotechnol.*, **7**, 89 (1996).
- 2 A.G. Mayes and K. Mosbach, *Trends Anal. Chem.*, **16**, 321 (1997).
- 3 D. Kriz, O. Ramström and K. Mosbach, *Anal. Chem.*, **71**, 345A (1997).
- 4 G. Wulff, In: *Frontiers in biosensorics 1: fundamental aspects*, F.W. Schiller, F. Schubert and J. Fedrowitz Eds, Birkhäuser Verlag, Basel, p. 13 (1997).
- 5 K. Haupt and K. Mosbach, *Biochem. Soc. Trans.*, **27**, 344 (1999).
- 6 J. Janata, M. Josowicz, P. Vanysek and D.M. DeVaney, *Anal. Chem.*, **70**, 179R (1998).
- 7 W. Göpel, J. Hesse and J.N. Zemel, *Sensors*, VCH: Weinheim (1995).
- 8 P. Fabry and E. Siebert, In: *The CRC handbook of solid-state electrochemistry*, P.J. Gellings and H.J.M. Bouwmeester Eds., CRC, Boca Raton, p. 329 (1997).
- 9 R.L. Solsky, *Anal. Chem.*, **62**, 21R (1990).
- 10 P. Schnierle, T. Kappes and P.C. Hauser, *Anal. Chem.*, **70**, 3585 (1998).
- 11 P. Zhao and W.-J. Kai, *Anal. Chem.*, **69**, 5052 (1997).
- 12 H.H. Möbius, P. Shuk and W. Zastrow, *Fresenius J. Anal. Chem.*, **356**, 221 (1996).
- 13 W. Kutner, J. Wang, M. L'Her and R.P. Buck, *Pure & Applied Chem.*, **70**, 1301 (1998).

- 14 K. Kalcher, J.-M. Kaufmann, J. Wang, I. Svancara, K. Vytras, C. Neuhold and Z. Yang, *Electroanalysis*, **7**, 7 (1995).
- 15 K.S. Alber, J.A. Cox and P.J. Kulesza, *Electroanalysis*, **9**, 97 (1997).
- 16 I. Fatt, *Polarographic oxygen sensors*, CRC Press, Cleveland (1976).
- 17 A.C. Partridge, P. Harris and M.K. Andrews, *Analyst*, **121**, 1349 (1996).
- 18 U. Lampe, M. Fleischer, N. Reitmeier, H. Meixner, J.B. Monagle and A. Marsh, *Sens. Update*, **2**, 1 (1996).
- 19 S. Bruckenstein and J.S. Symanski, *J. Chem. Soc., Faraday Trans. 1*, **82**, 1105 (1986).
- 20 H. Grange, C. Bieth, H. Boucher and G. Delappierre, *Sens. Actuators*, **12**, 291 (1987).
- 21 C. Cane, I. Gracia and A. Merlos, *Microelectron. J.*, **28**, 389 (1997).
- 22 M.M.G. Antonisse, R.J.W. Lugtenberg, R.J.M. Egberink, J.F.J. Engbersen and D.N. Reinhoudt, *NATO ASI Ser., Ser. C*, **492**, 23 (1997).
- 23 P. Bergveld, *Sens. Actuators*, **A56**, 65 (1996).
- 24 I. Lundström, *Sens. Actuators*, **A56**, 75 (1996).
- 25 E. Benes, M. Groschl, W. Burger and M. Schmid, *Sens. Actuators*, **A48**, 1 (1995).
- 26 O.S. Wolfbeis, in *Optical fiber sensors Volume 4*, B. Culshaw, J. Dakin Eds., Artech House, Norwood MA, p. 53 (1997).
- 27 M. Wortberg, M. Orban, R. Renneberg and K. Cummann, In: *Handbook of biosensors and electronic noses*, E. Kress-Rogers Ed., CRC, Boca Raton FL, p. 369 (1997).
- 28 G. Gauglitz, *Sens. Update*, **1**, 1 (1996).
- 29 J. Homola, S.S. Yee and G. Gauglitz, *Sens. Actuators*, **B54**, 3 (1999).
- 30 G.C.M. Meijer and A.W. van Herwaarden (Eds), *Thermal sensors*, Institute of Physics Publishing, Bristol (1994).
- 31 B. Danielsson and B. Xie, In: *Frontiers in biosensorics 1: Fundamental aspects*, F.W. Schiller, F. Schubert and J. Fedrowitz Eds., Birkhäuser Verlag, Basel, p. 71 (1997).
- 32 C.B. Kriz, K. Rådevik and D. Kriz, *Anal. Chem.*, **68**, 1966 (1996).
- 33 K. Kriz, J. Gehrke and D. Kriz, *Biosens. Bioelectron.*, **13**, 817 (1998).
- 34 M.E. Lyons (Ed.), *Electroactive polymers in electrochemistry*, Plenum, N.Y. (1994).
- 35 M. Nishizawa, T. Matsue and I. Uchida, *Anal. Chem.*, **44**, 2642 (1992).
- 36 F. Musio and M.C. Ferrara, *Sens. Actuators*, **B41**, 97 (1997).
- 37 S. Dong, Z. Sun and Z. Lu, *Analyst*, **113**, 1525 (1988).
- 38 R.S. Hutchins and L.G. Bachas, *Anal. Chem.*, **67**, 1654 (1995).
- 39 Y. Yan and T. Bein, *J. Phys. Chem.*, **96**, 9387 (1992).
- 40 B. Chen, N.-K. Goh and L.S. Chia, *Electrochim. Acta*, **42**, 595 (1997).
- 41 O. Schaf, H. Ghobarkar and U. Guth, *Ionics*, **3**, 282 (1997).
- 42 A.P.F. Turner, *Curr. Opin. Biotechnol.*, **5**, 49 (1994).
- 43 F.W. Scheller, U. Wollenberger, D. Pfeiffer and F. Schubert, *Adv. Mol. Cell Biol.*, **15B**, 353 (1996).
- 44 A.A. Suleimann and G.G. Guilbault, *Analyst*, **119**, 2279 (1994).
- 45 J. Janata, *J. Am. Chem. Soc.*, **97**, 2914 (1975).
- 46 V.M. Mirsky, M. Riepl and O.S. Wolfbeis, *Biosens. Bioelectron.*, **12**, 977 (1997).
- 47 P. Skladal, *Electroanalysis*, **9**, 737 (1997).
- 48 O.G. Davies and J.D.R. Thomas, *Chem. Anal. (Warsaw)*, **40**, 341 (1995).
- 49 E. Palmquist, C.B. Kriz, M. Khayyami, K. Svanberg and D. Kriz, *Biosens. Bioelectron.*, **10**, 283 (1995).
- 50 A. Heller, *Curr. Opin. Biotechnol.*, **7**, 50 (1996).
- 51 I. Willner, E. Katz and B. Willner, *Electroanalysis*, **9**, 965 (1997).
- 52 M. Trojanowicz, T. Krawczynski and T. Krawczynski vel Krawczyk, *Mikrochim. Acta*, **121**, 167 (1995).
- 53 L. Gorton, G. Marko-Varga, B. Persson, Z. Huan, H. Linden, E. Burestedt, S. Ghodabi, M. Smolander, S. Sahni and T. Skotheim, *Adv. Mol. Cell Biol.*, **15B**, 421 (1996).
- 54 B. Liu, R. Hu, J. Deng, *Anal. Chem.*, **69**, 2343 (1997).
- 55 D. Kriz, C. Berggren, A. Johansson and R.J. Ansell, *Instr. Sci. Technol.*, **26**, 45 (1998).

- 56 R. Breslow, *Chem. Biol.*, **5**, R27 (1998).
- 57 P. Buehlmann, E. Pretsch and E. Bakker, *Chem. Rev.*, **98**, 1593 (1998).
- 58 K.P. Xiao, P. Bühlmann, S. Nishizawa, S. Amemiya and Y. Umezawa, *Anal. Chem.*, **69**, 1038 (1997).
- 59 Y. Gufni, H. Weizman, J. Libman, A. Shanzer and I. Rubinstein, *Chem. Eur. J.*, **2**, 759 (1996).
- 60 A. Ion, I. Ion, A. Popescu, M. Ungureanu, J.C. Moutet and E. Saint-Aman, *Adv. Mater.*, **9**, 711 (1997).
- 61 A.P. de Silva, H.Q.N. Gunaratne, T. Gunnlaugsson, A.J.M. Huxley, C.P. McCoy, J.T. Rademacher and T.E. Rice, *Chem. Rev.*, **97**, 1515 (1997).
- 62 I. Chaiken, D. Myszkowski and T. Morton, *Adv. Mol. Cell Biol.*, **15B**, 553 (1996).
- 63 T. Wessa and W. Göpel, *Fresenius J. Anal. Chem.*, **361**, 239 (1998).
- 64 K. Odashima, P. Bühlmann, M. Sugawara, K. Tohda, K. Koga and Y. Umezawa, *Adv. Supramol. Chem.*, **4**, 211 (1997).
- 65 A.L. Ottova and H. Ti Tien, *Bioelectrochem. Bioenerg.*, **42**, 141 (1997).
- 66 A. Ciszewski, G. Milczarek, E. Kubaszewski and M. Lzynski, *Electroanalysis*, **10**, 628 (1998).
- 67 R. Zhou, F. Josse, W. Göpel, Z.Z. Oeztuerk and O. Bekaroglu, *Appl. Organomet. Chem.*, **10**, 557 (1996).
- 68 M.Y.K. Ho and G.A. Rechnitz, *Anal. Chem.*, **59**, 536 (1987).
- 69 D. Kriz, O. Ramström, A. Svensson and K. Mosbach, *Anal. Chem.*, **67**, 2142 (1995).
- 70 A.L. Jenkins, O.M. Uy and G.M. Murray, *Anal. Commun.*, **34**, 221 (1997).
- 71 M.E. Cooper, B.P. Hoag and D.L. Gin, *Polymer Preprints*, **38**, 209 (1997).
- 72 P. Turkewitsch, B. Wandelt, G.D. Darling and W.S. Powell, *Anal. Chem.*, **70**, 2025 (1998).
- 73 J. Matsui, Y. Tachibana and T. Takeuchi, *Anal. Commun.*, **35**, 225 (1998).
- 74 A.L. Jenkins, O.M. Uy and G.M. Murray, *Anal. Chem.*, **71**, 373 (1999).
- 75 L.I. Andersson, A. Miyabayashi, D.J. O'Shannessy and K. Mosbach, *J. Chromatogr.*, **516**, 323 (1990).
- 76 E. Hedborg, F. Winquist, I. Lundström, L.I. Andersson and K. Mosbach, *Sens. Actuators*, **A37–38**, 796 (1993).
- 77 D. Kriz and K. Mosbach, *Anal. Chim. Acta*, **300**, 71 (1995).
- 78 L.I. Andersson, R. Müller, G. Vlatakis and K. Mosbach, *Proc. Natl. Acad. Sci. USA*, **92**, 4788 (1995).
- 79 K. Kriz, N. Debeljak and D. Kriz, *Anal. Chem.*, submitted for publication.
- 80 D. Kriz, M. Kempe and K. Mosbach, *Sens. Actuators*, **B33**, 178 (1996).
- 81 S. Kröger, A.P.F. Turner, K. Mosbach and K. Haupt, *Anal. Chem.*, **71**, 3698 (1999).
- 82 C.-T. Chen, G. Chen, Z. Guan, D. Lee and F.H. Arnold, *Polymer Preprints*, **37**, 216 (1996).
- 83 G. Chen, Z. Guan, C.-T. Chen, L. Fu, V. Sundaresan and F.H. Arnold, *Nature Biotechnol.*, **15**, 354 (1997).
- 84 G. Chen, V. Sundaresan and F.H. Arnold, *Polym. Mater. Sci. Eng.*, **76**, 378 (1997).
- 85 S.A. Piletsky, I. Dubei, D.M. Fedoryak and V.P. Kukhar, *Biopolim. Kletka*, **6**, 55 (1990).
- 86 M. Yoshikawa, J.-I. Izumi, T. Kitao, S. Koya and S. Sakamoto, *J. Membrane Science*, **108**, 171 (1995).
- 87 J. Mathew-Krotz and K.J. Shea, *J. Am. Chem. Soc.*, **118**, 8154 (1996).
- 88 J.-M. Hong, P.E. Anderson, J. Quian and C.R. Martin, *Chem. Mater.*, **10**, 1029 (1998).
- 89 A. Dzgoev and K. Haupt, *Chirality*, **11**, 465 (1999).
- 90 S.A. Piletsky, I.A. Butovich and V.P. Kukhar, *J. Anal. Chem. USSR*, **47**, 1231 (1992).
- 91 S.A. Piletsky, Y.P. Parhometz, N.V. Lavryk, T.L. Panasyuk and A.V. El'skaya, *Sens. Actuators B*, **18–19**, 629 (1994).
- 92 S.A. Piletsky, E.V. Piletskaya, A.V. Elgersma, K. Yano, I. Karube, Y.P. Parhometz and A.V. El'skaya, *Biosens. Bioelectron.*, **10**, 959 (1995).

- 93 S.A. Piletsky, E.V. Piletskaya, T.L. Panasyuk, A.V. El'skaya, R. Levi, I. Karube and G. Wulff, *Macromolecules*, **31**, 2137 (1998).
- 94 T.A. Sergeyeva, S.A. Piletsky, A.A. Brovko, E.A. Slinchenko, L.M. Sergeeva, T.L. Panasyuk and A.V. El'skaya, *Analyst*, **124**, 331 (1999).
- 95 T.A. Sergeyeva, S.A. Piletsky, A.A. Brovko, E.A. Slinchenko, L.M. Sergeeva and A.V. El'skaya, *Anal. Chim. Acta*, **392**, 105 (1999).
- 96 A. Walcarius, C. Despas, P. Trens, M.J. Hudson and J. Bessiere, *J. Electroanal. Chem.*, **453**, 249 (1998).
- 97 G.-J. Li and S. Kawi, *Talanta*, **45**, 759 (1998).
- 98 J. Lin and C.W. Brown, *Trends Anal. Chem.*, **16**, 200 (1997).
- 99 K.S. Alber and J.A. Cox, *Mikrochim. Acta*, **127**, 131 (1997).
- 100 S.-W. Lee, I. Ichinose and T. Kutinake, *Langmuir*, **14**, 2857 (1998).
- 101 S.-W. Lee, I. Ichinose and T. Kutinake, *Chem. Lett.*, 1193 (1998).
- 102 M. Hunnius, A. Rufinska and W.F. Maier, *Microporous Mesoporous Mater.*, **29**, 389 (1999).
- 103 D. Avnir, *Acc. Chem. Res.*, **28**, 328 (1995).
- 104 M.M. Collinson, *Mikrochim. Acta*, **129**, 149 (1998).
- 105 R. Makote and M.M. Collinson, *J. Chem. Soc. Chem. Commun.*, 425 (1998).
- 106 J. Sagiv, *Isr. J. Chem.*, **18**, 346 (1979).
- 107 I. Tabushi, K. Kurihara, K. Naka, K. Yamamura and H. Hatakeyama, *Tetrahed. Lett.*, **28**, 4299 (1987).
- 108 K. Yamamura, H. Hatakeyama, K. Naha, I. Tabushi and K. Kurihara, *J. Chem. Soc. Chem. Commun.*, 79 (1988).
- 109 L.I. Andersson, C.F. Mandenius and K. Mosbach, *Tetrahed. Lett.*, **29**, 5437 (1988).
- 110 J.-H. Kim, T.M. Cotton and R.A. Uphaus, *J. Phys. Chem.*, **92**, 5575 (1988).
- 111 O. Chailapakul and R.M. Crooks, *Langmuir*, **9**, 884 (1993).
- 112 R. Bilewicz and M. Majda, *J. Am. Chem. Soc.*, **113**, 5464 (1991).
- 113 N.F. Starodub, S.A. Piletsky, N.V. Lavryk and A.V. El'skaya, *Sens. Actuators B.*, **13-14**, 708 (1993).
- 114 M. Morita, Y. Iwasaki, T. Horiuchi and O. Niwa, *Denki Kagaku*, **64**, 1239 (1996).
- 115 M. Morita, O. Niwa and T. Horiuchi, *Electrochim. Acta*, **42**, 3177 (1997).
- 116 M. Lahav, E. Katz, A. Doron, F. Patolsky and I. Willner, *J. Am. Chem. Soc.*, **121**, 862 (1999).
- 117 N. Kodakari, T. Sakamoto, K. Shinkawa, H. Funabiki, N. Katada and M. Niwa, *Bull. Chem. Soc. Jpn.*, **71**, 513 (1998).
- 118 G. Wulff, B. Heide and G. Helfmeier, *J. Am. Chem. Soc.*, **108**, 1089 (1986).
- 119 O. Norrlöw, M.-O. Månsson and K. Mosbach, *J. Chromatogr.*, **396**, 374 (1987).
- 120 M.S. Boeckl, T. Baas, A. Fujita, K.-O. Hwang, A.L. Bramblett, B.D. Ratner, J.W. Rogers and T. Sasaki, *Biopolymers*, **47**, 185 (1998).
- 121 V.M. Mirsky, T. Hirsch, S.A. Piletsky and O.S. Wolfbeis, *Angew. Chem. Int. Ed. Engl.*, **38**, 1108 (1999).
- 122 A. Deronzier and J.-C. Moutet, *Curr. Top. Electrochem.*, **3**, 159 (1994).
- 123 S.J. Higgins, *Chem. Soc. Rev.*, **26**, 247 (1997).
- 124 H. Shinohara, M. Aizawa and H. Shirawaka, *J. Chem. Soc. Chem. Commun.*, 87 (1986).
- 125 E.C. Hernandez, C. Mortensen and G.L. Bachas, *Electroanalysis*, **9**, 1049 (1997).
- 126 J. Wang, S.-P. Chen and M.S. Lin, *J. Electroanal. Chem.*, **273**, 231 (1989).
- 127 L.D. Spurlock, A. Jaramillo, A. Praserttham, J. Lewis and A. Brajter-Toth, *Anal. Chim. Acta*, **336**, 37 (1996).
- 128 G. Bidan, B. Divisia-Blohorn, M. Lapkowski, J.-M. Kern and J.-P. Sauvage, *J. Am. Chem. Soc.*, **114**, 5986 (1992).
- 129 E. Pringsheim, E. Terpetschnig, S.A. Piletsky and O.S. Wolfbeis, *Advanced Mater.*, **11**, 865 (1999).
- 130 C. Malitesta, I. Losito and P.G. Zambonin, *Anal. Chem.*, **71**, 1366 (1999).
- 131 S. Daunert, S. Wallace, A. Florido and L.G. Bachas, *Anal. Chem.*, **63**, 1676 (1991).

- 132 V. Campo Dall'Orto, C. Danilowicz, S. Sobral, A. Lo Balbo and I. Rezzano, *Anal. Chim. Acta*, **336**, 195 (1996).
- 133 S. Trevin, F. Bedioui and J. Devynck, *Talanta*, **43**, 303 (1996).
- 134 X.Z. Wu, Y.J. Li, B. Gruendig, N.T. Yu and R. Renneberg, *Electroanalysis*, **9**, 1288 (1997).
- 135 T. Panasyuk, V. Campo Dall'Orto, G. Marraza, A. El'skaya, S. Piletsky, I. Rezzano and M. Mascini, *Anal. Lett.*, **31**, 1809 (1998).
- 136 D. Kriz, L.I. Andersson, M. Khayyami, B. Danielsson, P.-O. Larsson and K. Mosbach, *Biomimetics*, **3**, 81 (1995).
- 137 Y. Okahata, K. Yasunaga and K. Ogura, *J. Chem. Soc. Chem. Commun.*, 469 (1994)
- 138 F.L. Dickert, P. Forth, P. Lieberzeit and M. Tortschanoff, *Fresenius J. Anal. Chem.*, **360**, 759 (1998).
- 139 M.A. Craven, J.W. Gardner and P.N. Bartlett, *Trends Anal. Chem.*, **15**, 486 (1996).
- 140 F. Winkvist, P. Wide and I. Lundström, *Anal. Chim. Acta*, **357**, 21 (1997).
- 141 J.J. Lavigne, S. Savoy, M.B. Clevenger, J.E. Ritchie, B. McDoniel, S.-J. Yoo, E.V. Anslyn, J.T. McDevitt, J.B. Shear and D. Neikirk, *J. Am. Chem. Soc.*, **120**, 6429 (1998).

## **Ionic sensors based on molecularly imprinted polymers**

GEORGE M. MURRAY AND O. MANUEL UY

### **19.1 INTRODUCTION**

The application of imprinted polymers to chemical sensing has been eagerly sought. Until recently, few successes have occurred and most of the published accounts for 'sensors' have described phenomena that may lead to a sensing device, not actual devices. While the production of recognition sites is relatively advanced, sensing has remained elusive. The difficulty in making sensors with imprinted polymers resides in finding a sensitive means by which chemical recognition can be coupled to signal transduction. The association between the polymer and the molecular, or ionic, template must produce a distinct physical or chemical change that can be measured with high precision. Unlike gas sensors, ionic sensing must be performed in solution. Mass-sensitive devices such as the quartz crystal microbalance or surface acoustic wave sensors (SAWs) cannot usually be employed. The two major methods used for signal transduction in ionic sensors are based on electrochemical and spectroscopic properties. A third approach for the rapid and selective determination of ions is flow injection analysis (FIA), which may involve molecular imprinting. This would likely be a system that uses the imprinted polymer for selective removal and pre-concentration of a target analyte. Detection schemes employed for FIA are still primarily broad range electrochemistry or spectroscopy.

The production of polymers exhibiting selective binding of a specific cation involves the formation of cavities equipped with complexing groups or 'ligands' so arranged as to match the charge, coordination number, coordination geometry and size of the target cation (see also Chapter 9). Anion-complexing polymers are made in a similar manner, but they often employ a coordinatively captured metal ion that has a large affinity for the anion in question and also provides a spectroscopic signature for anion binding. These cavity-containing polymers are produced using a specific ion as a template around which monomeric-complexing ligands are self-assembled and later polymerised. The complexing ligands are selected with the functional groups known to form stable complexes with a target ion and less stable ones with other ions. Larger organic ions may be approached using metal ion binding or, more commonly, using complementary organic functionalities (see Chapter 6).

Selectivity in ionic sensing is expected to be highest when the target analyte is a polyatomic ion. This allows a polymer to be constructed that will possess multiple

points of contact, yielding several geometric and size constraints on the imprinted site. However, the more complex the analyte ion, the more difficult it becomes to design a self-assembling complex that will result in a selective polymer. Conversely, the simpler metal ions easily form self-assembled polymerisable complexes, but impose severe restrictions on the choice of matrix monomers to avoid creating sites for non-specific binding. The combination of imprinting and transduction selectivities can result in sensors that are less likely to respond to interfering species. In certain cases, enough criteria of selectivity may be available to achieve the most favourable sensing situation, i.e. exclusivity.

## **19.2 SYNTHESIS OF ION-SELECTIVE MOLECULARLY IMPRINTED POLYMERS (MIPs)**

The process of producing an ion-sensing polymer includes the following steps: (i) selection and preparation of ligand monomers, (ii) synthesis of ion complexes of the monomers or linear copolymers of the complexing monomers, (iii) preparation of cross-linked copolymers with the monomeric complexes or linear copolymer complexes, (iv) the testing of the polymers for ion selectivity, (v) optimisation of polymer ionic selectivity and (vi) the use of the polymers in the construction of ion-selective electrodes (ISEs) and optical sensors.

### **19.2.1 Monomer selection and preparation**

The selection of monomers is contingent on the avenue of sensing. For an ion-selective optrode (optode) detecting the analyte with an intrinsic chromophore, the only requirements are binding affinity and stability. When, on the other hand, the polymer matrix is responsible for the optical signal, the selection is more complex, since selective binding has to be ensured at a site that influences the chromophore. Ligands for metals can be chosen that increase the metal ion's molar absorptivity or yield a coloured complex, such as  $\text{Pb}^{2+}$  with dithizone. Metal ions that do not exhibit colour can be coordinated by ligands that form fluorescent complexes, such as  $\text{Zn}^{2+}$  with benzoin. When the imprinted site is designed to sense a heavy metal ion, a fluorescent ligand may be induced to phosphoresce, *via* the external heavy atom effect, yielding a longer-lived band that is Stokes shifted. In the case of anions, it may be useful to choose a luminescent metal ion as a component of the binding site to acquire both a thermodynamic binding affinity and a suitable chromophore. In most cases, non-polymerisable analogues (lacking the vinyl groups) of the prospective ligands can be used for screening since vinyl substitution usually has little effect on the binding affinity or spectral properties of the compounds.

The selection of appropriate monomers requires a knowledge of ion association. Since selectivity is of primary interest in sensor development, the complexation need not be overly large as long as a substantial difference exists between the target and most other ions. A very useful compilation of association data is found in

Sillen and Martell's *Stability constants of metal-ion complexes* [1]. This compilation is sufficiently comprehensive to show data for a variety of ligands and generally includes either the proposed ligand or a very similar compound. There is also sufficient information to investigate selectivity for a diverse collection of metals, providing clues to selectivity. Other compendia of data are available, such as the *CRC handbook* and Yatsimirskii and Vasiliev's, *Instability constants of complex compounds* [2]. An especially useful source of data on complex compounds is Gmelin and Meyer [3].

### 19.2.2 Preparation of complexes

The synthesis of metal ion complexes with polymerisable ligands is relatively straightforward. With a careful choice of complexing ligands, this is accomplished by mixing stoichiometric amounts of a metal salt and the complexing ligand in an aqueous or alcoholic solution and evaporating to near dryness. Our experience with making complexes shows that water or alcohol/water mixtures of the metal and ligand in stoichiometric ratios, evaporated to dryness, result in near quantitative yield of many complex compounds. Linear copolymer complexes of metal ions can be prepared in a similar fashion and are more easily precipitated from aqueous solutions.

### 19.2.3 Preparation of polymers

Metal ion-binding polymers and metal ion-containing anion-binding polymers are made in a similar fashion. There are two approaches to the creation of an ion-selective imprinted polymer based on metal ion coordination. One approach relies on the imprinting process to provide the geometric arrangement needed for complexation of a specific ion. In this approach, the ligand monomers are little more than vinyl-substituted ligating functional groups attached to a supramolecular polymeric support. The second approach is to use a chelator or a macrocyclic ligand that already has geometric constraints predisposed to a certain metal ion size or coordination geometry. The imprinting process is then used to make small changes in the geometry to enhance the selectivity. The primary resource for information about any MIP is the database of the Society for Molecular Imprinting maintained by Håkan Andersson. The efforts of Lars I. Andersson, Ian A. Nicholls, Olof Ramström (Sweden), Andrew G. Mayes, Joachim Steinke, Richard J. Ansell, Michael J. Whitcombe (UK) and Sergey A. Piletsky (Ukraine) have contributed to the usefulness of this extensive database that can be accessed at <http://www.ng.hik.se/~SMI/SMIbase.htm>.

There are two variations of the first technique (see also Chapter 9). The two approaches differ in the sequence of the steps to make a polymer. In the first version, a linear copolymer is produced, allowed to complex metal ions and then cross-linked to obtain rigidity and site preservation. Examples of this approach are found in some of the works of the groups of Kabanov [4] and Nishide [5]. The Kabanov group prepared a linear polymer with equal amounts of diethyl



vinyl-phosphonate and acrylic acid. This polymer was then equilibrated with  $\text{Cu}^{2+}$  ions and the resulting compound separated. The copper complex was cross-linked with *N,N'*-methylene diacrylamide (for structure see Chapter 9). The  $\text{Cu}^{2+}$  ions were subsequently desorbed from the cross-linked polymer with 1 N acid. The Nishide group prepared poly(4-vinylpyridine) and equilibrated the polymer with  $\text{Cu}^{2+}$  ions (for structure see Chapter 9). The resulting complex was cross-linked using 1,4-dibromobutane and acid-washed to remove the  $\text{Cu}^{2+}$  ions. Polymers of this type were also prepared using  $\text{Fe}^{3+}$ ,  $\text{Co}^{2+}$ ,  $\text{Cd}^{2+}$  and  $\text{Zn}^{2+}$  ions and in the absence of cations. The metal ion used as a template was then taken up more effectively and preferentially by a given polymer than the other ions. Visible spectral and equilibrium data indicated that the association constant of the  $\text{Cu}^{2+}$  complex with the  $\text{Cu}^{2+}$ -conditioned polymer was higher than with the other cation-conditioned and the non-conditioned polymers. The investigators concluded that the ligand positions in the conditioned polymers were maintained at the optimum conformation for the template cation. Similar experiments were conducted with poly(1-vinylimidazole) and 1-vinyl-2-pyrrolidone using  $\text{Ni}^{2+}$ ,  $\text{Co}^{2+}$  and  $\text{Zn}^{2+}$  with comparable results.

The second variation on the technique is to form metal ion complexes with polymerisable ligands and to copolymerise the complexes in the presence of a cross-linker and a non-complexing matrix monomer. Examples of this approach are the works of Kuchen and Schram [6] (for structure see Chapter 9), Harkins and Schweitzer [7] and our own efforts [8]. This approach may be preferable for sensor applications since all sites are imprinted and there is less chance of making sites that would allow non-specific binding. The risk in pursuing this path is that metal complexation may adversely affect the reactivity of the monomer toward copolymerisation. To our knowledge, this problem has not been reported with simple monomer ligands, but has been shown with macrocyclic ligands [9].

Another technique for preparing metal ion coordinating polymers, involving coordinating ligands possessing inherent geometric constraints, has been pursued by the groups of Arnold [10] and Fish [9]. Both groups used vinyl-substituted forms of the ligand 1,4,7-triazacyclononane (TACN) (for structures see Chapter 9). The ligand was functionalised using 4-vinylbenzyl chloride to produce mono- and (in Fish's case) tri-substituted derivatives. Fish and his co-workers made polymers that were intended as sequestering agents. The imprinting process was able to change the affinity sequence from that of the free ligand for metal ion binding. The polymers produced exhibited rapid exchange kinetics and the monomer complex's single crystal X-ray structure was given. Arnold's group used the  $\text{Cu}(\text{styryl-TACN})^{2+}$  complex to prepare an imprinted site for glucose (see also Chapter 18). The glucose-selective polymer will be discussed in greater detail below. Both groups were unable to polymerise the  $\text{Cu}(\text{styryl-TACN})^{2+}$  without another ligand coordinating  $\text{Cu}^{2+}$ . This is thought to be due to electron transfer from the carbon radical chain to  $\text{Cu}^{2+}$  quenching the chain growth.

In many cases, the steps involved in the production of the polymerisable complex are given in the literature for the non-vinyl-substituted ligand analogues. There is a sizeable literature on metal-containing polymers. Metal ion inclusion can affect

reactivity ratios and care must be taken to select complexes that will incorporate well into the polymeric matrix. Optical sensing strategies tend to limit the relative loading of the chromophoric complex in the copolymer to avoid spectral broadening and self-quenching in the case of luminescence. This requires inclusion of a non-coordinating matrix monomer, i.e. one that will not result in non-specific binding sites. The avoidance of non-specific binding sites is the key to making a selective sensor. This is especially important in the area of metal ion sensing with an ISE because most polar functional groups exhibit metal ion affinity.

A common requirement for the production of an imprinted polymer is adequate cross-linking. The conventional approach has been to use a large amount of cross-linker, thus making the cross-linking monomer the bulk of the copolymer. When used with a large amount of porogen, highly cross-linked polymers have been reported to show high capacity and fast exchange kinetics for metal ions. Another approach uses lower levels of cross-linking without a porogen. In this case, the polymers produced are only surface-active and should exhibit faster exchange kinetics. While speed is an issue in sensing, the main reason for this approach is to reduce mechanical stresses and strains on the coordination site. In this way, when the metal ion is desorbed, the distortion of the resulting cavity should be minimised. Again, the purpose is to avoid the production of non-specific binding sites that could adversely affect sensor selectivity. A common side benefit is that the polymers are less crystalline and exhibit better optical properties.

### 19.2.4 Testing for selectivity

For metal ion sensors, the selectivity is usually evaluated by the relative capacities for binding competing metals. This is done employing batch extraction for measuring the uptake of various cations by a polymer prepared with a given cation. The exchange equilibria are approximated by measuring the capacity of the resin for the various cations involved in the following general reaction:



where HR represents the protonated resin and  $M^{n+}$  represents the metal ion. The steps involved in acquiring both capacity data and the equilibrium constant are given in Fig. 19.1. The data acquired in Fig. 19.1 are also used in the equation (3) to calculate the metal ion capacity and selectivity parameters. The quantities in the equations are derived from the solutions obtained by following the steps in the procedure as outlined in Fig. 19.1. For example,  $V_1$  is the total volume of the extracting solution,  $[M^{2+}]_1$  is the concentration of divalent metal ion in the first extracting solution,  $V_2$  is the volume of solution used to obtain  $M_1$ , etc.

$$capacity = \frac{[M^{2+}]_1 V_2 + [M^{2+}]_2 V_3}{W_1} \quad (2)$$

$$K = \frac{[H^+]^2 (capacity - [M^{2+}]_1 V_1/W_1)}{[M^{2+}]_1 (2[M^{2+}]_1 V_1/W_1)^2} \quad (3)$$

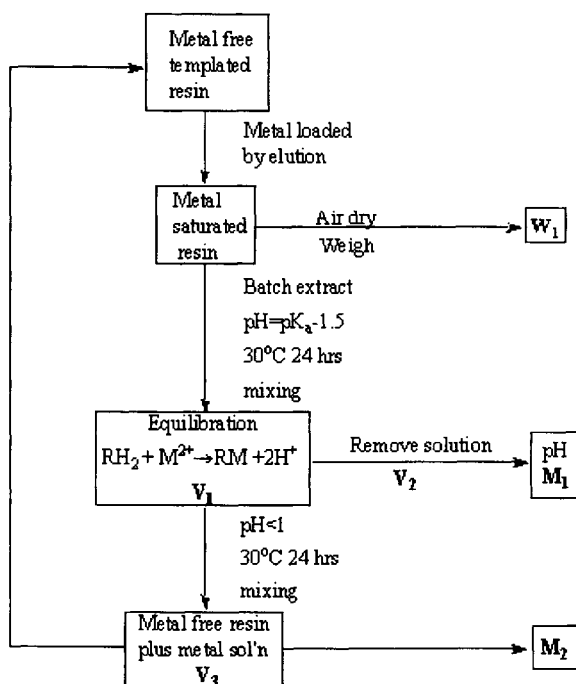


Fig. 19.1. Steps involved in ascertaining resin capacity.

$$\alpha_{M_1, M_2}(\text{selectivity}) = \frac{\text{capacity } M_1}{\text{capacity } M_2} \quad (4)$$

In addition to the cation used to prepare the polymer, other cations with differing charges, sizes, coordination numbers and/or coordination geometries are used in these selectivity quotient measurements to verify specificity. Measurements are also made using polymers prepared with no metal cation ( $H^+$  or  $NH_4^+$ ) as experimental controls. The measurements required for these studies are made using a pH meter for  $[H^+]$  and elemental analysis (inductively coupled plasma atomic emission spectrometry (ICP-AES) or inductively coupled plasma mass spectrometry (ICP-MS)) for  $[M^{n+}]$ .

One useful aspect of the ISE approach is the ease with which selectivity testing can be performed. Once the polymer is employed as the active ingredient in a polymer membrane electrode, the binding can be examined by measuring the potential of a cell as outlined below. We have seen that the selectivity obtained by batch extraction procedures gives the same affinity series as that measured by using the polymer in an electrode [11].

## 19.3 ELECTROCHEMICAL SENSORS

### 19.3.1 Conductivity

The simplest electrochemical approach to ion sensing that could employ imprinted polymers is to measure changes in polymer conductivity with ion binding. Binding ions to an organic polymer could increase conductivity by increasing the degree of conjugation. Wang and Wasielewski [12] suggested using bipyridyl components in a polymer backbone to produce metal ion-induced conjugation enhancement. Combining molecular imprinting to this approach should enhance selectivity. Piletsky *et al.* [13] produced conductometric sensors for the pesticide atrazine. While the analyte is not necessarily an ion, the mode of interaction with the sensor was suspected to be a function of the reorganisation of the polymer when the analyte was rebound, thus affecting the diffusion of co- and counter ions.

### 19.3.2 ISEs

Another approach to electrochemical transduction by chemical recognition is the incorporation of the imprinted polymer as the active ingredient in a membrane of an ISE. ISEs are devices which, when incorporated in an electrochemical cell with an appropriate reference electrode, produce a potential that varies predictably with the concentration of a certain ion in solution. If the response of the electrode follows theory, the response is Nernstian and is given by the Nernst equation:

$$E = K - \frac{RT}{nF} \ln \frac{\alpha^{ext}}{\alpha^{int}} \quad (5)$$

where  $E$  is the measured potential,  $K$  denotes an experimentally derived constant,  $R$  the gas constant,  $T$  the absolute temperature,  $n$  is ionic charge,  $F$  is Faraday's constant and the  $\alpha$ 's are the activities of the analyte ion in the external and internal (electrode filling) solutions. Inserting the numerical values of the constants, assuming room temperature, and changing logarithms to the base 10, the equation simplifies to:

$$E = K - 0.0592/n \log (\alpha) \quad (6)$$

and so the useful cell potential is:

$$E_{cell} = K - 0.0592/n \log (\alpha) - E_{ref} \quad (7)$$

ISEs are selective but not exclusive, so they may respond to other chemically similar ions and careful control of the cell contents is usually required. MIPs provide a means for selectivity enhancement and it is likely that electrodes made using imprinted polymers may more closely approach the exclusivity desired in such a device. A calibration plot for a typical imprinted polymer ISE is given in Fig. 19.2.

ISEs were first fabricated using crystalline materials. The selectivity was obtained using crystals that were sparingly soluble salts of the ion of interest. Later,

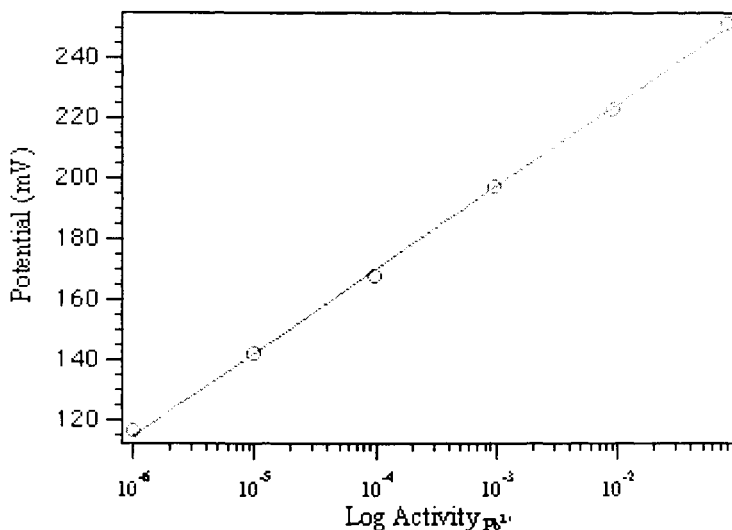


Fig. 19.2. The potential response of an imprinted polymer ISE for  $Pb^{2+}$  used in a cell with an Ag/AgCl reference electrode. The slope is 27.6 mV/decade and the line fitted to the data gives a correlation constant,  $r = 0.9996$ .

electrodes were fabricated from a variety of ion exchange materials. These materials were either liquid ion exchangers or selective ionophores dissolved in a polymer membrane. Size selectivity for certain ions was obtained by the use of crown ether ionophores. Crown ethers are useful for complexing hard metal ions or metal ions without directed bonding. Electrodes made using crown ethers have proven to be highly selective and show that ionic size plays an important role in ionic sensors. The basic crown is frequently modified by the addition of substituents, either to add ligating atoms or, more often, to strain the crown ring to effect slight changes in the size of the cavity. Using molecular imprinting is an obvious next step to more accurately set the cavity size for a specific ion.

Most polymer membrane ISEs are prepared by dissolving an ionophore in a polyvinylchloride (PVC) membrane. A large variety of plasticisers are used to increase the dielectric constant of the PVC and improve its hydrophilicity. Some membranes have complexes of the ions to be sensed to increase membrane conductivity, such as potassium tetraphenylborate in  $K^+$ -selective membranes. There is an extensive literature on the arcane arts of polymer membranes for electrodes with dissolved ionophores and a good review of this is given by Professor Ronald Armstrong in Section 3.7 of Gábor Harsányi's book, *Polymer films in sensor applications* [14].

The performance of electrodes is investigated by measuring the e.m.f. values produced by metal ion solutions at different activities. The activities of the metal ions are based on the activity coefficient ( $\gamma$ ) calculated from the modified form of the Debye-Hückel limiting law:

$$\log \gamma_{\pm} = -0.511 \times Z^2 \times \left[ \frac{\sqrt{I}}{1 + 1.5 \times \sqrt{I}} - 0.2 \times I \right] \quad (8)$$

where  $I$  is the ionic strength, and  $Z$  is the valence of the metal ion. For routine applications the ion concentration can be used in the place of activity.

The selectivity of ISEs is evaluated by calculating selectivity coefficients. Over the years, several different methods have been used to obtain these coefficients, the most common being the separate solution method, the fixed interference method [15] and the matched potential method [16]. In the separate solution method, the potential response is determined in each of the two separate solutions, one containing only the primary ion at an activity  $a_I$  and the other containing only the interfering ion at an activity  $a_J = a_I$ . The selectivity coefficient or the relative response of the electrode to the two ions I and J,  $K_{IJ}^{\text{pot}}$  is calculated from the following equation:

$$\log K_{IJ}^{\text{pot}} = \frac{E_J - E_I}{2.303 RT/z_I F} + (1 - z_I/z_J) \log a_I \quad (9)$$

where  $a_I$  is the activity of ion I,  $E_I$  and  $E_J$  are the measured electromotive forces for ions I and J, with  $z_I$  and  $z_J$  as their respective charges.

In the fixed interference method, the potential response is measured using solutions containing a constant activity of interfering ion J in the mixture of ions I and J. This is symbolised as  $a_J$  (IJ), the constant interferent ion activity in the mixture of I and J and  $a_I$  (IJ) the varying activities of the primary ion in the mixture of I and J. The potential values obtained are plotted against the activity of the primary ion. The intersection obtained from the extrapolation of the linear portions of this curve will indicate the value of  $a_I$  (IJ) that is to be used to calculate  $K_{IJ}^{\text{pot}}$  from the following:

$$K_{IJ}^{\text{pot}} = \frac{a_I(I)}{[a_J(J)]^{z_I/z_J}} \quad (10)$$

The selectivity coefficient in the matched potential method is defined as the activity ratio of primary and interfering ions which results in the same potential change as in a reference solution:

$$K_{IJ}^{\text{pot}} = \Delta a_I / a_J \quad (11)$$

where  $\Delta a_I = a'_I - a_I$ ,  $a_I$  is the initial background activity of primary ion in the reference solution,  $a'_I$  is the final activity of primary ion and  $a_J$  is the interfering ion activity which gives the same amount of potential change in the reference solution as  $\Delta a_I$ . The matched potential method is the method currently recommended by the International Union of Pure and Applied Chemistry (IUPAC) [17], but the other methods are commonly found in the literature and are sometimes used to make a direct comparison of electrode performances.

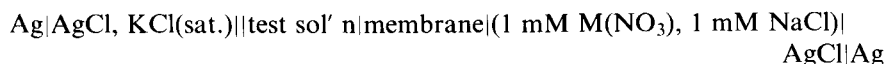
### 19.3.3 Imprinted polymer ISEs

The first imprinted polymer ISEs were prepared for calcium and magnesium ions by Mosbach's group [18]. The monomer used in the fabrication of the electrode was

a neutral ionophore *N,N'*-dimethyl-*N,N'*-bis(4-vinylphenyl)-3-oxapentadiamide. This was chosen as a  $\text{Ca}^{2+}$ -selective ionophore to produce a polymer cavity that would resemble a polyether site with imprinting being the means to acquire size selection (for structure see Chapter 9). The imprinting process enhanced the selectivity for  $\text{Ca}^{2+}$  by factors of 6 and 1.7 on  $\text{Ca}^{2+}$  binding using  $\text{Ca}^{2+}$  – and  $\text{Mg}^{2+}$  – imprinted polymers respectively, over an unimprinted polymer blank, as measured by batch extraction. A calibration curve (slope 27.15 mV/decade) and selectivity coefficients against alkali metals and alkaline earth metals for the  $\text{Ca}^{2+}$  electrode was provided. The membranes were prepared using a mixture of 32.1 wt% PVC, 65.3 wt% bis(2-ethylhexyl) sebacate, 1.85 wt% imprinted polymer and 0.7 wt% potassium tetrakis (*p*-chlorophenyl)borate. The electrode was evaluated with metal chloride solutions in a 1:1 methanol–water mixture (v/v) at an unspecified pH. The cell schematic was:



We have prepared ISEs for  $\text{Pb}^{2+}$  [19] and  $\text{UO}_2^{2+}$  [20]. The complex is illustrated in Fig. 19.3. The  $\text{Pb}^{2+}$  electrode was based on a  $\text{Pb}^{2+}$ -imprinted polymer that had been characterised previously as an ion exchange resin [8] and applied to the analysis of trace amounts of  $\text{Pb}^{2+}$  in seawater [21]. The uranyl ion electrodes were prepared from two polymers: one employing vinylbenzoate and the other vinylsalicylaldoxime as ligand (Fig. 19.4). Typical membranes were prepared by mixing 90 mg of PVC powder and 30 mg of imprinted polymer particles with 0.2 mL of plasticiser, either 2-nitrophenyl octyl ether or dioctyl phenylphosphonate. The tested electrodes were filled with 1 mM metal nitrate solution and 1 mM NaCl internal solution and conditioned for 24 h by soaking in a 1 mM  $\text{M}(\text{NO}_3)$  solution. Our measurements were made with a model 350 Corning pH/ion Analyzer. Rapid response was facilitated by the use of a high flow Ag/AgCl reference electrode, manufactured by Orion. The cell schematic was thus:



Although not an ion, glucose can be detected by virtue of an MIP-derived ion. The pH electrode is simply an ISE for  $\text{H}^+$ . Glass and ion-selective field effect transistors pH electrodes are the best characterised and the most successful ISEs. Many sensors employ chemical reactions to produce  $\text{H}^+$  or  $\text{OH}^-$  ions and employ pH electrodes for signal transduction. An imprinted sensor based on this approach is the glucose sensor produced by Arnold's group [10]. This polymer employs a metal ion ( $\text{Cu}^{2+}$ ) in the imprinted site and makes use of the metal's

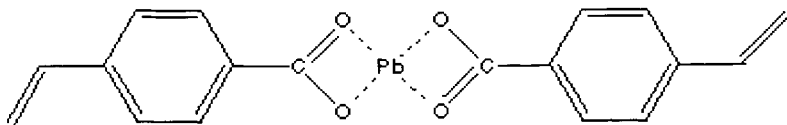


Fig. 19.3. Drawing of  $\text{Pb}(\text{vinylbenzoate})_2$ .

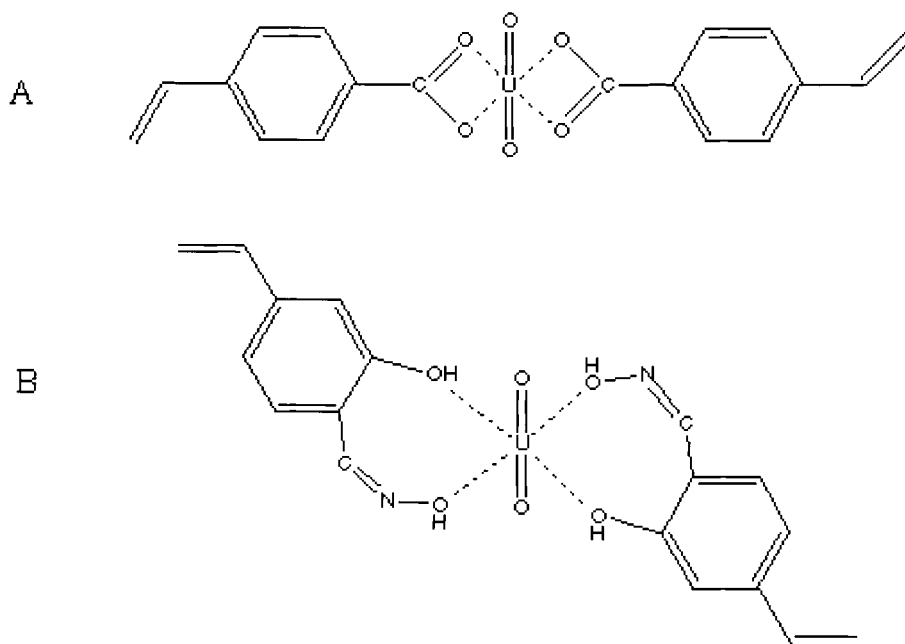


Fig. 19.4. Drawing of (A)  $\text{UO}_2(\text{vinylbenzoate})_2$  and (B)  $\text{UO}_2(\text{vinyl salicylaldoxime})_2$ .

directed bonding to obtain enhanced chemical selectivity (see Fig. 18.5 in Chapter 18). The imprinted polymer was synthesised using methyl- $\beta$ -glucopyranoside. The imprinting molecule is removed by replacement with  $\text{OH}^-$ . At pH above 8, the  $\text{Cu}^{2+}$  complex has water and hydroxide bound to the two coordination sites formerly occupied by the imprint molecule. At slightly higher pH values ( $>9$ ) glucose readily replaces the water and  $\text{OH}^-$ , liberating  $\text{H}^+$ . The increase in  $\text{H}^+$  is then measured and is proportional to the amount of glucose in solution. The pH change can be measured by a pH electrode or, alternatively, by a colorimetric or fluorimetric dye.

## 19.4 SPECTROSCOPIC SENSORS

Spectroscopic sensing requires that a chromophore must be available and be influenced by the rebinding of the imprinted analyte. This can be accomplished in a variety of ways, the simplest case being when the analyte is itself a chromophore. Sensors based on intrinsic analyte chromophores can benefit from molecular imprinting by both selectivity and sensitivity enhancement. In terms of selectivity, molecules similar to the analyte are likely to have similar spectroscopic parameters that could be the source of interference in a conventional sensing strategy. The inability of an interferent to bind to the imprinted polymer allows discrimination.



In terms of sensitivity, the analyte molecules can be effectively concentrated from the solution by the imprinted polymer. The degree of such concentration is controlled by the relevant binding constant. The target chromophore can be shielded from quenchers by the polymer matrix. The inclusion of non-complexing monomers isolates the chromophore, eliminates cross-talk and reduces concentration quenching. In the case of metal ion luminescence, the use of appropriate complexing ligands can enhance the intensity by several orders of magnitude through a variety of mechanisms.

#### **19.4.1 Transition metal ion chromophores**

Many metal ions are intrinsic chromophores and can be sensed by absorbance or luminescence. The transition metals exhibit colours based on inter-configurational d-electron transitions. The intensity and the positions of the spectral bands can be influenced with a judicious choice of coordinating ligand. The molar absorptivities are less than those of organic chromophores due to the 'forbidden' nature of the inter-configurational transitions, but the correct choice of coordinating ligands can improve the absorptivity. A variety of metal ion-sensing devices are based on the incorporation of an organic ligand dissolved in a polymer membrane. The film is then placed in a holder that is connected to optical fibres so that the colour can be registered with a remote spectrophotometer. An absorbance probe and a film employing a dithizone as the colorimetric reagent to measure the combination of a variety of soft metals is commercially available from Ocean Optics, Dunedin, FL, USA. It is a simple matter to exchange an imprinted polymer film and acquire a selective means for measuring a metal ion at trace levels.

The transition metals that do not possess intrinsic colour sometimes form coloured complexes, such as  $\text{Pb}^{2+}$  with the above mentioned dithizone ligand (Fig. 19.5). More importantly, from the stand point of sensitivity, colourless metal ions are compatible with organic ligands that luminesce. A large number of metal ion analyses rely on fluorimetry or phosphorimetry. In general, the coordination of a metal ion by an organic ligand results in changes in the degree of conjugation or planarity of the organic ligand. For fluorimetry, two factors limit the number of transition metal ions that form fluorescent chelates [22]. Many of the ions are paramagnetic allowing inter-system crossing to the triplet state with the possible result of phosphorescence. This situation is often labelled the 'external heavy atom effect'. The second factor is that the energy levels possessed by these ions may be closely spaced, leading to non-radiative decay. The first case can be advantageous to sensing, since the phosphorescence is generally red-shifted with respect to ligand fluorescence and the radiative lifetime is elongated, providing an opportunity for time resolution as another criterion of selectivity. Fluorimetric metal ion analyses are very sensitive but are prone to chemical interferences. The inclusion of molecular imprinting as a means to reduce interferences can result in highly sensitive and selective analyses. For example, Borovik's group has made an imprinted polymer based on a  $\text{Cu}^+$  complex that undergoes a dramatic colour change upon binding NO [23].

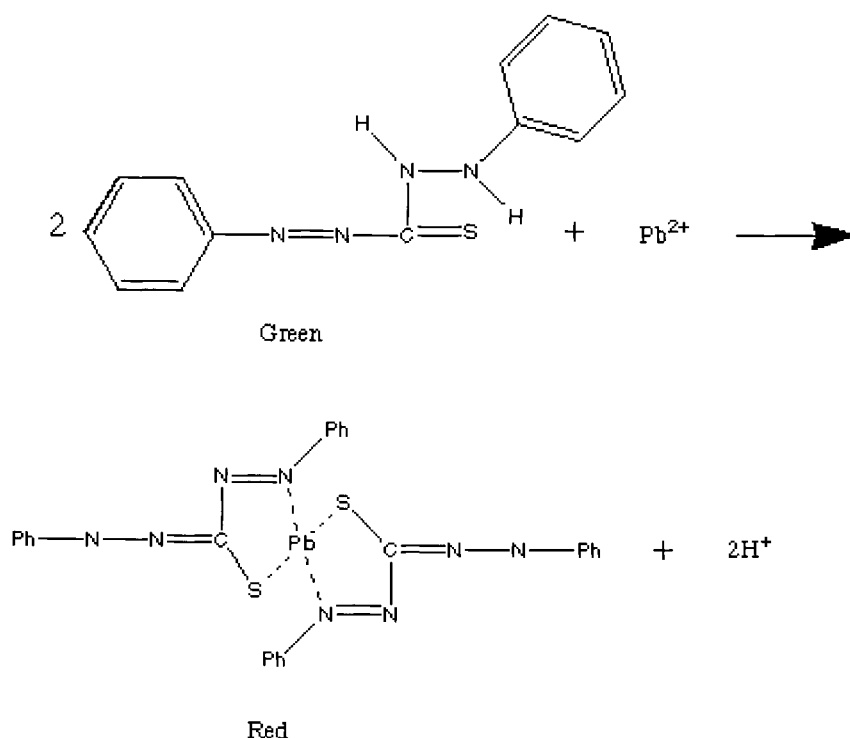


Fig. 19.5. Illustration of the mechanism of the colour change when  $\text{Pb}^{2+}$  is complexed by dithizone.

#### 19.4.2 Lanthanide ion chromophores

Lanthanide ions are useful as intrinsic and extrinsic chromophores. While it would be extremely difficult to imprint a polymer for a selected lanthanide ion, due to their hardness and lack of directed bonding, the use of a coordinatively captured lanthanide as a transducer for ligand binding has proved to be useful. Complexation by certain organic ligands enhances the luminescence intensity of the tripositive lanthanide  $\text{Ln(III)}$  ions. The enhancement of luminescence has been explained by a ligand to metal energy transfer mechanism. This mechanism was derived from a series of investigations by Crosby, Kasha and their co-workers [24]. Generally, when an excited triplet state of the coordinating ligand overlaps a lanthanide-excited electronic level, the lanthanide luminescence can be effectively pumped by a larger cross-section molecular absorbance, rather than by its own weak absorbance. This process is said to be much more efficient than direct absorption of light by the lanthanide, due to the poor absorptivities of the lanthanides (formally atomically forbidden absorbance for the intra-configurational  $f \rightarrow f$  transition).

Recognising the analytical potential of the influence which near neighbours (the analytes) have on the spectra of the lanthanide ions and realising that sensitivity and selectivity could be greatly enhanced by tuneable laser excitation, John C. Wright began important research in 1975 [25]. The major problem faced was the reproducible introduction of the analyte into the near environment of the lanthanide ion. He approached this problem by investigating the use of inorganic crystalline compounds as carriers of both the lanthanide probe ion and the analyte ion. We have approached this problem using organic coordinating ligands to immobilise the lanthanide ion and applied molecular imprinting to define the analyte association.

A large number of organic ligands have been used to enhance lanthanide luminescence intensity. When making an imprinted polymer sensor, the ligands must be chosen with sufficient affinity for the lanthanide so as to coordinatively hold the ion in the polymer as well as provide intense luminescence. Many mixed ligand lanthanide complexes have been studied, providing clues to how to make a suitable sensor. Lanthanide ions have a thermodynamic affinity for a variety of anions and this affinity can be exploited in making sensors for anions. Due to the relative hardness of lanthanides, the geometry of ligating atoms is a function of the steric strains imposed by the coordinating ligands. This is another avenue of exploitation for selectivity, since a careful selection of coordinating ligand can help define the line splitting by imposing a specific site symmetry on the lanthanide in the resulting compound. By imposing a certain coordination geometry on a complex, a large degree of change can be made to occur by ligand exchange, ensuring a significant change in the luminescence spectrum upon substitution.

We have prepared a variety of  $\text{Eu}^{3+}$  complexes with either a labile anion or a labile inorganic cation. Three series of compounds have been investigated. The first series was  $\text{Eu}(\text{1,10-phenanthroline})_2\text{X}_3$  (where  $\text{X} = \text{Cl}^-$ ,  $\text{NO}_3^-$ , acetate and benzoate), and the second was  $\text{M}[\text{Eu}(\text{benzoylacetone})_4]$  (where  $\text{M} = \text{Na}^+$ ,  $\text{K}^+$ ,  $\text{Rb}^+$  and  $\text{Cs}^+$ ) [26,27]. In order to investigate a more extensive list of cations, including divalent, a third series of compounds,  $\text{M}_3[\text{Eu}(\text{2,6-pyridinedicarboxylic acid})_3]_n$  (where  $\text{M} = \text{H}^+$ ,  $\text{Li}^+$ ,  $\text{Na}^+$ ,  $\text{K}^+$ ,  $\text{Rb}^+$ ,  $\text{Cs}^+$  and  $\text{NH}_4^+$  for  $n = 1$  and  $\text{M} = \text{Ca}^{2+}$  and  $\text{Mg}^{2+}$  for  $n = 2$ ), was prepared [27]. The preparation of the anion-containing complexes is generally straightforward, usually involving the combination of an aqueous or ethanol solution of a  $\text{Eu}^{3+}$  salt with an ethanol solution of the ligand. The desired complex usually precipitates, but if not, the addition of triethyl orthoformate or ethyl acetate promotes the precipitation. In some cases, methanol, acetone and acetonitrile have been substituted for ethanol. Preparations of the cation-containing complexes ordinarily involve the addition of a  $\text{Eu}^{3+}$  salt in ethanol, water/ethanol or water/acetone to the  $\beta$ -diketone chelating agent. Spectra of mixtures of the compounds were examined to verify that the luminescence features were clearly resolvable [26].

The equilibration of one of the  $\text{Eu}^{3+}$  complexes having a labile cation with a solution containing a small amount of a different cation, so as to bring about cation exchange, was performed. The methodology involved the use of a filter paper substrate to simulate a polymer immobilised reagent. The first experiments

using the filter substrate gave rise to band-broadened spectra. It was discovered that by washing the filter paper with butanol the spectra returned to the narrow bandwidth exhibited by the pure compound. It is suspected that the butanol wash eliminates surface interactions of the metal ion to the filter paper. The cations to be exchanged were selected carefully, since cations that are strongly complexed by the chelating ligands would tend to displace the  $\text{Eu}^{3+}$ . The first experiment of this sort involved the exchange of  $\text{Na}^+$  for the  $\text{Li}^+$  in  $\text{Li}_3[\text{Eu}(\text{2,6-pyridinedicarboxylic acid})_3]$  [26]. Subsequent to this success, a study was performed following the exchange of  $\text{Ca}^{2+}$ ,  $\text{NH}_4^+$ ,  $\text{Rb}^+$ ,  $\text{K}^+$  and  $\text{Li}^+$  for  $\text{Na}^+$  in  $\text{Na}_3[\text{Eu}(\text{2,6-pyridinedicarboxylic acid})_3]$  [28].

Success with ion exchange led to the use of  $\text{Eu}^{3+}$  as the basis of an imprinted polymer sensor for pinacolylmethylphosphonate (PMP), the hydrolysis product of the nerve agent Soman (see Fig. 20.11 in Chapter 20) [29]. Several  $\text{Eu}^{3+}$  compounds were prepared to find a complex that exhibited a luminescence spectrum suitable for a selective indication of PMP binding. Examples of the spectra of the two compounds deemed unsatisfactory for making the sensor are given in Fig. 19.6. Candidate compounds were synthesised using a stoichiometric ratio of 1 mole europium to 1 mole of PMP and 3 to 7 moles of ligating molecules. The number of ligating species was chosen to acquire a 9-coordinate  $\text{Eu}^{3+}$  complex. The calculated amount of each ligand was added to aqueous  $\text{EuCl}_3$  solutions. A 1:1 v/v water/methanol PMP solution was added to the europium/ligand solution. The resulting mixture was stirred for approximately 2 h and left overnight to allow the solvent to evaporate. Analogous compounds without PMP were also synthesised. The most clearly resolved difference in spectra was seen for the complexes employing 3,5-dimethyl methyl benzoate (DMMB). In order to make

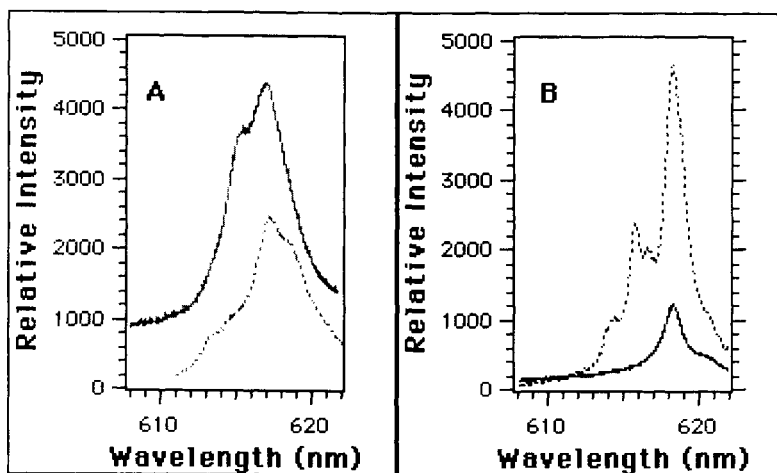


Fig. 19.6. Luminescence spectra of (A)  $\text{Eu}(\text{pyridine})_6(\text{NO}_3)_3$  and  $\text{Eu}(\text{pyridine})_6\text{PMP}(\text{NO}_3)_2$  and (B)  $\text{Eu}(\text{dipyridyl})_3(\text{NO}_3)_3$  and  $\text{Eu}(\text{dipyridyl})_3\text{PMP}(\text{NO}_3)_2$  excited at 465.8 nm with 1 mW.

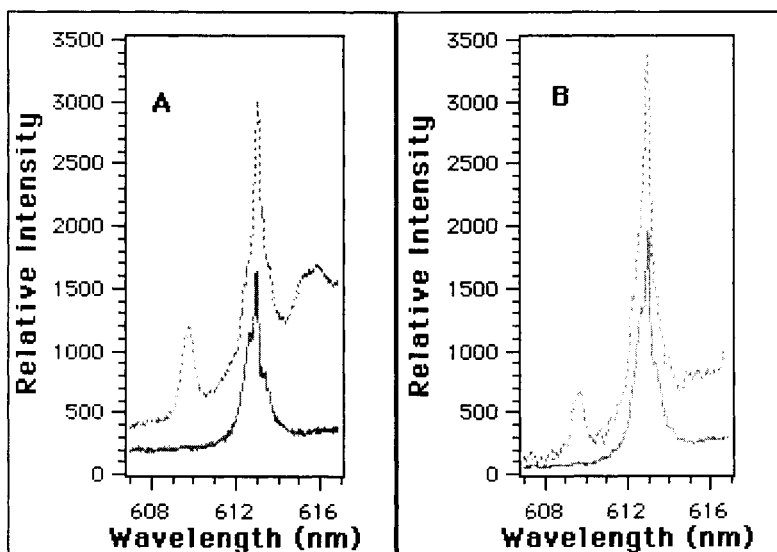


Fig. 19.7. Luminescence spectra of (A)  $\text{Eu}(\text{DMMB})_3(\text{NO}_3)_3$  (solid line) and  $\text{Eu}(\text{DMMB})_3\text{PMP}(\text{NO}_3)_2$  (dotted line) and (B)  $\text{Eu}(\text{DVMB})_3(\text{NO}_3)_3$  (solid line) and  $\text{Eu}(\text{DVMB})_3\text{PMP}(\text{NO}_3)_2$  (dotted line) excited at 465.8 nm with 1 mW.

polymerisable complexes, divinyl methylbenzoate (DVMB) was freshly prepared by the method of Shea and Stoddard [30] (for structure see **10** in Chapter 6).

The spectra of  $\text{Eu}(\text{DVMB})_3\text{PMP}(\text{NO}_3)_2$  and  $\text{Eu}(\text{DVMB})_3(\text{NO}_3)_3$  were identical to those employing DMMB, as seen in Fig. 19.7. The expected stoichiometry of  $\text{Eu}(\text{DVMB})_3\text{PMP}(\text{NO}_3)_2$  was verified using ICP-MS for Eu with a yield of 16.12% (calculated 16.36%).

The sensors were prepared using tapered 400  $\mu\text{m}$  multimode optical fibres, as shown in Fig. 19.8. The copolymer consisted of 3 mole %  $\text{Eu}(\text{DVMB})_3\text{PMP}(\text{NO}_3)_2$  complex, 1 mole % divinyl benzene, 1 mole % AIBN as initiator and the remaining matrix was styrene. The mixture was heated at 60°C in a sonicator until viscous, usually in about 1 h. The tapered fibres were dip-coated with one to three layers of the viscous copolymer, resulting in about 100  $\mu\text{m}$  of cured polymer. Polymerisation was completed by overnight UV irradiation. PMP was removed by a series of methanol/water washes, followed by washing with a weak nitric acid solution, and cleaning was verified by collecting the luminescence spectrum.

Initially, the performance of the PMP sensor was evaluated with a 1/2 metre monochromator equipped with a CCD detector to obtain figures of merit. The sensor was also evaluated using a fibre optic spectrometer from Ocean Optics, Model S2000. The sensor used to determine the limit of detection (LOD) consisted of a 400 mm optical fibre with a tapered end. A 50–75 mm layer of the 3 mole % complex polymer was directly deposited onto the tapered end without vinyl-silanisation. Using 1 mW of 465.8 nm for excitation, 200  $\mu\text{m}$  entrance slits of the

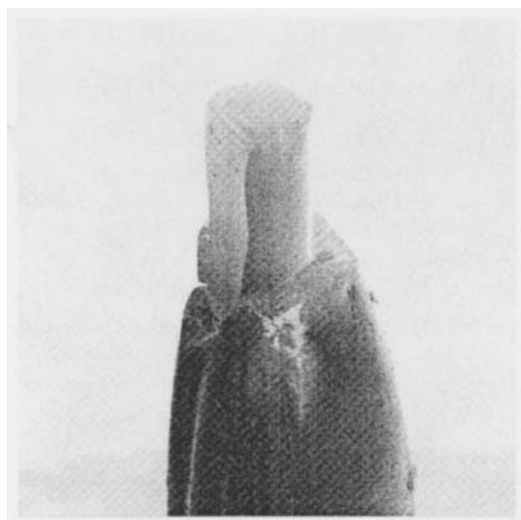


Fig. 19.8. SEM image of an imprinted polymer-coated tapered 400  $\mu\text{m}$  optical fibre at a magnification of 60  $\times$ .

monochromator and an exposure time of 5 s, the luminescence spectra of the sensor in a series of PMP solutions at pH 13 were obtained. The response of the sensor to increasing concentrations of PMP exhibits an increase in the luminescence intensity of the primary europium band as well as an increase in the intensity of the analyte peak. This increase in the luminescence is indicative of the rebinding of the PMP product into the primary coordination sphere of the lanthanide and the exclusion of water. The resulting peak areas in the 609 to 611 nm spectral region of the analyte were calculated and plotted as a function of concentration. Linear regression analysis was performed on the data and an LOD of 660 ppq calculated. The analytical figures of merit for the sensor with the each apparatus are given in Table 19.1. Concentrations below 660 ppq show no change in the intensity of either band. The residual 610 nm band remains visible even when the sensor is cleaned and should be subtracted out with the background for application purposes. Variations in the residual peak, the background or other slight differences between sensors appear to have little effect on the overall calibration curve, linear dynamic range and LOD. The typical 80% response time for the sensor was less than 8 min.

The effect of coating thickness on the response time of the sensor was also evaluated. The time dependent response of a sensor coated with a 100 micron layer and that of a sensor coated with a 200 micron layer to a 10 ppm PMP solution at pH = 13 was measured. The fibre with a 200 micron coating reached a maximum response within 14 min. The response time of the 100 micron coated fibre was decreased to 8 min. For an on-line monitor, the time for initial response is the most important factor. Using pH = 13, a distinct response occurred within 1 min.

TABLE 19.1

COMPARISON OF THE ANALYTICAL FIGURES OF MERIT FOR THE TWO DETECTORS FOR PMP

| Parameters            | Lab. bench system | Portable system                |
|-----------------------|-------------------|--------------------------------|
| LOD                   | 660 ppq           | 7 ppt                          |
| Linear dynamic range  | 750 ppq to 10 ppm | 10 ppt to 10 ppm               |
| Correlation ( $r^2$ ) | 0.9984            | 0.9973                         |
| Slope                 | 1.949 counts/ppt  | 1.484 $\mu\text{V}/\text{ppt}$ |
| 80% response time     | 8 min             | 8 min                          |

### 19.4.3 Organic chromophores

There does not appear to be an imprinted polymer ion sensor based on an intrinsic organic chromophore. The use of intrinsic organic chromophores has been demonstrated by Kriz *et al.* for an imprinted polymer fluorescence scheme for a specific enantiomer of dansyl-phenylalanine [31]. An alternative to using intrinsic chromophores or coordinated metal ions is to incorporate an organic chromophore into a binding site. The advantage in using an organic chromophore is in terms of sensitivity, since a variety of strongly absorbing and fluorescing dyes are available. The disadvantage is the unlikelihood of significant changes in the spectrum of an organic chromophore occurring through rebinding of an imprinted analyte. This is why the use of organic chromophores usually leads to quantitation by measuring fluorescence quenching. As stated previously, complexation of a metal ion by an organic chromophore may allow fluorescence or phosphorescence measurements.

An example of the use of organic chromophores in the production of an imprinted polymer sensor for  $\text{Pb}^{2+}$  is as follows [20]. In our initial screening of coordinating monomers for possible ISE enhancements, it was observed that DVMB luminesces blue-green and that the luminescence becomes yellow when a lead complex is formed. This observation suggested possible phosphorescence due to an external heavy atom effect. Since the lead-DVMB complexes rapidly polymerise in solution, it was decided to investigate the optical properties of the ligand precursor, DMMB. The lead complex was prepared by the method outlined above and dissolved in hexane to prevent complex dissociation. Luminescence spectra of the lead complex and free ligand were obtained with a spectrofluorimeter using a 467 nm excitation wavelength.

These observations, along with similar results obtained with a variety of complexing ligands, presented convincing evidence that a lead-sensing optrode could be made. The 3 mole %  $\text{Pb}(\text{DVMB})_2\text{Br}_2$  complex (2 mole % DVB) was bound by *in situ* copolymerisation on a 400  $\mu\text{m}$  optical fibre surface. The fibre was then used in the set-up schematically presented in Fig. 19.10. The luminescence

spectrum of the polymer-coated optical fibre showed the characteristic band of the Pb(II) complex, virtually identical to the one displayed in Fig. 19.9. The Pb(II) ion was then removed from the polymer by first swelling it in a mixture of methanol and water and then soaking in a stirred solution of EDTA; each process took about 1 h. The luminescence spectrum of the cleaned polymer no longer exhibited

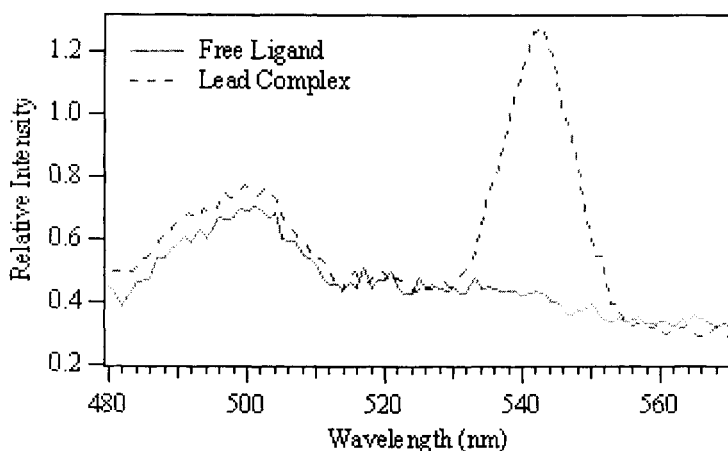


Fig. 19.9. Luminescence spectra of free ligand (DMMB) and its lead complex, excited at 467 nm.

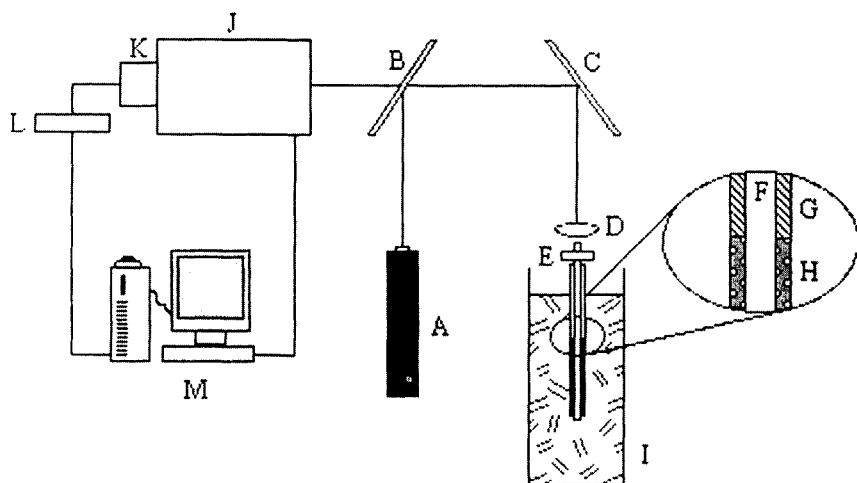


Fig. 19.10. Prototype of a lead ion measuring optrode system. Key to drawing: (A) Ar ion laser; (B) dichroic mirror; (C) mirror; (D) lens; (E) fibre mount; (F) optical fibre core; (G) fibre cladding; (H) templated polymer coating; (I) sample; (J) monochromator; (K) detector; (L) A/D converter; (M) computer.



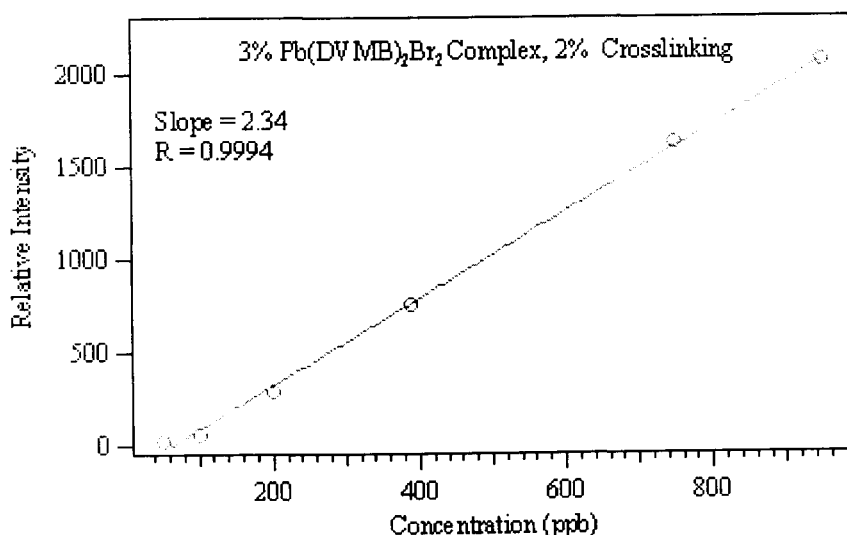


Fig. 19.11. Calibration curve obtained for the prototype lead optrode.

the characteristic lead complex luminescence band at 540 nm. The standard curve generated by the prototype optrode is given in Fig. 19.11. The luminescence was excited by the 488 nm line of an argon ion laser at a power of about 10 mW. Serial dilutions were used to obtain analytical figures of merit for a solution assay of the lead optrode. The calibration curve was linear for four decades of concentration from 50 to 1000 ppb complex with an LOD of 50 ppb complex (equivalent to 20 ppb lead), having a correlation coefficient of 0.9994.

A recent example of the use of organic chromophores to sense a polyatomic anion is given in the work of Turkewitsch *et al.* [32], with an attempt to make an imprinted polymer sensor for adenosine 3',5'-cyclic monophosphate (cAMP), a chemical messenger in cells. The imprinted polymer employed a fluorescent dye, *trans*-4-[*p*-(*N,N*-dimethylamino) styryl]-*N*-vinylbenzylpyridinium chloride as part of the binding site (for structure see Fig. 20.12 of Chapter 20). The association of the free dye with the target gave an increased fluorescence yield, while the polymer-bound dye fluorescence was quenched by complexation with the target. This was explained through steric factors within the polymer. Fluorescence measurements were performed in stirred and shaken solutions of polymer suspensions. The response, measured as the ratio of intensity of complexed polymer to a reference uncomplexed polymer was not linear with concentration and seemed to exhibit a substantial variance, as illustrated by a graph. This may be a function of the suspension process used to measure the fluorescence. Analytical figures of merit are not given. A time study showed that it required in excess of 30 min to reach an equilibrium intensity. Selectivity was measured with respect to a similar compound, guanosine 3',5'-cyclic monophosphate.

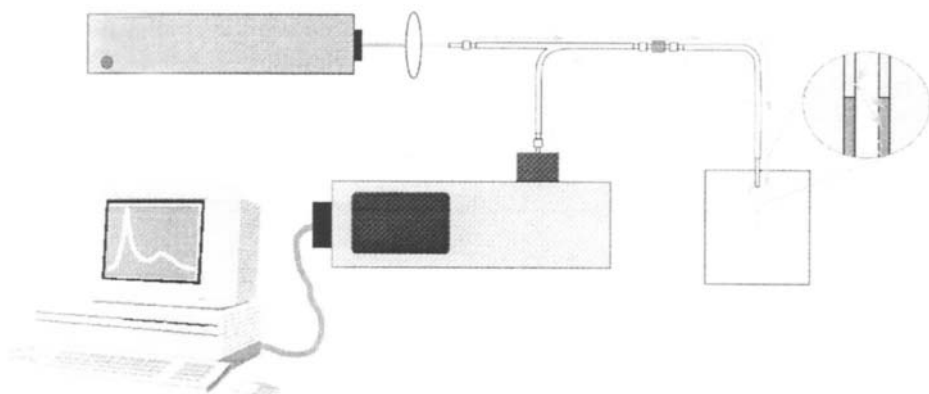


Fig. 19.12. Optrode configuration based on a bifurcated optical fibre.

#### 19.4.4 Optical probes

The quickest path to the fabrication of an optical sensor is to make a film that can be used in one of the commercially available film holders such as the one from Ocean Optics. Since absorbance-based probes require a differential measurement, they employ three fibres with source, signal and reference legs. The need for two spectroscopic channels is usually avoided by storing a reference spectrum. For luminescence measurements, the reference leg can be ignored or used to correct the spectra for variations in source intensity. A similar commercial probe was employed by Kriz and Mosbach [33].

Luminescence probes can be made by employing the polymer as a coating for an optical fibre. The polymer coating can be directly applied to the fibre as with the PMP sensor above, it can be bonded to a vinyl-silanised fibre surface or it can be implanted as a fine powder in a sol-gel coating. The fibre sensor can be addressed in a variety of ways [34], of which the simplest is to use a bifurcated fibre. In this configuration the sensor is attached to the common leg and the detector and source are attached to the bifurcated legs. This configuration is illustrated in Fig. 19.12.

#### 19.5 FIA

A common method for on-line monitoring of chemical compositions is the use of FIA. This approach is in essence a miniaturised wet chemical laboratory analysis. The approach was developed in the 1970s to adapt existing measurement methods to the task of rapid measurements. Typically, small pumps, tubes and mixing chambers combine to produce a flowing solution that is subjected to analysis by optical or electrochemical means using essentially the same reagents as in a normal-scale analytical determination. The key to sensitivity with these systems is to prevent dispersion in the stream. There are opportunities for imprinted polymers in both the sample purification and the detection of analytes.

The most developed areas for imprinted polymers are for sequestration and separation. Several reported imprinted polymer 'sensors' have in actuality been pre-treatments by separation to allow a selective determination using a general detection method. The adaptation of this to an FIA system would be relatively simple. For example, Kriz *et al.* [31] report a sensor for morphine (see Chapter 18). The method of morphine detection involved two steps. The first step was to immobilise the morphine by loading it on the imprinted polymer. In the detection step, the morphine was released from the column by elution of an electro-inactive competitor (codeine) and the released morphine was detected by an amperometric method. The polymer was tested after exposure to extremes of heat and chemicals and proved resilient. This method would probably be suitable for automation as a flow injection technique.

Metal ion-imprinted polymers can be applied to the pre-concentration and the sample clean-up stages for metal ion determinations. Most elemental techniques such as ICP-AES and ICP-MS suffer from the difficulties imposed by complex matrices that produce high dissolved salt concentrations. The use of imprinted resins for selective extraction of metal ions allows these methods to be used with greater flexibility and can significantly lower detection limits. The selectivity of some imprinted resins has been sufficient to allow selective and sensitive analyses of metal ions at ultra-trace levels using simpler and less expensive detection methods. By reducing the detection step to a simple colorimetric method, economy and simplicity are assured. The combination of imprinted polymer clean-up and colorimetric detection are attractive as the basis of an FIA system for the ultra-trace analysis of a specific metal or combination of metals.

The use of imprinted polymer ion separation and photometric detection has been demonstrated for  $\text{Pb}^{2+}$  [19] and for  $\text{UO}_2^{2+}$  [35]. In the case of  $\text{Pb}^{2+}$ , the imprinted  $\text{Pb}^{2+}$  resin described above was packed into columns and used to remove  $\text{Pb}^{2+}$  from tap and seawater at a variety of pH values [8]. The extraction efficiency of the imprinted resin was compared to the efficiency of an imidodiacetate resin (Chelex-100), a thiol-functionalised resin (Duolite G-73) and a high-capacity polyacrylic acid/polyvinyl alcohol resin (a proprietary NASA resin). The imprinted polymer's extraction efficiency was equal or better than the other resins and the effluents from the imprinted polymer resin were shown to be virtually free of contamination by other metal ions (Fig. 19.13). The purity of the effluent allowed the determination of  $\text{Pb}^{2+}$  using a very non-specific colorimetric reagent, dithizone. The method is suitable for automation as an FIA technique.

In the case of  $\text{UO}_2^{2+}$ , a similar study was performed. The photometric reagent used for  $\text{UO}_2^{2+}$  was dibenzoylmethane. Again, the imprinted resin was compared to other resins and performed exceedingly well. To verify the accuracy of the photometric method, a reference material was sought that would produce a very complex matrix. The NIST standard reference material, SRM 610 Trace Elements in Glass was selected for analysis. The glass samples were ground to a fine powder and dissolved by microwave digestion. A portion of the digest, diluted to reduce the acidity to a pH of 3.0, was passed through the imprinted resin and concentrated by a factor of 10. ICP-MS and UV/VIS spectrometry methods were used to determine

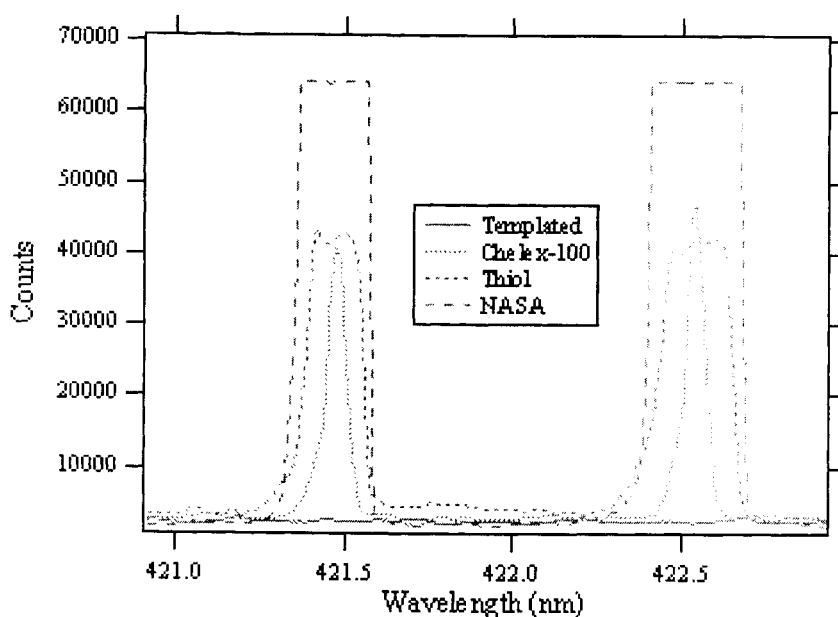


Fig. 19.13. ICP-AES spectra of ion exchange resin extracts showing the relative amounts of Sr and Ca in the extracts: Sr(II) line at 421.6 nm and Ca(I) line at 422.7 nm.

the concentration of  $\text{UO}_2^{2+}$ . The LOD for the dibenzoylmethane method was established as 160 ppt. Results obtained from the spectrophotometric analysis and the analysis by ICP-MS were in good agreement with the certified value ( $463.6 \pm 3.7$  ppm found by photometry versus the certified value of  $461.5 \pm 1.1$  ppm).

## 19.6 PROSPECTS

The application of molecular imprinting to the production of ionic and other types of sensors is in its infancy (Table 19.2). A recent review of sensors stated that 'its true value (molecular imprinting) in chemical sensing remains to be seen' [36]. This review, for the four year period from 1993 to 1997, gave 921 citations. Of these, three citations were mentioned in the molecular imprinting paragraph and two of these were reviews. A few molecularly imprinted sensors appeared scattered under the headings assigned by measurement method. Molecular imprinting has yet to receive much recognition as a means for chemical sensing.

The instrumental basis of chemical sensing has been extensively explored. Several methods have become favoured due to their ease of operation, sensitivity or cost. These methods are usually based on optics, resistance, capacitance or SAWs. All of these methods share one distinct problem, the need for chemical selectivity. Most of the accounts describing chemical sensors end with a statement that suggests other sensors could be fabricated similarly, if only a chemical recognition unit were

TABLE 19.2

## MOLECULARLY IMPRINTED IONIC SENSORS

| Analyte                       | Type           | Useful range                  | Reference |
|-------------------------------|----------------|-------------------------------|-----------|
| Pb <sup>2+</sup>              | ISE            | $\mu\text{M}$ –0.1 M          | [19]      |
| UO <sub>2</sub> <sup>2+</sup> | ISE            | $\mu\text{M}$ –0.1 M          | [20]      |
| Ca <sup>2+</sup>              | ISE            | $\mu\text{M}$ –0.1 M          | [18]      |
| Pb <sup>2+</sup>              | Lumin. optrode | 50–1000 ppb                   | [20]      |
| Glucose                       | pH             | < 1–15 mM                     | [10]      |
| PMP                           | Lumin. optrode | 10 ppt–10 ppm                 | [29]      |
| cAMP                          | Fluorescence   | $\sim \mu\text{M}$ (variable) | [32]      |

available. In the case of almost all existing sensors the chemical recognition is either fortuitous or the result of immuno-chemistry. What is lacking is a general approach to chemical recognition allowing the rational design and assembly of materials that provide both chemical recognition and signal transduction in a stable and reusable form. Molecular imprinting can provide the means for the synthesis of materials to function as the basis for chemical sensors in a needs-based fashion.

Historically, most of the MIPs practitioners are skilled in polymer chemistry and are more interested in polymers than sensing. Recently, analytical chemists have become aware of the potential of molecular imprinting as an analytical tool. As the methods of molecular imprinting get more exposure and become better understood, an even wider variety of practitioners will become interested. Still, the production of sensors by molecular imprinting is a cross-disciplinary pursuit. As polymer chemists and analytical chemists begin to meet and exchange ideas, one can expect that a wide variety of chemical sensors based on molecular imprinting will emerge.

## ACKNOWLEDGEMENTS

We wish to acknowledge Mr Steve Wajer of the Johns Hopkins University Applied Physics Research Laboratory for the SEM image. A portion of the work in this report was supported by a grant from the US Department of Energy's Environmental Management Science Program, DE-FG07-97ER14823, and a portion through the Johns Hopkins University Applied Physics Research Laboratory Internal Research and Development Fund.

## REFERENCES

- 1 L.G. Sillen and A.E. Martell, *Stability constants of metal-ion complexes*, 2nd edition, The Chemical Society, London (1964).
- 2 K.B. Yatsimirskii and V.P. Vasiliev, *Instability constants of complex compounds*, Plenum, New York, (1960).
- 3 L. Gmelin and R. Meyer (Eds), *Gmelins Handbuch der Anorganischen Chemie*, Deutsche Chemische Gesellschaft Verlag Chemie GMBH, Leipzig and Berlin (1995).

- 4 V.A. Kabanov, A.A. Efendiev and D.D. Oruiev, *J. Appl. Polym. Sci.*, **24**, 259 (1979).
- 5 H. Nishide and E. Tsuchida, *Makromol. Chem.*, **177**, 2295 (1976).
- 6 W. Kuchen and J. Schram, *Angew. Chem. Int. Ed. Engl.*, **27**, 1695 (1988).
- 7 D.A. Harkins and G.K. Schweitzer, *Sep. Sci. Tech.*, **26**, 345 (1991).
- 8 X. Zeng and G.M. Murray, *Sep. Sci. Tech.*, **31**, 2403 (1996).
- 9 R.H. Fish, H. Chen, M. Olmstead, R.L. Albrigh and J. Devenyi, *Angew. Chem. Int. Ed. Engl.*, **36**, 642 (1997).
- 10 G. Chen, Z. Guan, C.-T. Chen, L. Fu, V. Sundaresan and F. Arnold, *Nat. Biotech.*, **15**, 354 (1997).
- 11 X. Zeng, A.L. Jenkins, A.C. Bzhelyansky and G.M. Murray, submitted for publication.
- 12 B. Wang and M. Wasielewski, *J. Am. Chem. Soc.*, **119**, 12 (1997).
- 13 S.A. Piletsky, E.V. Piletskaya, A.V. Elgersma and L. Karube *Biosens. Bioelectron.*, **10**, 959 (1995).
- 14 G. Harsányi, *Polymer films in sensor applications*, Technomic Publishing Company, Inc., Lancaster (1995).
- 15 G.G. Guibault, R.A. Durst, M.S. Frant, H. Freiser, E.H. Hansen, E.T.S. Light, E. Pungor, G. Rechnitz, N.M. Rice, T.J. Rohm, W. Simon and J.D.R. Thomas, *Pure Appl. Chem.*, **46**, 129 (1976).
- 16 V.P.Y. Gadzekpo and G.D. Christian, *Anal. Chim. Acta.*, **164**, 279 (1984).
- 17 Y. Umezawa, K. Umezawa and H., *Pure Appl. Chem.*, **67**, 507 (1995).
- 18 T. Rosatzin, L. Andersson, W. Simon and K. Mosbach, *J. Chem. Soc. Perkin. Trans.*, **2**, 1261 (1991).
- 19 X. Zeng, A.C. Bzhelyansky and G.M. Murray, *Proc. of 1996 ERDEC Conf. on Chem. & Bio. Def. Res.*, Aberdeen Proving Ground, Maryland, p. 545 (1997).
- 20 G.M. Murray, A.L. Jenkins, A.C. Bzhelyansky and O.M. Uy, *JHUAPL Tech. Digest*, **18**, 432 (1997).
- 21 S.Y. Bae, X. Zeng and G.M. Murray, *J. Anal. At. Spec.*, **10**, 1177 (1998).
- 22 D.A. Skoog and J.J. Leary, *Principles of instrumental analysis*, Saunders, Fort Worth, 1992.
- 23 J.F. Krebs and A.S. Borovik, *J. Am. Chem. Soc.*, **117**, 10,593 (1995).
- 24 G.A. Crosby and M. Kasha, *Spectrochim. Acta*, **10**, 377 (1958).
- 25 J.C. Wright, In: *Modern fluorescence spectroscopy*, E.L. Wehry Ed., Plenum Press, New York, p. 51 (1981).
- 26 G.M. Murray, *Rare earth containing complex compounds for the determination of inorganic ions*, Dissertation, University of Tennessee (1988).
- 27 G.M. Murray, L.L. Pesterfield, N.A. Stump and G.K. Schweitzer, *Inorg. Chem.*, **28**, 1994 (1989).
- 28 N.A. Stump, L.L. Pesterfield, G.K. Schweitzer, J.R. Peterson and G.M. Murray, *Spec. Lett.* **28**, 1421 (1992).
- 29 A.L. Jenkins, O.M. Uy and G.M. Murray, *Anal. Comm.*, **34**, 221 (1997).
- 30 K.J. Shea and G.J. Stoddard, *Macromolecules*, **24**, 1207 (1991).
- 31 D. Kriz, O. Ramström, A. Svensson and K. Mosbach, *Anal. Chem.*, **67**, 2142 (1995).
- 32 P. Turkewitsch, B. Wandelt, G.D. Darling and W.S. Powell, *Anal. Chem.*, **70**, 2025 (1998).
- 33 D. Kriz and K. Mosbach, *Anal. Chim. Acta*, **300**, 71 (1995).
- 34 R.B. Thompson, In: *Topics in fluorescence spectroscopy*, J.R. Lakowicz Ed., International Society for Optical Engineering, Bellingham, p. 345 (1995).
- 35 S.Y. Bae, G. Southard and G. Murray, *Anal. Chim. Acta.*, **397**, 173 (1999).
- 36 J. Janata and M. Josowicz, *Anal. Chem.*, **70**, 179R (1998).

This Page Intentionally Left Blank

## Toward optical sensors for biologically active molecules

SCOTT MCNIVEN AND ISAO KARUBE

### 20.1 INTRODUCTION

Molecular imprinting [1] is now an established technique for the creation of polymeric matrices with predetermined affinity for particular substrates. The technique has been used for the creation of substrates with affinities for amino acids, peptides, proteins, nucleotides and nucleosides, carbohydrates, various drugs (e.g. opiates, alkaloids, antibiotics,  $\beta$ -blockers, tranquillisers) and other bioactive compounds (e.g. enkephalin, steroids, corticosteroids), herbicides, pesticides, as well as metal ions and a number of miscellaneous organic compounds [2–5].

An impressive arsenal of methods [6] has been developed for the creation of imprinted matrices but the basic technique entails polymerisation of a mixture of the molecule to be imprinted (the *template*), polymerisable monomer(s) with which the template can interact by hydrogen bonding, electrostatic interactions, metal ion coordination, etc. (the *functional monomer*) and a large excess of an inert monomer with two or more polymerisable functionalities which render it capable of cross-linking the polymer matrix (the *cross-linker*). The template is then extracted from the resulting polymer, thereby exposing binding sites which are complementary to the chemical functionality and three-dimensional structure of the template. Such molecularly imprinted polymers (MIPs) are robust recognition elements which retain their affinity for the template over lengthy periods of time, in both aqueous and organic solvents, and under extremes of temperature and pressure. Their high degree of cross-linking ensures they are far more robust than their biological counterparts (such as receptors, enzymes and antibodies) and, since they are able to be used in organic solvents, they constitute a *complementary* array of molecular recognition elements. Moreover, MIPs may be used as recognition elements for molecules for which the natural receptor is either unknown, difficult to purify, unstable or prohibitively expensive. It has been shown such MIPs may display affinities for their templates which are equal to those exhibited by antibodies and with similar levels of cross-reactivity [7].

These matrices have been used as chromatographic stationary phases for both enantiomeric and stereoisomeric separations [8], as artificial antibodies in immunoassay-type analyses [7], as microreactors for stereoselective synthesis [9] and as catalysts [10,11] and ‘equilibrium-shifters’ [12,13] for a variety of reactions. Since MIPs can be produced for such a wide variety of molecules, these characteristics have led many researchers to investigate the possibilities of employing MIPs as the



recognition elements in sensors [14,15]. However, while there have been many demonstrations of the *potential* of MIP-based sensors, they have yet to be routinely employed in practical applications.

This chapter deals, rather generally, with the use of MIPs in optically based analytical protocols, as well as in 'real' sensors, and concludes with a summary of recent progress in our laboratory toward the development of automated, flow injection type optical sensors.

## 20.2 OPTICAL SENSORS

There is no question that polymers which display high selectivity for their intended analyte can be synthesised using the molecular imprinting technique. For use in sensors, however, one of the fundamental difficulties is combining the recognition element with a suitable transducer, in order to convert the binding event into a detectable signal. To this end, a variety of instrumental techniques have been used in systems which exploit the potential of MIPs as recognition elements.

### 20.2.1 Ellipsometry

Perhaps the first demonstration of the use of MIPs in optical sensors was the work of Andersson *et al.* [16], using ellipsometry to quantify the amount of vitamin K<sub>1</sub> bound in a monolayer of octadecylsilane supported on a silicon wafer. Ellipsometry is a technique which relies upon the change in the polarisation of light reflected from a surface to measure the thickness of bound organic layers. They used a bait-and-switch approach, first 'imprinting' the monolayer with hexadecane which was subsequently extracted using chloroform. The monolayers were then exposed to methanolic solutions (2:3 H<sub>2</sub>O:MeOH) of various analytes (Fig. 20.1) for 10 min. Relative to a control experiment using solvent alone, neither vitamin K<sub>3</sub> (which lacks the isoprenoid tail of K<sub>1</sub>), adamantane nor cholesteryl oleyl carbonate gave any appreciable response. Vitamin K<sub>1</sub> could be determined in the concentration range 0.75–9  $\mu$ M and the monolayer was found to have an association constant of  $2.8 \times 10^5 \text{ M}^{-1}$ , with 1.9 binding sites per 100  $\text{\AA}^2$ .

Disappointingly, this promising work was not followed up, which casts doubt on both the efficacy and general utility of the 'imprinting' technique utilised herein, as well as the applicability of ellipsometry for measuring the extent of binding.

### 20.2.2 Linear dichroism

An intriguing report by Steinke *et al.* [17] describes the creation of 'molecularly imprinted anisotropic polymer monoliths'. Optically transparent blocks of MIP using either methacrylic acid (MAA) or 2-(acrylamido)-2-methylpropanesulphonic acid (AMPSA) as functional monomers and TRIM (trimethylolpropane trimethacrylate; 2-ethyl-2-(hydroxymethyl)-1,3-propanediol trimethacrylate) as the cross-linker were synthesised using the photoactive template Michler's ketone

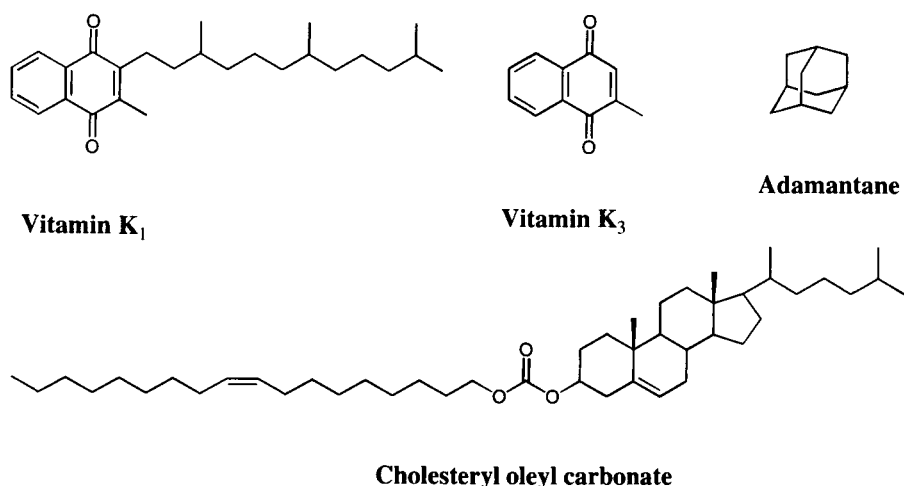


Fig. 20.1. Compounds examined in ellipsometry study.

[4,4'-bis(dimethylamino)benzophenone]. Prior to irradiation with plane-polarised light, the selectivity of these MIPs was tested in competitive batch binding experiments and it was found that MIPs employing either MAA or AMPSA had higher affinities for smaller and/or more basic analogues than for the template. The structures of these compounds and their separation factors ( $\alpha$ ) are shown in Fig. 20.2. This, however, is not so damning, as the template was chosen primarily for its photoreactivity (or, rather, the availability of a photoreactive analogue).

These monoliths were then irradiated with linearly polarised light, causing only those template molecules having a transitional dipole moment aligned with that of the light source to photoreact with the polymer backbone within the MIP binding site. This is shown schematically in Fig. 20.3.

The resulting monoliths displayed dichroism, with a maximum coinciding with that of the maximum of the absorption band of the (unreacted) template molecule. The observed anisotropy of the monoliths ( $\Delta A = A_{\parallel} - A_{\perp}$ , *ca.* 0.02 AU) was comparable with that of common oriented polymer films.

Subjecting the resulting monolithic MIPs to either heating or extended solvent extraction annulled the anisotropy, presumably due to changes in the orientation of the polymer backbone. The number of analytes to which this technique can be applied is rather limited but it is, nonetheless, an interesting concept.

The most outstanding feature of this work is that it describes the synthesis of MIPs which possess not only the attributes of typical imprinted polymers (number and strength of binding sites, pore size distribution) but that they are also transparent! It is rather surprising that this has not been further exploited. Such MIPs could conceivably be used for the determination of any analyte possessing a suitable chromophore. Alternatively, they could be used, in conjunction with a chromogenic reporter, in competitive assays.

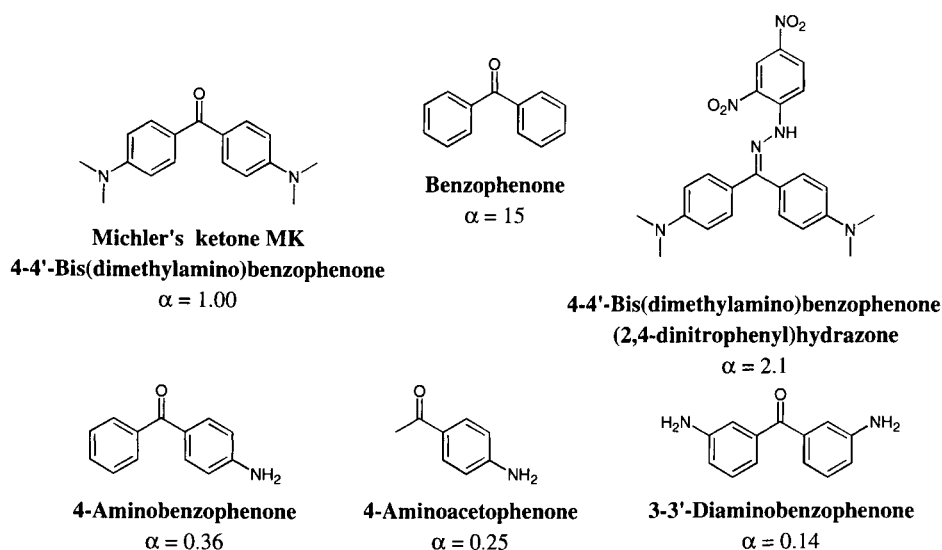


Fig. 20.2. Structures and separation values ( $\alpha$ ) of compounds examined in linear dichroism study. The capacity factor  $k'$  is calculated as  $(t_s - t_v)/t_v$ , where these terms refer to the retention times of the sample and the void marker, respectively. The separation factor  $\alpha$  is defined as  $k'_x/k'_y$ : the ratio of capacity factors for any two substances on the same column.

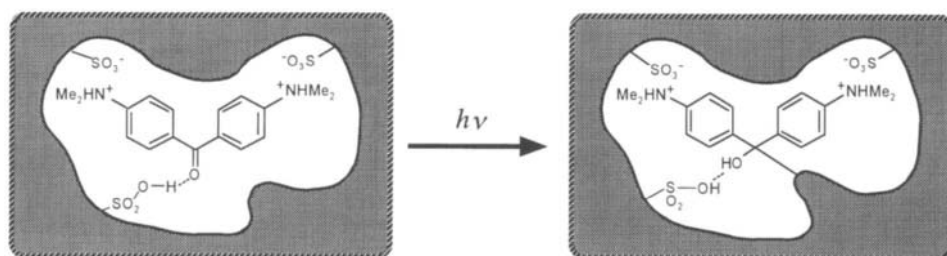


Fig. 20.3. Reaction of the template molecule (Michler's ketone) with the polymer backbone upon irradiation with plane-polarised light.

### 20.2.3 Colorimetric detection of solvent vapours using MIPs deposited on quartz crystals

Dickert and co-workers [18] have made an innovative advance by applying polyurethane-based MIPs to quartz crystals for the selective detection of solvent vapours (see also Section 20.2.5.8. and Chapter 21). Electrodes may be attached to quartz crystals to form quartz crystal microbalances (QCMs), wherein minute increases in the mass of the device (for example, upon adsorption of solvent vapour) result in a decrease of the resonant frequency of the crystal. For crystals

resonating at 10 MHz, frequency changes are measurable to an accuracy of greater than  $\pm 1$  Hz, with a frequency decrease of 1 Hz corresponding to a mass increase of slightly less than 1 ng. The superb sensitivity of QCMs permits the detection of extremely low concentrations of gaseous analytes, while the use of MIPs confers selectivity to the sensor. Our laboratory has independently developed QCMs for the detection of 2-methylisoborneol, a chemical responsible for the 'earthy' or 'musty' odour of stagnant waters [19,20].

Polymers were formed upon reaction of a 1:1 mixture of 4,4'-diisocyanatodiphenylmethane and 30% phenyltriisocyanate with bisphenol A (2,2-bis(4-hydroxyphenyl)-propane), diluted 1:20 with solvent, either  $\text{CHCl}_3$  or THF (for structures see Fig. 20.4). A MIP synthesised in THF showed no (frequency) response to ammonia vapour, whereas a non-imprinted polymer showed a response to ammonia (a much stronger electron donor) twice that to THF.

Dickert's group, however, has taken this concept a step further with the incorporation of a substituted phthalide dye into the MIP. Upon reaction with an acidic phenolic component of the polymer, e.g. bisphenol A, the lactone ring is cleaved, resulting in an intensely coloured carbenium ion. Diffusion of solvent vapours into the polymer matrix interferes with this reaction by binding to the free phenolic components and thereby diminishing the intensity of the colour. For optical measurements, the MIPs were formed as thin layers on quartz plates and the resulting composites had absorbances between 0.1 and 1 AU. Subsequently, MIPs incorporating phloroglucinol (1,3,5-trihydroxybenzene) as an additional cross-linker/phenolic compound were also prepared and applied to quartz crystals. Those

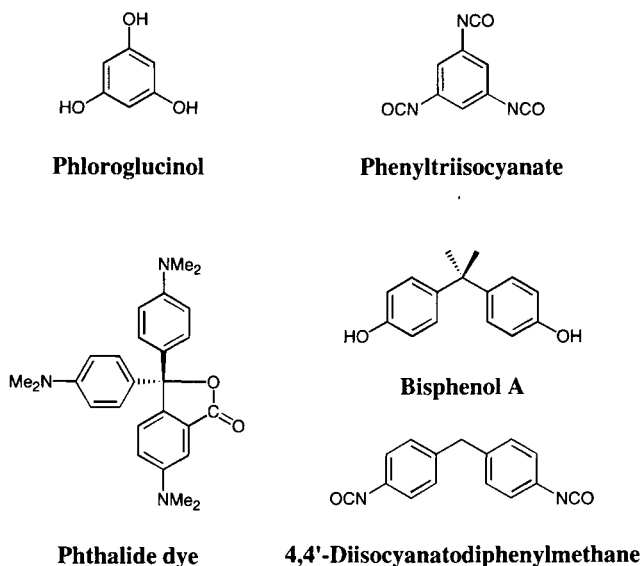


Fig. 20.4. Compounds used in solvent vapour sensor.

synthesised in ethanol showed only small changes in absorbance in response to exposure to ethyl acetate. The concentration of phloroglucinol was optimised to 10%, yielding MIPs with response times of a few minutes and a reported detection limit of several ppm ethyl acetate. It is noteworthy that these MIPs do not specifically employ a functional monomer to bind the template, although the unreacted phenol functionalities of the cross-linkers phloroglucinol and bisphenol A function as such. Indeed, by utilising the porogen itself as the template, the imprinting process is significantly simplified. The dual nature of these devices allows the confirmation of optical observations using extremely sensitive, independent mass-sensitive measurements. This approach has enormous potential (see Section 20.2.5.8. and Chapter 21 for further discussion). Indeed, a recent report uses a similar approach to examine the imprinting of 4-(4-propyloxyphenylazo)benzoic acid in  $\text{TiO}_2$  films [21].

#### 20.2.4 Surface plasmon resonance

Surface plasmon resonance (SPR) is a technique somewhat akin to ellipsometry, whereby the binding of organic molecules to a surface results in a change in the resonance angle of the incident light. This recently commercialised technique is commonly used to monitor binding events such as antibody–antigen interactions. Lai *et al.* [22] prepared MIPs against theophylline, caffeine and xanthine using MAA as the functional monomer and ethylene glycol dimethacrylate (EDMA) as the cross-linker and deposited these on silver-coated glass substrates. These 5–10 nm thick films were then exposed to aqueous solutions of the analytes for 60 min and dried in air overnight. The caffeine-imprinted polymer showed no response to theophylline at a concentration of 3 mg/mL and the xanthine MIP showed no response to 1 mg/mL aqueous theophylline. The response of the theophylline MIP to its template was approximately linear up to 6 mg/mL, with an estimated detection limit of 0.4 mg/mL. The theophylline MIP was treated with a variety of similar compounds (Fig. 20.5) to examine its cross-reactivity, but only theobromine at concentrations above 1 mg/mL gave any indication of interference.

These results should be compared with those of Vlatakis *et al.* [23]. As determined by an equilibrium binding method using radio-labelled substrates, their theophylline MIP reached binding equilibrium after 8 h, displayed negligible cross-reactivity with theobromine (but 7% with 3-methylxanthine), gave a linear response from 14–224  $\mu\text{M}$  ( $r^2 = 0.999$ ) and had a detection limit of 3.5  $\mu\text{M}$  (0.6  $\mu\text{g/mL}$ ) theophylline.

While the MIPs used in this work were inherently stable for at least 1 year, the silver films were prone to atmospheric degradation. Indeed, it was found that the application of the MIPs to the film protected it to some extent, but even when stored *in vacuo* these substrates were only stable for 5 days. The use of gold substrates is reportedly under investigation. Finally, it must be noted that the equipment used in this work was not a simple off-the-shelf commercial SPR system. These custom-made systems employed either highly sensitive photothermal deflection spectroscopy or a photodiode array to detect the changes in resonance

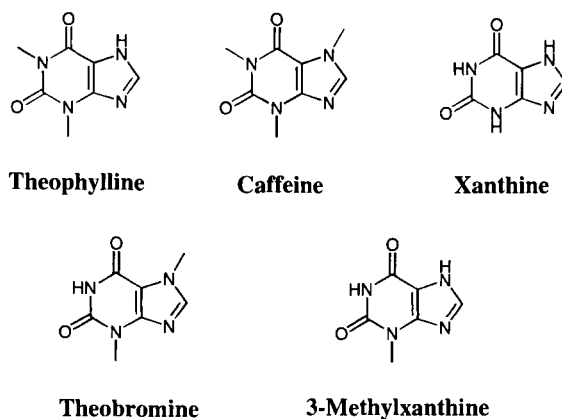


Fig. 20.5. Compounds examined in SPR study.

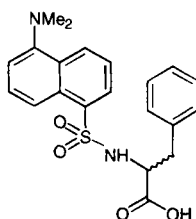
angles. Nonetheless, this is the first report of the use of SPR to detect the binding of substrates to MIPs. By judicious choice of analyte (and/or reporter) it may be possible to use MIPs in conjunction with standard SPR equipment, using either direct or competitive methods of detection.

### 20.2.5 Fluorimetry

Fluorimetry is perhaps the most sensitive optically based measurement technique and is capable of yielding very low detection limits ( $\leq 10^{-7}$  M). Consequently, many groups have tried to exploit this in the development of optically based sensors and thus the majority of reports deal with such techniques. We approach them in roughly chronological order.

#### 20.2.5.1 Fibre optic detection of fluorescent template

The first 'real' MIP-based optical sensor (and one of the very few which have been realised) was that of Kriz *et al.* [24]. MIPs using both MAA and 2-vinylpyridine (2-VP) as functional monomers were created against each enantiomer of *N*-dansyl phenylalanine (Fig. 20.6). Extracted particles sized to 75–105  $\mu\text{m}$  were then fixed against the quartz window of an optical fibre device using a nylon mesh held in place using an O-ring. The sensor was then immersed in 10 mL of MeCN for 4 h, whereupon a stable reading was obtained. The detector was then set to zero and increasing amounts of solid template were then added to the solution. The template then selectively bound to the MIP, increasing the local concentration of analyte and giving rise to a detectable response. Calibration curves (three points) were obtained upon addition of 100, 250 and 500  $\mu\text{g}$  (total) dansyl-Phe. Adequate differences between the responses to the D- and L-enantiomers were evident upon addition of 250  $\mu\text{g}$  (final concentration *ca.* 125  $\mu\text{M}$ ) of these compounds to a sensor



**Dansyl phenylalanine**

Fig. 20.6. Template examined using fibre optic sensor.

equipped with the 'anti L-MIP'. However, the time required for stabilisation of the fluorescence was approximately 4 h, far too lengthy for a sensor. Nonetheless, judicious choice of the analyte and optimisation of the mass-transfer properties of the MIP (e.g. use of smaller particles or membranes directly applied to the fibre optic cable) should improve the utility of such devices. Somewhat disappointingly, subsequent reports concerning this technique have not been forthcoming.

#### 20.2.5.2 Effect of template on formation of fluorophores within the MIP

Piletsky *et al.* [25] have reported the use of a MIP using allylamine (AA) and the 4-vinylphenylboronic acid adduct of sialic acid as functional monomers for the quantification of sialic acid. Very small particles (reported diameter 1–5  $\mu\text{m}$ ) of the sialic acid-imprinted polymer were suspended in 0.1 M borate buffer (pH 10) in the presence of carbohydrates and reagents ( $\beta$ -mercaptoethanol, *o*-phthalaldehyde) for the formation of fluorescent derivatives of primary amines. Presumably, the rationale behind this procedure was that the interaction of sialic acid with the amine functionalities within the binding cavities of the MIP should significantly hinder the formation of fluorophores. Thus, the fluorescence observed upon addition of the reagents should decrease with increasing concentrations of the template. Surprisingly, the fluorescence intensity was significantly *enhanced* in the presence of the template and, to a progressively lesser extent, the structurally similar hexoses galactose, glucose and mannose (Fig. 20.7). Sialic acid in the 0.5–10  $\mu\text{M}$  range could be detected within 40 min but the response to similar concentrations of galactose was practically identical to that of the template. Glucose and mannose, however, gave lesser responses. This lack of selectivity and the lengthy time required for equilibration severely limit the utility of this technique.

#### 20.2.5.3 Competition of template and fluorescent reporter

In subsequent work, Piletsky *et al.* [26] devised a somewhat simpler system for the fluorescent detection of the herbicide triazine. This technique was based upon the competition of the template and a fluorescent analogue (reporter) for the

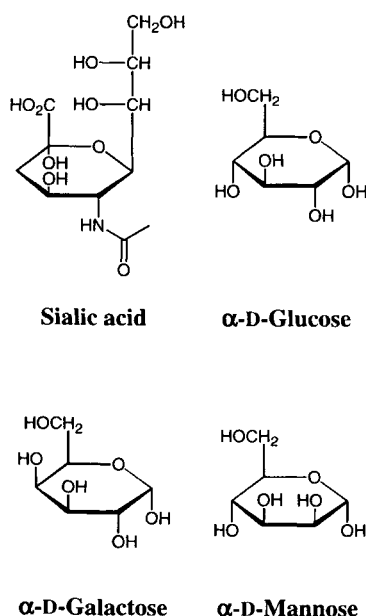


Fig. 20.7. Compounds examined using sialic acid-imprinted polymer.

binding sites within the MIP. Polymers were prepared in DMF using EDMA as cross-linker and either 2-(diethylamino)ethylmethacrylate (DEAEMA) or MAA as functional monomer. In typical experiments, 10 mg of the triazine-imprinted polymer (reported diameter 5–25  $\mu\text{m}$ ) were suspended in 500  $\mu\text{L}$  EtOH and incubated with 250  $\mu\text{L}$  of a 10  $\mu\text{M}$  ethanolic solution of 5-(4,6-dichlorotriazin-2-yl)aminofluorescein (the reporter) and various concentrations of triazine in a total volume of 1000  $\mu\text{L}$  EtOH for 3.5 h at ambient temperature. The solutions were then centrifuged and 100  $\mu\text{L}$  of supernatant were diluted to 3 mL with EtOH and the fluorescence measured. MIPs with DAM as the functional monomer were found to have a much lower affinity for the template than those using MAA. Using the latter, triazine could be detected in the range  $10^{-5}$ – $10^{-3}$  M. Batch binding experiments showed that the MIP was selective for triazine over atrazine and practically immune to interference from simazine (Fig. 20.8) over the same concentration range. While the selectivity seems sufficient, it is the lengthy equilibration time that limits the utility of this procedure.

#### 20.2.5.4 Imprinting of silicas with fluorophores

A report by Lulka and Chambers [27] describes the properties of surface-imprinted silicas using *N*-acetyltryptophanamide (NATA) or fluorescein (Fig. 20.9) as templates. Silica gel was mixed with bis(2-hydroxyethyl)-aminopropyltriethoxysilane (as functional monomer), tetraethoxysilane and the template and the slurry



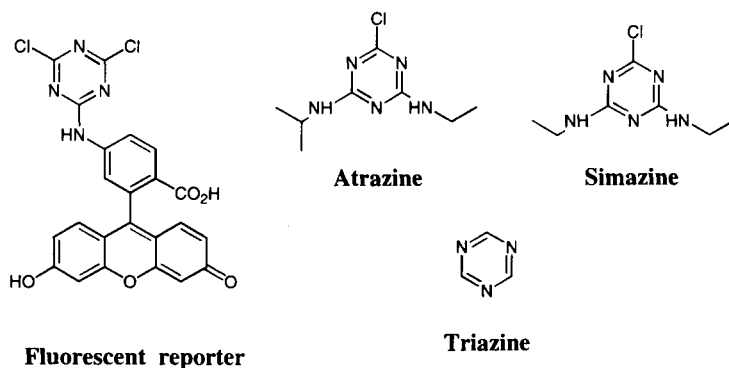


Fig. 20.8. Compounds examined using triazine-imprinted polymer.

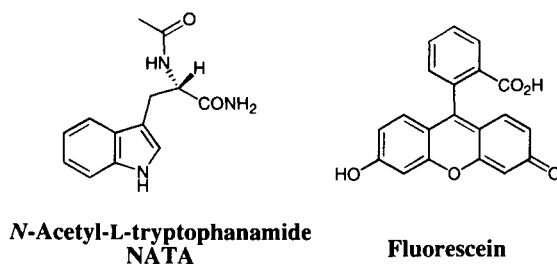


Fig. 20.9. Fluorescent template molecules used to imprint silicas.

allowed to polymerise for 8 h at 4°C. After extraction of the template, saturation of the polymer with substrate (the concentration of template was varied from 2 to 10  $\mu\text{M}$ ) and subsequent removal of non-specifically bound material, the polymers were glued to cards and their properties examined in a right-angle fluorescence detection configuration.

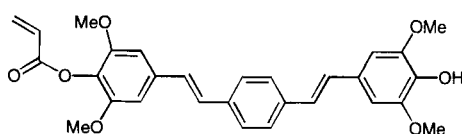
Scatchard analyses were carried out by incubating the MIPs with 3–300  $\mu\text{M}$  template for 1 h at 25°C. The NATA-imprinted polymer possessed two sets of binding sites with dissociation constants of 0.13 and 2.5  $\mu\text{M}$ , while the fluorescein-imprinted polymer had a single  $K_d$  of 192  $\mu\text{M}$ . The latter finding is encouraging, as Scatchard plots obtained from non-covalently imprinted polymers have typically indicated the existence of a small population of strong binding sites and a majority of much weaker sites, as found for the NATA-imprinted polymer. MIPs having a single affinity constant are much better models of their natural counterparts, such as enzymes, monoclonal antibodies and other proteinaceous receptors. Interestingly, the fluorescein-imprinted polymer showed higher affinities ( $K_d$ 's of 1.3 and 35 nM) for NATA than did the NATA MIP. These values are 10-fold those of the NATA MIP and, again, demonstrate the heterogeneity of the binding sites of typical MIPs.

Quenching experiments using both KI and acrylamide suggested that, as expected, MIP-bound substrates are somewhat shielded from their solvent environments, the effect being more noticeable for fluorescein than for NATA, perhaps due to the greater hydrophobicity of the former, but direct comparisons of results obtained from polymer-bound and solution measurements are somewhat precarious. For both polymers, iodide was found to be slightly more effective than acrylamide and NATA bound to the fluorescein-imprinted polymer was quenched to the same extent as NATA bound to its own MIP, indicating a similar degree of accessibility in both polymers.

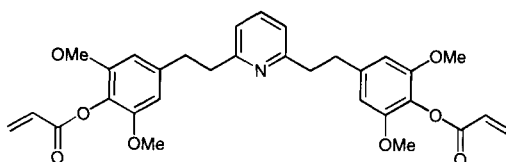
These results are rather preliminary, but illustrate an alternative method for the determination of inherently fluorescent molecules (such as NATA) or labelled compounds of low molecular weight. Further advances in the preparation of the MIPs (homogeneity of particles and binding sites), the measurement technique (preparation of the cards, direct measurement of suspended particles) and enhancement of their mass transfer characteristics and selectivity should greatly increase the utility of this technique.

#### 20.2.5.5 Covalent and non-covalent imprinting using fluorophores as functional monomers

In a short communication, Cooper *et al.* [28] report the utilisation of two novel fluorescent functional monomers (Fig. 20.10) in EDMA-based MIPs. Initially, a polymerisable phenolic compound was treated with cholesterol chloroformate (as per Whitcombe *et al.* [29]) and used to prepare a covalently imprinted polymer. Details are lacking, but this procedure was not successful; both the imprinted and the non-imprinted polymers had a similar affinity for cholesterol and no changes in



**Functional monomer for covalent imprinting**



**Functional monomer for non-covalent imprinting**

Fig. 20.10. Fluorescent functional monomers for covalent and non-covalent imprinting.

either the wavelength or the intensity of the fluorescence were observed upon exposure of the 'empty' MIP to the template.

A 2,6-disubstituted pyridine derivative was also synthesised and incorporated into an EDMA-based (the porogen was not disclosed) non-covalently imprinted polymer. The resulting polymer was reportedly sensitive to solvent, pH and the presence of 'organic additives' in solution. The example provided shows that cyclohexane suspensions of the polymer exhibit no diminution of fluorescence upon the addition of anisole, but show approximately 15% quenching in the presence of an equivalent concentration of phenol. Approaches such as these, wherein the fluorescent properties of the MIP itself are altered by interaction with the analyte, should prove extremely useful.

#### 20.2.5.6 Formation of fluorescent complex upon binding of metal ion template

Murray *et al.* [30] have further extended the scope of MIP-based sensors by developing a fluorescent sensor for  $\text{Pb}^{2+}$ . This and related work is treated in more detail in Chapter 19 by Murray *et al.*, but briefly, the fluorescence of methyl-3,5-divinylbenzoate (DVMB) changes from blue to yellow-green upon complexation of  $\text{Pb}^{2+}$ . A solution of 3% Pb-DVMB complex and 2% divinylbenzene in styrene was polymerised on the surface of a vinylised fibre-optical cable (see also Section 20.2.5.1.). Subsequently, the polymer matrix was first swollen in MeOH and then the  $\text{Pb}^{2+}$  ions were removed by soaking the probe in a stirred solution of EDTA. Each step took approximately 1 h. The device, excited at 488 nm using an argon laser, gave a linear response ( $r^2 = 0.9994$ ) from approximately 50 to 1000 ppb  $\text{Pb}^{2+}$ .

#### 20.2.5.7 Interaction of ancillary ligand with fluorescent metal complexes within the MIP

In a similar vein, Murray and co-workers [31,32] have produced a prototype MIP-based sensor for the detection of the chemical warfare agents sarin and soman or, rather, their hydrolysis products, e.g. pinacolyl methyl phosphonate (PMP, Fig. 20.11). This too is covered in more detail in Chapter 19. Their approach exploits the change in fluorescent properties effected by the binding of an ancillary ligand to a metal complex within the polymer matrix. MIPs were prepared by dissolving the pre-formed  $\text{Eu}(\text{DVMB})_3\text{PMP}(\text{NO}_3)_2$  complex (3%) in styrene and polymerising the mixture on the tip of a vinylised fibre-optical cable as above (see also Sections 20.2.5.1. and 20.2.5.6.), yielding a 60–80 nm thick layer. The polymers were then swollen in aqueous methanol, with sonication, and the PMP removed by the addition of nitric acid and further sonication.

The fluorescence of the DVMB- $\text{Eu}^{3+}$  complex within the MIP is significantly altered in the presence of PMP. The sharp 610 nm peak, present in the spectrum of the original polymer-bound DVMB- $\text{Eu}^{3+}$ -PMP complex and absent in the spectrum of the 'empty' polymer, is restored upon exposure of the polymer to 1 M NaOH solutions containing PMP. While a benchtop model of the sensor was more

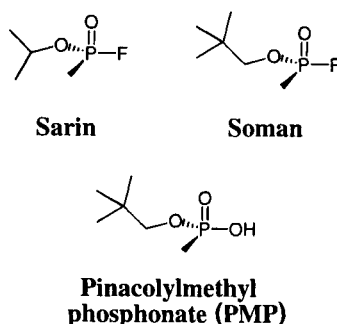


Fig. 20.11. Chemical warfare agents and one possible hydrolysis product.

sensitive, the actual portable sensor gave a linear response ( $r^2 = 0.9973$ ) from 10 ppt to 10 ppm PMP, with a detection limit of 7 ppt and 80% of response times of less than 8 min.

A number of commonly occurring pesticides and herbicides was also examined and found to cause no interference, even at extremely high concentrations. Such sensors, which combine the selectivity of MIPs with the extremely sensitive fluorescence properties of lanthanide complexes, ensure that this will be a very fruitful area of research.

#### 20.2.5.8 Determination of fluorophores using MIPs formed on quartz crystals

Subsequent to their earlier work (see Section 20.2.3. and Chapter 21), Dickert and co-workers [33] have created urethane-based MIPs for the detection of the polycyclic aromatic hydrocarbons (PAHs) pyrene and anthracene in aqueous solution. PAHs lack functional groups with which to interact with the functional monomers of a MIP, so binding and recognition were in this case achieved by a combination of  $\pi$ - $\pi$  aromatic stacking and size/shape selectivity. As above, MIPs synthesised using 4,4'-diisocyanatodiphenylmethane, phenyltriisocyanate, bisphenol A and phloroglucinol (Fig. 20.4) were formed on  $20 \times 10 \times 1$  mm quartz crystals. Imprinted polymers were, as expected, more responsive to their template than the other analyte. Interestingly, only about 80% of the template could be removed from the MIPs, but the residual molecules showed no fluorescence, presumably due to strong quenching by the polymer matrix. A parts-per-trillion detection limit was demonstrated for pyrene, with a linear response up to  $40 \mu\text{g/L}$  and a detection limit of *ca.* 30 ng/L, whereas non-imprinted polymers exhibited a response approximately 1% that of the MIP. Again, the response time is of the order of minutes.

Polymers imprinted against the sodium salts of anthraquinone 2-sulphonic acid and pyrene sulphonic acid both showed a 3- to 4-fold higher sensitivity to pyrene than to anthracene.

Clearly this technique has immense potential, especially when considered in conjunction with methods involving multiple sensors, in either optical- or

mass-sensitive mode. The combination of sensor arrays and neural networks or other data processing programs should overcome any lack of selectivity. The combination of 'traditional' imprinting techniques with QCMs and other mass-sensitive devices, such as surface acoustic wave sensors (SAWs) [34], should also prove to be extremely fruitful and, indeed, we are pursuing such work in our laboratories [19,20]. We await further developments with great interest.

#### 20.2.5.9 Quenching of functional monomer fluorescence upon binding of analyte

Turkewitsch *et al.* [35] have prepared a MIP for the fluorescent detection of the cellular secondary messenger cAMP (adenosine 3':5'-cyclic monophosphate) in aqueous media. The MIP employs TRIM as the cross-linker, HEMA (2-hydroxyethyl methacrylate) as a general hydrogen bonding functional monomer and uses the positively charged *trans*-4-[*p*-(*N,N*-dimethylamino)styryl]-*N*-vinylbenzylpyridinium moiety (Fig. 20.12) to act as both a fluorescent reporter and to bind the negatively charged cAMP by means of electrostatic interactions (aryl stacking is also possible).

The MIP was synthesised in methanol using a TRIM:HEMA:reporter ratio of 86:5.19:0.119, ground and wet sieved in water. Particles sized to 45–106  $\mu\text{M}$  were washed in a Soxhlet apparatus using a 7:3 v/v mixture of  $\text{H}_2\text{O}$ :MeOH for a minimum of 24 h, then with pure MeOH for at least 24 h.

One hundred and fifty milligrams of MIP were shaken in 4 mL of water overnight, centrifuged then resuspended in 1.25 mL of water and, in the absence of analyte, the fluorescence intensity  $I_0$  was measured at 595 nm upon excitation at 469 nm. The particles were then centrifuged, re-suspended in 1.25 mL of solutions of either cAMP or guanosine 3':5'-cyclic monophosphate (cGMP), shaken at 25°C for 1.5 h and then the fluorescence intensity  $I$  was measured.

Measurements revealed that the MIP became saturated with 1 mM cAMP after approximately 30 min, resulting in a 14% decrease in fluorescence intensity. The

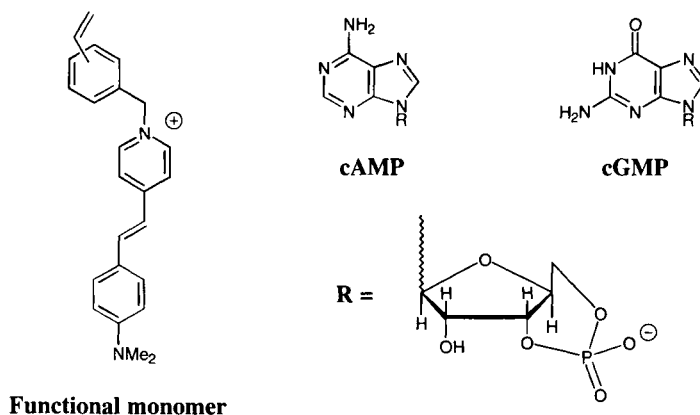


Fig. 20.12. Compounds involved in cAMP-imprinted polymer study.

effect of cAMP (0.01–1000  $\mu\text{M}$ ) and cGMP (1–1000  $\mu\text{M}$ ) on the fluorescence was then determined after 90–135 min equilibration. Using the imprinted polymer, quenching was observed at cAMP concentrations as low as 0.1  $\mu\text{M}$ . Both the imprinted and non-imprinted polymers showed a slight increase in the  $I_0/I$  ratio in the presence of increasing concentrations of cGMP, while the fluorescence of the non-imprinted polymer was basically unaffected by cAMP. The emission of the imprinted polymer, however, decreased appreciably ( $I_0/I$  increased) as the concentration of cAMP was raised. Interestingly, in a previous study the authors found the quantum yield of the functional monomer in aqueous solution to be greatly enhanced in the presence of purine nucleotides, but only slightly so in the presence of pyrimidine nucleotides. Upon fitting the data, the authors derived a single association constant of  $K_a = (3.5 \pm 1.7) \times 10^5 \text{ M}^{-1}$ . Alternatively, estimation of  $K_a$  using the concentration of cAMP, which produces a half-maximal response, gave a value of  $1.7 \times 10^5 \text{ M}^{-1}$ . These values are similar to those observed for other MIPs, although non-covalently imprinted polymers usually possess both high and low affinity binding sites. Nonetheless, Lulka's non-covalently fluorescein-imprinted polymer also had a single  $K_d$  of 192  $\mu\text{M}$  ( $K_a = 1/K_d = 5200 \text{ M}^{-1}$ ; see Section 20.2.5.4). For comparison, the association constant for the functional monomer and cAMP in aqueous solution is  $K_a = 13.8 \text{ M}^{-1}$ , but it should be noted that the environment within a MIP is far removed from that of bulk water. Nonetheless, the MIP, prepared in methanol, is able to distinguish between cAMP and cGMP in aqueous solution. This indicates that recognition is not based solely on electrostatic interactions between the analyte and the positively charged fluorescent reporter, but also involves a strong contribution from the imprinting effect.

#### 20.2.5.10 Competitive fluoroimmunoassay

In an extension of previous work [36] in which they developed an MIP-based radioimmunoassay, Haupt *et al.* [37] have devised a fluoroimmunoassay for the herbicide 2,4-dichlorophenoxyacetic acid (2,4-D) based on MIPs (see also Chapter 14). Polymers were prepared in a 4:1 mixture of MeOH:H<sub>2</sub>O, using 4-VP as the functional monomer and EDMA as the cross-linker, and particles with an average diameter of 1  $\mu\text{M}$ , usually discarded in chromatographic procedures, were used in the assay. The use of these 'fines' improves mass transport, decreasing the assay time, and results in a more compact pellet upon centrifugation. In a competitive batch binding protocol similar to that used by Piletsky *et al.* (see Section 20.2.5.3.), the MIP was allowed to equilibrate with a mixture of the analyte and the reporter compound 7-carboxymethoxy-4-methylcoumarin (CMMC) for 2 h in either 20 mM phosphate buffer (pH 7) or MeCN. Following centrifugation, the fluorescence of the supernatant was measured and the concentration of the analyte determined using a standard curve. This is shown schematically in Fig. 20.13. For comparison, MIP-based radioimmunoassays were performed using <sup>14</sup>C-labelled 2,4-D.

In aqueous buffer, 500 mg of polymer were required to bind 50% of the CMMC, whereas only 100 mg were needed to sequester 50% of the <sup>14</sup>C-2,4D. In

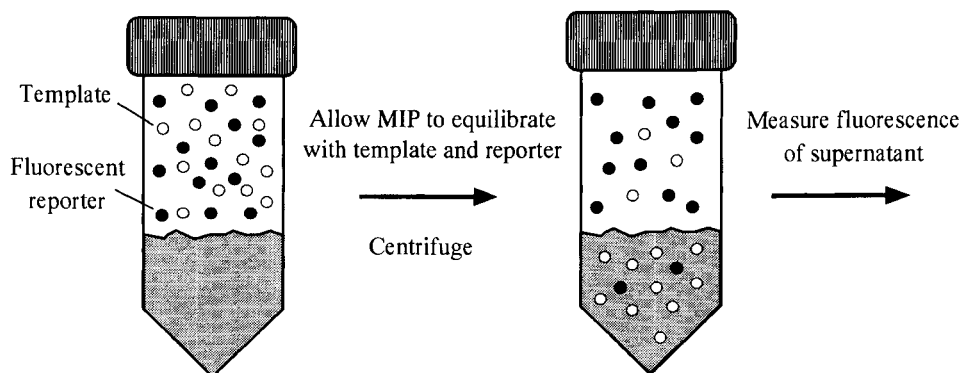


Fig. 20.13. Procedures involved in batch type competitive fluoroimmunoassays.

MeCN, these values were 230 and 200 mg, respectively, indicating that, while the level of binding was higher in the organic solvent (both imprinted and non-imprinted polymers), the relative preference for the template over the reporter was less than that observed in aqueous solution. These results demonstrate the differing selectivities resulting from hydrogen bonding in the organic solvent and electrostatic interactions in aqueous buffer.

Competitive binding experiments in the presence of 0.64 nM CMMC supported these findings. Based on the fluorescence of the supernatant, 2,4-D could be detected from 0.1 to 50  $\mu\text{M}$  in phosphate buffer and from 0.1 to 10  $\mu\text{M}$  in MeCN. The previous MIP-based radioimmunoassay, carried out in the same buffer, was able to detect the analyte over a similar range, from 0.135 to 45  $\mu\text{M}$ . As with the work of Piletsky *et al.* (see Sections 20.2.5.2. and 20.2.5.3.), the lengthy incubation time is a disadvantage of such systems.

The cross-reactivity of the assay was determined using a variety of compounds resembling the template (Fig. 20.14). Cross-reactivities determined in phosphate buffer were almost identical to those previously determined using the MIP-based radioimmunoassay, 2,4-DB (2,4-dichlorophenoxybutyric acid) showing an equally high affinity for the polymer (Table 20.1). In MeCN, however, binding of 2,4-DB was negligible, while CPOAc (4-chlorophenoxyacetic acid) showed a cross-reactivity of 50%. Significantly, monoclonal enzyme-linked immuno-sorbent assays (ELISAs) were unaffected by either of these compounds but showed cross-reactivities of 30–160% for 2,4-DOMe (2,4-dichlorophenoxyacetic acid methyl ester), presumably because the hapten used to raise the antibodies did not possess a free carboxylic acid functionality.

### 20.2.6 Sensors based on liquid chromatography (LC)

Each of the aforementioned applications of MIPs in optical sensors entails a batch-type incubation and/or measurement procedure. In our laboratories we set

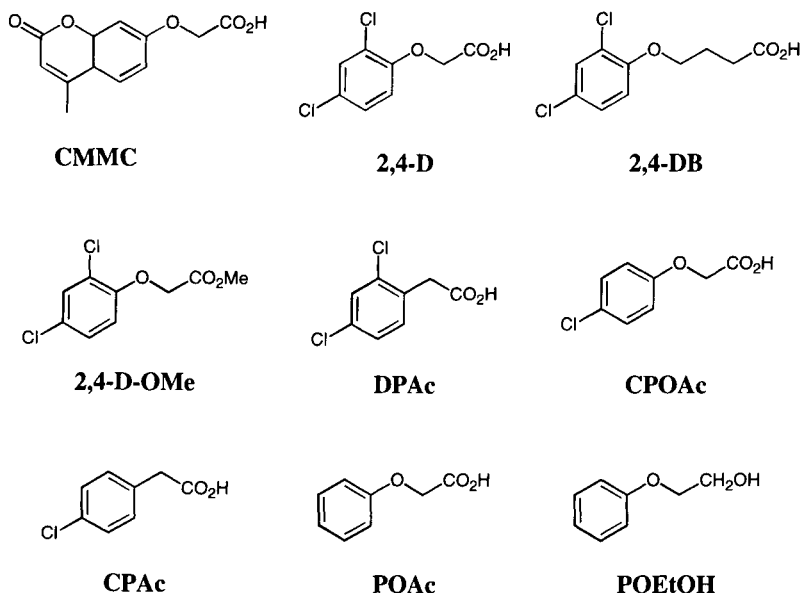


Fig. 20.14. Compounds examined in competitive fluoroimmunoassay.

TABLE 20.1

CROSS-REACTIVITIES OF VARIOUS COMPOUNDS ON 2,4-D-SELECTIVE MATRICES. CROSS-REACTIVITIES WERE CALCULATED BY COMPARING THE CONCENTRATIONS REQUIRED TO INHIBIT BINDING OF  $^{14}\text{C}$  2,4-D BY 50% ( $\text{IC}_{50}$  VALUES). ELISA RESULTS VARY DEPENDING ON ANTIBODY USED.

| Cross-reactivity with respect to 2,4-D (%) |                              |                            |                             |                  |
|--|------------------------------|----------------------------|-----------------------------|------------------|
| MIP-based assay                            |                              |                            |                             |                  |
| Compound                                   | Fluoroimmuno-assay in buffer | Fluoroimmuno-assay in MeCN | Radioimmuno-assay in buffer | Monoclonal ELISA |
| 2,4-D                                      | 100                          | 100                        | 100                         | 100              |
| 2,4-DB                                     | 100                          | 2                          | 95                          | 1.5–20           |
| 2,4-D-OMe                                  | 4                            | 1                          | 7                           | 30–160           |
| CPOAc                                      | 42                           | 50                         | 24                          | 0.5–2.8          |
| POAc                                       | 9                            | 14                         | 2                           |                  |
| DPAC                                       | 20                           | 2                          | 15                          |                  |
| CPAC                                       | 15                           | 1                          | 10                          |                  |
| POEtOH                                     | <0.1                         | <0.1                       | <0.1                        |                  |



out to develop flow injection-based systems capable of the rapid, continuous, automated detection of biologically active analytes.

The purpose of a sensor is to quantify an analyte with very high selectivity, even in the presence of considerable amounts of impurities or background material. Thus LC systems may be regarded as the simplest optical sensors. Selectivity is achieved by means of the column, which enables the temporal separation of the analyte from other components of the mixture which may interfere with the assay by absorbing/emitting light at the wavelength of detection. The analyte is then detected by virtue of its optical properties, i.e. its absorbance and/or fluorescence at a certain wavelength(s).

The use of MIPs in analytical systems is a facile and convenient means of achieving high selectivity for the analyte. MIPs can be regarded as chromatographic stationary phases with a predetermined selectivity for a particular compound. Thus, competitive batch binding assays are simply chromatographic separations involving a single theoretical plate. In addition to results obtained from batch binding and solid phase extraction studies, the selectivity of MIPs has been amply demonstrated using LC columns packed with imprinted polymers. Using such a system, the separation of molecules as closely related as enantiomeric amino acids has been achieved, obviating the need for expensive and fragile chiral sorbents. In addition, the order of elution on chiral columns is not known with certainty, whereas the template molecule is always eluted from MIPs *after* its stereoisomer and has a characteristic 'tailing' peak shape. Thus we sought to combine the excellent selectivity of MIPs and the practicality of LC in a displacement-type flow injection assay.

#### 20.2.6.1 Chloramphenicol (CAP) sensors

We have developed an LC-based sensor which relies upon the displacement of a drug-dye conjugate from a CAP-imprinted polymer upon application of samples containing the original template molecule (Fig. 20.15). This is essentially a competitive binding assay in a flow injection format. The increased number of theoretical plates available during the separation serves to greatly enhance the selectivity of the assay.

CAP is a useful broad spectrum antibiotic used in both human and veterinary medicine, but it is capable of producing toxic effects at high concentrations and, consequently, its use in food-producing animals has been banned. Thus the monitoring of drug levels in patients' blood and in foodstuffs is of great importance.

*Bulk imprinted polymers:* [38] Various combinations of porogens, functional monomers (MAA and DEAEMA) and functional monomer/template ratios were compared and the most selective MIP was that obtained using a mixture of DEAEMA, CAP (functional monomer:template ratio 2:1) and EDMA in THF. The mixture was polymerised, washed and particles sized to 25–63  $\mu\text{m}$  in diameter were packed into HPLC columns.

The columns were then equilibrated with MeCN, whereupon CAP and various derivatives (Fig. 20.16) were injected for analysis. At flow rates from 2 to 5 mL/min

CAP-imprinted polymer crushed, extracted and  
packed into HPLC columns

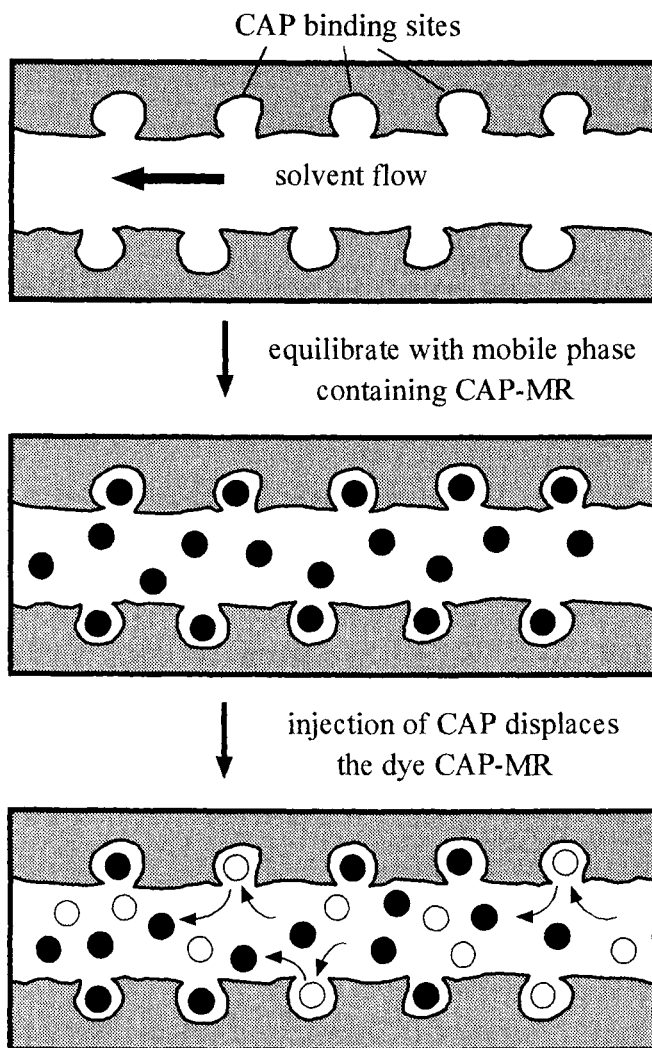


Fig. 20.15. Principle of flow-injection type competitive assays.

the order of elution was CAP-DA (CAP diacetate), CAP-MR (CAP methyl red), TAM (thiamphenicol) then, as expected, CAP. The diacetyl derivative CAP-DA was eluted practically in the void volume, while TAM, in which the aromatic nitro functionality was replaced by a methylsulphonyl group, was quite strongly retained ( $\alpha = 1.7\text{--}1.9$ ). The capacity factor  $k'$  is calculated as  $(t_s - t_v)/t_v$ , where these terms

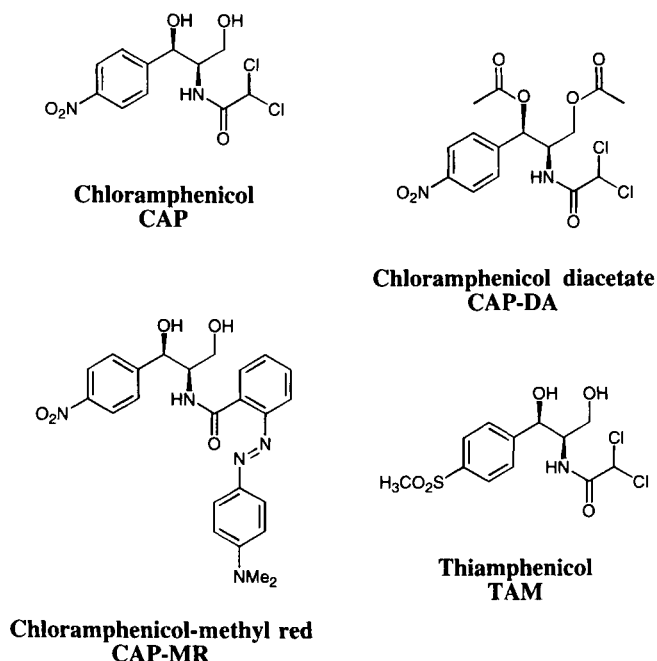


Fig. 20.16. Compounds examined using flow-injection type CAP sensor.

refer to the retention times of the sample and the void marker, respectively. The separation factor  $\alpha$  is defined as  $k'_x/k'_y$ , the ratio of capacity factors for any two substances on the same column. The behaviour of the dye conjugate was intermediate ( $\alpha = 3.0\text{--}3.3$ ). This indicated that the 1,3-dihydroxy moiety was responsible for the majority of the binding interactions, with lesser contributions from the aromatic nitro group and size/shape selectivity. Interestingly, the imprinting factor  $I = k_{\text{imp}}/k_{\text{non}}$  increased with the flow rate, indicating a lower level of non-specific interactions while, as expected,  $\alpha$  decreased.

The columns were then equilibrated with a solution of the dye conjugate CAP-MR in MeCN and solutions of CAP were injected to optimise the assay conditions. The concentration of the dye conjugate was varied from 0.1 to 0.8 mg/mL and a given amount of CAP injected at a flow rate of 2 mL/min. The highest responses were observed using CAP-MR concentrations of 0.4–0.6 mg/mL. Using a concentration of 0.6 mg/mL CAP-MR, the flow rate was then varied from 1 to 3 mL/min. As expected, higher responses were observed at the lower flow rates, but this led to the broadening of peaks (and less reliable peak areas) and longer assay times. Thus, a flow rate of 2 mL/min was considered optimal.

Calibration curves for the other compounds were then constructed under these conditions. Both CAP and TAM gave linear responses over an extremely wide range of concentrations (3–1000  $\mu\text{g/mL}$ ) while CAP-DA gave negligible responses, even at 1000  $\mu\text{g/mL}$ . The response of the sensor to TAM was approximately 40%

lower than that to CAP. However, this lack of specificity may actually be advantageous, as TAM is also a widely used antibiotic and the system is capable of detecting either compound.

Bovine serum samples spiked with various amounts of CAP were then extracted with ethyl acetate according to a standard procedure and the extracts analysed using our sensor. A linear response ( $r^2 = 0.990$ ,  $n = 6$ ) was observed from 5 to 160  $\mu\text{g/mL}$  CAP, which easily encompasses the therapeutic range of the drug (10–20  $\mu\text{g/mL}$  serum, potentially toxic above 25  $\mu\text{g/mL}$ ).

This is the first example of a continuous, automated, MIP-based method for the optical detection of an analyte. Using a 5 cm column, the time taken for a single determination was approximately 5 min.

*In situ-imprinted polymers:* [39] To further simplify construction of such sensors we investigated the use of *in situ* or 'rod' imprinted polymers using the technique pioneered by Matsui *et al.* (see Chapter 13). Solutions of template, either DEAEMA or AA as functional monomers, EDMA and initiator in the porogen (4:1 octanol:dodecanol, w/w) were introduced into 100  $\times$  4.6 mm (i.d.) HPLC columns and polymerised *in situ* at either 50 or 70°C. These 'rods' were then flushed with MeCN until a stable absorbance and back pressure were obtained. The most selective polymers were those polymerised at 50°C using DEAEMA as the functional monomer, with a functional monomer/template ratio of either 2:1 or 4:1. The latter was chosen for use in the sensor so as to directly compare the results obtained using bulk and *in situ* imprinted polymers.

As above, the order of elution was CAP-DA, TAM, then CAP. In this case, however, acetone was retained more strongly than CAP-DA, so the latter was used as the void marker. Capacity factors  $k'$  were much lower than previously observed, indicating that the *in situ* MIPs possess a lower density of binding sites. However, the separation factor  $\alpha$  between CAP and TAM was slightly greater, demonstrating that the *in situ* imprinted polymers contain binding sites of higher selectivity. This was somewhat surprising, but it must be recognised that the bulk and *in situ* imprinted polymers are intrinsically different materials. The porogen used in synthesis of the former was THF, while the *in situ* imprinted polymers were formed in a mixture of relatively hydrophobic fatty alcohols which, notwithstanding other effects, should have served to promote hydrogen bond formation between the template and the functional monomer.

The effect of the CAP-MR concentration on the response to injections of CAP was examined and, in contrast to results obtained using the bulk-imprinted polymer, the response did not display a maximum value but rose gradually from 0.3 to 0.6  $\mu\text{g/mL}$  then increased dramatically from 0.6 to 0.8  $\mu\text{g/mL}$  CAP-MR. However, the shape of the peaks became highly asymmetric at the higher concentrations, so a compromise of 0.5  $\mu\text{g/mL}$  was adopted. As with the bulk-imprinted polymer, lower flow rates produced dramatically greater responses, as a consequence of the increased time available for the template/analyte to interact with the polymer matrix. In order to facilitate comparison with the former study a flow rate of 2 mL/min was employed.

The columns were then equilibrated with 0.5  $\mu\text{g/mL}$  CAP-MR at a flow rate of 2 mL/min and calibration curves were constructed as before. Responses to CAP were reasonably linear ( $r^2 = 0.95$ ,  $n = 3$ ) from 3 to 30  $\mu\text{g/mL}$ , while those to TAM were slightly lower but equally linear ( $r^2 = 0.96$ ,  $n = 3$ ). Again, responses to the diacetylated derivative CAP-DA were negligible. The simplicity and versatility of the *in situ* imprinting technique greatly facilitates the development of MIP-based sensors such as these.

#### 20.2.6.2 Fluorescent detection of $\beta$ -estradiol [40]

Previous studies on the preparation of MIPs for testosterone [41,42] indicated that, among a number of other steroids,  $\beta$ -estradiol was also strongly retained on testosterone-imprinted polymers which employed MAA as the functional monomer. Further (unpublished) studies demonstrated that the use of DEAEMA as the functional monomer resulted in  $\beta$ -estradiol-imprinted polymers which bound the template *extremely* strongly. The choice of functional monomer determined which of the two functionalities of  $\beta$ -estradiol was responsible for the majority of the binding interactions: using MAA as the functional monomer caused the C-17 hydroxy group to become the predominant binding group, while the use of DEAEMA necessitated the presence of a C-3 phenol for efficient recognition. A recent report [43] indicates that the use of 4-VP as the functional monomer also results in MIPs which have reasonable selectivity for  $\beta$ -estradiol. In a logical extension of our previous work on CAP sensors, we sought to construct an automated, continuous sensor for  $\beta$ -estradiol based on the previously successful combination of LC and MIPs. The concentrations of steroids in biological fluids are extremely low (*ca.* nM), so an extremely sensitive reporter was required. Due to the tenacity with which  $\beta$ -estradiol bound to DEAEMA-containing MIPs, we chose to label  $\beta$ -estradiol at the C-3 position with a dansyl moiety, leaving the C-17 hydroxyl group free to interact with the MAA functional monomer. The moderately strong interactions between MAA and the C-17 hydroxyl group of  $\beta$ -estradiol were intended to strike a compromise between sufficient selectivity and short assay times, while the fluorescent label was incorporated to afford the assay the required sensitivity.

Polymers were formed by heating a solution of the template, MAA (functional monomer:template ratio of 8:1), EDMA and initiator in MeCN at 40°C for 16 h. Polymers were then ground, particles sized to 25–45  $\mu\text{m}$  were washed with EtOH until the template could no longer be detected and then packed into 100  $\times$  4.6 mm (i.d.) HPLC columns.

*Displacement technique:* [44] Initially, the polymer was equilibrated in MeCN and the template and a variety of compounds, including potential reporters (Fig. 20.17), were chromatographed. All of the reporter compounds examined displayed a low affinity for the MIP, giving  $k'$  values of at most 1.0, while that of  $\beta$ -estradiol was 3.5 ( $k_{\text{imp}}$   $\beta$ -estradiol dansylate = 0.73).

The polymer was then equilibrated in MeCN containing  $\beta$ -estradiol dansylate

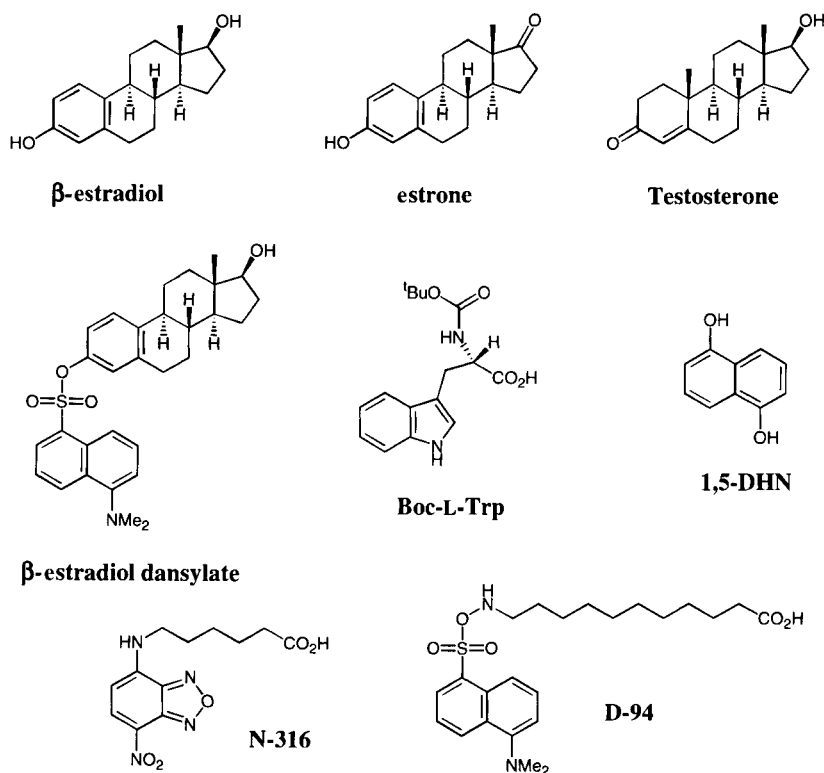


Fig. 20.17. Compounds examined using flow-injection type  $\beta$ -estradiol sensor.

and  $\beta$ -estradiol solutions of increasing concentrations were injected in order to displace the bound reporter and produce a peak. Disappointingly, no peak was observed even using  $\beta$ -estradiol concentrations as high as 100 nM.

Further attempts to produce a peak upon injection of  $\beta$ -estradiol solutions were made using various concentrations of  $\beta$ -estradiol dansylate in the mobile phase, but these were also unsuccessful. Thus, it appears that our designed reporter was not appreciably retained by the polymer and thus could not be displaced. Subsequently, we examined a variety of other non-specific reporters, varying their concentrations in the mobile phase from their fluorescence detection limit to levels at which they could easily be detected using UV spectroscopy (*ca.* 1–100 nM). Unfortunately, no peaks were observed.

Nevertheless, it may be possible to construct a displacement type system for the detection of  $\beta$ -estradiol by labelling the molecule at C-17 and using DEAEMA as the functional monomer. Alternatively, the reporter itself could be used as the template molecule. The smaller  $\beta$ -estradiol molecule should enjoy easy access to the binding sites and be able to compete effectively with the reporter. Finally, this technique may find more success for the analysis of corticosteroids [45], which possess

three or more functional groups, ensuring strong, multipoint binding and offering a number of possibilities for labelling.

*Direct measurement:* [44] In spite of the disappointing results above, we were able to use this system for the detection of  $\beta$ -estradiol by virtue of its inherent fluorescence. The use of a MIP as the chromatographic stationary phase greatly facilitates the separation of the analyte from other species. It is noteworthy that estrone, which fluoresces at approximately the same wavelength as  $\beta$ -estradiol due to its phenolic A-ring, was eluted in the void volume, while the fluorescence of  $\beta$ -estradiol reached a maximum after approximately 9 min in pure MeCN (flow rate 1 mL min<sup>-1</sup>). Thus, the only potential interfering species could be effectively removed from a sample containing a mixture of steroids.

In order to reduce the time required for the assay THF was added to the mobile phase. Increasing the proportion of this more polar solvent decreased both the retention time of the analyte and sharpened the resulting peaks which, in turn, increased the sensitivity of the assay. The best results were obtained using 5% THF. A linear response ( $r^2 = 0.998$ ,  $n = 4-5$ , average S.E.M. ca. 8%) was observed from 0.1 to 4  $\mu$ M  $\beta$ -estradiol and a single determination could be performed in 15 min. The advantages of this system are its potential for automation and reasonably short analysis time.

## 20.3 LATEST DEVELOPMENTS

Since the completion of the first draft of this chapter a number of interesting reports have appeared in the literature. These, too, will be considered in approximately chronological order.

### 20.3.1 Liquid chromatographic detection of L-phenylalanine amide

Using an approach similar to that outlined in Section 20.2.6.2. above, Piletsky *et al.* [46] have developed a sensor for the detection of L-phenylalanine amide. The system relies upon the displacement of the structurally unrelated dye, rhodamine B (Fig. 20.18), from an imprinted polymer upon injection of the template. MIPs were prepared in CHCl<sub>3</sub> using MAA as the functional monomer and EDMA as the cross-linker. Two other reporters, 4-nitrophenol and dansyl L-phenylalanine (Fig. 20.6), were also examined but proved to be unsuccessful. A number of interesting observations arise from this study. Firstly, using MeOH as the mobile phase, the non-imprinted polymer showed larger responses to phenylalanine than to the amide. Enantioselectivity was also observed, more so in the former case. Under the same conditions, the MIP exhibited a preference for the template, but negligible enantioselectivity was evident. The best results were obtained using 10  $\mu$ M rhodamine B in MeCN containing 0.5% AcOH as the mobile phase, where enantioselectivity was demonstrated for the amide. Unfortunately, the free amino acids were not soluble in this mobile phase. The time taken for a single measurement and

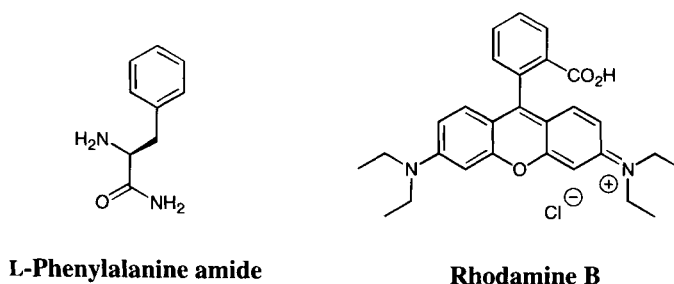


Fig. 20.18. The template (L-phenylalanine amide) and the fluorescent reporter dye used in this study. The other reporters examined (dansyl L-phenylalanine and 4-nitrophenol) were unsuccessful.

subsequent re-equilibration of the system was approximately 20 min. Basically linear relationships were observed between the area of the peak due to the displaced dye and the concentration of the analyte up to concentrations of 500  $\mu$ M. The ratio of responses due to the two enantiomers (L/D) ranged from 1.1 to 2.5, depending upon the concentration.

### 20.3.2 Fluorescent detection of PAHs in water

Dickert and co-workers [47] have expanded upon their earlier work (see Section 20.2.5.8.) on the detection of PAHs in water. Using similar procedures to those described above they have prepared a flow injection system for use with a number of imprinted polyurethanes (see Fig. 20.4) on quartz crystals, QCMs and SAWs, using a variety of PAHs of different sizes (Fig. 20.19). The most outstanding finding of these experiments is that the MIPs show maximum selectivity for analytes which are slightly larger than the actual templates. The optimum response to pyrene was observed when using polymers imprinted with the smaller templates acenaphthene and, to a lesser extent, phenanthrene (see Fig. 20.19 for relative responses). Polymers imprinted with anthracene or chrysene showed similar behaviour, binding molecules slightly larger than the template to a much greater extent (see Table 20.2). These fluorescence measurements were supported by data obtained using QCMs. In addition to the paper mentioned above, two reviews [48,49] have been published, although they tend to deal more with the application of polymers containing macromolecular hosts (e.g. calixarenes and cyclodextrins) to QCMs and SAWs.

### 20.3.3 MIPs and infrared evanescent wave spectroscopy

Haupt and co-workers have created a novel flow injection sensor by applying their 2,4-D MIP (see Section 20.2.5.10.) to the surface of ZnSe attenuated total reflectance crystals [50]. In this way, binding of the template could be monitored using FT-IR spectroscopy in the 3500–500  $\text{cm}^{-1}$  region. Three bulk MIPs were



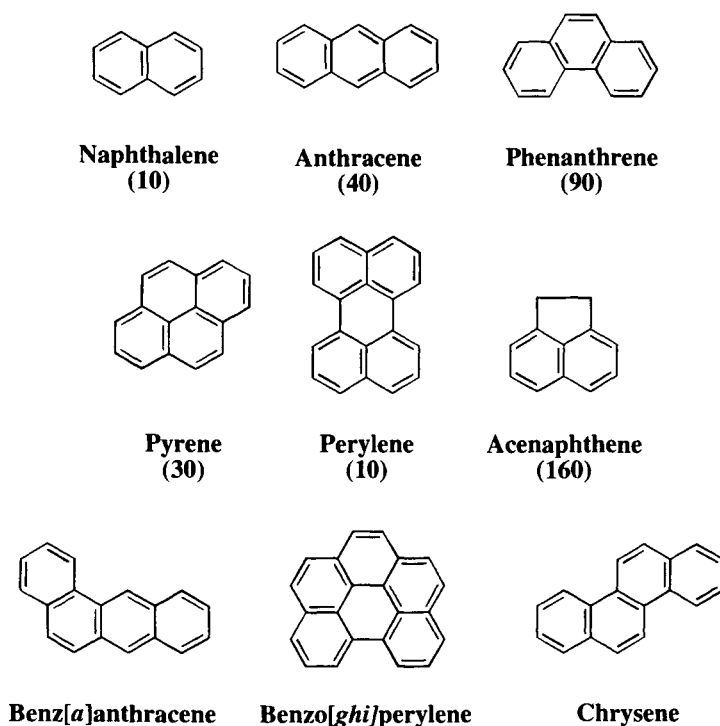


Fig. 20.19. Compounds used in the imprinting of polyurethanes. Where applicable, figures in parentheses represent the responses (fluorescence intensity, arbitrary units) to pyrene of polymers imprinted with various PAHs. The non-imprinted polymer gave a negligible response. See Table 20.2 for the behaviour of anthracene- and chrysene-imprinted polymers.

prepared by polymerising a 4/1 (v/v) MeOH/H<sub>2</sub>O solution containing EDMA as the cross-linker, 4-VP as the functional monomer and various amounts of methylmethacrylate (MMA) at 45°C overnight. Control polymers were prepared similarly, in the absence of the template. Keeping the template/4-VP ratio constant at 1/4, the molar proportions of EDMA and MMA were modified to examine the effects of the degree of cross-linking on the polymers. The resulting polymers had EDMA/MMA ratios of P1 = 20/0, P2 = 13/7 and P3 = 4/12.

These polymers were ground and wet-sieved through a 25  $\mu\text{m}$  sieve. They were then washed twice with 4/1 (v/v) MeOH/H<sub>2</sub>O solution and twice with MeOH, each time for 2 h. The particles were then repeatedly sedimented in acetone for 2 h to remove *coarse* particles. The *fine* particles were collected by centrifugation, dried in vacuo and used in radioligand binding assays to determine their affinity for the template. Imprinted polymer I1 exhibited the strongest binding, reaching saturation at approximately 1.5 mg mL<sup>-1</sup> <sup>14</sup>C-2,4-D. I2 also showed strong binding, reaching saturation at approximately 5 mg mL<sup>-1</sup> template. I3 exhibited binding only slightly greater than did the non-imprinted polymers (C1–C3).

TABLE 20.2

APPROXIMATE ENRICHMENT FACTORS OF POLYURETHANES IMPRINTED WITH EITHER ANTHRACENE OR CHRYSENE. ENRICHMENT FACTORS ARE CALCULATED AS THE RATIO OF THE CONCENTRATION OF THE ANALYTE WITHIN THE IMPRINTED POLYMER SUBSTRATES TO THAT WITHIN THE AQUEOUS PHASE.

| Analyte            | Enrichment factor<br>for anthracene MIP | Enrichment factor<br>for chrysene MIP |
|--------------------|---|---------------------------------------|
| Anthracene         | $4 \times 10^5$                         | Negligible                            |
| Benz[a]anthracene  | $1.0 \times 10^6$                       | $2 \times 10^5$                       |
| Chrysene           | $2.4 \times 10^6$                       | $6 \times 10^5$                       |
| Pyrene             | $2.0 \times 10^6$                       | $1.4 \times 10^6$                     |
| Perylene           | $9 \times 10^5$                         | $2.0 \times 10^6$                     |
| Benzo[ghi]perylene | $7 \times 10^5$                         | $1.0 \times 10^6$                     |

The polymer films were prepared by pipetting 20  $\mu\text{L}$  aliquots of the solution onto the ZnSe crystals, clamping a glass slide over these and polymerising the mixtures for 3 h at 50°C. Polymer I1 was too brittle and cracked easily, so I2 was used in further experiments. The polymer films were, on average, between 4 and 9  $\mu\text{m}$  thick, with a relative standard deviation of approximately 20% within one layer.

MIP-coated crystals were mounted in the flow cell and equilibrated with phosphate buffer (pH 7, 25 mM) for 60 min. Analyte solutions (4.5  $\mu\text{M}$ –4.5 mM) were then pumped through the system in the same buffer at 1.5 mL min<sup>-1</sup>, while spectra were recorded at 1 min intervals over the 1900–1000 cm<sup>-1</sup> region. Enrichment of the analyte could be observed by monitoring the areas of absorption bands specific to the analyte. Saturation was usually reached after approximately 15 min and the process could be reversed by rinsing the film with buffer. Despite the variations in thickness, the films showed reasonable reproducibility, with relative standard deviations ranging from 7.5% at the lowest concentrations to 24% at the highest. Binding of phenoxyacetic acid (POAc, see Fig. 20.14) to I2 was similar to or less than binding of 2,4-D to C2, while binding of POAc to C2 was negligible.

The data were fitted to a Langmuir binding model combined with a linear term and the analytes 2,4-D and POAc were found to have dissociation constants ( $K_D$ ) of approximately 190 and 370  $\mu\text{M}$  and critical concentrations (where concentrations due to specific- and non-specific binding are equal) of 4.0 and 5.5 mM, respectively. This selectivity is not as high as that observed in other experiments [36,37], perhaps due to the lower degree of cross-linking. The  $K_D$  of 2,4-D is also about two orders of magnitude higher than the *apparent* dissociation constant,  $K_{\text{app}}$  of 1.2  $\mu\text{M}$ , as determined by radioligand binding [51]. Limits of detection for 2,4-D range from 2.9 to 28  $\mu\text{M}$ , depending upon the wavenumber range examined. This should be compared with the detection limits of approximately 0.1  $\mu\text{M}$  determined in

radio- and fluoroimmunoassays. It is expected that a combination of improved spectroscopic transducers and MIPs should lead to more reproducible, more sensitive sensors.

### 20.3.4 Competitive chemiluminescence assay

In work similar to that described in Section 20.2.5.10., Haupt and co-workers have found yet another use for their 2,4-D-imprinted polymer [51]. Whereas in the work described above the competing analyte was CMMC (see Fig. 20.14), in these experiments 2,4-dichlorophenol (DCP) was used as the competitor. This compound is an enhancer of the peroxidase-catalysed chemiluminescence of the well known reaction of luminol and  $\text{H}_2\text{O}_2$ . Thus, in a certain concentration range, the amount of DCP present in solution is an indicator of the amount of template bound to the MIP. Competitive radioimmunoassays were used to determine the affinity of DCP for the 2,4-D-imprinted polymer and it was found that, while 500  $\mu\text{g}$  of MIP were required to bind 50% of the CMMC, only 250  $\mu\text{g}$  of polymer were required to bind 50% of the DCP. In order to verify this unexpected result, competitive binding assays were performed in the presence of  $^{14}\text{C}$ -2,4-D and it was found that the relative affinities of the polymer for CMMC and DCP were approximately 6 and 10% that of 2,4-D. However, while CMMC bound poorly to the non-imprinted polymer, DCP bound equally as well as to the MIP. This indicates that, in the latter case, binding is almost entirely non-specific. Thus DCP was a poor probe for this system. Fluorescein was also examined as a probe for polymers imprinted with 2,4-D, propranolol, atrazine and theophylline but, just as in our work (Section 20.2.6.2.) and that of Piletsky *et al.* (Section 20.3.1.), structurally unrelated probes are generally unsuitable. Incidentally, Haupt and co-workers have successfully used 2,5-dihydroxyphenylacetic acid (homogentisic acid) as a reporter in a 2,4-D MIP-based sensor using differential pulse voltammetry [52].

### 20.3.5 A fluorescent sensor for L-tryptophan

Wang and co-workers [53] have succeeded in constructing a novel sensor based on the displacement of a small, structurally unrelated quencher from a MIP comprising a fluorescent functional monomer (Fig. 20.20). The principle of detection relies upon the enhanced fluorescence observed upon displacement of the quencher, *p*-nitrobenzaldehyde, from the L-tryptophan (L-Trp) binding sites within the polymer.

MIPs were typically formed by mixing the template, a 4-fold excess of the fluorescent functional monomer and a 40-fold excess of the cross-linker EDMA in MeCN. Small amounts of AcOH and trifluoroacetic acid were then added to dissolve the template, the solution flushed with nitrogen for 45 min, initiator added and the solution stirred for 2 h before being polymerised at 45°C for 48 h. The resulting polymer was then ground, sieved through a 100  $\mu\text{m}$  sieve, washed with 100 mL 20% AcOH in MeOH, 200 mL 10% AcOH in MeOH and finally with 100 mL of MeOH. The MIP was then dried *in vacuo* at 35°C overnight to give yields of

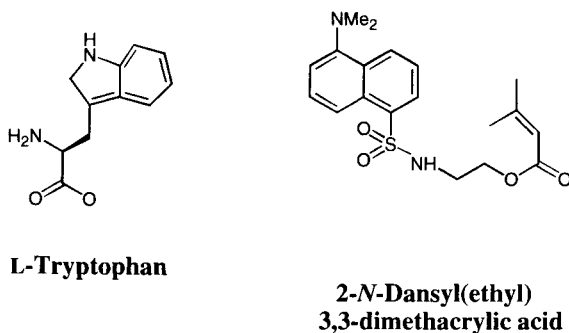


Fig. 20.20. The template (*L*-tryptophan) and the fluorescent functional monomer used in this study.

about 60%. Non-imprinted polymers were prepared similarly in the absence of the template.

Equilibration of the MIP and the template for 4 h in a two phase 1/1 (v/v)  $\text{CHCl}_3$ /citrate buffer (0.03 M) mixture showed negligible changes in the emission spectrum of the organic layer. Thus the effect of *p*-nitrobenzaldehyde on the emission spectra of the polymers was examined. Interestingly, the non-imprinted polymer was more readily quenched than the MIP, which is counter-intuitive, reinforcing the observation that the physical structures of the imprinted and non-imprinted polymers are intrinsically different. Quenching of the fluorescence of the imprinted polymer by *p*-nitrobenzaldehyde was weaker in the presence of *L*-Trp, indicating that the template was occupying and, therefore, 'protecting' some proportion of the binding sites within the MIP. Forty milligrams of the polymers were mixed with 4 mL of 3 mM *p*-nitrobenzaldehyde in  $\text{CHCl}_3$  and various concentrations of *L*-Trp in 4 mL of 0.03 M citrate buffer were mixed for 4 h and the fluorescence spectra of the organic layer recorded. In the absence of the template the fluorescence was reduced by more than 75%, but upon addition of 10 mM *L*-Trp the fluorescence increased by more than 40%. No change was observed upon addition of 3 mM of template to the non-imprinted polymer. A number of other amino acids were examined to determine the selectivity of the MIP. At concentrations of 10 mM, 3-indoleacetic acid, indole and *L*-alanine exhibited negligible effects, but the responses to *D*-Trp and *L*-phenylalanine were 70 and 60%, respectively, that to *L*-Trp, indicating the ability of the MIP to discriminate not only between the side chains of the amino acids but also the chirality of the template.

At low concentrations ( $< 10$  mM), tryptamine caused a small increase in the fluorescence intensity, presumably due to its ability to displace *p*-nitrobenzaldehyde from the binding sites by virtue of its resemblance to the template, but it was found that 10 mM tryptamine itself was able to quench the fluorescence of the MIP, albeit less than 1/10th as effectively as *p*-nitrobenzaldehyde. In spite of shortcomings, such as the long incubation period, the biphasic nature of the system, the need for a specially designed functional monomer and its rather high detection limit (*ca.* 0.1

mM), this method has demonstrated yet another means by which MIPs may be incorporated into sensors.

### 20.3.6 An enzyme-linked MIP sorbent assay

In yet another application of their 2,4-D MIP, Haupt and co-workers [54] have developed an MIP-based ELISA. Precipitation-polymerised microspheres were prepared by dissolving 2 mmol of the cross-linker TRIM, 4 mmol of the functional monomer 4-VP and 10 mmol of the template in 40 mL of 4/1 (v/v) MeOH/H<sub>2</sub>O, sonicating the solution for 5 min, cooling it in ice and sparging it with nitrogen for 3 min. The solution was then polymerised at 60°C for 16h. The fine particles were collected by centrifugation, washed three times in 7/3 (v/v) MeOH/AcOH, once in acetone and finally dried at 40°C. Non-imprinted polymers were prepared similarly but without the template. Note that in this procedure an unusually large amount of template was used. This is intended to drive the system toward the formation of template/functional monomer complexes prior to polymerisation. The imprinted microspheres were found to have average surface areas of 7 m<sup>2</sup> g<sup>-1</sup> (from BET measurements) and diameters of 600 nm (from SEM measurements).

Radioligand binding assays were performed basically as before [36,37] to determine the affinity of the microspheres for <sup>14</sup>C-2,4-D. As expected, the non-imprinted polymer exhibited very little affinity for the radioligand while the imprinted microspheres bound the analyte very strongly. Approximately 6 mg of the MIP was required to bind 50% of the radioligand (*cf.* 150 µg for the radioimmunoassay [36] and 100 µg for the fluoroimmunoassay [37]), indicating the extremely low binding capacity of the microspheres compared with the usual block polymers, even though the average diameters of the spheres were similar (600 nm *v.* 1000 nm, respectively).

Competitive radioassays indicated a slight preference for the template over CPOAc or 2,4-DB (see Fig. 20.14), giving cross-reactivities of 25 and 10% (*cf.* 24 and 95%; Table 20.1).

Having established the selectivity of the microspheres for 2,4-D, the template was then conjugated to tobacco peroxidase (TOP). Briefly, TOP was activated using NaIO<sub>4</sub> then coupled with diaminopropane. 2,4-D was converted to its *N*-hydroxysuccinimide ester and allowed to react with the derivatised TOP. After purification, the final 2,4-D/TOP ratio was estimated to be 8/1.

In colorimetric assays using *o*-phenylenediamine in H<sub>2</sub>O<sub>2</sub>, the analyte could be quantified from 40 to 600 µg mL<sup>-1</sup>, while in chemiluminescent assays using luminol and H<sub>2</sub>O<sub>2</sub> the range was 1–200 µg mL<sup>-1</sup>, corresponding to a lower detection limit of approximately 4.5 µM 2,4-D, a little higher than the MIP-based radio- or fluoroimmunoassays (*cf.* 0.1 µM, see Section 20.2.5.10.). Note that this technique differs from conventional ELISAs in that the activity of the enzyme in the supernatant is determined after removal of the MIP. Nonetheless, it has been demonstrated that MIP-based ELISA type assays are feasible, have detection limits similar to MIP-based radio- and fluoroimmunoassays and may obviate the use of the more expensive and fragile antibodies.

### 20.3.7 A fluorescent FIA sensor for flavonol

In a very thorough series of experiments, Suarez-Rodriguez and Diaz-Garcia [55] have developed an FIA system for the detection of 3-hydroxyflavone (flavonol, Fig. 20.21). In a typical procedure, MIPs were prepared by polymerising a nitrogen sparged solution of template (38  $\mu\text{M}$ ), MAA (302  $\mu\text{M}$ ) and EDMA (1.42 mM) in  $\text{CHCl}_3$  at 70°C for 14 h. The resulting polymer was ground and sieved to obtain particles with an average diameter of 80–160  $\mu\text{m}$ . Before use a 20 mg portion of the MIP was packed into a flow cell and washed with EtOH until the template was no longer observable in the effluent.

The optimal mobile phase was determined by equilibrating the MIP with hexane and injecting 150  $\mu\text{L}$  aliquots of 5.0  $\mu\text{M}$  flavonol in hexane. The time required to reach a maximal response of approximately double the initial intensity was about 12 min. However, the template could not be removed from the MIP until the mobile phase was changed to  $\text{CHCl}_3$ . A number of polar modifiers ( $\text{CHCl}_3$ , acetone, EtOH and dioxane) were then added to the hexane carrier to determine the optimal solvent mixture. The nature and proportion of the more polar solvent influenced both the relative fluorescence intensity as well as the time taken for the fluorescence intensity to return to its original level (the recovery time) and eventually a 70/30 (v/v) mixture of hexane/ $\text{CHCl}_3$ , which gave a recovery time of about 11 min, was chosen.

The ratio of EDMA cross-linker to MAA functional monomer was also examined.  $\text{CHCl}_3$  was again used as the porogen and 150  $\mu\text{L}$  aliquots of 5.0  $\mu\text{M}$  flavonol in a 70/30 (v/v) mixture of hexane/ $\text{CHCl}_3$  were injected into the system. Both the relative fluorescence intensity as well as the response time of the system generally decreased as the EDMA/MAA ratio was increased and, in particular, fluorescence intensities and response times for MIPs with EDMA/MAA ratios  $> 0.4$  were significantly reduced. Thus, the optimal polymer was deemed to be that with an EDMA/MAA ratio of approximately 0.25. This is unusual, as most MIPs, as well as the mixture indicated above, have an EDMA/MAA ratio of *ca.* 4/1.

Using the optimal conditions determined above, the effect of the volume of porogen used in the polymerisation was examined. Volumes of  $\text{CHCl}_3$  from 0.6 to 1.5 mL had little effect on the response times, while volumes of less than 0.8 mL

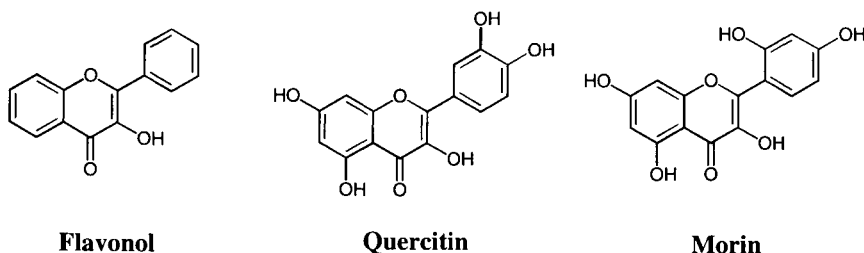


Fig. 20.21. Compounds examined using the flow-injection type flavonol sensor.

$\text{CHCl}_3$  decreased the fluorescence intensity dramatically. Thus, further MIPs were prepared using 1 mL of porogen. The template/functional monomer ratio was also examined and it was found that a maximum fluorescence intensity was observed for flavonol/MAA ratios of *ca.* 0.1, while ratios from 0.01 to 0.5 exhibited significantly decreased fluorescence intensities but similar or slightly higher response times. Thus, this ratio was employed in the preparation of subsequent MIPs.

After establishing the optimal conditions, the selectivity of the MIP for flavonol over some similar compounds (Fig. 20.21) was examined. It was found that the addition of either morin or quercetin to the template flavonol resulted in slightly higher relative fluorescence intensities than using the template alone. These additions gave enhancements of approximately 10% in the former case and about 5% in the latter, whether in ratios of 1:3, 1:6 or 1:9. Most curiously, neither of the other two compounds caused any response at all when injected alone. Thus, the sensor is specific for flavonol. Using data obtained from triplicate injections, the limit of detection was found to be 0.5 nM (signal/noise = 3), with a linear range up to 100 nM flavonol and a relative standard deviation of 2%.

The reproducibility of the sensor was also investigated by removing the template from the polymer and 'reloading' it into the system. After three cycles, the signals from a single batch of polymer had values 80–97% that of the initial response. Between different batches of the MIP, this figure was found to be 93%. Moreover, the polymers were found to be mechanically stable after more than 2 months of continuous use.

Finally, the sensor was used to determine the concentration of flavonol in olive oils. Samples were fortified with olive oil, diluted 4/1 (v/v) with the 70/30 (v/v) hexane/ $\text{CHCl}_3$  mixture and injected into the system. Responses were approximately 95% those of the pure solutions. Samples were also analysed using a traditional LC-based method. The two sets of results showed a correlation of  $r^2 = 0.998$ ,  $n = 6$ , conclusively demonstrating the utility of this system in practical applications.

## 20.4 OUTLOOK

There are a number of approaches to the development of optical MIP-based sensors and these can be classified according to the nature of the analyte:

1. Chromogenic analytes, either inherently chromogenic or labelled.
  - (a) Measurement of solution after equilibration with (or exposure to) the polymer.
  - (b) Measurement of bound analyte, in either the presence or absence of the supernatant.
2. Non-chromogenic analytes.
  - (a) Competition with a reporter molecule, measurement of solution or polymer.
  - (b) Alteration of wavelength and/or intensity of a chromogen within the MIP.
  - (c) Formation of a chromogenic compound within/without the MIP.

Of the many examples of the use of MIPs in optically based analytical techniques, by far the majority rely upon fluorescence measurements to achieve optimal sensitivity. Thus, it seems that fluorimetric techniques will continue to receive much interest.

The resounding success of Haupt's fluoroimmunoassay procedure (Section 20.2.5.10.) ensures that such extraordinarily simple yet selective techniques will receive a great deal of attention in the near future. The lengthy incubation times required to reach equilibrium may simply be shortened to more convenient exposure times.

Nonetheless, batch binding procedures require both exposure and analysis steps, whereas these are combined in our LC-based method. Although this was not entirely successful in the latter example given above (Section 20.2.6.2.), we look forward to the widespread adoption of this technique. The *in situ* imprinting technique simplifies the procedure to an enormous extent.

Direct measurement of MIPs (Sections 20.2.5.4., 20.2.5.5. and 20.2.5.9.) should also yield new opportunities. One envisages soaking a polymer film in a sample solution (or, as in Section 20.2.3., exposing the film to a gaseous analyte) then inserting the film into the appropriate device and, from the observed change in optical properties, calculating the concentration of analyte in the sample. Transparent MIPs such as those developed by Steinke *et al.* (Section 20.2.2.) should prove extremely useful in such techniques.

The use of fibre optics should also prove to be very interesting. The formation of imprinted matrices directly on the optic fibre (Sections 20.2.5.6. and 20.2.5.7.) should overcome the shortcomings of Kriz's prototype (Section 20.2.5.1.). Thin membranes of MIP should vastly increase mass-transfer rates, reducing incubation times as well as obviating the need for physical entrapment of polymer particles.

A very important field in the future is the development of portable devices for on-site analyses of, for example, lead ions (Section 20.2.5.6.), chemical warfare agents (20.2.5.7.), herbicides (Sections 20.2.5.3. and 20.2.5.10.) or PAHs (Section 20.2.5.8.). Improvements to the MIPs themselves, such as increasing the capacity, improving the mass-transfer rate and reducing the heterogeneity of the binding sites, can only serve to accelerate the development of MIP-based sensors. Finally, combinations of catalytically active MIPs and biological recognition elements or, alternatively, 'passive' MIPs and enzymes may prove to be extremely interesting. The future for MIP-based optical sensors appears undeniably bright!

## ACKNOWLEDGEMENTS

Thanks are due to H.-S. Ji, K.-H. Lee and K. Yano for their assistance in the preparation of this manuscript. Work in our laboratories was supported by the Japanese Ministry of Education, Science, Sports, and Culture: Large-scale Research Projects, under the New Program in Grants-in-Aid for Scientific Research.



## REFERENCES

- 1 J. Steinke, D.C. Sherrington and I.R. Dunkin, *Adv. Poly. Sci.*, **123**, 81 (1995).
- 2 G. Wulff, *Angew. Chem. Int. Ed. Engl.*, **34**, 1812 (1995).
- 3 K. Mosbach and O. Ramström, *Bio/Technology*, **14**, 163 (1996).
- 4 T. Takeuchi and J. Matsui, *Acta Polymer.*, **47**, 471 (1996).
- 5 J.-M. Lin, M. Yamada and T. Hobo, *Mem. Fac. Eng., Tokyo Metro. University*, **47**, 5603 (1997).
- 6 A.G. Mayes and K. Mosbach, *Trends Anal. Chem.* **16**, 321 (1997).
- 7 R.J. Ansell, O. Ramström and K. Mosbach, *Clin. Chem.*, **42**, 1506 (1996).
- 8 M. Kempe and K. Mosbach, *J. Chromatogr. A.*, **694**, 3 (1995).
- 9 S.E. Byström, A. Börje and B. Åkermark, *J. Am. Chem. Soc.*, **115**, 2081 (1993).
- 10 M.E. Davis, A. Katz and W.R. Ahmad, *Chem. Mater.*, **8**, 1820 (1996).
- 11 P.A. Brady and J.K. Sanders, *Chem. Soc. Rev.*, **26**, 327 (1997).
- 12 O. Ramström, Y. Ye and K. Mosbach, *Chromatographia*, **47**, 465 (1998).
- 13 Y. Ye, O. Ramström and K. Mosbach, *Anal. Chem.*, **70**, 2789 (1998).
- 14 G. Wulff, In: *Frontiers in biosensorics I: fundamental aspects*, F.W. Scheller, F. Schubert and J. Fedrowitz Eds, Birkhauser Verlag, Basel, p. 13 (1997).
- 15 D. Kriz, O. Ramström and K. Mosbach, *Anal. Chem.*, **69**, 345A (1997).
- 16 L.I. Andersson, C.F. Mandenius and K. Mosbach, *Tetrahedron Lett.*, **29**, 5437 (1988).
- 17 J.H.G. Steinke, I.R. Dunkin and D.C. Sherrington, *Macromolecules*, **29**, 407 (1996).
- 18 F.L. Dickert and S. Thierer, *Adv. Mater.*, **8**, 987 (1996).
- 19 H.-S. Ji, S. McNiven, K. Yano, K. Ikebukuro, U.T. Bornschauer, R.D Schmid and I. Karube, *Anal. Chim. Acta*, **387**, 39, (1999).
- 20 H.-S. Ji, S. McNiven, K. Ikebukuro and I. Karube, *Anal. Chim. Acta*, **390**, 93, (1999).
- 21 S.-W. Lee, I. Ichinose and T. Kunitake, *Langmuir*, **14**, 2857 (1998).
- 22 E.P.C. Lai, A. Fafara, V.A. Vandernoot, M. Kono and B. Polsky, *Can. J. Chem.*, **76**, 265 (1998).
- 23 G. Vlatakis, L.I. Andersson, R. Muller and K. Mosbach, *Nature*, **361**, 645 (1993).
- 24 D. Kriz, O. Ramström, A. Svensson and K. Mosbach, *Anal. Chem.*, **67**, 2142 (1995).
- 25 S.A. Piletsky, E.V. Piletskaya, K. Yano, A. Kugimiya, A.V. Elgersma, R. Levi, U. Kahlow, T. Takeuchi, I. Karube, T.I. Panasyuk and A.V. El'skaya, *Anal. Lett.*, **29**, 157 (1996).
- 26 S.A. Piletsky, E.V. Piletskaya, A.V. El'skaya, R. Levi, K. Yano and I. Karube, *Anal. Lett.*, **30**, 445 (1997).
- 27 M.F. Lulka and J.P. Chambers, *Anal. Lett.*, **30**, 2301 (1997).
- 28 M.E. Cooper, B.P. Hogg and D.L. Gin, *Polym. Prepr.*, **38**, 209 (1997).
- 29 M.J. Whitcombe, M.E. Rodriguez, P. Villar and E.N. Vulfson, *J. Am. Chem. Soc.*, **117**, 7105 (1995).
- 30 G.M. Murray, A.L. Jenkins, A. Bzhelyansky and O.M. Uy, *Johns Hopkins Technical Digest*, **18**, 464 (1997).
- 31 A.L. Jenkins, O.M. Uy and G.M. Murray, *Anal. Comm.*, **34**, 221 (1997).
- 32 A.L. Jenkins, O.M. Uy and G.M. Murray, *Anal. Chem.*, **71**, 373 (1999).
- 33 F.L. Dickert, H. Besenbock and M. Tortschanoff, *Adv. Mater.*, **10**, 149 (1998).
- 34 F.L. Dickert, P. Forth, P. Leiberzeit and M. Tortschanoff, *Fresenius J. Anal. Chem.*, **360**, 759 (1998).
- 35 P. Turkewitsch, B. Wandelt, G.D. Darling and W.S. Powell, *Anal. Chem.*, **70**, 2025 (1998).
- 36 K. Haupt, A. Dzgoev and K. Mosbach, *Anal. Chem.*, **70**, 628 (1998).
- 37 K. Haupt, A.G. Mayes and K. Mosbach, *Anal. Chem.*, **70**, 3936 (1998).
- 38 R. Levi, S. McNiven, S.A. Piletsky, S.H. Cheong, K. Yano and I. Karube, *Anal. Chem.*, **69**, 2017 (1997).
- 39 S. McNiven, M. Kato, R. Levi, K. Yano and I. Karube, *Anal. Chim. Acta*, **365**, 69, (1998).

- 40 A. Rachkov, S. McNiven, S.-H. Cheong, A. El'skaya, K. Yano and I. Karube, *Supramol. Chem.*, **9**, 317 (1998).
- 41 S.-H. Cheong, S. McNiven, A. Rachkov, R. Levi, K. Yano and I. Karube, *Macromolecules*, **30**, 1317 (1997).
- 42 S.-H. Cheong, A. Rachkov, J.-K. Park, K. Yano and I. Karube, *J. Poly. Sci. A*, **36**, 1725 (1998).
- 43 J. Haginaka and H. Sanbe, *Chem. Lett.*, 1089 (1998).
- 44 A. Rachkov, S. McNiven, A. El'skaya, K. Yano and I. Karube, *Anal. Chim. Acta*, **405**, 23, (2000).
- 45 O. Ramström, Y. Ye and K. Mosbach, *Chem. Biol.*, **3**, 471 (1996).
- 46 S.A. Piletsky, E. Terpetschnig, H.S. Andersson, I.A. Nicholls and O.S. Wolfbeis, *Frese-  
nius J. Anal. Chem.*, **364**, 512 (1999).
- 47 F.L. Dickert, M. Tortschanoff, W.E. Bulst and G. Fischerauer, *Anal. Chem.*, **71**, 4559 (1999).
- 48 F.L. Dickert and R. Sikorski, *Mater. Sci. Eng. C*, **10**, 39 (1999).
- 49 F.L. Dickert and O. Hayden, *Trends Anal. Chem.*, **18**, 192 (1999).
- 50 M. Jakusch, M. Janotta, B. Mizaikoff, K. Mosbach and K. Haupt, *Anal. Chem.*, **71**, 4786 (1999).
- 51 K. Haupt, *React. Funct. Polym.*, **41**, 125 (1999).
- 52 S. Kröger, A.P.F. Turner, K. Mosbach and K. Haupt, *Anal. Chem.*, **71**, 3698 (1999).
- 53 Y. Liao, W. Wang and B. Wang, *Bioorg. Chem.*, **27**, 463 (1999).
- 54 I. Surugui, L. Ye, E. Yilmaz, A. Dzgoez, B. Danielsson, K. Mosbach and K. Haupt, *Analyst*, **125**, 13 (2000).
- 55 J.L. Suarez-Rodriguez and M.E. Diaz-Garcia, *Anal. Chim. Acta*, **405**, 67 (2000).

This Page Intentionally Left Blank

## **Non-covalent molecularly imprinted sensors for vapours, polyaromatic hydrocarbons and complex mixtures**

FRANZ L. DICKERT AND OLIVER HAYDEN

### **21.1 INTRODUCTION**

Host-guest chemistry has enjoyed increased attention as an alternative to biological receptors. Although biological macromolecules as hosts exhibit very high affinities, generally only synthetic recognition elements are robust enough for durable field sensors. The study of artificial recognition systems has resulted in two major methodologies for the design of receptors. In one method, tailored supramolecular host molecules [1] are adapted for the use of a wide range of substance classes with remarkable selectivities. A second method involves molecular imprinting, which may be covalent and non-covalent. Imprinting techniques circumvent the synthetic effort by utilising a template-controlled synthesis of rigid polymers [2] or sol-gels [3,4]. Both approaches make use of the association of host and guest molecules to form an inclusion process through shape- or size-sensitive recognition.

The intriguing idea of molecular imprinting has been partially deduced from the early theories on antibody biosynthesis completed in the mid 1940s (see Chapter 1). One of the first experimental applications of molecular imprinting was reported by F.H. Dickey [5], but it was the work of G. Wulff [6] in 1972 which described the imprinting of organic polymers for the first time. Finally, K. Mosbach [7] developed the first selective non-covalent imprinted polymers (see Chapters 1 and 5). Recent advances in the optimisation of selectivity and sensitivity of non-covalent imprinting allow for effective design of molecularly imprinted polymers (MIPs) as coatings for sensor elements [8,9] and for solid phase extractions [10,11]. The results given in this chapter show the versatility of non-covalent MIPs with respect to certain sensing devices, in particular optical- and mass-sensitive sensor elements, and their promise as MIP detection systems of commercial interest.

### **21.2 CHEMICAL SENSORS**

The extensive literature on biosensors and chemosensory devices contains few reports on sensor elements with applicable advances in portability and in-the-field-ruggedness. Biosensors provide high affinities and therefore outstanding sensitivity

and selectivity, although the biological receptors lack stability and, often, reversibility (see also Chapter 10). In contrast, chemical sensors have the *forte* of thermal and chemical stability, which is useful for applications under harsh conditions where biosensors would be too fragile. Synthetic receptors based on MIPs can exhibit sensitivities comparable to those of biological receptors. However, generally speaking, it is obvious that the sensitivities and selectivities of common MIP sensors at this level are still not comparable to their biological counterparts. The imprinted layers described in this chapter are capable of a sufficient and selective sensor response to offer an alternative for a wide range of chemical analyses. A major strong point of molecular imprinting is the appropriate adaptation to analytes where there is no equivalent biological sensing element.

Chemical sensors are by definition small, inexpensive and preferably hand-held devices, capable of continuously monitoring chemical constituents in liquids or gases. MIP sensors usually consist of an imprinted sensitive layer and a transducer to convert the chemical information, in real time, into an electrical or optical signal which is further evaluated electronically [12]. Figure 21.1 shows the set-up of chemosensors and two typical mass-sensitive devices.

The selective enrichment of the analyte in the sensitive MIP layer alters the properties of the coating physicochemically. This effect, and the versatile handling of the imprinted polymers permits, the application of various detection principles to monitor the process of specific incorporation into the polymer matrix. Suitable properties for a sensor response include changes in mass, fluorescence, absorbance,

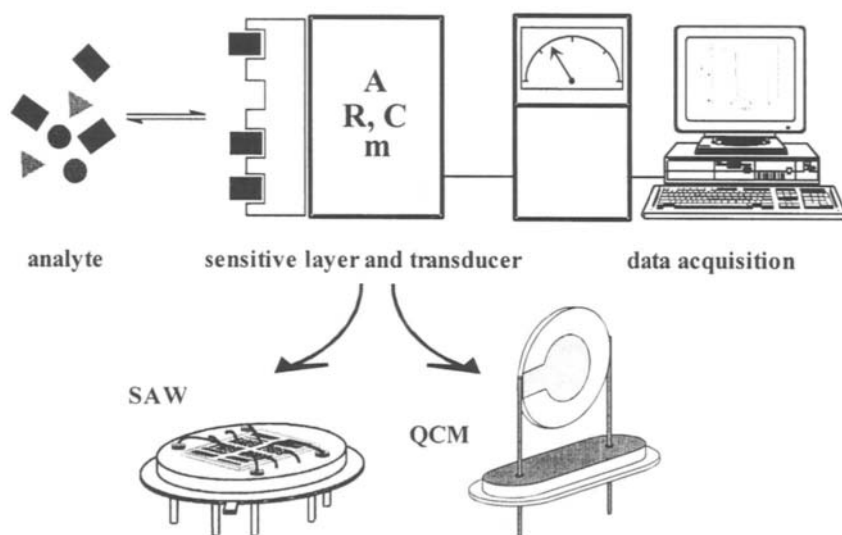


Fig. 21.1. Schematic structure of a chemosensory system. Various physical or optical properties can be used for sensory detection. Typical mass-sensitive transducer (QCM and SAW) are shown.

TABLE 21.1

## SUMMARY OF SUITABLE ULTRA-SENSITIVE AND INTEGRATED CHEMOSENSORY DEVICES

| Sensors                | Sensing scheme              | Particular advantages                            | Disadvantages                                |
|------------------------|-----------------------------|--|--|
| Optical sensor/optrode | Absorbance fluorescence     | Multiplex advantage, inexpensive one-way sensors | Bleaching                                    |
| SPR                    | Coupling angle reflectivity | Biosensor applications                           | Miniaturisation                              |
| FET                    | Field-effect                | Working range, detection limit                   | Reference electrode                          |
| QCM, SAW and STW       | Mass-sensitivity            | Inexpensive, universal detection principle       | Temperature cross-sensitivity, viscous media |

resistance or capacitance. Table 21.1 gives a brief summary of the most applicable sensing schemes for sensors, including considerations about true miniaturisation and sensitivity of chemosensors.

Chemically sensitive field-effect transistors (ChemFETs) are an example of an 'active' sensing device. ChemFETs [13] are well established for charged and polar species to monitor changes in field strength. These devices have some restrictions in implementation, such as the construction of small reference electrodes. Because of the high sensitivity and drift phenomena of these devices to minor changes in temperature or humidity, ChemFETs have to be 'sealed' properly in microelectronic circuits. This is a disadvantage of all highly sensitive transducers – the more sensitive, the more susceptible the sensors are to environmental conditions. Therefore, it is important to obtain good control of the environmental conditions through proper temperature and humidity control, e.g. in order to reduce cross-sensitivities.

Optical fibres and integrated optoelectronic devices for a wide spectral range are available making optical sensors feasible for the detection of various substance classes. In particular, MIP-coated optrodes, optical sensors with embedded labels, can be used for the detection of analytes which do not have suitable optical absorbance. Optical sensors are capable of simultaneously analysing different characteristic wavelengths, the so-called 'multiplex advantage'. Additionally, the length of the coated fibres, up to 1000 m, enables monitoring in difficult to access areas. Fourier-transform analysis of spectrophotometric data dramatically improves the speed of

gathering spectral information. However, multivariate data evaluation is required in order to extract the relevant information.

The detection of mass changes is also highly applicable, as mass is a fundamental quality of all analytes and thus independent of morphological, functional and optical aspects. The most favourable MIP sensors, therefore, are microelectronic transducers based on piezocrystals [14,15], such as quartz crystal microbalances (QCMs), shear transverse acoustic waves (STWs) [16] and surface acoustic waves (SAWs) [17]. High frequency devices for liquid applications are accessible with quartz analogue 428 MHz-LiTaO<sub>3</sub> substrates, working in the STW mode with a low damping in aqueous phases. The gravimetric sensing scheme of these resonators is linearly correlated with the sensor response, yielding a direct prediction about the imprinting effect. Viscosity and temperature effects can be compensated for measurements with dual or ternary sensors, which include an uncoated and/or reference channels coated with non-imprinted polymers.

### 21.3 EVIDENCE FOR MOLECULAR RECOGNITION

Evidence for a specific inclusion process promoted by molecular imprinting is directly given through sensor effects in comparison to non-imprinted layers of equivalent height. Detailed interpretation of specific inclusion or non-specific adsorption phenomena is accessible with the Brunauer–Emmett–Teller (BET) isotherm adsorption analysis [18]; a typical BET-isotherm is shown in Fig. 21.2.

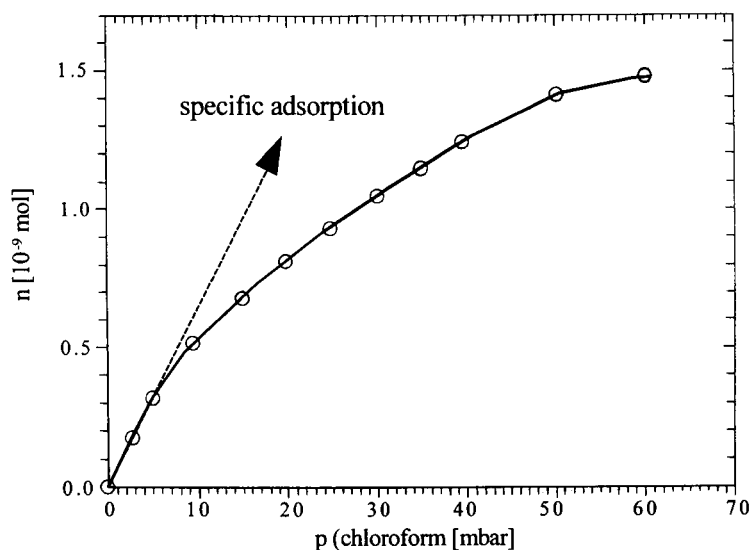


Fig. 21.2. Typical BET isotherm with specific analyte incorporation within the linear slope of the adsorption curve; number of moles chloroform  $n$  in a QCM layer as a function of the partial pressure  $p$ .

The adsorption analysis can be performed using the experimental sensor effect data from gravimetric QCM measurements. The frequency shift, which is proportional to the partial pressure of the analyte, is correlated to the number of specific incorporation sites in the linear range of the isotherm slope. Additional evidence for specific interactions between the analyte and the polymer matrix can be demonstrated using infrared spectroscopic analysis [19]. NMR [4,7] can also provide information about imprinting effects.

Many examples of specific inclusions are given by template synthesis studies [20,21]. Solvents are proposed to act as templates *via* non-covalent interactions. They therefore direct reactions towards the most 'solvated' shape of the product. Solvent-controlled synthesis is comparable to a sensory recognition phenomenon and hence can be treated as a template effect, just as non-covalent imprinting. Rebek and co-workers [22] have studied the solvent effect in detail, suggesting a process of preorganisation by weak intermolecular forces, which prevents the collapse of hydrogen-bonded assemblies. In the case of molecular imprinting, the solvent can act as both porogen and template during the polymerisation (see also Chapter 5). The primary difference between template-controlled synthesis and molecular imprinting is the rigid polymer lattice, which freezes the mobility of the template-monomer aggregates. As a result of the MIP structure, the molecular point of view has to be altered on a more macroscopic level, where the imprinted cavities are not identical but have various affinities for the templates. Regarding complex formation, both the variable affinity of imprinted sites and the mass transfer limitations have to be considered. In some cases the templates will be trapped within the thin sensor coatings. In other cases de- and adsorption take place on the porous surface of the polymer. Finally, the mobility of incorporated templates in the polymer matrix may be hindered by narrow diffusion pathways and collapsing pores.

The presented methods of examination focus on a comprehensive understanding of the imprinting effect. However, a reliable rule-based mechanism to predict the potential of target MIP structures for sensory applications is still not available and often, only experimental evaluations of MIPs provide useful rules of thumb for the development of selective coatings.

## 21.4 PRINCIPLES OF NON-COVALENT IMPRINTING FOR SENSORS

Conventional host-guest chemistry with supramolecular hosts depends on time-consuming and often sophisticated synthesis. This strategy leads to highly selective devices [23]. The effort involved in this synthesis, however, does not often lead to proper results concerning the sensor response.

The 'tailored' arrangement in non-covalent imprints is achieved by polymerisation in the presence of the template (analyte). The self-assembling process with non-covalent imprinting is performed mainly *via* hydrogen bonds and weaker forces, such as van der Waals' interactions, which leads to binding sites with more heterogeneous affinities when compared to covalent imprints. The incorporated



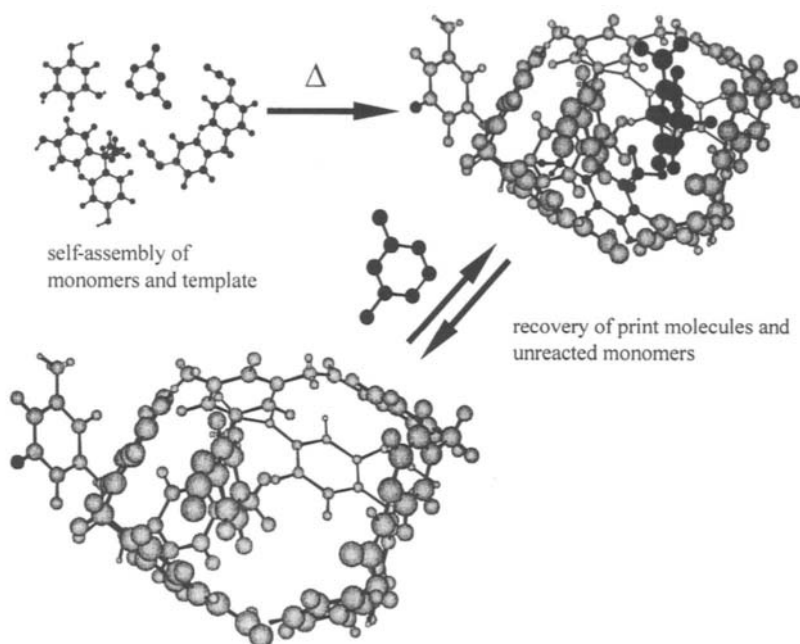


Fig. 21.3. Schematic figure of non-covalent imprinting of polyurethane with an organic solvent as template and porogen. Highly robust MIPs are best prepared over night at room temperature. Template removal is achieved by evaporation or dissolution. Due to the ultra-thin layers the print molecules are often removed completely.

templates are subsequently extracted by evaporation or dissolution, leaving binding sites complementary to the original template in the polymer. Figure 21.3 shows the process of imprinting in the case of poly(urethanes). Poly(urethanes) are formed by reaction of monomers with two different types of end group chemistry, i.e. – NCO groups reacting with – OH groups, to form the covalent ‘urethane’ linkage. Urethanes are robust, with good adhesion properties, and the attractive groups in the molecules are not readily attacked chemically. Additionally, the reactive groups are stable enough for extensive curing for hours (in other words good cross-linking) for (ultra-)thin coatings in the nm and lower  $\mu\text{m}$  range, qualities essential to gather reproducible bulk effects. The sensor coatings with imprinted polyurethanes provide greater hardness without brittleness compared to most other polymers, such as the extensively used imprinted vinyls and acrylics. Generally, radical polymerisation procedures for sensory MIPs are significantly less reproducible and thus depend on fast-evaporating solvents and strict control of the polymerisation conditions and coating procedures. Sensor layers from sol-gels have advantages comparable to polyurethanes. In addition to their chemical resistance and robustness, sol-gels allow polycondensation in aqueous solutions and functional groups can be chosen from a wide range of reactive components. The reaction time with urethanes and sol-gels, as well as the polymerisation temperature, can be chosen arbitrarily.

Most often, extremely robust coatings are achieved under room temperature conditions overnight.

Normally, the template can be completely removed in the case of thin coatings by extensive dissolution and the porous MIP structure inhibits template inclusion. Evaporation of the templates is preferred in the case of adequate volatility. The dissolution or evaporation of the templates is best observed spectroscopically.

It should be pointed out that not all binding sites are accessible during the analyte enrichment in the polymer because of the occasional collapse of pores and the formation of hindered diffusion pathways. Ageing phenomena, such as the inherent shrinkage of polymers, also contribute to limited sensitivity. In contrast to imprinted cavities, the monomeric host molecules, like cyclodextrins, have uniform pre-organised cavities. The macrocyclic hosts tend to crystallise during the evaporation of the solvent, which generates tension and eventually leads to cracks in the coating. Once again, cross-linking is the most suitable way to obtain an amorphous organisation of the coatings [24], but as with imprinting, the porosity of the layer is essential for a fast response time.

Low-weight organic molecules, such as volatile organic compounds (VOCs) [25], e.g. hydrocarbons without functionalities or anaesthetics, can be used as print molecules for non-covalent MIPs. If the print molecule is a suitable organic solvent, the print molecule itself is the porogen during the polymerisation process. Enhanced imprinting effects are promoted by  $\pi$ - $\pi$  interactions between aromatic moieties in monomers and analytes, such as polycyclic aromatic hydrocarbons (PAHs) or aromatic VOCs (xylene or toluene, for example).

Other classes of substances have also been studied for their suitability as print molecules for thin sensor layers. For example, I. Tabushi and co-workers [26] developed imprinted monolayers following the methodology of J. Sagiv [27], by building a silane monolayer in the presence of hexadecane, which is the print molecule. This idea has been shown to be fruitful for the detection of vitamins K and E, through intercalation in the monolayer. However, problems occurred due to the slow kinetics of the adsorption-desorption process in the narrow channels formed by the dense packing of silane chains. Chemosensors coated with self-assembled monolayers show reasonable sensor effects with mixed monolayers [28] consisting of aliphatic chains of different length. The main advantage of monolayer-coated sensors is their short response time, in the range of seconds, which is a highly desirable trait for the detection of hazardous compounds, such as nerve gases or explosives. For example, commercially available SAW/GC coupled sensor devices [29,30] detect ppt concentrations of warfare agents with suitable response times in the range of seconds. The application of sensors with non-covalent imprinted monolayers for analytes such as low-volatile nerve gas or surfactants is conceivable.

As will be seen in the next section, MIPs are highly suitable for the detection of low weight analytes due to suitable bulk effects, less hindered analyte diffusion, adequate polymer porosity and good recognition. On the other hand, very large molecules do not fit in the diffusion pathways. Surface interactions between polymer and analyte may be adequate for a reasonable imprinting effect [31]. Proteins or other biological molecules will be more readily detected using antibody

recognition. However, molecular imprinting is superior to natural recognition systems in that there are no suitable natural recognition systems for small organic molecules. If fast response times are to be achieved, extensive bulk effects cannot be utilised in a sensitive coating, therefore only ultra-sensitive devices can be considered for an appropriate sensor response.

MIP sensor elements are also suitable for the analysis of multicomponent samples. The cost-effective, miniaturised, non-covalent MIP sensor arrays, when combined with computational data evaluation, make weak artificial recognition phenomena highly applicable for smart sensors. In comparison to gas or liquid chromatography, the results with mass-sensitive MIP sensors are faster and cheaper to obtain [32]. For effective on-line monitoring, the ideal MIP sensor or actuator should allow reversible analyte enrichment without dependencies on intermediate washing procedures (with organic solvents, for example).

## 21.5 OPTICAL SENSOR APPLICATIONS

Optical devices are preferentially integrated in optoelectronic circuits. State-of-the-art microfabrications, such as with LIGA technology, miniaturised laser diodes, etc., make sophisticated, small and rigid optical sensors and actuators possible.

Analytes without pronounced inherent optical properties require a recognition system as well as the selective incorporation into the MIPs. The intercalation of organic dyes into MIPs leads to sensitive materials for optrodes. Using this approach, two ways of selective detection can be combined within the sensitive layer. Concave chemistry, which relates to the incorporation of analytes by size- and shape-sensitive recognition, is one approach. The other method is convex chemistry, realised by donor-acceptor interactions with the embedded dye. Covalent immobilisation of the dye prevents leaching, but the stability of optical devices primarily depends on the photochemical stability of the label. Therefore, pulsed fluorescence analysis, for instance, instead of continuous irradiation is favourably used to decrease photodegradation. In contrast to classical analytical applications, the indicator reagent is selected in view of less stable complexes, to guarantee chemosensory properties. This is the reason for non-linear calibration curves, which need computational data evaluation when a sizeable working range is required. The MIPs can be covalently linked to the optical substrate to further increase the long-term stability and ruggedness. For instance, suitable linkers can be thiol linkers to gold electrodes or more chemically robust silanes for covalent linkage to quartz substrates.

Imprinted polyurethanes as coatings for optrodes have been used for the detection of solvent vapours in air (see chapter 20). One per cent of substituted 3,3-diphenylphthalide as indicator has been intercalated within the polymer. The phthalide forms a highly coloured planar carbenium ion by interaction with an acidic component and a subsequent cleavage of the lactone ring – the unreacted phenolic groups in a polyurethane provide enough acidity for this reaction (Fig. 21.4). The incorporation of analytes reduces the acidity and the back-reaction

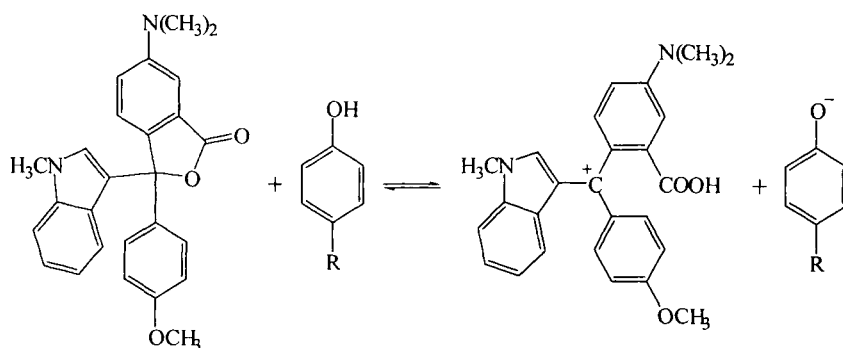


Fig. 21.4. Cleavage of the phthalide lactone ring, leading to a coloured carbenium ion.

occurs; hence the absorbance declines. This system has been used for the detection of ammonia and tetrahydrofuran [33] using tetrahydrofuran imprinted coatings. Ammonia, the better donor, did not change the absorbance, whereas tetrahydrofuran showed an appreciable sensor effect (Fig. 21.5). The reverse behaviour is observed with a non-imprinted layer, where the sensitivity for ammonia is twice that of tetrahydrofuran. Obviously, favourable inclusion only occurs with tetrahydrofuran as a result of the imprinting. Similar, but much more pronounced results, can be shown with analytes such as ethanol and ethyl acetate (Fig. 21.6), clearly indicating the impact of this type of non-covalent imprinting even with volatile

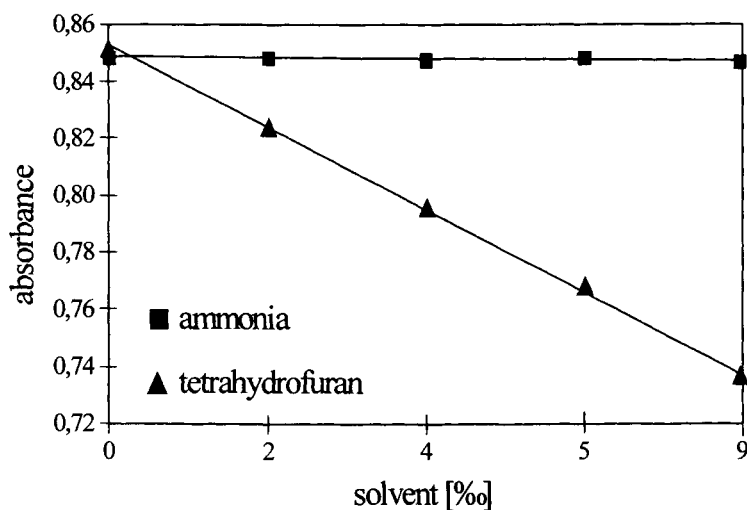


Fig. 21.5. Tetrahydrofuran imprinted polyurethane layer of 300 nm with embedded phthalide indicator shows a reasonable sensor effect with tetrahydrofuran – no effect occurs with ammonia vapour. Other solvents as template/porogen shift the sensitivity of the MIPs towards the analyte (former template) to be.

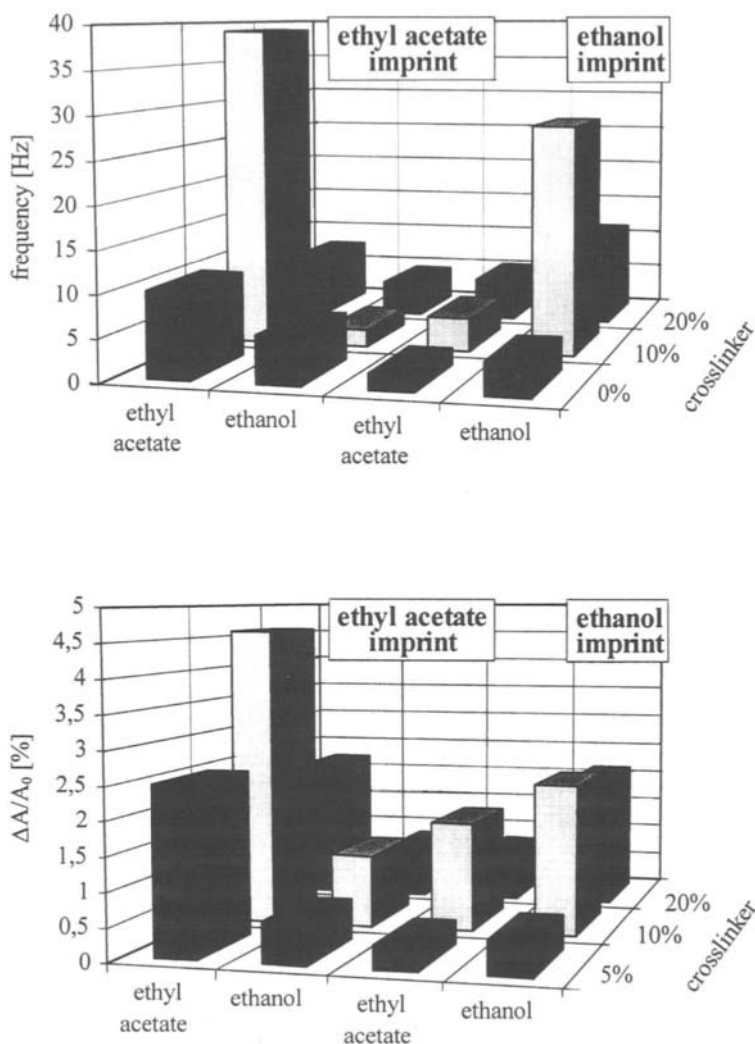


Fig. 21.6. Different print molecules and variable contents of cross-linker; QCM measurements (above) and changes in optical absorbance (below) due to 0.1% pulses of ethanol or ethyl acetate.

analytes of comparable molecular weights and chemical properties. Variable contents of cross-linker in the polyurethane matrix altered the selectivity and sensitivity pattern for the print molecule. The highest sensitivities with 10% cross-linker showed an optimum imprinting effect, whereas higher ratios of cross-linker seemed to impede the uptake of the analyte due to less accessible cavities. Again, non-imprinted polymers have equal sensitivity to both analytes. In this example, the mechanism of selective recognition is clearly due to the amount of cross-linker

added. Thus, the recognition process depends on hydrogen bonding between polymer and analyte, as well as sterically feasible incorporation.

If the analyte has optical properties useful for spectroscopic analysis, the embedding of a dye can be replaced (bleaching of the dye is avoided) by the direct detection of selectively incorporated analytes. Direct observation is also advantageous in the specific detection of characteristic wavelengths. In particular, luminescence methods, such as fluorescence spectroscopy, provide suitable spectroscopic data for trace analysis in the ppb range with a wide working range of great proportionality to the analyte concentration.

In liquid environmental analysis the detection of toxic compounds like PAHs [34], originating from incomplete combustion processes, such as in diesel engines, are of increasing interest. In addition, this substance class has the advantage of high fluorescence activity. Once again, the extended aromatic  $\pi$  systems of PAHs are useful for an analyte binding *via*  $\pi$ - $\pi$  interactions with a phenylated polymer matrix. Robust urethane polymers have been used as non-covalent MIPs for liquid applications. The removal of the PAH templates exceeded 80%, according to UV and fluorescence measurements. Residual template molecules did not show any fluorescence, possibly due to quenching by the polymer matrix. The enrichment factor of pyrene, for example, is about 107, and roughly 20% of the imprinted cavities are refilled. Improved sensitivities have been obtained using slightly smaller print molecules than the corresponding analyte, indicating that the swelling in the aqueous phase enlarges the binding sites to some extent. Micrometre layers led to detection limits for pyrene down to 30 ng/l possible, with an appropriate signal-to-noise ratio of 3:1. Saturation is additionally observed with UV measurements, as no quenching effect or self-absorption occurs within the layer. This detection model is highly suitable for environmental monitoring, since the MIP provides a separation of the PAHs from the complex sample matrix and thus from included quenchers and fluorescence active substances, such as ubiquitous humic acids. The layer thickness of 3  $\mu\text{m}$ , on the other hand, prolonged the response time up to 60 min, which is still a good performance compared to chromatographic analysis procedures. The linear working range of this coating ranges from 40  $\mu\text{g/l}$  down to 30 ng/l (Fig. 21.7). The low detection limit of 30 ng/l and the high selectivity can be compared to a synthetic antibody, as the detection limits of currently reported immunoaffinity chromatography [35] are in the 10 ng/l range. In Fig. 21.8 the sensitivity for pyrene is shown for single and double imprinted (pyrene and naphthalene) polyurethanes under various polymerisation temperatures. In most cases, high polymerisation temperatures allow increased curing of the cross-linked MIP and thus 'tighter pores'. Therefore, the addition of the smaller naphthalene as template reduces the analyte enrichment. Conversely, pure pyrene imprinting shows better incorporation properties with higher polymerisation temperatures, correlating with the results mentioned before with smaller template molecules. The examples given for optical sensor devices are suitable for a wide area of analytical applications. However, the dependence on either an optical label or suitable spectroscopical properties of the analyte restrict the application of optical sensors to definite substance classes.

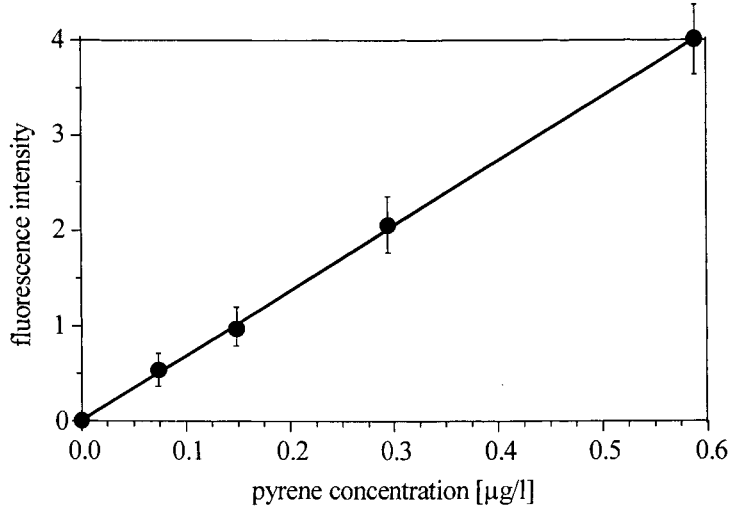


Fig. 21.7. Pyrene detection in the ng/l range with a 3  $\mu\text{m}$  MIP layer. Non-imprinted polyurethane shows negligible non-specific uptake of PAHs.

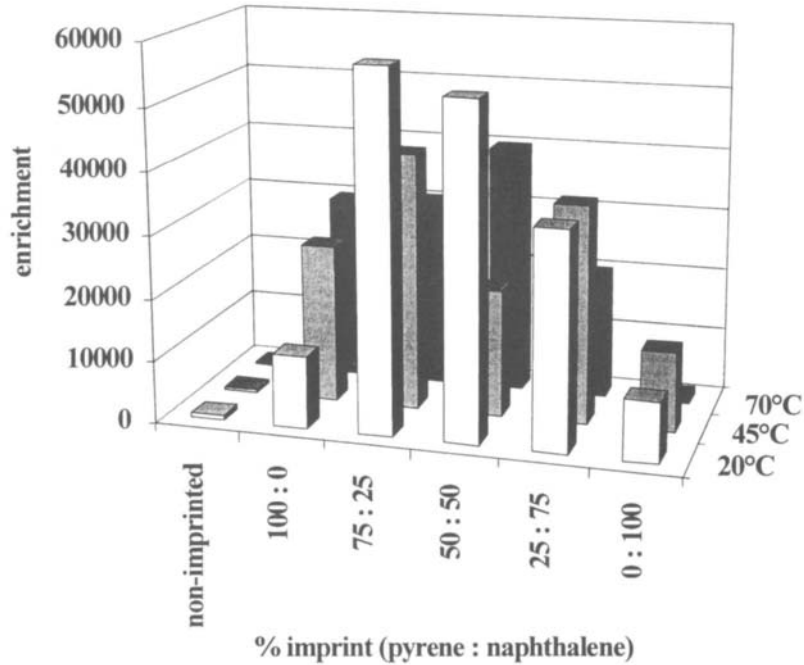


Fig. 21.8. Sensitivity pattern to pyrene of 100 nm layers of polyurethane imprinted with various ratios of pyrene/naphthalene and polymerised at different temperatures.

## 21.6 MASS-SENSITIVE DEVICES

The change of mass and the subsequent change in resonance frequency of the oscillating quartz plate is probably the most universally applicable sensing method. This is due to the fact that morphological, optical and functional aspects of the analyte do not interfere with the detection principle of the resonating transducer. Because of the high frequency resolution of 0.01 Hz, mechano-acoustic sensors are considered to be among the most sensitive transducers. The Sauerbrey [36] equation (1) provides a mathematical basis for the mass sensitivity.

$$\Delta f \propto f_0^2 \Delta m \quad (1)$$

Supposing an ultra-thin layer with a homogeneous distribution on the QCM with a resonance frequency  $f_0$ , we can assume a proportionality between mass loading  $\Delta m$  and frequency shift  $\Delta f$ . SAWs with operating frequencies up to 2.5 GHz yield detectable masses down to femtogram levels (see [37,38] for details about the mass sensitivity of SAWs). In practice, GHz SAWs have detection limits down to the lower ppb concentrations due to the increased mass resolution, which depends on the square of the operating frequency  $f_0$ . Figure 21.9 summarises sensor effects gathered with equally coated sensors (QCM and SAW) exposed to the same

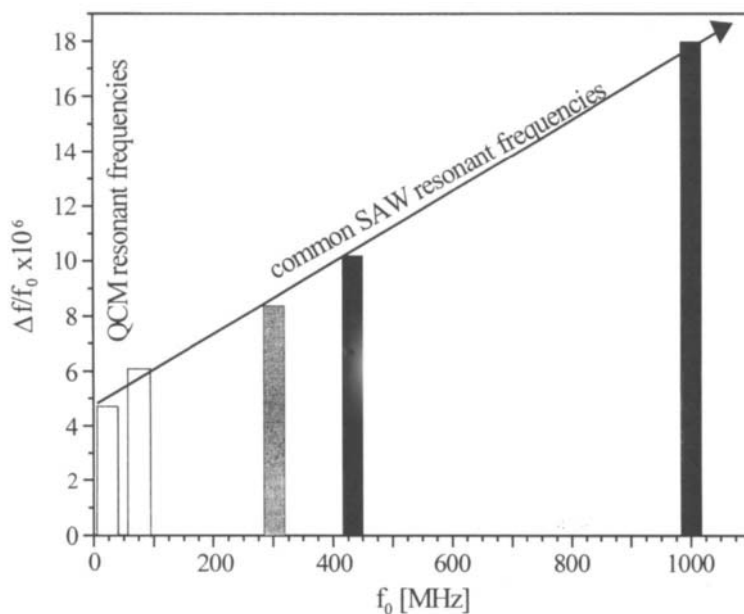


Fig. 21.9. Comparison of sensor responses of resonators with equivalent nanometre coatings to analyte pulses in the gas phase; the sensor response  $\Delta f$  as a function of the initial frequency  $f_0$ . The sensitivity increases with the square of the fundamental frequency (*cf.* Sauerbrey equation).



analyte concentrations. These outstanding detection limits are highly suitable for the on-line monitoring of small amounts of analytes. Thickness shear wave QCMs have applicable frequencies up to 20 MHz. These transducers are much more independent of viscoelastic interferences compared to the more sensitive SAWs. In contrast to QCMs, the SAWs are also damped inoperatively as a result of the energy loss from the surface waves to the surrounding liquid phase, unless STWs [16] are used.

Equivalent working ranges of mass-sensitive devices are only surmounted with ChemFETs and ion-selective electrodes. The resonating transducers are cheap and easily integrated due to their universal applications in electronic circuits. The ease of on-chip preparation of the MIP coatings is an additional advantage. The devices are coated by airbrush, spinning techniques or by dip-coating. The resulting layers, from a few up to several hundred nanometres, provide response times in the range of seconds or minutes respectively. Gas phase analysis with mass-sensitive devices is a well-established application [39]. However, usage in aqueous phases is still a tricky and controversial topic [40]. Numerous problems occur with additional viscosity effects, air bubbles, conductivity, etc.

In particular, the detection of neutral or inert analytes, such as anaesthetics, odours or hazardous compounds *via* weak complex formation within the MIPs is the *forte* of mass-sensitive devices due to the ultra-low detection limits, such as 1 pg for a 1GHz SAW. It is important that the sensitive layer is tightly bound to the metal electrode (QCM) or covalently linked to the piezo substrate (SAW) in order to achieve a stable coating in liquids. A stable link is sometimes crucial, for example when using polystyrenes (PSts).

Like the optical sensors for the detection of VOCs, polyurethane-coated resonators have been used for the detection of ethanol and ethyl acetate (Fig. 21.6). QCMs and SAWs have been coated with 100 nm layers. The response time, selectivity and sensitivity pattern of these devices outperform the results from the optrode measurements due to their independence from a label. Both analytes are best detected with 10% cross-linker in the coating. The optrodes described in the previous section show ageing by light and thermal exposure. The sensor response with gravimetric sensors is maintained. Usually, the long-term stability of the mass-sensitive elements exceeds that of the optrodes. Comparing the detection limits and the signal-to-noise-ratio of the QCMs and SAWs for the detection of organic solvents, a sensitivity increase of a factor of 40 was observed using identical conditions and layer thickness [41]. With the results given for the gas phase analysis, commercial implementation is imaginable. The toxic levels of most industrially used volatile compounds are in the lower ppm range – a concentration for practical long-term monitoring with integrated mass-sensitive devices. Moreover, coated mechano-acoustic actuators are applicable for process control; as an example, the endpoint of organic syntheses can be controlled by observing an excess of a particular reagent [42]. PAH detection using coated 10 MHz QCMs [43] is performed analogously to the polyurethane MIPs used for the fluorescence detection. The detection limits with fluorescence have proven to be superior to QCM measurements.

At this stage QCM applications in aqueous media are still a vivid research area. Further sensitivity improvements can be obtained by an STW resonator. However, the real time observation of the incorporation processes, either specific or non-specific, in comparison to a non-imprinted device is performed much more easily utilising QCMs than with optical devices. In particular, non-specific adsorption of cross-sensitive substances can be excluded by the use of suitable materials, such as polyurethanes, for mass-sensitive devices. In the case of optical sensing, the responses might be influenced by quenching or self-absorption.

Applications in organic liquids are another suitable field for coated resonators and are much more easily performed than in aqueous surroundings. In contrast to the complex effects in aqueous phases, the main interference to the mass effect in organic liquids occurs from viscosity, which can be compensated for using a dual array with an uncoated transducer and/or a non-imprinted coated device, as in the gas phase. The best compensation for non-specific effects and temperature fluctuations is achieved with a dual/ternary electrode geometry on one quartz plate.

The stability of mass-sensitive MIP sensors is appropriate for long-term monitoring of the degradation processes of lubricants [44]. Modern high-performance engines would not function without proper lubrication. A modern engine oil consists of a base oil and a package of additives, where the amount of additives in the oil can be up to 30%. This highly complex multicomponent mixture can still be analysed by artificial recognition systems. Highly cross-linked polyurethanes have shown suitable properties for imprinting with fresh or degraded oil. These MIPs, shown in Figs 21.10 and 21.11, have remarkably constant sensitivities, even after a year. In addition, non-imprinted layers showed similar performance to uncoated devices (bare gold electrodes seem to be more attractive for particle adhesion). The imprinting with fresh and waste oil enabled us to observe an overall picture of the degradation processes within a commercially applicable 6 kHz frequency range, which is the result of a mass effect and increased viscosity. The results given for the detection of motor oil degradation show the versatility of non-covalent imprinting even with multicomponent mixtures, pointing out the ease of preparation and the long-term stability of the coating.

An alternative to MIPs is a merger between conventional host-guest chemistry and molecular imprinting for a selective measure to increase selectivities. Tailor-made molecules [45], such as cyclodextrins and calixarenes, have been studied thoroughly as host molecules for low-weight organic molecules. These hosts have hydroxy functionalities which can be used for covalent embedding in a polymer matrix. The molecular cavities of the host molecule have defined interactions with the incorporated analyte in contrast to the heterogeneous affinities of imprinted binding sites as mentioned previously. Layers consisting of supramolecular host molecules often have higher sensitivities, due to the higher binding site density and the absence of occasionally collapsing hollows in imprinted layers. However, the development of adapted host molecules depends on time-consuming and often sophisticated synthesis to obtain the spatial arrangements needed for an optimum host-guest interaction. Covalent embedding of host molecules should be favourable in view of robust coatings, an additional porogen effect, minimised crystallisation

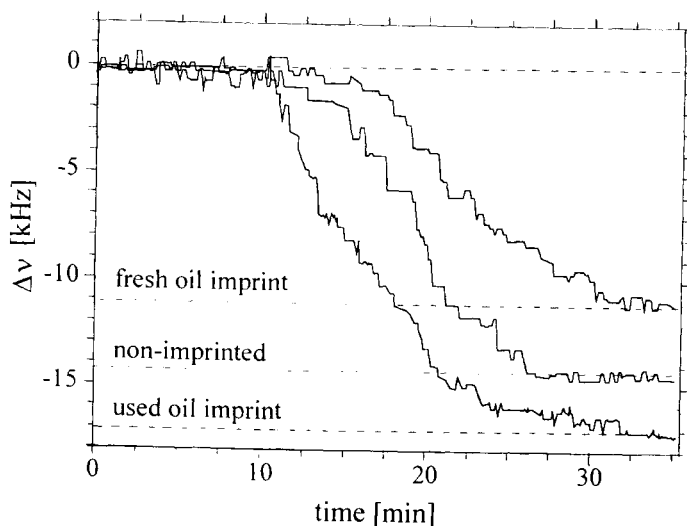


Fig. 21.10. Viscous and mass effect of equal non-imprinted, fresh oil and waste oil MIPs on QCMs. The sensor responses are the results going from fresh to degraded motor oil. An equal sensor response for non-imprinted and bare gold electrode is observed. The sensor effects can be related to a selective incorporation of different oils by the MIPs.

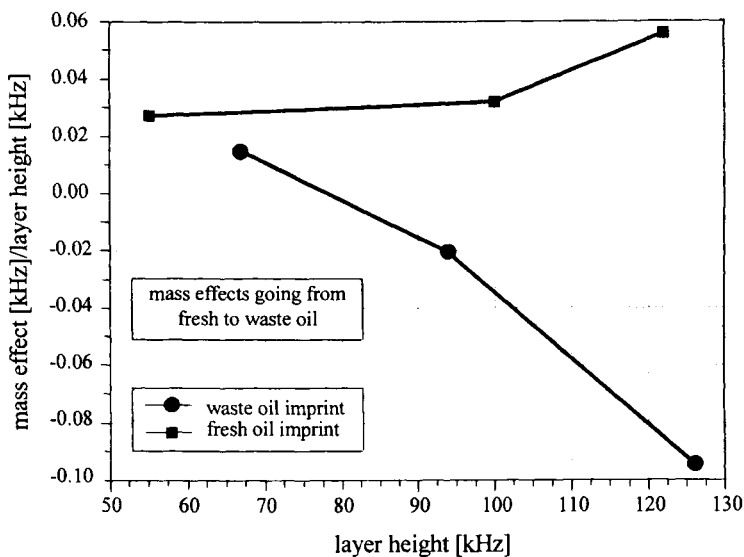


Fig. 21.11. Oil-sensitive MIPs: sensitivity increases with the layer thickness of the QCM coatings. Sensor effects have been gathered by differential measurements between uncoated and MIP-coated electrodes (difference eliminates viscosity and temperature effects).

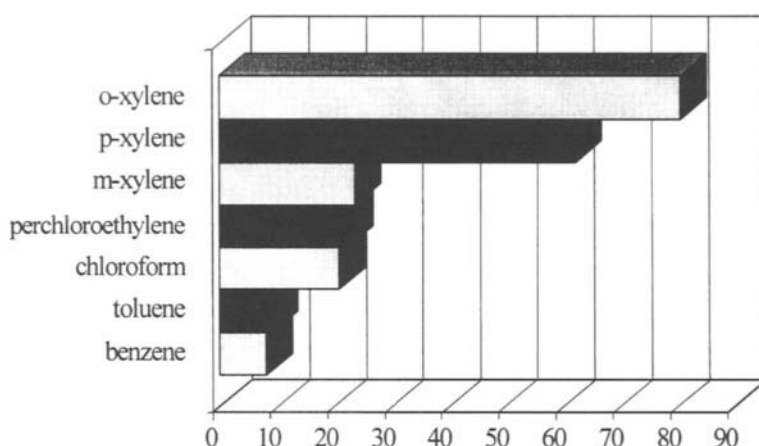


Fig. 21.12. Sensitivity pattern of QCM coated with a *p*-xylene imprinted polyurethane to 0.1% solvent pulses. Other templates for the polymerisation results in increased sensitivity to the corresponding analyte and to sterically comparable neutral molecules.

of the supramolecular hosts and lower cross-sensitivity to water due to the removal of the hydroxy functionalities. Furthermore, the covalent embedding prevents wash out and enables the development of suitable combinations of MIPs and host molecules for application in liquids. The analyte may diffuse into the bulk polymer to be trapped in an imprinted or a pre-organised binding site. The analyte may be preferentially incorporated in the host molecules, if high concentrations of embedded hosts are used. The number of imprinted binding sites will decrease with increasing ratio of hosts; an extreme example would be pure linkages between the hosts. In addition, the embedded supramolecular host molecules act as a porogen and improve the porosity of the MIP coating. As an example, Figs 21.12 and 21.13 show the summarised sensor effects of a *p*-xylene imprinted polyurethane with and without 42% covalently embedded calix[6]arenes. The inversion of sensor responses, shown in Fig. 21.13, due to certain xylene isomers as print molecules and 42% embedded calix[6]arene is a vivid example of the effectiveness of supramolecular methodologies, even with isomer analytes.

## 21.7 DIFFERENCES BETWEEN CHROMATOGRAPHIC AND CHEMOSENSORY APPLICATIONS

Most progress in the methods and usage of functional monomers for imprinting has been made in the field of chromatography. Recent analytical applications in the liquid phase often involve chiral separation problems (see Chapter 17). Non-covalently imprinted polymers offer suitable solutions, as imprinted polymers with

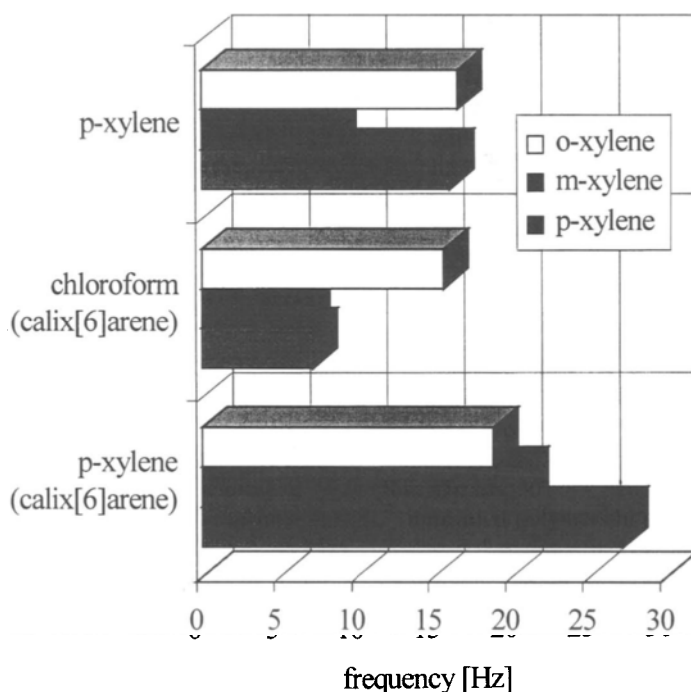


Fig. 21.13. QCM responses to coatings polymerised from different porogens (acting as print molecules) with/without embedded calix[6]arene in brackets. The sensor response of 70 nm layers to 500 ppm of xylene isomers is shown. Compared to the layer polymerised in chloroform, the pronounced imprint effect for xylene can be seen. *o*-Xylene has the lowest volatility of the xylene isomers and therefore is equally detected in all layers.

enantio- and stereo-selectivity have already been successfully adapted for a number of chiral compounds [46]. Other applications use the recognition abilities of non-covalent MIPs for thin-layer chromatography [47], electrodialysis [48] or for molecular recognition at the electrode/solution interface [49].

Imprinting in the field of chromatography or catalysis [50] has to be distinguished from the imprinting of coatings for sensor devices. For example, the catalytically active cavities in the polymer have to stabilise a distinct transition state. In chromatography, the affinity and the mass transfer rates in the coatings/beads have to be modified to give suitable separation efficiency and less peak broadening.

In most cases, chromatography and solid phase extractions with MIPs are performed with organic eluants. The rigidity of the backbone structure is critically important when considering the mechanical stress that occurs during HPLC separations. The macroscopic polymer beads are optimised with regards to monodispersity and mechanical stability. GC on the other hand relies on thermally stable coatings.

A crucial factor in chromatographic MIP applications is the extensive peak broadening and tailing that results from the bulk effect in the polymer matrix. This is a critical limitation for MIPs in chromatography. Bulk effects are essential in sensory applications, where the sensitivity of sensor coatings depends on a one-step enrichment for an applicable selective incorporation. Instead, chromatographic columns have thousands of plates for an entire separation and hence the inclusion process can be weaker and less selective in comparison to sensor layers.

The principal advantage of sensors is therefore their fast response time in comparison to the retention time in chromatography, but the sensor response is partially a sum signal of the favourably enriched analyte and the cross-sensitive compounds, which makes a independent calibration necessary. Furthermore, it is essential for the sensor layer to allow a completely reversible inclusion process, while still maintaining high selectivities and high enrichment factors.

Chemosensory applications will normally take place in an environment of complex composition. Humidity and other varying ambient conditions are in sharp contrast to the well-defined environment most typically found in related applications of imprinted polymers. Moreover, the trend in sensor technology towards miniaturisation, with the aim of future nano-scale dimensions, is a primary reason for rising perturbation sensitivity, such as new interfering forces that can be neglected in the macro range. Chemical sensors can be influenced by numerous factors, such as electrostatic effects (ChemFETs) or non-specific adsorption (SAW, surface plasmon resonance).

In contrast to this technological progress, the energy supply and the equipment for the data analysis still remain quite large for most chemosensory systems. Few sensing schemes, such as integrated optical and mass-sensitive elements, are capable of a real size reduction to small hand-held devices for relatively trouble-free operation.

The dimensions of the sensor layers are not comparable to the macroscopic polymer beads in HPLC columns. The common height of the sensor coatings never exceeds more than a few micrometres. In fact, if the sensitivity of the MIP to a single analyte is good, the sensor coatings are in the range of a hundred nanometres. The bulk effect, which allows sensitivity increase by an enhancement of the layer thickness, is normally adapted to the desired sensor sensitivity and response time. In particular, with complex analyte mixtures or increased selectivities, thicker coatings have shown to be more suitable. Fig. 21.11 demonstrates the sensitivity for the incorporation of the former print molecule mixture (fresh or waste oil). The data show the mass effect differences when changing between fresh and waste oil. The sensor effect disproportionately exceeds the layer thickness, indicative of selectivity enhancement. The sensitivity is much higher for waste oil enrichment in waste oil MIPs than in fresh oil MIPs, although using the same amount of templates. The observed selectivity increase can result from two different effects. Either the sensor effect by non-specific adsorption on the polymer surface decreases in proportion to the layer thickness increase, or imprinted sites become more selective the longer it takes to diffuse into the MIP.

Swelling/shrinkage is an inherent property of even highly cross-linked polymers.

It can reduce the analyte enrichment in the bulk because of collapsing pores or diffusion hindrances. Contrary to chromatography, sensory applications mainly depend on bulk effects (exceptions are surface imprinting techniques). Therefore, it is important to carefully design the MIPs in view of the analyte media. In aqueous surroundings swelling can often be disregarded, whereas organic solutions will affect the polymer properties.

The ageing of polymers can be a crucial factor in imprinted polymers. The properties of the coatings will be altered, due to the influence of oxygen, humidity or light exposure. These changes affect the sensor characteristics as well as the cross-sensitivity, particularly with regard to the ambient humidity. Moreover, unreacted monomer functionalities may undergo certain consequent reactions. The sensor unit itself is affected by minor abrasions. As a consequence of these phenomena drift effects occur. The electronic drift or the drift of chemosensory elements cannot be forestalled completely because of the nature of the polymer and the temperature fluctuations in electronic circuits. A drift compensation can be performed using an extrapolation process or by a dual arrangement with an uncoated reference sensor. Experimental set-ups with ternary electrode geometry on a single, QCM are even more suitable. The third electrode can be coated, for instance, with a non-imprinted material, which allows direct comparison of imprint effects, non-specific adsorption or incorporation in relation to the 'sensitive' electrode under equivalent conditions.

Sensors should normally have short response times, with the exception of sensors for long-term monitoring or chemical dosimeters. The response time also depends on whether the measurement occurs in the gas phase or in the liquid phase. High mass-transfer between the MIPs and liquids has to be guaranteed for liquid measurements; sufficient wetting of the MIPs in aqueous samples is particularly critical. Generally, the optimisation of the non-covalent imprinted polymer tends to raise the selectivity more than the sensitivity, as the ratio of accessible binding sites in the MIPs will always be limited. In other words, the amount of template added to the monomer solution is always limited. In the end, only sensors that are less prone to ageing phenomena and with minimum drift effects will evoke commercial interest. The design of MIP sensor elements is primarily a precise balance of sensitivity (bulk effect and sensing scheme), response time (rate of mass transfer), affinity (reversible inclusion or antibody analogue binding) and selectivity (MIP, ageing phenomena) for the desired requirements, such as working range and the time-scale of monitoring (long-term or one-time use).

## **21.8 CONCLUSIONS**

In summary, non-covalently imprinted polymers offer a universal tool for sensor technology, besides the main applications in HPLC and solid phase extraction. The examples discussed above are but a few of the potential applications of smart chemosensory devices coated with non-covalent MIPs. The strategy of non-covalent imprinting is highly appropriate for sensory applications. Antibody-like

affinities for analytes should even allow for clinical applications in the future. The versatility and ease of preparation is best promoted with mass-sensitive transducers. If the analyte has inherent optical properties, optrodes are also suitable. Improved detection limits can be obtained with SAWs (gas phase), operating in the GHz

TABLE 21.2

MULTICOMPONENT ANALYSIS OF XYLENE MIXTURES IN THE PRESENCE OF HUMIDITY OF A NON-COVALENT MIP SENSOR ARRAY WITH IMPRINTED PST AND PMA (Cf. FIG. 21.14). THE RESULTS OF A BACK-PROPAGATION NETWORK (ANN) AND A PLS ARE GIVEN AS ROOT MEAN SQUARED ERRORS OF PREDICTION IN PER CENT

| Error of prediction (%) | <i>o</i> -Xylene | <i>p</i> -Xylene | Relative humidity |
|-------------------------|------------------|------------------|-------------------|
| ANN                     | 4.3              | 4                | 0.3               |
| PLS                     | 9.2              | 9.8              | 0.2               |

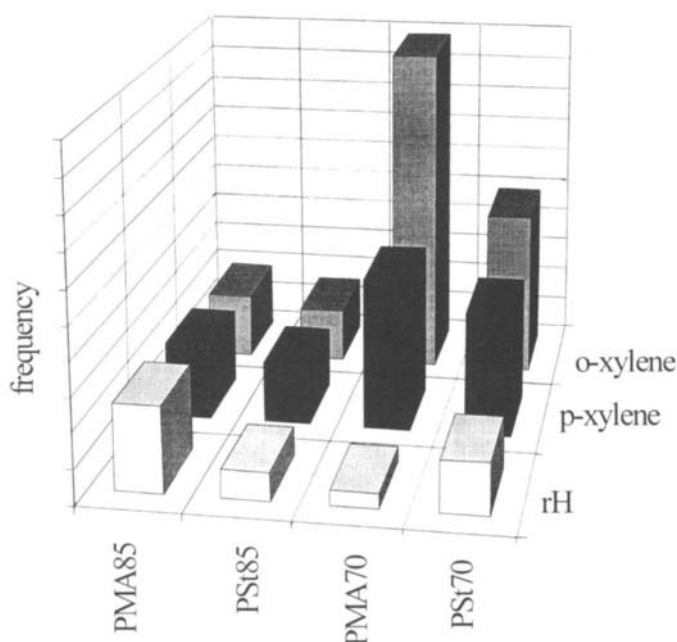


Fig. 21.14. Sensitivity pattern to xylenes and ambient humidity (rH) of a non-covalent MIP array PMA (MAA and EDMA) and PSt (styrene and divinylbenzene) with 85 and 70% cross-linker. PMA85/PSt85 is *p*-xylene and PMA70/PSt70 *o*-xylene imprinted. Data evaluation is shown in Table 21.2.



range, and STWs (gas or liquid phase) for resolutions down to the ppt level. The most promising MIP detection elements are for small organic hydrocarbons. For these substance classes, non-covalent MIP sensors are quickly reaching the stage of commercial implementation. Combined with multivariate data evaluation, MIP sensor arrays have the potential for work-place monitoring or process control under harsh and variable conditions.

An example of a non-covalent MIP sensor array is shown in Fig. 21.14. Xylene imprinted poly(styrenes) (PSt) and poly(methacrylates) (PMA) with 70 and 85% cross-linker have been used for the detection of *o*- and *p*-xylene. The detection has been performed in the presence of 20–60% relative humidity to simulate environmental conditions. In contrast to the calixarene/urethane layers mentioned before, *p*-xylene imprinted PSTs still show a better sensitivity to *o*-xylene. The inversion of the xylene sensitivities can be gathered with PMAs and higher cross-linker ratios. As a consequence of the humidity, multivariate calibration of the array with partial least squares (PLS) and artificial neural networks (ANN) is performed. The evaluated xylene detection limits are in the lower ppm range (Table 21.2), whereas neural networks with back-propagation training and sigmoid transfer functions provide the most accurate data for *o*- and *p*-xylene concentrations as compared to PLS analyses.

## REFERENCES

- 1 J.C. Lockhart, In: *Chemical sensors: comprehensive supramolecular chemistry*, G.W. Gokel Ed., Elsevier, Oxford, Vol 1, p. 605 (1996).
- 2 F.L. Dickert and O. Hayden, *Trends Anal. Chem.*, **18**, 192 (1999).
- 3 F.L. Dickert, W. Greibl, P.A. Lieberzeit, A. Rohrer, P. Forth and G. Voigt, *SPIE*, **3857**, 14 (1999).
- 4 A. Katz and M.E. Davis, *Nature*, **403**, 286 (2000).
- 5 F.H. Dickey, *Proc. Natl. Acad. Sci.*, **35**, 227 (1949).
- 6 G. Wulff and A. Sarhan, *Angew. Chem. Int. Ed. Engl.*, **11**, 341 (1972).
- 7 B. Sellergren, M. Lepistö and K. Mosbach, *J. Am. Chem. Soc.*, **110**, 5853 (1988).
- 8 B. Sellergren, *Trends Anal. Chem.*, **16**, 310 (1997).
- 9 A.G. Mayes and K. Mosbach, *Trends Anal. Chem.*, **16**, 321 (1997).
- 10 B. Sellergren, *Trends Anal. Chem.*, **18**, 164 (1999).
- 11 D. Stevenson, *Trends Anal. Chem.*, **18**, 154 (1999).
- 12 M. Otto, In: *Analytical chemistry*, R. Kellner, J.-M. Mermet, M. Otto and H.M. Widmer Eds, Wiley-VCH, Weinheim, p. 359 (1998).
- 13 M. Josowicz and J. Janata, *Anal. Chem.*, **58**, 514 (1986).
- 14 F.L. Dickert, P. Forth, P. Lieberzeit and M. Tortschanoff, *Fresenius J. Anal. Chem.*, **360**, 759 (1998).
- 15 J.W. Grate, S.J. Martin and R.M. White, *Anal. Chem.*, **65**, 987A (1993).
- 16 M. Tom-Moy, R.L. Baer, D. Spira-Solomon and T.P. Doherty, *Anal. Chem.*, **67**, 1510 (1995).
- 17 F.L. Dickert, W. Greibl, R. Sikorski, M. Tortschanoff and K. Weber, *SPIE*, **3539**, 114 (1998).
- 18 F.L. Dickert, U. Geiger, M. Keppler, M. Reif, W.-E. Bulst, U. Knauer and G. Fischer-auer, *Sens. Actuat., B*, **26–27**, 199 (1995).
- 19 T. Kobayashi, H.Y. Wang and N. Fujii, *Anal. Chim. Acta*, **365**, 81 (1998).

- 20 E.E. Simanek, M. Mammen, D.M. Gordon, D. Chin, J.P. Mathias, C.T. Seto and G.M. Whitesides, *Tetrahedron*, **51**, 607 (1995).
- 21 R. Hoss and F. Vögtle, *Angew. Chem. Int. Ed. Engl.*, **33**, 357 (1994).
- 22 Y. Tokunaga, D.M. Rudkevich, J. Santamaria, G. Hilmersson and J. Rebek Jr., *Chem. Eur. J.*, **4**, 1499 (1998).
- 23 J.C. Lockhart, In: *Chemical sensors: comprehensive supramolecular chemistry*, G.W. Gokel Ed., Elsevier, Oxford, Vol. 1, p. 187 (1996).
- 24 F.L. Dickert, U. Geiger and K. Weber, *Fresenius J. Anal. Chem.*, **364**, 128 (1999).
- 25 F.L. Dickert, P. Forth, P. Lieberzeit and M. Tortschanoff, *Fresenius J. Anal. Chem.*, **360**, 759 (1998).
- 26 K. Yamamura, H. Hatakeyama, K. Naka, I. Tabushi and K. Kurihara, *J. Chem. Soc. Chem. Commun.*, 79 (1988).
- 27 J. Sagiv, *J. Am. Chem. Soc.*, **102**, 92 (1980).
- 28 F.L. Dickert, P. Achatz, W.E. Bulst, W. Greibl, O. Hayden, L. Ping, R. Sikorski and U. Wolff, *SPIE*, **3857**, 116 (1999).
- 29 G.W. Watson, W. Horton and E.J. Staples, Proceedings of the 1991 Ultrasonic Symposium, 305 (1991).
- 30 R.A. McGill, M.H. Abraham and J.W. Grate, *Chemtech.*, **24**, 27 (1994).
- 31 H. Shi, W.-B. Tsai, M.D. Garrison, S. Ferrari and B.D. Ratner, *Nature*, **398**, 593 (1999).
- 32 T. Wessa and W. Göpel, *Fresenius J. Anal. Chem.*, **361**, 239 (1998).
- 33 F.L. Dickert and S. Thierer, *Adv. Mater.*, **8**, 987 (1996).
- 34 F.L. Dickert, H. Besenböck and M. Tortschanoff, *Adv. Mater.*, **10**, 149 (1998).
- 35 M. Cichna, D. Knopp and R. Niessner, *Anal. Chim. Acta*, **339**, 241 (1997).
- 36 G. Sauerbrey, *Z. F. Physik*, **155**, 206 (1959).
- 37 B.A. Auld (Ed.), In: *Acoustic fields and waves in solids*, Wiley & Sons Inc., New York, Vol. 2 (1973).
- 38 A. Mauder, *Sens. Actuat. B*, **26**, 187 (1995).
- 39 F.C.J.M. Van Veggel, In: *Mass sensors in supramolecular technology*, D.N. Reinhoudt Ed., *Comprehensive Supramolecular Chemistry 10*, Elsevier, Oxford, p. 171 (1996).
- 40 *Faraday Discuss.* **107** (1997).
- 41 F.L. Dickert, P. Forth, W.-E. Bulst, G. Fischerauer and U. Knauer, *Sens. Actuat. B*, **46**, 120 (1998).
- 42 F.L. Dickert, M. Tortschanoff, K. Weber and M. Zenkel, *Fresenius J. Anal. Chem.*, **362**, 21 (1998).
- 43 F.L. Dickert, M. Tortschanoff and W.E. Bulst, *G. Fischerauer Anal. Chem.*, **71**, 4559 (1999).
- 44 N.L. Jarvis, H. Wohltjen, M. Klusty, N. Gorin, C. Fleck, G. Shay and A. Smith, *Lubric. Engineer.*, **50**, 689 (1994).
- 45 F.L. Dickert and A. Haunschild, *Adv. Mater.*, **5**, 887 (1993).
- 46 M. Kempe and K. Mosbach, *J. Chromatogr. A*, **694**, 3 (1995).
- 47 D. Kriz, C.B. Kriz, L.I. Andersson and K. Mosbach, *Anal. Chem.*, **66**, 2636 (1994).
- 48 M. Yoshikawa, T. Fujisawa, J. Izumi, T. Kitao and S. Sakamoto, *Anal. Chim. Acta*, **365**, 59 (1998).
- 49 M.T. Rojas and A.E. Kaifer, *J. Am. Chem. Soc.*, **117**, 5883 (1995).
- 50 E. Toorisaka, M. Yoshida, K. Uezu, M. Goto and S. Furusaki, *Chem. Lett.*, 387 (1999).

This Page Intentionally Left Blank

# INDEX

Note: Figures and Tables are indicated (in this index) by *italic page numbers*; abbreviation 'MIP' = 'molecularly imprinted polymer'

- Acenaphthene, 492
- Acetonitrile, as mobile phase, 168
- N*-Acetyl-L-phenylalanine amide, as template, 276, 277
- N*-Acetyl-D-tryptophan, 276, 277
- N*-Acetyltryptophanamide-imprinted silicas, 475–477
- N*-Acetyltryptophanamide (NATA), structure, 476
- 2-Acetyl-5-(*p*-vinylbenzyloxy)phenol, metal ion complexes, 249
- Acrylamide, as functional monomer, 22, 141, 144, 287, 397, 398, 405
- Acrylamide–methyl diacrylamide (pAA–MDA) copolymers, 22
- Acrylamide MIPs, 65
- 2-(Acrylamido)-2-methylpropanesulphonic acid (AMPSA), as functional monomer, 140, 398, 468
- Acrylic acid
  - as functional monomer, 287, 290, 291, 398
  - separated from maleic acid, 274
- N*-Acryloyl-L-alanine, as chiral functional monomer, 383
- Adamantane, 219, 468, 469
- Adenine-responsive films, 432
- Adenines, retention by 9EA-imprinted polymers, 128, 130
- Adenosine 3',5'-cyclic monophosphate (cAMP)
  - fluorescence sensor for, 141, 460, 464, 480–481
  - structure, 143, 480
- Adenosine monophosphate (AMP), imprinted enzymes activated by, 275
- Adenosine triphosphate (ATP) imprinted beads, 315
- $\beta$ -Adrenergic antagonists, analysis of, 335, 391
- Adsorption–desorption kinetics, 132–133
- Adsorption isotherms, 51–52, 126
  - bi-Langmuir isotherm, 66, 126, 130, 131
  - determination of, 127–128
  - fitting of L-PA data, 130–132
  - Freundlich isotherm, 66, 126, 130, 131, 132
  - Langmuir type isotherm, 52, 53, 126, 129, 130, 131
  - metal adsorption on metal ion imprinted resins, 257–260
  - Scatchard plot, 127, 128, 204, 288
  - tri-Langmuir isotherm, 126, 132
- Aerogels, 216
- Aerosol polymerisation
  - advantages and disadvantages, 309, 319
  - imprinted beads produced by, 319–320
- Affinity chromatography, 11
  - antibodies isolated by, 122–123
  - protein purification by, 285
  - stationary phases, 82
- Affinity-imprinting, 288
- Agarose gel, MIP particles trapped in, 425
- Ageing of polymers, in sensors, 522
- D,L-Alanine *p*-nitroanilide, resolution of, 121, 122
- Albumins
  - catalytic activity in, 281, 282
  - see also* Bovine serum albumin
- Aldehydes, as binding groups, 85, 88
- Alkyl orange dyes

- adsorption on molecularly imprinted silicas, 6, 10, 218, 223, 226
- structures, 6, 222
- Allylamine, as functional monomer, 141, 143, 474
- Alternating copolymers, 28
- Alumina thin films, 234
- Aluminosilicates *see* Zeolites
- Amberlite XAD-2 resin, 250
- Ambient pressure aerogels, 216
- Ametryn
  - chromatographic retention on MIPs, 152, 178
  - recognition by MIPs, 169, 170
  - structure and properties, 169, 337, 339
- Ametryn-imprinted polymers, 152, 336–339
  - chromatographic retention of triazines on, 152
  - rebinding behaviour, 337
  - selectivity, 170, 338
- Amide-based cross-linking monomers, 43
- Amidines
  - in binding sites, 79, 98, 99, 100, 103
  - catalytic effects, 103
  - imprinting by, 98, 99–100, 138
- Amidopyrazoles, as binding site monomers, 98–99
- Amines
  - as binding groups, 85, 88, 95, 96
  - discrimination between primary and tertiary, 118, 119
- 4-Aminoacetophenone, 470
- Amino acid derivatives
  - imprinting with, 85
  - resolution of enantiomers, 121, 122, 407
- Amino acids
  - aromatic, resolution of enantiomers, 194, 409, 410
  - chiral, recognition of, 188
  - p*-nitrophenyl esters, 197
  - N*-protected, imprinting of, 119, 120, 141, 144, 170–172, 188, 197, 407
  - optically active, preparation of, 92–93
  - resolution of enantiomers, 194–195, 265, 388, 389, 404, 406–407, 409
- Amino acid specific polymers, 208–211
- Aminoalcohols, imprinting of, 119, 120
- p*-Aminoazobenzene imprinted gels, 226, 227
- 4-Aminobenzophenone, 470
- 2-Aminoethyl methacrylate (AEMA), as functional monomer, 142
- Amino-functionalised silicas, 90, 229
- p*-Aminophenylalanine anilide, 147
- 3-Aminopropyl triethoxysilane, as functional monomer, 286
- Amperometric enzyme sensors, 422
- Amperometric sensors, 419
  - recognition elements, 422, 423
- Amperometric solution-phase sensors, 430
- Amylose-based molecularly imprinted matrices, 282–283
- Androstane-3,17-dione, 94
- Animal cells, cultivation of, 302, 303
- Anthracene
  - detection of, 479, 491, 493
  - structure, 492
- Antibodies, 122
  - catalytic, 281, 282, 292
  - MIPs compared with, 102, 121–125, 208, 325, 343
  - production of, 5, 71–72, 122–124
    - against haptens, 122, 343–344
    - compared with synthesis of MIPs, 125, 325
  - silica analogues, 6
- Antibody–antigen interactions
  - in competitive immunoassays, 341, 342
  - monitoring by optical sensors, 472
  - in non-competitive immunoassays, 341, 342
  - on/off kinetics, 132–133
- Antibody-formation theories, 3–5
  - instructional theory, 4
  - selective theory, 4
- Antibody mimics, MIPs as, 102, 121–125, 325, 342–344
- Antigens, 122, 341
  - selectivity of antibodies, 122
  - theories, 3–5
- Aqueous buffer-based assays, 346–348
- Aqueous two-step swelling method
  - advantages and disadvantages, 309
  - imprinted beads produced by, 317–319
- Artificial antibodies, 325
  - combinatorial approach for, 336
- Artificial enzymes, 13–14, 102
  - in biomimetic sensors, 423
- Artificial neural networks, 524
- Aryl-1,3-diketones, 154, 155

- Aspartic acid, 118, 406  
  resolution of enantiomers, 406, 410
- Z-L-Aspartic acid-imprinted polymer, 406
- Aspergillus oryzae* protease, bio-imprinted, 277
- Association mechanism, 9–10  
  objections to, 10–11
- Atenolol, resolution of enantiomers, 390
- Atomic force microscopy (AFM), composite materials for sensors, 434, 435
- Atrazine  
  association constant of complex with acetic acid, 158  
  chromatographic retention on MIPs, 152, 177, 178  
  conductometric sensors for, 447  
  determination of, 345, 346  
  recognition by MIPs, 169, 170  
  selection of best functional monomer for imprinting, 169–170, 336–339  
  site of interaction with carboxylic acids, 169, 170  
  solid phase extraction of, 352, 359, 367, 368  
  structure and properties, 169, 337, 339, 476
- Atrazine-imprinted membranes, 427–428
- Atrazine-imprinted polymers, 152, 336–339  
  preparation of, 336, 365  
  rebinding behaviour, 337  
  selectivity, 170, 338  
  in solid phase extraction, 365
- Atropine-imprinted silicas, 13
- Attenuated total reflectance (ATR) crystals, 2,4-D MIP on, 491
- Automated batch *in situ* polymer preparation, 335, 336
- Azobenzene dyes  
  imprinting by, 222, 224  
  *see also* Alkyl orange dyes
- 2,2'-Azobis(2,4-dimethylvaleronitrile) (ABDV), as free radical initiator, 25, 116
- 2,2'-Azobisisobutyronitrile (AIBN), as free radical initiator, 23, 24, 25, 39, 116, 334, 381
- 2,2'-Azobis(4-methoxy-2,4-dimethylvaleronitrile), as free radical initiator, 116
- Azo-initiators, 24, 25, 116
- Bacillus mycoides* imprinted silica, 14–15
- Bacteria-imprinted polymers, 288–289, 295–303  
  applications, 301–302  
  methodology, 296–301
- Bacteria-imprinted silica, 14–15
- Bacteria-mediated lithography, 288–289, 296–303  
  applications, 301–302, 303  
  methodology, 288–289, 296–301
- Bait-and-switch approach, 194, 200, 468
- Barbiturates, as templates, 98, 141, 144
- Batch rebinding experiments  
  adsorption–desorption kinetics, 132–133  
  adsorption isotherms, 127–129
- Batch-type *in situ* polymer preparation  
  procedure, 335, 336
- Beads  
  advantages over crushed bulk material, 305–306  
  production of, 307–321, 326  
  *see also* Molecularly imprinted polymer beads; Silica beads
- Bentazone  
  solid phase extraction of, 360  
  structure, 361
- Bentazone-imprinted polymers, in solid phase extraction, 365
- Benzaldehyde, as template, 220
- Benzamidine-imprinted polymers  
  in CE/CEC, 334, 381–382, 389  
  compared with pentamidine-imprinted polymers, 332, 334, 381–382
- Benz[a]anthracene  
  detection of, 493  
  structure, 492
- Benzenesulphonamide, as template, 236–237, 238
- Benzoic anhydride, esterification of, catalysis of, 236
- Benzo[ghi]perylene  
  detection of, 493  
  structure, 492
- Benzophenone, 470
- Benzoquinoline, as template, 224
- Benzylamine-imprinted polymer, chromatographic behaviour, 173–174

- (*S*)-Benzyl benzodiazepine-imprinted polymer, as chiral stationary phase, 402
- Benzylmalonic acid, as template, 142
- Benzyltriphenylphosphonium ions, determination of, 425–426
- BET *see* Brunauer–Emmett–Teller...
- Beta-blockers
- analysis of, 335, 349
  - resolution of enantiomers, 387, 388–389, 390, 391, 401–402, 403
  - see also* Atenolol; Metoprolol; Pindolol; Prenalterol; Propranolol; Timolol
- Bi-Langmuir adsorption isotherm, 66, 126
- fitting of L-PA data, 130, 131
- Binding site
- accessibility, 35–36, 75
  - distribution
    - in metal-coordinating imprinting, 188
    - in non-covalent imprinting, 126–127  - formation of, mechanism for, 32
  - heterogeneity, 126, 161
  - integrity, 35, 36
  - interactions, 81–82, 186
  - location, 46–47
  - one-point interaction model, 232
  - stability, 35, 36
  - three-point interaction model, 127, 195, 232, 265
  - two-point interaction model, 82, 127, 206, 232
  - types, 36, 37, 222
- Binding site monomers *see* Functional monomers
- Bio-imprinting, 271–293
- early studies, 5
- Biological macromolecules
- as matrix-forming materials, 272–283
  - molecular imprinting of, 283–289
- Biological recognition systems, 422–423
- Biomimetic applications
- hydrogels, 289
  - metal ion imprinted resins, 264–265
- Biomimetic chemistry, meaning of term, 423
- Biomimetic recognition elements, 423
- Biosensors
- advantages, 503–504
  - disadvantages, 422, 504
- Biphenyl-4,4'-dialdehyde, 90
- 2,2'-Bipyridine, as template, 224
- 2,6-(Bisacrylamido)pyridine, as cross-linker, 399
- N,N'*-Bisacryloyldiaminopyridine, as functional monomer, 144
- N,O*-Bisacryloyl-L-phenylalaninol, 399
- N,N'*-Bisalkylamidines, 100
- Bisazomethines, 87
- 4,4'-Bis(dimethylamino)benzophenone
- structure, 470
  - as template, 468–469, 470
- 4,4'-Bis(dimethylamino)benzophenone (2,4-dinitrophenyl)hydrazone, 470
- Bisepoxysilicone, as functional monomer, 319
- Bis(2-hydroxyethyl)-aminopropyltriethoxysilane, 475
- 2,2-Bis(4-hydroxyphenyl)-propane, 471
- Bisimidazole derivatives, as templates, 189–190, 191, 264, 285
- Bis[*N*-(5-methacryloylamino)salicylidene-*S*-norsalinate] Co(III) complexes, as functional monomers, 187–188
- N,N'*-Bismethacryloyl-1,3-diaminobenzene, as functional monomer, 144
- Bisphenol A, as cross-linker, 471, 472, 479
- 1,4-Bis-(3/4-vinylbenzoxo)-benzene, 207, 208
- Blaschke-type chiral stationary phases, 395
- Block copolymers, 28
- B-lymphocytes, 122
- Boc-L-Phe *see tert*-Butoxycarbonyl-L-phenylalanine
- Boc-L-Trp, 402, 489
- Borane-derived catalysts, 106–107
- Boronic acid-containing binding sites, 74, 82–85, 86–87, 233
- Bovine erythrocyte haemoglobin, as matrix-forming protein, 274
- Bovine pancreatic chymotrypsinogen, as matrix-forming protein, 274
- Bovine serum albumin (BSA)
- catalytic activity in, 281, 282
  - imprinted gels/polymers, 227, 228, 284
  - as matrix-forming protein, 273–274, 275
- Brunauer–Emmett–Teller (BET) adsorption isotherm method, 53, 506
- Brush-type selectors, 145–146
- Bubble fractionation, 413
- Bulk preparation techniques, 22, 246, 305, 326, 399

- limitations, 22, 246, 305, 399–400
- metal ion-imprinted polymers, 246
- silica gels, 222–233
- transfer to preformed beads method, 310
- tert*-Butoxycarbonylphenylalanine (Boc-Phe), resolution of enantiomers, 314, 407
- tert*-Butoxycarbonyl-L-phenylalanine (Boc-L-Phe) imprinted polymers, 142
  - beads, 310, 314, 316
  - chromatographic behaviour, 171–172, 314
- Butylene dimethacrylate (BDMA), as cross-linker, 77
- Butyl orange, 6, 10, 222
- Cadmium(II)-binding isotherms, on metal ion imprinted resins, 259
- Cadmium(II)-imprinted polymers/resins
  - metal adsorption behaviour, 247–248, 257–260, 283
  - preparation of, 256, 257
- Caffeine
  - determination of, 352
  - separation from theophylline, 329, 348
  - structure, 473
- Caffeine-imprinted polymer, 472
- Calcium(II)-selective ionophore, 248–249, 450
- Calixarenes, effect on *p*-xylene imprinted polyurethane MIP, 519, 520
- D,L-Camphorsulphonic acid, resolution of enantiomers, 11, 12, 233
- Candida cylindracea* lipase, 280
- Candida rugosa* lipase, 279
- Capacity factors
  - BOC-L-phenylalanine MIP, 171
  - calculation of, 485–486
  - chloramphenicol MIP, 485–486, 487
  - guanidine-functionalised silica xerogels, 230
  - L-PA imprinted polymers, 150
  - theophylline-imprinted polymer rod column, 329
  - triazine-imprinted polymers, 152, 170
- Capillary electrochromatography (CEC), 377–380
  - chiral separations in, 387–391, 412–413
  - compared with conventional liquid chromatography, 379, 391
  - imprinted fused silica capillaries in, 118
  - instrumentation, 378, 379–380
  - MIP-based, 381–391
    - electrochromatographic separations, 387–391
    - gel-entrapped MIP particles, 382–383, 413
    - in situ* dispersion polymerisation used, 381–382, 413
    - in situ* prepared MIP monoliths, 383–386, 413
    - MIP coatings, 383, 413
    - preparation of MIPs, 381–386
    - pseudo-stationary phase, MIPs as, 383
  - principles, 377–379
  - stationary phases
    - in situ* prepared monolithic, 333, 335, 380
    - packed stationary phases, 379–380
- Capillary electrophoresis (CE)
  - chiral separations in, 412–413
  - in situ* imprinted polymers in, 333–334
- Carbohydrate-based molecularly imprinted matrices, 282–283
- Carbonate esters, 95
- Carbon dioxide, supercritical, polymerisation in, 321–322
- Carbon monoxide gas sensor, 199
- 3-Carboxybenzisoxazoles, decarboxylation of, 103
- N*-(4-Carboxybenzoyl)-phenylglycine imprinted polymers, 100
- Carboxylic acid esters, as binding groups, 91–92, 95
- Carboxylic acids, as templates, 98, 139–140, 141
- 7-Carboxymethoxy-4-methylcoumarin, 481, 483
- Catalysis
  - imprinted metal oxides in, 235–239
  - metal-coordinated imprinted polymers in, 197
  - MIPs in, 102–107
  - molecularly imprinted protein matrices in, 276–282
  - molecularly imprinted silicas in, 13–14
- Catalytic antibodies, 281, 282, 292
- Catechol-imprinted electrodes, 430
- Cation exchange resins



- chitosan-containing, 247, 283
- functional group titrations, 44–46
- CBS reaction, 106
- N*-CBZ-Tyr-PNP, 291
- Cell-imprinted polymers
  - applications, 301–302
  - method of production, 296–301
- Cell-mediated lithography, 288–289, 297, 299
  - on planar surfaces, 302, 303
- Chain transfer, in free radical polymerisation, 26–27
- Characterisation techniques, 47–55
  - elemental analysis, 48
  - fluorescence spectroscopy, 49–50, 51
  - gas sorption measurements, 51–52
  - gravimetric analysis, 48
  - infrared spectroscopy, 49, 50
  - mercury penetration measurements, 52
  - NMR spectroscopy, 49, 231
  - thermal analysis, 55
  - thermoporosimetry, 54
- Chemically modified electrodes (CMEs), 419
  - recognition elements for, 421–422
- Chemically sensitive field effect transistors (CHEMFETs), 420, 505
- Chemical sensors, 265–266, 417–418, 503–506
  - principles, 418, 504
- Chemical vapour deposited (CVD) films, 218, 220
- Chemical warfare agents, detection of, 63, 198, 478–479, 509
- Chemiluminescent assays, 494, 496
- Chewing gum, determination of nicotine in, 368–370
- Chicken egg ovalbumin, as matrix-forming protein, 274
- Chiral cavities, 79–80, 188
  - asymmetric syntheses in, 92–94
- Chiral chromatography, 188, 314, 400–413
  - in CE and CEC, 412–413
  - in HPLC, 401–410
  - in TLC, 410–412
- Chiral stationary phases (CSPs)
  - examples, 11–12, 118–121, 233, 395, 402
    - high-enantioselectivity/high-substrate-selectivity, 118–121
    - high-enantioselectivity/low-substrate-selectivity, 121
  - metal-coordinating MIPs as, 188
- Chitosan, 282
- Chitosan-epichlorohydrin polymers/resins, 247–248, 283
- Chloramphenicol
  - determination of, 345, 352, 484–488
  - medical uses, 484
  - as template, 141, 142, 484, 487
- Chloramphenicol diacetate
  - flow injection analysis, 484–488
  - structure, 486
- Chloramphenicol-methyl red
  - flow injection analysis, 484–488
  - structure, 486
- Chloramphenicol sensors, 484–488
  - with bulk imprinted polymers, 484–487
  - with *in situ* imprinted polymers, 487–488
- Chloride ions, sensor for, 432
- Chloroform, as mobile phase, 171
- 4-Chlorophenoxyacetic acid, (CPOAc), 482, 483
- Chlorotriazines
  - discrimination from S-triazines, 169–170, 366
  - solid phase extraction of, 367
  - see also* Atrazine; Cyanazine; Terbutylazine
- Cholesterol-imprinted beads, 311, 312
- Cholesterol-imprinted polymers, 143, 145, 153
  - binding of structural analogues, 205
  - preparation of, 204, 205, 283
- 2-Cholesteryl-3,6-dioxadecyl carbonate, 219
- Cholesteryloleyl carbonate, 468, 469
- Chromatography
  - band broadening with MIP phases, 133–138, 521
    - effect of sample load, 134, 163
    - in polymer rod columns, 330
  - chiral, 188, 314, 400–413
  - chiral stationary phases, 118–121, 188, 395, 402
  - column efficiencies, 310
  - compared with chemosensory applications, 519–522
  - diode array detection (DAD) in, 363, 368
  - height equivalent to theoretical plate, 134
  - limitations of MIPs, 521

- mobile phases
  - aqueous mobile phases, 176–179
  - optimisation of, 179
  - organic mobile phases, 167–173
- molecularly imprinted silicas in, 11–12
- number of theoretical plates, 83, 84, 117, 310
  - effect of Joule heating, 379
- resolution of enantiomers, 11, 83, 118, 387–391
- retention modes
  - electrostatic interactions, 166, 167–173
  - hydrophobic interactions, 166, 176–179
  - ion exchange retention mode, 166, 173–176
- retention of template on MIP, 134, 158, 159
- stationary phases, 21, 326
  - beads compared with crushed polymers, 305
  - in situ* imprinted polymer rods as, 327–330
  - metal-coordinating imprinted polymers, 188, 193–195
- transport model, 129, 136
- see also* Capillary electrochromatography; High-performance liquid...; Thin layer chromatography
- Chromophores
  - lanthanide ion, 453–457
  - transition metal ion, 442, 452, 453
- Chrysene, detection of, 491, 493
- $\alpha$ -Chymotrypsin
  - bio-imprinted, 277
    - mechanistic evaluation of catalytic activities, 279
  - MIPs compared with, 102, 197, 290
  - non-uptake on trypsin-imprinted gels, 288
  - polymeric mimics, 290, 291
  - X-ray crystallographic studies, 276
- Cibachron Blue, as template, 142
- Cinchonidine, distinguished from cinchonine, 331
- Cinchonidine- and cinchonine-imprinted polymer rods, 330–331
- Cinchonidine- and cinchonine-imprinted silica, 225
- Coated wire electrodes (CWEs), 419
- Coatings of MIPs
  - in capillary columns, 383
  - on silica beads, 196–197, 284, 287
- Cobalt complexes
  - in enzyme-like polymers, 290
  - in metal-coordinating imprinted polymers, 63, 187–188, 197
- Cobalt(II)-imprinted microspheres, metal adsorption behaviour, 252
- Codeine, effect on morphine MIPs, 348, 425
- Colorimetric detection
  - of metal ions, 462
  - of solvent vapours, 470–472
- Colorimetric reagents, 452, 462
- Combinatorial techniques, 125, 335–339, 346
- Competitive chemiluminescence assay, 494
- Competitive immunoassays, antibody–antigen interactions in, 341, 342
- Competitive ligand binding assays
  - MIPs in, 342–348, 352
  - see also* Molecularly imprinted sorbent assays
- Composite materials, in electrochemical sensors, 434
- Concanavalin A-labelled lectin, 299, 300, 301
- Concave chemistry, 510
- Condensation, gelation by, 215
- Conducting polymers, in electrochemical sensors, 431–433
- Conductometric sensors, 419–420, 447
- Confocal laser microscopy, cell-mediated lithography, 297, 298, 300
- Controlled-distance imprinting methods, 16, 85, 87, 89, 90, 229
- Controlled-pore glass beads, 307
- Convex chemistry, 510
- Copolymers, 27–28
  - alternating, 28
  - block, 28
  - divinyl monomers with monovinyl monomers, 29–35
  - GMA–EDMA, 34–35
  - MAA–EDMA, 32–33
  - MMA–EDMA, 22, 26, 27, 29–31, 29–32
  - statistical, 28
  - styrene–divinylbenzene, 22, 33–34
  - styrene–methyl methacrylate, 32
- Copper(II), amperometric detection of, 428
- Copper(II)-binding isotherms, on metal ion imprinted resins, 258

- Copper(II)–imidazole interactions, 63, 186, 189
- Copper(II)–iminodiacetic acid complex, as functional monomer, 189, 193, 409
- Copper(II)-imprinted microspheres  
metal adsorption behaviour, 252–253  
pH effects, 253
- Copper(II)-imprinted polymers/resins  
metal adsorption behaviour, 247, 249, 257–260  
phase transition behaviour, 290  
preparation of, 247, 248, 256, 257, 444
- Copper(II)-loaded microspheres  
ESR studies, 255  
FTIR studies, 254  
preparation of, 253–254
- Copper(II)–methacrylic acid complex, 250
- Corticosteroid-imprinted polymers, 206, 346  
selectivity, 348
- Corticosteroids, analysis of, 345, 489–490
- Cotinine, solid phase extraction of, 359, 369
- Cotinine-imprinted polymers, in MISPE, 365
- Coumarin derivatives, as fluorescent tracers, 350, 481
- Covalent approach to imprinting, 16, 81, 82–97, 380, 396  
advantages and disadvantages, 204  
and bead production technique, 306  
binding-site distribution, 126–127  
boronic acid-containing binding sites, 82–85, 86–87  
with disulphides, 89–90, 89  
with esters, 89, 91–92  
fluorescent functional monomers for, 477–478  
with ketals, 88, 90–91  
and non-covalent binding during equilibration, 95–97  
sacrificial spacer approach, 204–206  
with Schiff bases, 85, 88
- Covalent rebinding, 114
- Creatinine, as template, 144
- Cross-linking monomers, 41–43, 75–76, 77, 380, 398, 399  
polymer properties affected by, 75, 77, 398, 445  
*see also* Divinylbenzene; Ethylene glycol dimethacrylate; Trimethylolpropane trimethacrylate
- Cross-polarisation magic angle spinning (CP-MAS) NMR technique, 39, 49, 229
- Crown ether ionophores, 448
- Crown ethers and derivatives, 64
- CSPs *see* Chiral stationary phases
- Curing steps, post-treatment, 161, 164
- Cyanazine  
chromatographic retention on MIPs, 152, 178  
recognition by MIPs, 169, 170  
structure and properties, 169
- Cyclic adenosine monophosphate (cAMP)  
fluorescence sensor for, 141, 460, 464, 480–481  
imprinting of, 141, 143
- Cyclic voltammetry (CV), 218, 419
- Cyclobarbitol, as template, 144
- Cyclodextrin-based functional monomers, 64, 98, 101, 141, 143, 282, 391, 517
- Cyclodextrins, modified, chiral separation using, 334
- Cyclodicarboxylic acids, 91
- Cyclosporin, 344, 346  
determination of, 344, 345, 346, 352
- Cyclosporin-imprinted polymer, 346
- D-94, 489
- 2-*N*-Dansyl(ethyl)-3,3-dimethacrylic acid, 495
- Dansyl phenylalanine  
resolution of enantiomers, 383, 389, 473–474  
structure, 474
- Darifenacin  
solid phase extraction of, 352, 360, 366  
structure, 361
- Darifenacin-imprinted polymers, in solid phase extraction, 365
- Debye–Hückel limiting law, 448–449
- Debye–Scherrer spectroscopy, 11
- Decyladamantane-1-carboxylate, as template, 219
- Dehydrofluorination, catalysis of, 102–103, 141, 281, 282
- Detection limits  
in competitive ligand binding assays, 345, 349–350, 493–494  
2,4-D sensors, 482, 493–494, 496  
PMP sensors, 458

- polycyclic aromatic hydrocarbons, 479, 513
- surface acoustic wave sensors, 515
- 1,5-DHN, 489
- Diabetes mellitus, 199
- Diacrylamides, as cross-linkers, 42
- N,N'*-Diacryloyl-1,4-diaminobenzene, as cross-linker, 42
- Diacryloyldiaminopyridines, as functional monomers, 141, 144
- N,O*-Diacryloylphenylalaninol, as cross-linker, 42
- Dialdehydes, imprinting of, 87, 96
- N,N*-Dialkyl-*p*-phenylazoanilines, as templates in imprinted silicas, 226
- 2,6-Diaminoanthraquinone, as template, 140
- 3,3'-Diaminobenzophenone, 470
- Diaminonaphthalenes-imprinted beads, 318
- Diaminopyridines, as binding site monomers, 98
- Diazepam, 344
  - determination of, 344, 345, 352
- Diazepam-imprinted polymers, 123, 208, 314
- Diazomethane, esterification by, 164
- Dibenzamide, as template, 234
- Dibenzoylmethane, as photometric reagent, 462
- 1,4-Dibromobutane (DB), as cross-linker, 247
- Dicarboxylic acids, separation on silica, 87, 91
- 2,4-Dichlorophenol (DCP), in competitive chemiluminescence assay, 494
- 2,4-Dichlorophenoxyacetic acid (2,4-D)
  - detection limits, 482, 493–494, 496
  - determination of
    - by enzyme-labelled assay, 345, 350–351, 496
    - by fluoroimmunoassay, 345, 350, 481–482
    - and FT-IR spectroscopy, 491–494
  - structure, 151, 483
  - as template, 142
- 2,4-Dichlorophenoxyacetic acid-imprinted polymers
  - in ATR/FTIR method, 491
  - in competitive chemiluminescence assay, 494
  - in competitive fluoroimmunoassay, 481
  - in electrochemical sensor, 426
  - preparation of, 150, 151, 306, 347, 481
- 2,4-Dichlorophenoxyacetic acid methyl ester, (2,4-DOMe), 482, 483
- 2,4-Dichlorophenoxybutyric acid (2,4-DB), 482, 483
- Dickey, Frank H., 5, 6, 72, 213, 222, 380, 503
- N,N*-Diethyl-2-aminoethyl methacrylate (DEAEMA)
  - as functional monomer, 141, 142, 153, 315, 475, 487
  - in fluorescent detection of  $\beta$ -estradiol, 488, 489
- N,N'*-1,2-Diethylenebisacrylamide, as cross-linker, 287
- Diethylene glycol dimethacrylate (DEGDMA), as cross-linker, 76, 77
- Diethylvinylphosphonate-acrylic acid copolymers, 247, 248, 443–444
- Differential pulse voltammetry, 426, 494
- Differential scanning calorimetry (DSC), 55, 164
- 2,5-Dihydroxyphenylacetic acid, 494
- Diimines, as templates, 229
- 4,4'-Diisocyanatodiphenylmethane, 471, 479
- m*-Diisopropenylbenzene, as cross-linker, 42, 46
- Diketones
  - rebinding to imprinted polymers, 46–47
  - as templates, 88, 90
- Diluents
  - MIP selectivity affected by, 153, 154
  - polymer porosity affected by, 34–35, 154
  - polymer specific surface area affected by, 35, 154
- Dimethacrylamides, as cross-linkers, 42
- 3 $\alpha$ ,7 $\alpha$ -Dimethacryloylcholic acid, as functional monomer, 145
- N,O*-Dimethacryloylphenylglycinol, as functional monomer, 144
- N,N*-Dimethyl-2-aminoethyl acrylate, as functional monomer, 142
- trans*-4-[*p*-(*N,N*-Dimethylamino)styryl]-*N*-vinylbenzylpyridinium ion, 460, 480
- 4-(*N,N*-Dimethylamino)-4'-sulphonamidoazobenzene, 224

- N,N'*-Dimethyl-*N,N'*-bis(4-vinylphenyl)-3-oxapentadiamide, 248, 450
- 3,5-Dimethyl methyl benzoate (DMMB)  
complexes, with europium, 455, 456  
luminescence spectrum, 459
- N*-(3,5-Dinitrobenzoyl)- $\alpha$ -methylbenzylamine, 143, 144, 410, 411
- Diode array detection (DAD), 363, 368
- Diolel hydrogen phosphate, as functional monomer, 256
- Diolel phosphate (DOLPA), as functional monomer, with  $\gamma$ -ray irradiation, 263–264
- Diols, as templates, 84, 86, 87
- Dip-coating techniques, 221, 235, 516
- Dipeptides  
binding with amidopyrazoles, 98–99  
binding to tripeptide-imprinted polymer, 210  
resolution of enantiomers, 401, 403, 405  
separation of diastereomers, 143, 410
- Diphenyl phosphate, hydrolysis of, 105
- 3,3-Diphenylphthalide, 510
- Dispersion polymerisation  
advantages and disadvantages, 309  
beads produced by, 309, 315–317, 400  
*in situ* polymers produced by, 332–335, 381–382, 400
- Displacement techniques  
fluorescent detection of  $\beta$ -estradiol, 488–490  
fluorescent detection of L-phenylalanine amide, 490–491
- Disulphide cross-linkages, effect on MIPs, 16–17
- Disulphides, as templates, 89–90, 92
- Dithizone  
as colorimetric reagent, 452, 462  
complexes with metals, 442, 452, 453
- Diurea derivatives, as templates, 207
- Divinylbenzene (DVB)  
copolymers with styrene, 22, 77  
effect of diluent, 34  
as cross-linker, 22, 41–42, 42, 75, 77, 316, 383, 399  
properties of resultant polymers, 78  
structure, 42, 399
- Divinyl methyl benzoate (DVMB)  
complexes  
with europium, 198, 456, 478  
with lead, 458–460, 478  
fluorescence, 478  
luminescence, 458
- Divinyl monomers, copolymerisation with monovinyl monomers, 29–35
- DNA base adducts, attack by carcinogens, 155
- DNA imprinted matrices, 292
- 1,12-Dodecanediol-*O,O'*-diphenylphosphonic acid (DDDPA), as functional monomer, 260–261
- L-DOPA-imprinted polymers, 85, 86, 93
- Dopamine-imprinted metal oxide gels, 221, 429
- Drug bioanalysis, MIPs in, 345, 352
- Dubinín equation, 53
- Early developments  
by Dickey and Pauling, 3–6  
by Polyakov, 1–3
- Electrochemical sensors, 265, 418–420  
with conducting polymers, 431–433  
gate sites in surface monolayers, 429–431  
with inorganic templated materials, 428–429  
with MIPs  
with accumulation of analyte in polymer, 424–426  
early approaches, 424  
by permeation through polymer, 426–428  
with molecularly imprinted recognition sites, 423–434  
recognition elements, 422, 423  
with redox polymers, 433–434  
*see also* Amperometric...; Conductometric; Potentiometric sensors
- Electronic noses, 13, 436
- Electron spin resonance (ESR) spectroscopy  
copper(II)-loaded microspheres, 255  
 $\text{Cu}^{2+}$ –imidazole interactions, 189
- Electro-osmotic flow (EOF), 378
- Electrophoresis  
*in situ* imprinted polymers in, 333–335  
*see also* Capillary electrophoresis
- Electrostatic interactions  
in chromatographic retention, 167–173  
ligand recognition affected by, 65

- polymer selectivity affected by, 63
- Elemental analysis, 48
- Ellipsometry, imprinted films studied by, 219, 430, 468
- Emulsion polymerisation
  - oil/water emulsion polymerisation, 255–256, 311–312
  - seed emulsion polymerisation, 250, 251, 320
  - water/oil emulsion polymerisation, 260, 261, 311
  - see also* Suspension polymerisation
- Enantiomer separation
  - by ligand exchange chromatography, 265
  - by metal-coordinating MIPs, 188
  - by MIP beads, 314
  - by MIP-CE/CEC, 387–391, 412–413
  - by molecularly imprinted silicas, 11, 12, 233
- Enantioselective catalysts, MIPs as, 106–107
- Enantioselectivity
  - effect of solvents, 348–349
  - in imprinted ligand-exchange materials, 265, 266
  - in ion exchange mode, pH effects, 174–176
- Enkephalin-imprinted polymers, 63, 123
- Enzyme-labelled assay, of 2,4-D, 345, 350–351
- Enzyme-linked immuno-sorbent assay (ELISA), 359
  - clean-up before, 367
  - with 2,4-D MIPs, 496
  - compared with other assay methods, 482, 483
- Enzyme-mimetic imprinted hydrogels, 290–291
- Enzymes
  - active sites in, 71, 72, 276
  - behaviour in non-aqueous media, 276
  - bio-imprinted
    - activity in non-aqueous media, 273, 276, 277–278
    - applications, 278–279, 292
    - mechanistic evaluation of catalytic activities, 279
    - photostimulation of catalytic activities, 280–281
    - preparation of, 273, 275, 278
  - conformational characteristics, 289
  - cross-linked, 275
  - key-and-lock model, 72
  - MIPs mimicking, 102, 197, 290–291
  - molecularly imprinted silicas as, 13–14
  - synthetic/semi-synthetic, 281
- Enzyme selectivity, imprinted metal oxides, 236, 237
- Enzyme sensors, 422
- Enzyme thermistors, 421
- Ephedrine-imprinted polymers, 119, 120, 402
- 1,2-Epoxydodecane, recognition of, 219
- Epoxysilicone beads, 319–320
- Ester hydrolysis, catalysis of, 103–105
- Esterification
  - of anhydrides, catalysis of, 235–236
  - of boronic acids, 82
  - MIPs treated by, 164–165
- $\beta$ -Estradiol
  - determination of, 345, 488–490
  - fluorescent detection of, 488–490
  - direct measurement, 490
  - displacement technique, 488–490
- $\beta$ -Estradiol dansylate, 488, 489
- $\beta$ -Estradiol-imprinted polymers, 317, 319, 488
- Estrone, 489, 490
- Ethanol vapour, detection of, 512, 516
- Ethyl acetate vapour, detection of, 512, 516
- 9-Ethyladenine (9EA), association constants
  - of complexes with butyric acid, 158
- 9-Ethyladenine (9EA) imprinted polymers
  - monomer-template solution complexes, 159–161
  - rebinding experiments
    - adsorption isotherms, 127–128, 129
    - association constants, 158
    - effect of mobile phases, 172
    - kinetics, 133
- Ethylene glycol dimethacrylate (EDMA)
  - as cross-linker, 22, 42–43, 42, 61, 75, 116, 189, 197, 332, 334, 380, 383, 398, 399, 475, 477, 481, 488, 490, 492, 494, 497
  - properties of resultant polymers, 76, 78, 290
  - in imprinted polymer beads, 312, 315
  - structure, 42, 399
  - see also* Glycidoxypropyl methacrylate–...(GMA–EDMA); Methacrylic acid–...(MAA–EDMA); Methyl

- methacrylate-...(MMA-EDMA)  
copolymers
- Ethyl orange, 6, 222
  - templates mimicking, 226
- Europium(III)-based chromophores, 454–456
- Europium(III) ion based metal-complexing imprinted polymers, 63, 198, 456, 478–479
- External heavy atom effect, 452, 458
- Extraction techniques *see* Liquid–liquid extraction; Solid phase extraction
- Fibre optic sensors, 456, 457, 461, 473–474, 478, 499, 505
- Field effect transistor-based sensors, 420, 505
- Fischer, Emil, 72
- Flavonol
  - determination of, 352, 497–498
  - structure, 497
- Flavour esters, synthesis of, 278–279
- Flexibility
  - of binding groups, effect on resolving power of polymers, 84–85
  - of polymers, effect on template rebinding, 76, 78
- Flow injection analysis (FIA), 441, 461–463
  - chloramphenicol determination, 484–488
  - in combinatorial method, 335
  - $\beta$ -estradiol determination, 488–490
  - flavonol determination, 497–498
  - fluorescent detection of PAHs in water, 491
  - lead-ion determination, 462
  - metal ion-imprinted polymers in, 462–463
  - morphine determination, 462
  - uranyl ion determination, 462–463
- Fluorescein, 476, 494
- Fluorescein-imprinted silica, 475–477
- Fluorescence
  - of  $\beta$ -estradiol, 490
  - of methyl-3,5-divinylbenzoate, 478
  - quenching of functional monomer, 480–481
- Fluorescence sensor, for cAMP, 141, 460, 464, 480–481
- Fluorescence spectroscopy, characterisation of MIPs, 49–50, 51, 226
- Fluorescent complexes
  - formation on binding of metal ion template, 452, 478
  - interaction with ancillary ligands, 455–456, 478–479
  - selection of monomers, 442
- Fluorescent ligand displacement assay, for MIPs, 345, 350
- Fluorescent reporter, competition with template, 474–475
- Fluorescent templates
  - fibre optic detection of, 473–474
  - imprinting of silica with, 475–477
- Fluorimetric metal ion analysis, 452
- Fluorimetry, 473–482
  - competition of template and fluorescent reporter, 474–475
  - competitive fluoroimmunoassay, 481–482
  - determination of fluorophores using MIPs formed on quartz crystals, 479–480, 491
  - effect of template on formation of fluorophores in MIP, 474
  - fibre optic detection of fluorescent template, 473–474
  - fluorophores as functional monomers, 477–478
  - formation of fluorescent complex on binding of metal ion template, 478
  - imprinting of silicas with fluorophores, 475–477
  - interaction of ancillary ligand with fluorescent complex in MIP, 478–479
  - quenching of functional monomer fluorescence, 480–481
- Fluorocarbon liquids
  - properties, 312
  - suspension polymerisation in, 308, 312–315, 347
- Fluoroimmunoassay, 345, 350, 481–482
  - compared with other assay methods with 2,4-D MIP, 482, 483
  - limits of detection, 493–494
- 4-Fluoro-4-(4-nitrophenyl)butanone, dehydrofluorination of, 102–103
- Fluorophores
  - determination using MIPs formed on quartz crystals, 479–480, 491
  - effect of template on formation of, 474

- as functional monomers, 477–478, 494
- as templates in imprinting of silica, 475–477
- Footprint catalysts, 236, 237, 238
- Footprint theory, 9
  - in structure elucidation, 13
  - support of, 10–11
- Fourier transform analysis, 505–506
- Fourier transform infrared (FTIR) spectroscopy
  - copper(II)-loaded microspheres, 254
  - 2,4-dichlorophenoxyacetic acid-MIP, 491
  - molecularly imprinted protein-based matrices, 275
  - surface-modified metal-coordinating imprinted polymers, 192
- Free energy changes, 60, 65
- Free radical initiators, 24, 25
- Free radical polymerisation, 23–28, 113, 508
- Freeze drying, template-mediated, molecularly imprinted proteins prepared by, 273
- Freundlich adsorption isotherm, 66, 126
- Frontal analysis, 129–132
  - L-PA model system, 129–132, 136, 137
- Fructose-6-phosphate, as template, 275
- Fullerenes, C<sub>60</sub>, saccharides attached to, 85, 86
- Functional group complementarity, 139–140, 185
- Functional group titrations, 44–46
- Functional monomers
  - acidic, 140, 398
  - basic, 142–143, 398
  - charged, 143
  - effect of concentration on MIP selectivity, 83–84, 149
  - fluorophores as, 477–478, 494
  - quenching fluorescence on binding of analyte, 480–481
  - selection of, 138–146, 380, 397–398
    - in batch-type *in situ* molecular imprinting, 336–339
    - for *in situ* rods, 330–331
  - in stoichiometric non-covalent interactions, 98
  - uncharged, 144–145, 398
  - see also Methacrylic acid; Methyl methacrylate; Vinylpyridine
- Functional monomer–template interactions, 60–61, 126–127, 138
  - factors affecting, 138, 169, 186, 330, 334
  - studies of solution structures, 156–161
- Galactose, 474, 475
- $\beta$ -D-Galactosidase, 279–280
- Gas sensors, 198–199, 419, 516
- Gas separation membranes, 235
- Gas sorption measurements, 51–52
- Gate sites in surface monolayers, 218–219, 429–431
- Gel-entrapped MIP particles
  - in capillary electrochromatography, 382–383, 413
  - in electrochemical sensors, 425
- Geotrichum candidum* lipase, 279
- Gibbs free energy changes, 60, 65
- Glass transition temperature, heat treatment at temperatures exceeding, 162, 372
- Glucose
  - determination of, 352
  - sensor(s) for, 199, 200, 422, 426, 474
  - structure, 475
- Glucose-containing complex, polymerisation of, 200, 426, 427
- Glucose oxidase
  - as template, 287
  - on trypsin-imprinted gel, 288
- Glucose-selective polymer, 199, 200, 426, 427, 444, 450–451
- Glutamic acid, 118, 406
  - resolution of enantiomers, 406
- D-Glyceric acid, chiral recognition of, 16
- Glyceric acid derivatives, as templates, 16, 85, 86
- Glycidoxypyrrol methacrylate–ethylene glycol dimethacrylate (GMA–EDMA) copolymers
  - kinetics of copolymerisation, 31
  - porosity, 34–35
- Glycoproteins, as templates, 86
- Graphitised carbon black (GCB), 356
- Gravimetric analysis, 48
- Groundwater pollutants, 168, 366
- Guanidine-functionalised silica gel, 101, 229–232
- Guanidines, as binding site monomers, 98, 101



- Guanine, attack by carcinogens, 155, 157  
Guanines, alkylated, discrimination between, 155, 157  
Guanosine 3',5'-cyclic monophosphate  
  sensor for, 460, 480–481  
  structure, 480
- Haemoglobin, as matrix-forming protein, 274
- Halogenated solvents, 27
- Haptens  
  formation of antibodies from, 122, 343–344  
  imprinting technique compared with, 71–72, 125, 344
- Harmane derivatives, resolution of, 11–12
- Henderson–Hasselbach equation, 174
- Herbicides  
  assay of, 66, 168, 336, 346  
  *see also* Bentazone; 2,4-Dichlorophenoxyacetic acid (2,4-D); Triazines
- Hexadecane, as template, 219
- High-performance liquid chromatography (HPLC)  
  chiral chromatography, 401–410  
  imprinted beads as stationary phase, 318, 520  
  *in situ* imprinted polymer columns, 332  
  resolution of Boc-Phe, 314  
  separation of dicarboxylic acids, 91  
  UV detection technique, 359, 360, 367
- High-pressure polymerisation, 62, 152–153
- High-temperature polymerisation, 62, 150
- Historical background, 1–17
- Homogentisic acid, 426, 494
- Hoogsteen type interactions, 160
- Hydrogels, responsive, 289–291
- Hydrogenation catalysts, 197
- Hydrogen bond donor parameter, of mobile phase modifier, effect on MIP selectivity, 171
- Hydrogen bonding  
  IR spectroscopy, 49  
  multiple, in binding interactions, 98, 99, 146–147, 274  
  in solvents, 38, 54
- Hydrolysis  
  gelation by, 215  
  MIPs treated by, 165
- Hydrophobic interactions  
  in chromatographic retention on MIPs, 176–179  
  in MIP–ligand interactions, 65–66, 125  
  in preparation of MIPs, 63, 150–151
- Hydroquinone, as polymerisation inhibitor, 27
- $\alpha$ -Hydroxycarboxylic acids, as templates, 85, 86
- 7-Hydroxycoumarin  
  solid phase extraction of, 352, 359, 364  
  structure, 361
- 7-Hydroxycoumarin-imprinted polymers, in solid phase extraction, 365
- 2-Hydroxyethyl methacrylate (HEMA), as functional monomer, 141, 144, 153, 197, 290, 480
- 3-Hydroxyflavone *see* Flavonol
- N*-[2-Hydroxy-3-(tripropoxysilyl)propoxy]propyl-3-aminobenzenboronic acid, as functional monomer, 283, 284
- Ibuprofen  
  separation from related compounds, 408  
  structure, 408
- Imidazole–Cu<sup>2+</sup> interactions, 63, 186, 189
- Iminodiacetic acid (IDA)–Cu<sup>2+</sup> complexes, MIPs prepared using, 189, 190, 191, 264
- Immunoaffinity chromatography, detection limits, 513
- Immunoassays  
  meaning of term, 341  
  types, 341
- Immunoglobulin G (IgG), structure, 123, 125
- Immunoglobulins, 122
- Immunosensors, 422
- Indium–tin oxide electrodes, 430
- Inductively coupled plasma atomic emission spectrometry (ICP-AES), 446, 462
- Inductively coupled plasma mass spectrometry (ICP-MS), 446, 462
- Information-theory interpretations, selectivity of imprinted silicas, 13
- Infrared evanescent wave spectroscopy, MIPs and, 491–494
- Infrared spectroscopy, 38, 49, 50

- Inhibition, of free radical polymerisation, 27
- Inhibitor–enzyme interactions, 288
- Initiation, of free radical polymerisation, 23–25, 381
- Initiators, 23, 24, 25, 39, 116, 334, 381
- Inorganic matrices
- molecularly imprinted, 213–241
  - in electrochemical sensors, 428–429
- see also* Silica; Zeolites
- In situ* dispersion polymers, 332–335
- applications
- capillary electrochromatography, 333, 335, 381–382
  - capillary electrophoresis, 333–334
  - solid phase extraction, 332–333
- preparation of, 332, 381–382, 400
- In situ* imprinted polymer rods
- chloramphenicol MIP, 487–488
  - as chromatographic stationary phases, 327–330, 487–488
  - in capillary electrochromatography, 383–386
  - in flow injection analysis, 487–488
  - preparation of, 328, 400
  - selection of functional monomer for, 330–331
- In situ* imprinted polymers
- applications, 327
- preparation of
- for batch applications, 335
  - as dispersive polymers, 332
  - as rods, 327–330
- In situ* molecular imprinting, 326–327
- for batch applications, 335–339
- Instructional/instructive theory, 4, 125
- Interfacial activation technique, bio-imprinted enzymes prepared by, 278, 288
- Interfacial polycondensation, 288, 296–297
- Iodomethane, enzymes deactivated by, 279
- Ion exchange chromatographic retention mode, 173–176
- Ion exchange resins, reduced plate height vs mobile phase velocity, 135
- Ionic sensors, 441–464
- see also* Electrochemical sensors
- Ion-selective electrodes (ISEs), 419, 447–449
- fabrication of, 447–448
  - imprinted polymer ISEs, 449–451
  - calibration plot, 448
  - membrane ISEs, 448
  - recognition elements, 421
  - selectivity testing, 446, 449
  - fixed interference method, 449
  - matched potential method, 449
  - separate solution method, 449
- Ion-selective MIPs
- synthesis of, 442–446
  - preparation of complexes, 443
  - preparation of polymers, 443–445
  - selection of monomers, 442–443
  - testing for selectivity, 445–446
- Ion sieving, 431–432
- sensors using, 432
- Iron(II)–imidazole interactions, 63
- 2-([(Isobutyrylamino)caproyl]-L-phenylalanyl)-2-aminopyridine, 197, 290
- N*-Isopropylacrylamide, 290, 291
- Itaconic acid (ITA), as functional monomer, 140, 398
- Kelvin equation, 53
- Ketal bond formation, 46, 88, 90
- Ketones, enantioselective reduction of, 106–107
- Ketoprofen
- separation from related compounds, 408
  - structure, 408
- Kinetics
- adsorption–desorption, 132–133
  - free radical copolymerisation, 28
- $\beta$ -Lactoglobulin, imprinted, 282
- Lactonisation, effect of imprinted silica gels, 237
- Langmuir–Blodgett films/monolayers, 217, 430
- Langmuir type isotherm, 52, 53, 126
- fitting of data, 130, 131, 493
- Lanthanide ion chromophores, 453–457
- Latex particles, surface rearrangement of, 250–251, 320–321
- Lead(II)-based chromophores, 442, 452, 453, 458–460
- Lead(II) selective electrodes, 265, 464
- calibration plot for, 448
- Lead(II) selective matrices, 63, 462

- Lead(II) selective optrode, 458–460, 464, 478  
  prototype  
    calibration plot, 460  
    equipment setup, 459
- Leucine-enkephalin, determination of, 345
- D,L-Leucine *p*-nitroanilide, resolution of, 121, 122
- Lichrosphere beads, 310
- Ligand-exchange chromatography, 187, 265  
  benefits, 193
- Linear dichroism, 468–469
- Lipases  
  lipid coating of, 279–280  
  effect of imprinting, 280
- Liquid chromatography  
  optical sensors in, 482–490  
  *see also* High-performance liquid chromatography
- Liquid–liquid extraction  
  of biological samples, 344, 357  
  of metal ions, selectivity compared with imprinted resins, 261–262
- Listeria monocytogenes*-imprinted polymer beads, 288, 297, 298, 300, 301
- Listeria monocytogenes*-imprinted polymers, on planar surface, 302, 303
- Lithography  
  cell-mediated, 288–289, 297, 299  
  on planar surfaces, 302, 303
- Local anaesthetics, resolution of enantiomers, 389, 391
- L-PA *see* L-Phenylalanine anilide (L-PA)  
  model system
- Lubricants, monitoring of degradation processes, 517
- Luminescence probes, 461
- Luminol, 494
- Magnetic beads, 314–315, 347
- Magnetometric transducers, 421
- Maleic acid, separated from acrylic acid, 274
- L-Malic acid, as template, 273–274, 275
- Mandelic acid  
  resolution of enantiomers, 11, 85, 233  
  stereospecific inversion of, 92
- Mannose, 474, 475
- Mass-sensitive transducers, 420, 423, 505, 506, 515–519  
  *see also* Piezoelectric sensors; Quartz crystal microbalances; Surface acoustic wave sensors
- Mass transfer kinetics  
  effect of mobile phase, 173  
  photoinitiated compared with thermoinitiated polymerisation, 40–41
- MCM-41 zeolite, 240, 241, 428
- Membrane ion-selective electrodes, 448
- Membranes  
  molecularly imprinted  
    chiral separation using, 413  
    in electrochemical sensors, 426–428
- (–)-Menthol-imprinted tetraethoxysilane gels, 226
- Mercury(II), amperometric detection of, 428
- Mercury penetration measurements, 52
- Metal-coordinated imprinted polymers  
  applications, 192–199  
  catalysis, 197  
  recognition and binding of proteins, 195–197  
  sensors, 197–199  
  sorbents for separation media, 193–195  
  preparation by bulk polymerisation approach, 187–190  
  surface modified polymers, 191–192
- Metal-coordination interactions, 63, 81, 97, 185–201, 284–285, 286  
  advantages, 186–187  
  design of MIPs based on, 187–192  
  bulk polymerised imprinted polymers, 187–190  
  surface-modified imprinted polymers, 191–192
- Metal ion-binding polymers, preparation of, 246–250, 443–445
- Metal ion complexes, preparation of, 249, 443
- Metal ion coordination, 63, 81, 97, 185–201
- Metal ion imprinted microspheres  
  metal adsorption behaviour, 252–253  
  pH effects, 253  
  physicochemical characterisation of, 251–252  
  preparation of, by seed emulsion polymerisation, 250–251, 320–321
- Metal ion-imprinted polymers/resins, 114, 245  
  applications, 264–267

- biomimetic applications, 264–265
- early studies, 247–250
- in flow injection analysis, 462–463
- preparation of, 245–247
  - by oil/water emulsion polymerisation, 256–260
  - by water/oil emulsion polymerisation, 260, 261
- types, 245
- Metal ion-mediated rebinding, 114
- Metal ions, molecular imprinting of, 17
- Metal oxide gels
  - characterisation of, 216–217
  - cross-linking of, 216
  - post-functionalisation of, 213
  - preparation of, 213, 214–217
  - properties, 213–214
  - see also* Silica
- Methacrylic acid (MAA)
  - compared with acrylamide, in chiral stationary phases, 405
  - compared with trifluoromethylacrylic acid in imprinting of cinchona alkaloids, 330–331
  - in imprinting of triazines, 169–170, 336–339
  - compared with vinylpyridines, in chiral stationary phases, 405
  - as functional monomer, 100, 138, 140, 169, 290, 330–331, 336–339, 380, 397, 398, 468, 473
  - sites of interaction with atrazine, 169, 170
  - structure, 140, 337
- Methacrylic acid–ethylene glycol dimethacrylate (MAA–EDMA) copolymers, 32–33
- Methacrylic acid–ethylene glycol dimethacrylate (MAA–EDMA) imprinted beads, 313, 316
- Methacrylic acid–ethylene glycol dimethacrylate (MAA–EDMA) MIPs, 116
  - catalytic behaviour, 290
  - in chiral stationary phases, 401–405
  - electrostatic interactions in, 65
  - hydrolysis of cross-links in, 165, 166
  - in situ* dispersion polymers, 332, 334
  - in L-PA model system, 116
  - metal ion imprinted, 249
  - in MISPE, 365
  - in optical sensors, 488, 490, 497
  - primary structure, 32
  - secondary structure, 32–33
  - templates, 138
  - in MISPE, 365
- 3-Methacryloxypropyltrimethoxysilane, 334, 335, 384
- 3- $\beta$ -Methacryloylcholesterol, as functional monomer, 145
- N*-Methacryloylhistidine, 197, 290
- (*R,S*)-Methoxyamidotetralin (MAT), elution profiles when applied on (*S*)-MAT imprinted stationary phase, 173
- 1-Methoxy-3,5-bis-(4-vinylbenzoxy)-benzene, 207, 208
- 3-(2'-Methoxymethyl-1'-hydroxycyclohexyl-1'-methyl)norharmane, 12
- Methyl-3,5-divinylbenzoate, 478
  - see also* Divinyl methyl benzoate (DVMB)
- Methylene Blue, as template, 5, 282
- N,N'*-Methylenediacrylamide
  - as cross-linker, 42, 115, 187, 247, 287, 291, 399, 426, 444
  - structure, 42, 399
- Methyl- $\alpha$ -D-glucoside, determination of, 345
- 2-Methylisoborneol, detection of, 471
- Methyl methacrylate (MMA)
  - free radical addition polymerisation of
    - initiation of, 23
    - propagation of, 23
    - termination of, 26
  - as functional monomer, 22, 26, 27, 29–32, 398, 492
- Methyl methacrylate–ethylene glycol dimethacrylate (MMA–EDMA) copolymers, 22, 26, 27, 29–32
  - kinetics of copolymerisation, 30
- N*-Methyl-3-methoxymorphine-imprinted silica gels, 225
- Methyl orange, 6, 222
  - sulphonamide derivative, 224
  - templates mimicking, 226
- d,l*  $\alpha$ -Methylphenylamine, resolution of, 195
- Methyltriethoxysilane/tetraethoxysilane (MTES/TEOS) sol-gels, 235
- 3-Methylxanthine, 473

- Metoprolol, resolution of enantiomers, 347, 388, 389
- Michaelis–Menten kinetics, 105, 106, 236
- Michler's ketone, as template, 468–469, 470
- Microorganisms  
   surface imprinting of, 295–303  
   *see also* Bacteria-imprinted polymers
- Molecular imprinting  
   biological macromolecules as matrix-forming materials, 272–283  
   carbohydrates as precursors, 282–283  
   proteins as precursors, 272–282  
   capillary electrochromatography based on, 381–391  
   combinatorial method for, 335–339  
   compared with antibody formation, 125, 325  
   covalent approach, 16, 81, 82–97, 380, 396  
   evidence for, 506–507  
   first discovered, 1–3  
   general principles, 21, 71, 72–74, 203, 245, 272, 380–381, 395–396, 467, 507–508  
   *in situ*, 326–327  
   limitations, 161  
   literature on, 1, 2, 17  
   metal-ion chelation approach, 63, 81, 97, 185–201, 245, 284–285, 380  
   non-covalent approach, 17, 21, 60, 113–180, 380–381, 396–397, 507–510  
   schematic representation, 61, 72
- Molecularly imprinted polymer beads  
   near-monodisperse, 318  
   production of, 307–321  
     by aerosol polymerisation, 309, 319–320  
     considerations affecting suitability, 306–307  
     by dispersion/precipitation  
       polymerisation, 309, 315–317, 322, 496  
     preformed beads used, 307, 308, 310–311  
     by surface rearrangement of latex particles, 309, 320–321  
     by suspension polymerisation in fluorocarbon liquids, 308, 312–315, 400  
     by suspension polymerisation in water, 21–22, 308, 311–312, 400  
       by two-step swelling method, 309, 317–319, 400, 408, 409
- Molecularly imprinted polymers (MIPs)  
   as antibody mimics, 102, 121–125, 325, 342–344  
   characteristics, 343  
   characterisation of, 47–55  
   in electrochemical sensors, 424–428  
   factors influencing recognition properties, 138–161  
     choice of functional monomer, 138–146  
     concentration of functional monomer and template, 149  
     diluent properties, 153, 154  
     monomer–template rigidity, 139, 156  
     monomer–template solution structures, 156–161  
     number of template interaction sites, 146–147  
     polymerisation pressure, 151–153  
     polymerisation temperature, 149–151  
     template shape, 139, 154–155  
     thermodynamic considerations, 147–154  
   first reported, 15, 71
- MAA–EDMA copolymers  
   primary structure, 32  
   secondary structure, 32–33
- molecular-level design, 325
- morphology design, 325–326
- preparation of, 32–47, 113–118, 380–381, 399–400  
   compared with formation of antibodies, 125, 325  
   cross-linking monomers for, 41–43  
   extraction of template, 43–44, 343  
   metal-coordinating imprinted polymers, 187–190  
   physical principles underlying, 59–64  
   solvents for, 38  
   surface-modified metal-coordinating imprinted polymers, 191–192
- recognition properties  
   chromatographic evaluation of, 117  
   factors influencing, 138–161  
   thermodynamic considerations, 64–67, 147–154
- selectivity  
   effect of cross-linking, 75–76, 77

- effect of monomer–template rigidity, 156
- effect of rigid templates, 63
- effect of solvents, 348–349
- estimation of, 348
- Molecularly imprinted solid phase extraction (MISPE), 358–373
  - affinity mode, 367
  - cartridge format for MIPs, 358, 359–360
  - coupled column approaches, 362, 363, 370
  - drying of MIP cartridges, 362, 370
  - elution solvents, 364
    - examples, 359–360
  - examples of applications, 359–360
  - of nicotine, 368–370
  - off-line protocols
    - extraction of analytes of environmental concern, 366–368
    - sample clean-up of biological fluids, 364–366
  - on-line protocols
    - coupled column approaches, 362, 363, 370
    - extraction of nicotine, 368–370
    - with pulsed elution, 370
  - reversed-phase mode, 358, 362, 367
  - steps in development of new protocols, 370–371
  - template bleeding problems, 371–372
  - validation of method, 371
    - results for example protocols, 365
  - wash procedures, 358
    - examples, 359–360
- Molecularly imprinted sorbent assays (MIAs), 342–343
  - aqueous buffer-based, 346–348
  - organic solvent-based, 344–346
  - sensitivity, 349–350
- Molecular printing (of proteins), 196
- Monoalcohols, as templates, 85, 87
- Monoclonal antibodies, preparation of, 123–124, 344
- Monodisperse polymer imprinted beads, production of, 317, 322
- Monolayer-coated sensors, 218, 219, 430, 468, 509
- Monolayer films, 217–220
  - octadecyltrichlorosilane-based, 218–219
  - Monolithic imprinted polymer capillary columns, 327–331, 383–386, 400
- Monolithic stationary phases, 380
- Monolith technique, 22
  - see also* Bulk preparation techniques
- Monomer–template assemblies
  - in metal-coordinating imprinted polymers, 189, 193, 194
  - stabilisation of, 139, 507
  - thermodynamic considerations, 147–154, 371
- Monomer–template interactions, 60–61, 126–127, 138
  - factors affecting, 138, 169, 186, 330, 334
  - studies of solution structures, 156–161
- Monomer–template rigidity, MIP selectivity affected by, 139, 156
- Monomer-type surfactants, surface imprinting using, 266–267
- Monosaccharides, imprinting of, 119
- Morin
  - effect on flavonol sensor, 498
  - structure, 497
- Morphine
  - binding to carrier protein, 348
  - determination of, 345, 424–425, 462
  - structure, 348
- Morphine-imprinted polymers, 63, 123, 316, 348, 424–425, 434
- Morphine-imprinted silicas, 13
- Morphine-responsive electrochemical sensor(s), 424–425, 434, 462
- Multicomponent samples, analysis of, 510, 524
- Multiple coordinating monomers, in molecular imprinting, 62–63
- Multiplex advantage, 505
- Multivariate analysis, 13, 506, 524
- Myosmine, solid phase extraction of, 359, 369
- Myosmine-imprinted polymers, in MISPE, 365
- N-316, 489
- Naphthalene, 492
- Naproxen
  - determination of, 352, 409
  - separation from related compounds, 408

- Naproxen-imprinted beads/polymers, 318–319, 402, 408
- NATA *see* *N*-Acetyltryptophanamide
- Nernst equation, 447
- Nerve agents, detection of, 63, 198, 478–479, 509
- Neural networks, 480, 524
- Nickel(II)-imprinted microspheres  
metal adsorption behaviour, 252–253  
pH effects, 253
- Nickel(II)-imprinted polymers, 248
- Nicotinamide adenine dinucleotide (NAD), as template, 233–234
- Nicotine  
solid phase extraction of, 352, 359, 368–370  
structure, 361
- Nicotine-imprinted polymers, 67  
preparation of, 365, 368  
in solid phase extraction, 365, 368–370
- Nicotine-imprinted silica, 15, 225
- $\beta$ -Nicotyrine, 369
- NIST standard reference material SRM-610, 462
- Nitrate ions, sensor for, 432
- Nitric oxide gas sensor, 199
- p*-Nitrobenzaldehyde, as fluorescence quencher, 494, 495
- Nitrobenzene-selective sensor, 433–434
- Nitrogen bases, interaction with boronic acid-containing binding sites, 83, 87
- Nitrogen heterocycles, imprinting of, 121, 123, 156, 224
- Nitrogen oxides, sensing of, 199, 432, 452
- p*-Nitrophenyl esters, catalysed hydrolysis of, 197, 290
- Non-aqueous media  
enzymes in, 276  
proteins in, 272  
suspension polymerisation in, 79
- Non-competitive immunoassays, antibody–antigen interactions in, 341, 342
- Non-covalent approach to imprinting, 17, 21, 113–180, 380–381, 396–397  
advantages and disadvantages, 203–204  
and bead production technique, 306  
binding-site distribution, 126  
combined with covalent monomer–template bonds, 64  
effect of monomer–template ratios, 62  
functional monomers, 138–146, 330  
fluorescent functional monomers, 477–478  
limitations, 64, 117–118  
for sensors, 507–510  
structure–binding relationships, 118–125
- Non-covalent binding, during equilibration, 95–97
- Non-covalent rebinding, 95–97, 114
- Non-polar solvents, disadvantages, 63
- Non-radioactive assays, 345, 350–351  
*see also* Enzyme-labelled assay;  
Fluorescent...assay
- Non-steroidal anti-inflammatory drugs *see* Ibuprofen; Ketoprofen; Naproxen
- Norephedrine imprinted hydrogels, 291
- Nuclear magnetic resonance (NMR) spectroscopy  
binding interactions studied by, 49, 231–232  
for characterisation of MIPs, 49  
monomer–template interactions studied by, 60, 61, 158, 160  
surface-modified metal-coordinating imprinted polymers studied by, 192
- Nucleotides  
effect on cAMP-imprinted polymer, 481  
recognition of, 208–209  
as templates, 141, 142, 233–234
- Octadecylsilane based monolayer films, 218–219, 430, 468
- Octadecylsulphonate based monolayer films, 220
- Octadecyltrimethoxysilane based monolayer films, 220
- 4-(Octyloxy)phenylphenyliodonium hexafluoroantimonate, as initiator, 319
- Oil-sensitive MIPs, 517, 518
- Oil/water emulsion polymerisation, surface imprinting using, 255–260
- Oil/water suspension polymerisation, 21–22, 311–312
- Oligopeptides  
recognition of, 208–209  
as templates, 98
- Olive oils, determination of flavonol in, 498

- On-line monitoring, of chemical composition, 461
- Optical probes, 461
- Optical rotation
- of imprinted polymers, after template removal, 80
  - measurement of, 79–80
- Optical sensors, 265, 420–421, 467–490, 505–506, 510–514
- colorimetric detection of solvent vapours, 470–472
  - ellipsometry, 468
  - fluorimetry, 473–482
  - linear dichroism, 468–469
  - in liquid chromatography, 482–490
  - recognition elements, 422, 423
  - surface plasmon resonance, 472–473
- Organic chromophores, 458–460
- Organic liquids, sensors in, 517
- Organic polymers
- molecular imprinting in, 15–17
  - see also* Molecularly imprinted polymers
- Organic solvent-based assays, 344–346
- Ormosils, 231
- Ovalbumin, as matrix-forming protein, 274
- Oxazaborolidines, as catalysts, 107
- Oxygen gas sensor, 199
- PA *see* Phenylalanine anilide
- Papain, imprinted, 282
- Particle sizes, beads, 310, 314, 315, 318, 319
- Pattern recognition, 13, 436
- Pauling, Linus, 3–6, 203
- Pentaerythritol tetraacrylate (PETEA), as cross-linker, 386, 399
- Pentaerythritol triacrylate (PETRA)
- as cross-linker, 42, 386, 398, 399, 405
  - structure, 42, 399
- Pentafluorostyrene, 207, 208
- Pentamidine
- solid phase extraction of, 352, 359, 364
  - structure, 361
- Pentamidine-imprinted polymers, 99–100, 138
- in CE/CEC, 334, 381–382, 389
  - compared with benzamidine-imprinted polymers, 334, 381–382
  - preparation of, 316, 332, 365
  - in solid phase extraction, 365
- Peptides, imprinting of, 13–14, 43, 98, 119, 120, 143, 145
- Perfluorocarbons, suspension polymerisation in, 308, 312–315, 347
- Perfluorosulphonamidoethyl acrylate, 313
- Peroxides, as free radical initiators, 25, 27
- Persulphates, as free radical initiators, 25
- Perylene
- detection of, 493
  - structure, 492
- pH effects
- guanidine-functionalised silica xerogels, 230–231
  - in ion exchange mode, 174–176
- Phenanthrene
- structure, 492
  - as template, 234
- 1,10-Phenanthroline, as template, 224
- Phenoxyacetic acid (POAc)
- binding to 2,4-D MIP, 483, 493
  - structure, 483
- Phenylalanine
- determination of, 345
  - resolution of enantiomers, 194–195, 406, 407, 410
- L-Phenylalanine, as template, 195, 265, 266, 389, 406
- L-Phenylalanine amide, liquid
- chromatographic detection of, 490–491
- D,L-Phenylalanine anilide (D,L-PA)
- fitting of adsorption isotherms, 129–132
  - protonation-states model, 176
  - resolution of, 14, 84, 122, 129
  - separation of enantiomers
    - chromatographic band broadening, 134–137
    - by thin-layer chromatography, 411
- L-Phenylalanine anilide (L-PA)
- adsorption isotherms, 129–132
  - minimum-energy conformation, 119
  - molecular imprinting of, 116
  - photochemically initiated polymerisation
    - of, 39, 41, 116, 150
    - as template, 116, 144, 166, 328, 382
    - thermochemically initiated polymerisation
      - of, 41, 116, 149–150
- L-Phenylalanine anilide (L-PA) imprinted polymers
- in capillary electrochromatography, 389



- characterisation of, 44, 45
- effect of diluents, 37
- in electrochemical sensors, 424
- esterification of carboxylic groups, 164, 165
- ion exchange retention mode in resolution of, D,L-PA, 173–175
- photo- vs thermo-initiation, 41
- protonation-states model, 176
- L-Phenylalanine anilide (L-PA) model system, 116
  - effect of thermal annealing, 162, 163
  - factors affecting chromatographic response, 66, 134–137, 149–151, 162, 163
  - model of binding site, 158, 160
  - monomer–template interactions, 60
- Phenylalanine derivatives, molecular imprinting of enantiomers, 146–147
- L-Phenylalanine ethyl ester, as template, 118, 140, 146
- L-Phenylalanine-imprinted membranes, 427
- L-Phenylalanine-*N*-methylanilide (L-PMA), 118
  - minimum-energy conformation, 119
- D,L-Phenylalanine *p*-nitroanilide, resolution of, 122
- D,L-Phenylalanyl glycine anilide, resolution of, 121
- N,N'*-1,4-Phenylenediacrylamide, as cross-linker, 115, 399
- Phenyl- $\alpha$ -D-mannopyranoside, as template, 72–73, 84
- Phenylphosphonic acid (PPA), binding to guanidine-functionalised silica xerogels, 231–232
- 2-Phenylpropionic acid, resolution of enantiomers, 334, 389
- Phenyltriisocyanate, 471, 479
- Phenyltrimethoxysilane, in metal oxide thin films, 221, 429
- Phloroglucinol, as cross-linker, 471, 472, 479
- Phosphate receptors on silica xerogels, 101, 229–232
- Phospholipase D, 279
- Phosphonamides, as templates, 237, 238
- Phosphonate receptors on silica xerogels, 101, 229–232
- Phosphonic acid esters, as templates, 98, 101
- Phosphoric esters, as templates, 98, 101, 105
- Photochemically initiated polymerisation, 24
  - compared with thermochemically initiated polymerisation, 39–41, 150
  - in monolithic imprinted polymer capillary columns, 385, 386
  - in suspension polymerisation, 313–314
- Photometric reagents, 462
- Photosensitive hydrogels, 291–292
- Photostimulation, of bio-imprinted enzymes, 280–281
- Phthalide dye
  - incorporation into MIPs, 471, 510–513
  - structure, 471, 511
- Phthalocyanines, in amperometric sensors, 423
- Physicochemical recognition elements, 421–422
- Piezoelectric transducers, 420, 506
- Pinacolyl methyl phosphonate (PMP)
  - imprinted polymer sensor(s), 455–457, 458, 478–479
  - effect of coating thickness on response time, 457
  - evaluation of performance, 456–457
  - fibre-optic tip, 456, 457, 478
  - performance data, 458, 479
  - preparation of, 456
  - structure, 479
- Pindolol, resolution of enantiomers, 390
- Pirkle-type chiral stationary phases, 395
- Plasma deposition technique, surface imprinting by, 292
- Plastic antibodies, 208
- Pneumococcus* polysaccharide Type III, 5
- Polyacrylamide gels
  - in MIP-based capillary electrochromatography, 382–383
  - molecular imprinting of, 115–116, 287
- Polyakov, M.V., 1–3
- Polyamines, in interfacial polycondensation, 296
- Polyaniline, as sensor material, 433
- Polychlorinated aromatic compounds, 206–207
- Polyclonal antibodies, preparation of, 344
- Polyclonal nature of MIPs, 125, 349, 401
- Polycyclic aromatic hydrocarbons (PAHs)
  - detection of, 479–480, 491, 513, 516

- sources, 513
- see also* Anthracene; Pyrene
- Polyethylene glycol, in interfacial polycondensation, 296
- Polymerisation
  - of amino acid esters, 13–14
  - binding-site interactions during, 81
  - chain transfer in, 26–27
  - copolymerisation, 27–28
  - in fluorocarbons, 308, 312–315
  - free-radical addition, 23–28
  - for imprinted beads, 307–321
  - inhibition of, 27
  - initiation of, 23–25, 381
  - kinetics of copolymerisation of MMA and EDMA, 30, 31
  - for metal ion imprinted resins, 255–264
  - propagation of, 25
  - of silica, pH control of, 2, 7
  - steady state, 26
  - in supercritical carbon dioxide, 321–322
  - tacticity of polymers, 28
  - termination of, 25–26
  - see also* Aerosol...; Dispersion...; Emulsion...; Interfacial...; Precipitation...; Suspension polymerisation
- Polymerisation diluents
  - MIP selectivity affected by, 153, 154
  - polymer properties affected by, 33–35, 153, 154
- Polymerisation pressure, effect on MIP selectivity, 62, 151–153
- Polymerisation solvents, 398–399
  - see also* Porogens
- Polymerisation temperature, effect on MIP selectivity, 62, 149–151
- Polymers, optimisation of structure, 74–80
- Poly(metalloporphyrin)s, 433–434
- Poly(4-methyl-4'-vinyl-2,2'-bipyridine), 248
- Polyols, as templates, 86
- Polypeptides, effect of imprinted silica on formation of, 13–14
- Polypyrrole
  - with complexing cavities, 432–433
  - composites, 434
  - in electrochemical sensors, 422, 431–432
- Polysaccharide-based molecularly imprinted matrices, 282–283
- Polysiloxanes, imprinted, 218, 219, 286–287
- Polyurethane-based MIPs, 508
  - effect of cross-linker content, 512
  - in optical sensors, 471, 510–513, 516
  - on quartz crystals, 470–471, 479, 491
  - p*-xylene imprinted, 519, 520
- Poly(vinyl alcohol), as suspension stabiliser, 311, 312
- Poly(vinyl chloride) membrane ion-selective electrodes, 448
- Poly(vinylimidazole), 248, 444
- Poly(4-vinylpyridine) (PVP), interaction with metal ions, 247, 444
- Poly(vinylpyrrolidone), 17, 311
- Pore size
  - distribution, determination of, 53
  - factors affecting, 33–34
- Pore volume, determination of, 53
- Porogen imprinting effects, 155, 156, 172
- Porogens (solvents), 33, 153 *see also* diluent
  - effect on *in situ* prepared MIP monolithic columns, 384, 386
  - effect on polymer properties, 33–34, 78, 329–330, 381, 398–399
  - as MISPE wash solvents, 362, 366
  - in suspension polymerisation, 313
- Porosity, polymer, factors affecting, 33, 38–39, 40, 153, 330
- Porous structure
  - build-up of, 33–35
  - characterisation of
    - in dry state, 50–53
    - in swollen state, 54–55
- Porphyrin-imprinted polymers, 219
- Porphyrins, in electrochemical sensors, 423, 433–434
- Portable analysers, 458, 479, 499
- Post-treatments, 161–165
  - esterification, 164–165
  - hydrolysis, 165
  - thermal annealing/curing, 161–164
- Potassium oleate, as functional monomer, 256
- Potentiometric sensors, 418–419
- Potentiometric titrations, 44–46
- Precipitation polymerisation, beads/
  - microspheres produced by, 315–317, 322, 496

- Preformed beads, polymerisation in, 307, 308, 310–311
- Prenalterol, resolution of enantiomers, 390
- Preparative chromatographic separations, 84
- Prometryn
- chromatographic retention on MIPs, 177, 178
  - recognition by MIPs, 170
  - structure and properties, 169
  - as template, 140, 166
- Propagation, free radical polymerisation, 25
- Propazine, solid phase extraction of, 368
- Propranolol, enantiomer separation by CE/CEC, 387, 388–389, 388, 412, 413
- S-Propranolol
- determination of, 345
  - solid phase extraction of, 352, 359, 364
  - structure, 123, 349, 361
- R-Propranolol-imprinted polymers, in capillary electrochromatography, 387, 388–389, 390
- S-Propranolol-imprinted polymers, 123, 314, 316, 319, 347
- in capillary electrochromatography, 335
  - enantioselectivity, 349
  - in solid phase extraction, 365, 371
- Propyl orange, 6, 10, 218, 222
- 4-(4-Propyloxyphenylazo)benzoic acid-imprinted titanium oxide films, 221, 428, 472
- Protein-based molecularly imprinted matrices
- applications
    - in catalysis, 276–282
    - for recognition and separation, 273–276
- preparation of, 272–273
- by chemical cross-linking, 274–275
  - by freeze drying, 273
- Protein binding assays, 341
- Proteins
- recognition and binding of, 195–197, 284–287
  - two-dimensional crystallisation of, 196
- Protolytic functional groups, templates with, chromatographic retention mode for, 173–176
- Pseudoephedrine-imprinted polymers, 119, 120, 402
- Pseudomonas fluorescens* imprinted silica, 14–15
- Purines, retention by 9EA-imprinted polymers, 128, 130
- Pyrene
- detection of, 479, 493, 513, 514
  - structure, 492
- trans*-3-(3-Pyridyl)-acrylic acid, as functional monomer, 383
- Pyrimidines, retention by 9EA-imprinted polymers, 128, 130
- Quartz crystal microbalances, 504, 505, 506
- MIPs deposited on, 470–471, 491, 516–519
  - oil-sensitive MIPs, 517, 518
- Quartz crystals
- MIPs on
    - colorimetric detection of solvent vapours using, 470–471
    - determination of fluorophores using, 479–480, 491
- Quaternary ammonium compounds, as functional monomers, 143
- Quercitin
- effect on flavonol sensor, 498
  - structure, 497
- Quinidine/quinine-imprinted silica, 13, 225
- Quinoline, as template, 224
- Racemic resolution, 11–12, 73
- boronic acid-containing imprinted polymers first used, 83
- Radical polymerisation, 23–28, 113, 508
- Radioimmunoassay
- compared with other assay methods with 2,4-D MIP, 482, 483
  - limits of detection, 493–494
- Radioligand binding assays
- imprinted polymer beads, 314, 316, 496
  - MIPs, 123, 132, 345
- Rebinding of templates to MIPs
- adsorption isotherms, 127–128
  - binding-site interactions during, 81, 127–128
  - medium dependence in, 165–179
- Recognition elements, MIPs as, 125, 423, 467
- generation by combinatorial techniques, 125

- Recognition elements in sensors, 421–423  
  biological, 422–423  
  biomimetic, 423  
  physicochemical, 421–422
- Recognition properties of MIPs  
  factors affecting, 138–161  
  *see also* Molecularly imprinted polymers,  
    recognition properties
- Redox polymers, in electrochemical sensors,  
  433–434
- Regioselective reactions, 94
- Restricted-access materials, 219, 357
- Rhodamine B, 490, 491
- Rhodanile Blue, imprinting by, 227, 228
- Rhodium complexes, catalysts based on, 197
- Ribonuclease A, as template, 196, 286
- Rigidity  
  monomer–template, MIP selectivity  
    affected by, 139, 156  
  of polymers, MIP selectivity affected by,  
    75  
  of templates, MIP selectivity affected by,  
    63
- RNA imprinted matrices, 292
- Rods, imprinted polymer, as  
  chromatographic stationary phases,  
  327–330, 383–386, 487–488
- (S)-Ropivacaine-imprinted polymers, in  
  capillary electrochromatography, 387–  
  388, 389
- Ruthenium complexes, as templates, 106
- Saccharides  
  resolution of free sugars, 84  
  as templates, 84, 86, 87
- Sacrificial spacer method, 204–206, 311  
  combined with non-covalent imprinting,  
  206–208, 209
- Safranin O  
  imprinting of, 115, 227, 228  
  structure, 115, 228
- Salicylic acid, as template, 144
- Sameridine  
  solid phase extraction of, 352, 359, 364  
  structure, 361
- Sample clean-up  
  of biological fluids, MISPE used, 364–366  
  for metal ion determinations, 462
- Sarin (nerve agent)  
  detection of, 198, 478  
  structure, 479
- Saturation capacities  
  in L-PA model system, 131–132  
  typical values, 128
- Sauerbrey equation, 515
- Scanning electron microscopy (SEM)  
  cell-mediated lithography, 297, 300  
  silica xerogels, 216  
  surface-modified metal-coordinating  
    imprinted polymers, 192
- Scatchard plots, 127, 128  
  of cholesterol-imprinted polymer, 204  
  of fluorescein- and NATA-imprinted  
    silica, 476  
  of trypsin-imprinted gel, 288
- Schiff bases, 85, 88, 92, 95, 188
- Seawater, lead ions in, 450, 462
- Seed emulsion polymerisation, 250–251, 320
- Selective theory (of antibody formation), 4
- Selectivity  
  mechanisms, 7, 9–11  
  of metal ion imprinted resins, 260, 261  
  of MIPs  
    effect of cross-linking, 75–76, 77  
    effect of monomer–template rigidity,  
      156  
    effect of rigid templates, 63  
    effect of solvents, 348–349  
    estimation of, 348  
  of silicas, factors affecting, 2–3  
  of triazine-imprinted polymers, 169, 170,  
    338
- Self-assembled monolayers (SAMs), 217–218  
  gate sites in, 218–219, 429–431, 509
- Self-association model, for template–  
  template interactions, 66–67
- Semiconducting oxide gas sensors, 419–420
- Sensitivity, molecularly imprinted assays,  
  349–350
- Sensor arrays, 480, 510, 524
- Sensors  
  application areas, 418  
  compared with chromatographic  
    applications, 519–522  
  environmental considerations, 521  
  metal-coordinated imprinted polymers in,  
    197–199  
  metal ion imprinted resins in, 265–266

- with molecularly imprinted recognition sites, 423–434
- non-covalent molecularly imprinted, 503–524
- performance parameters, 418
- principles, 418, 504
- recognition elements, 421–423
  - biological, 422–423
  - biomimetic, 423
  - physicochemical, 421–422
- required characteristics, 522
- transducers, 418–421, 505
  - electrochemical, 418–420
  - field effect transistor-based, 420, 505
  - mass-sensitive, 420, 506
  - optical, 420–421, 505–506
- see also* Amperometric...; Chemical...; Electrochemical...; Ionic...; Mass-sensitive...; Optical...; Potentiometric sensors
- Serine proteases, MIPs mimicking, 197, 290
- Severinghaus-type electrodes, 419
- Shape complementarity, 119, 154–155
- Shear transverse acoustic wave (STW) sensors, 506
- Sialic acid–boronic acid complex, membrane imprinted with, 428
- Sialic acid-imprinted polymer, 86, 141, 143, 474
- Silane-containing boronic acids, coupling by, 85, 86
- Silanes, gelation of, 215
- Silica
  - amino-functionalised, 90, 229
  - boronate-functionalised, 233–234
  - factors affecting surface properties, 223
  - guanidine-functionalised, 229–232
  - hydrophobised, 356
  - methacrylate-functionalised, 287
    - with metal-coordinating sites, 192, 194, 196–197, 286
  - molecularly imprinted
    - applications, 11–15
    - in catalysis, 13–14
    - chiral resolution using, 11–12, 233
    - in chromatography, 11–13
    - commercial applications, 15
    - confirmatory studies, 224
    - controlled distance method, 87, 90, 229
    - Dickey's method of preparation, 7, 8, 222, 224
    - early studies, 2–3, 222
    - effect of ageing, 224
    - with fluorophores as templates, 475–477
    - limitations, 15
    - methods of preparation, 6–7, 8, 222–233
    - microporosities, 10
    - Polyakov's method of preparation, 7, 8
    - selective adsorption of alkyl orange dyes, 6, 223
      - in structure elucidation, 13
    - polymers coated onto, 79, 115, 192
    - silane-functionalised, 226–227
    - silanol groups and siloxane bonds on surface, 216, 217
  - Silica beads, 307
    - imprinted polymers in pores, 310, 400
    - thin polymer coating on, polymer recognition by, 196–197, 284, 287
- Silicates, imprinted, adsorption of alkyl orange dyes, 224, 231
- Silicone oil, suspension polymerisation in, 315
- Simazine
  - response of atrazine sensor, 428
  - response of triazine sensor, 475
  - solid phase extraction of, 359, 367, 368
  - structure, 361, 476
- Simazine-imprinted polymers, in solid phase extraction, 365
- Size exclusion effect, 119
- Smart gels, 289
- Society for Molecular Imprinting (SMI), database, 443
- Sodium dodecyl sulphate (SDS), effect on selectivity of metal ion imprinted resins, 256, 260
- Soil pollutants, 168, 366
- Sol-gels, for sensors, 428, 508
- Sol-gel techniques, 7, 213, 214–217, 286
- Solid phase extraction (SPE)
  - advantages, 351–352, 356
  - high-affinity phases, 358
  - mixed-mode sorbents in, 356, 357
  - molecularly imprinted, 352, 358–373, 520
    - in situ* imprinted dispersion polymers, 332–333
  - multi-purpose phases, 356–357

- 96-well format, 357
- principles, 355–356
- see also Molecularly imprinted solid phase extraction (MISPE)
- Solubility parameters
  - of polymers, 38, 39, 54
  - of solvents, 38, 54
- Solvation, determination of, by fluorescence probes, 49–50
- Solvation model, for template–template interactions, 66–67
- Solvent extraction, of metal ions, selectivity compared with imprinted resins, 261–262
- Solvent memory effect, 362, 507
- Solvents
  - chain transfer in free radical polymerisation, 27
  - effects
    - on binding to protein-based molecularly imprinted matrices, 274, 275
    - on polymer porous structure, 33, 38–39, 40, 78, 398–399
    - in suspension polymerisation, 313
    - solubility parameters, 38
- Solvent vapours, detection of, 470–472, 510–513
- Soman (nerve agent)
  - detection of, 63, 198, 478–479
  - hydrolysis product, 455, 478
  - structure, 479
- Specific pore volume, determination of, 53
- Specific surface area
  - determination of, 53
  - factors affecting, 35, 36
- Spectrophotometry, MIPs for ion separation, 462–463
- Spectroscopic sensors, 451–461
  - lanthanide ion chromophores, 453–457
  - optical probes for, 461
  - organic chromophores, 458–460
  - transition metal ion chromophores, 442, 452–453
- Spin-casting techniques (for preparation of thin films), 221, 516
- Spiropyran–merocyanine isomerisation, photostimulated, 281
- SSZ-26 (zeolite), 240
- Staphylococcus aureus*-imprinted polymer
  - beads, 297, 300, 301
- Starch, cross-linked, 282
- Statistical copolymers, 28
- Steady state, in free radical polymerisation, 26
- Stereoselective adsorbents, 118–121, 188, 224–225
- Stereoselective reactions, 94
- Steroid-imprinted polymers, 64, 94, 98, 101, 206
- Steroids
  - separation of, 12
  - as templates, 206, 346, 488
- Stoichiometric non-covalent interactions, 97–107
  - examples, 98
- Structure–binding relationships, 118–125
- Structure elucidation, molecularly imprinted silica used in, 13
- Structure–selectivity relationships, in molecularly imprinted silicas, 13
- Styrene–divinylbenzene copolymers, 22
  - porosity, 33–34
  - in solid phase extraction, 356
- Styrene–methyl methacrylate (S–MMA) copolymers, 32
- Subtilisin, bio-imprinted, 273, 276, 277–278
- Sugars see Saccharides
- Sulphonamides, as templates, 236–237, 238
- Supercritical carbon dioxide, polymerisation in, 321–322
- Supramolecular imprinting, 240, 241
  - concentration threshold for, 220
- Surface acoustic wave (SAW) sensors, 420, 480, 491, 504, 505, 506
  - detection limits, 515, 516
- Surface area of polymers, factors affecting, 35, 36
- Surface imprinting, 246–247, 250, 292
  - of microorganisms, 295–303
  - using monomer-type surfactants, 266–267
  - using oil/water emulsion polymerisation, 255–260
  - using plasma deposition technique, 292
  - using seed emulsion polymerisation, 250–251, 320–321
  - using water/oil emulsion polymerisation, 260–262

- Surface-modified metal-coordinating  
  imprinted polymers, 191–192
- Surface plasmon resonance (SPR) sensors,  
  423, 472–473
- Surface rearrangement method, for metal ion  
  imprinted beads/microspheres, 250–251,  
  320–321
- Surfactants  
  monomer-type, in surface imprinting, 266–  
  267  
  polymeric, in suspension polymerisation,  
  313
- Suspension polymerisation, 21–22, 79  
  in fluorocarbon liquids, imprinted beads  
  produced by, 308, 312–315, 347,  
  400  
  in non-aqueous media, 79  
  partitioning of components, 306–307  
  in water, imprinted beads produced by,  
  308, 311–312, 400  
  *see also* Emulsion polymerisation
- Swelling of polymers  
  effect on binding sites, 36–37  
  effect on sensors, 521–522  
  factors affecting, 36, 54–55, 154, 162, 165–  
  167, 171  
  in imprinted gels, 289–291  
  in MISPE, 362
- Swollen polymers, determination of porosity,  
  54–55
- Synthetic enzymes, 281
- Synthetic receptors, 271
- Tacticity of polymers, 28
- Tamoxifen  
  solid phase extraction of, 352, 360, 366  
  structure, 361
- Tamoxifen-imprinted polymers, in solid  
  phase extraction, 365
- Template  
  bleeding  
  effects, 43, 161  
  in MISPE protocols, 371–372  
  prevention of, 43  
  competition with fluorescent reporter,  
  474–475  
  effect of concentration on MIP selectivity,  
  149  
  effect on formation of fluorophores, 474  
  extraction of, 7, 43–44, 73, 74  
  binding-site interactions during, 43, 81  
  number of interaction sites, 146–147  
  polymer chain conformation affected by,  
  32, 33  
  polymer chain growth affected by, 32, 33  
  preparative amounts required, 161  
  quantification of, 44  
  racemic, 143  
  remaining/residual, 7, 222  
  effect on MIP recognition, 158–159  
  rigid, selectivity affected by, 63  
  shape, MIP selectivity affected by, 154–  
  155
- Template–functional monomer interactions,  
  60–61, 126–127, 138  
  effect of porogens, 330, 334  
  factors affecting, 138, 169, 186, 330, 334  
  study by optical techniques, 219, 472–473
- Template–metal ion interactions, 63
- Template–monomer assemblies *see*  
  Monomer–template assemblies
- Template polymerisation *see* Molecular  
  imprinting
- Template–template self-association, 66–67
- Terbutylazine  
  chromatographic retention on MIPs, 177,  
  178  
  recognition by MIPs, 170  
  structure and properties, 169
- Terbutylazine-imprinted polymers, in solid  
  phase extraction, 367, 368
- Terephthalic acid, imprinting by, 87, 91
- Termination, free radical polymerisation,  
  25–26
- Testosterone and derivatives  
  separation of, 12  
  structure, 489
- Testosterone-imprinted polymers, 206, 488
- 2,3,7,8-Tetrachlorodibenzodioxin (TCDD),  
  receptors for, 207–208
- Tetraethoxysilane (TEOS) gels, 215  
  fluorophore-imprinted, 475  
  (–)-menthol-imprinted, 226
- Tetrahydrofuran-imprinted coatings, 511
- Tetramethoxysilane, in metal oxide thin  
  films, 429
- Tetramethylene dimethacrylate, as cross-  
  linker, 75

- Thebaine-imprinted beads, 319–320
- Theobromine, 472, 473
- Theophylline, 344
- determination of, 344, 345
  - immunoassay compared with MIA, 344
  - recognition of, 267
  - separation from caffeine, 329, 348
  - solid phase extraction of, 352, 360, 364, 370
  - structure, 361, 473
- Theophylline-imprinted polymers/resins, 123, 208, 316, 317, 344
- response to xanthine and derivatives, 329, 348, 472
  - in rod form, 328, 329
  - in solid phase extraction, 365
- Thermal annealing, as post-treatment, 161–164
- Thermal curing, 161, 164
- Thermal gravimetric analysis (TGA), 55, 164
- Thermochemically initiated polymerisation, 24
- compared with photochemically initiated polymerisation, 39–41, 150
- Thermodynamic considerations, 59–68
- of MIP–ligand recognition, 64–67
  - in preparation of MIPs, 59–64
  - stabilisation of monomer–template assemblies affected by, 147–154
- Thermometric sensors, 421, 422
- Thermoporosimetry, 54
- Thermoresponsive imprinted gels, 291
- Thiamphenicol
- flow injection analysis, 484–488
  - structure, 486
- Thin films
- metal ion imprinted resins, 267
  - metal oxide gels, 221
- Thin layer chromatography
- chiral chromatography, 410–412
  - molecularly imprinted silicas used in, 12–13
- Three-dimensional matrices for molecular imprinting, 221–239
- Thymidine imprinted enzyme, 278
- Timolol
- resolution of enantiomers, 401, 403
  - as template, 140, 402
- Tin dioxide substrate, in monolayers, 218, 219, 220
- Tin(IV) oxide electrodes, silane monolayers on, 218, 219, 430
- Titanium oxide films, 4-(4-propyloxyphenylazo)benzoic acid-imprinted, 221, 428, 472
- Tobacco peroxidase, 2,4-D MIP conjugated to, 350–351, 496
- Transducers
- electrochemical, 418–420
  - field effect transistor-based, 420
  - magnetometric, 421
  - mass-sensitive, 420
  - optical, 420–421
  - thermometric, 421
- Transesterification, effect of imprinted silica gels, 237, 238
- Transferrin-imprinted gels, 227, 228, 284
- Transition metal ion chromophores, 442, 452, 453
- Transition metal ions, separation of, 247–255
- Transition state analogues, 237, 282
- Trialdehydes, as templates, 89
- 1,4,7-Triazacyclononane (TACN), 265–266, 444
- Triazine, structure, 476
- Triazine-imprinted polymer, 475
- Triazines, 168, 366
- chromatographic retention on MIPs, 152, 177, 178
  - combinatorial approach for MIPs, 336–339
  - determination of, 345
  - fluorescent detection of, 474–475
  - hydrophobicity, 169, 178
  - properties, 169
  - recognition by MIPs, 170
  - solid phase extraction of, 352, 359, 364
  - solution complexes, 159–160
  - structures, 169, 361
  - as templates, 152, 168–170
  - see also* Ametryn; Atrazine; Cyanazine; Prometryn; Terbutylazine
- Tricarbamates, as templates, 233
- Triethylamine (TEA), 364
- Triethylene glycol dimethacrylate (TEGDMA), as cross-linker, 76, 77



- Trifluoroacetic acid (TFA), 364
- 2-(Trifluoromethyl)acrylic acid (TFM)  
   compared with methacrylic acid  
     in imprinting of cinchona alkaloids, 330–331  
     in imprinting of triazines, 169–170, 336–339  
   as functional monomer, 63, 140, 169–170, 330–331, 336–339, 397, 398  
   structure, 140, 337
- 1,3,5-Trihydroxybenzene, 471
- Tri-Langmuir adsorption isotherm, 126, 132
- Trimethoxysilylpropylguanidinium chloride, 101, 229
- N,N,N*-Trimethyl-2-aminoethyl methacrylate, 141
- Trimethylolpropane trimethacrylate (TRIM)  
   as cross-linker, 42, 43, 76, 398, 399, 468, 480  
   in chiral stationary phases, 405  
   polymer  
     effect of thermal annealing, 162  
     preformed beads, 307, 310  
     with surface-modified metal-coordinating imprinted polymers, 192, 193  
   structure, 42, 399
- Trimethylsilane monolayers, 219
- Tripeptides, binding to MIPs, 209–210
- Triquat cation, as template, 240
- Tröger's Base MIP, interactions with ligands, 65
- Tromsdorff effect, 29
- Trypsin-imprinted gels, 288
- Tryptamine, effect on fluorescence, 495
- L-Tryptophan  
   fluorescent sensor for, 494–496  
   structure, 495
- Tryptophan anilide, resolution of enantiomers, 122
- Two-dimensional matrices for molecular imprinting, 217–220, 286  
   *see also* Chemical vapour deposited (CVD) films; Langmuir–Blodgett (LB) films; Self-assembled monolayers (SAMs)
- Two-phase suspension... *see* Oil/water suspension polymerisation
- Two-step swelling method, imprinted beads produced by, 317–319, 400
- Tyrosine, resolution of enantiomers, 195
- Tyrosine anilide, resolution of enantiomers, 122
- Uranyl ion  
   photometric determination of, 462–463  
   selective electrodes, 265, 450, 464
- Urea sensors, 422
- UV-initiated polymerisation  
   bulk polymerisation, 24, 314  
   suspension polymerisation, 313–314
- Vapours, detection of, 470–472, 510–513
- 4-Vinylbenzamidines, as functional monomers, 139, 143
- p*-Vinylbenzoic acid, as functional monomer, 140, 398, 450, 451
- N*-(4-Vinylbenzyl)iminodiacetic acid, as functional monomer, 398, 409, 410
- 4-Vinylbenzyl thioacetate, 90, 92
- 1-(4'-Vinylbenzyl)-1,4,7-triazacyclononane Cu(II) methyl- $\beta$ -D-glucopyranoside, 200, 426, 427
- 4-Vinyl-1-(*N,N'*-dialkylamidino)benzene  
   association constant for complex with 4-methylbenzoic acid, 158  
   as functional monomer, 143
- 1-Vinylimidazole, as functional monomer, 398
- Vinylimidazole–Co<sup>2+</sup> complexes, 188, 197
- Vinylimidazole–Ni(II) complexes, 248
- 4-Vinylphenylboronic acid, 72, 73, 74, 143, 474  
   polymers, 82
- 10-(*p*-Vinylphenyl)decanoic acid, as monomer-type surfactant, 267
- 2-Vinylpyridine (2VPY), as functional monomer, 141, 142, 209, 380, 398, 473
- 4-Vinylpyridine (4VPY)  
   as functional monomer, 141, 142, 151, 209, 247, 318, 347, 380, 398, 481, 488, 492  
   in fluorescent detection of  $\beta$ -estradiol, 488  
   metal ion complexes, 247, 250  
   *see also* Poly(4-vinylpyridine)

- 1-Vinyl-2-pyrrolidone, as functional monomer, 144, 248, 444
- Vinylsalicylaldoxime, 450, 451
- Vitamin K<sub>1</sub>  
determination of, 218, 219, 430, 468, 509  
structure, 219, 469
- Vitamin K<sub>3</sub>, 219, 469
- Volatile organic compounds (VOCs), 509
- Water  
polycyclic aromatic hydrocarbons in, 479–480, 491  
as solvent of polymerisation, 63–64  
stagnant, odour compound, 471  
suspension polymerisation in, imprinted beads produced by, 308, 311–312, 400
- Water-compatible polymers, 64
- Water/oil emulsion polymerisation, surface imprinting using, 260–262
- Watson–Crick type interactions, 160
- Xanthine, structure, 473
- Xanthine derivatives  
selectivity of theophylline MIP, 328, 329, 348  
*see also* Caffeine; Methylxanthine; Theobromine; Theophylline
- Xanthine-imprinted polymer, 472
- Xerogels, silica-containing, 216
- X-ray photoelectron spectroscopy (XPS), surface-modified metal-coordinating imprinted polymers studied by, 192
- x* reciprocal plot *see* Scatchard plot
- Yohimbine-imprinted polymers, 63
- Zeolites, 239  
molecular imprinting of, 239–240, 428
- Zinc(II)-imprinted polymers/resins  
metal adsorption behaviour  
adsorption isotherms, 257–260  
pH effects, 261, 262, 263  
preparation of, 256, 257, 260
- Zinc selenide crystals, 2,4-D MIP on, 491, 493
- ZSM-18 (zeolite), 240
- Zwitterionic species, 64

This Page Intentionally Left Blank